CYTOKINE-MEDIATED ORGAN DYSFUNCTION AND TISSUE DAMAGE INDUCED BY VIRUSES

EDITED BY: Michael H. Lehmann, Piotr Religa and Juliet Spencer
PUBLISHED IN: Frontiers in Immunology

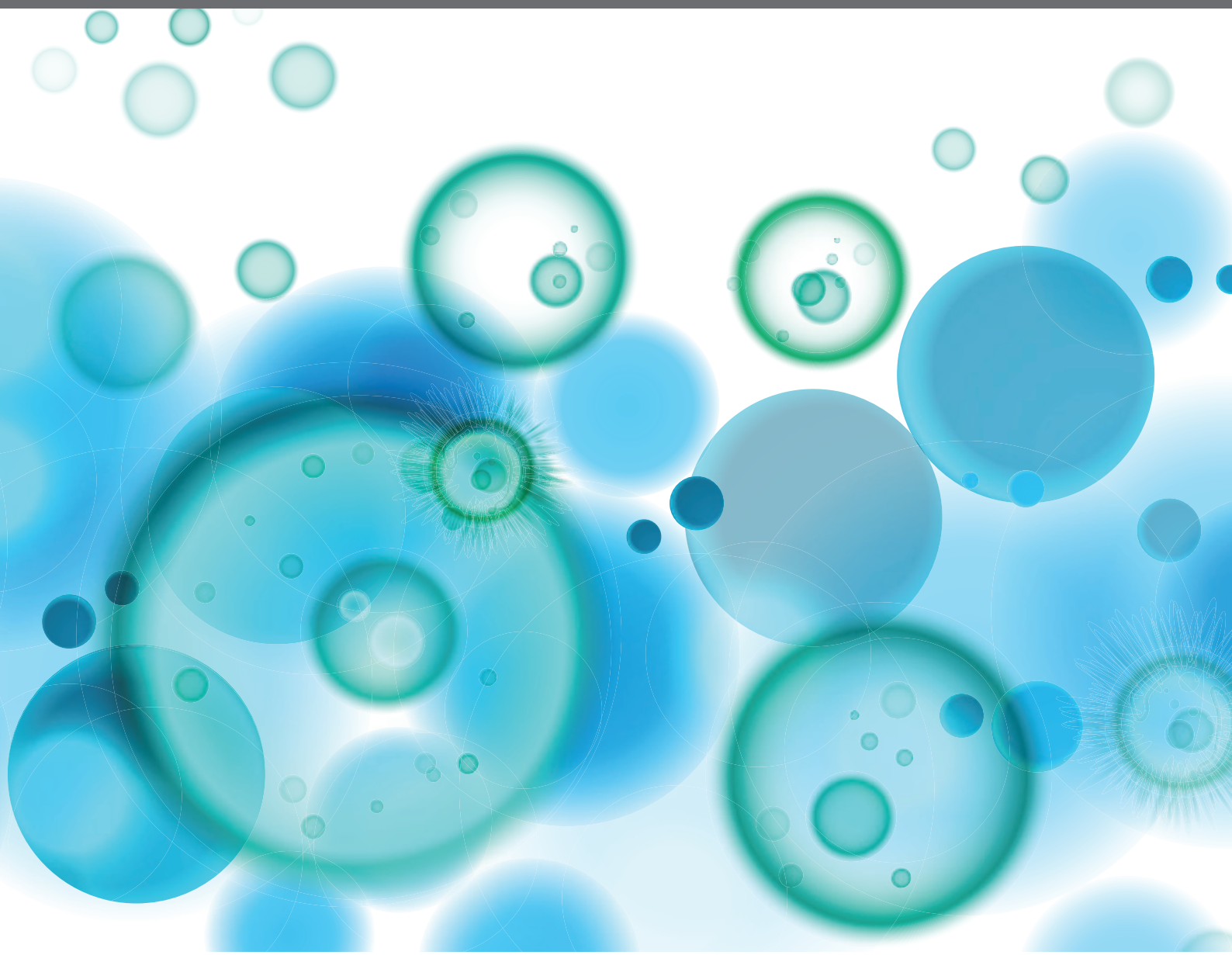

frontiers Research Topics

ISSN 1664-8714
ISBN 978-2-88963-519-1
DOI 10.3389/978-2-88963-519-1

About Frontiers

Frontiers is more than just an open-access publisher of scholarly articles: it is a pioneering approach to the world of academia, radically improving the way scholarly research is managed. The grand vision of Frontiers is a world where all people have an equal opportunity to seek, share and generate knowledge. Frontiers provides immediate and permanent online open access to all its publications, but this alone is not enough to realize our grand goals.

Frontiers Journal Series

The Frontiers Journal Series is a multi-tier and interdisciplinary set of open-access, online journals, promising a paradigm shift from the current review, selection and dissemination processes in academic publishing. All Frontiers journals are driven by researchers for researchers; therefore, they constitute a service to the scholarly community. At the same time, the Frontiers Journal Series operates on a revolutionary invention, the tiered publishing system, initially addressing specific communities of scholars, and gradually climbing up to broader public understanding, thus serving the interests of the lay society, too.

Dedication to Quality

Each Frontiers article is a landmark of the highest quality, thanks to genuinely collaborative interactions between authors and review editors, who include some of the world's best academicians. Research must be certified by peers before entering a stream of knowledge that may eventually reach the public - and shape society; therefore, Frontiers only applies the most rigorous and unbiased reviews.
Frontiers revolutionizes research publishing by freely delivering the most outstanding research, evaluated with no bias from both the academic and social point of view. By applying the most advanced information technologies, Frontiers is catapulting scholarly publishing into a new generation.

What are Frontiers Research Topics?

Frontiers Research Topics are very popular trademarks of the Frontiers Journals Series: they are collections of at least ten articles, all centered on a particular subject. With their unique mix of varied contributions from Original Research to Review Articles, Frontiers Research Topics unify the most influential researchers, the latest key findings and historical advances in a hot research area! Find out more on how to host your own Frontiers Research Topic or contribute to one as an author by contacting the Frontiers Editorial Office: researchtopics@frontiersin.org

CYTOKINE-MEDIATED ORGAN DYSFUNCTION AND TISSUE DAMAGE INDUCED BY VIRUSES

Topic Editors:
Michael H. Lehmann, Ludwig-Maximilians-Universität München, Germany
Piotr Religa, Karolinska Institutet, Sweden
Juliet Spencer, Texas Woman's University, United States

Citation: Lehmann, M. H., Religa, P., Spencer, J., eds. (2020). Cytokine-Mediated Organ Dysfunction and Tissue Damage Induced by Viruses. Lausanne: Frontiers Media SA. doi: 10.3389/978-2-88963-519-1

Table of Contents

frontiers in Immunology

EDITORIAL
published: 22 January 2020
doi: 10.3389/fimmu.2020.00002

Editorial: Cytokine-Mediated Organ Dysfunction and Tissue Damage Induced by Viruses

Juliet V. Spencer[1], *Piotr Religa*[2] *and Michael H. Lehmann*[3]*

[1] Department of Biology, Texas Woman's University, Denton, TX, United States, [2] Department of Medicine, Karolinska Institutet, Stockholm, Sweden, [3] Institute for Infectious Diseases and Zoonoses, Ludwig-Maximilians-Universität München, Munich, Germany

Keywords: coxsackievirus, hantavirus, HCMV, HIV, influenza, MHV, RSV, TMEV

Editorial on the Research Topic

Cytokine-Mediated Organ Dysfunction and Tissue Damage Induced by Viruses

Cytokines are small proteins, mostly secreted into the extracellular environment, that bind to specific cell surface receptors, which mediate cell differentiation, migration, growth, and death. Gene expression and cellular release of cytokines are strictly regulated to assure proper function of cells, tissues, and organs. Upon virus infection, a cell starts producing type I interferons (IFN) and inflammatory cytokines (ICs) to restrict spread and replication of the respective virus. Ideally, the virus is completely eliminated by the immune system and the antiviral mechanisms are turned off within a reasonable time frame. However, there are different scenarios where this process does not work efficiently or does not happen at all, leading to cytokine-mediated organ dysfunction and tissue damage.

First, if a virus inhibits type I IFN production and signaling but does not prevent expression of ICs, then this virus spreads further, and more viral components are in the system, which continuously amplifies ICs production. The lung is one organ that is especially vulnerable to such a "cytokine storm," triggered, for example, by infection with respiratory syncytial virus (RSV) or influenza virus. In a comprehensive review article, Bohmwald et al. describe in detail where and which cytokines are induced during human RSV infection and their potential contribution to damage of not only the lung but also the brain. The pathophysiological production of ICs is most probably also due to the ability of RSV to induce the expression of Toll-like receptor (TLR) 4 in human airway epithelial cells, which normally do not respond to endotoxin (1).

Aflatoxin B_1 (AFB_1), a mycotoxin produced by *Aspergillus flavus*, increases TLR4 expression as well as TLR2, IL-1β, and IL-6 expression in human monocyte-derived dendritic cells (2). Sun et al. confirmed upregulation of TLR4 expression by AFB_1 in porcine alveolar macrophages (PAMs) and mice infected with swine influenza virus (SIV) subtype H1N1. Importantly, they show that AFB_1 exacerbates lung damage in mice during SIV infection, caused by a TLR4-dependent increase in viral replication and TNF levels. Consequently, uptake of AFB_1, for example by contaminated food (3), could aggravate the course of flu.

Experimental evidence suggests that extrarespiratory induction of ICs such as TNF, IL-6, and IL-8 contributed to deadly infection with the 1918 H1N1 influenza A virus (IAV) strain (4), which hit mankind during World War I, a period when not sufficient food was available (5). Similarly, systemic high levels of IL-6 and IL-8 were detected in humans infected with IAV subtype H5N1, especially in those with fatal outcome, but not in humans infected with IAV subtype H3N2 or H1N1 (6). Hence, it appears that an IAV which just passed the animal-human barrier is much more harmful than a human adapted strain. In this respect, Krischuns et al. discovered that infection

Edited and reviewed by:
Vitaly V. Ganusov, The University of Tennessee, Knoxville, United States

***Correspondence:**
Michael H. Lehmann
Michael.Lehmann@lmu.de; Orlataler@web.de

Specialty section:
This article was submitted to Viral Immunology, a section of the journal Frontiers in Immunology

Received: *26 November 2019*
Accepted: *02 January 2020*
Published: *22 January 2020*

Citation:
Spencer JV, Religa P and Lehmann MH (2020) Editorial: Cytokine-Mediated Organ Dysfunction and Tissue Damage Induced by Viruses. Front. Immunol. 11:2. doi: 10.3389/fimmu.2020.00002

of human alveolar epithelial cells with highly pathogenic avian influenza virus (HPAIV) strains, but not with human adapted IAV strains, leads to constitutive phosphorylation of tripartite motif (TRIM) 28 at S473 and increased production of IFN-β, IL-6, and IL-8. TRIM28 negatively regulates transcription in a number of ways (7), and the inability of the non-human adapted influenza strains to prevent its deactivation could well explain the dysregulated cytokine expression observed in individuals infected with the IAV subtype H5N1 or the 1918 pandemic H1N1 IAV. In conclusion, severe organ damage can occur if a virus passes from its natural host to another species where it can or gains the ability to replicate without having an effective mechanism to block immunity of the other species. such a scenario is frequently observed in humans when they are infected with hantavirus (8). Possibly, activation of bystander CD8+ T cells after hantavirus infection, as shown in an original article by Raftery et al., could be a reason for the organ damages in humans. Indeed, viral-activated bystander memory CD8+ T cells can cause organ damage in a T cell receptor independent manner (9). In contrast, no apparent disease is observed in rodents, the natural reservoir hosts of all hantavirus species, which is similar to humans where a lifelong, persistent infection with human cytomegalovirus (HCMV) remains normally inconspicuous. However, there are several situations in which HCMV induces damage to organs and tissues, and Clement and Humphreys review the involvement of cytokines therein.

The cellular tropism of human and simian immunodeficiency virus is limited, but dysfunctions and damages also occur in the hearts, lungs, kidneys, and brains of infected individuals. Lehmann et al. provide a model to understand the complexity of these pathologies based on recent cell biology findings about systemic distribution of the viral Nef protein and improved understanding of C-C motif chemokine ligand 2 (CCL2) dependent transendothelial cell migration. The focus of this Mini Review is on the brain, where non-physiological induction of CCL2 expression not only drives encephalitis but also affects signaling and survival of neuronal cells. Indeed, antiviral and anti-inflammatory cytokine expression have to be well-coordinated during a viral infection in order to enable elimination of the pathogen on the one hand, and to avoid tissue and organ damage on the other hand. This problem is discussed by Savarin and Bergmann on the basis of a murine model of encephalomyelitis induced by a neurotropic strain of mouse hepatitis virus where the interplay of IFN and IL-10 dictates the extent of viral control and tissue pathology.

Type I IFN is required to restrict coxsackievirus B3 (CVB3) replication (10), and Liu et al. found that functional TRIM21 is important for high level type I IFN expression *in vitro* and *in vivo*. Additionally, they show that TRIM21 deficiency leads to higher viral titers, stronger cardiac and pancreatic damages, and higher levels of ICs including CCL2 in mice infected with CVB3. Meyer et al. detected increased levels of colony stimulating factor 1 (CSF-1) in heart biopsies of patients with myocarditis, and by using nanoparticle-encapsulated siRNA directed against CSF-1 they could decrease CVB3-induced monocyte infiltration and heart damage in mice. Beling and Kespohl suggest that therapeutic targeting the proteasome could help to prevent immunopathology of the heart, which can be triggered by many different viruses. Theiler's murine encephalitis virus (TMEV) induces myocarditis in mice, but this virus can also induce demyelination of neurons depending on the mouse strain. A Hypothesis and Theory article by Omura et al. summarizes findings about the different nature of these diseases and provides evidence that TMEV induces cell-type specific innate immune responses and distinct organ-specific pathology. Thus, the choice of the right animal model to study virus induced immunopathology can be challenging. For that, Manickam et al. provide a thorough review of non-human primate models for understanding the extent of cytokine-mediated tissue damage during many different types of virus infection, including dengue virus, HCMV, hepatitis B and C virus, HIV, influenza virus, and Zika virus.

Collectively, this Research Topic introduces some of the complex virus-host interactions that can tip the scales toward immunopathology. The common themes that emerge from this collection include the potential for use of cytokines as markers of disease and the manipulation of certain cellular molecules as therapeutic options.

AUTHOR CONTRIBUTIONS

All authors listed have made a substantial, direct and intellectual contribution to the work, and approved it for publication.

ACKNOWLEDGMENTS

We extend our gratitude to the authors for their excellent contributions to the Research Topic, and we thank the reviewers for their time, effort, and helpful feedback.

REFERENCES

1. Monick MM, Yarovinsky TO, Powers LS, Butler NS, Carter AB, Gudmundsson G, et al. Respiratory syncytial virus up-regulates TLR4 and sensitizes airway epithelial cells to endotoxin. *J Biol Chem.* (2003) 278:53035–44. doi: 10.1074/jbc.M308093200
2. Mohammadi A, Mehrzad J, Mahmoudi M, Schneider M. Environmentally relevant level of aflatoxin B1 dysregulates human dendritic cells through signaling on key toll-like receptors. *Int J Toxicol.* (2014) 33:175–86. doi: 10.1177/1091581814526890
3. Mahato DK, Lee KE, Kamle M, Devi S, Dewangan KN, Kumar P, et al. Aflatoxins in food and feed: an overview on prevalence, detection and control strategies. *Front Microbiol.* (2019) 10:2266. doi: 10.3389/fmicb.2019.02266
4. de Wit E, Siegers JY, Cronin JM, Weatherman S, van den Brand JM, Leijten LM, et al. 1918 H1N1 influenza virus replicates and induces proinflammatory cytokine responses in extrarespiratory tissues of ferrets. *J Infect Dis.* (2018) 217:1237–46. doi: 10.1093/infdis/jiy003
5. Richardson M. *The Hunger War: Food, Rations and Rationing 1914-1918.* Barnsley: Pen and Sword Books (2015). p. 272.

6. de Jong MD, Simmons CP, Thanh TT, Hien VM, Smith GJ, Chau TN, et al. Fatal outcome of human influenza A (H5N1) is associated with high viral load and hypercytokinemia. *Nat Med.* (2006) 12:1203–7. doi: 10.1038/nm1477
7. Cheng CT, Kuo CY, Ann DK. KAPtain in charge of multiple missions: emerging roles of KAP1. *World J Biol Chem.* (2014) 5:308–20. doi: 10.4331/wjbc.v5.i3.308
8. Jiang H, Zheng X, Wang L, Du H, Wang P, Bai X. Hantavirus infection: a global zoonotic challenge. *Virol Sin.* (2017) 32:32–43. doi: 10.1007/s12250-016-3899-x
9. Kim J, Chang DY, Lee HW, Lee H, Kim JH, Sung PS, et al. Innate-like cytotoxic function of bystander-activated CD8(+) T cells is associated with liver injury in acute hepatitis A. *Immunity.* (2018) 48:161–73.e5. doi: 10.1016/j.immuni.2017.11.025
10. Kandolf R, Canu A, Hofschneider PH. Coxsackie B3 virus can replicate in cultured human foetal heart cells and is inhibited by interferon. *J Mol Cell Cardiol.* (1985) 17:167–81. doi: 10.1016/s0022-2828(85)80019-5

Conflict of Interest: The authors declare that the research was conducted in the absence of any commercial or financial relationships that could be construed as a potential conflict of interest.

frontiers in Immunology

REVIEW
published: 18 March 2019
doi: 10.3389/fimmu.2019.00452

Contribution of Cytokines to Tissue Damage During Human Respiratory Syncytial Virus Infection

*Karen Bohmwald[1], Nicolás M. S. Gálvez[1], Gisela Canedo-Marroquín[1], Magdalena S. Pizarro-Ortega[1], Catalina Andrade-Parra[1], Felipe Gómez-Santander[1] and Alexis M. Kalergis[1,2]**

[1] Millenium Institute on Immunology and Immunotherapy, Departamento de Genética Molecular y Microbiología, Facultad de Ciencias Biológicas, Pontificia Universidad Católica de Chile, Santiago, Chile, [2] Departamento de Endocrinología, Facultad de Medicina, Pontificia Universidad Católica de Chile, Santiago, Chile

The human respiratory syncytial virus (hRSV) remains one of the leading pathogens causing acute respiratory tract infections (ARTIs) in children younger than 2 years old, worldwide. Hospitalizations during the winter season due to hRSV-induced bronchiolitis and pneumonia increase every year. Despite this, there are no available vaccines to mitigate the health and economic burden caused by hRSV infection. The pathology caused by hRSV induces significant damage to the pulmonary epithelium, due to an excessive inflammatory response at the airways. Cytokines are considered essential players for the establishment and modulation of the immune and inflammatory responses, which can either be beneficial or harmful for the host. The deleterious effect observed upon hRSV infection is mainly due to tissue damage caused by immune cells recruited to the site of infection. This cellular recruitment takes place due to an altered profile of cytokines secreted by epithelial cells. As a result of inflammatory cell recruitment, the amounts of cytokines, such as IL-1, IL-6, IL-10, and CCL5 are further increased, while IL-10 and IFN-γ are decreased. However, additional studies are required to elicit the mediators directly associated with hRSV damage entirely. In addition to the detrimental induction of inflammatory mediators in the respiratory tract caused by hRSV, reports indicating alterations in the central nervous system (CNS) have been published. Indeed, elevated levels of IL-6, IL-8 (CXCL8), CCL2, and CCL4 have been reported in cerebrospinal fluid from patients with severe bronchiolitis and hRSV-associated encephalopathy. In this review article, we provide an in-depth analysis of the role of cytokines secreted upon hRSV infection and their potentially harmful contribution to tissue damage of the respiratory tract and the CNS.

Keywords: human respiratory syncytial virus, cytokines, chemokines, tissue damage, inflammation

OPEN ACCESS

Edited by:
Michael H. Lehmann, Ludwig Maximilian University of Munich, Germany

Reviewed by:
Peter J. M. Openshaw, Imperial College London, United Kingdom
Yashoda M. Hosakote, The University of Texas Medical Branch at Galveston, United States

***Correspondence:**
Alexis M. Kalergis
akalergis@bio.puc.cl;
akalergis@icloud.com

Specialty section:
This article was submitted to Cytokines and Soluble Mediators in Immunity, a section of the journal Frontiers in Immunology

Received: *21 September 2018*
Accepted: *19 February 2019*
Published: *18 March 2019*

Citation:
Bohmwald K, Gálvez NMS, Canedo-Marroquín G, Pizarro-Ortega MS, Andrade-Parra C, Gómez-Santander F and Kalergis AM (2019) Contribution of Cytokines to Tissue Damage During Human Respiratory Syncytial Virus Infection. Front. Immunol. 10:452. doi: 10.3389/fimmu.2019.00452

INTRODUCTION

Prevalence of hRSV Infection Worldwide

The human respiratory syncytial virus (hRSV) is one of the primary viral agents causing hospitalizations due to acute lower respiratory tract infection (ALRTI) in young children, immunocompromised and elderly individuals worldwide (1, 2). The epidemic period for hRSV infections usually takes place during the winter season in areas with temperate climates (3).

This pathogen causes pulmonary manifestations mainly in the upper and lower respiratory tract, promoting the development of bronchiolitis and pneumonia (**Figure 1**) (4, 5). Some of the risk factors associated with the development of hRSV-associated ALRTI are premature birth, low birth weight, maternal smoking, history of atopy and no history of breastfeeding in infancy, among others (6). A recent report estimated that -during 2015- hRSV-associated ALRTI episodes reached a global burden of 33.1 million, resulting in 3.2 millions hospital admissions and around 60,000 in-hospital deaths in children under the age of 5 (1), although, no global studies of other populations such as the elderly or patients with underlying medical conditions have been conducted (7). Reinfections during childhood and adulthood are very common, and the severity of hRSV infections in healthy adults is mild. This decrease in severity has been related to higher neutralizing antibody titers induced by constant challenges with the virus throughout life (8). Besides children, the elderly have been described as another high-risk population, probably because of their senescent immune system (9). In this population, hRSV is the leading viral pathogen, which causes morbidity and mortality, followed by influenza A (10).

Besides the airway pathologies caused by hRSV, neurologic complications have also been described after infection with this virus, although less frequently (11–13). The etiology of the neurological alterations remains unknown. However, it has been proposed that inflammatory mediators, such as cytokines could be playing an essential role in the development of neurologic alterations (14, 15).

The hRSV is a highly contagious virus, as it can live outside of the host for about 6 h on hard surfaces, and as much as 20 min on the skin (16). Also, people that are infected with this virus remain contagious up to 8 days starting from the day of infection (17). Studies have shown that at least a third of the children experiencing hRSV infection within their first year of life will get re-infected during their second or third year of life (18). Patients infected with this virus cannot promote an adequate immunological response and, therefore, can get infected again with the same virus in the same cohort (19). In this regard, it has been described that this virus can impair the assembly of a proper immunological synapse between the antigen-presenting cells (APC), such as the dendritic cells, and T cells (**Figure 1B**) (20). In this way, hRSV renders T cells unable to respond correctly, which may lead to a poor adaptive immune response against the virus and, consequently, the reinfections mentioned above (**Figure 1**).

Most studies, aimed to determine the economic burden associated with hRSV, measure its immediate impact on health-care resources, such as hospitalizations, ambulatory care, and emergency department visits, focusing primarily on infant populations (21–23). It is noteworthy that hRSV has been associated with long-term illness such as asthma and recurrent wheezing (24, 25), which could represent a substantial increase in the economic burden related to this pathogen (26, 27).

Currently, there are no licensed vaccines available for preventing hRSV infection although several groups are working in the development of potentially effective vaccines and therapies. Nowadays, the only drug available on the market designed to ameliorate this disease is palivizumab, a humanized monoclonal antibody against the fusion protein (F-protein) of the virus. This product is used as a prophylactic option, along with ribavirin as a therapeutic option, although this strategy is only used in high-risk patients, such as children born after $\leq$29 weeks of gestation and preterm infants with chronic pulmonary disease (28, 29). Because this treatment fails to target most of the population susceptible to hRSV-caused disease, (i.e., healthy infants, children, and the elderly), the development of an effective vaccine is imperative (21, 22, 30). Several studies have concluded that the cost-effectiveness of palivizumab might not be enough to recommend the massive use of this antibody (22, 31–33). However, other studies have concluded that it does reduce the severity of infection and long-term effects on children, suggesting that it can diminish the spending of health-care resources (34, 35).

hRSV: General Characteristics and Infective Cycle

The hRSV has been recently defined as a member of the *Orthopneumovirus* genus from the *Pneumoviridae* family being also recently renamed as human Orthopneumovirus and is an enveloped, negative-sense and single-stranded RNA virus with a genome of about 15.2 kb, possessing 10 genes that encode for 11 proteins (36–38). The viral particle displays 3 surface proteins, the F-protein, the glycoprotein (G) and the small hydrophobic (SH) protein (**Figure 1A**). Of all these, the G-protein is responsible for the attachment with the membrane of the host cell (39), mainly by binding to the CX3CR1 receptor on ciliated epithelial cells (40, 41). The fpre F-protein is responsible for the fusion of the viral membrane with the host cell membrane and further entry of the viral genetic material into the cytosol, apparently by its interaction with the surface protein nucleolin, although other receptors have been described to play a role in this process (42).

This virus can be transmitted by aerosol particles person-to-person, or via direct contact of these aerosol particles with the exposed mucosa, such as conjunctival (43). After infection, the incubation period can vary between 2 and 8 days in healthy individuals (44). At the beginning of hRSV infection, the virus meets the first line of defense of the organism, consisting of epithelial cells from the nasal and upper respiratory tract (45, 46).

The airway epithelium presents the apical junctional complex (AJC), which seals the space between the layer of epithelial cells and acts as a barrier that prevents the entry of pathogens into the organism (47). It has been described that hRSV infection induces a dysfunction in the epithelial barrier in a protein kinase D (PKD)-dependent manner (48). After infection by hRSV, cells exhibit a disruption of the AJC, which can be prevented when PKD-inhibitors are added, as described previously (48). As mentioned above, once hRSV reaches the apical side of the ciliated epithelial cells, the G and F proteins allow the attachment and fusion of the virus to the host membrane, respectively (39, 42).

After the virus has fused with the membrane of the host cells, it then begins the mechanism of entering the cells. The entry of

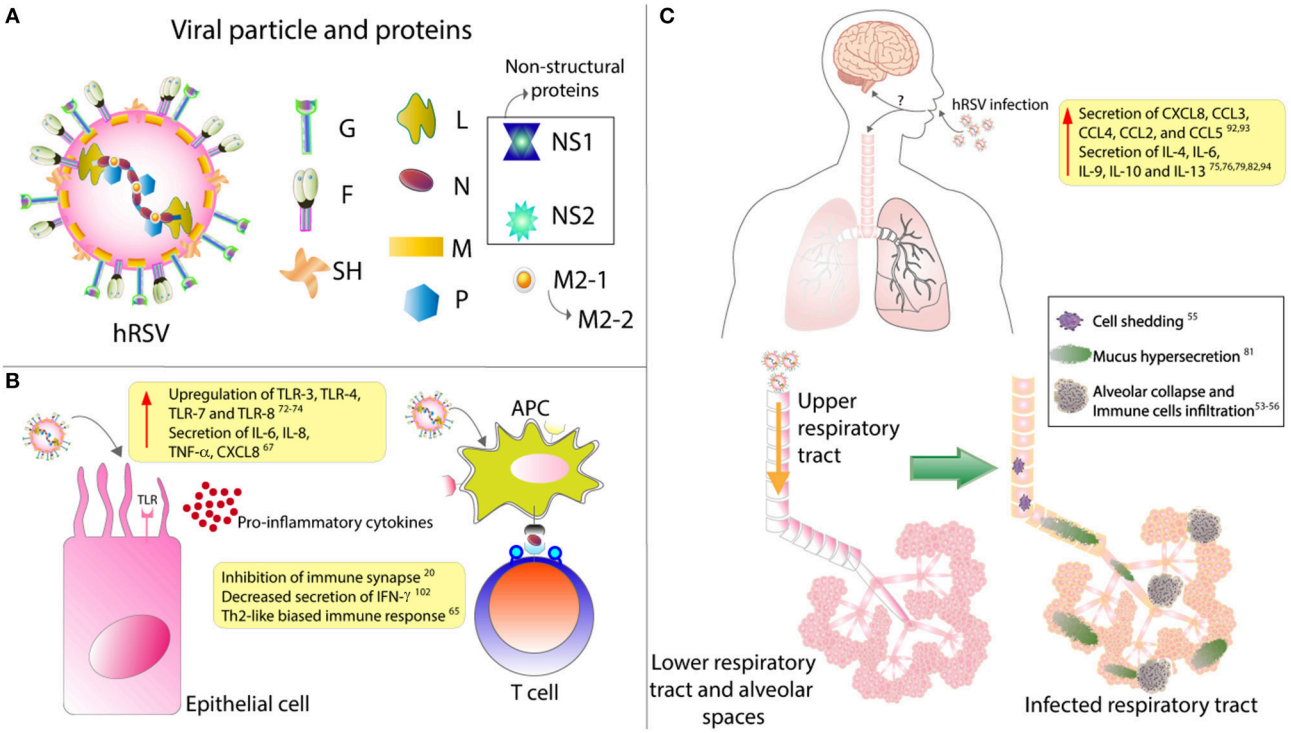

FIGURE 1 | hRSV structure and impact over epithelial cells and respiratory tract. **(A)** The viral particle is composed of 9 structural proteins: 3 in the surface (F, G, and SH) and the other 5 inside the particle (L, N, P, M, M2.1, and M2.2). **(B)** Upon infection, it has been described that epithelial cells upregulates their expression of several TLRs and secrete mainly pro-inflammatory cytokines. Remarkably, it has also been described that hRSV infection of antigen presenting cells (APC) renders them unable to properly activate T cells, as this virus is able to inhibit the assembly of an immunological synapse. **(C)** hRSV infection induces the secretion of several pro-inflammatory cytokines that will induce the infiltration of many immune cells. These immune cells, along with the hypersecretion of mucus and the shedding of the infected epithelial cells, will induce the collapse of the lower respiratory tract. Finally, it has been described that hRSV infection can cause CNS pathologies, although the mechanism underlying this have not been described.

the virus is through an endocytosis-dependent mechanism and allows the entering of the whole virus, including its lipid envelope (49). Then, the virus is carried within endocytic vacuoles, and undergoes a second fusion, this time with the vacuole itself, that occurs when the F-protein is cleaved by a furin-like convertase, to render the virus able to infect the cell (49). Then the virus reaches the cytoplasmic inclusion bodies (IBs) of the cells, where it can replicate its RNA using the viral RNA-dependent RNA polymerase (RdRp) complex, which is composed of the large protein (L) and the phosphoprotein (P) of the virus (50). As transcription goes on, the viral protein M2-1 is added to the complex allowing the synthesis of the mRNA (50, 51). The virus starts the replication of its RNA in the nasal epithelial cells and then it moves toward the bronchioles, where the replication becomes more effective (44). The virus spreads via intercellular extensions between two cells or through the cell to cell transmission, and in both cases, the infected cell is the one who passes the virus to the target cell (52).

To study the pathology associated with hRSV and the immune response during the infection, the use of several animal models has shown to be extremely important (53, 54). Lately, mice have been the animal model of choice for most immunology studies on this virus (53), although it is important to emphasize that the immune response observed in mice is not necessarily identical to the one observed in human patients. Some of these differences in the immune response between mice and humans are remarkable, for instance, the fact that older mice are more susceptible to hRSV-infection as compared to younger mice (55). Some techniques and methods to determine hRSV disease severity used in murine models are also different from those used to evaluate these parameters in humans. For instance, recording the body weight changes as a parameter of disease severity (more weight loss implies a more severe disease) is frequently used in the murine model, but it is not used as a parameter in humans disease (53). Also, obtaining bronchoalveolar lavage fluid (BALF) samples from mice is a standard procedure to evaluate inflammatory parameters, and these results can vary significantly from those observed in humans (53, 56). Although some differences can be observed, the data relative to cytokines and chemokines in the lower respiratory tract of mice and humans varies little, and to our knowledge, no published studies are describing these molecules in the upper respiratory tract and central nervous system (CNS) of mice (**Table 1**).

Further, in this review, we will provide an in-depth analysis of the current information available regarding the inflammatory mediators that are induced upon hRSV infection, and which ones are produced, up-regulated and down-regulated in the different sections of the respiratory tract and the CNS (**Table 1**).

TABLE 1 | Effect of hRSV infection on the expression profile of cytokines in the upper and lower respiratory tract and entral nervous system.

Organism	Upper respiratory tract	Lower respiratory tract	Central nervous system
Human		↑IL-6 (57, 58)	↑IL-6 (14, 15, 59)
		↑TNF-α (57, 58)	
		↑IL-4 (60–62)	
	↑TNF-α (63, 64)	↑IL-6 (60)	
	↑IL-12 (65)	↑IL-9 (60, 66)	
	↑IL-23 (65)	↓IL-10 (60–62, 67–69)	
		↑IL-13 (60–62)	
		↓IFN-γ (66)	
		↑IL-17 (70, 71)	
		↑TSLP (72)	
		↑CXCL8 (57, 58, 73)	
	↑CXCL8 (74)	↑CCL3 (57, 58, 75)	↑CCL2 (15)
	↑CCL5 (74)	↑CCL4 (57, 58)	↑CCL4 (15)
	↑CXCL10 (74)	↑CCL2 (57, 58)	↑CXCL8 (15)
		↑CCL5 (57, 58, 75)	
Mouse	–	↑IL-6 (76)	–
		↑IL-1β (77)	
		↑TNF-α (77)	
		↑IFN-γ (77)	
		↑IL-12 (77)	
		↑TSLP (78)	
	–	↑CCL3 (77)	–
		↑CCL5 (77)	

Additionally, we will discuss the contribution of cytokines to the immune response and immunopathology observed after hRSV infection.

CYTOKINES ELICITED BY hRSV INFECTION

Among the inflammatory mediators that have been described to play an essential role in the hRSV pathology are cytokines and chemokines. Cytokines are small secreted molecules that contribute significantly to the modulation of the immune response and T cells differentiation (79). Several cell types can produce and secrete cytokines including immune cells, epithelial cells, and endothelial cells, amongst others (80, 81). Depending on the effect that they generate over immune cells, they can be classified into two groups; pro-inflammatory and anti-inflammatory (79). Interleukin (IL)-1, tumor necrosis factor alpha (TNF-α), interferon-gamma (IFN-γ), and IL-6, among others (79, 82, 83) belong to the pro-inflammatory group, IL-10 is anti-inflammatory, and IL-12 can be pro- and anti-inflammatory cytokine (**Figure 1C**) (84, 85).

Among cytokines, chemokines are a group of proteins with chemoattractant properties and are characterized by three to four cysteine residues present in their structure (80, 84). These proteins can be classified -according to the position of the cysteines residues in their N-terminal portion- into four families. The first family is the C-C chemokines present the cysteine residues continuously. The second family is the C-X-C chemokines present one amino acid between the two cysteine residues. The third family is the X-C chemokine only present one cysteine residue in a conserved position (this family is composed of only one member; XCL1). Finally, the four family is the C-X-3-C chemokine, which presents two cysteine residues separated by three interchangeable amino acids (This family possesses only one member; CX3CL1) (84, 86). Another relevant characteristic of chemokines is that they are considered to be promiscuous proteins, as they can interact with more than one chemokine receptor and one receptor can bind more than one chemokine (86). Additionally to their chemoattractant function, chemokines play an essential role in maintaining the homeostasis during the development of the brain, heart, and hematopoietic system, among others (86). Besides, they are also critical players in the modulation of the immune response during infections, as they are responsible for the infiltration of immune cells into the site of injury (84, 86).

CYTOKINES INDUCED BY hRSV INFECTION IN THE UPPER RESPIRATORY TRACT

As mentioned above, the hRSV infection starts with the virus reaching the mucous membranes of the eyes, nose or mouth, allowing it to enter the organism (87). The first zone of infection is the upper respiratory tract, where it targets the ciliated epithelium of the nasopharynx, and then it moves toward the lungs, blocking the airways as the infection proceeds (**Figure 1C**) (88). This inflammation -known as bronchiolitis or pneumonia, accordingly to the degree of the disease- involves infiltration of polymorphonuclear cells (PMNs) such as neutrophils and eosinophils. Moreover, the rounding and shedding of the infected epithelial cells apparently caused by the NS2 protein, as described by Liesman et al. (74) inducing the collapse of the alveolar spaces and, therefore, impaired oxygen exchange (89). Remarkably, humans are born with at least a third of the alveoli that they will possess once the lungs are fully developed, with alveolar walls similar to the ones seen in an adult (90, 91). However, during childhood, these structures exhibit a lower area/volume ratio when compared with a fully developed lung, a rate that is increased until adolescence. Therefore, the useful space for gas exchange is reduced in early stages of human development. This phenomenon could explain for the exacerbated pathology observed in children, compared to teenagers and adults, with even further complications the younger they are (90, 91).

Several reports have described the changes in the ciliated epithelium upon infection with this virus. For instance, Wong et al. described that, upon infection, total loss of cilia is reported, mainly associated with microtubule damage (92). These could be in direct relation with reports indicating that this virus replicates in the apical cell surface of these cells (93). Remarkably, Smith et al. described that infection with hRSV could induce ciliary dyskinesia and ciliary loss of epithelial cells early during the infection, impairing in this way the clearance of the respiratory tract (94). Interestingly, Jumat et al. recently described the morphogenesis of hRSV in epithelial cells, using a primary culture of nasal epithelial cells as a model. They detected the presence of the F-protein of hRSV predominantly in cilia, but not the N-protein, observing this and several other proteins in the non-cilia locations of the cells, indicating that, probably the hRSV-F protein may be responsible for the damage to the cilia (46). Therefore, upon infection, hRSV seems to replicate and exit from non-cilia locations in the apical side of epithelial cells, somehow causing loss of ciliary function.

In response to all this damage, the airway epithelium generates cytokines and chemokines to recruit effector cells to the site of infection and restrict its propagation (95), causing an exacerbated immune response where infiltrating immune cells such as PMNs, T cells and inflammatory mediators cause damage to the tissues (63, 84). This exaggerated inflammatory response is increased as the infection progresses, with hRSV inducing a Th2-like immune response, promoting the inflammation (64). Notably, it has been described that primary infection with hRSV induces the transcription of nuclear factor kappa B (NF-κB) mainly through its M2-1 protein (96). This factor, in turn, produces the secretion of IL-8/CXCL8, TNF-α, CCL5, and CXCL10, among others. Accordingly, transcription factor AP-1 is also required for the expression of IL-8, as described by Dey et al. (97). Both NF-κB and AP-1 are regulated in their expression by the TGF-ß activation kinase 1 (TAK1), as deletion or inactivation of this kinase reduce gene expression of the transcription factors and decrease their nuclear translocation and DNA-binding activity (97), suggesting that the virus could be modulating these pathways. Finally, it has also been reported that STAT1 regulates the secretion of IL-4 by basophils upon infection with hRSV. In this line, Moore et al. described that KO mice for STAT1 showed higher levels of IL-4 in lungs, upon infection; a phenomenon that was reverted when mice were depleted from basophils. Remarkably, this increase in the expression of IL-4 correlated with more marked lung histopathology (98).

In light of all this, Das et al. reported that human nasal epithelial cells infected with hRSV exhibits increased levels of IL-6, CXCL8, and CCL5, as compared to non-infected cells (65). Remarkably, IL-2 levels in nasopharyngeal aspirates do not seem to correlate with hRSV infection, as Giugno et al. described that the concentration of this cytokine was heterogeneous among infected and non-infected children (99). The secretion of these pro-inflammatory cytokines may be adding to the exacerbated inflammation described in this disease (**Figures 1C**, **2**).

Since hRSV-infected children are only brought onto health centers once the disease has reached an advanced development stage, it is hard to determine the temporality of the secretion of cytokines and chemokines in humans, during this disease. In this line, Blanco *et al.* performed a study in cotton rats where they measured the transcription levels of several of these molecules during primary and secondary infection (100). Therein the authors show an increase in the transcription levels of all the cytokines measured except for IL-10 during the first day post-infection. A peak for IL-6, IFN-α, and TNF-α, was detected during day 1 post-primary infection, decreasing the first two by day 3, while the latter remained high up until day 10. Likewise, IL-1β, CCL5, CXCL1, and CXCL10 transcription levels peaked at day 2, remaining high up until days 5 or 6. The cytokines that peaked during day 3 were IL-10 and CCL4, recovering normal levels by day 7. The last molecule to reach its peak was IFN-γ, at day 4 post-primary infection which correlates with previous studies indicating that this virus inhibits the expression of this cytokine. Then, at day 14, the levels of IFN-γ were returned to normal levels (100). Remarkably, infectious virus was not detected in the lungs of cotton rats challenged in a secondary infection; however, changes in the lung structure were detected even earlier than in primarily infected cotton rats (100). Despite all this, and as indicated above, these data are all related to transcript expression level, and it is not a direct measure of proteins. Therefore, this information must be taken into account cautiously.

Another work performed by Legg et al. examined the cytokine response to the hRSV through nasal lavage fluid in infants (101). In this study when some respiratory symptoms the research team visited the infant to whom they performed a clinical examination and nasal lavage, considering this collection of samples days 1 and 2. The same procedure was performed at day 5 and 6 since the development of the symptoms. They found that IL-4/IFN-γ ratio was elevated at day 1–2 and 5–6, and during the first two days, the IL-10/IL-12 ratio reached its peak (101). The results obtained with IFN-γ in infants correlates with the results obtained in mice since during the first couple of days the secretion of this cytokine has a similar pattern, suggesting that the other cytokines should behave similarly in humans as it does in cotton rats.

Toll-like receptors (TLRs) are pathogen recognition receptors (PRRs) that are activated upon the recognition of pathogen-associated molecular patterns (PAMPs) (102). They are expressed in several cell types such as immune cells and epithelial cells. Moreover, they are significant players in the early response against pathogens, as they can regulate the secretion of several cytokines and chemokines (103, 104). In this line, the role of TLRs in the innate immune response against hRSV is significant, as TLR3, TLR4, TLR7, and TLR8 are upregulated upon infection (**Figure 1B**) (105–107). TLR4 has been described to interact with the F-hRSV protein, leading to the activation of NF-κB and the secretion of the cytokines mentioned above, such as CXCL8 and TNF-α (108, 109). In humans, mutations in TLR4 impair the activation of this pathway and, in mice this renders the organism unable to clear the virus, and the persistence of the virus has been described in TLR4 deficient mice (57, 58). TLR3, which recognizes viral double-stranded RNA, induces the secretion of type I IFN and the activation of the NF-κB pathway (105). Remarkably, TLR3 deficient mice have shown a Th2-like biased immune response, further exacerbating the

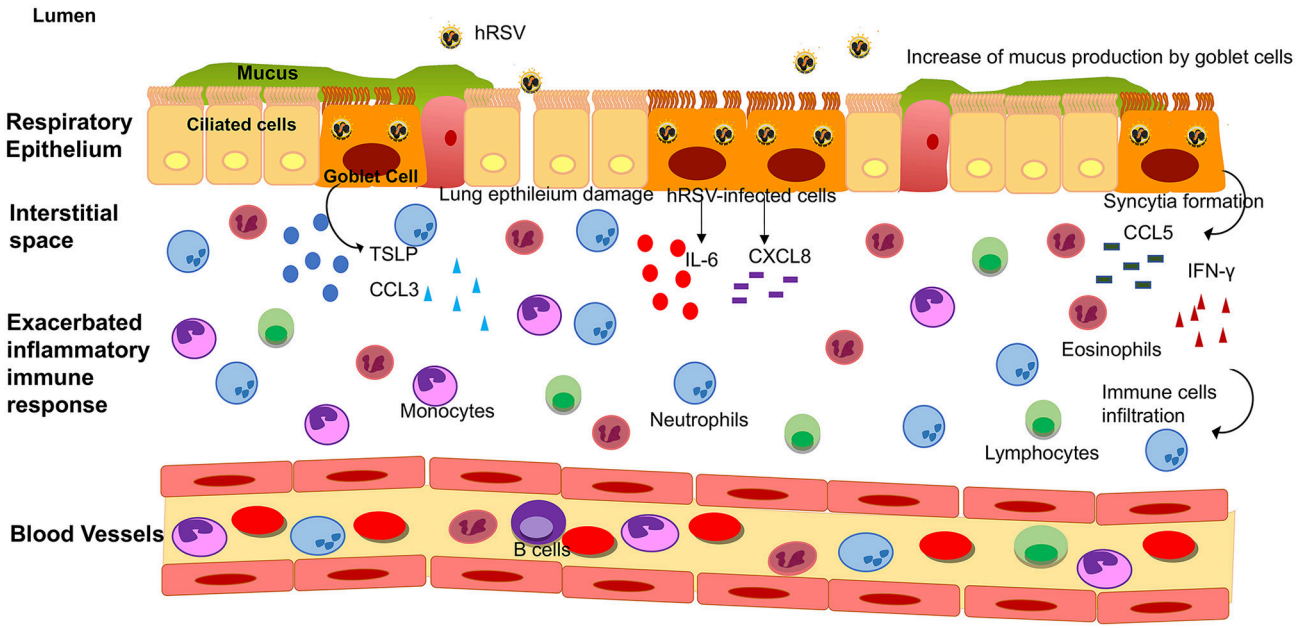

FIGURE 2 | Lower respiratory tract inflammatory response induced by hRSV infection**.** Upon hRSV infection in the lower respiratory tract, the epithelial cells secrete IL-6, IFN-γ, CCL3, CCL5, CXCL8, and TSLP among others inflammatory mediators. This inflammatory immune response promotes the infiltration of immune cells (such as monocytes, eosinophil, neutrophils and lymphocytes, among other) into the lungs, causing an obstruction of the airways and damage to the tissue.

eosinophils infiltration and mucus secretion (60). TLR7, in turn, recognizes viral single-stranded RNA and induces the secretion of T cells-activator and mucus-secreting cytokines such as IL-12 and IL-23 (61).

Mucus secretion is also a significant factor associated with hRSV infection. The production of this thick layer that works as another defense mechanism of the organism is performed by goblet cells (**Figures 1C**, **2**) (62). These cells are activated by cytokines such as IL-13, IL-17, and IL-23 (67), TLRs such as TLR3, and TLR7 (60) and immune receptors such as CXCR2 (68). As described above, TLR3 upregulation, secretion of IL-13 by infiltrating eosinophils and activation of several immune receptors are hallmarks of hRSV infection. Therefore, higher production of mucus usually correlates with more severe disease. Remarkably, Mukherjee et al. described that upon blockade of IL-17 through neutralizing antibodies, the secretion of mucus by hRSV-infected mice was significantly reduced, leading to a less exacerbated obstruction of the airways (69).

As it can be seen, the immune response against hRSV may be redundant at some points, but this redundancy itself is in part aiding the exacerbated inflammation and the production of pro-inflammatory cytokines. Although the organism exhibits several mechanisms to impede the advance of hRSV throughout the upper respiratory tract, this virus can avoid and even take advantage of many of these, eventually reaching the lower respiratory tract, where it will continue to replicate and progress in its pathology.

Cytokines Induced by hRSV Infection in the Lower Respiratory Tract

It has been described that hRSV is a mucosa-restricted virus, as in natural infections it initially replicates in the epithelium of the nasopharynx (110). In immunologically naïve infants, hRSV spreads through a cell to cell transfer and extracellular binding, producing discontinuous foci of infection in the tracheal epithelium (110). The lower respiratory tract is essential for the respiratory system and is composed of trachea, bronchi (primary and secondary) and alveoli (111). Under normal conditions, inhaled pathogens are cleared via the mucociliary escalator from ciliated epithelial cells. This defense mechanism is coordinated with the actions of the airway lining fluid, rich in antioxidants, defensins, and lysozyme secreted by Clara cells and submucosal glands, along with mucous glycoproteins secreted by goblet cells (**Figure 2**) (66).

An exacerbated hRSV infection is characterized by several symptoms including severe chesty cough, wheezing, apnea and cyanosis and all of these symptoms can be signs of a lower respiratory tract infection (LRTI) (112). In infants, the leading pathology caused by LRTI is bronchiolitis, which has been described to involve an acute inflammation—mainly associated with exacerbated infiltration of neutrophils- necrosis of epithelial airway cells and increased production of mucus, among others (113, 114). Additionally, it has been described that the damage observed in the respiratory tract is not only induced by the viral infection itself, but also by the local production of cytokines (88). In the bronchioles samples from post-mortem patients, hRSV was detected mainly in the ciliated cells (115). Moreover,

the majority of inflammation observed was at the submucosa level (115).

To understand the nature of this inflammation, the majority of the studies that have been performed in patients are focused on the analysis of the production of cytokines that coordinate the infiltration of immune cells. Since it is difficult to obtain bronchoalveolar lavage fluids (BALFs) samples from patients, these studies have been performed on ventilated hRSV-infected infants (116, 117). McNamara et al. collected these samples from term and pre-term infants to determine the inflammatory mediator profile in these children. An increase of the transcript and protein levels of cytokines such as IL-6, TNF-α, CXCL8, CCL3, CCL4, CCL2, and CCL5 was observed, as compared to control groups (**Figure 2**) (116, 117).

It has been reported that cytokines associated with a Th2-like response, such as IL-4, IL-6, IL-9, IL-10, and IL-13, are elevated in nasal washes and lungs of children with hRSV-induced LRTI (**Figure 2**) (72). Among these, IL-6 is a pro-inflammatory cytokine which has been described to play an essential role in the host immune response against hRSV infection (116). McNamara *et al*. also showed in pre-term and term infants with hRSV-induced bronchiolitis that IL-6 levels were elevated at day 1 of intubation, in term infants as compared to pre-term and control group (116). According to this observation, it is possible that IL-6 plays a relevant role in the hRSV pathogenesis in the lung of infected infants. When comparing the concentration of chemokines on the first day of intubation and the extubating day, no differences were found between these critical days (57). During another study performed in children under the age of 2 with clinical manifestations of respiratory obstruction and distress due to viral infection, different cytokines related to hRSV-infection were evaluated at three-time points: admission-hospitalization, discharge and 1 month after release (70). At the beginning of the study, the children admitted exhibited an increase in Th2-like cytokines such as IL-4, IL-5, and IL-13 (70). The increase in these cytokines decayed progressively until 1 month after discharge. In another study in children with signs of severe LRTI and positive for hRSV infection (71), cytokines were evaluated at two points: discharge and 1 year after release. Th2-like cytokines, such as IL-4 and IL-6, decayed 1 year after the infection. Surprisingly, IL-13 levels remained higher in the initially infected group when compared with the control group 1 year after the viral infection, although the authors could not rule out the effects of other diseases or environmental factors (71). Furthermore, children admitted in hospital with bronchiolitis due to hRSV-infection exhibited higher concentrations of IL-6 in nasal swabs as compared with their older siblings (118).

IL-10 has also been described as a key cytokine in the response against this virus (119–121). The varying levels and the role of IL-10 during hRSV infection have not been entirely determined, as IL-10 fluctuates with the age of children (120). Importantly, a study found that lower levels of IL-10 correlate with the severity of the hRSV disease in infants (120). Additionally, it has been described that in infants older than 3 months of age with mild hRSV infection exhibit high IL-10 levels, which can be related to a protector effect. Nonetheless, in infants below 3 months of age, high IL-10 levels were reported in those with severe bronchiolitis, therefore being considered as a hallmark of disease (121).

Interestingly, it has been reported that infants younger than 3 months, hospitalized with hRSV-induced bronchiolitis, presented elevated amounts of Th2-related cytokines in BALF samples, such as IL-3, IL-4, IL-10, and IL-13 (75). Furthermore, an increase of pro-inflammatory cytokines such as IL-1β, IL-6, TNF-α, and also IL-12-p40 -a Th1-like related cytokine- was also reported (75). Importantly, IL-3 -which is involved in the infiltration of immune cells that are related to the asthma development- and IL-12p40 are necessary for the secretion of IFN-γ. Therefore, the increase of both cytokines correlates with recurrent episodes of wheezing in hRSV infection (75).

IFN-γ is a cytokine that stimulates viral clearance by promoting anti-viral immune effector responses. Therefore, low levels of this cytokine in patients have been associated with a higher severity index in the bronchiolitis caused by hRSV (**Figure 2**) (122). Semple *et al*. reported that in infants hospitalized due to hRSV-induced bronchiolitis who needed oxygenation or ventilated support, IFN-γ levels in BALF were low when compared with the infants that never required oxygenation (122). These low IFN-γ levels correlated with increased severity of the disease and its reduction is significant in the development of the bronchiolitis (122). Contrary to these findings, recent studies performed by Thwaites *et al*. shows high levels of IFN-γ in patients from the pediatric intensive care unit (PICU) with hRSV-infection, along with high levels of IL-1 and IL-10 respect to the healthy controls (123). Also, reduced IFN-γ levels were detected in children with moderate bronchiolitis; however, in children with severe bronchiolitis, the levels of IL-17A and MUC5AC were increased (123). Considering the data mentioned above, the amount of IFN-γ in patients with hRSV-bronchiolitis is controversial.

Additionally, Semple et al. also analyzed the production of IL-9 (122). This cytokine is produced in Th9-like immune response and has been implicated in the severity of the hRSV pathology (124). The data obtained showed that IL-9 levels in BALF were increased in infants with severe bronchiolitis that required oxygenation. However, no differences were found when compared with infants that never needed oxygen supplementation (122). In another study performed in pre-term and term infants with hRSV bronchiolitis, the expression of the IL-9 mRNA in BALF was increased in both groups, as compared to control groups (124). Moreover, no significant differences were found in the levels of IL-9 transcript among pre-term and term infants. However, the protein secretion was increased in term infants when compared to both pre-term and control groups (124). Furthermore, the primary source of these cytokines in the lungs of hRSV-infected infants were neutrophils (124). Remarkably, it has been reported that IL-9 can upregulate genes involved in the mucus production in goblet cells, which could explain the elevated amounts of mucus in patients with hRSV-induced bronchiolitis (124). Additionally, it has been reported that IL-9 polymorphism has a different effect in the hRSV disease severity in boy and girls (125). The single nucleotide polymorphism (SNP) rs2069885 of the IL-9 gene was associated

with higher susceptibility of severe disease caused by hRSV while in boys, is associated with a lower susceptibility (125).

Also, it has been described an association of the polymorphism of the IL-4 and IL-4Rα genes with hRSV disease severity (73). Hoebee *et al.* found that the−590T allele of the IL-4 gene was expressed more frequently in infants hospitalized by hRSV bronchiolitis compared to the control group (73). Moreover, the authors found an association of the hRSV disease severity and the IL-4 locus in children older than 6 months that were hospitalized by hRSV bronchiolitis (73). Additionally, this study found that 2 polymorphisms of the IL-4Rα gene, the I50V, and the Q551R. Only the Q551R SNP show an association with the children older than 6 months who were hospitalized by a severe hRSV bronchiolitis (73).

Another relevant cytokine reported upon hRSV infection is the thymic stromal lymphopoietin (TSLP), a cytokine associated with asthma development (126). Also, a strong association in Th2-like effector cytokines, such as IL-4 and IL-5, and IL-13 has been reported (127, 128). TSLP is secreted by epithelial cells associated with barriers (129) and bronchial smooth muscle cells (130, 131). In infants with hRSV-induced bronchiolitis, this cytokine was elevated as compared to healthy controls, suggesting that TSLP could play an essential role in the hRSV immunopathology (132).

Importantly, the response associated with IL-17 can be harmful to the patients, as mentioned above. Higher levels of IL-17 have been reported in patients with mechanic ventilation due to hRSV-induced bronchiolitis (76, 78). IFN-λ is a cytokine discovered in the year 2003 (77) and it has been reported to play a role in the establishment of the adaptive response to hRSV, with an increase in the secretion of IL-6, CXCL8, and IL-10 in peripheral blood mononuclear cells (PBMC) (133). Moreover, a deleterious effect of IFN-λ in hRSV infection has been seen (134), as a study of acute bronchiolitis-patients reported a significant increase in the transcription of IFN-λ in patients with increased respiration rate, a sign of acute bronchiolitis induced by hRSV-infection (134).

As we described earlier, chemokines are also involved in the inflammatory response elicited by hRSV-infection. One of these is CCL3, a small pleiotropic chemoattractant protein whose function is to attract or activate immune cells such as eosinophils, monocytes, basophils and lymphocyte subpopulations (135). This chemokine was increased in lower respiratory tract secretions from infants under 2 months old that were hospitalized with hRSV-induced bronchiolitis (135). Interestingly, this increase was correlated with the detection of eosinophil degranulation products, which suggests that CCL3 has an active role in this process during hRSV-induced bronchiolitis (135). In addition to this, it was also reported that CCL5 was increased in these infants (135). CCL5 is a chemoattractant cytokine that principally recruits monocytes, T cells, and eosinophils, acting via three chemokine receptors: CCR1, CCR3, and CCR5 (136). Evidence obtained from children with hRSV infection shows an increase of the CCL5 protein levels in both upper and lower airway secretions, and levels of CCL5 in upper airway secretions correlate positively with disease severity (137, 138). Recently a prospective study of 173 patients with bronchiolitis caused by hRSV was performed, holding 536 healthy controls whose samples of nasopharyngeal aspirate were taken (139). Therein, the authors found a single SNP in CCL5 (rs2107538*CT), exhibiting an association with hRSV-bronchiolitis and also with the need for mechanical ventilation (139). These data suggest that CCL5 contributes to bronchiolitis leading to airways damage in patients.

Furthermore, McNamara et al. also evaluated this chemokine in BALF from infants that required ventilation support and found an increase at the first day of the mechanical ventilation, but these levels decreased over time (117). This phenomenon was also observed for CXCL8 (117), which is a chemokine that attracts mainly neutrophils, one of the most frequent immune cells found in the airways of hRSV-infected infants (140). Subsequently to these results, another study performed in BALF samples from intubated infants reported elevated levels of CXCL8 transcript, which also correlates with the finding of this chemokine in nasopharyngeal aspirates (NPA) (141). Thus, the NPA samples might be an excellent alternative to study the implications of the infection caused by hRSV in the respiratory tract (**Figure 2**).

CYTOKINES SECRETED BY EPITHELIAL CELLS IN RESPONSE TO THE hRSV INFECTION *IN VITRO*

The majority of the knowledge available about the induction of pro-inflammatory cytokines and chemokines production upon hRSV infection has been described *in vitro* using airway epithelial cells (AECs) models such as A549, primary human small airway epithelial cells (SAECs), BEAS-2B and primary normal human bronchial epithelial cells (NHBE), among others (88, 142, 143). The data obtained using these models can vary depending on the cell line. According to this, experiments in the A549 cell line (human alveolar type II-like epithelial) with the Long strain of hRSV showed that infection with hRSV induces the secretion of IL-6, CCL3, and CCL5 at 48 h post-infection as compared to non-infected cells (144, 145). On the other hand, a study performed in this cell line but with a different strain and subgroup of hRSV obtained from clinical isolates showed that the induction of IL-6 and CCL5 could be variable and dependent on the virus strain used (146).

BEAS-2B is an SV40 transformed human normal bronchial epithelium cell line that exhibits a limited susceptibility to hRSV-infection and profile of virus resistance as compared to the A549 cell line (142). Infection of this cell line with the hRSV Long strain showed an increase in the transcript levels for CXCL8 at 4 h post-infection, which was observed up to 24 h post-infection (143). Regarding the upregulation of IL-6, it was observed only at 96 h post-infection (143). However, another study performed using the hRSV Long strain showed that CXCL8 levels were not changed upon infection with hRSV, while CCL3 and CCL5 levels were increased (64). Importantly, the authors observed that the amounts of CCL5 produced by the epithelial cells were enough to attract eosinophils (64). Furthermore, infected BEAS-2B cells with the hRSV strain A2 also exhibited an induction in

the secretion of IL-6 and CXCL8 as compared to non-infected cells (145).

Currently, primary or normal epithelial cells are the most used model for hRSV infection as it is thought to be representative of the effects of hRSV infection in the respiratory tract. Accordingly, it has been reported that primary AECs obtained from hRSV-infected infants exhibited higher viral titers as compared to the BEAS-2B cell line when infected with the same virus (147). Besides, the amounts of IL-6 and CXCL8 were higher in the primary AECs as compared to BEAS-2B cells (147). Considering these data, AECs can be considered as an excellent model for understanding the effects of hRSV-infection and the production of cytokines and chemokines as may occur in infants.

Additionally, in a study *in vitro* using a WT hRSV A2 strain (6340WT) and a recombinant strain that lacks the G-protein gene (6340ΔG), infection of NHBEs cells induced the secretion of CCL2, CCL5, and CXCL8 by both viruses (148). However, only the recombinant virus was able to promote the secretion of CXCL10 in NHBEs (148). On the other hand, both F- and G-protein promoted the secretion of CXCL8 and CXCL10, whereas only G-protein induced the secretion CCL5 (148). In contrast to these findings, infection with the hRSV Long strain in NHBEs cells did not lead to the secretion of CCL2 and CCL3, but the levels of CCL5 were increased as compared to uninfected cells (149). Additionally, it has been described that hRSV infection in NHBEs cells induced the expression of TSLP transcript at 12 h post-infection and TSLP secretion exhibited a peak at 24 h post-infection as compared to ultraviolet (UV)-hRSV inactivated (150). This phenomenon was also seen in NHBEs cells obtained from asthmatic patients and infected with hRSV, as TSLP concentration were high when compared to healthy patients with hRSV-infection (150). Moreover, studies using A549 cells co-transfected with the human TSLP promoter with a reporter, and a dominant-negative form of RIG-I (DN-RIG-I), showed that hRSV-infection could induce activation of this pathway to increase TSLP expression (150).

hRSV INDUCED CYTOKINE PRODUCTION AND TISSUE DAMAGE IN MICE

It has been described that hRSV-infected BALB/c mice can exhibit increased levels of IL-6 in BALFs at 12 h post-infection that remains elevated up until 14 days post-infection (59). Similar results were observed in lungs parenchyma and sera of hRSV-infected mice (59). The contribution of IL-6 to the hRSV immunopathology was evaluated by the depletion of this cytokine one day before hRSV infection, parameters of disease, such as weight loss were more severe (59). Furthermore, in these hRSV-infected mice the lung vascular permeability was evaluated by measurement of albumin in the airways, which was increased as compared to the isotype control at 7, 11, and 14 days post-infection (59). Further, in the absence of IL-6, hRSV-infected mice displayed an increase of lymphocyte recruitment at 7 days post-infection, while neutrophil infiltration was similar to the isotype control (59). These results suggest that the early production of IL-6 is essential to control the severity of the disease and to limit lung damage.

Furthermore, it has also been described that hRSV infection promotes an increase of IL-1β, TNF-α, IFN-γ IL-12, IL-6, CCL3, and CCL5 in BALF samples from mice (151). The elevated levels of IL-1β and TNF-α on the first day of hRSV infection correlate with the peak of weight loss, whereas increased levels of IL-12 were found before the induction of IFN-γ (151). Besides, histological analyses have shown that hRSV infection produces changes in the lung that are associated with airway and vascular cuffing and interstitial pneumonia (144). On the other hand, an effect of TNF-α alone over the hRSV-infection has not been demonstrated with knockout mice. However, in a study in BALB/cJ mice with pretreatment with antibody for TNF-α before the hRSV-infection, mice showed a significant increase of weight loss and slow recovery as compared to control mice (152). Therefore, these observations suggest that TNF-α can be established as a participant in the hRSV-infection, and in the absence of this cytokine the mice showed a delay in the viral clearance.

The role of IFN-γ during hRSV pathogenesis was evaluated using both an IFN-γ knockout mice model and the blockade of IFN-γ (153). The data obtained from this study shows that, both in IFN-γ knockout (IFN-$\gamma^{-/-}$) mice and in the anti-IFN-γ treated mice, the immune cell infiltration (principally neutrophils and eosinophils) in BALF samples were higher than in control mice. However, when the respiratory rate was evaluated [the ratio between inspiration time and expiration time (Ti/Te)] the anti-IFN-γ treated hRSV-infected mice shows no difference in the ratio compared to control mice (153). Besides, in the absence of IFN-γ also increase the viral load of these mice compared to control mice. These results suggest that IFN-γ plays a dual role during hRSV infection, been necessary to control the viral replication and also prevents the obstruction of the airways (153).

Regarding to the role of chemokines, has been reported that elevated concentrations of CCL3 and CCL5 at day one post-infection are consistent with recruitment of monocytes and lymphocytes into the mice lungs (151, 154). Additionally, it has been described that CCL5 induction by hRSV infection contributes to a subsequent allergic pulmonary inflammation (155). Moreover, in mice, the secretion of CCL5 in the lungs was correlated with airway hyperreactivity (AHR). This association was evaluated by antibody neutralization of CCL5, showing that while viral loads were not affected by this treatment, a significant decrease for hRSV-induced AHR was observed, down to control mice levels (156). Furthermore, it was described that CCL5 exhibits a biphasic response during the hRSV infection, with an initial phase of innate immune response and a second phase consisting of lymphocyte-mediated responses (157). Besides, mice sensitized with recombinant vaccinia expressing G-hRSV protein (rVV-G) showed a significant increase of both mRNA and protein levels for CCL5 during the first 24 h post-infection (157). Then, CCL5 is also increased in the second phase of hRSV infection at 168 h post-infection (157). To understand the role of CCL5 when viral replication was eliminated, an inhibitory analog of CCL5, Met-RANTES, was used to treat hRSV-infected mice. These studies showed that mice treated with Met-RANTES

exhibited a significant reduction of $CD4^+$ and $CD8^+$ T cell recruitment into the lungs after infection (157). Along these lines, blockage of CCL5 reduced both weight loss and eosinophilia, suggesting that this cytokine plays an essential role during lung inflammation (157). Accordingly, the induction of CCL5 by hRSV infection is involved in lung inflammation, although there is no evidence of a contribution or a direct role in airway damage.

Regarding the contribution of CCL3 to hRSV infection, it was shown that equivalent to CCL5, CCL3 displays a biphasic expression both for mRNA and protein, at day 1 and 7 post-infection (158). Moreover, blockage of CCL3 with a neutralizing antibody showed no change in the recruitment of NK cells and did not affect viral loads in the lungs of hRSV-infected mice after 4 days of infection (158). However, at 7 days post-infection, the number of $CD4^+$ and $CD8^+$ T cells was reduced in the lungs of infected mice (158). Accordingly, hRSV-infected BALB/c WT mice exhibited an infiltration of about 80% of mononuclear cells close to vessels and bronchioles, while $CCL3^{-/-}$ hRSV-infected mice exhibited a decrease of infiltrating cells in the lungs. Interestingly, in both mice, the viral loads were equivalent (154). Additionally, in $CCL3^{-/-}$ hRSV-infected mice the mRNA of CCL5, CCL2, and CXCL2 were decreased as compared to their wildtype littermates, suggesting that CCL3 is required for the development of the hRSV-induced immunopathology (154). Despite these data, there is no direct evidence of the pulmonary damage caused by CCL3, which be relevant to determine.

Related with the production of TSLP in hRSV-infected mice, it has been reported that at the peak of the immunopathology, high amounts of this cytokine are produced (150). The contribution of TSLP to the hRSV pulmonary immunopathology was analyzed using TSLP KO mice and results showed that expression of Gob5, IL-13, and mucus production decreased as compared to hRSV-infected WT mice (150). Moreover, Stier et al. showed that knockout mice for the TLSP receptor (TSLPR KO) infected with hRSV displayed moderate mucous cell metaplasia, as the WT hRSV-infected mice. However, the accumulation of intraluminal mucus was lower when compared to WT mice (159). The airways obstruction of both hRSV-infected WT and TSLPR KO mice, was evaluated by methacholine challenge. Consistently, hRSV-infected WT mice displayed an increase in the airway reactivity (increased amounts of methacholine) as compared to the hRSV-infected TSLPR KO mice. These later animals showed only minor symptoms of the disease, which were equivalent to the mock-treated mice (159). Accordingly, these results suggest that TSLP activity is relevant for the hRSV immunopathology and that also contributes to lung damage in murine models (150).

As described above, most of the work in this field suggests what cytokines are either up- or down-modulated during hRSV infection. However, little or nothing has been reported about the direct contribution of these mediators to the airway damage caused by hRSV. The development of new methodological approaches is still necessary to achieve a better understanding of the effects that this virus produces on the respiratory tract by inducing inflammatory mediators. However, it could be possible to suggest that, like what is seen for the upper respiratory tract, hRSV exhibits several redundant mechanisms that induce damage and inflammation in the lower respiratory tract.

hRSV INFECTION IS ASSOCIATED WITH ELEVATED LEVELS OF CYTOKINES IN THE CNS

As described above, hRSV infection induces cytokines that damage the respiratory tract, but also these cytokines could affect the CNS. Years ago, a small number of hRSV-infected patients were reported to exhibit clinical signs associated with neurological complications, such as seizures (160, 161), apnea (12), encephalopathy (162) and encephalitis (163, 164). Nowadays, the cases of neurological abnormalities related to hRSV infection reported are increasing. However, our knowledge regarding the mechanisms involved in this phenomenon remains limited and controversial (**Figure 1**).

One of the first findings in patients with neurological manifestations associated with hRSV infection was the detection of virus-specific antibodies in cerebrospinal fluid (CSF) (165). Later, after many efforts to find viral genetic material in CSF, hRSV RNA belonging to the serogroup B was detected in the CSF of an infant with febrile convulsion and pneumonia (13). Researchers not only have focused on hRSV detection, but also on the possible production of cytokines that could be a consequence of viral infection and that could explain the symptoms affecting the CNS. Accordingly, an increase of IL-6 in CSF from an hRSV-infected patient was reported (14). The observation that serum IL-6 levels in these patients were normal (14) would suggest that this cytokine is produced locally in the CNS, most likely by CNS-resident cells, such as microglia and astrocytes. A report about 3 clinical cases where children infected by hRSV suffered from seizures, showed that the levels of IL-6 were increased and that the serogroup of hRSV found in the CFS belonged to the serogroup A (166). Additionally, the same authors also found viral RNA in the CSF of a different cohort of hRSV-infected patients, with increased levels of IL-6, IL-8, CCL2, and CCL4, suggesting that these inflammatory mediators may play a critical role during the hRSV-infection in the CNS pathogenesis (15). Importantly, the increased levels of IL-6 correlate with the severity of the CNS encephalitis mediated by a cytokine storm, which can be useful as a molecular marker of neurological prognosis (167). Based on all the data described above, it is possible that hRSV spreads from the lungs to the CNS and infects local cells, initiating an inflammatory immune response mediated by cytokines.

As we mentioned above, there is controversy in this field due to reports in which hRSV-derived genetic material was not found in CSF samples from patients with severe bronchiolitis (168). Analyses of blood and CSF samples from 10 patients with apneas showed that only 7 were positive for hRSV (168). This study showed that hRSV RNA was detected in PBMC of two patients, but was not found in their CSF (168). Possible explanations for this controversy could be due to differences in the clinical signs of the patients, to the hRSV serogroups found infecting them and also to technical differences used by the researchers.

Although there is clinical relevance in the CNS pathologies caused by hRSV infection, there is little research in this aspect that could provide conclusive evidence. A study using the mouse

model described that hRSV could infect sensory neurons in the lungs through the interaction of the G-hRSV glycoprotein with the chemokine receptor CX3CR1 located at the surface of these cells (169). Experiments with mouse neuronal primary cultures showed that hRSV infected about 5% of these cells and this percentage decrease when CX3CR1 was blocked (169). Nevertheless, in this study, the authors did not evaluate the effect of hRSV infection in these cells or whether the neurons secreted inflammatory mediators. To approach these questions, neuronal N2a cells were infected with hRSV showing that these cells secrete IL-6 and TNF-α *in vitro* (170).

While these reports advance the knowledge in this field, there is still no evidence of neuronal infection by hRSV *in vivo*. In this regard, Espinoza *et al.* described that hRSV could be detected in several areas of the brain from infected mice, such as the cortex, ventromedial hypothalamic nucleus, and hippocampus (171). Interestingly, the finding of the virus in the hippocampus led to hypothesize that behavioral and learning processes may be altered. Marble burying (MB) and Morris Water Maze (MWM) test were performed 30 days after hRSV infection to test this hypothesis. In both trials, behavioral (MB) and spatial learning (MWM), performance was altered in hRSV-infected mice (171). The authors also evaluated the possible impairment in the functionality of the synaptic plasticity in the hippocampus. The data shows that the long-term potentiation (LTP) and the long-term depression (LTD) were altered in hRSV-infected mice, suggesting damage in the brain of these animals (171). It is possible to think that impairment in the behavior and learning is due to the neuronal infection by hRSV, which alters the normal function of these cells. Besides, it is also possible that hRSV infection promotes the secretion of several cytokines in the CNS, either by neurons or other resident cells, which could contribute to this neurological-associated phenomenon. However, more research is still necessary in this field to further advance our knowledge of the effects that this virus has on our CNS.

CONCLUDING REMARKS

HRSV remains one of the primary viral agents causing respiratory tract infections worldwide, for which there is no vaccine available. Once hRSV infection reaches the epithelium of the respiratory tract, it produces several symptoms such as wheezing, apnea, cyanosis, and bronchiolitis, related to acute lower tract infection. Most of the damage seen in patients with complications associated with hRSV infection is caused by an exacerbated immune response triggered mainly by the cytokines secreted by the infected cells of the respiratory tract epithelium.

In human studies, cytokines and chemokines have been detected in nasopharyngeal aspirates, tracheobronchial aspirates or bronchoalveolar lavage fluids, in children with mechanic ventilation due to bronchiolitis associated with hRSV infection. In these patients -usually children younger than 2 years of age- the cytokines that predominated were IL-4, IL-5, IL-6, IL-10, and IL-13. A low concentration of cytokines associated with a Th1-like response such as IFN-γ is also seen, which could be considered as a severity index. Also, chemokines such as CCL3, CCL5, and CXCL8 are increased in the lower respiratory tract of individuals infected with hRSV. These components contribute to generating a severe pathology in the patients, which is associated with an unbalance between Th1- and Th2-like cytokines, and an increase in chemokines that attract more inflammatory cells like granulocytes, which in turn generates a deleterious effect on the patient. Moreover, the secretion of many of the cytokines described above has also been seen in mice models, with associated tissue damage, although further studies are still required to fully elicit the specific role of each cytokine in this pathology.

Furthermore, infection by hRSV seems to reach CNS, which produces high levels of IL-6 in the zone. This infection might generate problems in the behavior and learning process of the children, but further studies are required to elucidate more information in this regard.

AUTHOR CONTRIBUTIONS

All authors listed have made a substantial, direct and intellectual contribution to the work, and approved it for publication.

FUNDING

This work was supported by FONDECYT grants N° 3180570, N° 1150862, N° 1190830 and the Millennium Institute on Immunology and Immunotherapy (P09/016-F). AMK is a Helen C. Levitt Visiting Professor, Department of Microbiology and Immunology, University of Iowa.

REFERENCES

1. Shi T, McAllister DA, O'Brien KL, Simoes EAF, Madhi SA, Gessner BD, et al. Global, regional, and national disease burden estimates of acute lower respiratory infections due to respiratory syncytial virus in young children in 2015: a systematic review and modelling study. *Lancet*. (2017) 390:946–58. doi: 10.1016/S0140-6736(17)30938-8
2. Kestler M, Muñoz P, Mateos M, Adrados D, Bouza E. Respiratory syncytial virus burden among adults during flu season: an underestimated pathology. *J Hosp Infect*. (2018) 100:463–8. doi: 10.1016/j.jhin.2018.03.034
3. Moura FE, Borges LC, Augusta S, Portes R, Antônio E. Respiratory syncytial virus infections during an epidemic period in salvador, brazil. viral antigenic group analysis and description of clinical and epidemiological aspects. *Mem Inst Oswaldo Cruz Rio Janeiro*. (2003) 98:739–43. doi: 10.1590/S0074-02762003000600005
4. Bohmwald K, Espinoza JA, Becerra D, Rivera K, Lay MK, Bueno SM, et al. Inflammatory damage on respiratory and nervous systems due to hRSV infection. *Curr Opin Immunol*. (2015) 36:14–21. doi: 10.1016/j.coi.2015.05.003
5. Espinoza JA, Bueno SM, Riedel CA, Kalergis AM. Induction of protective effector immunity to prevent pathogenesis caused by the respiratory syncytial virus. Implications on therapy and vaccine design. *Immunology*. (2014) 143:1–12. doi: 10.1111/imm.12313
6. Shi T, Balsells E, Wastnedge E, Singleton R, Rasmussen ZA, Zar HJ, et al. Risk factors for respiratory syncytial virus associated with acute lower respiratory infection in children under five years: systematic review

and meta–analysis. *J Glob Health*. (2015) 5:020416. doi: 10.7189/jogh.05.020416
7. Amand C, Tong S, Kieffer A, Kyaw MH. Healthcare resource use and economic burden attributable to respiratory syncytial virus in the United States: a claims database analysis. *BMC Health Serv Res*. (2018) 18:294. doi: 10.1186/s12913-018-3066-1
8. Walsh EE. Respiratory syncytial virus infection: an illness for all ages. *Clin Chest Med*. (2017) 38:29–36. doi: 10.1016/j.ccm.2016.11.010
9. Malloy AMW, Falsey AR, Ruckwardt TJ. Consequences of immature and senescent immune responses for infection with respiratory syncytial virus. *Curr Top Microbiol Immunol*. (2013) 372:211–31. doi: 10.1007/978-3-642-38919-1-11
10. Falsey AR, Hennessey PA, Formica MA, Cox C, Walsh EE. Respiratory syncytial virus infection in elderly and high-risk adults. *N Engl J Med*. (2005) 48:377–82. doi: 10.1056/NEJMoa043951
11. Eisenhut M. Extrapulmonary manifestations of severe respiratory syncytial virus infection–a systematic review. *Crit Care*. (2006) 10:R10. doi: 10.1186/cc4984
12. Kho N, Kerrigan JF, Tong T, Browne R, Knilans J. Respiratory syncytial virus infection and neurologic abnormalities: retrospective cohort study. *J Child Neurol*. (2004) 19:859–64. doi: 10.1177/08830738040190110301
13. Zlateva KT, Van Ranst M. Detection of subgroup B respiratory syncytial virus in the cerebrospinal fluid of a patient with respiratory syncytial virus pneumonia. *Pediatr Infect Dis J*. (2004) 23:1065–6. doi: 10.1097/01.inf.0000143654.12493.c9
14. Otake Y, Yamagata T, Morimoto Y, Imi M, Mori M, Aihara T, et al. Elevated CSF IL-6 in a patient with respiratory syncytial virus encephalopathy. *Brain Dev*. (2007) 29:117–20. doi: 10.1016/j.braindev.2006.06.008
15. Kawashima H, Kashiwagi Y, Ioi H, Morichi S, Oana S, Yamanaka G, et al. Production of chemokines in respiratory syncytial virus infection with central nervous system manifestations. *J Infect Chemother*. (2012) 18:827–31. doi: 10.1007/s10156-012-0418-3
16. Brown PM, Schneeberger DL, Piedimonte G. Biomarkers of respiratory syncytial virus (RSV) infection: Specific neutrophil and cytokine levels provide increased accuracy in predicting disease severity. *Paediatr Respir Rev*. (2015) 16:232–40. doi: 10.1016/j.prrv.2015.05.005
17. Greenberg D. Respiratory syncytial virus (RSV) - A key player for severe infections in special populations. *J Microbiol Immunol Infect.* (2015) 48:S12. doi: 10.1016/j.jmii.2015.02.139
18. Kazakova A, Teros-Jaakkola T, Kakkola L, Toivonen L, Peltola V, Waris M, et al. Prospective clinical and serological follow-up in early childhood reveals a high rate of subclinical RSV infection and a relatively high reinfection rate within the first 3 years of life. *Epidemiol Infect*. (2016) 144:1622–33. doi: 10.1017/S0950268815003143
19. Hall CB, Powell KR, MacDonald NE, Gala CL, Menegus ME, Suffin SC, et al. Respiratory syncytial viral infection in children with compromised immune function. *N Engl J Med.* (1986) 315:77–81. doi: 10.1056/NEJM198607103150201
20. Gonzalez PA, Prado CE, Leiva ED, Carreno LJ, Bueno SM, Riedel CA, et al. Respiratory syncytial virus impairs T cell activation by preventing synapse assembly with dendritic cells. *Proc Natl Acad Sci USA*. (2008) 105:14999–5004. doi: 10.1073/pnas.0802555105
21. Paramore LC, Ciuryla V, Ciesla G, Liu L. Economic impact of respiratory syncytial virus-related illness in the US. *Pharmacoeconomics*. (2004) 22:275–84. doi: 10.2165/00019053-200422050-00001
22. Hall CB, Weinberg GA, Iwane MK, Blumkin AK, Edwards KM, Staat MA, et al. The burden of respiratory syncytial virus infection in young children. *N Engl J Med.* (2009) 360:588–98. doi: 10.1056/NEJMoa0804877
23. Stockman LJ, Curns AT, Anderson LJ, Fischer-Langley G. Respiratory Syncytial Virus-associated Hospitalizations among infants and young children in the United States, 1997–2006. *Pediatr Infect Dis J*. (2012) 31:5–9. doi: 10.1097/INF.0b013e31822e68e6
24. Sigurs N, Bjarnason R, Sigurbergsson F, Kjellman B. Respiratory syncytial virus bronchiolitis in infancy is an important risk factor for asthma and allergy at Age 7. *Am J Respir Crit Care Med.* (2000) 161:1501–7. doi: 10.1164/ajrccm.161.5.9906076
25. Sigurs N, Gustafsson PM, Bjarnason R, Lundberg F, Schmidt S, Sigurbergsson F, et al. Severe respiratory syncytial virus bronchiolitis in infancy and asthma and allergy at age 13. *Am J Respir Crit Care Med*. (2005) 171:137–41. doi: 10.1164/rccm.200406-730OC
26. Carbonell-Estrany X, Pérez-Yarza EG, García LS, Guzmán Cabañas JM, Bòria EV, Atienza BB. Long-term burden and respiratory effects of respiratory syncytial virus hospitalization in preterm infants—The SPRING Study. *PLoS ONE*. (2015) 10:e0125422. doi: 10.1371/journal.pone.0125422
27. Fauroux B, Simões EAF, Checchia PA, Paes B, Figueras-Aloy J, Manzoni P, et al. The burden and long-term respiratory morbidity associated with respiratory syncytial virus infection in early childhood. *Infect Dis Ther*. (2017) 6:173–97. doi: 10.1007/s40121-017-0151-4
28. Jorquera PA, Tripp RA. Respiratory syncytial virus: prospects for new and emerging therapeutics. *Exp Rev Respir Med*. (2017) 11:609–15. doi: 10.1080/17476348.2017.1338567
29. PATH. RSV Vaccine and mAb Snapshot. *PATH Vaccine Resour Libr*. (2018). Available online at: https://www.path.org/resources/rsv-vaccine-and-mab-snapshot/
30. Report T. Updated guidance for palivizumab prophylaxis among infants and young children at increased risk of hospitalization for respiratory syncytial virus infection. *Pediatrics*. (2014) 134:e620–38. doi: 10.1542/peds.2014-1666
31. Hampp C, Kauf TL, Saidi AS, Winterstein AG. Cost-effectiveness of respiratory syncytial virus prophylaxis in various indications. *Arch Pediatr Adolesc Med*. (2011) 165:498–505. doi: 10.1001/archpediatrics.2010.298
32. Wegner S, Vann JJ, Liu G, Byrns P, Cypra C, Campbell W, et al. Direct cost analyses of palivizumab treatment in a cohort of at-risk children: evidence from the north carolina medicaid program. *Pediatrics*. (2004) 114:1612–9. doi: 10.1542/peds.2004-0959
33. ElHassan NO, Sorbero MES, Hall CB, Stevens TP, Dick AW. Cost-effectiveness analysis of palivizumab in premature infants without chronic lung disease. *Arch Pediatr Adolesc Med*. (2006) 160:1070. doi: 10.1001/archpedi.160.10.1070
34. Mochizuki H, Kusuda S, Okada K, Yoshihara S, Furuya H, Simões EAF, et al. Palivizumab prophylaxis in preterm infants and subsequent recurrent wheezing: Six-year follow-up study. *Am J Respir Crit Care Med.* (2017) 196:29–38. doi: 10.1164/rccm.201609-1812OC
35. Blanken MO, Rovers MM, Molenaar JM, Winkler-Seinstra PL, Meijer A, Kimpen JLL, et al. Respiratory syncytial virus and recurrent wheeze in healthy preterm infants. *N Engl J Med*. (2013) 368:1791–9. doi: 10.1056/NEJMoa1211917
36. Afonso CL, Amarasinghe GK, Bányai K, Bào Y, Basler CF, Bavari S, et al. Taxonomy of the order *Mononegavirales*: update 2016. *Arch Virol*. (2016) 161:2351–60. doi: 10.1007/s00705-016-2880-1
37. Graham BS, Rutigliano JA, Johnson TR. Respiratory syncytial virus immunobiology and pathogenesis. *Virology*. (2002) 297:1–7. doi: 10.1006/viro.2002.1431
38. Hacking D, Hull J. Respiratory syncytial virus—viral biology and the host response. *J Infect*. (2002) 45:18–24. doi: 10.1053/jinf.2002.1015
39. Levine S, Kaliaber-Franco R, Paradiso PR. Demonstration that glycoprotein G is the attachment protein of respiratory syncytial virus. *J Gen Virol*. (1987) 68:2521–4. doi: 10.1099/0022-1317-68-9-2521
40. Johnson SM, McNally BA, Ioannidis I, Flano E, Teng MN, Oomens AG, et al. Respiratory syncytial virus uses CX3CR1 as a receptor on primary human airway epithelial cultures. *PLoS Pathog*. (2015) 11:e1005318. doi: 10.1371/journal.ppat.1005318
41. Zhivaki D, Lemoine S, Lim A, Morva A, Vidalain PO, Schandene L, et al. Respiratory syncytial virus infects regulatory b cells in human neonates via chemokine receptor CX3CR1 and promotes lung disease severity. *Immunity*. (2017) 46:301–14. doi: 10.1016/j.immuni.2017.01.010
42. Tayyari F, Marchant D, Moraes TJ, Duan W, Mastrangelo P, Hegele RG. Identification of nucleolin as a cellular receptor for human respiratory syncytial virus. *Nat Med*. (2011) 17:1132–5. doi: 10.1038/nm.2444
43. Hall CB, Douglas RG. Modes of transmission of respiratory syncytial virus. *J Pediatr*. (1981) 99:100–3. doi: 10.1016/S0022-3476(81)80969-9
44. Piedimonte G, Perez MK. Respiratory Syncytial Virus Infection and Bronchiolitis. *Pediatr Rev*. (2014) 35:519–30. doi: 10.1542/pir.35-12-519
45. Obata K, Kojima T, Masaki T, Okabayashi T, Yokota S, Hirakawa S, et al. Curcumin prevents replication of respiratory syncytial virus and the

epithelial responses to it in human nasal epithelial cells. (2013) 8:e70225. doi: 10.1371/journal.pone.0070225
46. Jumat MR, Yan Y, Ravi LI, Wong P, Huong TN, Li C, et al. Morphogenesis of respiratory syncytial virus in human primary nasal ciliated epithelial cells occurs at surface membrane microdomains that are distinct from cilia. *Virology*. (2015) 484:395–411. doi: 10.1016/j.virol.2015.05.014
47. Turner JR. Intestinal mucosal barrier function in health and disease. *Nat Rev Immunol*. (2009) 9:799–809. doi: 10.1038/nri2653
48. Rezaee F, DeSando SA, Ivanov AI, Chapman TJ, Knowlden SA, Beck LA, et al. Sustained protein kinase d activation mediates respiratory syncytial virus-induced airway barrier disruption. *J Virol.* (2013) 87:11088–95. doi: 10.1128/JVI.01573-13
49. Krzyzaniak MA, Zumstein MT, Gerez JA, Picotti P, Helenius A. Host cell entry of respiratory syncytial virus involves macropinocytosis followed by proteolytic activation of the F Protein. *PLoS Pathog.* (2013) 9:e1003309. doi: 10.1371/journal.ppat.1003309
50. Sourimant J, Rameix-Welti M-A, Gaillard A-L, Chevret D, Galloux M, Gault E, et al. Fine Mapping and characterization of the l-polymerase-binding domain of the respiratory syncytial virus phosphoprotein. *J Virol.* (2015) 89:4421–33. doi: 10.1128/JVI.03619-14
51. Fearns R, Collins PL. Role of the M2-1 transcription antitermination protein of respiratory syncytial virus in sequential transcription. *J Virol*. (1999) 73:5852–64
52. Cifuentes-Muñoz N, Dutch RE, Cattaneo R. Direct cell-to-cell transmission of respiratory viruses: the fast lanes. *PLoS Pathog*. (2018) 14:e1007015. doi: 10.1371/journal.ppat.1007015
53. Openshaw PJ. The mouse model of respiratory syncytial virus disease. In: Anderson GBL, editor. *Challenges and Opportunities for Respiratory Syncytial Virus Vaccines*, Current Topics in Microbiology and Immunology, Vol 372. Berlin: Springer.
54. Taylor G. Animal models of respiratory syncytial virus infection. *Vaccine*. (2017) 35:469–80. doi: 10.1016/j.vaccine.2016.11.054
55. Graham DBS, Perkins MD, Wright PF, Karzon DT. Primary respiratory syncytial virus infection in mice. *J Med Virol.* (1988) 26:153–62. doi: 10.1002/jmv.1890260207
56. Gharib SA, Nguyen E, Altemeier WA, Shaffer SA, Doneanu CE, Goodlett DR, et al. Of mice and men: comparative proteomics of bronchoalveolar fluid. *Eur Respir J.* (2010) 35:1388–95. doi: 10.1183/09031936.00089409
57. Jakubzick C, Tacke F, Llodra J, van Rooijen N, Randolph GJ. Modulation of dendritic cell trafficking to and from the airways. *J Immunol*. (2006) 176:3578–84. doi: 10.4049/jimmunol.176.6.3578
58. Tulic MK, Hurrelbrink RJ, Prele CM, Laing IA, Upham JW, Le Souef P, et al. TLR4 polymorphisms mediate impaired responses to respiratory syncytial virus and lipopolysaccharide. *J Immunol.* (2007) 179:132–40. doi: 10.4049/jimmunol.179.1.132
59. Pyle CJ, Uwadiae FI, Swieboda DP, Harker JA. Early IL-6 signalling promotes IL-27 dependent maturation of regulatory T cells in the lungs and resolution of viral immunopathology. *PLOS Pathog.* (2017) 13:e1006640. doi: 10.1371/journal.ppat.1006640
60. Rudd BD, Smit JJ, Flavell RA, Alexopoulou L, Schaller MA, Gruber A, et al. Deletion of TLR3 alters the pulmonary immune environment and mucus production during respiratory syncytial virus infection. *J Immunol.* (2006) 176:1937–42. doi: 10.4049/jimmunol.176.3.1937
61. Lindell DM, Morris SB, White MP, Kallal LE, Lundy PK, Hamouda T, et al. A novel inactivated intranasal respiratory syncytial virus vaccine promotes viral clearance without TH2 associated Vaccine-Enhanced disease. *PLoS ONE*. (2011) 6:e21823. doi: 10.1371/journal.pone.0021823
62. Stokes KL, Currier MG, Sakamoto K, Lee S, Collins PL, Plemper RK, et al. The Respiratory Syncytial Virus Fusion Protein and Neutrophils Mediate the Airway Mucin Response to Pathogenic Respiratory Syncytial Virus Infection. *J Virol*. (2013) 87:10070–82. doi: 10.1128/JVI.01347-13
63. Moreno-Solis G, Torres-Borrego J, de la Torre-Aguilar MJ, Fernandez-Gutierrez F, Llorente-Cantarero FJ, Perez-Navero JL. Analysis of the local and systemic inflammatory response in hospitalized infants with respiratory syncitial virus bronchiolitis. *Allergol Immunopathol*. (2014) 43:264–71. doi: 10.1016/j.aller.2014.02.002
64. Becker S, Soukup JM. Airway epithelial cell-induced activation of monocytes and eosinophils in respiratory syncytial viral infection. *Immunobiology*. (1999) 201:88–106. doi: 10.1016/S0171-2985(99)80049-7
65. Das S, Palmer OP, Leight WD, Surowitz JB, Pickles RJ, Randell SH, et al. Cytokine amplification by respiratory syncytial virus infection in human nasal epithelial cells. *Laryngoscope*. (2005) 115:764–8. doi: 10.1097/01.MLG.0000159527.76949.93
66. Chalovich JM, Eisenberg E. Respiratory epithelial cells orchestrate pulmonary innate immunity. *Magn Reson Imag.* (2013) 31:477–9. doi: 10.1016/j.immuni.2010.12.017
67. Peebles RS, Sheller JR, Collins RD, Jarzecka K, Mitchell DB, Graham BS. Respiratory syncytial virus (RSV)-induced airway hyperresponsiveness in allergically sensitized mice is inhibited by live RSV and exacerbated by formalin-inactivated RSV. *J Infect Dis.* (2000) 182:671–7. doi: 10.1086/315783
68. Miller AL, Strieter RM, Gruber AD, Ho SB, Lukacs NW. CXCR2 Regulates Respiratory syncytial virus-induced airway hyperreactivity and mucus overproduction. *J Immunol.* (2003) 170:3348–56. doi: 10.4049/jimmunol.170.6.3348
69. Mukherjee S, Lindell DM, Berlin AA, Morris SB, Shanley TP, Hershenson MB, et al. IL-17Induced pulmonary pathogenesis during respiratory viral infection and exacerbation of allergic disease. *Am J Pathol.* (2011) 179:248–58. doi: 10.1016/j.ajpath.2011.03.003
70. Ungvári I, Tölgyesi G, Semsei ÁF, Nagy A, Radosits K, Keszei M, et al. CCR5Δ32 mutation, Mycoplasma pneumoniae infection, and asthma. *J Allergy Clin Immunol.* (2007) 119:1545–7. doi: 10.1016/j.jaci.2007.03.014
71. Pino M, Kelvin DJ, Bermejo-Martin JF, Alonso A, Matías V, Tenorio A, et al. Nasopharyngeal aspirate cytokine levels 1 yr after severe respiratory syncytial virus infection. *Pediatr Allergy Immunol.* (2009) 20:791–5. doi: 10.1111/j.1399-3038.2009.00868.x
72. Bermejo-Martin JF, Bernardo D, Dominguez-Gil M, Alonso A, Garcia-Arevalo MC, Pino M, et al. Interleukin (IL)-1β, IL-6 and IL-8 in nasal secretions: A common role for innate immunity in viral bronchial infection in infants? *Br J Biomed Sci.* (2006) 63:173–5. doi: 10.1080/09674845.2006.11978093
73. Hoebee B, Rietveld E, Bont L, Van Oosten M, Hodemaekers HM, Nagelkerke NJD, et al. Association of Severe Respiratory Syncytial Virus Bronchiolitis with Interleukin-4 and Interleukin-4 Receptor α Polymorphisms. *J Infect Dis.* (2003) 187:2–11. doi: 10.1086/345859
74. Liesman RM, Buchholz UJ, Luongo CL, Yang L, Proia AD, DeVincenzo JP, et al. RSV-encoded NS2 promotes epithelial cell shedding and distal airway obstruction. *J Clin Invest.* (2014) 124:2219–33. doi: 10.1172/JCI72948
75. Bertrand P, Lay MK, Piedimonte G, Brockmann PE, Palavecino CE, Hernández J, et al. Elevated IL-3 and IL-12p40 levels in the lower airway of infants with RSV-induced bronchiolitis correlate with recurrent wheezing. *Cytokine*. (2015) 76:417–23. doi: 10.1016/j.cyto.2015.07.017
76. Stoppelenburg AJ, Salimi V, Hennus M, Plantinga M, Huis in 't Veld R, Walk J, et al. Local IL-17A Potentiates early neutrophil recruitment to the respiratory tract during severe rsv infection. *PLoS ONE*. (2013) 8:078461. doi: 10.1371/journal.pone.0078461
77. Sheppard P, Kindsvogel W, Xu W, Henderson K, Schlutsmeyer S, Whitmore TE, et al. IL-28, IL-29 and their class II cytokine receptor IL-28R. *Nat Immunol.* (2003) 4:63–8. doi: 10.1038/ni873
78. Faber T, Groen H, Welfing M, Jansen KJ., Bont LJ. Specific Increase in Local IL-17 production during recovery from primary RSV bronchiolitis. *J Med Virol.* (2012) 84:1084–8. doi: 10.1002/jmv.23291
79. Shachar I, Karin N. The dual roles of inflammatory cytokines and chemokines in the regulation of autoimmune diseases and their clinical implications. *J Leukoc Biol.* (2013) 93:51–61. doi: 10.1189/jlb.0612293
80. Tripp RA, Oshansky C, Alvarez R. Cytokines and respiratory syncytial virus infection. *Proc Am Thorac Soc.* (2005) 2:147–9. doi: 10.1513/pats.200502-014AW
81. Gulati K, Guhathakurta S, Joshi J, Rai N, Ray A. MOJ Immunology cytokines and their role in health and disease: a brief overview. (2016) 4:00121. doi: 10.15406/moji.2016.04.00121
82. Holdsworth SR, Gan P-Y. Cytokines: names and numbers you should care about. *Clin J Am Soc Nephrol.* (2015) 10:2243–54. doi: 10.2215/CJN.07590714

83. Cavaillon JM. Pro- versus anti-inflammatory cytokines: myth or reality. *Cell Mol Biol.* (2001) 47:695–702.
84. Turner MD, Nedjai B, Hurst T, Pennington DJ. Cytokines and chemokines: At the crossroads of cell signalling and inflammatory disease. *Biochim Biophys Acta - Mol Cell Res.* (2014) 1843:2563–82. doi: 10.1016/j.bbamcr.2014.05.014
85. Chang HD, Radbruch A. The pro- and anti-inflammatory potential of interleukin-12. in *Anna N Y Acad Sci.* (2007) 1109:40–6. doi: 10.1196/annals.1398.006
86. Hughes CE, Nibbs RJB. A guide to chemokines and their receptors. *FEBS J.* (2018) 285:2944. doi: 10.1111/febs.14466
87. Akhter J, Al S. "Epidemiology and Diagnosis of Human Respiratory Syncytial Virus Infections," in *Human Respiratory Syncytial Virus Infection*. (InTech). doi: 10.5772/29105
88. Villenave R, Shields MD, Power UF. Respiratory syncytial virus interaction with human airway epithelium. *Trends Microbiol.* (2013) 21:238–244. doi: 10.1016/j.tim.2013.02.004
89. Knudson CJ, Hartwig SM, Meyerholz DK, Varga SM. RSV Vaccine-Enhanced Disease Is Orchestrated by the Combined Actions of Distinct CD4 T Cell Subsets. *PLoS Pathog.* (2015) 11:1–23. doi: 10.1371/journal.ppat.1004757
90. Hislop AA. Airway and blood vessel interaction during lung development. *J Anat.* (2002) 201:325–34. doi: 10.1046/j.1469-7580.2002.00097.x
91. Griffiths C, Drews SJ, Marchant DJ. Respiratory syncytial virus: Infection, detection, and new options for prevention and treatment. *Clin Microbiol Rev.* (2017) 30:277–319. doi: 10.1128/CMR.00010-16
92. Wong JYW, Rutman A, O'Callaghan C. Recovery of the ciliated epithelium following acute bronchiolitis in infancy. *Thorax.* (2005) 60:582–7. doi: 10.1136/thx.2004.024638
93. Wright PF, Ikizler MR, Gonzales RA, Carroll KN, Johnson JE, Werkhaven JA. Growth of respiratory syncytial virus in primary epithelial cells from the human respiratory tract. *J Virol.* (2005) 79:8651–4. doi: 10.1128/JVI.79.13.8651-8654.2005
94. Smith CM, Kulkarni H, Radhakrishnan P, Rutman A, Bankart MJ, Williams G, et al. Ciliary dyskinesia is an early feature of respiratory syncytial virus infection. *Eur Respir J.* (2014) 43:485–96. doi: 10.1183/09031936.00205312
95. Guo-Parke H, Canning P, Douglas I, Villenave R, Heaney LG, Coyle PV, et al. Relative respiratory syncytial virus cytopathogenesis in upper and lower respiratory tract epithelium. *Am J Respir Crit Care Med.* (2013) 188:842–51. doi: 10.1164/rccm.201304-0750OC
96. Reimers K, Buchholz K, Werchau H. Respiratory syncytial virus M2-1 protein induces the activation of nuclear factor kappa B. *Virology*. (2005) 331:260–8. doi: 10.1016/j.virol.2004.10.031
97. Dey N, Liu T, Garofalo RP, Casola A. TAK1 regulates NF-KB and AP-1 activation in airway epithelial cells following RSV infection. *Virology*. (2011) 418:93–101. doi: 10.1016/j.virol.2011.07.007
98. Moore ML, Newcomb DC, Parekh VV, Van Kaer L, Collins RD, Zhou W, et al. STAT1 negatively regulates lung basophil IL-4 expression induced by respiratory syncytial virus infection. *J Immunol.* (2009) 183:2016–26. doi: 10.4049/jimmunol.0803167
99. Giugno KM, Machado DC, Amantéa SL, Barreto SSM. Concentrations of interleukin-2 in the nasopharyngeal secretion of children with acute respiratory syncytial virus bronchiolitis. *J Pediatr*. (2004) 80:315–20. doi: 10.2223/1206
100. Blanco JCG, Richardson JY, Darnell MER, Rowzee A, Pletneva L, Porter DD, et al. Cytokine and chemokine gene expression after primary and secondary respiratory syncytial virus infection in cotton rats. *J Infect Dis.* (2002) 185:1780–5. doi: 10.1086/340823
101. Legg JP, Hussain IR, Warner JA, Johnston SL, Warner JO. Type 1 and type 2 cytokine imbalance in acute respiratory syncytial virus bronchiolitis. *Am J Respir Crit Care Med.* (2003) 168:633–9. doi: 10.1164/rccm.200210-1148OC
102. Takeda K, Akira S. Toll-like receptors in innate immunity. *Int Immunol.* (2005) 17:1–14. doi: 10.1093/intimm/dxh186
103. Kumar H, Kawai T, Akira S. Toll-like receptors and innate immunity. *Biochem Biophys Res Commun.* (2009) 388:621–5. doi: 10.1016/j.bbrc.2009.08.062
104. Kolli D, Velayutham T, Casola A. Host-viral interactions: role of pattern recognition receptors (PRRs) in human pneumovirus infections. *Pathogens*. (2013) 2:232–63. doi: 10.3390/pathogens2020232
105. Dou Y, Zhao Y, Zhang Z, Mao H, Tu W, Zhao X. Respiratory syncytial virus infection induces higher toll-like receptor-3 expression and TNF-α production than human metapneumovirus infection. *PLoS ONE.* (2013) 8:e73488. doi: 10.1371/journal.pone.0073488
106. Johnson TR, Rao S, Seder RA, Chen M, Graham BS. TLR9 agonist, but not TLR7/8, functions as an adjuvant to diminish FI-RSV vaccine-enhanced disease, while either agonist used as therapy during primary RSV infection increases disease severity. *Vaccine*. (2009) 27:3045–52. doi: 10.1016/j.vaccine.2009.03.026
107. Marr N, Turvey SE. Role of human TLR4 in respiratory syncytial virus-induced NF-κB activation, viral entry and replication. *Innate Immun.* (2012) 18:856–65. doi: 10.1177/1753425912444479
108. Kurt-Jones EA, Popova L, Kwinn L, Haynes LM, Jones LP, Tripp RA, et al. Pattern recognition receptors TLR4 and CD14 mediate response to respiratory syncytial virus. *Nat Immunol.* (2000) 1:398–401. doi: 10.1038/80833
109. Haynes LM, Moore DD, Kurt-Jones EA, Finberg RW, Anderson LJ, Tripp RA. Involvement of toll-like receptor 4 in innate immunity to respiratory syncytial virus. *J Virol.* (2001) 75:10730–7. doi: 10.1128/JVI.75.22.10730-10737.2001
110. Yingxin Z, Jamaluddin M, Zhang Y, Sun H, Ivanciuc T, Garofalo RP et al. Systematic analysis of cell-type differences in the epithelial secretome reveals insights into the pathogenesis of rsv- induced lower respiratory tract infections. (2018) 198:3345–64. doi: 10.4049/jimmunol.1601291
111. Mercer RR, Crapo JD. Lower respiratory tract structure of laboratory animals and humans: Dosimetry implications. *Aerosol Sci Technol.* (1993) 18:257–271. doi: 10.1080/02786829308959603
112. Stein RT, Sherrill D, Morgan WJ, Holberg CJ, Halonen M, Taussig LM, et al. Respiratory syncytial virus in early life and risk of wheeze and allergy by age 13 years. *Lancet*. (1999) 354:541–5.
113. American Academy of Pediatrics Subcommittee on Diagnosis and Management of Bronchiolitis S on D and M of. Diagnosis and management of bronchiolitis. *Pediatrics*. (2006) 118:1774–93 doi: 10.1542/peds.2006-2223
114. Del Vecchio A, Ferrara T, Maglione M, Capasso L, Raimondi F. New perspectives in respiratory syncitial virus infection. *J Matern Neonatal Med.* (2013) 26:55–9. doi: 10.3109/14767058.2013.831282
115. Johnson JE, Gonzales RA, Olson SJ, Wright PF, Graham BS. The histopathology of fatal untreated human respiratory syncytial virus infection. *Mod Pathol.* (2007) 20:108–19. doi: 10.1038/modpathol.3800725
116. McNamara PS, Flanagan BF, Selby AM, Hart CA, Smyth RL. Pro- and anti-inflammatory responses in respiratory syncytial virus bronchiolitis. *Eur Respir J.* (2004) 23:106–12. doi: 10.1183/09031936.03.00048103
117. McNamara PS, Flanagan BF, Hart CA, Smyth RL. Production of Chemokines in the Lungs of Infants with severe respiratory syncytial virus bronchiolitis. *J Infect Dis.* (2005) 191:1225–32. doi: 10.1086/428855
118. Ugonna K, Douros K, Bingle CD, Everard ML. Cytokine responses in primary and secondary respiratory syncytial virus infections. *Pediatr Res.* (2016) 79:946–50. doi: 10.1038/pr.2016.29
119. Breindahl M, Rieneck K, Nielse C, Justesen T, Bendtzen K, Müller K. Cytokine responses in infants infected with respiratory syncytial virus. *Open J Immunol.* (2012) 2:40–8. doi: 10.4236/oji.2012.21005
120. Fan R, Wen B, Liu W, Zhang J, Liu C, Fan C, Qu X. Cytokine Altered regulatory cytokine pro fi les in cases of pediatric respiratory syncytial virus infection. *Cytokine*. (2018) 103:57–62. doi: 10.1016/j.cyto.2017.12.028
121. Vieira RA, Diniz EM de A, Ceccon MEJR. Correlation between inflammatory mediators in the nasopharyngeal secretion and in the serum of children with lower respiratory tract infection caused by respiratory syncytial virus and disease severity. *J Bras Pneumol.* (2010) 36:59–66. doi: 10.1111/anae.13774
122. Semple MG, Dankert HM, Ebrahimi B, Correia JB, Booth JA, Stewart JP, et al. Severe respiratory syncytial virus bronchiolitis in infants is associated with reduced airway interferon gamma and substance P. *PLoS ONE*. (2007) 2:1–8. doi: 10.1371/journal.pone.0001038
123. Thwaites RS, Ito K, Chingono JMS, Coates M, Jarvis HC, Tunstall T, et al. Nasosorption as a minimally invasive sampling procedure: mucosal viral load and inflammation in primary RSV bronchiolitis. *J Infect Dis.* (2017) 215:1240–4. doi: 10.1093/infdis/jix150

124. McNamara PS, Flanagan BF, Baldwin LM, Newland P, Hart CA, Smyth RL. Interleukin 9 production in the lungs of infants with severe respiratory syncytial virus bronchiolitis. *Lancet*. (2004) 363:1031–7. doi: 10.1016/S0140-6736(04)15838-8
125. Schuurhof A, Bont L, Siezen CLE, Hodemaekers H, van Houwelingen HC, Kimman TG, et al. Interleukin-9 polymorphism in infants with respiratory syncytial virus infection: An opposite effect in boys and girls. *Pediatr Pulmonol.* (2010) 45:608–13. doi: 10.1002/ppul.21229
126. Ying S, O'Connor B, Ratoff J, Meng Q, Mallett K, Cousins D, et al. Thymic Stromal Lymphopoietin Expression Is Increased in Asthmatic Airways and Correlates with Expression of Th2-Attracting Chemokines and Disease Severity. *J Immunol.* (2005) 174:8183–90. doi: 10.4049/jimmunol.174.12.8183
127. Soumelis V, Reche PA, Kanzler H, Yuan W, Edward G, Homey B. Human epithelial cells trigger dendritic cell-mediated allergic inflammation by producing TSLP. *Nat Immunol.* (2002) 3:673–80. doi: 10.1038/ni805
128. Rochman Y, Dienger-Stambaugh K, Richgels PK, Lewkowich IP, Kartashov AV, Barski A, et al. TSLP signaling in CD4+ T cells programs a pathogenic T helper 2 cell state. *Sci Signal.* (2018) 11:eaam8858. doi: 10.1126/scisignal.aam8858
129. Ziegler SF, Artis D. Sensing the outside world: TSLP regulates barrier immunity. *Nat Immunol.* (2010) 11:289–93. doi: 10.1038/ni.1852
130. Allakhverdi Z, Comeau M, Jessup H, Delespesse G. Thymic stromal lymphopoietin as a mediator of crosstalk between bronchial smooth muscles and mast cells. *J Allergy Clin Immunol.* (2009) 123:958–60. doi: 10.1016/j.jaci.2009.01.068
131. Harada M, Hirota T, Jodo AI, Doi S, Kameda M, Fujita K, et al. Functional analysis of the thymic stromal lymphopoietin variants in human bronchial epithelial cells. *Am J Respir Cell Mol Biol.* (2009) 40:368–74. doi: 10.1165/rcmb.2008-0041OC
132. García-García ML, Calvo C, Moreira A, Cañas JA, Pozo F, Sastre B, et al. Thymic stromal lymphopoietin, IL-33, and periostin in hospitalized infants with viral bronchiolitis. *Medicine*. (2017) 96:e6787. doi: 10.1097/MD.0000000000006787
133. Jordan WJ, Eskdale J, Boniotto M, Rodia M, Kellner D, Gallagher G. Modulation of the human cytokine response by interferon lambda-1 (IFN-λ1/IL-29). *Genes Immun.* (2007) 8:13–20. doi: 10.1038/sj.gene.6364348
134. Selvaggi C, Pierangeli A, Fabiani M, Spano L, Nicolai A, Papoff P, et al. Interferon lambda 1-3 expression in infants hospitalized for RSV or HRV associated bronchiolitis. *J Infect*. (2014) 68:467–77. doi: 10.1016/j.jinf.2013.12.010
135. Harrison AM, Bonville CA, Rosenberg HF, Domachowske JB. Respiratory syncytical virus–induced chemokine expression in the lower Airways. *Am J Respir Crit Care Med*. (1999) 159:1918–24. doi: 10.1164/ajrccm.159.6.9805083
136. Culley FJ, Pennycook AMJ, Tregoning JS, Hussell T, Openshaw PJM. Differential Chemokine Expression following Respiratory Virus Infection Reflects Th1- or Th2-Biased Immunopathology Differential Chemokine Expression following Respiratory Virus Infection Reflects Th1- or Th2-Biased Immunopathology. *J Virol.* (2006) 80:4521–7. doi: 10.1128/JVI.80.9.4521
137. Hornsleth A, Loland L, Larsen LB. Cytokines and chemokines in respiratory secretion and severity of disease in infants with respiratory syncytial virus (RSV) infection. *J Clin Virol.* (2001) 21:163–70. doi: 10.1016/S1386-6532(01)00159-7
138. Sung RY, Hui SH, Wong CK, Lam CW, Yin J. A comparison of cytokine responses in respiratory syncytial virus and influenza A infections in infants. *Eur J Pediatr.* (2001) 160:117–22. doi: 10.1007/s004310000676
139. Alvarez AE, Marson FAL, Bertuzzo CS, Bastos JCS, Baracat ECE, Brandão MB, et al. Association between single nucleotide polymorphisms in TLR4 , TLR2 , TLR9 , VDR , NOS2 and CCL5 genes with acute viral bronchiolitis. *Gene*. (2018) 645:7–17. doi: 10.1016/j.gene.2017.12.022
140. Jones A, Qui JM, Bataki E, Elphick H, Ritson S, Evans GS, et al. Neutrophil survival is prolonged in the airways of healthy infants and infants with RSV bronchiolitis. *Eur Respir J.* (2002) 20:651–7. doi: 10.1183/09031936.02.00278902
141. Smyth RL, Mobbs KJ, O'Hea U, Ashby D, Hart CA. Respiratory syncytial virus bronchiolitis: Disease severity, interleukin-8, and virus genotype. *Pediatr Pulmonol.* (2002) 33:339–46. doi: 10.1002/ppul.10080
142. Hillyer P, Shepard R, Uehling M, Krenz M, Sheikh F, Thayer KR, et al. Differential responses by human respiratory epithelial cell lines to respiratory syncytial virus reflect distinct patterns of infection control. *J Virol.* (2018) 92:JVI.02202-17. doi: 10.1128/JVI.02202-17
143. Noah TL, Hill C, Carolina N, Respiratory SB. Respiratory syncytial virus-induced cytokine production by a human bronchial epithelial cell line. *Am J Physiol.* (1993) 265:L472–8. doi: 10.1152/ajplung.1993.265.5.L472
144. Carubelli CM, Jafri HS, Sanchez PJ, Ramilo O. Ribavirin suppresses pro-inflammatory cytokin production in pulmonary epithelial cells infected with respiratory syncytial virus (RSV). *Pediatr Res.* (1999) 45:158A. doi: 10.1203/00006450-199904020-00939
145. Yoon JSJ-S, Kim H, Lee Y, Lee J-SJS. Cytokine induction by respiratory syncytial virus and adenovirus in bronchial epithelial cells. *Pediatr Pulmonol.* (2007) 42:277–282. doi: 10.1002/ppul.20574
146. Levitz R, Wattier R, Phillips P, Solomon A, Lawler J, Lazar I, et al. Induction of IL-6 and CCL5 (RANTES) in human respiratory epithelial (A549) cells by clinical isolates of respiratory syncytial virus is strain specific. *Virol J.* (2012) 9:190. doi: 10.1186/1743-422X-9-190
147. Fonceca AM, Flanagan BF, Trinick R, Smyth RL, McNamara PS. Primary airway epithelial cultures from children are highly permissive to respiratory syncytial virus infection. *Thorax*. (2012) 67:42–8. doi: 10.1136/thoraxjnl-2011-200131
148. Oshansky CM, Barber JP, Crabtree J, Tripp RA. Respiratory syncytial virus f and g proteins induce interleukin lα, cc, and cxc chemokine responses by normal human bronchoepithelial cells. *J Infect Dis.* (2010) 201:1201–7. doi: 10.2307/40599271
149. Olszewska-Pazdrak B, Casola A, Saito T, Alam R, Crowe SE, Mei F, et al. Cell-specific expression of RANTES, MCP-1, and MIP-1alpha by lower airway epithelial cells and eosinophils infected with respiratory syncytial virus. *J Virol.* (1998) 72:4756–64.
150. Lee H-C, Headley MB, Loo Y-M, Berlin A, Gale M, Debley JS, et al. Thymic stromal lymphopoietin is induced by respiratory syncytial virus–infected airway epithelial cells and promotes a type 2 response to infection. *J Allergy Clin Immunol.* (2012) 130:1187–96.e5. doi: 10.1016/j.jaci.2012.07.031
151. Bolger G, Lapeyre N, Dansereau N, Lagacé L, Berry G, Klosowski K, et al. Primary infection of mice with high titer inoculum respiratory syncytial virus: characterization and response to antiviral therapy. *Can J Physiol Pharmacol.* (2005) 83:198–213. doi: 10.1139/y05-007
152. Neuzil KM, Tang YW, Graham BS. Protective role of TNF-α in respiratory syncytial virus infection *in vitro* and *in vivo*. *Am J Med Sci.* (1996) 311(5):201–4. doi: 10.1097/00000441-199605000-00001
153. van Schaik SM, Obot N, Enhorning G, Hintz K, Gross K, Hancock GE, et al. Role of interferon gamma in the pathogenesis of primary respiratory syncytial virus infection in BALB/c mice. *J Med Virol.* (2000) 62:257–66. doi: 10.1002/1096-9071(200010)62:2<257::AID-JMV19>3.0.CO;2-M
154. Haeberle HA, Kuziel WA, Dieterich HJ, Casola A, Gatalica Z, Garofalo RP. Inducible expression of inflammatory chemokines in respiratory syncytial virus-infected mice: role of MIP-1alpha in lung pathology. *J Virol.* (2001) 75:878–90. doi: 10.1128/JVI.75.2.878-890.2001
155. John AE, Berlin AA, Lukacs NW. Respiratory syncytial virus-induced CCL5/RANTES contributes to exacerbation of allergic airway inflammation. *Eur J Immunol.* (2003) 33:1677–85. doi: 10.1002/eji.200323930
156. Tekkanat KK, Maassab H, Miller A, Berlin A, Kunkel SL, Lukacs NW. Rantes (CCL5) production during primary respiratory syncytial virus infection exacerbates airway disease. *Eur J Immunol*. (2002) 32(11):3276–84. doi: 10.1002/1521-4141(200211)32:11<3276::AID-IMMU3276>3.0.CO;2-5
157. Culley FJ, Pennycook AM, Tregoning JS, Dodd JS, Walzl G, Wells TN, et al. Role of CCL5 (RANTES) in Viral Lung Disease. *J Virol.* (2006) 80:8151–8157. doi: 10.1128/JVI.00496-06
158. Tregoning JS, Pribul PK, Pennycook AMJ, Hussell T, Wang B, Lukacs N, et al. The chemokine MIP1α/CCL3 determines pathology in primary RSV infection by regulating the balance of t cell populations in the murine lung. *PLoS ONE*. (2010) 5:09381. doi: 10.1371/journal.pone.0009381

159. Stier MT, Bloodworth MH, Toki S, Newcomb DC, Goleniewska K, Boyd KL, et al. Respiratory syncytial virus infection activates IL-13–producing group 2 innate lymphoid cells through thymic stromal lymphopoietin. *J Allergy Clin Immunol.* (2016) 138:814–24.e11. doi: 10.1016/j.jaci.2016.01.050
160. Antonucci R, Chiappe S, Porcella A, Rosatelli D, Fanos V. Bronchiolitis-associated encephalopathy in critically-ill infants: An underestimated complication? *J Matern Neonatal Med.* (2010) 23:431–6. doi: 10.3109/14767050903184181
161. Millichap JJ, Wainwright MS. Neurological complications of respiratory syncytial virus infection: case series and review of literature. *J Child Neurol.* (2009) 24:1499–503. doi: 10.1177/0883073808331362
162. Morichi S, Kawashima H, Ioi H, Yamanaka G, Kashiwagi Y, Hoshika A, et al. Classification of acute encephalopathy in respiratory syncytial virus infection. *J Infect Chemother.* (2011) 17:776–81. doi: 10.1007/s10156-011-0259-5
163. Xu L, Gao H, Zeng J, Liu J, Lu C, Guan X, et al. A fatal case associated with respiratory syncytial virus infection in a young child. *BMC Infect Dis.* (2018) 18:217. doi: 10.1186/s12879-018-3123-8
164. Ng Y, Cox C, Atkins J, Butler IJ. Encephalopathy Associated With Respiratory Syncytial Virus Bronchiolitis. *J Child Neurol.* (2001) 16:105–8. doi: 10.1177/088307380101600207
165. Cappel R, Thiry L, Clinet G. Viral Antibodies in the CSF After Acute CNS Infections. *Arch Neurol.* (1975) 32:629–31. doi: 10.1001/archneur.1975.00490510085008
166. Kawashima H, Ioi H, Ushio M, Yamanaka G, Matsumoto S, Nakayama T. Cerebrospinal fluid analysis in children with seizures from respiratory syncytial virus infection. *Scand J Infect Dis.* (2009) 41:228–31. doi: 10.1080/00365540802669543
167. Morichi S, Morishita N, Ishida Y, Oana S, Yamanaka G, Kashiwagi Y, et al. Examination of neurological prognostic markers in patients with respiratory syncytial virus-associated encephalopathy. *Int J Neurosci.* (2017) 127:44–50. doi: 10.3109/00207454.2016.1138951
168. O'Donnell DR, McGarvey MJ, Tully JM, Balfour-Lynn IM, Openshaw PJM. Respiratory syncytial virus RNA in cells from the peripheral blood during acute infection. *J Pediatr.* (1998) 133:272–4. doi: 10.1016/S0022-3476(98)70234-3
169. Li X, Fu ZF, Alvarez R, Henderson C, Tripp RA. Respiratory syncytial virus (RSV) infects neuronal cells and processes that innervate the lung by a process involving RSV G protein. *J Virol.* (2006) 80:537–40. doi: 10.1128/JVI.80.1.537-540.2006
170. Yuan X, Hu T, He H, Qiu H, Wu X, Chen J, et al. Respiratory syncytial virus prolifically infects N2a neuronal cells, leading to TLR4 and nucleolin protein modulations and RSV F protein co-localization with TLR4 and nucleolin. *J Biomed Sci.* (2018) 25:13. doi: 10.1186/s12929-018-0416-6
171. Espinoza JA, Bohmwald K, Cespedes PF, Gomez RS, Riquelme SA, Cortes CM, et al. Impaired learning resulting from Respiratory Syncytial Virus infection. *Proc Natl Acad Sci USA.* (2013) 110:9112–7. doi: 10.1073/pnas.1217508110

Conflict of Interest Statement: The authors declare that the research was conducted in the absence of any commercial or financial relationships that could be construed as a potential conflict of interest.

frontiers in Immunology

ORIGINAL RESEARCH
published: 04 October 2018
doi: 10.3389/fimmu.2018.02297

Aflatoxin B_1 Promotes Influenza Replication and Increases Virus Related Lung Damage via Activation of TLR4 Signaling

Yuhang Sun[1,2], *Jiarui Su*[1,2], *Zixuan Liu*[1,2], *Dandan Liu*[1,2], *Fang Gan*[1,2], *Xingxiang Chen*[1,2] *and Kehe Huang*[1,2*]

[1] *Department of Animal Nutrition and Immunology, College of Veterinary Medicine, Nanjing Agricultural University, Nanjing, China,* [2] *Institute of Nutritional and Metabolic Disorders in Domestic Animals and Fowls, Nanjing Agricultural University, Nanjing, China*

Aflatoxin B_1 (AFB_1), which alters immune responses to mammals, is one of the most common mycotoxins in feeds and food. Swine influenza virus (SIV) is a major pathogen of both animals and humans. However, there have been few studies about the relationship between AFB_1 exposure and SIV replication. Here, for the first time, we investigated the involvement of AFB_1 in SIV replication *in vitro* and *in vivo* and explored the underlying mechanism using multiple cell lines and mouse models. *In vitro* studies demonstrated that low concentrations of AFB_1 (0.01–0.25 μg/ml) markedly promoted SIV replication as revealed by increased viral titers and matrix protein (M) mRNA and nucleoprotein (NP) levels in MDCK cells, A549 cells and PAMs. *In vivo* studies showed that 10–40 μg/kg of AFB_1 exacerbated SIV infection in mice as illustrated by significantly higher lung virus titers, viral M mRNA levels, NP levels, lung indexes and more severe lung damage. Further study showed that AFB_1 upregulated TLR4, but not other TLRs, in SIV-infected PAMs. Moreover, AFB_1 activated TLR4 signaling as demonstrated by the increases of phosphorylated NFκB p65 and TNF-α release in PAMs and mice. In contrast, TLR4 knockdown or the use of BAY 11-7082, a specific inhibitor of NFκB, blocked the AFB_1-promoted SIV replication and inflammatory responses in PAMs. Furthermore, a TLR4-specific antagonist, TAK242, and TLR4 knockout both attenuated the AFB_1-promoted SIV replication, inflammation and lung damage in mice. We therefore conclude that AFB_1 exposure aggravates SIV replication, inflammation and lung damage by activating TLR4-NFκB signaling.

Keywords: aflatoxin B_1, swine influenza virus, replication, inflammation, lung damage, TLR4, NFκB, TNF-α

OPEN ACCESS

Edited by:
Michael H. Lehmann, Ludwig-Maximilians-Universität München, Germany

Reviewed by:
Florian Krammer, Icahn School of Medicine at Mount Sinai, United States
Dunja Bruder, Universitätsklinikum Magdeburg, Germany

***Correspondence:**
Kehe Huang
khhuang@njau.edu.cn

Specialty section:
This article was submitted to Viral Immunology, a section of the journal Frontiers in Immunology

Received: *19 May 2018*
Accepted: *17 September 2018*
Published: *04 October 2018*

Citation:
Sun Y, Su J, Liu Z, Liu D, Gan F, Chen X and Huang K (2018) Aflatoxin B_1 Promotes Influenza Replication and Increases Virus Related Lung Damage via Activation of TLR4 Signaling. Front. Immunol. 9:2297. doi: 10.3389/fimmu.2018.02297

INTRODUCTION

Swine influenza virus (SIV), a single-stranded negative-sense RNA virus, causes severe systemic effects, resulting in significant economic losses in the animal husbandry industry. SIV also causes human disease and can even give rise to human pandemics, including the pandemic caused by the H1N1/2009 virus (1). Increasing evidence indicates that viral infection is associated with several environmental, nutritional, and immune factors, such as mycotoxin contamination (2, 3), selenium deficiency (4, 5), and macrophage polarization (6). The involvement of these factors may partly

explain the differences in morbidity and mortality in infected animals and humans all over the world.

Aflatoxin B_1 (AFB_1), which is produced by *Aspergillus flavus*, is one of the most common mycotoxins in contaminated food and plant products from tropical and subtropical areas with high temperature and humidity (7, 8). It is well known that AFB_1 is harmful to the liver and kidney of mammals and is regarded as a representative orally ingested carcinogen (9, 10). However, increasing evidence indicates that AFB_1 can also affect immune responses in mammals (11, 12); these evidences show that low doses of AFB_1 ($\leq$0.025 mg/kg) significantly increase the secretion of pro-inflammatory cytokines by T cells and NK cells in rats, but high doses of AFB_1 (0.4–0.8 mg/kg) markedly decrease macrophage migration and the lymphocyte response to mitogens in pigs. Specifically, some reports propose that mycotoxins can eventually decrease resistance to infectious diseases (13), and aflatoxins are thought to feature prominently in the progression of some viral diseases, such as HIV (3). However, so far, there have been no studies investigating whether influenza virus infection in mammals exposed to AFB_1 is more severe than infection in unexposed mammals.

Toll-like receptors (TLRs) compose a main family of pattern recognition receptors with a critical role in the activation of the innate immune response (14). To date, there are at least 13 members (TLR1-TLR13) of this family in mammals that recognize specific components of pathogenic microorganisms. TLR4 is a unique receptor for pathogen recognition that was initially found in various cell types, including porcine alveolar macrophages, and in mice. In the past, many studies have focused on TLR4 structure and function. On the one hand, TLR4 activation leads to nuclear factor kappa (NFκB) translocation and the expression of proinflammatory cytokines, including tumor necrosis factor (TNF-α), which is responsible for activating the innate immune system (15). On the other hand, the overexpression or continuous activation of TLR4 leads to excessive inflammatory responses and/or tissue injury in the body (16–19). Interestingly, viruses can evade the host immune response when TLR4 is inhibited, thereby enhancing viral replication, and one study has shown that a TLR4 antagonist can protect mice from lethal influenza infection (20). Nevertheless, few studies are available regarding the role played by TLR4 in AFB_1–promoted SIV replication.

Thus, given the differences in morbidity and mortality following SIV infection, we hypothesized that AFB_1 promotes SIV replication. In this study, multiple cell lines and mouse models were established to assess the involvement of AFB_1 in SIV replication *in vitro* and *in vivo* and to elucidate the underlying mechanism of such involvement.

MATERIALS AND METHODS

Ethics Statement

This research protocol was approved by the Ethics Committee for Animal Experimentation of Nanjing Agricultural University (approval number: SYXK-SU-2011-0036). All animal care and use procedures were conducted in strict accordance with the Animal Research Committee guidelines of the College of Veterinary Medicine at Nanjing Agricultural University, and all efforts were made to minimize animal suffering and to reduce the number of animals used.

Reagents

AFB_1 (1 mg/mL; Sigma-Aldrich, USA), BAY 11-7082 (10 mM; MCE, USA) and TAK-242 (50 mM; ApexBio, USA) were dissolved in dimethyl sulfoxide (DMSO), packaged, and stored frozen at −20°C until use. For *in vitro* studies, the dissolved AFB_1 was diluted with serum-free medium, and equal concentrations of DMSO were used in the vehicle and in the control solution. For *in vivo* studies, the dissolved AFB_1 was diluted in fresh sterile endotoxin-free saline daily, and the solution was then injected intraperitoneally (i.p.) at concentrations of 10, 20, and 40 μg/kg b.w.; diluted TAK-242 was also prepared daily and then injected i.p. (3 mg/kg b.w.) 1 h prior to other treatments as previously described (16, 17, 21).

Cell Culture

Madin-Darby canine kidney (MDCK, NBL-2) cells, human lung cancer cells (A549) and porcine alveolar macrophages (PAMs, 3D4/21) that were free of any respiratory or systemic diseases were purchased from the China Institute of Veterinary Drug Control (Beijing, China). MDCK and A549 cells were grown in Dulbecco's modified Eagle's medium (Gibco, USA) containing 10% fetal calf serum (FCS; Gibco, USA) and 1% penicillin-streptomycin (Solarbio, China) at 37°C in 5% CO_2. PAMs were cultured in Roswell Park Memorial Institute-1640 medium (Gibco, USA) supplemented with 10% FCS, 1% penicillin-streptomycin and 1% nonessential amino acids (Gibco, USA) at 37°C in 5% CO_2. Cells and serum and culture medium were tested for mycoplasma using MycoTestTM kit (Seebio, China). During viral infection, all cell lines were transferred to serum-free medium supplemented with 1 μg/ml tolylsulfonyl phenylalanyl chloromethyl ketone (TPCK)-treated trypsin (Sigma, USA).

Cell Viability Determination by MTT and LDH Assays

MDCK cells, A549 cells and PAMs were cultured in 96-well plates for 24 h and were then exposed to various concentrations of AFB_1 or to 1 μg/ml DMSO for an additional 24 h before being subjected to colorimetric 3-(4,5-dimethylthiazol-2-yl)-2,5-diphenyltetrazolium bromide (MTT) assay. Subsequently, the absorbance was measured at 490 nm with a reference wavelength of 655 nm, and all experiments were performed in triplicate.

Lactate dehydrogenase (LDH) release was also measured using commercially available kits to assess cell viability. Briefly, cells were seeded in 96-well plates and exposed to various concentrations of AFB_1 or to 1 μg/ml DMSO. After 24 h of incubation, the supernatant was collected for the measurement of LDH release according to the manufacturer's protocol (Jiancheng, China). The absorbance was measured at a wavelength of 450 nm, and all samples were measured in triplicate.

Apoptosis Assay by DAPI Staining

4′,6-diamidino-2-phenylindole (DAPI) staining was performed as described previously (22) with a minor modification. Briefly, PAMs were seeded on coverslips (WHB, China) into 12-well culture plates and incubated with AFB_1 and DMSO for 24 h. Next, the PAMs were washed three times with PBS and fixed with 4% paraformaldehyde for 20 min at 4°C. After three washes, cell nuclei were counterstained with DAPI (Beyotime, China) for 5 min in the dark. Finally, the stained PAMs were washed three times and examined by fluorescence microscopy (Nikon Ti-S, Japan).

Viral Titration by $TCID_{50}$

Influenza virus strain A/swine/Guangxi/18/2011 (H1N1) was kindly provided by Dr. Weiye Chen, Harbin Veterinary Research Institute, Chinese Academy of Agricultural Sciences (Harbin, China). The virus was propagated in MDCK cells, and the supernatant was harvested at 72 h post infection (hpi) to ensure that enough virus was obtained. The viral titers were determined by the 50% tissue culture infectious doses ($TCID_{50}$) in MDCK cells, A549 cells and PAMs. Briefly, the MDCK cells, A549 cells and PAMs were seeded in a 96-well plate (Corning, USA) for 24 h, infected with 10-fold serial dilutions of virus in serum-free medium supplemented with 1 μg/ml TPCK-treated trypsin and then exposed to various concentrations of AFB_1. The cytopathic effect induced by the virus was observed and recorded after 24 hpi to calculate the virus titers by the method of Reed and Muench. A biosafety level 2 facility was used for all the experiments with the H1N1 virus.

Animals and Study Design

Male TLR4 knockout (C57BL/10ScNJNju, $TLR4^{-/-}$) and wild-type (C57BL/10JNju, WT) mice, 6–8 weeks old and weighing 18–20 g, were purchased from Nanjing University (Nanjing, China). $TLR4^{-/-}$ mice do not express functional TLR4 or TLR4 mRNA because of the TLR4 lps-del mutation. All mice were housed in a specific pathogen-free environment (22 ± 2°C) with a 12 h light/dark cycle. Water and food were available *ad libitum* throughout the whole study. All mice were acclimatized for 1 week before the onset of experiments. Body weight changes and illnesses were monitored daily.

For the first randomized trial, WT mice were randomly divided into 6 groups (each group included 3 replicates, with 4 mice per replicate): 4 groups were challenged intranasally with a nonlethal dose of H1N1 virus (1000 $TCID_{50}$) (23) prior to treatment with AFB_1 on d 1, d 7, and d 14 as described previously (24, 25), and the other two groups were given equivalent amounts of PBS intranasally. Among the 4 infected groups, three groups were given 10, 20, and 40 μg/kg b.w. AFB_1 i.p. daily for 15 days, and the fourth group was given an equivalent amount of PBS i.p. Likewise, two uninfected groups were injected with equivalent amounts of PBS or AFB_1 (40 μg/kg).

For the second randomized trial, WT mice were randomly divided into 2 groups (each group included 3 replicates, with 3 mice per replicate): the first group was given 3 mg/kg of TAK242 i.p.1 h prior to the other treatments, and the other group was given an equivalent amounts of PBS i.p.

For the third randomized trial, $TLR4^{-/-}$ and WT mice were likewise divided into 2 groups (each group included 3 replicates, with 3 mice per replicate).

All mice from the second and third randomized trials were treated with equivalent amounts of H1N1 virus and 40 μg/kg of AFB_1 as described for the first randomized trial.

Histopathological Examination and Immunohistochemical Staining

At the end of the experiments, mice were euthanized. Lung and spleen tissues were taken from each mouse. Approximately 75% of the lung tissue was stored at −80°C for the subsequent experiments, and the other 25% of the lung tissue was fixed in 4% formaldehyde for hematoxylin-eosin staining (H&E) according to standard protocols as described previously (26, 27) with some modifications. Briefly, lung tissue was fixed in 10-fold volume of 4% formaldehyde for 48 h. Next, samples were embedded in paraffin and cut into 4-μm-thick sections. One section from each tissue sample was stained with H&E.

For immunohistochemical staining, spleen tissues were incubated with a monoclonal antibody for TLR4 (Abcam, UK) and then incubated with an appropriate horseradish peroxidase (HRP)-conjugated secondary antibody. Subsequently, the HRP conjugates were visualized using a diaminobenzidine solution. Images were captured with a Pannoramic viewer (Pannoramic MIDI, 3D HISTECH), and data were analyzed using DensitoQuant software (QuantCenter, 3DHISTECH). A histochemistry score (H-score) was calculated according to a previously reported equation (28, 29).

Fluorescent Quantitative Real-Time PCR (qRT-PCR) Analysis

Cells and lung and spleen tissues were collected to determine the relative mRNA expression levels of viral matrix (M) protein, TLRs, TNF-α and IL-10. Primers for the reference genes and target genes (**Table 1**) were designed and synthesized by Invitrogen based on known sequences. Briefly, total RNA was first extracted from tissues and cells using an RNAiso Plus kit (TaKaRa, Japan). First-strand cDNA was synthesized using a reverse transcription kit (TaKaRa, Japan). Subsequently, the samples of cDNA were subjected to qRT-PCR (TaKaRa, Japan) using specific primers with a no-cDNA template as a calibrator. The relative expression levels of the target genes were calculated by the $2^{-\Delta\Delta CT}$ method with 18S or GAPDH as an endogenous reference gene.

Western Blot Analysis

Cells and lung and spleen tissues were collected for western blotting analysis to assess the relative expression levels of viral nucleoprotein (NP), phosphorylated NFκB p65 (pp65) and TLR4. Briefly, total protein was extracted, and the protein concentration was measured with a BCA kit (Beyotime, China). The proteins were denatured, subjected to 10–15% of sodium dodecyl sulfate-polyacrylamide gel electrophoresis and then transferred to polyvinylidene difluoride membranes (Bio-Rad, USA). Next, the membranes were blocked for 2 h at room temperature (RT) in 5% bovine serum albumin (BSA) in Tris-buffered saline containing

TABLE 1 | Primers sequences for real-time PCR.

Source	Gene	Forward (5′-3′)	Reverse (3′-5′)
Virus	*M*	GGGAAGAACACCGATCTTGA	CTCCGTTCCCATTAAGAGCA
Pig	*TLR1*	GAAACTACAAGGGCAGCTGG	GGGAAACTGAACACCTCCCT
	TLR2	AGACGCTGGAGGTGTTGG	AACGAAGCATCTGGGAGT
	TLR3	AAAACCAGCAACACGACT	TTGGAAAGCCCATAAAGA
	TLR4	AGAATGAGGACTGGGTGA	TGTAGTGAAGGCAGAGGT
	TLR5	GGCTCAACCAAACCAACG	GGGTGATGACGAGGAATAG
	TLR6	AACTCACCAGAGGTCCAA	TCTTCCCTGTCGATTCTC
	TLR7	GGCAAGTAGAGGACAT	GGTAGACCCTGAACAT
	TLR8	CGGCACCAGAAGAACG	GGCAGGTCAGGAGCAA
	TLR9	GGCCTTCAGCTTCACCTTGG	GGTCAGCGGCACAAACTGAG
	TLR10	ATGATTCGGCCTGGGTAAAG	TTGCCAGGATCAGAGTTTCC
	IL-10	CTGCCTCCCACTTTCTCTTG	TCAAAGGGGCTCCCTAGTTT
Mouse	*TNF-α*	GACTCAGATCATCGTCTC	GGAGTAGATGAGGTACAG
	GAPDH	CCACCCAGAAGACTGTGGAT	AAGCAGGGATGATGTTCTGG
	TLR4	CACTGTTCTTCTCCTGCCTGAC	CCTGGGGAAAAACTCTGGATA
	18S	TTGACGGAAGGGCACCACCAG	GCACCACCACCCACGGAATCG

M, influenza A virus matrix protein; TLR, toll-like receptor; IL-10, interleukin 10; TNF-α, tumor necrosis factor-α; GAPDH, glyceraldehyde-phosphate dehydrogenase.

0.1% Tween 20 (TBST), incubated overnight at 4°C with specific primary antibodies from (anti-NP, ab128193; anti-TLR4, ab13556; anti-pp65, ab76302 or anti-actin, ab14128; Abcam, UK), and then incubated for 1 h at RT with appropriate secondary antibodies (horseradish peroxidase-labeled anti-mouse or anti-rabbit secondary antibodies; Cell Signaling Technology, USA). Finally, the bound antibodies were visualized using an enhanced chemiluminescence kit (Beyotime, China).

Determinations of TNF-α and IL-10 by ELISA

Whole blood from mice was collected from the retro-orbital plexus in heparinized tubes by a trained individual and was allowed to clot at RT. Sera were separated by centrifugation and stored at −80°C until analysis. The contents of TNF-α and IL-10 in sera were measured using ELISA kits (Jiancheng, China) according to the manufacturer's instructions.

Short Interfering RNA (siRNA) Transfection

A pig TLR4-specific siRNA sequence, 5′-GGAUUUAUCCAGAUGUGAATT-3′, and a control siRNA sequence were obtained from a paper published by our coauthor (18). qRT-PCR was performed to determine the interfering efficiency of siTLR4. The siRNA experiment was carried out as our coauthor described previously (4). Briefly, PAMs were seeded in 12-well plates and were transfected for 6 h with X-tremeGENE siRNA transfection reagent (Roche, USA), siTLR4 and negative control siTLR4 diluted in medium according to the manufacturer's protocol, when the cells had reached approximately 70–80% confluence. Next, PAMs were infected with H1N1 virus and exposed to AFB_1 for an additional 24 h for further experiments.

Statistical Analysis

Statistical analysis was conducted using Prism 6 (GraphPad Software, La Jolla, CA). Data are presented as the means ± SEM. Unpaired two-tailed Student's *t*-tests were performed to evaluate statistical significance for two-group comparisons, and ordinary one-way (nonparametric) ANOVA with Tukey's posttests and two-way ANOVA with Dunnett's posttests were performed to evaluate statistical significance for multigroup comparisons. A value of $P < 0.05$ was considered significant, and $P < 0.01$ was considered strongly significant.

RESULTS

The Cytotoxic Effects of Various Concentrations of AFB_1 on MDCK Cells, A549 Cells and PAMs

To remove the effects of AFB_1-induced cytotoxicity on viral replication, the effects of various concentrations of AFB_1 on cell viability were determined by MTT and LDH assays. As shown in **Figures S1A–C**, the viability of MDCK cells, A549 cells and PAMs decreased significantly when the AFB_1 concentrations were greater than 0.5, 0.5, and 0.1 μg/ml, respectively. Correspondingly, LDH assay showed that LDH release increased markedly in MDCK cells, A549 cells, and PAMs when the AFB_1 concentrations were greater than 0.5, 0.5, and 0.1 μg/ml, respectively (**Figures S1D–F**). Afterwards, DAPI staining was performed to determine the extent of apoptosis and thus to further assess the cytotoxicity of AFB_1 on PAMs. As shown in **Figure S1G**, apoptosis began to occur when the AFB_1 concentration reached 0.1 μg/ml and was identified by the condensation and fragmentation of nuclei. In addition, given that AFB_1 was dissolved in DMSO, the effects of DMSO on MDCK cells, A549 cells and PAMs were also measured, and no significant differences were observed between the DMSO (1 μg/ml) group and either of the control groups (no DMSO and no AFB_1). Taken together, these results suggest that AFB_1 at concentrations between 0.01 and 0.25 μg/ml, 0.01 and 0.25 μg/ml, and 0.01 and 0.05 μg/ml are not toxic to MDCK cells, A549 cells and PAMs, respectively. Thus, for subsequent experiments, AFB_1 was used at concentrations of 0.01, 0.05, and 0.25 μg/ml in both MDCK and A549 cells and at concentrations of 0.01, 0.025, and 0.05 μg/ml in PAMs.

AFB_1 Promotes SIV Replication in MDCK Cells, A549 Cells and PAMs

To investigate the potential role AFB_1 plays in SIV replication, viral titers, viral M mRNA expression levels and NP expression levels were measured by $TCID_{50}$, qRT-PCR and western blotting, respectively, as described previously (30). All cells were infected with SIV and then treated with various concentrations of AFB_1 for 24 h. As shown in **Figure 1**, viral titers, M mRNA expression levels and NP levels were significantly increased in SIV-infected MDCK (**Figures 1A,D,G**) and A549 cells (**Figures 1B,E,G**) treated with 0.01–0.25 μg/ml AFB_1 compared with levels in cells without AFB_1 treatment. Correspondingly, viral titers, M mRNA expression levels and NP levels were also markedly increased

in SIV-infected PAMs (**Figures 1C,F,G**) treated with 0.025–0.05 μg/ml AFB_1 compared with levels in non-AFB_1-treated PAMs. To confirm that the increase in SIV replication induced by AFB_1 was not due to the presence of DMSO, we compared viral M mRNA expression of the three cell lines exposed to DMSO to that of the three cell lines exposed to medium and demonstrated that viral M mRNA expression in the three DMSO-exposed cell lines was identical to that in the cell lines exposed to medium alone (data not shown). Taken together, our results suggest that AFB_1 exposure promotes SIV replication *in vitro*.

AFB_1 Upregulates TLR4-NFκB Signaling and Promotes Inflammatory Responses in SIV-Infected PAMs

TLRs are a main family of pattern recognition receptors with a critical role in the activation of innate immune responses, but it has been proven that the overexpression or continuous activation of TLR4 can lead to excessive inflammatory responses or to injury in the body (16–18). To determine whether the promotion of SIV replication by AFB_1 is associated with TLRs-induced innate immune responses or injury, the expression levels of TLRs 1-10 in SIV-infected PAMs were investigated. As shown in (**Figure 2A**), the relative expression of TLR4 mRNA was significantly elevated following exposure to 0.025–0.05 μg/ml AFB_1 compared with the expression in the control group. This finding was confirmed by the marked increases in TLR4 protein levels (**Figure 2B**). TLR4 induces NFκB activation (15), and a previous study indicated that NFκB signaling involves pathogen- or cytokine-induced immune and inflammatory responses (31). To further confirm whether TLR4-NFκB was activated, the levels of pp65 were also determined. The results showed that 0.025–0.05 μg/ml AFB_1 significantly increased the relative protein levels of pp65 (**Figure 2C**). The inflammatory response was quantified based on the expressions of the TNF-α and IL-10 genes, and the results indicated that 0.025–0.05 μg/ml AFB_1 significantly increased the relative TNF-α mRNA level but decreased the relative IL-10 mRNA level (**Figures 2D,E**). Taken together, our results

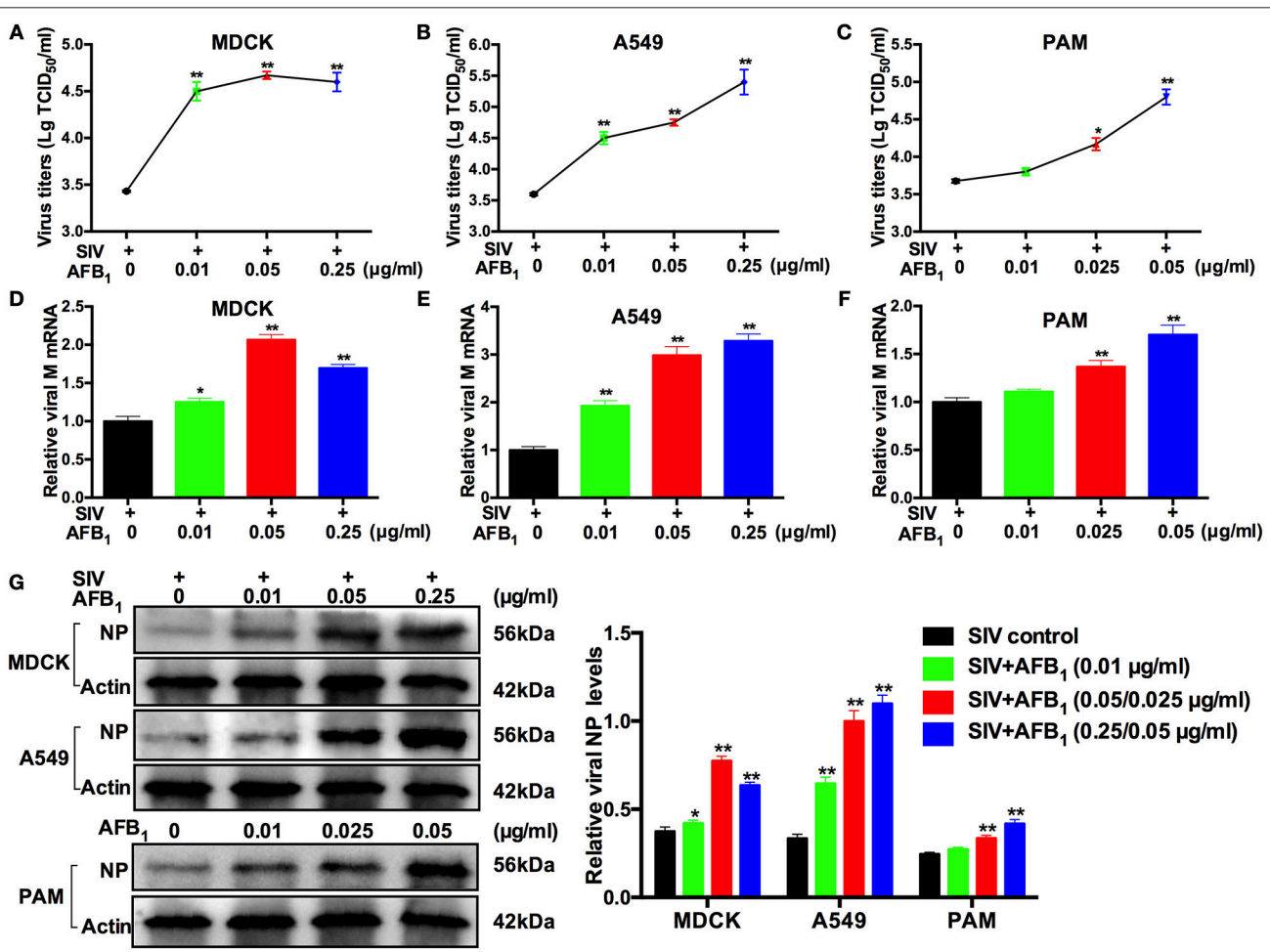

FIGURE 1 | AFB_1 promotes swine influenza virus (SIV) replication in multiple cell lines. Cells were infected with SIV (MOI = 1), and then incubated with various concentrations of AFB_1 for 24 h. **(A–C)** Viral titers. Infectious virus particles were quantified by $TCID_{50}$. **(D–F)** Viral M protein mRNA and **(G)** nucleoprotein (NP) levels were analyzed by qRT-PCR and western blotting, respectively. Data are presented as the means ± SEM of three independent experiments. Significance compared with the SIV control group, $^*P < 0.05$ and $^{**}P < 0.01$.

demonstrated that AFB_1 upregulated TLR4-NFκB signaling and promoted inflammatory responses in the SIV-infected PAMs.

TLR4 Knockdown and BAY 11-7082 Administration Block the AFB_1-Promoted SIV Replication and Inflammatory Responses in SIV-Infected PAMs

To further investigate the mechanism of SIV promotion by AFB_1, a TLR4-specific siRNA sequence was used to remove the effects of TLR4, and a control siRNA sequence was used as a negative control. The interfering efficiency of siTLR4 was determined by qRT-PCR. As shown in (**Figure 3A**), TLR4 knockdown significantly decreased TLR4 mRNA expression by >70% compared with the expression in the blank; no significant difference in TLR4 mRNA expression was observed between the blank and siControl groups. In addition, our results demonstrated that 0.05 μg/ml AFB_1 significantly elevated viral titers (**Figure 3B**), M mRNA expression (**Figure 3C**) and NP levels (**Figure 3D**) in SIV-infected PAMs compared to the corresponding parameters in control cells without AFB_1. In contrast, TLR4 knockdown significantly reduced AFB_1-promoted SIV replication, as indicated by lower viral titers, M mRNA expression and NP levels in the TLR4 knockdown group than in the siControl group; no significant difference in SIV replication was observed between the TLR4 knockdown and control groups (**Figures 3B–D**). These findings indicated that TLR4 knockdown blocked the promotion of SIV replication induced by AFB_1. Likewise, TLR4 knockdown significantly reduced pp65 protein and TNF-α mRNA levels compared with the levels in the siControl group and even compared with the levels in the control group (**Figures 3E,F**), suggesting that TLR4 knockdown drastically counteracted the AFB_1-promoted inflammatory responses in the SIV-infected PAMs.

Furthermore, our previous study indicated that BAY 11-7082 (10 μM), a specific inhibitor of NFκB, significantly reduces pp65 in PAMs and does not have cytotoxicity in PAMs (32). In the present study, BAY 11-7082 was used to further confirm the mechanism of SIV promotion by AFB_1. The results showed that compared with medium alone, BAY 11-7082 significantly reduced the elevations in viral titers (**Figure 3G**), M mRNA levels (**Figure 3H**), and TNF-α mRNA levels (**Figure 3I**) promoted by AFB_1 in SIV-infected PAMs, and no significant differences in the above parameters were observed between the BAY 11-7082 group and the control groups. Taken together, the results indicated that TLR4 knockdown and BAY 11-7082 blocked the AFB_1-promoted SIV replication and inflammatory responses.

AFB_1 Promotes SIV Replication and Lung Damage Induced by SIV in Mice

To further verify the *in vitro* results, lung tissues were taken from SIV-infected mice exposed to AFB_1 to assess viral replication

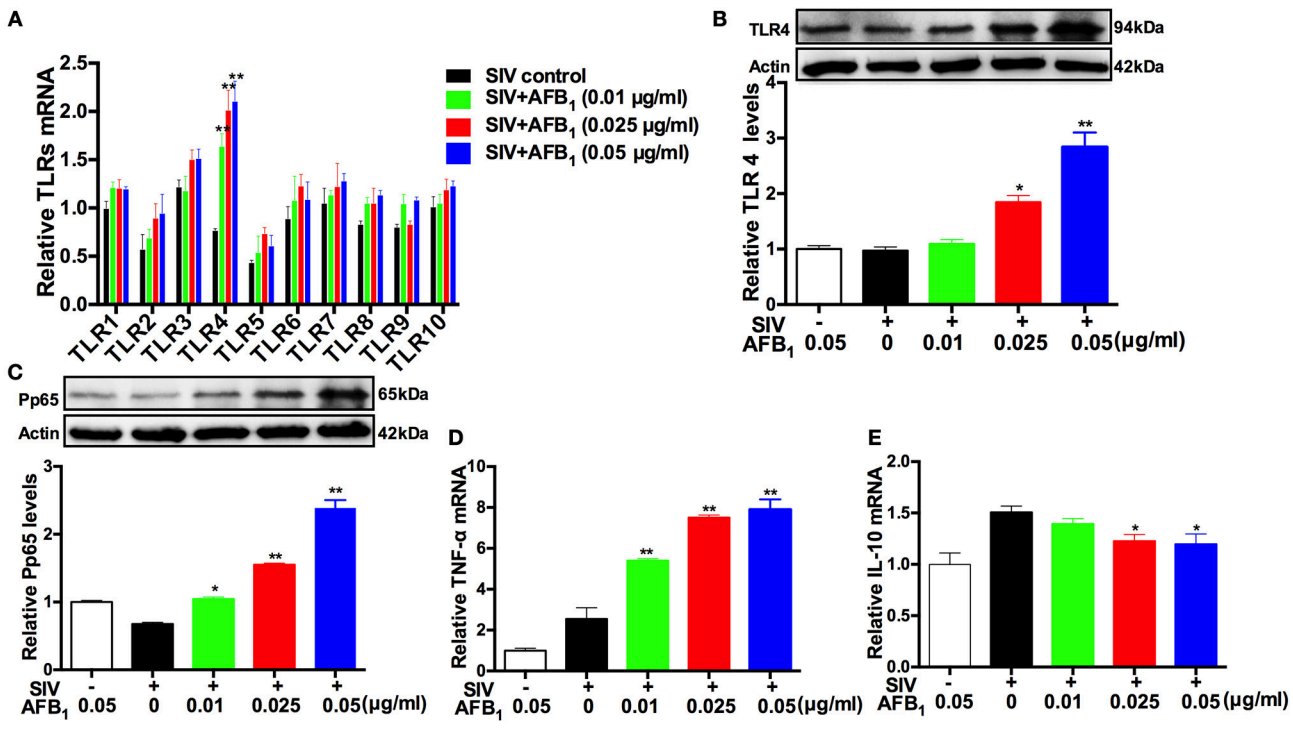

FIGURE 2 | AFB_1 upregulates TLR4-NFκB signaling and promotes inflammatory responses in SIV-infected PAMs. PAMs were incubated with or without SIV (MOI = 1), and then, the SIV-infected PAMs were incubated with various concentrations of AFB_1 for 24 h. **(A)** Relative TLRs mRNA, **(B)** TLR4 protein, **(C)** phosphorylated NF-κB p65 (pp65), **(D)** TNF-α mRNA levels and **(E)** IL-10 mRNA levels. Data are presented as the means ± SEM of three independent experiments. Significance compared with the SIV control group, $^*P < 0.05$ and $^{**}P < 0.01$.

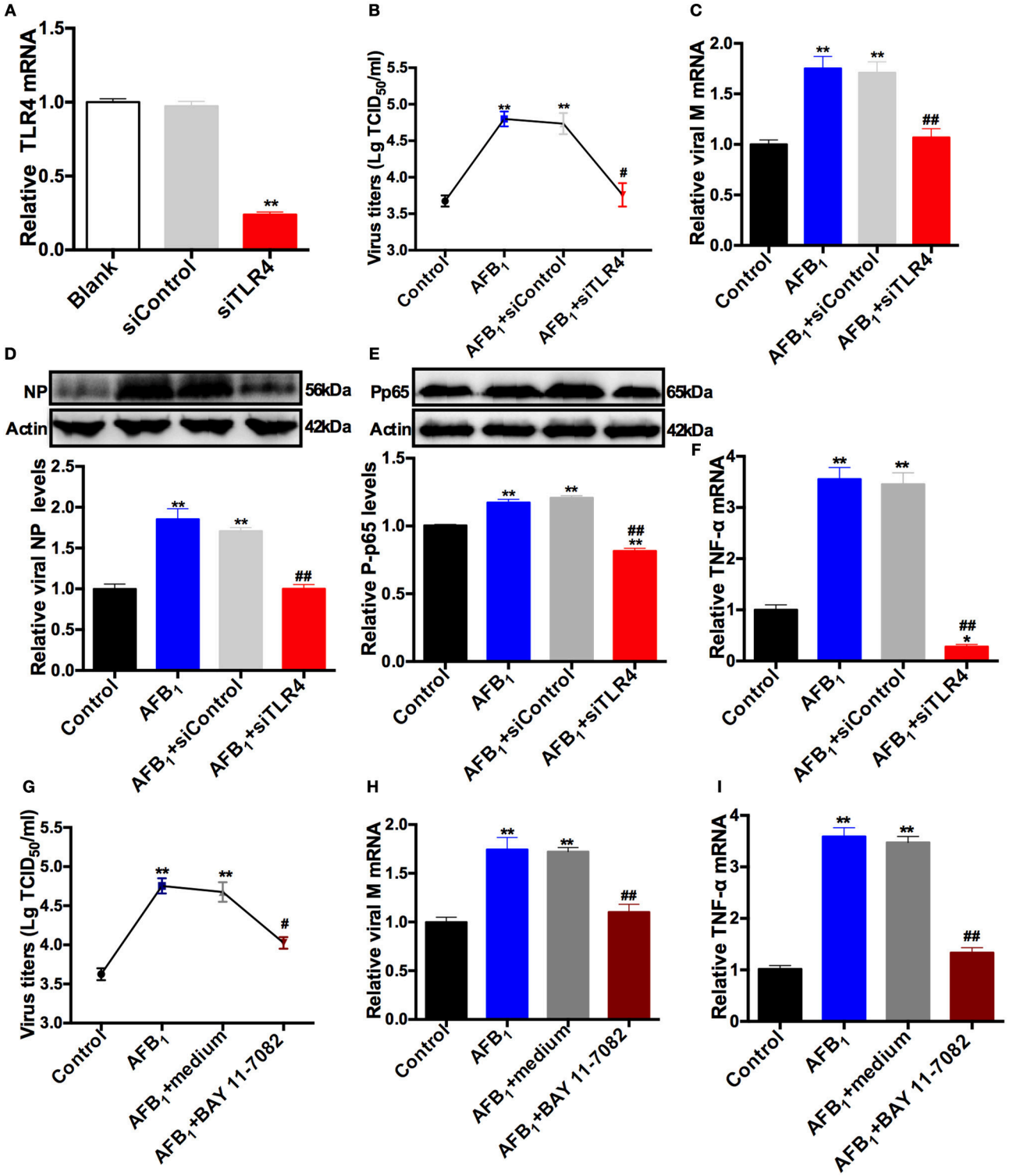

FIGURE 3 | TLR4 knockdown and BAY 11-7082 reduce the AFB_1-promoted SIV replication and inflammatory responses. PAMs were infected with SIV (MOI = 1) and then treated with (AFB_1 group) or without (control group) 0.05 μg/ml AFB_1. A TLR4-specific siRNA sequence was used to remove the effects of TLR4, and a control siRNA sequence was used as a negative control. **(A)** The knockdown efficiency of TLR4 siRNA in PAMs. **(B)** Viral titers and **(C)** relative viral M mRNA levels, **(D)** NP, **(E)** pp65 and **(F)** TNF-α mRNA levels. A specific inhibitor of NFκB, BAY 11-7082 (10 μM), was added to remove the effects of NFκB, and medium was used as a negative control. **(G)** Viral titers, **(H)** relative viral M mRNA levels, and **(I)** TNF-α mRNA levels. Data are presented as the means ± SEM of three independent experiments. Significance compared with the control group, $^{*}P < 0.05$, $^{**}P < 0.01$; significance compared with the negative control group, $^{\#}P < 0.05$ and $^{\#\#}P < 0.01$.

as indicated by viral titers (**Figure 4A**), M mRNA levels (**Figure 4B**) and NP levels (**Figure 4C**). As expected, AFB_1 at doses of 10–40 μg/kg markedly increased viral titers, M mRNA levels and NP levels in lungs of SIV-infected mice compared with the levels in lungs of mice without AFB_1. To further assess the impact of AFB_1 on viral replication, weight gain (**Figure 4D**), the lung index (**Figure 4E**) and histological damage (**Figures 4F,G**) were determined. As expected, SIV-infected mice exhibited decreased weight gain, but enhanced the lung index and inflammatory cell infiltration compared with mice from the blank group, and these changes were aggravated following exposure to 10–40 μg/kg AFB_1. In addition, 40 μg/kg AFB_1 had no effects on these parameters in mice from the blank group (**Figures 4D-G**). Taken together, our data suggest that AFB_1 promotes SIV replication and SIV-induced lung damage in mice.

AFB_1 Promotes TLR4 Expression and the Inflammatory Response in SIV-Infected Mice

To further verify the *in vitro* results, spleen tissues were taken from SIV-infected mice exposed to AFB_1 to assess TLR4 expressions as indicated by TLR4 protein and mRNA levels. The immunohistochemical assay demonstrated that AFB_1 at doses of 10–40 μg/kg significantly increased TLR4 expression

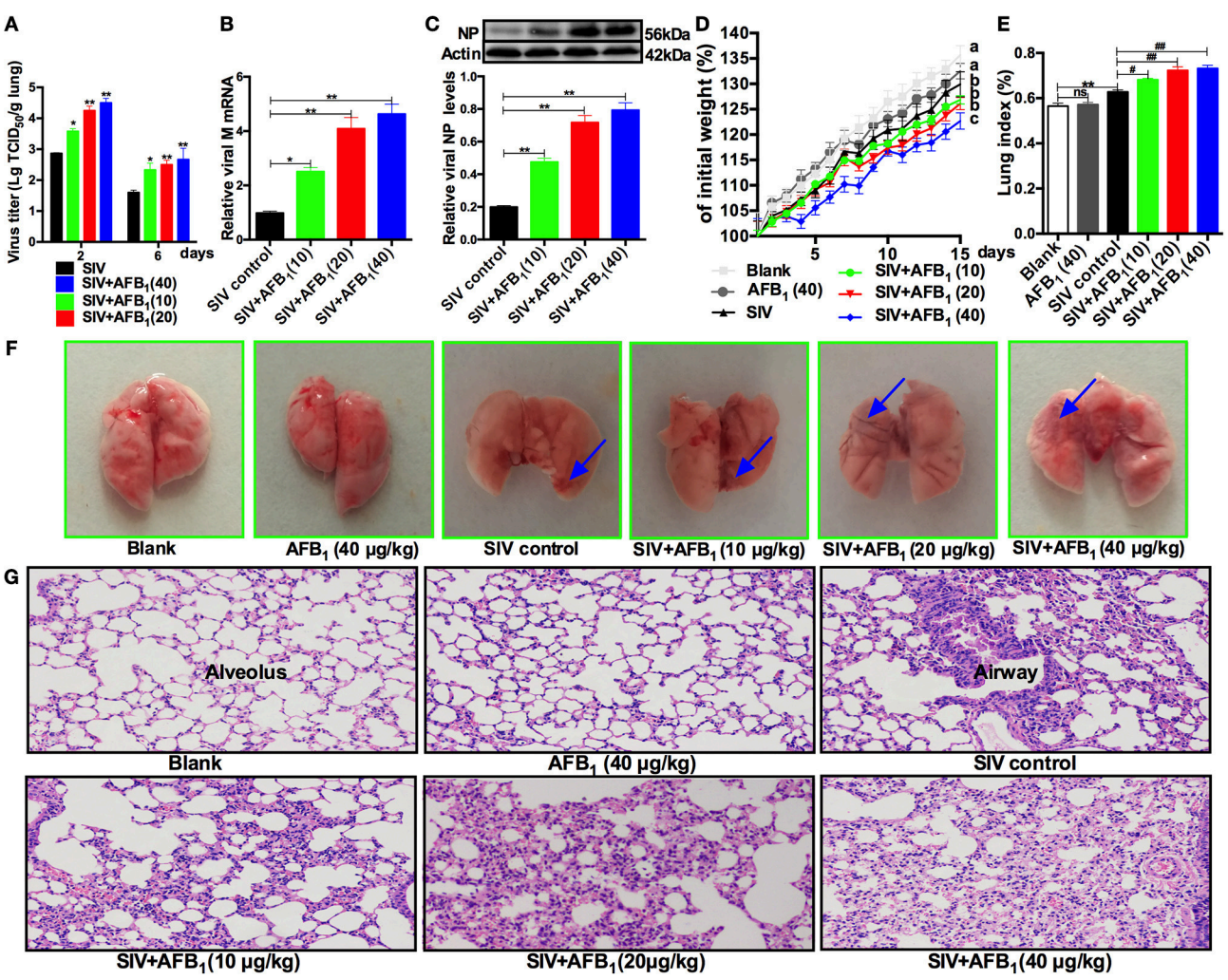

FIGURE 4 | AFB_1 promotes SIV replication and lung damage in mice. Anesthetized mice were infected intranasally with 1000 $TCID_{50}$ of SIV or PBS on d 1, d 7, and d 14; injected intraperitoneally with various concentrations of AFB_1 daily; and sacrificed at 15 days post infection (dpi). **(A)** Viral titers in the lung homogenates were determined by $TCID_{50}$ on MDCK cells at 2 and 6 dpi. Data are shown as mean log_{10} $TCID_{50}$ per gram of lung for three mice per group. The lung tissues were harvested at 15 dpi to assess viral replication as measured by **(B)** viral M mRNA and **(C)** NP levels. **(D)** Comparison of weight change expressed as a percentage of starting weight. **(E)** The lung index was calculated as the ratio of lung weight and body weight. **(F)** Representative images taken from nine mice in six groups as indicated. The areas of hemorrhage are denoted with the blue arrows. **(G)** Pathological changes in lungs. The mouse lungs were removed at 15 dpi, sectioned and stained with H&E for histological examination. Representative images from nine mice in each group were obtained at 200 × magnification. Data are presented as the means ± SEM of nine mice in each group; Different lowercase letters indicate significant differences ($P < 0.05$). $^{*,\#}P < 0.05$, $^{**,\#\#}P < 0.01$, ns, not significant.

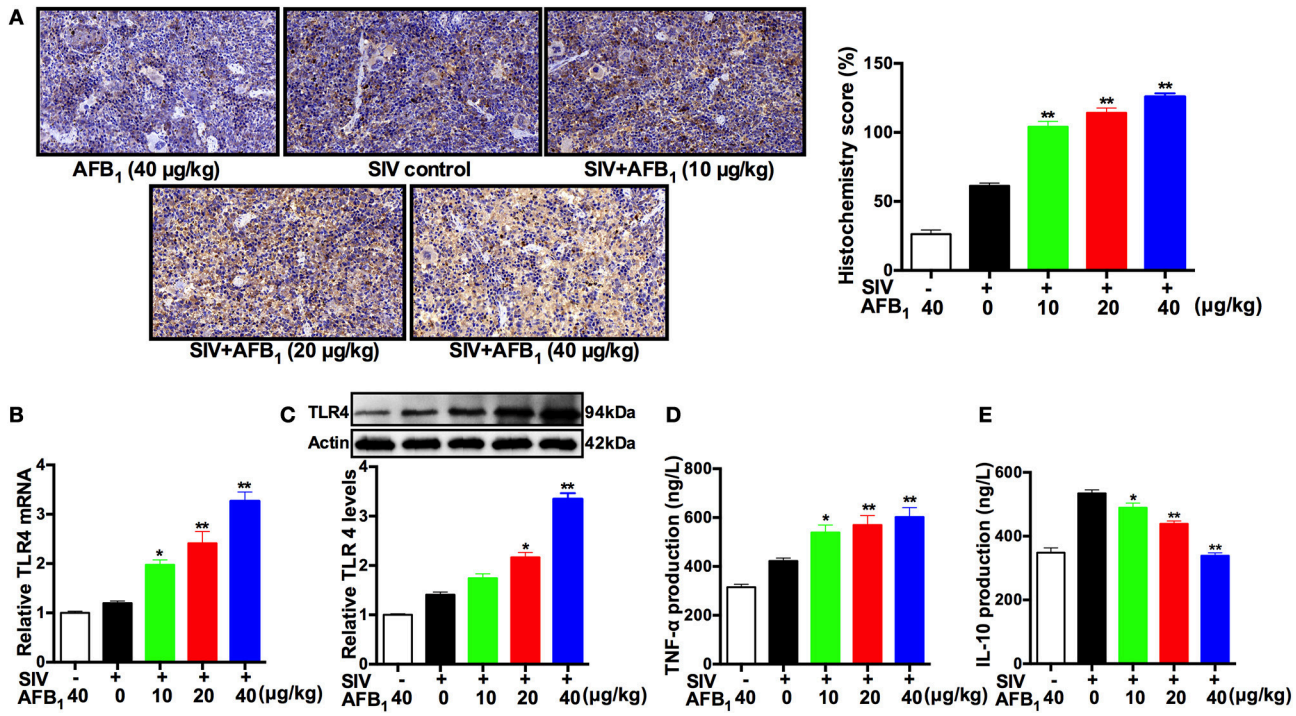

FIGURE 5 | AFB_1 promotes TLR4 expression and inflammatory responses in mice. Anesthetized mice were infected intranasally with 1000 $TCID_{50}$ of SIV or PBS at d 1, d 7, and d 14; injected intraperitoneally with various concentrations of AFB_1 daily; and sacrificed at 15 dpi. The spleen tissues were harvested at 15 dpi to assess TLR4 expression as measured by **(A)** TLR4 protein staining, **(B)** relative TLR4 mRNA levels and **(C)** TLR4 protein levels using immunohistochemistry, qRT-PCR and western blotting, respectively. **(D)** Serum TNF-α and **(E)** IL-10 levels. Representative immunohistochemistry images from nine mice in each group were obtained at 400 × magnification. Data are presented as the means ± SEM of three independent experiments. Significance compared with the SIV control group, $^*P < 0.05$ and $^{**}P < 0.01$.

(H-score) in the spleens of SIV-infected mice (**Figure 5A**). As expected, qRT-PCR and western blot assays supported the above results, demonstrating that AFB_1 at doses of 10–40 μg/kg markedly increased TLR4 mRNA (**Figure 5B**) and protein levels (**Figure 5C**) in the SIV-infected mice compared with the levels in mice without AFB_1. In addition, the inflammatory response was quantified by the release of TNF-α and IL-10, and the results showed that AFB_1 at doses of 10 to 40 μg/kg markedly increased TNF-α release but significantly decreased IL-10 release in sera (**Figures 5D,E**). Taken together, our data suggest that AFB_1 promotes TLR4 expression and the inflammatory response in SIV-infected mice.

TAK242 and TLR4 Knockout Alleviates AFB_1-Promoted SIV Replication, Inflammation and Lung Damage in SIV-Infected Mice

To determine the roles TLR4 plays in the promotion of SIV replication by AFB_1 *in vivo*, the TLR4 inhibitor, TAK242, was used to treat mice (16). The results showed that TLR4 mRNA (**Figure 6A**), viral M mRNA (**Figure 6B**) and NP levels (**Figure 6C**) were markedly reduced in the presence of TAK242 compared with the levels in the no-TAK242 group, suggesting that TLR4 activation is required for the promotion of SIV replication by AFB_1. However, no significant differences in weight gain (**Figure 6D**) or the lung index (**Figure 6E**) were observed between the TAK242 and control groups. Histological examination of lungs demonstrated that lung damage was alleviated after TAK242 administration (**Figures 6F–G**). In addition, TAK242 significantly reduced TNF-α content in sera (**Figure 6H**). Taken together, our results indicated that TAK242 alleviated AFB_1-promoted SIV replication, inflammation and lung damage in SIV-infected mice.

To further confirm the roles TLR4 plays in the promotion of SIV replication by AFB_1, $TLR4^{-/-}$ mice were used in this study. The results showed that $TLR4^{-/-}$ mice exhibited decreased TLR4 mRNA (**Figure 6I**), viral M mRNA (**Figure 6J**) and NP levels (**Figure 6K**) compared with WT mice, suggesting that TLR4 activation is indeed required for the promotion of SIV replication by AFB_1. Likewise, no significant differences in weight gain (**Figure 6L**) and the lung index (**Figure 6M**) were observed between WT and $TLR4^{-/-}$ mice. As expected, histological examination of lungs from $TLR4^{-/-}$ mice did not reveal obvious lung damage (**Figures 6N–O**). In addition, the TNF-α content in sera of $TLR4^{-/-}$ mice was lower than that in sera of WT mice (**Figure 6P**). Taken together, our results indicated that TLR4 knockout attenuated AFB_1-promoted SIV replication, inflammation and lung damage in SIV-infected mice.

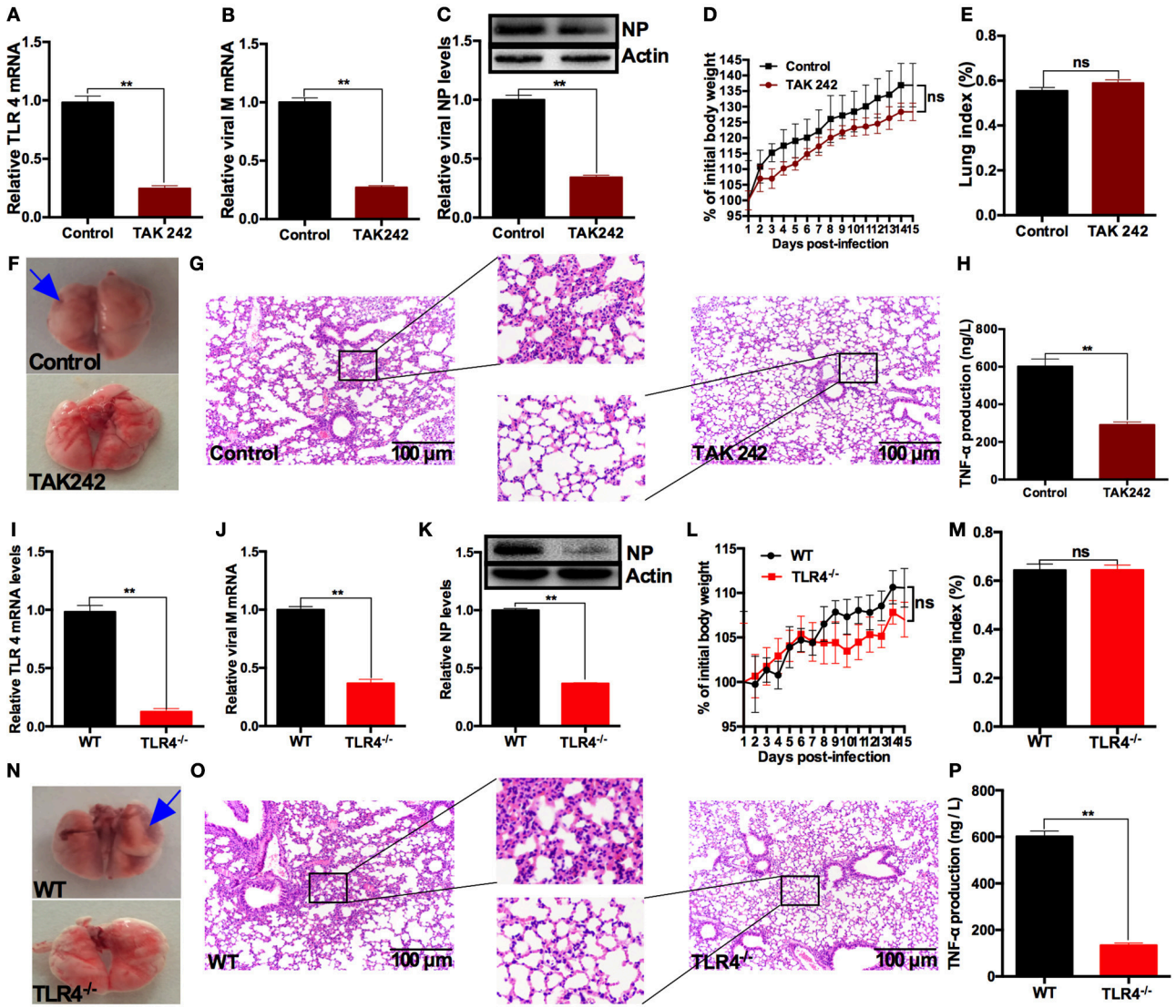

FIGURE 6 | TLR4 deficiencies alleviate AFB_1-promoted SIV replication, inflammation and lung damage in mice. Anesthetized mice were infected intranasally with 1000 $TCID_{50}$ of SIV on d 1, d 7, and d 14 and were injected intraperitoneally with 40 μg/kg AFB_1 daily. Mice from the TAK242 group were injected with 3 mg/kg TAK242 daily, and the mice from control group were given PBS. Mice were sacrificed at 15 dpi. **(A)** Relative TLR4 mRNA levels, **(B)** viral M mRNA levels, **(C)** viral NP levels, **(D)** body weight and **(E)** the lung index. **(F)** Representative images taken from mice in the control and TAK242 groups. The areas of hemorrhage are denoted with the blue arrows. **(G)** Pathological changes in lungs and **(H)** serum TNF-α in mice. $TLR4^{-/-}$ and WT mice were infected intranasally with 1000 $TCID_{50}$ of SIV on d 1, d 7, and d 14; injected intraperitoneally with 40 μg/kg AFB_1 daily; and sacrificed at 15 dpi. **(I)** Relative TLR4 mRNA levels, **(J)** viral M mRNA levels, **(K)** viral NP levels, **(L)** body weight, and **(M)** the lung index. **(N)** Representative images taken from mice in the TLR4 knockout ($TLR4^{-/-}$) and wild-type (WT) groups. The areas of hemorrhage are denoted with the blue arrows. **(O)** Pathological changes in lungs and **(P)** serum TNF-α in $TLR4^{-/-}$ and WT mice. Data are presented as the means ± SEM. Significance compared with control/WT mice, $^{**}P < 0.01$; ns, not significant.

DISCUSSION

Swine are one of the species most sensitive to AFB_1, and the maximum tolerance level of AFB_1 for pigs is approximately 0.385 mg/kg of feed (33). On the contrary, mice are highly resistant to AFB_1 (TD_{50} > 5,400 mg/kg b.w.) (34). According to the World Health Organization, in humans, AFB_1 at concentrations of 30 to 50, 50 to 100, and 100 to 1,000 μg/kg b.w. produces mild, moderate and severe toxicity, respectively. According to the guidelines of the US Food and Drug Administration and the National Food Safety Standard (GB2761-2017, China), the maximum allowable dietary AFB_1 concentrations for humans and animals are 20 and 300 μg/kg, respectively. However, it was previously unknown whether low-dose AFB_1 could cause or exacerbate secondary diseases. Therefore, concentrations of 10, 20, and 40 μg/kg b.w. were used in this study. Our findings confirmed that 40 μg/kg AFB_1 has no effects on the weight gain and lung function

of mice, which is consistent with a previous study (34) and suggests that the promotion of SIV replication by AFB_1 is not due to AFB_1 toxicity. In addition, to remove the potential effects of AFB_1-induced cytotoxicity on SIV replication, the safe concentrations of AFB_1 were also determined by MTT and LDH assays and DAPI staining for further *in vitro* experiments.

Since the initial report in 1979 that AFB_1 decreases interferon production by the influenza virus (35), few studies have been performed to determine its effects on SIV replication. Our study shows that AFB_1 promotes SIV replication *in vivo* and *in vitro*. First, enhanced viral replication was observed in the MDCK cells, A549 cells and PAMs. Correspondingly, the *in vivo* results supported the conclusion of the *in vitro* experiments that AFB_1 promotes SIV replication in mice. In addition, SIV-infected mice exposed to AFB_1 also exhibited decreased weight gain but increased the lung index and lung damage. Our findings are consistent with the outcomes of SIV infection (36–38), suggesting that SIV infection is aggravated by AFB_1.

Toll-like receptors (TLRs), which exist in porcine alveolar macrophages and in mice, are associated with the innate immune response (14, 39). Interestingly, viruses can evade the host immune response, thereby enhancing viral replication, when TLR4 is inhibited, but TLR4 antagonists can protect mice from lethal influenza infection (20). Therefore, the role of TLRs in the AFB_1-induced promotion of viral replication was examined in our present study. Our data showed that AFB_1 upregulated TLR4, but not other TLRs, in the SIV-infected PAMs. We investigated the underlying mechanism by using TLR4 knockdown and $TLR4^{-/-}$ mice. The results showed that TLR4 knockdown and the inhibition of NFκB significantly reduced the AFB_1-promoted SIV replication and inflammatory responses in PAMs, and TLR4 deficiencies also attenuated the AFB_1-promoted SIV replication, inflammation and lung damage in mice. This may appear counterintuitive at first because the TLR4 pathway is often required for protection against influenza infection (40). Generally, TLR4 plays a critical role in the activation of innate immune responses to defend the body against pathogens. However, an increasing number of studies have shown that the overexpression and/or continuous activation of TLR4 can lead to excessive inflammatory responses or tissue damage in the body (16–18, 41). Our results are the first to suggest that AFB_1 promotes SIV replication and SIV-related lung damage by activating the TLR4-NFκB pathway. This finding is supported by previous studies demonstrating that TLR4 antagonists or TLR4 knockout can prevent lethal influenza infection (20, 42). Therefore, we infer that AFB_1 might promote TLR4 overexpression and excessive inflammatory responses and reduce tolerance (43), thereby promoting SIV replication.

Previous study indicated that the effects of proinflammatory cytokines were antagonized by anti-inflammatory cytokines such as IL-10 (43). In addition, a delicate balance between pro- and anti-inflammatory cytokine production is essential for the recovery from and defense against viral infection (44), which has roles in the maintenance of homeostasis and immunity. Accordingly, our data suggested that the inflammatory response was aggravated to defend against SIV infection, and IL-10 decreased and was not enough for the maintenance of homeostasis and immunity, thereby reducing the tolerance and increasing viral replication. On the contrary, excessive inflammatory responses can induce anti-inflammatory responses (19), and M2 macrophage polarization (anti-inflammatory macrophage phenotype) is TLR4 dependent (45). Therefore, it is likely that AFB_1 promotes SIV replication via the TLR4-dependent induction of M2 macrophage polarization, but this possibility needs to be further studied.

In conclusion, our data suggest that AFB_1 promotes SIV replication and SIV-induced lung damage by activating TLR4-NFκB signaling *in vitro* and *in vivo* or at least promotes these processes in a TLR4-dependent manner. This finding suggests a new risk of AFB_1 exposure and reveals the vital role of TLR4-induced inflammation in the promotion of SIV replication and lung damage by AFB_1, pointing to TLR4 as a potential therapeutic target for preventing lethal influenza infection.

AUTHOR CONTRIBUTIONS

YS, FG, XC, and KH designed this project. YS, JS, ZL, and DL conducted the experiments. YS, KH, and DL wrote and revised the manuscript. FG, XC, KH, and DL gave helpful advice regarding the project. All authors reviewed the manuscript.

FUNDING

This work was also supported by Jiangsu Agricultural science and technology independent innovation foundation of China (CX (15) 1067).

ACKNOWLEDGMENTS

We thank Weiye Chen from the Harbin Veterinary Research Institute, Chinese Academy of Agricultural Sciences (Harbin, China), for kindly providing the H1N1 virus. This work was supported by the National Natural Science Foundation of China (Nos. 31472253 and 31772811).

SUPPLEMENTARY MATERIAL

The Supplementary Material for this article can be found online at: https://www.frontiersin.org/articles/10.3389/fimmu.2018.02297/full#supplementary-material

Figure S1 | Effects of various concentrations of AFB_1 on cells. Cells were exposed to various concentrations of AFB_1 for 24 h, and then subjected to **(A–C)** MTT, **(D–F)** LDH, and **(G)** DAPI staining assays for the detection of cell viability. A DMSO group was included to remove the effects of DMSO on cell viability, as the AFB_1 was dissolved in DMSO. Cells without any AFB_1 and DMSO were used as the control group. Cell nuclei were counterstained with DAPI to assess apoptosis, and the apoptotic cells were identified by the condensation and fragmentation of nuclei (yellow arrows). Data are presented as the means ± SEM of three independent experiments. Significance compared with the control group, $^{*}P < 0.05$ and $^{**}P < 0.01$.

REFERENCES

1. Vijaykrishna D, Smith GJ, Pybus OG, Zhu H, Bhatt S, Poon LL, et al. Long-term evolution and transmission dynamics of swine influenza A virus. *Nature* (2011) 473:519–22. doi: 10.1038/nature10004
2. Gan F, Zhang Z, Hu Z, Hesketh J, Xue H, Chen X, et al. Ochratoxin A promotes porcine circovirus type 2 replication *in vitro* and *in vivo*. *Free Radical Bio Med.* (2015) 80:33–47. doi: 10.1016/j.freeradbiomed.2014.12.016
3. Jolly PE. Aflatoxin: does it contribute to an increase in HIV viral load? *Future Microbiol.* (2014) 9:121–4. doi: 10.2217/fmb.13.166
4. Chen X, Ren F, Hesketh J, Shi X, Li J, Gan F, et al. Selenium blocks porcine circovirus type 2 replication promotion induced by oxidative stress by improving GPx1 expression. *Free Radical Bio Med.* (2012) 53:395–405. doi: 10.1016/j.freeradbiomed.2012.04.035
5. Steinbrenner H, Al-Quraishy S, Dkhil MA, Wunderlich F, Sies H. Dietary selenium in adjuvant therapy of viral and bacterial infections. *Adv Nutr.* (2015) 6:73–82. doi: 10.3945/an.114.007575
6. Zhao X, Dai J, Xiao X, Wu L, Zeng J, Sheng J, et al. PI3K/Akt signaling pathway modulates influenza virus induced mouse alveolar macrophage polarization to M1/M2b. *PloS ONE* (2014) 9:e104506. doi: 10.1371/journal.pone.0104506
7. Battilani P, Toscano P, Van der Fels-Klerx HJ, Moretti A, Camardo Leggieri M, Brera C, et al. Aflatoxin B1 contamination in maize in Europe increases due to climate change. *Sci Rep.* (2016) 6:24328. doi: 10.1038/srep24328
8. Chen J, Wen J, Zhuang L, Zhou S. An enzyme-free catalytic DNA circuit for amplified detection of aflatoxin B1 using gold nanoparticles as colorimetric indicators. *Nanoscale* (2016) 8:9791–7. doi: 10.1039/C6NR01381C
9. Kim J, Park SH, Do KH, Kim D, Moon Y. Interference with mutagenic aflatoxin B1-induced checkpoints through antagonistic action of ochratoxin A in intestinal cancer cells: a molecular explanation on potential risk of crosstalk between carcinogens. *Oncotarget* (2016) 7:39627–39. doi: 10.18632/oncotarget.8914
10. Wang Y, Zhang Z, Wang H, Zhang Y, Ji M, Xu H, et al. miR-138-1* regulates aflatoxin B1-induced malignant transformation of BEAS-2B cells by targeting PDK1. *Arch Toxicol.* (2016) 90:1239–49. doi: 10.1007/s00204-015-1551-4
11. Qian G, Tang L, Guo X, Wang F, Massey ME, Su J, et al. Aflatoxin B1 modulates the expression of phenotypic markers and cytokines by splenic lymphocytes of male F344 rats. *J Appl Toxicol.* (2014) 34:241–9. doi: 10.1002/jat.2866
12. Miller DM, Stuart BP, Crowell WA, Cole JR Jr, Goven AJ, Brown J. Aflatoxicosis in swine: its effect on immunity and relationship to salmonellosis. *Proc Am Assoc Vet Lab Diagnost.* 21:135–46. (1978).
13. Oswald IP, Marin DE, Bouhet S, Pinton P, Taranu I, Accensi F. Immunotoxicological risk of mycotoxins for domestic animals. *Food Addit Contam A* (2005) 22:354–60. doi: 10.1080/026520305000 58320
14. Fabris TF, Laporta J, Corra FN, Torres YM, Kirk DJ, McLean DJ, et al. Effect of nutritional immunomodulation and heat stress during the dry period on subsequent performance of cows. *J Dairy Sci.* (2017) 100:6733–42. doi: 10.3168/jds.2016-12313
15. Vaure C, Liu Y. A comparative review of toll-like receptor 4 expression and functionality in different animal species. *Front Immunol.* (2014) 5:316. doi: 10.3389/fimmu.2014.00316
16. Hua F, Tang H, Wang J, Prunty MC, Hua X, Sayeed I, et al. TAK-242, an antagonist for Toll-like receptor 4, protects against acute cerebral ischemia/reperfusion injury in mice. *J Cerebr Blood F Met.* (2015) 35:536–42. doi: 10.1038/jcbfm.2014.240
17. Sha T, Sunamoto M, Kitazaki T, Sato J, Ii M, Iizawa Y. Therapeutic effects of TAK-242, a novel selective Toll-like receptor 4 signal transduction inhibitor, in mouse endotoxin shock model. *E J Pharmacol.* (2007) 571:231–9. doi: 10.1016/j.ejphar.2007.06.027
18. Xu H, Hao S, Gan F, Wang H, Xu J, Liu D, et al. *In vitro* immune toxicity of ochratoxin A in porcine alveolar macrophages: a role for the ROS-relative TLR4/MyD88 signaling pathway. *Chemi Biol Interact.* (2017) 272(Suppl. C):107–16. doi: 10.1016/j.cbi.2017.05.016
19. Ma L, Dong F, Zaid M, Kumar A, Zha X. ABCA1 protein enhances Toll-like receptor 4 (TLR4)-stimulated interleukin-10 (IL-10) secretion through protein kinase A (PKA) activation. *J Biol Chem.* (2012) 287:40502–12. doi: 10.1074/jbc.M112.413245
20. Shirey KA, Lai W, Scott AJ, Lipsky M, Mistry P, Pletneva LM, et al. The TLR4 antagonist Eritoran protects mice from lethal influenza infection. *Nature* (2013) 497:498–502. doi: 10.1038/nature12118
21. Tramullas M, Finger BC, Moloney RD, Golubeva AV, Moloney G, Dinan TG, et al. Toll-like receptor 4 regulates chronic stress-induced visceral pain in mice. *Biol Psychiat.* (2014) 76:340–8. doi: 10.1016/j.biopsych.2013.11.004
22. Zhang Q, Liu J, Chen S, Liu J, Liu L, Liu G, et al. Caspase-12 is involved in stretch-induced apoptosis mediated endoplasmic reticulum stress. *Apoptosis* (2016) 21:432–42. doi: 10.1007/s10495-016-1217-6
23. LeMessurier KS, Lin Y, McCullers JA, Samarasinghe AE. Antimicrobial peptides alter early immune response to influenza A virus infection in C57BL/6 mice. *Antivir Res.* (2016) 133:208–17. doi: 10.1016/j.antiviral.2016.08.013
24. Ghoneim HE, Thomas PG, McCullers JA. Depletion of alveolar macrophages during influenza infection facilitates bacterial superinfections. *J Immunol.* (2013) 191:1250–9. doi: 10.4049/jimmunol.1300014
25. Huang L, Qin T, Yin Y, Gao X, Lin J, Yang Q, et al. Bacillus amyloliquefaciens SQR9 induces dendritic cell maturation and enhances the immune response against inactivated avian influenza virus. *Sci Rep.* (2016) 6:21363. doi: 10.1038/srep21363
26. Jiang P, Zhou N, Chen X, Zhao X, Li D, Wang F, et al. Integrative analysis of differentially expressed microRNAs of pulmonary alveolar macrophages from piglets during H1N1 swine influenza A virus infection. *Sci Rep.* (2015) 5:8167. doi: 10.1038/srep08167
27. Xu G, Zhang X, Sun Y, Liu Q, Sun H, Xiong X, et al. Truncation of C-terminal 20 amino acids in PA-X contributes to adaptation of swine influenza virus in pigs. *Sci Rep.* (2016) 6:21845. doi: 10.1038/srep21845
28. Yeo W, Chan SL, Mo FK, Chu CM, Hui JW, Tong JH, et al. Phase I/II study of temsirolimus for patients with unresectable Hepatocellular Carcinoma (HCC)- a correlative study to explore potential biomarkers for response. *BMC Cancer* (2015) 15:395. doi: 10.1186/s12885-015-1334-6
29. Azim HA, Peccatori FA, Brohée S, Branstetter D, Loi S, Viale G, et al. RANK-ligand (RANKL) expression in young breast cancer patients and during pregnancy. *Breast Cancer Res.* (2015) 17:24. doi: 10.1186/s13058-015-0538-7
30. Morita M, Kuba K, Ichikawa A, Nakayama M, Katahira J, Iwamoto R, et al. The lipid mediator protectin D1 inhibits influenza virus replication and improves severe influenza. *Cell* (2013) 153:112–25. doi: 10.1016/j.cell.2013.02.027
31. Song S, Bi J, Wang D, Fang L, Zhang L, Li F, et al. Porcine reproductive and respiratory syndrome virus infection activates IL-10 production through NF-kappaB and p38 MAPK pathways in porcine alveolar macrophages. *Dev Comp Immunol.* (2013) 39:265–72. doi: 10.1016/j.dci.2012.10.001
32. Hou L, Gan F, Zhou X, Zhou Y, Qian G, Liu Z, et al. Immunotoxicity of ochratoxin A and aflatoxin B1 in combination is associated with the nuclear factor kappa B signaling pathway in 3D4/21 cells. *Chemosphere* (2018) 199:718–27. doi: 10.1016/j.chemosphere.2018.02.009
33. Southern LL, Clawson AJ. Effects of aflatoxins on finishing swine. *J Anim Sci.* (1979) 49:1006–11. doi: 10.2527/jas1979.4941006x
34. Rawal S, Kim JE, Coulombe R. Aflatoxin B1 in poultry: toxicology, metabolism and prevention. *Res Vet Sci.* (2010) 89:325–31. doi: 10.1016/j.rvsc.2010.04.011
35. Hahon N, Booth JA, Stewart JD. Aflatoxin inhibition of viral interferon induction. *Antimicrob Agents Chemother.* (1979) 16:277–82. doi: 10.1128/AAC.16.3.277
36. Wang J, Li F, Wei H, Lian Z-X, Sun R, Tian Z. Respiratory influenza virus infection induces intestinal immune injury via microbiota-mediated Th17 cell–dependent inflammation. *J Exp Med.* (2014) 211:2397–410. doi: 10.1084/jem.20140625
37. Chandler JD, Hu X, Ko E-J, Park S, Lee Y-T, Orr M, et al. Metabolic pathways of lung inflammation revealed by high-resolution metabolomics (HRM) of H1N1 influenza virus infection in mice. *Am J Physiol Regul Integr Comp Physiol.* (2016) 311:R906–16. doi: 10.1152/ajpregu.00298.2016
38. Bi Y, Xie Q, Zhang S, Li Y, Xiao H, Jin T, et al. Assessment of the internal genes of influenza A (H7N9) virus contributing to high pathogenicity in mice. *J Virol.* (2015) 89:2–13. doi: 10.1128/JVI.02390-14
39. Xie SZ, Hao R, Zha XQ, Pan LH, Liu J, Luo JP. Polysaccharide of dendrobium huoshanense activates macrophages via toll-like receptor 4-mediated signaling pathways. *Carbohydr Polym.* (2016) 146:292–300. doi: 10.1016/j.carbpol.2016.03.059

40. Shinya K, Ito M, Makino A, Tanaka M, Miyake K, Eisfeld AJ, et al. The TLR4-TRIF pathway protects against H5N1 influenza virus infection. *J Virol.* (2011) 86:19–24. doi: 10.1128/JVI.06168-11
41. Chakraborty D, Zenker S, Rossaint J, Holscher A, Pohlen M, Zarbock A, et al. Alarmin S100A8 activates alveolar epithelial cells in the context of acute lung injury in a TLR4-Dependent manner. *Front Immunol.* (2017) 8:1493. doi: 10.3389/fimmu.2017.01493
42. Imai Y, Kuba K, Neely GG, Yaghubian-Malhami R, Perkmann T, van Loo G, et al. Identification of oxidative stress and toll-like receptor 4 signaling as a key pathway of acute lung injury. *Cell* (2008) 133:235–49. doi: 10.1016/j.cell.2008.02.043
43. Iwasaki A, Pillai PS. Innate immunity to influenza virus infection. *Nat Rev Immunol.* (2014) 14:315–28. doi: 10.1038/nri3665
44. Frazier WJ, Hall MW. Immunoparalysis and adverse outcomes from critical illness. *Pediat Cli N Am.* (2008) 55:647–68. doi: 10.1016/j.pcl.2008.02.009
45. Li X, Wang Z, Zou Y, Lu E, Duan J, Yang H, et al. Pretreatment with lipopolysaccharide attenuates diethylnitrosamine-caused liver injury in mice via TLR4-dependent induction of Kupffer cell M2 polarization. *Immunol Res.* (2015) 62:137–45. doi: 10.1007/s12026-015-8644-2

Conflict of Interest Statement: The authors declare that the research was conducted in the absence of any commercial or financial relationships that could be construed as a potential conflict of interest.

frontiers in Immunology

ORIGINAL RESEARCH
published: 28 September 2018
doi: 10.3389/fimmu.2018.02229

Phosphorylation of TRIM28 Enhances the Expression of IFN-β and Proinflammatory Cytokines During HPAIV Infection of Human Lung Epithelial Cells

*Tim Krischuns[1,2], Franziska Günl[1,2], Lea Henschel[1,2], Marco Binder[3], Joschka Willemsen[3], Sebastian Schloer[2,4], Ursula Rescher[2,4], Vanessa Gerlt[1,2], Gert Zimmer[5,6], Carolin Nordhoff[1,2], Stephan Ludwig[1,2] and Linda Brunotte[1,2]**

[1] Institute of Virology Muenster, Westfaelische Wilhelms-University Muenster, Muenster, Germany, [2] Cluster of Excellence "Cells in Motion", Westfaelische Wilhelms-University Muenster, Muenster, Germany, [3] Research Group "Dynamics of Early Viral Infection and the Innate Antiviral Response", Division Virus-Associated Carcinogenesis (F170), German Cancer Research Center (DKFZ), Heidelberg, Germany, [4] Center for Molecular Biology of Inflammation, Institute of Medical Biochemistry, Westfaelische Wilhelms-University Muenster, Muenster, Germany, [5] Institute of Virology and Immunology (IVI), Bern, Switzerland, [6] Department of Infectious Diseases and Pathobiology (DIP), Vetsuisse Faculty, University of Bern, Bern, Switzerland

OPEN ACCESS

Edited by:
Michael H. Lehmann,
Ludwig-Maximilians-Universität München, Germany

Reviewed by:
David Kong Ann,
City of Hope National Medical Center/Beckman Research Institute, United States
Kenrie PY Hui,
University of Hong Kong, Hong Kong

***Correspondence:**
Linda Brunotte
brunotte@uni-muenster.de

Specialty section:
This article was submitted to Cytokines and Soluble Mediators in Immunity, a section of the journal Frontiers in Immunology

Received: 31 May 2018
Accepted: 07 September 2018
Published: 28 September 2018

Citation:
Krischuns T, Günl F, Henschel L, Binder M, Willemsen J, Schloer S, Rescher U, Gerlt V, Zimmer G, Nordhoff C, Ludwig S and Brunotte L (2018) Phosphorylation of TRIM28 Enhances the Expression of IFN-β and Proinflammatory Cytokines During HPAIV Infection of Human Lung Epithelial Cells. Front. Immunol. 9:2229. doi: 10.3389/fimmu.2018.02229

Human infection with highly pathogenic avian influenza viruses (HPAIV) is often associated with severe tissue damage due to hyperinduction of interferons and proinflammatory cytokines. The reasons for this excessive cytokine expression are still incompletely understood, which has hampered the development of efficient immunomodulatory treatment options. The host protein TRIM28 associates to the promoter regions of over 13,000 genes and is recognized as a genomic corepressor and negative immune regulator. TRIM28 corepressor activity is regulated by post-translational modifications, specifically phosphorylation of S473, which modulates binding of TRIM28 to the heterochromatin-binding protein HP1. Here, we identified TRIM28 as a key immune regulator leading to increased IFN-β and proinflammatory cytokine levels during infection with HPAIV. Using influenza A virus strains of the subtype H1N1 as well as HPAIV of subtypes H7N7, H7N9, and H5N1, we could demonstrate that strain-specific phosphorylation of TRIM28 S473 is induced by a signaling cascade constituted of PKR, p38 MAPK, and MSK1 in response to RIG-I independent sensing of viral RNA. Furthermore, using chemical inhibitors as well as knockout cell lines, our results suggest that phosphorylation of S473 facilitates a functional switch leading to increased levels of IFN-β, IL-6, and IL-8. In summary, we have identified TRIM28 as a critical factor controlling excessive expression of type I IFNs as well as proinflammatory cytokines during infection with H5N1, H7N7, and H7N9 HPAIV. In addition, our data indicate a novel mechanism of PKR-mediated IFN-β expression, which could lay the ground for novel treatment options aiming at rebalancing dysregulated immune responses during severe HPAIV infection.

Keywords: influenza, TRIM28, KAP1, TIF1-beta, innate immunity, IFN-β, RIG-I, PKR

INTRODUCTION

Influenza A viruses (IAV) are the leading cause of annually recurring respiratory infections affecting millions of people worldwide. Infection by seasonal viruses is accompanied by mild to severe symptoms, such as fever, headache and dry cough but immunocompetent patients usually recover within 2–3 weeks. In contrast, infections with highly pathogenic avian influenza viruses (HPAIV), such as H5N1 often cause severe viral pneumonia as well as multiple organ failure and can lead to death, as exemplified by the "bird flu" outbreak in Hong Kong in 1997 with an overall mortality rate of 33% (1–3). Uncontrolled expression of type I and type II interferons (IFNs) and high levels of proinflammatory cytokines, such as TNF-α, IL-1ß, IL-6, und IL-8 due to a hyperinduction of the innate immune and inflammatory responses are the suspected reasons for HPAIV-induced immunopathology (reviewed in (4)). The underlying molecular mechanisms and signaling pathways, which are responsible for the increased and sustained expression of IFNs and proinflammatory cytokines during HPAIV infection are still not fully understood. However, a virus-induced imbalance of stimulatory and inhibitory factors, which normally regulate the controlled onset and resolution of immune responses, is hypothesized (5).

The innate immune response to IAV is rapidly initiated by pathogen recognition receptors (PRRs), such as RIG-I, which recognize viral RNA in the cytoplasm of infected cells and activate a signal transduction cascade involving the adaptor protein MAVS and the transcription factors IRF3/7. Upon phosphorylation, IRF3/7 dimerize and translocate into the cell nucleus where they bind to the IFN-α/β promotor and facilitate gene transcription. Alternatively, membrane associated toll-like receptors (TLRs) can detect viral glycoproteins or sense viral RNA in endosomal compartments and signal via the adaptor protein MyD88 resulting in the activation of IRF3/5/7 and subsequently in IFN-α/β expression (6, 7). Secreted IFN-α/β bind to the interferon-α/β receptor on neighboring cells resulting in STAT1/2 phosphorylation by the receptor-associated Jak/Tyk kinases (8). This mediates the nuclear translocation of STATs and upregulation of the expression of hundreds of interferon-stimulated genes (ISGs), among them antiviral proteins, chemokines and proinflammatory cytokines. This allows the recruitment and activation of immune cells at the site of infection. To resolve the ongoing immune reaction and prevent immunopathology, negative immune regulators, such as the recently identified death-associated protein kinase 1 (DAPK1) (9) and others interfere with further signal transduction and cytokine expression.

Here, we have identified the host factor and transcriptional corepressor Tripartite motif-containing 28 (TRIM28/KAP1/TIF1β) as a critical regulator of IFN-β, IFN-γ and cytokine expression during infection with HPAIV. TRIM28 belongs to the family of TRIM proteins (10) of which most members are involved in the regulation of the immune response to diverse viruses (11, 12). Like most of the TRIM family members, TRIM28 possesses E3 ubiquitin ligase activity located in its N-terminal RBCC-domain. Its C-terminus contains a rather unique arrangement of functional domains including a heterochromatin protein 1 binding domain (HP1 BD), a plant homeodomain (PHD) and a bromodomain (Bromo), which is only shared by the three other TRIM-family members TRIM24/TIF1α, TRIM33/TIF1γ and TRIM66/TIF1δ. All four proteins are known for their function as transcriptional regulators and constitute the TRIM subfamily VI (13–15).

Functionally, TRIM28 is described as a universal genome regulator involved in embryonic and stem cell development, cell cycle regulation, apoptosis, cancer, diverse stress responses and immunity (16–18). Mice lacking TRIM28 die at an early embryonic stage emphasizing its crucial role during embryonic development (19). In addition, TRIM28 facilitates silencing of endogenous retroviruses (20), restricts pro-viral gene activation and suppresses lytic gene expression of Kaposi's sarcoma-associated herpes virus, Murine leukemia virus and human T-cell lymphotropic virus-1 (21–23). It possesses E3 SUMO ligase activity and interacts with diverse transcription factors and other proteins to modulate their activity. These functions of TRIM28 are suspected to be regulated by post-translational modification (PTM) including SUMOylation, phosphorylation and others, which often occur at acceptor sites located in close proximity to the functional domains in the C-terminus (24–26). In contrast to the majority of TRIM proteins, which comprise immune enhancing activities, TRIM28 is associated with immunosuppression (27). The protein was reported to downregulate the activity of several immune-related transcription factors, such as IRF7, IRF5 and IRF1 as well as STAT3 by varying mechanisms (28–30). A role of TRIM28 during IAV replication has not been investigated until today. First evidence for a possible functional relevance derives from a global SUMO-screening demonstrating that TRIM28 is deSUMOylated during IAV infection (31). Nevertheless, this study did not address whether TRIM28 is involved in the immune response to IAV infection.

In the present study, we demonstrate that TRIM28 is phosphorylated at serine 473 (S473), a site known to regulate TRIM28 corepressor activity, during infection of human lung epithelial cells with HPAIV. Furthermore, we establish a link of S473 phosphorylation to elevated IFN-β expression and provide compelling evidence that TRIM28 is a key factor in the development of cytokine overexpression during HPAIV infection. These results could be the starting point for the development of new immunomodulatory strategies targeting TRIM28 post-translational modification to control the expression of type I IFNs as well as proinflammatory cytokines.

MATERIAL AND METHODS

Cells and Viruses

Human alveolar epithelial cells (A549), African green monkey kidney epithelial cell (Vero), HEK293T, HEK293T-Phoenix and Madin-Darby canine kidney type II cells (MDCK-II) were cultivated in Dulbecco's modified Eagle's Medium (DMEM) (Sigma, Germany) supplemented with 10% fetal bovine serum (Merck, Germany) and 1% Penicillin/Streptomycin (P/S) (Merck, Germany) at 37°C and 5% CO_2. Human Umbilical Vein

Endothelial Cells (HUVECs) were isolated from umbilical cords by dispase treatment and cultured on CellBIND® dishes (Corning, USA) in HUVEC-medium [50% EGM2 and 50% M199 (Biochrom, Germany) supplemented with 10% fetal calf serum (Sigma, Germany), 30 µg/mL gentamycin (Cytogen, Germany), 15 ng/mL amphotericin B (Biochrom, Germany), 100 IE Heparin (Ratiopharm, Germany), 2 mM L-glutamine (Lonza, Switzerland)] at 5% CO_2 and 37°C. Upon infection HUVECs were cultured in M199 medium containing 1% BSA, 30 µg/ml gentamicin and 15 ng/ml amphotericin B. All work with HUVECs was conducted with the formal approval of the Ethics Committee of North Rhine-Westphalia and the University of Muenster. A/Thailand/KAN-1/2004 (H5N1) (KAN-1) was kindly provided by P. Puthavathana (Bangkok, Thailand). A/FPV/Bratislava/79 (H7N7) (FPV) was obtained from the virus depository of the Institute of Virology in Giessen, Germany. A/Hamburg/04/2009 (H1N1pdm) was a kind gift of the German National Reference Centre for Influenza (Brunhilde Schweiger, Berlin, Germany). A/Vietnam/1203/2004 (H5N1) (VN) and A/Anhui/1/2013 (H7N9) (Anhui) were kindly offered by Thorsten Wolff (RKI, Berlin). Recombinant A/Puerto Rico/8/34 (H1N1) (PR8), A/seal/Mass/1-SC35M/80 (H7N7) (SC35M) and A/WSN/33 (H1N1) (WSN) were generated using the pHW2000 reverse genetics system (32). All influenza viruses were propagated on MDCK-II cells in infection medium [DMEM supplemented with 1% P/S, 0.25% bovine serum albumin (BSA, Sigma) and 0.01% $MgCl_2$ and $CaCl_2$ (Roth, Germany)]. Infections were carried out by incubating cells in infection PBS (PBS supplemented with 1% P/S, 0.25% BSA and 0.01% $MgCl_2$ and $CaCl_2$) at the indicated multiplicity of infection (MOI) for 30 min. Experiments involving HPAIV were conducted in a biosafety level (BSL) 3 approved laboratory. Recombinant VSV (serotype Indiana) encoding firefly luciferase (VSV-luc) was generated by replacing the GFP gene in the previously described VSV-GFP vector by the firefly luciferase gene according to published procedures (33). VSV-luc was propagated on Vero cells and titrated by immunostaining with a rabbit polyclonal anti-VSV serum as described previously (34).

Plasmids

Guide RNAs (gRNA) targeting TRIM28 and mCherry were designed with *Bbs*I overhang sequences. The gRNA oligonucleotides were ordered phosphorylated, annealed and ligated into *Bbs*I digested pSpCas9(BB)-2A-GFP plasmid (Addgene #48138) (35). For MyD88 and PKR, gRNAs were annealed, phosphorylated by PNK and cloned into *Bsm*BI digested lentiCRISPR v2 vector (Addgene #52961) (36). Oligonucleotide sequences are included in **Supplementary Table S1**. Full-length human TRIM28 was subcloned from pEGFP-TRIM28 (Addgene #45568) into *Not*I and *Xho*I (NEB, USA) digested pBluescript II SK(+/–) vector. In pBluescript II SK(+/–), TRIM28 mutants (S473A, S473E) were obtained by site-directed mutagenesis with non-overlapping primers. Subsequently, TRIM28 wildtype and the phospho-mutants were cloned into *Not*I and *Eco*RI (NEB, USA) digested retroviral vector pQCXIP. PCR primer sequences are included in **Supplementary Table S2**.

Generation of Knockout Cells

A549 TRIM28 CRISPR-Cas9 knockout (KO) and control cells (Ctrl) were generated by transient transfection. In brief, A549 cells were transfected with either pSpCas9(BB)-2A-GFP harboring a gRNA targeting TRIM28 or a control gRNA targeting mCherry (plasmids were kindly provided by Nicole Fischer, Hamburg, Germany). Positively transfected cells were selected by fluorescence-activated cell sorting (FACS) and clonal cell lines were analyzed for TRIM28 KO by western blot. A549 PKR, RIG-I KO, MAVS KO and MyD88 KO cells were generated by lentiviral transduction as described elsewhere (9, 37). In brief, lentiviral particles were produced on HEK293T cells by transfection with the following three plasmids at a 3:1:3 ratio; (i) pCMV-DR8.91 (ii) pMD2.G (iii) lenti-CRISPR-vector. Virus particle-containing supernatants were harvested 48, 56, and 72 h post-transfection (h p.t.) and used for transduction of target cells. Successfully transduced cells were selected with 1 µg/ml puromycin (Sigma, Germany). Gene knockout in single cell clones was validated by western blot.

Retroviral Gene Transfer

The empty retroviral vector pQCXIP or pQCXIP-TRIM28 expressing the different phospho-mutants were transfected into HEK293T-Phoenix packaging cells (Orbigen, USA). Retrovirus-containing supernatants were harvested 48 and 60 h p.t., supplemented with polybrene (Santa Cruz Biotechnology, USA) to a final concentration of 4 µg/ml and used for transduction of A549 TRIM28 KO cells. Transduced cells were selected with 1 µg/ml puromycin for 5 days to obtain stable cell lines and TRIM28 expression levels were analyzed by western blot. Stable TRIM28 mutant-expressing cells were subcloned to obtain single cell clones with equal expression of TRIM28 as measured by western blot.

Cell Treatments

Cells were treated with inhibitors for 1 h prior to infection, RNA transfection or induction of genotoxic stress. After removal of the inoculum, transfection mix or chemicals, inhibitors were added to the infection medium. The following inhibitors were used: ATM (KU-60019, Selleckchem, Germany), Chk2 (Chk2 inhibitor II, Abcam, Germany), p38 MAPK (SB202190, Calbiochem, USA), PKR (2-Aminopurine, Sigma, Germany), MEK (U0126, Taros Chemicals, Germany), MK2 (PF-3644022, Sigma, Germany), MSK1 (SB747651A, Axon Medchem, Netherlands) and the ROS-scavenging agent N-Acetyl-L-cysteine (NAC) (Sigma, Germany). Cells were stimulated by exposure to 1 kJ/m^2 UVC-light using a Stratalinker 2400 UV Crosslinker (BioSurplus, USA), or incubation with H_2O_2, etoposide (Sigma, Germany) or IFN-β (R&D Systems, Germany) for the indicated times and concentrations. For RNA and HMW poly(I:C) (Invivogen, USA) stimulations, A549 cells were transfected using Lipofectamine 2000™ (Invitrogen, USA) according to the manufacturer's instructions. Therefore, total RNA from

MDCK-II cells either infected with WSN at an MOI of 5 for 8 h or non-infected cells was isolated using the RNeasy Kit™ according to the manufacturer's instructions (Qiagen, Germany).

MTT-Assay

For cytotoxicity measurements, MTT [3-(4,5-dimethylthiazol-2-yl)-2,5-diphenyltetrazolium bromide] (Sigma, Germany) was added to the cells at a final concentration of 5 mg/ml for 4 h at 37°C and 5% CO_2. As a positive control, 2 μM staurosporine (Sigma, Germany) was added for 10 h. Supernatants were aspirated and DMSO (Roth, Germany) was added for 5 min before the optical density (OD) was measured at a wavelength of 562 nm (MicroLumat Plus LB96V, Berthold Technologies, Germany).

Western Blot and Antibodies

Cells were lysed with ice cold radioimmunoprecipitation assay (RIPA) buffer (25 mM TRIS pH 7.5, 150 mM NaCl, 0.1% SDS, 0.5% sodium deoxycholate, 1% Triton X-100) supplemented with the following protease and phosphatase inhibitors; 10 μM leupeptin (Sigma, Germany), 200 nM aprotinin (Roth, Germany), 5 mM benzamidine (Sigma, Germany), 2.5 mM pefabloc (Sigma, Germany), 10 mM beta-glycerophosphate (Sigma, Germany), 1 mM sodium orthovanadate (Sigma, Germany), 10 mM sodium fluoride (Roth, Germany) and 2.5 mM sodium pyrophosphate (Sigma, Germany). Lysates were sonicated for 20 s (pulse 50%, amplitude 30%) and pelleted at 4°C, 14.000 g for 15 min. Protein amounts were adjusted to 20 μg, mixed with 4× sample buffer (0.25 M TRIS pH 6.8, 40% glycerol, 8% SDS, 10% β-mercaptoethanol, 0.01% bromophenol blue) and separated by SDS-PAGE. Proteins were transferred to nitrocellulose membranes and detected by using primary antibodies targeting tubulin (Sigma, Germany), PB1 (GeneTex, USA), TRIM28, TRIM28 S473-P, TRIM28 S824-P (Abcam, UK), CREB S133-P, RIG-I, eIF2α S51-P, ERK1/2, ERK1/2 T202/Y204-P, HSP27, HSP27 S82-P (Cell signaling Technologies, USA) and anti-mouse or anti-rabbit IgG secondary antibodies either conjugated to fluorophores (Licor, Germany) or horseradish peroxidase (Cell Signaling Technology, USA). Selected bands were densitometrically quantified using Licor Image studio software (Licor, Germany).

Immunofluorescence

A549 cells were seeded on glass coverslips and fixed with 4% paraformaldehyde (Sigma, USA). Cells were permeabilized with 0.1% Triton X-100, and blocked for 30 min in 3% BSA. Slides were incubated overnight at 4°C with primary antibodies against IAV nucleoprotein (NP) (GeneTex, USA) and TRIM28 S473-P. Secondary antibodies anti-rabbit Alexa Fluor 488 (Invitrogen, USA) and anti-mouse Alexa Fluor 568 (Invitrogen, USA) were incubated for 1 h at room temperature. Cell nuclei were stained for 20 min with DAPI (Thermo Fisher Scientific, USA). Coverslips were mounted on glass slides in Mounting Medium S3023 (Dako Omnis, USA) and examined using a LSM-800 Airyscan confocal microscope (Carl Zeiss, Germany).

Phosphoproteomic Screen

A549 cells were stably labeled with "light" lysine ($^{12}C_6$, $^{14}N_2$) and arginine ($^{12}C_6$, $^{14}N_4$), "medium" lysine ($^{13}C_6$, $^{14}N_2$) and arginine ($^{13}C_6$, $^{14}N_2$) or "heavy" lysine ($^{13}C_6$, $^{15}N_2$) and arginine ($^{13}C_6$, $^{15}N_4$). Labeled cells were infected with either PR8, FPV or KAN-1 at an MOI of 5 for 2, 4, 6, and 8 h. "Light"-labeled cells were used as non-infected control (0 h), whereas "medium"- and "heavy"-labeled cells were infected for 2 or 6 h and 4 or 8 h, respectively. Lysates from non-infected, 2, 4 h infected cells (Mix 1) and non-infected, 6, 8 h infected cells (Mix 2) were subjected to tryptic digestion. Phosphopeptides were purified by cation exchange chromatography and TiO_2-enrichment followed by LC-MS/MS analysis on a Proxeon Easy-nLC coupled to an LTQ-Orbitrap XL mass spectrometer. Data analysis was performed using Mascot and MaxQuant (v1.2.2.9) as previously described (38–40). Phosphorylation intensities of TRIM28 residues were quantified in relation to the phosphorylation of TRIM28 in non-infected cells in both lysate mixtures.

Cytokine Analysis

A549 TRIM28 KO and Ctrl cells were stimulated by transfection with 200 ng of viral or cellular RNA. The LEGENDplex™ Human Anti-Virus Response Panel (BioLegend Cat. No. 740350) was used for the simultaneous determination of the concentrations of IFN-α, -β, -γ, -λ1 and λ2/3 as well as IL-1β, IL-6, IL-8, IL-10, IL-12p70, TNF-α, IP-10, and GM-CSF in the supernatant. Cytokine capturing was performed according to the manufacturer's protocol in filter plates. Bead-bound cytokines were measured on a FACSCalibur Cytometer (Becton Dickinson) and concentrations were calculated using the LEGENDplex™ Data Analysis Software (BioLegend, USA).

RNA Isolation and Quantitative Real-Time PCR (qRT-PCR)

RNA was isolated using peqGOLD TriFast™ according to the manufacturer's instructions (VWR, USA). Total RNA was reverse transcribed with oligo(dT) primers and RevertAid H Minus Reverse Transcriptase (Thermo Fisher Scientific, USA). RT-PCR was carried out in duplicates using a LightCycler® 480 II (Roche, Germany). Primer sequences are provided in **Supplementary Table S3**. Commercially available primers were used for analysis of IFN-β mRNA (Qiagen, Germany). Expression data were normalized to the housekeeping gene glyceraldehyde 3-phosphate dehydrogenase (GADPH) and analyzed using the $2^{-\Delta\Delta CT}$ method as described elsewhere (41).

IFN-Bioassay

A549 TRIM28 KO and Ctrl cells were stimulated by transfection of 250 ng of viral or cellular RNA and at 6 h p. t. supernatants were harvested. The cell-free supernatants were diluted 1:10 and added to Vero cells for another 16 h. Subsequently, Vero cells were infected with VSV-luc at an MOI of 5 for 5 h. Supernatants were aspirated, cells were lysed in passive lysis buffer (Promega,

USA) and luciferase assay substrate (Promega, USA) was added. VSV-luc reporter gene expression was determined by measuring luminescence using a MicroLumat Plus LB96V luminometer (Berthold Technologies, Germany).

RESULTS

Phosphorylation of TRIM28 Is Induced by HPAIV Infection

Viruses activate diverse signaling pathways in infected cells. To elucidate whether human adapted and highly pathogenic avian-derived IAV strains differentially activate kinase-governed signaling pathways a quantitative phosphoproteomic screen was performed (40). Human lung epithelial cells (A549) were infected with the human IAV strain A/Puerto Rico/8/34 (PR8, H1N1), the HPAIV strain A/Thailand/KAN-1/2004 (KAN-1, H5N1), which was isolated from a fatal human case following direct avian-to-human transmission and the HPAIV avian isolate A/FPV/Bratislava/79 (FPV, H7N7). This revealed that the host factor TRIM28 was increasingly phosphorylated at S473 during infection with KAN-1 and FPV but not with PR8 (**Figure 1A**, upper panel). For the neighboring serine 471 (S471), increased phosphorylation was only detected during FPV infection (**Figure 1A**, lower panel). These results were confirmed by western blot analysis using an antibody specific for phosphorylated TRIM28 S473 (**Figure 1B**). Based on these data, we speculated that TRIM28 phosphorylation could be a strain-dependent mechanism. To support this hypothesis, additional IAV strains were tested. We observed that TRIM28 S473 was also phosphorylated upon infection with the mouse-adapted HPAIV variant A/seal/Mass/1-SC35M/80 (SC35M, H7N7) and the HPAIV strains A/Vietnam/1203/2004 (VN, H5N1), A/Anhui/1/2013 (Anhui, H7N9) but not with the human-adapted 2009 pandemic H1N1 strain A/Hamburg/04/2009 (H1N1pdm) (**Figure 1C** upper panels). Quantitative western blot analysis further demonstrated that SC35M, KAN-1, and FPV induced S473 phosphorylation to different degrees, suggesting that all three strains have individual capacities to induce S473 phosphorylation (**Figures 1B,C**, lower panels). Plotting the virus strains according to the intensity of the induced S473-P signals indeed suggests that the degree of human adaptation inversely correlates with the capacity to induce S473 phosphorylation (**Figure 1D**). Like H5N1 viruses, H7N7 viruses can cross the species barrier from birds to humans and may cause severe to lethal respiratory disease in humans (42–44). As we observed S473 phosphorylation during infection with the mouse-adapted HPAIV variant SC35M, we used this strain as a representative for HPAIV in many experiments. This had the advantage that we could perform the experiments under BSL2 conditions. Interestingly, phosphorylation at S473 and S471 could be detected at 6 h p.i in the phosphoproteomic screen as well as in western blot analysis, indicating that it is not induced at an early stage of viral infection like viral entry or nuclear replication but rather at a later step. S473 phosphorylation was also observed at a low MOI of 0.1 (**Supplementary Figure S1A**). In addition, strain-dependent phosphorylation was also observed in primary HUVECs (**Supplementary Figure S1B**). Immunofluorescence data showed that the occurrence of nuclear S473 phosphorylation correlates with the cytoplasmic localization of the viral nucleoprotein (NP) 10 h after infection. In contrast, in cells infected for 5 h, only background phosphorylation was observed in the nucleus (**Figures 1E,F**). In summary, these results demonstrate that HPAIV of the H5N1, H7N7, and H7N9 subtypes induce phosphorylation of TRIM28 S473 at a late time point during infection. Furthermore, our data indicate that the capacity of IAV strains to phosphorylate TRIM28 inversely correlates with the degree of human adaptation.

HPAIV-Induced Phosphorylation of TRIM28 Is Mediated by a Signaling Pathway not Related to the DNA Damage Response (DDR)

Phosphorylation of TRIM28 at positions S473 and serine 824 (S824) is widely described to occur in response to DNA damage and can be experimentally induced by various genotoxic stresses including treatment with H_2O_2, UV-radiation and etoposide (45–47). During DNA damage, phosphorylation at these sites is mediated by the kinase ataxia-telangiectasia mutated (ATM) and the checkpoint kinases 1 und 2 (Chk1/2) (48, 49) (**Figure 2A**). Phosphorylation is associated with different biological outcomes. While S473 is located in close proximity to the HP1 BD, which mediates the interaction with HP1 and repression of Krüppel-associated box zinc finger protein (KRAB-ZNF)-dependent genes, S824 lies next to the C-terminal bromodomain. Functionally, phosphorylation of S473 has been demonstrated to ablate binding of TRIM28 to HP1 and TRIM28-mediated repression of KRAB-ZNF-dependent genes. In contrast, S824 phosphorylation facilitates local chromatin relaxation (48) and, in combination with TRIM28 deSUMOylation, leads to the de-repression of DDR-responsive genes (25). Because infection with IAV has been reported to induce DDR (50, 51), we examined whether infection with SC35M induces the same phosphorylation pattern on TRIM28 compared to UV-radiation, H_2O_2 or etoposide treatment. Remarkably, we found that the induced phosphorylation patterns during IAV infection and DNA damage are different. Infection with SC35M induced phosphorylation of S473 but not S824 while all three genotoxic agents readily induced phosphorylation at both sites (**Figure 2B**). We further investigated whether ATM and Chk2 are also the responsible kinases for TRIM28 phosphorylation during IAV infection. Treatment of A549 cells with non-toxic concentrations of the inhibitors for ATM and Chk2 prior to stimulation with H_2O_2, etoposide or infection with SC35M clearly demonstrated that these kinases are not involved in IAV-mediated TRIM28 S473 phosphorylation (**Figure 2C**; **Supplementary Figures S2A–D**). Using NAC to scavenge reactive oxygen species (ROS) we could also exclude ROS as cause of TRIM28 S473 phosphorylation during SC35M infection (**Figure 2D**). In summary, these results demonstrate that during IAV infection TRIM28 S473 is not phosphorylated by the DDR-related kinases ATM and Chk2, which suggests that

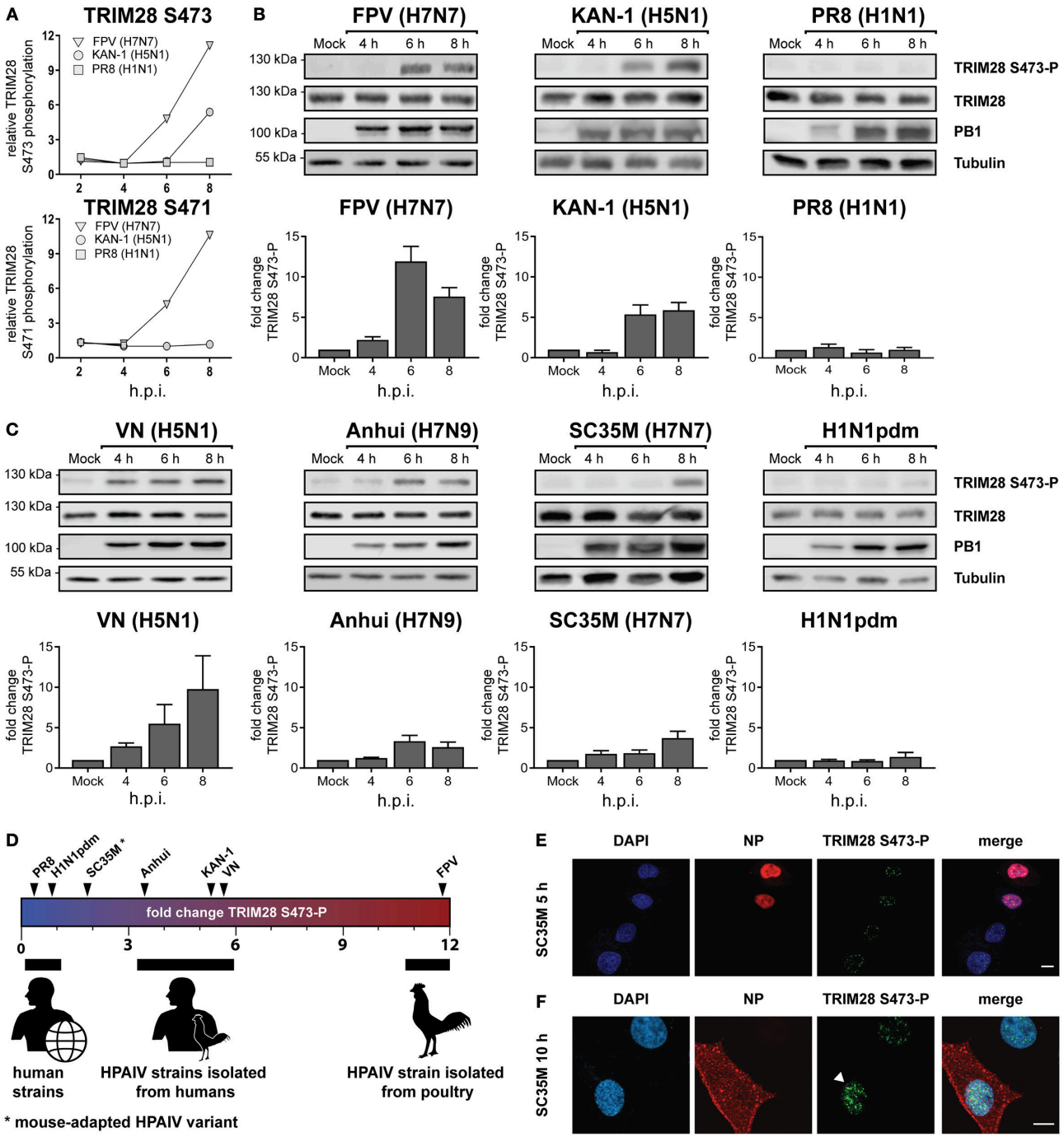

FIGURE 1 | Phosphorylation of TRIM28 during HPAIV infection. **(A)** SILAC-labeled human A549 cells were infected with FPV (H7N7), KAN-1 (H5N1), and PR8 (H1N1) for the indicated times at an MOI of 5. Phosphorylated peptides were enriched and analyzed by mass spectrometry. The relative phosphorylation of TRIM28 at serine 473 (S473) and serine 471 (S471) are depicted. Western blot of A549 cells infected with **(B)** FPV, KAN-1, PR8 and **(C)** VN (H5N1), Anhui (H7N9), SC35M (H7N7), H1N1pdm at an MOI of 5 for the indicated time points. Phosphorylation of TRIM28 S473 was detected using a phospho-specific antibody. Detection of total TRIM28 and tubulin served as loading controls. Densitometric quantifications of S473 phosphorylation were normalized to tubulin intensities and are depicted as mean fold change (±SEM). **(D)** Schematic representation of mean fold changes of TRIM28 S473 phosphorylation compared to non-infected cells at 6 h p.i. A549 cells were infected with SC35M **(E)** at an MOI of 5 for 5 h or **(F)** at an MOI of 0.5 for 10 h. Nuclei were stained with DAPI. Viral nucleoprotein (NP) and TRIM28 S473 phosphorylation were stained using specific antibodies. Cells were analyzed by confocal laser scanning microscopy.

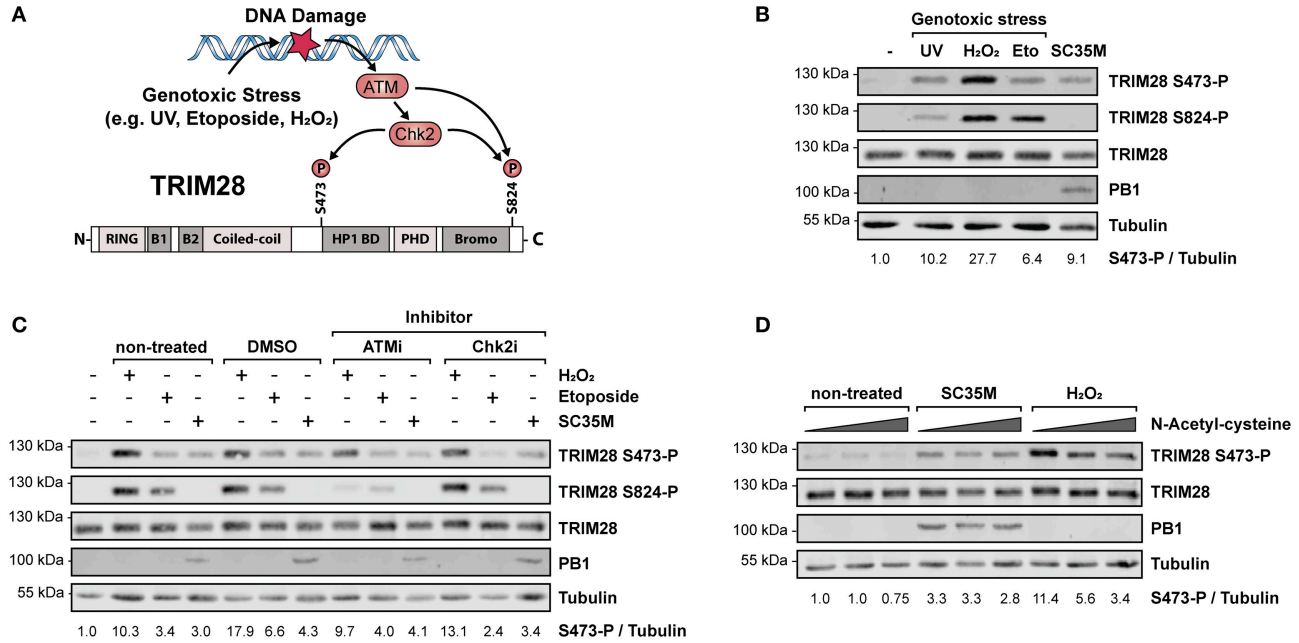

FIGURE 2 | Phosphorylation of TRIM28 S473 occurs by non-DDR related kinases during HPAIV infection. **(A)** Schematic representation of the involved kinases leading to TRIM28 S473 and S824 phosphorylation during DNA damage response. **(B)** A549 cells were treated with 250 μM H_2O_2 for 3 h, 100 μM etoposide for 6 h, infected for 10 h with SC35M at an MOI of 20 or treated with 1 kJ/m^2 ultraviolet light 30 min prior to western blot analysis. TRIM28 phosphorylation was detected using antibodies specific for TRIM28 phosphorylated at S473 or S824, respectively. Total TRIM28 and tubulin served as loading controls. Infection was validated using an antibody targeting the viral protein PB1. **(C)** A549 cells were treated with inhibitors for ATM (KU-60019, 2.5 μM), Chk2 (Chk2 Inhibitor II, 10 μM) and the solvent control (DMSO, 10 μM) 1 h prior to stimulation with H_2O_2, etoposide and SC35M infection in the presence of the corresponding inhibitors. **(D)** A549 cells were treated with increasing amounts of the reactive oxygen species scavenger NAC (5, 10, 15 mM) for 1 h following stimulation with 500 μM H_2O_2 for 2 h and infection with SC35M for 10 h at an MOI of 20 in the presence of NAC. TRIM28 S473 phosphorylation was monitored by western blot.

TRIM28 has a yet non-described, non-DDR related function in IAV infected cells.

TRIM28 Is a Negative Regulator of the Innate Immune Response to IAV

To gain insight into the general function of TRIM28 during viral infection, TRIM28 KO cells were generated using CRISPR-Cas9 (**Figure 3A**). Growth curve analyses demonstrated no pronounced effect on viral replication of SC35M and FPV in cells lacking TRIM28 compared to control cells (**Supplementary Figures S3A,B**). Because TRIM28 is described as a negative immune regulator, we analyzed the expression of IFN-β in these cells. Intriguingly, infection with PR8, SC35M or FPV resulted in elevated levels of IFN-β compared to infected control cells (**Figure 3B**). Elevated levels of IFN-β as well as the proinflammatory cytokines IL-6 and IL-8 were also observed during infection of TRIM28 KO cells with KAN-1 (**Figure 3C**). In addition, transfection of viral RNA (vRNA), as a trigger for the innate immune response, also resulted in higher mRNA levels of IFN-β, IL-6 and IL-8 in the absence of TRIM28 (**Figure 3D**). Importantly, we could also demonstrate that transcriptional upregulation correlated with significantly increased secretion of IFN-β, IL-6, IL-8 and IFN-γ in vRNA-treated TRIM28 KO cells at 8 and 24 h p.t. (**Figure 3E**; **Supplementary Figures S4A,B**). Because we did not observe an effect on SC35M and FPV replication, the biological function of increased IFN levels was manifested in an IFN-bioassay using a luciferase-expressing vesicular stomatitis virus (VSV-luc), which is highly sensitive to the action of IFNs. To induce an antiviral state, Vero cells were pre-treated with the supernatants from vRNA-stimulated TRIM28 KO and control cells. Infection with VSV-luc revealed a pronounced inhibition of viral replication in Vero cells that have been treated with the supernatant from stimulated TRIM28 KO cells compared to Vero cells treated with control cell supernatant, indicating that the increased IFN levels induced a more potent antiviral state (**Figure 3F**). In summary, these results demonstrate that TRIM28 functions as an important negative regulator of the expression of IFN-β, IFN-γ, IL-6 and IL-8 during IAV infection.

Phosphorylation of TRIM28 S473 Occurs in Response to Viral RNA but Is Independent of RIG-I

The previous results demonstrated that TRIM28 negatively regulates the expression of IFN-β, IFN-γ, IL-6 and IL-8 during IAV infection. However, the role and biological function of S473 phosphorylation and the source of activation remained elusive. During IAV infection IFN-β is majorly expressed in response to sensing of viral RNA by cytosolic RIG-I (52, 53).

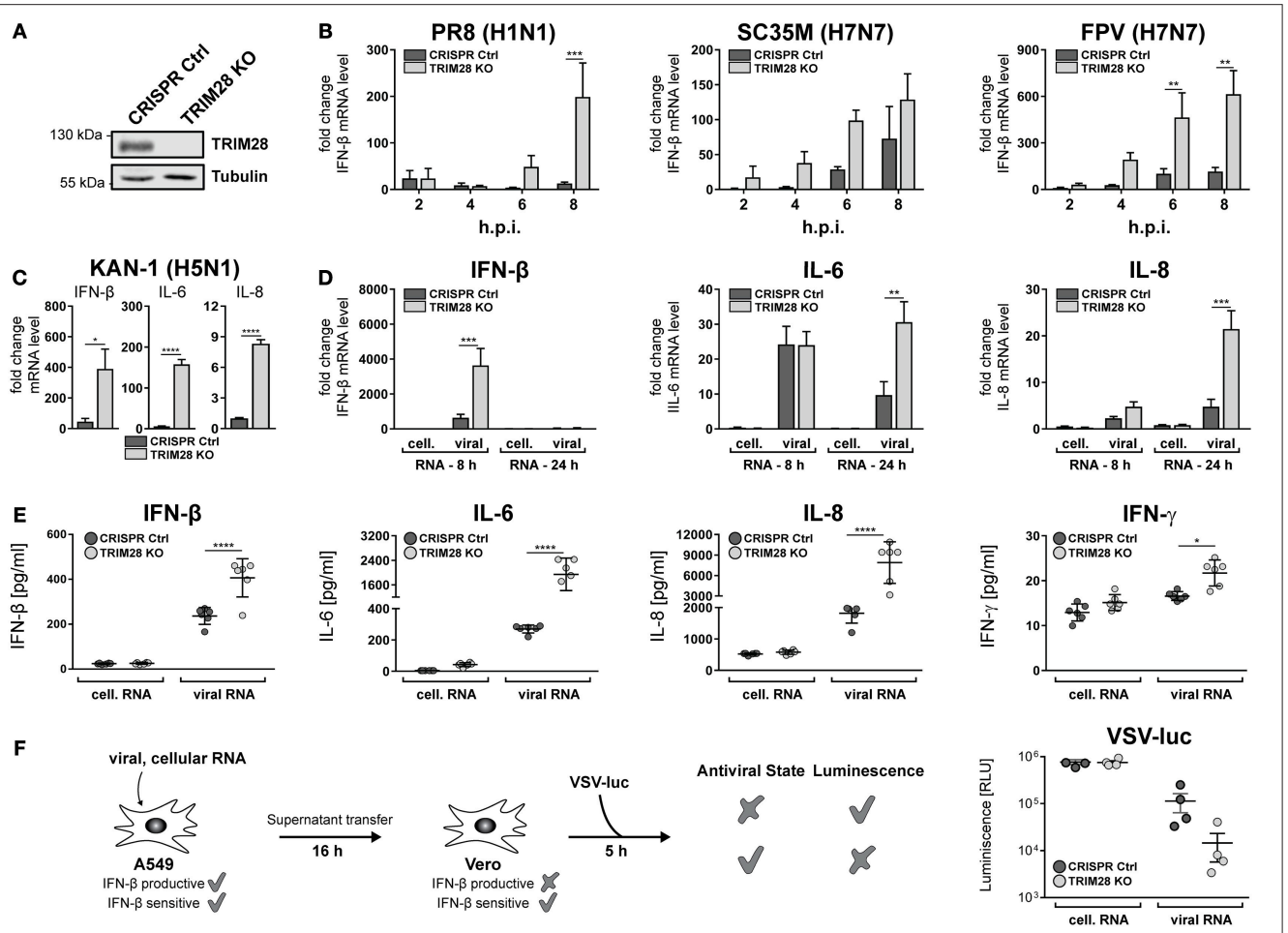

FIGURE 3 | TRIM28 is a negative regulator of the innate immune response during influenza A virus infection. **(A)** Western blot of A549 TRIM28 KO cells. **(B)** Infection of TRIM28 KO cells with PR8, SC35M and FPV at an MOI of 5. Total RNA was isolated at the indicated time points and IFN-β mRNA levels were analyzed by qRT-PCR. IFN-β levels are depicted as mean *n*-fold change (±SEM) compared to non-infected cells. $^{**}p \leq 0.002$; $^{***}p \leq 0.0002$; two-way ANOVA; Sidak's multiple comparisons test. **(C)** TRIM28 KO cells were infected with KAN-1 (H5N1) at an MOI of 0.01 for 24 h. IFN-β, IL-6 and IL-8 mRNA levels were determined as described in **(B)**. $^{*}p \leq 0.03$; $^{****}p \leq 0.0001$; two-tailed unpaired *t*-test. **(D)** TRIM28 KO cells were transfected with 200 ng viral or cellular RNA. Total RNA was isolated 24 h p.t. and IFN-β, IL-6 and IL-8 mRNA levels were determined by qRT-PCR. Results are shown as mean *n*-fold change (±SEM) over non-treated cells. $^{**}p \leq 0.0021$; $^{***}p \leq 0.0002$; two-way ANOVA; Sidak's multiple comparisons test. **(E)** TRIM28 KO cells were treated as in **(D)**. Supernatants were analyzed using LEGENDplex^{TM} bead immunoassay for the indicated cytokines at 24 h p.t. Results of six independent experiments are plotted as well as the mean (±SD). $^{*}p \leq 0.03$; $^{****}p \leq 0.0001$; two-way ANOVA; Tukey's multiple comparisons test. **(F)** A549 cells were transfected with 250 ng viral or cellular RNA for 6 h. Supernatants were harvested and transferred to Vero cells for 16 h. Stimulated Vero cells were infected with a luciferase-encoding vesicular stomatitis virus (VSV-luc) at an MOI of 5 for 5 h. Cells were harvested and virus replication was determined by luciferase assay. Results of four independent experiments are plotted as well as the mean (±SEM).

Because our results demonstrate that TRIM28 is also involved in the expression of IFN-β, we speculated that TRIM28 S473 phosphorylation could be induced by a similar mechanism. Therefore, we analyzed whether transfection of vRNA induces S473 phosphorylation. We observed that TRIM28 S473 was markedly phosphorylated following transfection of vRNA or poly(I:C) (**Figure 4A**; **Supplementary Figure S5A**). Importantly, using RIG-I knockout cells (RIG-I KO) (**Figure 4B**), we could demonstrate that S473 phosphorylation during vRNA transfection (**Figure 4C**) and SC35M infection (**Figures 4D,E**) is retained in the absence of RIG-I. This provides evidence that S473 phosphorylation occurs independent of the RIG-I signaling pathway. To support the idea that RIG-I independent mechanisms contribute to the expression of IFN-β during infection with HPAIV, we infected wildtype and RIG-I KO cells with PR8, SC35M as well as FPV and measured the induction of IFN-β. This revealed that IFN-β expression was rather low in PR8 infected wildtype cells and seems to primarily depend on RIG-I as 6.2-fold less IFN-β was induced in the absence of RIG-I. In contrast, IFN-β was upregulated by 25-fold and 75-fold in SC35M and FPV infected wildtype cells, respectively. However, lack of RIG-I reduced IFN-β induction only by 2-fold in SC35M infected cells and 1.5-fold in FPV infected cells (**Figure 4F**). This indicates that the expression of IFN-β during FPV infection is not exclusively dependent on RIG-I but involves other signaling pathways.

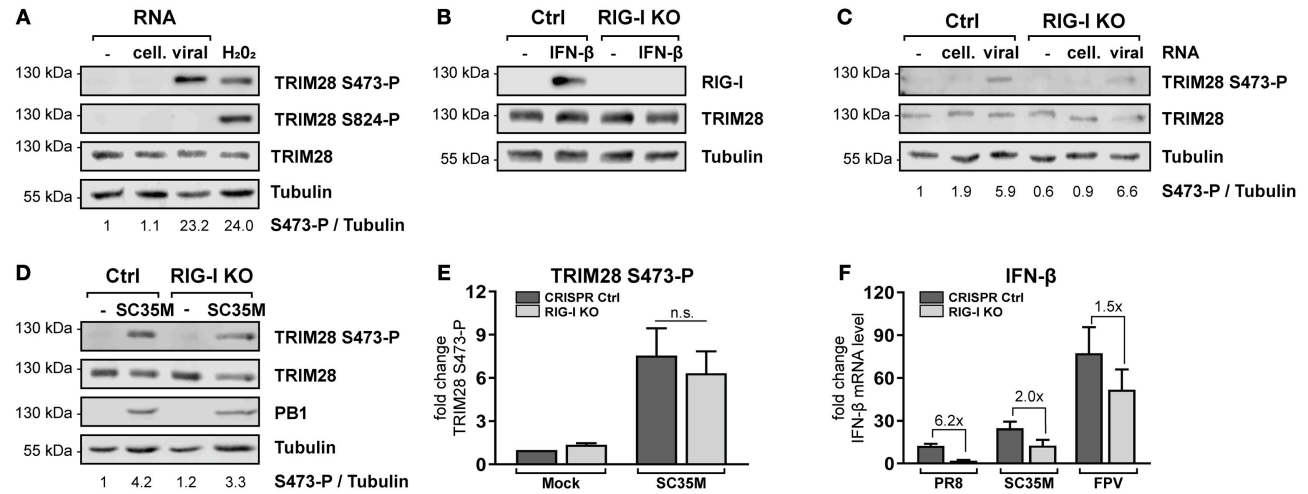

FIGURE 4 | TRIM28 S473 phosphorylation is induced by viral RNA in a RIG-I independent manner. **(A)** A549 cells were transfected with 1 μg viral or cellular RNA. Lysates were harvested 4 h p.t. and TRIM28 S473 and S824 phosphorylation was analyzed by western blot. As a control, cells were treated with 250 μM H_2O_2 for 3 h. **(B)** Western blot of A549 RIG-I KO cells treated for 24 h with 500 U/ml IFN-β. **(C)** RIG-I KO cells were transfected with 500 ng viral or cellular RNA. TRIM28 S473 phosphorylation was monitored by western blot. **(D)** Western blot of TRIM28 S473 phosphorylation in RIG-I KO cells infected with SC35M for 10 h at an MOI of 20. **(E)** Densitometric quantifications of S473 phosphorylation in RIG-I KO cells infected as in **(D)**. TRIM28 S473-P levels were normalized to tubulin intensities. Results are plotted as mean *n*-fold change (±SEM) over mock-infected cells. n.s. $p > 0.03$; two-way ANOVA; Tukey's multiple comparisons test. **(F)** Infection of RIG-I KO cells with PR8, SC35M or FPV at an MOI of 5. Total RNA was isolated 8 h p.i. and IFN-β mRNA levels were measured by qRT-PCR. IFN-β levels are depicted as mean *n*-fold change (±SEM) over mock-infected cells.

These data suggest that alternative RNA sensing receptors are responsible for the induction of S473 phosphorylation and contribute to the high levels of IFN-β during infection with HPAIV.

Detection of Viral RNA by the Cytoplasmic RNA Sensor PKR Induces TRIM28 S473 Phosphorylation

To further specify which immune recognition pathway comes into consideration for S473 phosphorylation and modulation of IFN-β expression during HPAIV infection, A549 cells lacking the adaptor proteins MAVS and MyD88 were examined. Infection with SC35M clearly demonstrated that TRIM28 S473 was still phosphorylated in cells lacking the RIG-I downstream effector MAVS, which supported the previous results obtained in RIG-I KO cells (**Figure 5A**, lane 7). Of note, RIG-I could not be detected in this western blot due to low induction by SC35M infection. However, RIG-I knockout in these cells was demonstrated following IFN-β treatment in **Figure 4B**. S473 phosphorylation was also retained despite lack of MyD88, which rules out the majority of TLRs as candidate receptors for mediating TRIM28 S473 phosphorylation (**Figure 5A**, lane 8). Another protein that is described to have RNA sensing capacity is the double-stranded RNA sensing protein kinase R (PKR), which also binds to double-stranded RNAs in the cytosol (54). Interestingly, inhibition of PKR using 2-Aminopurine (2-AP) impeded S473 phosphorylation in response to viral infection in a concentration dependent manner (**Figure 5B**) and following vRNA transfection (**Figure 5D**). Furthermore, **Figure 5C** shows that PKR inhibition also resulted in decreased levels of IFN-β, IL-6, and IL-8 during infection. As a genetic approach, A549 cells lacking PKR (PKR KO) were generated. Intriguingly, in these cells S473 phosphorylation after vRNA transfection was strongly reduced (**Figure 5E**). Infecting PKR KO cells with PR8, SC35M, and FPV revealed that the induction of IFN-β is differentially dependent on PKR. Although all three viruses induce less IFN-β in PKR KO cells, we observed a clear tendency that IFN-β induction is more dependent on PKR during infection with SC35M and FPV compared to PR8 (**Figure 5F**). This fits to our hypothesis that IFN-β induction in HPAIV but not PR8 infected cells is potentiated by a PKR activated signaling cascade. In summary, these results demonstrate that viral RNA sensing by PKR leads to TRIM28 S473 phosphorylation during HPAIV infection and presumably contributes to the high IFN-β levels.

p38 MAPK and MSK1 Phosphorylate TRIM28 S473 During HPAIV Infection

In order to elucidate the signaling cascade responsible for TRIM28 S473 phosphorylation during viral infection, we concentrated further on kinases which are reported to be involved in the expression of IFN-β and proinflammatory cytokines during HPAIV infection and are known to be activated by PKR (55–57). This led us to investigate the stress inducible mitogen-activated protein kinase (MAPK) p38. Treatment of A549 cells with the p38 inhibitor SB202190 at specific and non-toxic concentrations efficiently blocked TRIM28 S473 phosphorylation during SC35M infection (**Figure 6A**; **Supplementary Figure S6A**) demonstrating that p38 plays a major role in this process. In contrast, treating cells with an inhibitor of MEK, thus blocking the ERK MAPK pathway, did

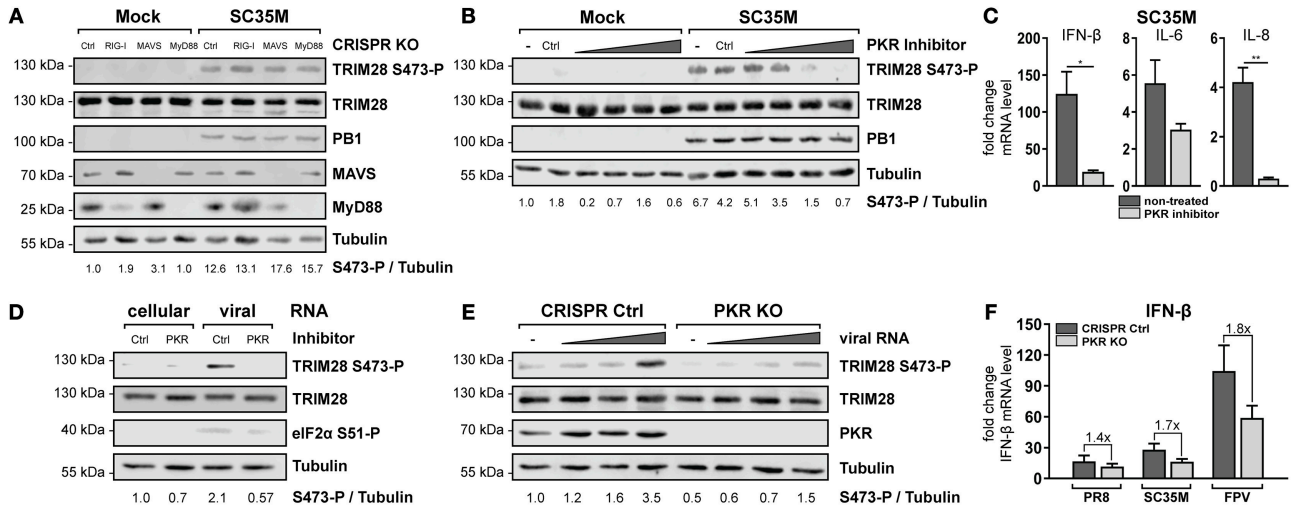

FIGURE 5 | PKR inhibition ablates TRIM28 S473 phosphorylation. **(A)** A549 RIG-I, MAVS, and MyD88 KO cells were infected with SC35M at an MOI of 20 for 10 h. TRIM28 S473 phosphorylation was analyzed with a phospho-specific antibody by western blot. Total TRIM28 and tubulin served as loading controls. The viral protein PB1 was used to verify IAV infection. Expression of MAVS and MyD88 was detected using specific antibodies. **(B)** A549 cells were treated for 1 h with the PKR inhibitor 2-AP (0.5, 1, 5 and 10 mM). Subsequently, cells were infected with SC35M at an MOI of 20 for 10 h in the presence of 2-AP. **(C)** A549 cells were pre-treated with 10 mM 2-AP and subsequently infected with SC35M at an MOI of 0.1 for 24 h in the presence of 2-AP. mRNA levels of IFN-β, IL-6 and IL-8 were determined by qRT-PCR. Results are depicted as mean *n*-fold change (±SEM) over non-infected cells. $*p \leq 0.03$; $**p \leq 0.002$; two-tailed unpaired *t*-test. **(D)** A549 cells pre-treated with 10 mM 2-AP for 1 h were transfected with 500 ng viral or cellular RNA. Lysates were harvested 4 h p.t. and TRIM28 S473 phosphorylation was analyzed by western blot. PKR inhibition was controlled by detection of eIF2α S51 phosphorylation. **(E)** A549 PKR KO cells were transfected with 50, 250, and 500 ng viral RNA or 500 ng cellular RNA. Lysates were harvested 8 h p.t. and TRIM28 S473 phosphorylation was analyzed by western blot. **(F)** Infection of PKR KO cells with PR8, SC35M or FPV at an MOI of 5. Total RNA was isolated 8 h p.i. and IFN-β mRNA levels were measured by qRT-PCR. IFN-β levels are depicted as mean *n*-fold change (±SEM) over non-infected cells.

not reduce S473 phosphorylation, excluding crosstalk from the classical MEK1/2-ERK1/2 MAP kinase pathway (**Figure 6B**; **Supplementary Figure S6B**). Well-described downstream kinases of p38 MAPK are MSK1 and MK2, which are both reported to be involved in the transcriptional regulation of cytokine expression (58, 59). Chemical inhibition of MSK1 but not MK2 resulted in the loss of S473 phosphorylation (**Figures 6C,D**; **Supplementary Figures S6C,D**). Importantly, inhibition of p38 MAPK and MSK1 led to reduced TRIM28 S473 phosphorylation during infection with the HPAIV KAN-1 and Anhui in primary HUVECs (**Supplementary Figures S6F,G**). This led us to conclude that MSK1 is the responsible kinase for S473 phosphorylation during IAV infection. Induction of S473 phosphorylation by transfection of vRNA was similarly abolished by inhibition of p38 and MSK1 but not by inhibiting MEK and MK2 (**Figure 6E**). Most importantly, loss of TRIM28 S473 phosphorylation by inhibition of p38 and MSK1 also resulted in decreased levels of IFN-β, IL-6, and IL-8 during infection with SC35M (**Figure 7A**), which was not caused by an inhibition of viral replication (**Figure 7B**). In conclusion, these data provide compelling evidence that TRIM28 S473 phosphorylation in response to PKR-dependent sensing of vRNA is mediated by the p38/MSK1-cascade during infection with HPAIV. Furthermore, these results strongly indicate that TRIM28 S473 phosphorylation results in enhanced expression of IFN-β and proinflammatory cytokines.

Constitutive Phosphorylation of TRIM28 S473 Leads to Increased Induction of IFN-β, IL-6 and IL-8 During HPAIV Infection

To establish the functional link between TRIM28 S473 phosphorylation and IFN-β expression, we reconstituted TRIM28 KO cells with either wildtype TRIM28 or the phospho-mutants S473A and S473E. Infection of TRIM28 KO cells with VSV-luc resulted in decreased viral replication. Most importantly, reconstitution of TRIM28 KO cells with the wildtype protein rescued VSV-luc replication (**Figure 8A**). Substitution of S473 with alanine (S473A) eliminates the phospho-acceptor site, while substitution with glutamic acid (S473E) mimics constitutive phosphorylation. As our previous data suggested that S473 phosphorylation regulates TRIM28-mediated repression of IFN-β, expression of these mutants should affect VSV-luc replication. Indeed, infection with VSV-luc demonstrated that reconstitution with TRIM28 S473E resulted in significantly decreased viral replication compared to cell expressing wildtype TRIM28 and TRIM28 S473A (**Figure 8B**). To proof that expression levels of IFN-β, IL-6, and IL-8 are also increased in the TRIM28 S473E expressing cells we infected the reconstituted cells with KAN-1 and performed qRT-PCR analysis. As seen in **Figure 8C**, the infected S473E expressing cells express higher levels of IFN-β, IL-6, and IL-8 compared to cells reconstituted with wildtype TRIM28 and TRIM28 S473A. Of note, also the non-phosphorylated form of TRIM28 harboring S473A showed increased levels of IFN-β,

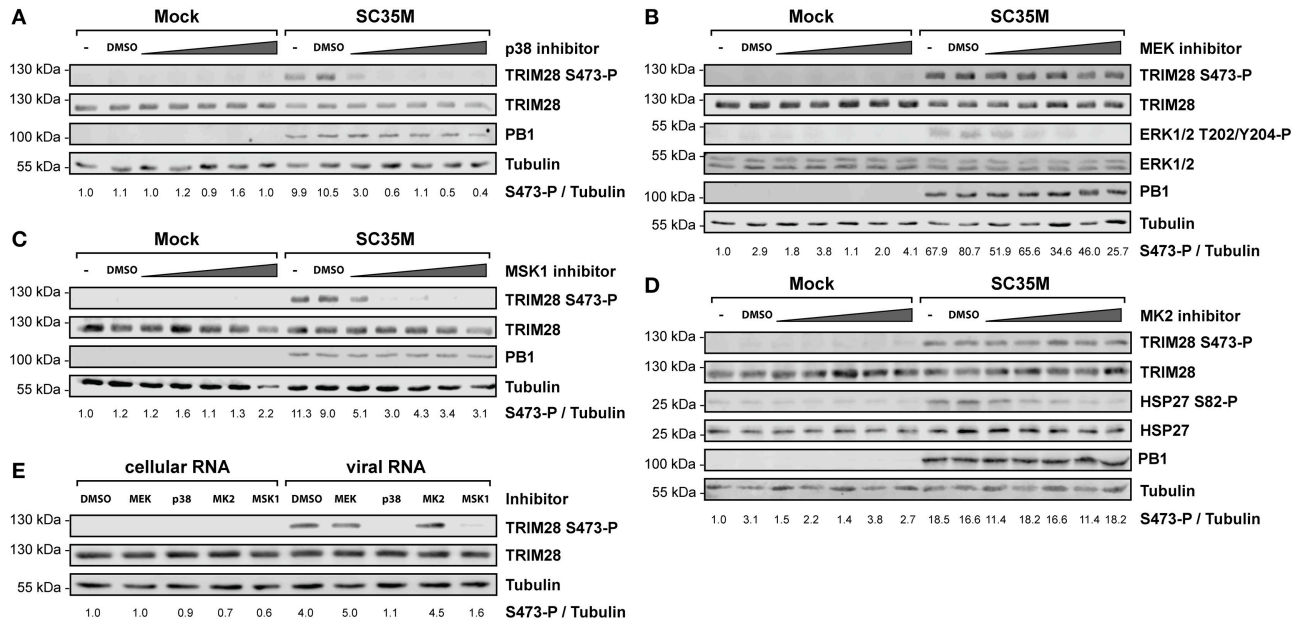

FIGURE 6 | Inhibition of p38 and MSK1 ablates TRIM28 S473 phosphorylation. A549 cells were pre-treated with inhibitors for **(A)** p38 (SB202190), **(B)** MEK (U0126), **(C)** MSK1 (SB747651), and **(D)** MK2 (PF-3644022) at 0.1 μM, 0.5 μM, 1 μM, 5 μM and 10 μM before infection with SC35M at an MOI of 20 for 10 h and further incubation with the inhibitors. Lysates were examined with a phospho-specific antibody for TRIM28 S473 phosphorylation. Infection was verified by detection of the viral PB1 protein. Tubulin and total TRIM28 served as loading controls. MEK and MK2 inhibition was controlled by detection of ERK T202/Y204, and HSP27 S82 phosphorylation, respectively. **(E)** A549 cells were pre-treated with p38 (SB202190), MEK (U0126), MSK1 (SB747651) and MK2 (PF-3644022) inhibitors at 1 μM for 30 min. Pre-treated cells were transfected with 500 ng viral or cellular in the presence of the corresponding inhibitors. Lysates were harvested 4 h p.t. and TRIM28 S473 phosphorylation was analyzed by western blot.

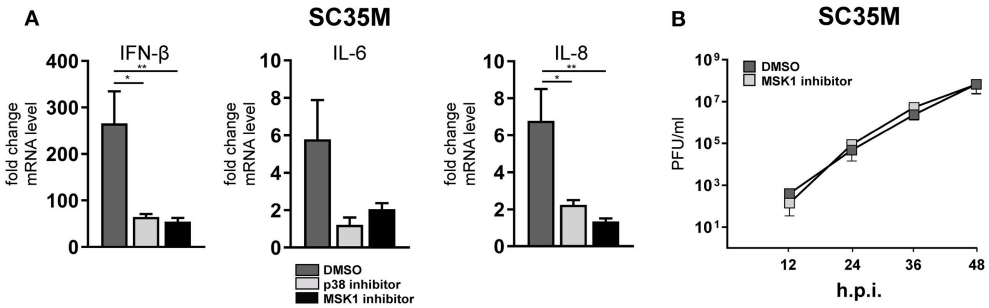

FIGURE 7 | Inhibition of p38 and MSK1 downregulates IFN-β, IL-6 and IL-8 expression. **(A)** A549 cells were pre-treated with inhibitors for p38 (SB202190) and MSK1 (SB747651) and infected with SC35M at an MOI of 0.1 for 24 h in the presence of the inhibitors. IFN-β, IL-6 and IL-8 mRNA levels were determined by qRT-PCR. Results are depicted as mean *n*-fold change (±SEM) over non-infected cells. $*p \leq 0.03$; $**p \leq 0.0021$ one-way ANOVA; Dunnett's multiple comparisons test. **(B)** A549 cells were pre-treated with the MSK1 inhibitor SB747651 for 1 h and subsequently infected with SC35M at an MOI of 0.001. Supernatants were analyzed at the indicated time points by plaque assay.

IL-6, and IL-8 compared to the cells expressing the wildtype protein. The reason for this is unknown. We speculate, that other phosphorylation sites, such as S471 and/or others, compensate for the lack of S473 phosphorylation. The phosphorylation dynamics of other phosphorylation sites of TRIM28 are not well-understood and require further investigation. In summary, our data demonstrate that S473 phosphorylation is functionally linked to increased expression of IFN-β, IL-6, and IL-8 and support our hypothesis, that phosphorylation at S473 modulates the corepressor activity of TRIM28 during infection with HPAIV.

DISCUSSION

Infection of humans with HPAIV is often associated with severe tissue damage and multiple organ failure caused by excessive production of IFNs and proinflammatory cytokines. The involved pathways as well as the underlying mechanisms leading to cytokine overexpression are not yet fully resolved. This knowledge gap impairs the development of new immunomodulatory treatment options due to the lack of suitable targets for efficient immunomodulatory therapies.

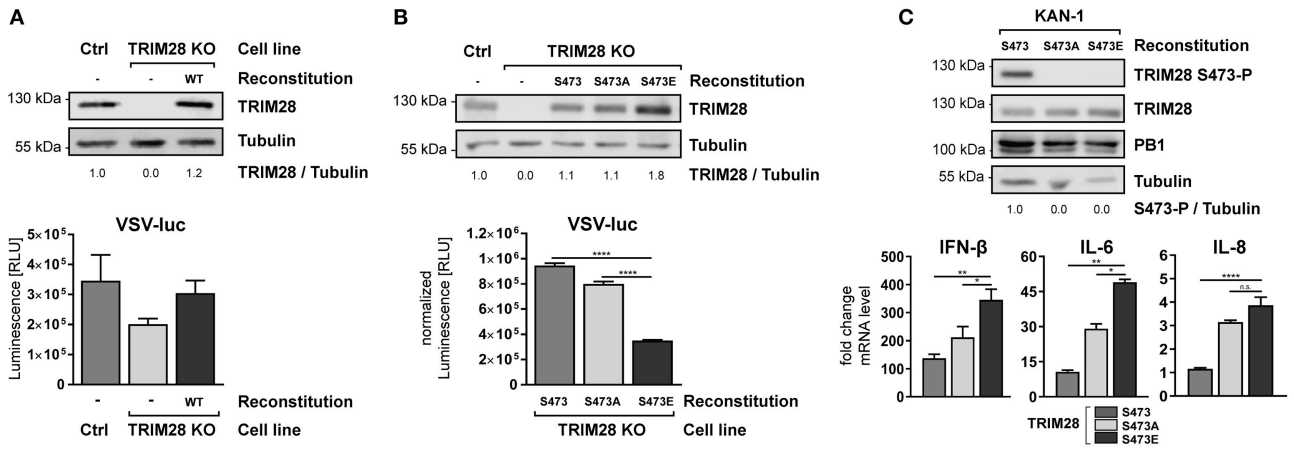

FIGURE 8 | Constitutive TRIM28 S473 phosphorylation potentiates the innate immune response. **(A)** TRIM28 KO cells were stably reconstituted with wildtype TRIM28 by retroviral transduction. Reconstituted cells were infected with VSV-luc at an MOI of 0.01 for 15 h. Cells were harvested and luciferase activity was measured. **(B)** In addition to wildtype TRIM28, phospho-mimetic variants (S473A and S473E) were stably reconstituted in TRIM28 KO cells. VSV-luc infection was carried out as described in **(A)**. Results are depicted as mean RLU (±SEM) normalized to TRIM28 expression. $^{****}p \leq 0.0001$; one-way ANOVA; Dunnett's multiple comparisons test. **(C)** Stably reconstituted TRIM28 KO cells were infected with KAN-1 at an MOI of 0.01. Total RNA was isolated 24 h p.i. and IFN-β, IL-6 and IL-8 mRNA levels were measured by qRT-PCR. mRNA levels are depicted as mean *n*-fold change (±SEM) over non-infected cells. n.s. $p > 0.03$, $^{*}p \leq 0.03$; $^{**}p \leq 0.002$; $^{****}p \leq 0.0001$; one-way ANOVA; Dunnett's multiple comparisons test.

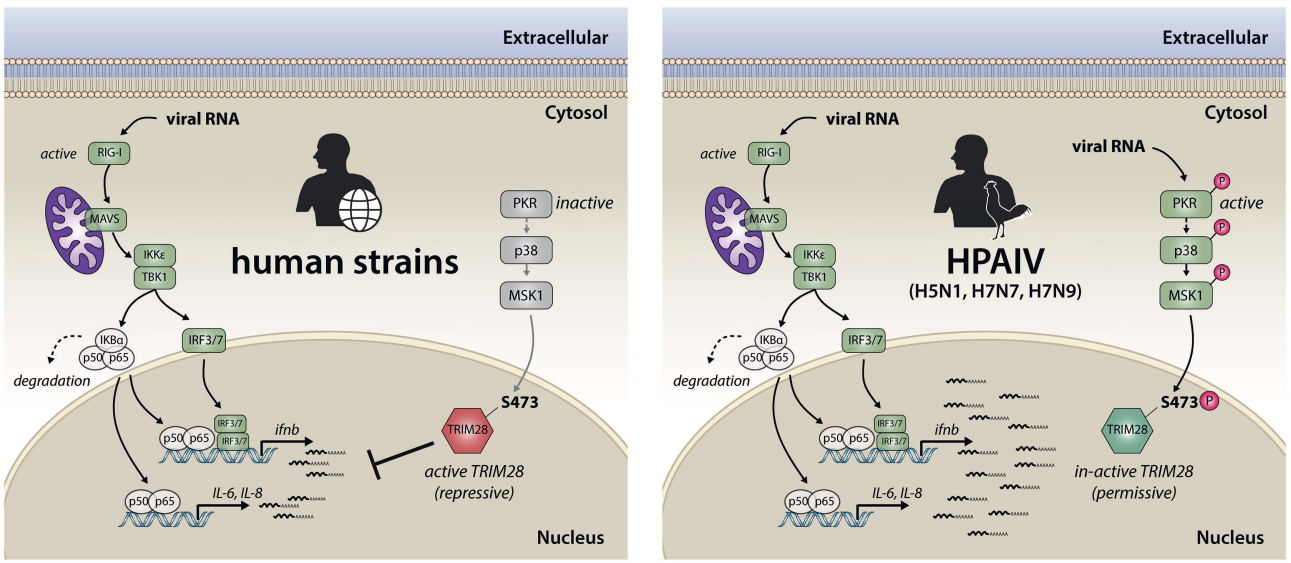

FIGURE 9 | Model for TRIM28-mediated upregulation of IFN-β and proinflammatory cytokines during infection with the HPAIV subtypes H5N1, H7N9 and H7N7. Early during IAV infection, viral RNAs are sensed by RIG-I. This initiates a signaling cascade, which includes the adaptor protein MAVS and results in the dimerization and nuclear translocation of the transcription factors IRF3/7. During infection with human adapted strains, this leads to non-pathological levels of IFN-β and proinflammatory cytokines, which usually leads to the clearance of IAV infection (left). In contrast, during infection with the HPAIV of the subtypes H5N1, H7N7 and H7N9 (right), the expression of IFN-β, IL-6 and IL-8 is potentiated. This is facilitated by PKR-mediated sensing of viral RNA followed by signal transduction via p38 and MSK1 resulting in phosphorylation of the transcriptional corepressor TRIM28 at serine 473. This leads to the release of TRIM28 corepressor activity and finally results in elevated expression of IFN-β, IL-6 and IL-8, which is commonly associated with tissue damage und high mortality during HPAIV infections.

Here, we report for the first time, that the cellular corepressor and negative immune regulator TRIM28 is the direct target of a signaling cascade involving the kinases PKR/p38/MSK1 during infection of human alveolar epithelial cells with HPAIV and contributes to the high expression levels of IFN-β, IL-6 and IL-8. Based on our results we hypothesize that TRIM28 is a key determinant for IFN-β overexpression and cytokine-mediated tissue damage and may represent a potential therapeutic target for the treatment of HPAIV-induced hypercytokinemia in humans.

TRIM28 is widely described as a genomic corepressor and negative immune regulator of cytokine expression in response to different immune stimuli. The described mechanisms of action involve its intrinsic E3 SUMO ligase activity as well as HP1-BD-mediated corepressor activity, which are assumed to be fine-tuned by SUMOylation and phosphorylation (24). The exact contribution of SUMOylation and phosphorylation to the regulation of TRIM28 activities has remained enigmatic. However, several reports have established an attractive regulatory model. While SUMOylation might control the general and genome wide repressor function of TRIM28, stimulus-dependent phosphorylation presumably regulates the de-repression of specific gene subsets (25) to allow stimulus- and stress-specific host responses. In line with this, Kubota et al. reported that tyrosine phosphorylation at positions Y449, Y458, and Y517 regulates HP1-binding and the controlled de-repression of genes required for stress tolerance and repair processes (60) and Li et al. demonstrated that phosphorylation of S824 regulates the expression of genes involved in cell cycle control and apoptosis in response to genotoxic stresses (25). Intriguingly, the authors of this report observed that the level of TRIM28 SUMOylation was decreased when S824 was mutated to aspartic acid to mimic constitutive phosphorylation, suggesting PTM crosstalk (25). Our own data suggest that phosphorylation of TRIM28 at S473 regulates the de-repression of IFN-β, IL-6 and IL-8. Nevertheless, we assume that additional sites could be involved, as we observed phosphorylation of the neighboring serine 471 in our phosphoproteomic screen (**Figure 1A**, lower panel). Supportive evidence for the biological relevance of phosphorylation of S473 and S471 comes from other proteomic studies in which these sites have been identified as phospho-acceptor sites (61, 62). In addition, both sites are also highly conserved in mice, rats and dogs, suggesting a biological important function. The p38/MSK1/TRIM28 signaling-axis was described previously to play a central role in myoblast differentiation. In these cells, TRIM28 phosphorylation controls the activity of the central transcriptional activator MyoD and thereby differentiation of myoblasts into myotubes (63). In addition, this report convincingly demonstrated that TRIM28 is a bona fide target of MSK1 in an *in vitro* kinase assay.

The detailed mechanism of TRIM28-mediated cytokine amplification during HPAIV infection remained unsolved. Based on available reports we assume that phosphorylation at S473 attenuates HP1- and chromatin-binding of TRIM28, which results in the loss of its corepressor function and leads to the de-repression of the described genes (49). However, other mechanism cannot be excluded. Because TRIM28 itself does not possess DNA binding activity, it is likely that cytokine repression occurs through the interaction with other transcription factors and chromatin remodeling enzymes. Indeed, TRIM28 was shown to interact and modulate the activity of diverse immune-related proteins, including NF-κB (64), STAT1 (28), STAT3 (29), IRF7 (30), and IRF5 (65). Nevertheless, a conjoint conclusion for the mode of action of TRIM28 is difficult to extract because diverse cell lines and immune stimuli were employed and the impact of S473 phosphorylation was not addressed. Thus, it needs to be investigated whether one of these factors facilitates TRIM28-mediated cytokine upregulation upon S473 phosphorylation. Recently, a novel model for TRIM28-mediated control of gene expression was proposed (66, 67). In this model, TRIM28 is involved in tethering of the 7SK snRNP complex to the promotor proximal regions of many rapid response genes that contain paused RNA Polymerase II (Pol II). Thereby, TRIM28 facilitates recruitment of the positive transcription elongation factor P-TEFb, which releases paused Pol II by phosphorylating serine 2 in the pol II C-terminal domain (CTD) and allows rapid elongation of transcription (62, 67, 68). Most intriguingly, TRIM28 was found to be associated with more than 13,000 promotor proximal regions, giving a rough estimation of how many genes might be regulated by TRIM28 (69). So far, the importance of S473 phosphorylation and SUMOylation for the control of immune-related genes has not yet been addressed in this model.

Phosphorylation of TRIM28 S473 was induced in a strain-dependent manner. This suggests that the degree of human adaptation as well as the reported characteristic to induce hypercytokinemia and tissue damage in humans might be determinants for TRIM28 phosphorylation during infection. To challenge this theory, we included the pandemic 2009 H1N1 virus in our analysis because it is a triple reassortant virus containing genes derived from humans, swine and birds and has acquired stepwise human adaptation in pigs prior to human transmission. In contrast to other pandemic IAV strains, H1N1pdm demonstrated weak virulence and low mortality rates (70) and human infections with this virus are not necessarily associated with hypercytokinemia and tissue damage. Thus, we expected that this strain would not trigger S473 phosphorylation. Indeed, we could not detect S473 phosphorylation with H1N1pdm, supporting our hypothesis (**Figure 1C**). The reasons for strain-dependent phosphorylation of TRIM28 on a molecular level are not known. It is tempting to speculate that it is mediated by virus intrinsic properties, such as avian specific protein signatures, differences in the NS1-mediated inhibition of PKR activation or other factors that underlie human adaptation. Alternatively, differences in replication speed or nuclear export of vRNPs, leading to accumulation of cytosolic vRNA cannot be excluded.

In addition to the novel role of TRIM28, our results suggest a new mechanism for PKR-mediated cytokine expression. Here, PKR senses viral RNA at a late time point during infection with HPAIV and provokes TRIM28 S473 phosphorylation via p38 and MSK1 with the consequence of excessive production of IFN-β, IL-6 and IL-8. PKR-mediated regulation of IFN-β expression in virus infected cells is described to be facilitated by activation of the translation elongation factor eIF2α as well as by compromised IFN-β mRNA stability (71, 72). Here we show, that in HPAIV-infected cells, PKR signals via p38/MSK1 to inactivate TRIM28 and potentiates the expression of IFN-β, IL-6 and IL-8 in human lung epithelial cells. At this moment, it remains unknown whether this pathway is also present in other IAV susceptible cell types, such as macrophages and dendritic cells, which could have severe immunopathological consequences as these cells are the main producers of IFNs and

cytokines. The results from the phosphoproteomic screen as well as western blot analysis demonstrate that S473 phosphorylation occurs at a surprisingly late time point during infection. We assume that PKR activation requires the accumulation of viral RNA in the cytoplasm, possibly in the form of exported vRNPs, in order to boost IFN-β and cytokine expression through S473 phosphorylation. This mechanism of PKR activation has been previously suggested for Influenza B viruses (73) but is not described for IAV. Although our results convincingly show that TRIM28 phosphorylation is mediated by PKR, we can currently not exclude that other signaling pathways and receptors, such as TLR3, which signals independently of the adaptor proteins MyD88 and MAVS, are also involved.

In summary, we propose a model for the TRIM28-mediated potentiation of cytokine expression during HPAIV infection. During infection with human adapted IAV strains, viral RNA is detected early during infection by RIG-I, which leads to the expression of non-pathological levels of IFN-β and proinflammatory cytokines (**Figure 9**, left side). In contrast, during infection with HPAIV of the H5N1, H7N7, and H7N9 subtypes cytosolic viral RNA is recognized by PKR, in addition to the RIG-I-dependent antiviral response. This leads to the activation of p38 and MSK1 and subsequently to phosphorylation of TRIM28 at S473 with the consequence of exacerbation of the ongoing immune response by amplification of IFN-β, IL-6 and IL-8 expression, which may lead to excessive immune cell recruitment and tissue inflammation (**Figure 9**, right side). We therefore propose, that controlling phosphorylation of TRIM28 by therapeutic interventions could prevent uncontrolled cytokine expression during HPAIV infections in humans.

AUTHOR CONTRIBUTIONS

TK and LB are responsible for the concept and designed the experiments. TK, FG, VG, LH, SS, and CN conducted the experiments. MB and JW generated knockout cell lines. GZ generated recombinant VSV-luc. LB and TK wrote the manuscript. LB, TK, SL, and UR discussed and edited the manuscript.

FUNDING

This project was funded by the Young Investigator fund Innovative Medizinische Forschung of the Medical Faculty Muenster (granted to LB), several grants of the Deutsche Forschungsgemeinschaft (DFG) (BR 5189/1-1 to LB and LU 47723/1 to SL) and SFB/CRC 1009/B2 and A6.

ACKNOWLEDGMENTS

We would like to thank René Riedke, Maria Bethke, Sebastian Kordes and Ludmilla Wixler for technical assistance and Martin Stehling for FACS-based isolation of single cell clones. We are grateful for discussion and critical comments to Martin Schwemmle and Yvonne Börgeling. We acknowledge support by Open Access Publication Fund of University of Muenster.

SUPPLEMENTARY MATERIAL

The Supplementary Material for this article can be found online at: https://www.frontiersin.org/articles/10.3389/fimmu.2018.02229/full#supplementary-material

REFERENCES

1. Claas EC, Osterhaus AD, van Beek R, De Jong JC, Rimmelzwaan GF, Senne DA, et al. Human influenza A H5N1 virus related to a highly pathogenic avian influenza virus. *Lancet* (1998) 351:472–7. doi: 10.1016/S0140-6736(97)11212-0
2. Yuen KY, Chan PK, Peiris M, Tsang DN, Que TL, Shortridge KF, et al. Clinical features and rapid viral diagnosis of human disease associated with avian influenza A H5N1 virus. *Lancet* (1998) 351:467–71. doi: 10.1016/S0140-6736(98)01182-9
3. de Jong MD, Simmons CP, Thanh TT, Hien VM, Smith GJ, Chau TN, et al. Fatal outcome of human influenza A (H5N1) is associated with high viral load and hypercytokinemia. *Nat Med.* (2006) 12:1203–7. doi: 10.1038/nm1477
4. Tisoncik JR, Korth MJ, Simmons CP, Farrar J, Martin TR, Katze MG. Into the eye of the cytokine storm. *Microbiol Mol Biol Rev.* (2012) 76:16–32. doi: 10.1128/MMBR.05015-11
5. Liu Q, Zhou YH, Yang ZQ. The cytokine storm of severe influenza and development of immunomodulatory therapy. *Cell Mol Immunol.* (2016) 13:3–10. doi: 10.1038/cmi.2015.74
6. Alexopoulou L, Holt AC, Medzhitov R, Flavell RA. Recognition of double-stranded RNA and activation of NF-kappaB by Toll-like receptor 3. *Nature* (2001) 413:732–8. doi: 10.1038/35099560
7. Pichlmair A, Reis e Sousa C. Innate recognition of viruses. *Immunity* (2007) 27:370–83. doi: 10.1016/j.immuni.2007.08.012
8. Darnell JE Jr., Kerr IM, Stark GR. Jak-STAT pathways and transcriptional activation in response to IFNs and other extracellular signaling proteins. *Science* (1994) 264:1415–21. doi: 10.1126/science.8197455
9. Willemsen J, Wicht O, Wolanski JC, Baur N, Bastian S, Haas DA, et al. Phosphorylation-Dependent Feedback Inhibition of RIG-I by DAPK1 Identified by Kinome-wide siRNA Screening. *Mol Cell* (2017) 65:403–15 e408. doi: 10.1016/j.molcel.2016.12.021
10. Reddy BA, Etkin LD, Freemont PS. A novel zinc finger coiled-coil domain in a family of nuclear proteins. *Trends Biochem Sci.* (1992) 17:344–5. doi: 10.1016/0968-0004(92)90308-V
11. Rajsbaum R, Garcia-Sastre A, Versteeg GA. TRIMmunity: the roles of the TRIM E3-ubiquitin ligase family in innate antiviral immunity. *J Mol Biol.* (2014) 426:1265–84. doi: 10.1016/j.jmb.2013.12.005
12. van Tol S, Hage A, Giraldo MI, Bharaj P, Rajsbaum R. The TRIMendous Role of TRIMs in Virus-Host Interactions. *Vaccines (Basel)* (2017) 5:E23. doi: 10.3390/vaccines5030023
13. Khetchoumian K, Teletin M, Mark M, Lerouge T, Cervino M, Oulad-Abdelghani M, et al. TIF1delta, a novel HP1-interacting member of the transcriptional intermediary factor 1 (TIF1) family expressed by elongating spermatids. *J Biol Chem.* (2004) 279:48329–41. doi: 10.1074/jbc.M404779200
14. Short KM, Cox TC. Subclassification of the RBCC/TRIM superfamily reveals a novel motif necessary for microtubule binding. *J Biol Chem.* (2006) 281:8970–80. doi: 10.1074/jbc.M512755200
15. Sripathy SP, Stevens J, Schultz DC. The KAP1 corepressor functions to coordinate the assembly of de novo HP1-demarcated microenvironments of heterochromatin required for KRAB zinc finger protein-mediated transcriptional repression. *Mol Cell Biol.* (2006) 26:8623–38. doi: 10.1128/MCB.00487-06
16. Iyengar S, Farnham PJ. KAP1 protein: an enigmatic master regulator of the genome. *J Biol Chem.* (2011) 286:26267–76. doi: 10.1074/jbc.R111.252569

17. Czerwinska P, Mazurek S, Wiznerowicz M. The complexity of TRIM28 contribution to cancer. *J Biomed Sci.* (2017) 24:63. doi: 10.1186/s12929-017-0374-4
18. Miles DC, de Vries NA, Gisler S, Lieftink C, Akhtar W, Gogola E, et al. TRIM28 is an epigenetic barrier to induced pluripotent stem cell reprogramming. *Stem Cells* (2017) 35:147–57. doi: 10.1002/stem.2453
19. Cammas F, Mark M, Dolle P, Dierich A, Chambon P, Losson R. Mice lacking the transcriptional corepressor TIF1beta are defective in early postimplantation development. *Development* (2000) 127:2955–63.
20. Rowe HM, Jakobsson J, Mesnard D, Rougemont J, Reynard S, Aktas T, et al. KAP1 controls endogenous retroviruses in embryonic stem cells. *Nature* (2010) 463:237–40. doi: 10.1038/nature08674
21. Wolf D, Goff SP. TRIM28 mediates primer binding site-targeted silencing of murine leukemia virus in embryonic cells. *Cell* (2007) 131:46–57. doi: 10.1016/j.cell.2007.07.026
22. Wolf D, Hug K, Goff SP. TRIM28 mediates primer binding site-targeted silencing of Lys1,2 tRNA-utilizing retroviruses in embryonic cells. *Proc Natl Acad Sci USA.* (2008) 105:12521–6. doi: 10.1073/pnas.0805540105
23. Chang PC, Fitzgerald LD, Van Geelen A, Izumiya Y, Ellison TJ, Wang DH, et al. Kruppel-associated box domain-associated protein-1 as a latency regulator for Kaposi's sarcoma-associated herpesvirus and its modulation by the viral protein kinase. *Cancer Res.* (2009) 69:5681–9. doi: 10.1158/0008-5472.CAN-08-4570
24. Ivanov AV, Peng H, Yurchenko V, Yap KL, Negorev DG, Schultz DC, et al. PHD domain-mediated E3 ligase activity directs intramolecular sumoylation of an adjacent bromodomain required for gene silencing. *Mol Cell* (2007) 28:823–37. doi: 10.1016/j.molcel.2007.11.012
25. Li X, Lee YK, Jeng JC, Yen Y, Schultz DC, Shih HM, et al. Role for KAP1 serine 824 phosphorylation and sumoylation/desumoylation switch in regulating KAP1-mediated transcriptional repression. *J Biol Chem.* (2007) 282:36177–89. doi: 10.1074/jbc.M706912200
26. Mascle XH, Germain-Desprez D, Huynh P, Estephan P, Aubry M. Sumoylation of the transcriptional intermediary factor 1beta (TIF1beta), the Co-repressor of the KRAB Multifinger proteins, is required for its transcriptional activity and is modulated by the KRAB domain. *J Biol Chem.* (2007) 282:10190–202. doi: 10.1074/jbc.M611429200
27. Versteeg GA, Rajsbaum R, Sanchez-Aparicio MT, Maestre AM, Valdiviezo J, Shi M, et al. The E3-ligase TRIM family of proteins regulates signaling pathways triggered by innate immune pattern-recognition receptors. *Immunity* (2013) 38:384–98. doi: 10.1016/j.immuni.2012.11.013
28. Kamitani S, Ohbayashi N, Ikeda O, Togi S, Muromoto R, Sekine Y, et al. KAP1 regulates type I interferon/STAT1-mediated IRF-1 gene expression. *Biochem Biophys Res Commun.* (2008) 370:366–70. doi: 10.1016/j.bbrc.2008.03.104
29. Tsuruma R, Ohbayashi N, Kamitani S, Ikeda O, Sato N, Muromoto R, et al. Physical and functional interactions between STAT3 and KAP1. *Oncogene* (2008) 27:3054–9. doi: 10.1038/sj.onc.1210952
30. Liang Q, Deng H, Li X, Wu X, Tang Q, Chang TH, et al. Tripartite motif-containing protein 28 is a small ubiquitin-related modifier E3 ligase and negative regulator of IFN regulatory factor 7. *J Immunol.* (2011) 187:4754–63. doi: 10.4049/jimmunol.1101704
31. Domingues P, Golebiowski F, Tatham MH, Lopes AM, Taggart A, Hay RT, et al. Global Reprogramming of host SUMOylation during influenza virus infection. *Cell Rep.* (2015) 13:1467–80. doi: 10.1016/j.celrep.2015.10.001
32. Hoffmann E, Neumann G, Kawaoka Y, Hobom G, Webster RG. A DNA transfection system for generation of influenza A virus from eight plasmids. *Proc Natl Acad Sci USA.* (2000) 97:6108–13. doi: 10.1073/pnas.100133697
33. Hoffmann M, Wu YJ, Gerber M, Berger-Rentsch M, Heimrich B, Schwemmle M, et al. Fusion-active glycoprotein G mediates the cytotoxicity of vesicular stomatitis virus M mutants lacking host shut-off activity. *J Gen Virol.* (2010) 91:2782–93. doi: 10.1099/vir.0.023978-0
34. Halbherr SJ, Ludersdorfer TH, Ricklin M, Locher S, Berger Rentsch M, Summerfield A, et al. Biological and protective properties of immune sera directed to the influenza virus neuraminidase. *J Virol.* (2015) 89:1550–63. doi: 10.1128/JVI.02949-14
35. Ran FA, Hsu PD, Wright J, Agarwala V, Scott DA, Zhang F. Genome engineering using the CRISPR-Cas9 system. *Nat Protoc.* (2013) 8:2281–308. doi: 10.1038/nprot.2013.143
36. Sanjana NE, Shalem O, Zhang F. Improved vectors and genome-wide libraries for CRISPR screening. *Nat Methods* (2014) 11:783–4. doi: 10.1038/nmeth.3047
37. Bender S, Reuter A, Eberle F, Einhorn E, Binder M, Bartenschlager R. Activation of type, I., and III interferon response by mitochondrial and peroxisomal MAVS and Inhibition by hepatitis C virus. *PLoS Pathog.* (2015) 11:e1005264. doi: 10.1371/journal.ppat.1005264
38. Olsen JV, Macek B. High accuracy mass spectrometry in large-scale analysis of protein phosphorylation. *Methods Mol Biol.* (2009) 492:131–42. doi: 10.1007/978-1-59745-493-3_7
39. Carpy A, Krug K, Graf S, Koch A, Popic S, Hauf S, et al. Absolute proteome and phosphoproteome dynamics during the cell cycle of Schizosaccharomyces pombe (Fission Yeast). *Mol Cell Proteomics* (2014) 13:1925–36. doi: 10.1074/mcp.M113.035824
40. Kathum OA, Schrader T, Anhlan D, Nordhoff C, Liedmann S, Pande A, et al. Phosphorylation of influenza A virus NS1 protein at threonine 49 suppresses its interferon antagonistic activity. *Cell Microbiol.* (2016) 18:784–91. doi: 10.1111/cmi.12559
41. Livak KJ, Schmittgen TD. Analysis of relative gene expression data using real-time quantitative PCR and the 2(-Delta Delta C(T)) method. *Methods* (2001) 25:402–8. doi: 10.1006/meth.2001.1262
42. Fouchier RA, Schneeberger PM, Rozendaal FW, Broekman JM, Kemink SA, Munster V, et al. Avian influenza A virus (H7N7) associated with human conjunctivitis and a fatal case of acute respiratory distress syndrome. *Proc Natl Acad Sci USA.* (2004) 101:1356–61. doi: 10.1073/pnas.0308352100
43. Belser JA, Lu X, Maines TR, Smith C, Li Y, Donis RO, et al. Pathogenesis of avian influenza (H7) virus infection in mice and ferrets: enhanced virulence of Eurasian H7N7 viruses isolated from humans. *J Virol.* (2007) 81:11139–47. doi: 10.1128/JVI.01235-07
44. Puzelli S, Rossini G, Facchini M, Vaccari G, Di Trani L, Di Martino A, et al. Human infection with highly pathogenic A(H7N7) avian influenza virus, Italy, (2013). *Emerg Infect Dis.* (2014) 20:1745–9. doi: 10.3201/eid2010.140512
45. Blasius M, Forment JV, Thakkar N, Wagner SA, Choudhary C, Jackson SP. A phospho-proteomic screen identifies substrates of the checkpoint kinase Chk1. *Genome Biol.* (2011) 12:R78. doi: 10.1186/gb-2011-12-8-r78
46. Bolderson E, Savage KI, Mahen R, Pisupati V, Graham ME, Richard DJ, et al. Kruppel-associated Box (KRAB)-associated co-repressor (KAP-1) Ser-473 phosphorylation regulates heterochromatin protein 1beta (HP1-beta) mobilization and DNA repair in heterochromatin. *J Biol Chem.* (2012) 287:28122–31. doi: 10.1074/jbc.M112.368381
47. King CA. Kaposi's sarcoma-associated herpesvirus kaposin B induces unique monophosphorylation of STAT3 at serine 727 and MK2-mediated inactivation of the STAT3 transcriptional repressor TRIM28. *J Virol.* (2013) 87:8779–91. doi: 10.1128/JVI.02976-12
48. Ziv Y, Bielopolski D, Galanty Y, Lukas C, Taya Y, Schultz DC, et al. Chromatin relaxation in response to DNA double-strand breaks is modulated by a novel ATM- and KAP-1 dependent pathway. *Nat Cell Biol.* (2006) 8:870–6. doi: 10.1038/ncb1446
49. Hu C, Zhang S, Gao X, Gao X, Xu X, Lv Y, et al. Roles of Kruppel-associated Box (KRAB)-associated Co-repressor KAP1 Ser-473 phosphorylation in DNA damage response. *J Biol Chem.* (2012) 287:18937–52. doi: 10.1074/jbc.M111.313262
50. Vijaya Lakshmi AN, Ramana MV, Vijayashree B, Ahuja YR, Sharma G. Detection of influenza virus induced DNA damage by comet assay. *Mutat Res.* (1999) 442:53–8. doi: 10.1016/S1383-5718(99)00058-3
51. Li N, Parrish M, Chan TK, Yin L, Rai P, Yoshiyuki Y, et al. Influenza infection induces host DNA damage and dynamic DNA damage responses during tissue regeneration. *Cell Mol Life Sci.* (2015) 72:2973–88. doi: 10.1007/s00018-015-1879-1
52. Kato H, Takeuchi O, Sato S, Yoneyama M, Yamamoto M, Matsui K, et al. Differential roles of MDA5 and RIG-I helicases in the recognition of RNA viruses. *Nature* (2006) 441:101–5. doi: 10.1038/nature04734
53. Rehwinkel J, Tan CP, Goubau D, Schulz O, Pichlmair A, Bier K, et al. RIG-I detects viral genomic RNA during negative-strand RNA virus infection. *Cell* (2010) 140:397–408. doi: 10.1016/j.cell.2010.01.020
54. Clemens MJ. PKR–a protein kinase regulated by double-stranded RNA. *Int J Biochem Cell Biol.* (1997) 29:945–9. doi: 10.1016/S1357-2725(96)00169-0

55. Lee DC, Cheung CY, Law AH, Mok CK, Peiris M, Lau AS. p38 mitogen-activated protein kinase-dependent hyperinduction of tumor necrosis factor alpha expression in response to avian influenza virus H5N1. *J Virol.* (2005) 79:10147–54. doi: 10.1128/JVI.79.16.10147-10154.2005
56. Taghavi N, Samuel CE. Protein kinase PKR catalytic activity is required for the PKR-dependent activation of mitogen-activated protein kinases and amplification of interferon beta induction following virus infection. *Virology* (2012) 427:208–16. doi: 10.1016/j.virol.2012.01.029
57. Borgeling Y, Schmolke M, Viemann D, Nordhoff C, Roth J, Ludwig S. Inhibition of p38 mitogen-activated protein kinase impairs influenza virus-induced primary and secondary host gene responses and protects mice from lethal H5N1 infection. *J Biol Chem.* (2014) 289:13–27. doi: 10.1074/jbc.M113.469239
58. Rouse J, Cohen P, Trigon S, Morange M, Alonso-Llamazares A, Zamanillo D, et al. A novel kinase cascade triggered by stress and heat shock that stimulates MAPKAP kinase-2 and phosphorylation of the small heat shock proteins. *Cell* (1994) 786:1027–1037. doi: 10.1016/0092-8674(94)90277-1
59. Mayer TZ, Simard FA, Cloutier A, Vardhan H, Dubois CM, McDonald PP. The p38-MSK1 signaling cascade influences cytokine production through CREB and C/EBP factors in human neutrophils. *J Immunol.* (2013) 191:4299–307. doi: 10.4049/jimmunol.1301117
60. Kubota S, Fukumoto Y, Aoyama K, Ishibashi K, Yuki R, Morinaga T, et al. Phosphorylation of KRAB-associated protein 1 (KAP1) at Tyr-449, Tyr-458, and Tyr-517 by nuclear tyrosine kinases inhibits the association of KAP1 and heterochromatin protein 1alpha (HP1alpha) with heterochromatin. *J Biol Chem.* (2013) 288:17871–83. doi: 10.1074/jbc.M112.437756
61. Beausoleil SA, Jedrychowski M, Schwartz D, Elias JE, Villen J, Li J, et al. Large-scale characterization of HeLa cell nuclear phosphoproteins. *Proc Natl Acad Sci USA.* (2004) 101:12130–5. doi: 10.1073/pnas.0404720101
62. Molina H, Horn DM, Tang N, Mathivanan S, Pandey A. Global proteomic profiling of phosphopeptides using electron transfer dissociation tandem mass spectrometry. *Proc Natl Acad Sci USA.* (2007) 104:2199–204. doi: 10.1073/pnas.0611217104
63. Singh K, Cassano M, Planet E, Sebastian S, Jang SM, Sohi G, et al. A KAP1 phosphorylation switch controls MyoD function during skeletal muscle differentiation. *Genes Dev.* (2015) 29:513–25. doi: 10.1101/gad.254532.114
64. Kamitani S, Togi S, Ikeda O, Nakasuji M, Sakauchi A, Sekine Y, et al. Kruppel-associated box-associated protein 1 negatively regulates TNF-alpha-induced NF-kappaB transcriptional activity by influencing the interactions among STAT3, p300, and NF-kappaB/p65. *J Immunol.* (2011) 187:2476–83. doi: 10.4049/jimmunol.1003243
65. Eames HL, Saliba DG, Krausgruber T, Lanfrancotti A, Ryzhakov G, Udalova IA. KAP1/TRIM28: an inhibitor of IRF5 function in inflammatory macrophages. *Immunobiology* (2012) 217:1315–24. doi: 10.1016/j.imbio.2012.07.026
66. Bunch H, Calderwood SK. TRIM28 as a novel transcriptional elongation factor. *BMC Mol Biol.* (2015) 16:14. doi: 10.1186/s12867-015-0040-x
67. McNamara RP, Reeder JE, McMillan EA, Bacon CW, McCann JL, D'Orso I. KAP1 Recruitment of the 7SK snRNP Complex to Promoters Enables Transcription Elongation by RNA Polymerase, I. *I Mol Cell* (2016) 61:39–53. doi: 10.1016/j.molcel.2015.11.004
68. Zhu Y, Pe'ery T, Peng J, Ramanathan Y, Marshall N, Marshall T, et al. Transcription elongation factor P-TEFb is required for HIV-1 tat transactivation *in vitro*. *Genes Dev.* (1997) 11:2622–32. doi: 10.1101/gad.11.20.2622
69. McNamara RP, Guzman C, Reeder JE, D'Orso I. Genome-wide analysis of KAP1, the 7SK snRNP complex, and RNA polymerase II. *Genom Data* (2016) 7:250–5. doi: 10.1016/j.gdata.2016.01.019
70. Wang TT, Palese P. Unraveling the mystery of swine influenza virus. *Cell* (2009) 137:983–5. doi: 10.1016/j.cell.2009.05.032
71. Levin D, Ernst V, London IM. Effects of the catalytic subunit of cAMP-dependent protein kinase (type II) from reticulocytes and bovine heart muscle on protein phosphorylation and protein synthesis in reticulocyte lysates. *J Biol Chem.* (1979) 254:7935–41.
72. Schulz O, Pichlmair A, Rehwinkel J, Rogers NC, Scheuner D, Kato H, et al. Protein kinase R contributes to immunity against specific viruses by regulating interferon mRNA integrity. *Cell Host Microbe* (2010) 7:354–61. doi: 10.1016/j.chom.2010.04.007
73. Dauber B, Martinez-Sobrido L, Schneider J, Hai R, Waibler Z, Kalinke U, et al. Influenza B virus ribonucleoprotein is a potent activator of the antiviral kinase PKR. *PLoS Pathog.* (2009) 5:e1000473. doi: 10.1371/journal.ppat.1000473

Conflict of Interest Statement: The authors declare that the research was conducted in the absence of any commercial or financial relationships that could be construed as a potential conflict of interest.

frontiers in Immunology

ORIGINAL RESEARCH
published: 03 December 2018
doi: 10.3389/fimmu.2018.02560

Hantavirus-Driven PD-L1/PD-L2 Upregulation: An Imperfect Viral Immune Evasion Mechanism

*Martin J. Raftery, Mohammed O. Abdelaziz, Jörg Hofmann and Günther Schönrich**

Berlin Institute of Health, Institute of Virology, Charité–Universitätsmedizin Berlin, Humboldt-Universität zu Berlin, Berlin, Germany

Viruses often subvert antiviral immune responses by taking advantage of inhibitory immune signaling. We investigated if hantaviruses use this strategy. Hantaviruses cause viral hemorrhagic fever (VHF) which is associated with strong immune activation resulting in vigorous CD8+ T cell responses. Surprisingly, we observed that hantaviruses strongly upregulate PD-L1 and PD-L2, the ligands of checkpoint inhibitor programmed death-1 (PD-1). We detected high amounts of soluble PD-L1 (sPD-L1) and soluble PD-L2 (sPD-L2) in sera from hantavirus-infected patients. In addition, we observed hantavirus-induced PD-L1 upregulation in mice with a humanized immune system. The two major target cells of hantaviruses, endothelial cells and monocyte-derived dendritic cells, strongly increased PD-L1 and PD-L2 surface expression upon hantavirus infection *in vitro*. As an underlying mechanism, we found increased transcript levels whereas membrane trafficking of PD-L1 was not affected. Further analysis revealed that hantavirus-associated inflammatory signals and hantaviral nucleocapsid (N) protein enhance PD-L1 and PD-L2 expression. Cell numbers were strongly reduced when hantavirus-infected endothelial cells were mixed with T cells in the presence of an exogenous proliferation signal compared to uninfected cells. This is compatible with the concept that virus-induced PD-L1 and PD-L2 upregulation contributes to viral immune escape. Intriguingly, however, we observed hantavirus-induced CD8+ T cell bystander activation despite strongly upregulated PD-L1 and PD-L2. This result indicates that hantavirus-induced CD8+ T cell bystander activation bypasses checkpoint inhibition allowing an early antiviral immune response upon virus infection.

Keywords: bystander activation, hantaviruses, viral immune evasion, PD-L1, PD-L2, PD-1, CD86

OPEN ACCESS

Edited by:
Michael H. Lehmann, Ludwig-Maximilians-Universität München, Germany

Reviewed by:
Tony Schountz, Colorado State University, United States
Dimitris Lagos, University of York, United Kingdom
Jorg Goronzy, Stanford University, United States

****Correspondence:***
Günther Schönrich
guenther.schoenrich@charite.de

Specialty section:
This article was submitted to Cytokines and Soluble Mediators in Immunity, a section of the journal Frontiers in Immunology

Received: *25 May 2018*
Accepted: *17 October 2018*
Published: *03 December 2018*

Citation:
Raftery MJ, Abdelaziz MO, Hofmann J and Schönrich G (2018) Hantavirus-Driven PD-L1/PD-L2 Upregulation: An Imperfect Viral Immune Evasion Mechanism. Front. Immunol. 9:2560. doi: 10.3389/fimmu.2018.02560

INTRODUCTION

The immune response to infection is regulated not only by signaling through antigen receptors but also by co-receptors (1). The principal stimulatory co-receptor CD28 is constitutively expressed on T cells and interacts with CD80 and CD86 expressed on activated professional antigen-presenting cells (APCs) such as dendritic cells (DCs) (2). In contrast, programmed death-1 (PD-1), a member of the CD28 family, is a key negative regulator of immune responses (3). PD-1 is expressed on activated T cells whereas the known PD-1 ligands, PD-L1 and PD-L2, are detected on professional APCs similar to CD80 and CD86 (4). In addition, PD-L1 is expressed by non-hematopoietic cells such as endothelial cells (5–8). PD-L1

is further upregulated by proinflammatory cytokines that are released during virus infections such as type I and type II interferon (9). These pro-inflammatory cytokines also enhance PD-L2 expression, which is usually expressed at only low levels by a restricted number of cell types such as dendritic cells (DCs) (9).

Viruses have evolved mechanisms to exploit host inhibitory receptor signaling for subversion of host immune responses (10). Persisting viruses such as human immunodeficiency virus type 1 (HIV-1), hepatitis B virus (HBV) and hepatitis C virus (HCV) drive virus-specific CD8+ T cells into a dysfunctional or "exhausted" phenotype that is characterized by increased PD-1 expression (11, 12). In accordance, blockade of PD-1 or its ligands in chronic viral infection can enhance virus-specific $CD8^+$ T-cell responses and reduce the viral load. The functional consequences of PD-L1 upregulation during acute viral infection are less clear (13). For example, CD8+ T cell responses are impaired and immunopathology is attenuated by the PD-1 pathway during acute virus infections of the lower respiratory tract (14). On the other hand, it has been reported that PD-L1 upregulation on DCs contribute to the antiviral defense during acute HSV-1 infection (15). Moreover, during acute Friend retrovirus infection CD8+ T cells expressing high levels of PD-1 were both cytotoxic and critical for virus control (16).

Viral hemorrhagic fever (VHF) is a term for a group of similar but distinct zoonotic human diseases that are caused by RNA viruses including hantaviruses. Humans are infected with hantaviruses after inhalation of aerosols that contain virions derived from the natural host reservoirs, mostly rodents (17). The hallmarks of VHF are increased vascular permeability and loss of platelets (18). Hantaviruses are known to replicate without causing obvious cytopathic effects. As with other VHFs dysregulated immune responses play a role in hantavirus-associated diseases (19, 20). Paradigmatic experiments with lymphocytic choriomeningitis virus (LCMV)-infected mice have shown that PD-L1 is critical for prevention of immunopathology and virus-induced dysfunction such as vascular leakage (21, 22). Thus, it is important to understand how hantavirus replication modulates PD-L1 and PD-L2. In this study, we investigated how hantavirus replication affects the key stimulatory and inhibitory checkpoints of immune responses and explored the functional consequences thereof.

MATERIALS AND METHODS

Ethics Statement

The analyses of human sera were in accordance with the ethical standards of the institutional research committee and with the 1964 Helsinki declaration and its later amendments or comparable ethical standards. For this retrospective study, formal consent is not required. Buffy coat preparations were purchased from German Red Cross (Dresden). Blood samples were taken with the approval of the ethics committee of the Charité–Universitätsmedizin Berlin. Written informed consent was obtained from all donors.

Cells

Vero E6 and RPE-1 cells were cultured in Dulbecco's MEM (Gibco) supplemented with 10% hiFCS (BioWhittaker), 2 mM L-glutamine, penicillin and streptomycin (PAA). HUVECs were generated and cultivated as described (23). Adherent cells were passaged by first washing with PBS (Biochrom), addition of trypsin until cells detached and finally addition of FCS-containing medium to stop trypsin. HEL cells, an erythroleukemia suspension cell line, were cultured in RPMI 1640 (Gibco) with 10% hiFCS, 2 mM L-glutamine, penicillin and streptomycin (PAA). Huh7.5 cells is a human hepatoma cell line, which expresses an endogenous RIG-I with a mutation (T55I) in the first caspase-recruiting domain. This mutated RIG-I acts as a dominant-negative inhibitor (24). Transduced Huh7.5 clones overexpressing constitutive active RIG-I have been generated previously and were cultured as described (25). Huh7.5 cells were cultured as previously described (26).

Density gradient centrifugation using Ficoll-Paque was used to isolate PBMCs from buffy coat units (DRK, Dresden). In short, blood diluted 1:1 with RPMI wash (RPMI 1640, 2% heat-inactivated FCS and 0.2 mM EDTA) was layered onto Ficoll (PAA) and centrifuged at 800 *g*, 30 min RT. PBMC were isolated from the interface, washed twice and CD14+ cells isolated using Blood CD14 isolation kit (Miltenyi Biotec). CD14+ monocytes were used to generate immature DCs by cultivation in RPMI1640 with 10% hiFCS (Hyclone), 2 mM L-glutamine, penicillin and streptomycin (PAA) and further supplemented with 500 IU/ml GM-CSF (ImmunoTools) and 200 IU/ml IL-4 (ImmunoTools). Medium and cytokines were changed every 2–3 days, cells were used for experiments at day 6.

Cytokines And Pathogen-Associated Molecular Patterns (PAMPs)

IFN-α, IFN-β, and IFN-γ were provided by ImmunoTools. Further samples of IFN-β were supplied by R&D Systems. TLR3 agonist polyinosinic:polycytidylic acid [poly(I:C)] and polydeoxyadenylic:polydeoxythymidylic acid [poly(dA:dT)], which indirectly stimulates retinoic acid–inducible gene I (RIG-I), were obtained from InvivoGen. Poly(I:C) was used at 10 μg/ml and poly(dA:dT) at 1 μg/ml.

Serum Samples And ELISAs

Samples from patients infected with Puumala virus (PUUV) or Dobrava-Belgrade virus (DOBV) were collected for diagnostic purposes and were anonymized and stored before being tested retrospectively. Routine diagnostic testing included qPCR of the L segment of hantavirus from RNA isolated from the sera, positivity indicating the presence of active viral infection and thus an acute infection. All serum samples were stored at −80°C before use. The histone/dsDNA complexes were determined using Cell Death Detection $ELISA^{PLUS}$ (Roche) for quantification of neutrophil extracellular traps (NETs) in the serum as previously described (27). Human sPD-L1 and sPD-L2 levels were determined by using ELISA kits from R&D Systems, whereas the ELISA for measuring soluble CD86 (sCD86) was provided by PromoKine.

Flow Cytometry of Surface Molecules

Cells were harvested and washed twice in ice-cold FACS washing solution. Cells were then resuspended in 50 μl FACS blocking solution, containing the primary antibody in appropriate dilution, and incubated for 1 h. Cells stained with directly-coupled antibodies were washed and analyzed. For uncoupled primary antibodies after incubation cells were again washed twice with FACS wash and secondary antibody, diluted in FACS block solution, was added. After 45 min the cells were washed with FACS wash solution and resuspended in FACS fixation solution. For quantifying fluorescence of labeled cells a FACSCalibur® (BD Biosciences) was used. Results were evaluated with the flow cytometry analysis software programs CellQuestPro® and FlowJo V10 (BD Biosciences).

Transfection

Transfection was undertaken using plasmid pcDNA3.1 HTNV N or empty pcDNA3.1 as control (1 μg) using Lipofectamine 3000 transfection reagent according to the manufacturer's protocol, including Optimem medium (Thermo Fischer Scientfic).

Antibodies And Staining Reagents

For flow cytometry and functional studies, respectively, the following antibodies and staining reagents were used: anti-CD40 (clone 5C3), anti-CD54 (clone HA58), anti-CD80 (L307.4), anti-CD83 (clone HB15e), anti-CD107a (H4A3), and anti-B7-H2 (clone 2D3) were supplied by BD PharMingen; anti-PD-1 (clone J116), anti-PD-L1 (clone MIH1), and anti-PD-L2 (clone MIH18), anti- B7-H3 (clone H74), anti-B7-H4 (clone MIH35) were purchased from eBioscience; anti-CD86 (clone IT2.2) was supplied by ImmunoTools; anti-DC-SIGN (Clone MR-1) was purchased from Acris; anti-MHC class I (clone w6/32) and II (clone L243) were produced in-house; HCMV pp65 495-503 loaded NTA HLA-A2 tetramer reagents were obtained from TCMetrix. Secondary antibodies coupled to fluorochromes were supplied by Dianova. Blocking monoclonal antibodies directed against human IL-15 (clone 34559) and anti-human IFNR chain 2 (clone MMHAR-2) were supplied by R&D Systems. Cells were incubated with blocking antibodies or isotype-matched control antibodies for 1 h before exposure to virus. Isotype-matched control antibodies were supplied by BD PharMingen. For immunohistochemistry human-specific FITC-coupled anti-MPO (clone 7.17; ImmunoTools) and polyclonal goat anti human PD-L1 (R&D Systems) were used with bovine anti goat Fab fragment Alexa 594-coupled (Dianova) as secondary antibody, all used at 1:300 dilution.

PD-L1 Uptake Protocol

Cells were incubated with PE-coupled anti-PD-L1 antibody for 1 h at 4°C or 37°C for 4 h before being washed and analyzed by flow cytometry. Uptake was calculated by subtracting MFI at 37°C from MFI at 4°C. Uptake of HTNV infected cells was then compared to uninfected cells.

T Cell Assay

CD4+ cells were isolated from PBMCs using CD4-coupled beads (Miltenyi) and frozen on liquid nitrogen until use. HUVECs infected with HTNV at a MOI of 1.5 were incubated in flat-bottom 96-well plates for 4 days before being were mixed with allogenic CD4+ cells at a ratio of 1:4 and treated with PHA at 5ug/ml for 2 days. Proliferation was measured by MTT dye test (EZ4U-test).

Viruses

Virus stocks of Hantaan virus (HTNV, strain 76-118) and Tula virus (TULV, strain Moravia) were propagated on VeroE6 cells in a biosafety level 3 (BSL3) laboratory as previously described (28). For virus titration, supernatants from hantavirus-infected cells were incubated with Vero E6 cells and subsequently focus-forming units (FFU) were counted in a chemiluminescence detection assay (29). Virus stocks were regularly tested for mycoplasma by PCR and stored at −80°C before use. In order to infect cells virions were allowed to adsorb to cells for 1 h. After infection cells were washed three times with medium before incubation in a humidified incubator at 37°C. Uninfected cells treated with medium instead of virions were used as mock control. Herpes simplex virus type 1 *(HSV-1)* strain KOS and Vesicular stomatitis virus (VSV, strain Indiana) was propagated and titrated as previously described. Titres were determined by plaque assay on Vero E6 cells and expressed as PFU per milliliter (30). UV inactivation was performed for 5 min and the remaining titer was tested and found to be less than 1 FFU/ml.

qPCR

RNA was isolated from cells using RNeasy Plus mini kit (Quiagen) and reverse transcribed using SuperScript III (Thermo Fisher Scientific). qPCR was performed on a qTOWER^3 (Analytik Jena) using PrimeTime gene expression master mix and PrimeTime primers (IDT). The input RNA was normalized using average expression of β-actin and cyclophilin B housekeeping genes.

Humanized Mouse Model

The generation of mice with a humanized immune system has been described elsewhere (31). Briefly, NSG mice expressing HLA-A2, a human MHC class I molecule, were humanized by reconstitution with HLA-A2+ human CD34+ hematopoietic stem cells isolated from umbilical cord blood. Engraftment was evaluated at 11 weeks post inoculation by cytofluorimetric analysis of PBMCs. Successfully engrafted mice were infected i.p. with 10^5 focus-forming units (FFU) of HTNV (strain 76-118). Infection was successful as determined by qPCR from sera. Twenty-Two days post infection mice were sacrificed and liver, kidney, lungs and spleen fixed and mounted in paraffin blocks. The infection experiments were approved by the governmental animal-welfare committee of the state Berlin, Germany (G 0013/12).

ImageJ Analysis

Six cell-rich areas of five to twelve cells each were analyzed on each slide. Cell density was determined blind using DAPI staining and subsequently the mean intensity of staining of human PD-L1 (Texas Red) was determined.

Statistical Analysis

Student's *t*-test and 1 way ANOVA test with Bonferroni correction were used to determine statistical significance. *P*-values below 0.05 (95% confidence) were considered to be significant. Prism 6 software (GraphPad) was used for statistical analysis.

RESULTS

Strong Upregulation of PD-1 Ligands in Hantavirus-Infected Patients and in an Animal Model of Hantavirus Infection

Initially we tested if hantaviruses modulate the expression of the ligands of checkpoint inhibitor PD-1 during clinical infection of humans. For this purpose, we measured the amount of soluble PD-L1 (sPD-L1) and soluble PD-L2 (sPD-L2) in sera from hantavirus-infected patients. The level of both sPD-L1 (**Figure 1A**) and sPD-L2 (**Figure 1B**) were strongly upregulated in sera from hantavirus-infected patients as compared to normal healthy individuals. Sequential samples from the same patients indicate that for both PUUV and DOBV sPD-L1 levels decrease with time indicating active regulation and that acute samples still with active virus replication (hantavirus RNA positive) have high sPD-L1 levels (**Figure 1C**). Similarly, PUUV samples early in convalescence (IgM > IgG) had significantly raised sPD-L1 compared to samples taken later (IgG > IgM) (**Figure 1D**). We also detected elevated levels of neutrophil extracellular traps (NETs), a marker for recent hantavirus infection, in these sera (**Figure 1E**) (27, 32). The level of sPD-L1 detected in culture supernatants and plasma of patients is known to correlate with the level of membrane-bound PD-L1 (33, 34). Taken together, PD-L1 and PD-L2 are strongly upregulated in hantavirus infected patients. Using a previously established animal model of hantavirus-induced immunopathology we analyzed the spleen of hantavirus-infected mice with a humanized immune system as previously published (31). We observed enhanced expression of human PD-L1 in the spleen (**Figure 1F**) in addition to high levels of human myeloperoxidase (MPO)-expressing cells, presumably neutrophils (data not shown). Taken together this data shows that PD-L1 and PD-L2 are strongly upregulated during hantavirus infection *in vivo*.

Hantavirus-Infected Human Dendritic Cells Upregulate Both Costimulatory Molecules as Well as PD-L1/PD-L2

Next we investigated the possible source of sPD-L1 and sPD-L2 seen in sera from hantavirus-infected patients. The production of sPD-L1 by proteolytic cleavage of membrane-bound PD-L1 is a feature of activated monocyte-derived DCs (35). This important immunoregulatory cell type is susceptible to hantavirus infection (36–39). As previously reported, immature DCs infected with Hantaan virus (HTNV), the most common cause of human hantavirus infections, upregulated adhesion molecules and MHC molecules (**Figure 2A**). In addition, HTNV increased expression of costimulatory molecules on the surface of immature DCs (**Figure 2B**). Intriguingly, HTNV infection resulted in enhanced expression of both PD-L1 and PD-L2 whereas PD-1 was barely detectable on the surface of uninfected and HTNV-infected immature DCs (**Figure 3A**). In contrast, HTNV-infected DCs did not upregulate other members of the B7 family such as B7-H2, B7-H3, and B7-H4. (**Figure 3B**) (40). In summary, hantavirus replication in DCs drives surface expression of both T cell costimulatory molecules such as CD86 as well as the T cell inhibitory molecules PD-L1/PD-L2.

Hantavirus Regulates PDL1/PDL2 Expression on the Transcription Level

In further experiments we analyzed the mechanism upregulating PD-L1 and PD-L2 during hantavirus infection of DCs. PD-L1 expression can be regulated on the genetic, transcriptional, post-transcriptional and post-translational level (41). We first determined the number of PD-L1 and PD-L2 transcripts in HTNV-infected DCs and DCs exposed to IFN-α by qPCR. HTNV increased the number of transcripts encoding PD-L1 and PD-L2 (**Figure 4A**). IFN-α also upregulated PD-L1 and PD-L2 transcripts. We also tested whether HTNV modulates DCs trafficking of PD-L1. As shown in **Figure 4B** HTNV-infected DCs endocytosed PD-L1 as efficiently as uninfected control cells excluding altered endocytosis kinetics as a mechanism of PD-L1 upregulation. In conclusion, hantaviruses increase the number of PD-L1/PD-L2 transcripts but do not modulate endocytosis of the corresponding proteins.

Hantavirus-Associated Inflammatory Signals Including Hantaviral N Protein Drive PD-L1 Expression

Next we examined which hantavirus-associated inflammatory stimuli modulate PD-L1 expression on immature DCs. IFN-γ and to a lesser extent IFN-α upregulated cell-surface PD-L1 (**Figure 5A**). Hantavirus replication triggers pattern recognition receptors (PRRs) such as toll-like receptor 3 (TLR3) and retinoic acid–inducible gene I (RIG-I) (30, 42, 43). Strikingly, TLR3 agonist poly(I:C) strongly increased PD-L1 expression on immature DCs (**Figure 5A**). Poly(I:C) similarly induced PD-L2 (data not shown). In contrast, immature DCs treated with RIG-I activating signals such as UV-inactivated VSV or poly(dA:dT) did not show increased PD-L1 expression (**Figure 5A**). The absence of PD-L1 upregulation after stimulation of the RIG-I pathway was confirmed by using Huh7.5 cells expressing a constitutive active RIG-I molecule (RIG-CA) (25). These cells did not express elevated PD-L1 levels compared to the untreated cells whereas Huh7.5 cells treated with IFN-γ upregulated PD-L1 compared to untreated Huh7.5 cells (**Figure 5B**). We also tested the effect of hantaviral nucleocapsid (N) protein, which has many diverse functional activities during the viral life cycle (44). As shown in **Figure 5C** expression of N protein in HEL cells, a human erythroleukemia cell line, resulted in PD-L1 upregulation. In summary, type I IFN, hantaviral N protein, and TLR3 signaling induced PD-L1 expression whereas RIG-I signaling had no effect.

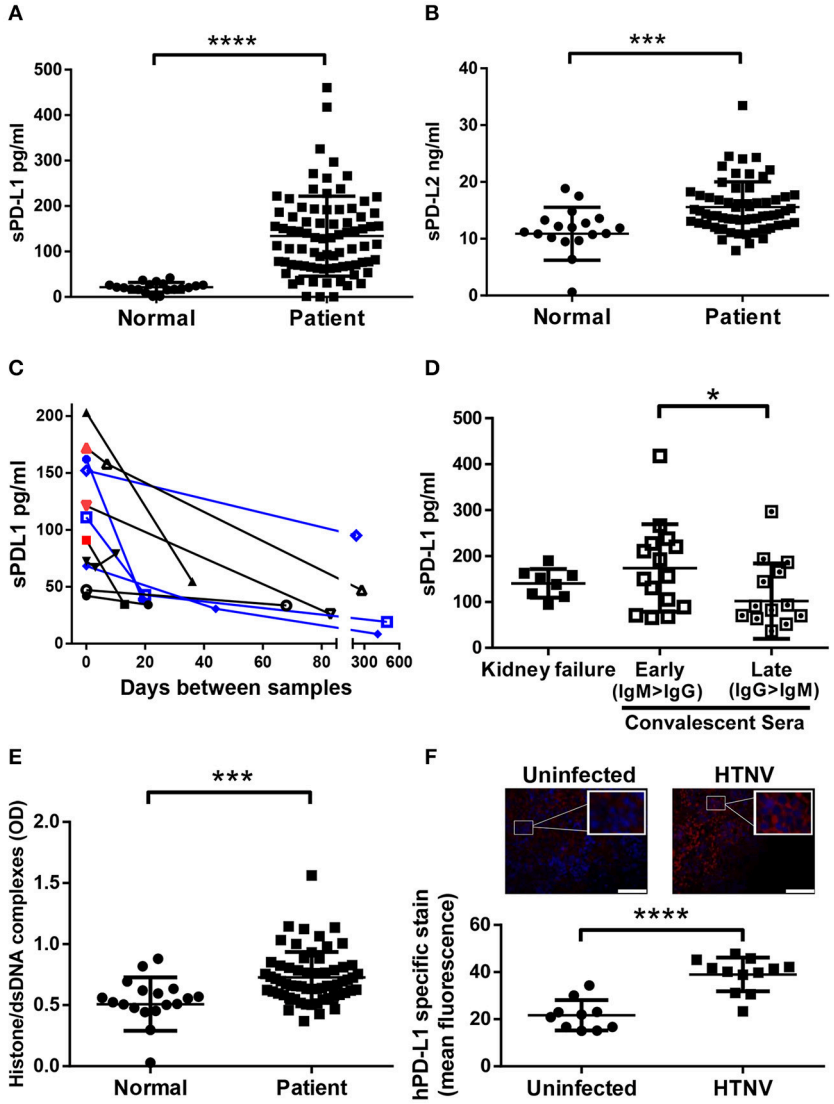

FIGURE 1 | Levels of sPD-L1, sPD-L2, hantavirus-specific IgG and NETs in sera from hantavirus-infected patients. Sera from normal healthy individuals or convalescent hantavirus-infected patients (after the viremic phase) was tested by ELISA for levels of **(A)** sPD-L1 and **(B)** sPD-L2. Error bars represent the mean ± SD (****$p < 0.0001$, ***$p < 0.001$, paired Student's t-test). **(C)** Sequential sera samples from patients with PUUV (black) or DOBV (blue) were tested for sPD-L1. Red samples also tested additionally positive for hantavirus RNA and are therefore acute infections. **(D)** Levels of sPD-L1 in patients with kidney failure or in convalescence were further analyzed. Convalescent sera were separated into early convalescent (IgM dominant) or late convalescent (IgG dominant). Error bars represent the mean ± SD (*$p < 0.05$, paired Student's t-test). **(E)** The level of NETs in sera from normal healthy individuals or convalescent hantavirus-infected patients was determined as previously described (27). Error bars represent the mean ± SD (***$p < 0.001$, paired Student's t-test). **(F)** Spleen sections from uninfected or HTNV-infected humanized mice were stained for human PD-L1 (red) and nuclei (blue). HTNV-infected spleen sections show large areas of human cells with enhanced PD-L1 expression in comparison to uninfected spleen sections (upper left and right panel; inserts show higher magnification of cells; bars represent 100 μm). Slides from uninfected and HTNV-infected humanized and unreconstituted mice animals (N = 3 each group; 12 total) were analyzed using ImageJ to determine the intensity of human PD-L1 staining (Lower panel). Error bars represent the mean ± SEM (****$p < 0.0001$, paired Student's t-test). The samples from unreconstituted mice were used to determine the background staining. No significant difference was found in background staining in HTNV-infected or uninfected unreconstituted mice.

Subversion of T Cell Responses by Hantavirus-Induced Checkpoint Inhibitors

We next analyzed whether PD-L1 and PD-L2 is upregulated on hantavirus-infected endothelial cells, which play a pivotal role in hantavirus pathogenesis (45, 46). Upon hantavirus infection human umbilical vein endothelial cells (HUVECs) upregulated both PD-L1 and PD-L2 (**Figure 6A**). PD-L1 expression started to increase on HTNV-infected cells at 12 h post infection similar to MHC class I expression (**Figure 6B**). PD-L1 expression further increased at later time points post infection (**Figure 6B**). We also tested whether hantavirus-induced PD-L1 and PD-L2 modulate T cell responses. For this purpose, HTNV-infected

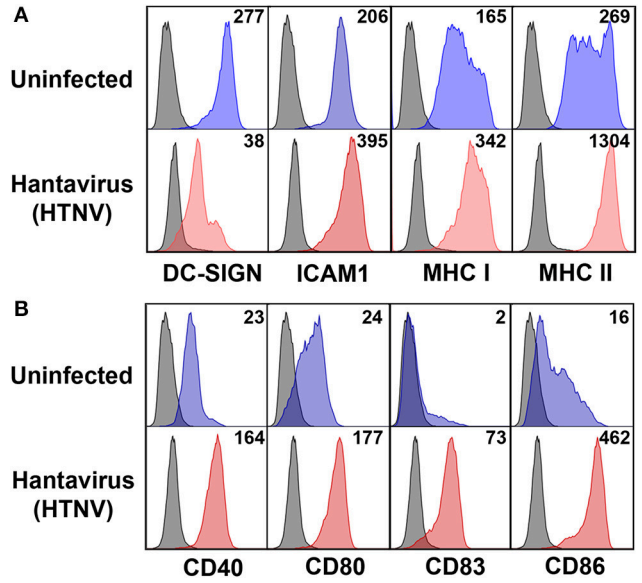

FIGURE 2 | Mature DC phenotype after hantavirus infection. Immature DCs were infected with HTNV at MOI of 1.5 and incubated for 4 days before staining for **(A)** maturation markers and **(B)** costimulatory markers. The results shown are representative of three independent experiments using three different donors.

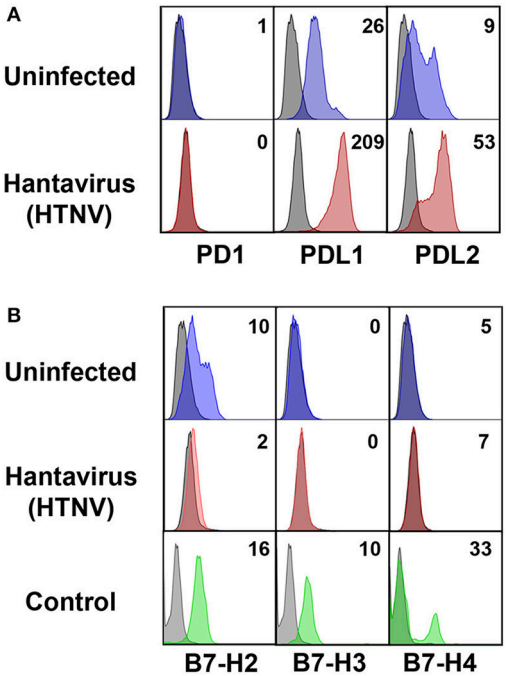

FIGURE 3 | Hantavirus-induced upregulation of PD-L1 and PD-L2 on immature DCs. **(A)** Immature DCs were infected with HTNV at a MOI of 1.5 and incubated for 4 days before staining for PD-1, PD-L1 or PD-L2. **(B)** Immature DCs infected as for **(A)** were stained for members of the B7 family other than PD-L1/PD-L2. The results shown are representative of three independent experiments using three different donors. Positive controls are given in the lower panel (B7-H2 and B7-H3 from HUVEC, B7-H4 from HEK293 cells transfected with a B7-H4 plasmid).

HUVECs were mixed with allogeneic CD4+ cells and stimulated with PHA. T cells strongly upregulate PD-1 upon stimulation with PHA (47). As shown in **Figure 6C** the numbers of surviving T cells and endothelial cells was strongly reduced in comparison to control T cells exposed to uninfected HUVECs, suggesting that T cell proliferation may be reduced. These results indicate that hantaviruses upregulate both PD-L1 and PD-L2 on endothelial cells which has a functional effect on T cells.

Hantavirus-Induced Bystander Activation Despite Upregulation of Checkpoint Inhibitors

To test the functional consequences of PD-1 ligand upregulation we investigated the behavior of T cells when exposed to infected autologous myeloid cells. We infected PBMCs from healthy human donors with HTNV and subsequently stained T cells for expression of the C-type lectin CD69 as an early marker of T-cell activation (48). Recently, it has been shown that CD69 regulates the metabolism and migration-retention ratio of T cells as well as the acquisition of T cell effector or regulatory phenotypes (49). Surprisingly, we observed increased percentages of activated cells especially in the CD8+ T cell population early after infection of PBMCs with HTNV (**Figure 7A**). Bystander activation of T cells during viral infections is common and is initiated by stimulated professional APCs such as DCs (50). In order to identify the responding cells, we tested whether heterologous memory CD8+ T cells are activated in this experimental setting.

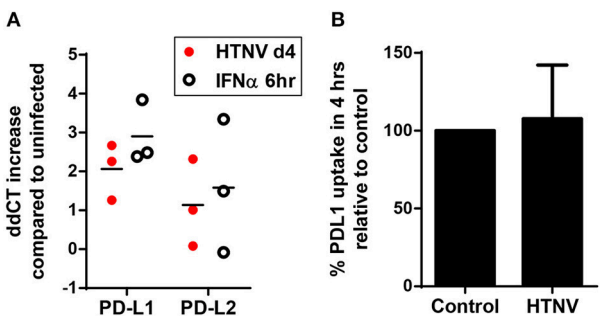

FIGURE 4 | Increase in PD-L1 and PD-L2 transcripts but not cellular uptake in hantavirus-infected immature DCs. **(A)** Immature DCs were infected with HTNV at MOI of 1.5 and incubated for 4 days or exposed to IFN-α for 6 h at 2,000 U/ml before being harvested. Subsequently, RNA was isolated and the number of indicated transcripts quantified by qPCR according to the delta-delta-Ct (ddCt) method. **(B)** Immature DCs infected as for **(A)** were incubated with PE-coupled anti-PD-L1 antibody at 4°C 1 h or at 37°C for 4 h before being washed and analyzed by flow cytometry. Uptake was calculated by subtracting MFI at 37°C from MFI at 4°C. Uptake of HTNV infected cells was then compared to uninfected cells. Results are derived from three independent experiments, error bars represent the mean ± SD.

For this purpose we infected PBMCs derived from HLA-A2+ human healthy donors that were seropositive for human cytomegalovirus (HCMV), a member of the human herpesvirus family. A HLA-A2 tetramer loaded with a immunodominant

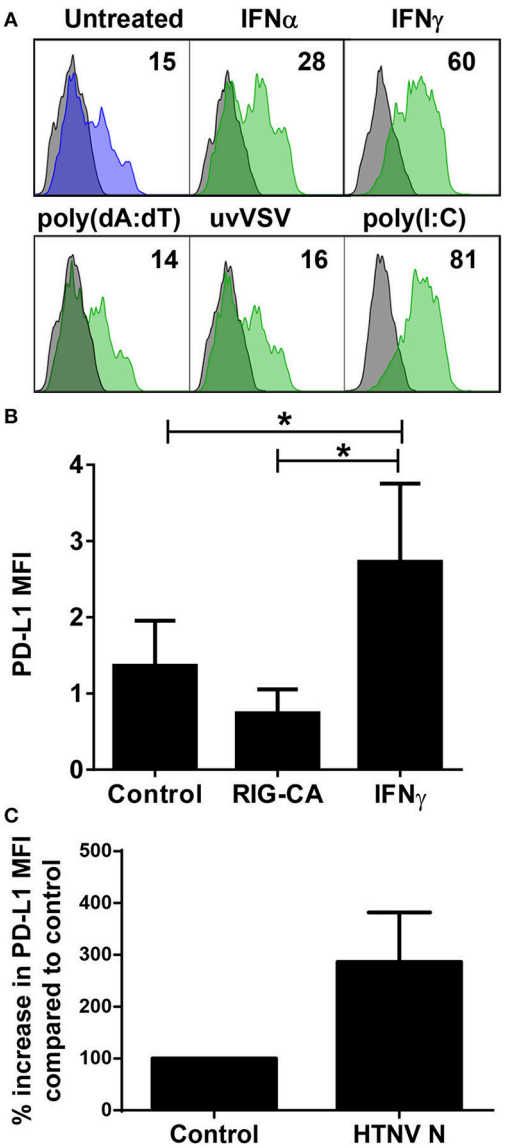

FIGURE 5 | Control of PD-L1 expression by inflammatory stimuli. **(A)** Immature DCs were exposed to the following inflammatory stimuli before staining for PD-L1: type I IFN (IFN-α at 1,000 U/ml), type II IFN (IFN-γ at 1,000 U/ml), poly(dA:dT), UV-inactivated VSV or poly(I:C) for 24 h. The results shown are representative of three independent experiments using three different donors. **(B)** Huh7.5 cells (control), Huh7.5 cells permanently expressing a constitutively active form of RIG-I (RIG-CA) or Huh7.5 cells stimulated with IFN-γ at 1,000 U/ml for 24 h were stained for PD-L1 and analyzed by flow cytometry. Results are derived from three independent experiments, error bars represent the mean ± SEM (*$p < 0.05$, paired Student's t-test). **(C)** HEL cells were transfected with HTNV N-expressing plasmids or empty plasmids (Control). After 2 days cells were stained for PD-L1. Results are given as a percentage of control and are derived from three independent experiments, error bars represent the mean ± SD.

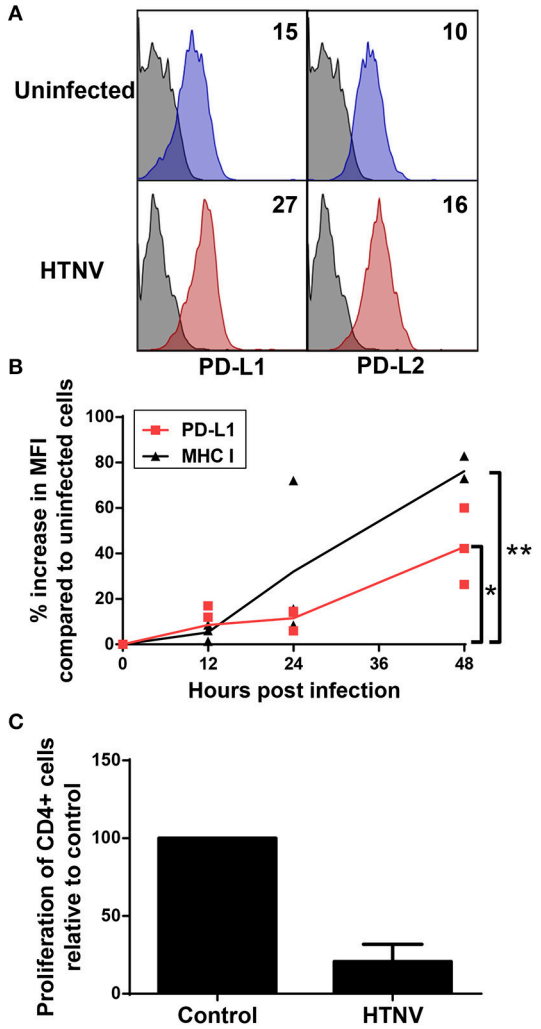

FIGURE 6 | Upregulation of functional PD-L1 and PD-L2 on HTNV-infected endothelial cell lines. **(A)** HUVECs were infected with HTNV at a MOI of 1.5 and incubated for 4 days before staining for PD-L1 or PD-L2. The results shown are representative of 4 independent experiments using 4 different donors. **(B)** Human primary fibroblasts (Fi301) cells were infected at a MOI of 1.5 and incubated for 12, 24 or 48 h before staining for PD-L1 or MHC class I molecules. Results are derived from three independent experiments (*$p < 0.05$, **$p < 0.01$, paired Student's t-test). **(C)** HUVECs infected as for **(A)** were mixed with allogeneic CD4+ cells at a ratio of 1:4 and treated with PHA at 5 μg/ml. After 2 days the number cells was measured by MTT dye test (EZ4U-test). Results are derived from three independent experiments using three different donors, error bars represent the mean ± SD.

peptide derived from pp65 (CMVpp65TET) was used to detect HCMV-specific CD8+ memory T cells. After HTNV infection of PBMCs the percentage of CMVpp65TET+ CD8+ T cells that expressed CD107a (LAMP-1), a marker for degranulation of activated CD8+ T cells (51), significantly increased in PBMCs as compared to uninfected PBMCs (**Figure 7B**). In contrast, in PBMCs infected with herpes simplex virus type 1 (HSV-1), another member of the human herpesvirus family, no significant increase in activated CMVpp65TET+ CD8+ T cells was observed (**Figure 7B**). In conclusion, heterologous T cells are activated at an early time point after hantavirus infection despite increased expression of PD-L1 on antigen-presenting cells.

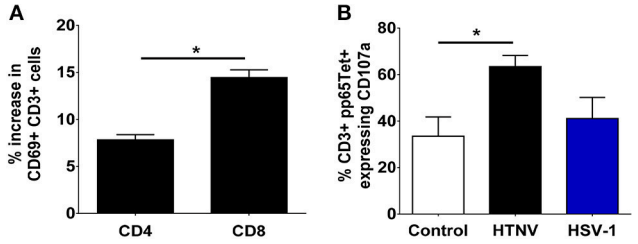

FIGURE 7 | Monocyte-dependent bystander activation of CD8+ T lymphocytes by hantavirus. PBMCs isolated from blood of healthy human donors were mock-infected or infected with HTNV. After 3–4 days cells were analyzed by flow cytometry. **(A)** HTNV-specific increase in CD69+ cells in the CD4+ and CD8+ subset of CD3+ cells after 4 days of incubation. Results are from three independent experiments. Error bars represent the mean ± SEM (*$p < 0.05$, paired Student's *t*-test). **(B)** PBMCs from HLA-A2+ HCMV-seropositive healthy human donors were exposed to HTNV or HSV-1 for 4 days before being stained for HCMV-specific CD3+ cells using a pp65 loaded tetramer reagent (CMVpp65TET). Degranulation was determined by CD107a staining. Results are derived from three independent experiments. Error bars represent the mean ± SEM (*$p < 0.05$, paired Student's *t*-test).

CD86-Dependency of Hantavirus-Induced Bystander Activation

We next examined the mechanisms by which hantavirus-infected DCs cause bystander activation despite checkpoint inhibitors. First, we tested whether hantavirus-infected DCs express inflammatory cytokines that can cause bystander activation of memory CD8+ T cells in the absence of cognate antigen such as IL-15, IL-18, and IL-21 (52). For this purpose RNA from immature DCs infected with HTNV or exposed to IFN-α was isolated and subjected to qPCR. As shown in **Figure 8A** HTNV upregulated production of mRNA encoding IL-15, IL-18, and IL-21 in immature DCs. This finding is in line with cytokine-drive bystander activation of T cells during hantavirus infection of PBMCs. In order to further dissect the mechanism we used antibodies to block IL-15 as this cytokine has been implicated in hantavirus-induced natural killer (NK) cell activation (53). We also blocked type I IFN, which also can contribute to bystander activation of T cells (52). The IL-15 block had no significant effect whereas the type I IFN block significantly reduced T cell bystander activation (**Figure 8B**). In comparison depletion of CD14+ cells completely abrogated hantavirus-induced bystander activation (**Figure 8B**). CD14 serves as marker for monocytes which are detected in PBMCs at frequencies of 10–20% (54) and represent the major hantavirus-permissive cell type in PBMCs. In addition, by blocking the T cell costimulatory molecule B7-2 (CD86) during HTNV infection of PBMCs we could also prevent bystander activation of CD8+ T cells (**Figure 8C**). In contrast, blocking of MHC class I molecules had no effect (**Figure 8C**). These result suggested that CD86 expressed by CD14+ cells plays a major role in hantavirus-induced bystander activation whereas interaction of T cell receptors (TCRs) with MHC-bound peptides interactions is not required (**Figure 8C**). In accordance, CD14+ cells strongly upregulated CD86 during infection with HTNV (**Figure 8D**) and high levels of soluble CD86 were detected in hantavirus-infected patients (**Figure 8E**). Taken together, these results demonstrate that CD14+ monocytes are inducing hantavirus-driven bystander T cell activation in a CD86-dependent manner.

DISCUSSION

In this study, we detected high amounts of sPD-L1 and sPD-L2 in sera of hantavirus-infected patients. Hantaviruses strongly upregulated PD-L1 and PD-L2 on endothelial cells, which play a pivotal role in hantavirus-induced pathogenesis. In line with an inhibitory role of PD-L1/PD-L2 hantavirus-infected endothelial cells did not induce T cell proliferation. Hantaviruses also strongly increased expression of PD-L1 and PD-L2 on monocyte-derived DCs. However, monocyte-derived inflammatory cells could still activate heterologous CD8+ T cells in a CD86-dependent fashion. This indicates that hantavirus-induced CD8+ T cell bystander activation bypasses inhibitory checkpoints.

Gene expression of PD-L1 and PD-L2 is controlled by inflammatory signals (9). Hantavirus-induced upregulation of PD-L1 and PD-L2 could be indirect due to release of IFNs. In line with this view, endothelial cells and DCs predominantly produce IFN-β upon infection with pathogenic hantaviruses (37, 38, 55, 56). PD-L2 is upregulated equally well by IFN-β and IFN-γ whereas PD-L1 is especially sensitive to IFN-γ (57). In hantavirus-infected patients vigorous responses of NK cells and CD8+ T cells resulting in increased levels of IFN-γ are observed (19, 58–61). In addition to this, we show that hantaviral N protein in HEL cells resulted in PD-L1 upregulation although the underlying mechanism is unclear. Thus, IFN-independent mechanisms may contribute to hantavirus-induced PD-L1/PD-L2 expression as recently shown for MHC class I molecules (62). In conclusion, PD-L1/PD-L2 upregulation in hantavirus-infected patients is due to both IFNs and additional IFN-independent mechanisms.

Hantavirus infection is detected by pattern recognition receptors, primarily TLR-3 (42) and RIG-I. (30, 43). We found that the TLR3 ligand poly(I:C) strongly increased PD-L1 levels on immature DCs. In accordance, poly(I:C) has been reported to upregulate PD-L1 on DCs (63, 64) as well as endothelial cells (65) and airway epithelial cells (66). In contrast, PD-L1 was not upregulated upon stimulating RIG-I. Taken together, our *in vitro* observations would fit with hantavirus infection strongly inducing PD-L1 and PD-L2 by triggering TLR-3, which transmits downstream signals through the TIR-domain-containing adapter-inducing IFN-β (TRIF) pathway. Production of IFN-β by both TLR3 and RIG-I induced signaling would be expected to further increase expression of PD-1 ligands later in infection.

Other viruses have also been reported to modulate checkpoint inhibitors. Similar to hantaviruses the Japanese encephalitis virus nonlytically infects monocyte-derived DCs thereby inducing phenotypic maturation and a significant increase in PD-L1 expression (67). Replication competent but not inactivated KSHV induces PD-L1 expression in human monocytes in a dose-dependent manner although the precise mechanism has

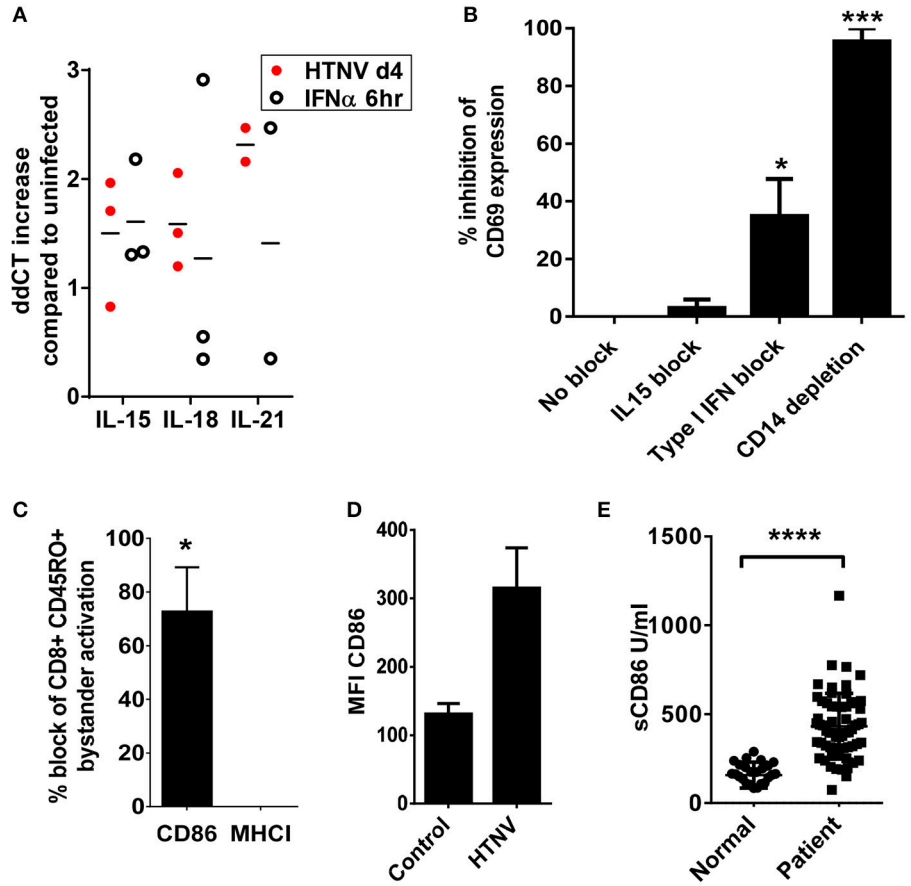

FIGURE 8 | Dependency of hantavirus-induced bystander activation on costimulatory CD86 molecules. **(A)** Immature DCs were infected with HTNV at a MOI of 1.5 and incubated for 4 days or exposed to IFN-α for 6 h at 2,000 U/ml before being harvested. Subsequently, cellular RNA was isolated and the number of indicated cytokine-encoding transcripts quantified by qPCR according to the delta-delta-Ct (ddCt) method. **(B)** PBMCs treated with anti-IL15 (20 μg/ml) or anti-IFN-α (20 μg/ml) and PBMCs depleted of CD14+ cells were exposed to HTNV at a MOI of 1.5 for 4 days before CD69 expression on CD8+ cells was measured by cytofluorimetric analysis. Results are derived from three independent experiments, error bars represent the mean ± SEM (*$p < 0.05$, ***$p < 0.001$, 1 way ANOVA test with Bonferroni correction). **(C)** PBMCs treated with anti-CD86 or anti-MHC (both 10 μg/ml) were exposed to HTNV at a MOI of 1.5 for 4 days before CD69 expression on CD8+ CD45RO+ cells was determined by cytofluorimetric analysis. Error bars represent the mean ± SEM (*$P < 0.05$, Student's t-test). **(D)** PBMC infected with MOI 1.5 of TULV or HTNV were analyzed 3 days post infection for the expression of CD86 on the surface of CD14+ cells. **(E)** Sera from normal healthy individuals or convalescent hantavirus-infected patients were tested by ELISA for levels of sCD86. Error bars represent the mean ± SD (****$p < 0.0001$, paired Student's t-test).

not been defined (68). Akhmetzyanova et al. observed a type I IFN-dependent increase in PD-L1 expression after infection of spleen cells with the murine Friend retrovirus (FV) (69). PD-1 and PD-L1 are also up-regulated in monocytic cells upon HIV-1 infection (70, 71). In accordance, the HIV-1 Tat protein has been observed to increase PD-L1 expression on DCs through TNF-α and TLR4 (72). The HCV core protein up-regulates PD-L1 expression on Kupffer cells, which binds PD-1 to promote T cell dysfunction and development of viral persistence (73). A subset of macrophages upregulated PD-L1 expression via type I IFN during infection with LCMV (74). In addition, influenza virus enhances PD-L1 expression of lung macrophages through type I IFN signaling (75). Taken together, it appears that PD-L1 upregulation is a relatively common consequence of viral infection which is driven by type I IFN and viral PRR triggering.

PD-L1 expression on professional APCs facilitates the induction of regulatory T cells (Tregs) and enhances expression of the key transcription factor forkhead box p3 (Foxp3) (76, 77). Tregs not only regulate effector T cell function but also humoral immunity (78). A recent report has shown that the severity of hantavirus-associated disease correlates with expression of Foxp3 (79). This strongly suggests that hantavirus-induced upregulation of PD-L1 on DCs induces Tregs. In accordance, other investigators have shown that virus-induced PD-L1 upregulation on monocyte-derived DCs leads to expansion of Tregs (67).

We observed that hantavirus-infected human endothelial cells upregulate surface expression of PD-L1 and PD-L2 and inhibit proliferation of PHA-stimulated T cells. Other investigators detected increased amounts of PD-L1 in hantavirus-infected cultures of rat endothelial cells (80). In HFRS patients, hantavirus-induced PD-L1 may be responsible for the contraction of a newly identified highly cytotoxic T cell subset that strongly upregulates PD-1 in the late phase of hantavirus

infection (81). Hantavirus-induced expression of PD-L1 and PD-L2 may contribute to the recently described protection of hantavirus-infected endothelial cells from cytotoxic attack by CD8+ T cells and NK cells (82). In line with this notion, antibody blockade of PD-L1 and PD-L2 on IFN-γ treated endothelial cells enhanced cytolytic activity of antigen-specific CD8+ T lymphocytes (8). Similarly, failure of the inhibitory PD-1/PD-L1 axis during hantavirus infection of vascular tissue may lead to unbalanced immunostimulation and immunopathology as proposed for inflammatory blood vessel diseases (83).

Despite checkpoint inhibition we observed bystander activation in a subset of T cells. Bystander activation of T lymphocytes represents a first line of antiviral defense and may contribute to hantavirus-induced immunopathogenesis. In line with his view, bystander T cells responding to dengue virus, another VHF virus, secrete IFN-γ (84). It has been reported that virus-induced bystander T cell activation bypasses control checkpoints such as Tregs (85). In accordance, we observed that hantavirus-induced bystander T cell activation is not prevented by PD-Ll/PD-L2 upregulation on monocyte-derived inflammatory DCs. This can be explained by the fact that bystander CD8+ T cell activation does not result in TCR-induced PD-1 upregulation. In contrast, TCR signaling induced by cognate antigen upregulates PD-1 expression on CD8+ T cells within the first 24 h during infection (86). This may ensure that virus-specific T cells are excluded from innate responses and differentiate into effector T cells of the adaptive immunity.

Hantavirus-induced bystander activation was strictly dependent on CD14+ cells. This may be explained firstly by the fact that monocyte-derived cells are needed for hantavirus infection in PBMCs. Secondly, CD86 is expressed almost exclusively on monocyte-derived cell types and we could show that CD86 was required for hantavirus-induced bystander activation. Thus, CD86 on hantavirus-infected DCs may activate heterologous CD8+ T cells through CD28. The importance of CD28 for bystander activation of CD8+ T cells has been previously described (87). It is unlikely that hantaviruses directly activate T lymphocytes through PRRs. However, previous reports demonstrated that inflammatory cytokines such as type I contribute to innate T cell activation (88–90). In accordance, we observed that blocking of type I IFN reduced bystander activation of CD8+ T cells upon hantavirus infection.

Many acute viral infections are known to trigger bystander activation of heterologous CD8+ T cells (91–93). Often CD8+ T cells specific for human herpesviruses contribute to the heterologous antiviral immune response (92). In line with this view, we observed activation of HCMV-specific memory CD8+ T cells in PBMCs from HCMV-seropositive patients after hantavirus infection. In fact, bystander activation of CD8+ T cells represent an early line of antiviral defense (94). Bystander activated CD8+ T lymphocytes control early pathogen load in virus-infected tissue by a NKG2D-dependent mechanism (95). In accordance with this concept, cytotoxic CD8+ T cells strongly expressing NKG2D were detected in the lung of hantavirus-infected patients (96). NKG2D ligands are upregulated by PRRs that sense viral replication (97). These include RIG-I, which has been shown to detect hantaviruses (30). Interestingly, a strong plasmablast response with reactivity against virus-unrelated antigens has recently been detected in patients with acute hantavirus pulmonary syndrome (98). Whether this heterologous B cell response has a pathogenic or protective role is unclear.

In conclusion, hantavirus-infected patients suffer from immunopathology in the face of immunosuppressive PD-L1 upregulated by hantaviral N protein and most likely hantavirus-induced TLR3 signaling. This apparent discrepancy could be explained by rapid cleavage and removal of PD-L1 from the surface of hantavirus-infected cells *in vivo*. In accordance, we detected large quantities of sPD-L1 in the serum of patients with hantavirus-associated disease. Moreover, the lack of opportunistic infections in these patients implies that PD-L1 does not globally suppress the immune system. Finally, early activation of heterologous CD8+ T cells during acute virus infections bypasses or overwhelms the inhibitory PD-1/PD-L1 axis and represents a means of eluding viral immune subversion at least in the short term (99).

AUTHOR CONTRIBUTIONS

MR designed research, performed all experiments, analyzed data, contributed to writing, and prepared figures. MA analyzed data and contributed to manuscript revision. JH provided serum samples from hantavirus-infected patients, contributed to manuscript revision and provided intellectual input. GS was involved in experiment conception, wrote the paper, analyzed data, provided intellectual input, and contributed to figure preparation.

ACKNOWLEDGMENTS

We acknowledge support from the German Research Foundation (DFG) and the Open Access Publication Fund of Charité–Universitätsmedizin Berlin. This work was also supported by a grant (GALHANT) from the Federal Ministry of Education and Research (BMBF) and the FAZIT foundation. We thank M. Binder for providing the Huh7.5 RIG-CA cells and C. Priemer for assistance in culturing cells.

REFERENCES

1. Attanasio J, Wherry EJ. Costimulatory and coinhibitory receptor pathways in infectious disease. *Immunity* (2016) 44:1052–68. doi: 10.1016/j.immuni.2016.04.022
2. Esensten JH, Helou YA, Chopra G, Weiss A, Bluestone JA. CD28 costimulation: from mechanism to therapy. *Immunity* (2016) 44:973–88. doi: 10.1016/j.immuni.2016.04.020
3. Sharpe AH, Pauken KE. The diverse functions of the PD1 inhibitory pathway. *Nat Rev Immunol.* (2018) 18:153–67. doi: 10.1038/nri.2017.108
4. Keir ME, Butte MJ, Freeman GJ, Sharpe AH. PD-1 and its ligands in tolerance and immunity. *Annu Rev Immunol.* (2008) 26:677–704. doi: 10.1146/annurev.immunol.26.021607.090331
5. Eppihimer MJ, Gunn J, Freeman GJ, Greenfield EA, Chernova T, Erickson J, et al. Expression and regulation of the PD-L1 immunoinhibitory

molecule on microvascular endothelial cells. *Microcirculation* (2002) 9:133–45. doi: 10.1038/sj/mn/7800123
6. LaGier AJ, Pober JS. Immune accessory functions of human endothelial cells are modulated by overexpression of B7-H1 (PDL1). *Hum Immunol.* (2006) 67:568–78. doi: 10.1016/j.humimm.2006.04.013
7. Mazanet MM, Hughes CC. B7-H1 is expressed by human endothelial cells and suppresses T cell cytokine synthesis. *J Immunol.* (2002) 169:3581–8. doi: 10.4049/jimmunol.169.7.3581
8. Rodig N, Ryan T, Allen JA, Pang H, Grabie N, Chernova T, et al. Endothelial expression of PD-L1 and PD-L2 down-regulates CD8+ T cell activation and cytolysis. *Eur J Immunol.* (2003) 33:3117–26. doi: 10.1002/eji.200324270
9. Sun C, Mezzadra R, Schumacher TN. Regulation and function of the PD-L1 checkpoint. *Immunity* (2018) 48:434–52. doi: 10.1016/j.immuni.2018.03.014
10. Ong EZ, Chan KR, Ooi EE. Viral manipulation of host inhibitory receptor signaling for immune evasion. *PLoS Pathog.* (2016) 12:e1005776. doi: 10.1371/journal.ppat.1005776
11. Hofmeyer KA, Jeon H, Zang X. The PD-1/PD-L1 (B7-H1) pathway in chronic infection-induced cytotoxic T lymphocyte exhaustion. *J Biomed Biotechnol.* (2011) 2011:451694. doi: 10.1155/2011/451694
12. Shin H, Wherry EJ. CD8 T cell dysfunction during chronic viral infection. *Curr Opin Immunol.* (2007) 19:408–15. doi: 10.1016/j.coi.2007.06.004
13. Brown KE, Freeman GJ, Wherry EJ, Sharpe AH. Role of PD-1 in regulating acute infections. *Curr Opin Immunol.* (2010) 22:397–401 doi: 10.1016/j.coi.2010.03.007
14. Erickson JJ, Gilchuk P, Hastings AK, Tollefson SJ, Johnson M, Downing MB, et al. Viral acute lower respiratory infections impair CD8+ T cells through PD-1. *J Clin Invest.* (2012) 122:2967–82. doi: 10.1172/JCI62860
15. Bryant-Hudson KM, Carr DJ. PD-L1-expressing dendritic cells contribute to viral resistance during acute HSV-1 infection. *Clin Dev Immunol.* (2012) 2012:924619. doi: 10.1155/2012/924619
16. Zelinskyy G, Myers L, Dietze KK, Gibbert K, Roggendorf M, Liu J, et al. Virus-specific CD8+ T cells upregulate programmed death-1 expression during acute friend retrovirus infection but are highly cytotoxic and control virus replication. *J Immunol.* (2011) 187:3730–7. doi: 10.4049/jimmunol.1101612
17. Kruger DH, Figueiredo LT, Song JW, Klempa B. Hantaviruses–globally emerging pathogens. *J Clin Virol.* (2015) 64:128–36. doi: 10.1016/j.jcv.2014.08.033
18. Paessler S, Walker DH. Pathogenesis of the viral hemorrhagic fevers. *Annu Rev Pathol.* (2013) 8:411–40. doi: 10.1146/annurev-pathol-020712-164041
19. Schonrich G, Rang A, Lutteke N, Raftery MJ, Charbonnel N, Ulrich RG. Hantavirus-induced immunity in rodent reservoirs and humans. *Immunol Rev.* (2008) 225:163–89. doi: 10.1111/j.1600-065X.2008.00694.x
20. Vaheri A, Strandin T, Hepojoki J, Sironen T, Henttonen H, Makela S, et al. Uncovering the mysteries of hantavirus infections. *Nat Rev Microbiol.* (2013) 11:539–50. doi: 10.1038/nrmicro3066
21. Barber DL, Wherry EJ, Masopust D, Zhu B, Allison JP, Sharpe AH, et al. Restoring function in exhausted CD8 T cells during chronic viral infection. *Nature* (2006) 439:682–7. doi: 10.1038/nature04444
22. Frebel H, Nindl V, Schuepbach RA, Braunschweiler T, Richter K, Vogel J, et al. Programmed death 1 protects from fatal circulatory failure during systemic virus infection of mice. *J Exp Med.* (2012) 209:2485–99. doi: 10.1084/jem.20121015
23. Raftery MJ, Schwab M, Diesner S, Egerer G, Schonrich G. Dendritic cells cross-presenting viral antigens derived from autologous cells as a sensitive tool for visualization of human cytomegalovirus-reactive CD8+ T cells. *Transplantation* (2002) 73:998–1002. doi: 10.1097/00007890-200203270-00031
24. Sumpter R Jr., Loo YM, Foy E, Li K, Yoneyama M, Fujita T, et al. Regulating intracellular antiviral defense and permissiveness to hepatitis C virus RNA replication through a cellular RNA helicase, RIG-I. *J Virol.* (2005) 79:2689–99. doi: 10.1128/JVI.79.5.2689-2699.2005
25. Binder M, Kochs G, Bartenschlager R, Lohmann V. Hepatitis C virus escape from the interferon regulatory factor 3 pathway by a passive and active evasion strategy. *Hepatology* (2007) 46:1365–74. doi: 10.1002/hep.21829
26. Quinkert D, Bartenschlager R, Lohmann V. Quantitative analysis of the hepatitis C virus replication complex. *J Virol.* (2005) 79:13594–605. doi: 10.1128/JVI.79.21.13594-13605.2005
27. Raftery MJ, Lalwani P, Krautkrmer E, Peters T, Scharffetter-Kochanek K, Kruger R, et al. beta2 integrin mediates hantavirus-induced release of neutrophil extracellular traps. *J Exp Med.* (2014) 211:1485–97. doi: 10.1084/jem.20131092
28. Kraus AA, Priemer C, Heider H, Kruger DH, Ulrich R. Inactivation of Hantaan virus-containing samples for subsequent investigations outside biosafety level 3 facilities. *Intervirology* (2005) 48:255–61. doi: 10.1159/000084603
29. Heider H, Ziaja B, Priemer C, Lundkvist A, Neyts J, Kruger DH, et al. A chemiluminescence detection method of hantaviral antigens in neutralisation assays and inhibitor studies. *J Virol Methods* (2001) 96:17–23. doi: 10.1016/S0166-0934(01)00314-7
30. Lee MH, Lalwani P, Raftery MJ, Matthaei M, Lutteke N, Kirsanovs S, et al. RNA helicase retinoic acid-inducible gene I as a sensor of Hantaan virus replication. *J Gen Virol.* (2011) 92(Pt 9):2191–200. doi: 10.1099/vir.0.032367-0
31. Kobak L, Raftery MJ, Voigt S, Kuhl AA, Kilic E, Kurth A, et al. Hantavirus-induced pathogenesis in mice with a humanized immune system. *J Gen Virol.* (2015) 96(Pt 6):1258–63. doi: 10.1099/vir.0.000087
32. Strandin T, Makela S, Mustonen J, Vaheri A. Neutrophil activation in acute hemorrhagic fever with renal syndrome is mediated by hantavirus-infected microvascular endothelial cells. *Front Immunol.* (2018) 9:2098. doi: 10.3389/fimmu.2018.02098
33. Chen Y, Wang Q, Shi B, Xu P, Hu Z, Bai L, et al. Development of a sandwich ELISA for evaluating soluble PD-L1 (CD274) in human sera of different ages as well as supernatants of PD-L1+ cell lines. *Cytokine* (2011) 56:231–8. doi: 10.1016/j.cyto.2011.06.004
34. Frigola X, Inman BA, Lohse CM, Krco CJ, Cheville JC, Thompson RH, et al. Identification of a soluble form of B7-H1 that retains immunosuppressive activity and is associated with aggressive renal cell carcinoma. *Clin Cancer Res.* (2011) 17:1915–23. doi: 10.1158/1078-0432.CCR-10-0250
35. Frigola X, Inman BA, Krco CJ, Liu X, Harrington SM, Bulur PA, et al. Soluble B7-H1. differences in production between dendritic cells and T cells. *Immunol Lett.* (2012) 142:78–82. doi: 10.1016/j.imlet.2011.11.001
36. Markotic A, Hensley L, Daddario K, Spik K, Anderson K, Schmaljohn C. Pathogenic hantaviruses elicit different immunoreactions in THP-1 cells and primary monocytes and induce differentiation of human monocytes to dendritic-like cells. *Coll Antropol.* (2007) 31:1159–67.
37. Marsac D, Garcia S, Fournet A, Aguirre A, Pino K, Ferres M, et al. Infection of human monocyte-derived dendritic cells by ANDES Hantavirus enhances pro-inflammatory state, the secretion of active MMP-9 and indirectly enhances endothelial permeability. *Virol J.* (2011) 8:223. doi: 10.1186/1743-422X-8-223
38. Raftery MJ, Kraus AA, Ulrich R, Kruger DH, Schonrich G. Hantavirus infection of dendritic cells. *J Virol.* (2002) 76:10724–33. doi: 10.1128/JVI.76.21.10724-10733.2002
39. Scholz S, Baharom F, Rankin G, Maleki KT, Gupta S, Vangeti S, et al. Human hantavirus infection elicits pronounced redistribution of mononuclear phagocytes in peripheral blood and airways. *PLoS Pathog.* (2017) 13:e1006462. doi: 10.1371/journal.ppat.1006462
40. Li J, Lee Y, Li Y, Jiang Y, Lu H, Zang W, et al. Co-inhibitory molecule B7 superfamily member 1 expressed by tumor-infiltrating myeloid cells induces dysfunction of anti-tumor CD8(+) T Cells. *Immunity* (2018) 48:773–786e5. doi: 10.1016/j.immuni.2018.03.018
41. Zerdes I, Matikas A, Bergh J, Rassidakis GZ, Foukakis T. Genetic, transcriptional and post-translational regulation of the programmed death protein ligand 1 in cancer. biology and clinical correlations. *Oncogene* (2018) 37:4639–61. doi: 10.1038/s41388-018-0303-3
42. Handke W, Oelschlegel R, Franke R, Kruger DH, Rang A. Hantaan virus triggers TLR3-dependent innate immune responses. *J Immunol.* (2009) 182:2849–58. doi: 10.4049/jimmunol.0802893
43. Zhang Y, Liu B, Ma Y, Yi J, Zhang C, Zhang Y, et al. Hantaan virus infection induces CXCL10 expression through TLR3, RIG-I, and MDA-5 pathways correlated with the disease severity. *Mediators Inflamm.* (2014) 2014:697837. doi: 10.1155/2014/697837
44. Reuter M, and Kruger D, H. The nucleocapsid protein of hantaviruses: much more than a genome-wrapping protein. *Virus Genes* (2018) 54:5–16. doi: 10.1007/s11262-017-1522-3

45. Hepojoki J, Vaheri A, Strandin T. The fundamental role of endothelial cells in hantavirus pathogenesis. *Front Microbiol.* (2014) 5:727. doi: 10.3389/fmicb.2014.00727
46. Schonrich G, Kruger DH, Raftery MJ. Hantavirus-induced disruption of the endothelial barrier: neutrophils are on the payroll. *Front Microbiol.* (2015) 6:222. doi: 10.3389/fmicb.2015.00222
47. Saunders PA, Hendrycks VR, Lidinsky WA, Woods ML. PD-L2:PD-1 involvement in T cell proliferation, cytokine production, and integrin-mediated adhesion. *Eur J Immunol.* (2005) 35:3561–9. doi: 10.1002/eji.200526347
48. Ziegler SF, Ramsdell F, Alderson MR. The activation antigen CD69. *Stem Cells* (1994) 12:456–65. doi: 10.1002/stem.5530120502
49. Cibrian D, Sanchez-Madrid F. CD69. from activation marker to metabolic gatekeeper. *Eur J Immunol.* (2017) 47:946–53. doi: 10.1002/eji.201646837
50. Fujinami RS, von Herrath MG, Christen U, Whitton JL. Molecular mimicry, bystander activation, or viral persistence: infections and autoimmune disease. *Clin Microbiol Rev.* (2006) 19:80–94. doi: 10.1128/CMR.19.1.80-94.2006
51. Betts MR, Brenchley JM, Price DA, De Rosa SC, Douek DC, Roederer M, et al. Sensitive and viable identification of antigen-specific CD8+ T cells by a flow cytometric assay for degranulation. *J Immunol Methods* (2003) 281:65–78. doi: 10.1016/S0022-1759(03)00265-5
52. Soudja SM, Chandrabos C, Yakob E, Veenstra M, Palliser D, Lauvau G. Memory-T-cell-derived interferon-gamma instructs potent innate cell activation for protective immunity. *Immunity* (2014) 40:974–88. doi: 10.1016/j.immuni.2014.05.005
53. Braun M, Bjorkstrom NK, Gupta S, Sundstrom K, Ahlm C, Klingstrom J, et al. NK cell activation in human hantavirus infection explained by virus-induced IL-15/IL15Ralpha expression. *PLoS Pathog.* (2014) 10:e1004521. doi: 10.1371/journal.ppat.1004521
54. Heideveld E, Masiello F, Marra M, Esteghamat F, Yagci N, von Lindern M, et al. CD14+ cells from peripheral blood positively regulate hematopoietic stem and progenitor cell survival resulting in increased erythroid yield. *Haematologica* (2015) 100:1396–406. doi: 10.3324/haematol.2015.125492
55. Geimonen E, Neff S, Raymond T, Kocer SS, Gavrilovskaya IN, Mackow ER. Pathogenic and nonpathogenic hantaviruses differentially regulate endothelial cell responses. *Proc Natl Acad Sci USA.* (2002) 99:13837–42. doi: 10.1073/pnas.192298899
56. Kraus AA, Raftery MJ, Giese T, Ulrich R, Zawatzky R, Hippenstiel S, et al. Differential antiviral response of endothelial cells after infection with pathogenic and nonpathogenic hantaviruses. *J Virol.* (2004) 78:6143–50. doi: 10.1128/JVI.78.12.6143-6150.2004
57. Garcia-Diaz A, Shin DS, Moreno BH, Saco J, Escuin-Ordinas H, Rodriguez GA, et al. Interferon receptor signaling pathways regulating PD-L1 and PD-L2 expression. *Cell Rep.* (2017) 19:1189–201. doi: 10.1016/j.celrep.2017.04.031
58. Bjorkstrom NK, Lindgren T, Stoltz M, Fauriat C, Braun M, Evander M, et al. Rapid expansion and long-term persistence of elevated NK cell numbers in humans infected with hantavirus. *J Exp Med.* (2011) 208:13–21. doi: 10.1084/jem.20100762
59. Khaiboullina SF, Martynova EV, Khamidullina ZL, Lapteva EV, Nikolaeva IV, Anokhin VV, et al. Upregulation of IFN-gamma and IL-12 is associated with a milder form of hantavirus hemorrhagic fever with renal syndrome. *Eur J Clin Microbiol Infect Dis.* (2014) 33:2149–56. doi: 10.1007/s10096-014-2176-x
60. Lindgren T, Ahlm C, Mohamed N, Evander M, Ljunggren HG, Bjorkstrom NK. Longitudinal analysis of the human T cell response during acute hantavirus infection. *J Virol.* (2011) 85:10252–60. doi: 10.1128/JVI.05548-11
61. Terajima M, Ennis FA. T cells and pathogenesis of hantavirus cardiopulmonary syndrome and hemorrhagic fever with renal syndrome. *Viruses* (2011) 3:1059–73. doi: 10.3390/v3071059
62. Lalwani P, Raftery MJ, Kobak L, Rang A, Giese T, Matthaei M, et al. Hantaviral mechanisms driving HLA class I antigen presentation require both RIG-I and TRIF. *Eur J Immunol.* (2013) 43:2566–76. doi: 10.1002/eji.201243066
63. Boes M, Meyer-Wentrup F. TLR3 triggering regulates PD-L1 (CD274) expression in human neuroblastoma cells. *Cancer Lett.* (2015) 361:49–56. doi: 10.1016/j.canlet.2015.02.027
64. Pulko V, Liu X, Krco CJ, Harris KJ, Frigola X, Kwon ED, et al. TLR3-stimulated dendritic cells up-regulate B7-H1 expression and influence the magnitude of CD8 T cell responses to tumor vaccination. *J Immunol.* (2009) 183:3634–41. doi: 10.4049/jimmunol.0900974
65. Cole JE, Navin TJ, Cross AJ, Goddard ME, Alexopoulou L, Mitra AT, et al. Unexpected protective role for Toll-like receptor 3 in the arterial wall. *Proc Natl Acad Sci USA.* (2011) 108:2372–7. doi: 10.1073/pnas.1018515108
66. Tsuda M, Matsumoto K, Inoue H, Matsumura M, Nakano T, Mori A, et al. Expression of B7-H1 and B7-DC on the airway epithelium is enhanced by double-stranded RNA. *Biochem Biophys Res Commun.* (2005) 330:263–70. doi: 10.1016/j.bbrc.2005.02.161
67. Gupta N, Hegde P, Lecerf M, Nain M, Kaur M, Kalia M, et al. Japanese encephalitis virus expands regulatory T cells by increasing the expression of PD-L1 on dendritic cells. *Eur J Immunol.* (2014) 44:1363–74. doi: 10.1002/eji.201343701
68. Host KM, Jacobs SR, West JA, Zhang Z, Costantini LM, Stopford CM, et al. Kaposi's sarcoma-associated herpesvirus increases PD-L1 and proinflammatory cytokine expression in human monocytes. *MBio* (2017) 8:e00917-17. doi: 10.1128/mBio.00917-17
69. Akhmetzyanova I, Drabczyk M, Neff CP, Gibbert K, Dietze KK, Werner T, et al. PD-L1 Expression on retrovirus-infected cells mediates immune escape from CD8+ T Cell Killing. *PLoS Pathog.* (2015) 11:e1005224. doi: 10.1371/journal.ppat.1005224
70. Rodriguez-Garcia M, Porichis F, de Jong OG, Levi K, Diefenbach TJ, Lifson JD, et al. Expression of PD-L1 and PD-L2 on human macrophages is up-regulated by HIV-1 and differentially modulated by IL-10. *J Leukoc Biol.* (2011) 89:507–15. doi: 10.1189/jlb.0610327
71. Said EA, Dupuy FP, Trautmann L, Zhang Y, Shi Y, El-Far M, et al. Programmed death-1-induced interleukin-10 production by monocytes impairs CD4+ T cell activation during HIV infection. *Nat Med.* (2010) 16:452–9. doi: 10.1038/nm.2106
72. Planes R, BenMohamed L, Leghmari K, Delobel P, Izopet J, Bahraoui E. HIV-1 Tat protein induces PD-L1 (B7-H1) expression on dendritic cells through tumor necrosis factor alpha- and toll-like receptor 4-mediated mechanisms. *J Virol.* (2014) 88:6672–89. doi: 10.1128/JVI.00825-14
73. Tu Z, Pierce RH, Kurtis J, Kuroki Y, Crispe IN, Orloff MS. Hepatitis C virus core protein subverts the antiviral activities of human Kupffer cells. *Gastroenterology* (2010) 138:305–14. doi: 10.1053/j.gastro.2009.09.009
74. Shaabani N, Duhan V, Khairnar V, Gassa A, Ferrer-Tur R, Haussinger D, et al. CD169(+) macrophages regulate PD-L1 expression via type I interferon and thereby prevent severe immunopathology after LCMV infection. *Cell Death Dis.* (2016) 7:e2446. doi: 10.1038/cddis.2016.350
75. Staples KJ, Nicholas B, McKendry RT, Spalluto CM, Wallington JC, Bragg CW, et al. Viral infection of human lung macrophages increases PDL1 expression via IFNbeta. *PLoS ONE* (2015) 10:e0121527. doi: 10.1371/journal.pone.0121527
76. Francisco LM, Salinas VH, Brown KE, Vanguri VK, Freeman GJ, Kuchroo VK, et al. PD-L1 regulates the development, maintenance, and function of induced regulatory T cells. *J Exp Med.* (2009) 206:3015–29. doi: 10.1084/jem.20090847
77. Francisco LM, Sage PT, Sharpe AH. The PD-1 pathway in tolerance and autoimmunity. *Immunol Rev.* (2010) 236:219–42. doi: 10.1111/j.1600-065X.2010.00923.x
78. Weingartner E, Golding A. Direct control of B cells by Tregs: an opportunity for long-term modulation of the humoral response. *Cell Immunol.* (2017) 318:8–16. doi: 10.1016/j.cellimm.2017.05.007
79. Koivula TT, Tuulasvaara A, Hetemaki I, Makela SM, Mustonen J, Sironen T, et al. Regulatory T cell response correlates with the severity of human hantavirus infection. *J Infect.* (2014) 68:387–94. doi: 10.1016/j.jinf.2013.11.007
80. Li W, Klein SL. Seoul virus-infected rat lung endothelial cells and alveolar macrophages differ in their ability to support virus replication and induce regulatory T cell phenotypes. *J Virol.* (2012) 86:11845–55. doi: 10.1128/JVI.01233-12
81. Liu B, Ma Y, Zhang Y, Zhang C, Yi J, Zhuang R, et al. CD8low CD100- T cells identify a novel CD8 T cell subset associated with viral control during human hantaan virus infection. *J Virol.* (2015) 89:11834–44. doi: 10.1128/JVI.01610-15
82. Gupta S, Braun M, Tischler ND, Stoltz M, Sundstrom KB, Bjorkstrom NK, et al. Hantavirus-infection confers resistance to cytotoxic lymphocyte-mediated apoptosis. *PLoS Pathog.* (2013) 9:e1003272. doi: 10.1371/journal.ppat.1003272

83. Weyand CM, Berry GJ, Goronzy JJ. The immunoinhibitory PD-1/PD-L1 pathway in inflammatory blood vessel disease. *J Leukoc Biol.* (2018) 103:565–75. doi: 10.1189/jlb.3MA0717-283
84. Suwannasaen D, Romphruk A, Leelayuwat C, Lertmemongkolchai G. Bystander T cells in human immune responses to dengue antigens. *BMC Immunol.* (2010) 11:47. doi: 10.1186/1471-2172-11-47
85. Bangs SC, McMichael AJ, Xu XN. Bystander T cell activation–implications for HIV infection and other diseases. *Trends Immunol.* (2006) 27:518–24. doi: 10.1016/j.it.2006.09.006
86. Ahn E, Araki K, Hashimoto M, Li W, Riley JL, Cheung J, et al. Role of PD-1 during effector CD8 T cell differentiation. *Proc Natl Acad Sci USA.* (2018) 115: 4749–54. doi: 10.1073/pnas.1718217115
87. Gilbertson B, Germano S, Steele P, Turner S, de St Groth Fazekas B, Cheers C. Bystander activation of CD8+ T lymphocytes during experimental mycobacterial infection. *Infect Immun.* (2004) 72:6884–91. doi: 10.1128/IAI.72.12.6884-6891.2004
88. Freeman BE, Hammarlund E, Raue HP, Slifka MK. Regulation of innate CD8+ T-cell activation mediated by cytokines. *Proc Natl Acad Sci USA.* (2012) 109:9971–6. doi: 10.1073/pnas.1203543109
89. Lauvau G, Goriely S. Memory CD8+ T cells: orchestrators and key players of innate immunity? *PLoS Pathog.* (2016) 12:e1005722. doi: 10.1371/journal.ppat.1005722
90. Tough DF, Sun S, Zhang X, Sprent J. Stimulation of naive and memory T cells by cytokines. *Immunol Rev.* (1999) 170:39–47.
91. Doisne JM, Urrutia A, Lacabaratz-Porret C, Goujard C, Meyer L, Chaix ML, et al. CD8+ T cells specific for EBV, cytomegalovirus, and influenza virus are activated during primary HIV infection. *J Immunol.* (2004) 173:2410–8. doi: 10.4049/jimmunol.173.4.2410
92. Sandalova E, Laccabue D, Boni C, Tan AT, Fink K, Ooi EE, et al. Contribution of herpesvirus specific CD8 T cells to anti-viral T cell response in humans. *PLoS Pathog.* (2010) 6:e1001051. doi: 10.1371/journal.ppat.1001051
93. Sckisel GD, Tietze JK, Zamora AE, Hsiao HH, Priest SO, Wilkins DE, et al. Influenza infection results in local expansion of memory CD8(+) T cells with antigen non-specific phenotype and function. *Clin Exp Immunol.* (2014) 175:79–91. doi: 10.1111/cei.12186
94. Lauvau G, Boutet M, Williams TM, Chin SS, Chorro L. Memory CD8(+) T Cells: innate-like sensors and orchestrators of protection. *Trends Immunol.* (2016) 37:375–85. doi: 10.1016/j.it.2016.04.001
95. Chu T, Tyznik AJ, Roepke S, Berkley AM, Woodward-Davis A, Pattacini L, et al. Bystander-activated memory CD8 T cells control early pathogen load in an innate-like, NKG2D-dependent manner. *Cell Rep.* (2013) 3:701–8. doi: 10.1016/j.celrep.2013.02.020
96. Rasmuson J, Pourazar J, Mohamed N, Lejon K, Evander M, Blomberg A, et al. Cytotoxic immune responses in the lungs correlate to disease severity in patients with hantavirus infection. *Eur J Clin Microbiol Infect Dis.* (2016) 35:713–21. doi: 10.1007/s10096-016-2592-1
97. Esteso G, Guerra S, Vales-Gomez M, Reyburn HT. Innate immune recognition of double-stranded RNA triggers increased expression of NKG2D ligands after virus infection. *J Biol Chem.* (2017) 292:20472–80. doi: 10.1074/jbc.M117.818393
98. Garcia M, Iglesias A, Landoni VI, Bellomo C, Bruno A, Cordoba MT, et al. Massive plasmablast response elicited in the acute phase of hantavirus pulmonary syndrome. *Immunology* (2017) 151:122–35. doi: 10.1111/imm.12713
99. Holmgren AM, McConkey CA, Shin S. Outrunning the Red Queen: bystander activation as a means of outpacing innate immune subversion by intracellular pathogens. *Cell Mol Immunol.* (2017) 14:14–21. doi: 10.1038/cmi.2016.36

Conflict of Interest Statement: The authors declare that the research was conducted in the absence of any commercial or financial relationships that could be construed as a potential conflict of interest.

frontiers in Immunology

MINI REVIEW
published: 29 January 2019
doi: 10.3389/fimmu.2019.00078

Cytokine-Mediated Induction and Regulation of Tissue Damage During Cytomegalovirus Infection

*Mathew Clement and Ian R. Humphreys**

Division of Infection and Immunity/Systems Immunity University Research Institute, Cardiff, United Kingdom

Human cytomegalovirus (HCMV) is a β-herpesvirus with high sero-prevalence within the human population. Primary HCMV infection and life-long carriage are typically asymptomatic. However, HCMV is implicated in exacerbation of chronic conditions and associated damage in individuals with intact immune systems. Furthermore, HCMV is a significant cause of morbidity and mortality in the immunologically immature and immune-compromised where disease is associated with tissue damage. Infection-induced inflammation, including robust cytokine responses, is a key component of pathologies associated with many viruses. Despite encoding a large number of immune-evasion genes, HCMV also triggers the induction of inflammatory cytokine responses during infection. Thus, understanding how cytokines contribute to CMV-induced pathologies and the mechanisms through which they are regulated may inform clinical management of disease. Herein, we discuss our current understanding based on clinical observation and *in vivo* modeling of disease of the role that cytokines play in CMV pathogenesis. Specifically, in the context of the different tissues and organs in which CMV replicates, we give a broad overview of the beneficial and adverse effects that cytokines have during infection and describe how cytokine-mediated tissue damage is regulated. We discuss the implications of findings derived from mice and humans for therapeutic intervention strategies and our understanding of how host genetics may influence the outcome of CMV infections.

Keywords: cytokine, cytomegalovirus infection, immunopathologic process, virus, mcmv

OPEN ACCESS

Edited by:
Juliet Spencer,
Texas Woman's University,
United States

Reviewed by:
Mary Hummel,
Northwestern University, United States
Sarah Rowland-Jones,
University of Oxford, United Kingdom
Laura Kay Hanson,
Texas Woman's University,
United States

****Correspondence:***
Ian R. Humphreys
humphreysir@cardiff.ac.uk

Specialty section:
This article was submitted to Viral Immunology, a section of the journal Frontiers in Immunology

Received: *14 September 2018*
Accepted: *11 January 2019*
Published: *29 January 2019*

Citation:
Clement M and Humphreys IR (2019) Cytokine-Mediated Induction and Regulation of Tissue Damage During Cytomegalovirus Infection. Front. Immunol. 10:78. doi: 10.3389/fimmu.2019.00078

INTRODUCTION

Human cytomegalovirus (HCMV) is a ubiquitous beta-herpesvirus that has co-evolved with its host for millions of years and acquired multiple immune evasion functions that manipulate and hide the virus from host immunity (1, 2). Primary HCMV infection and latency in immune-competent hosts is usually asymptomatic (3). Thus, HCMV is typically thought to establish lifelong infection without inducing overt pathology often triggered by other viruses. It is becomingly apparent, however, that chronic HCMV carriage in 'healthy individuals' may exacerbate conditions from general frailty (4) to cardiovascular disease (5).

HCMV causes morbidity and mortality in immune-compromised patients including transplant recipients and HIV co-infected individuals. Solid-state organ or human stem cell transplantation remains challenging as immune suppression can facilitate uncontrolled HCMV reactivation from host and/or donor tissue, resulting in organ pathology and systemic disease (6). HCMV co-infection is the leading cause of vision loss in untreated HIV/AIDS individuals (7, 8) and

remains an issue in patients receiving anti-retroviral therapy (9). HCMV causes gastrointestinal and neurological diseases during HIV co-infection (7, 10). Further examples of viral-induced morbidity include congenital infection where HCMV is the leading infectious cause of all congenital birth defects (11, 12). Life-long neurological defects ensue, including microcephaly, encephalitis, seizures, and blindness, and HCMV is the leading cause of congenital deafness (6, 12, 13).

The fact that HCMV preferentially causes disease in immune compromised individuals highlights the importance of immune control of virus replication. Indeed, many HCMV-associated disease manifestations correlate with viral replication and respond to antiviral drug treatment. However, certain syndromes, particularly chronic diseases, do not typically correlate with high HCMV load (14), suggesting that direct cellular destruction by virus is not the sole cause of tissue damage.

Cytokines participate in immune responses to viruses that activate innate immune responses and orchestrate the development of adaptive antiviral immunity. However, uncontrolled cytokine production can cause off-target effects, participating in various immune-driven pathological processes. Due to the limitations of what can be investigated in humans, the murine CMV (MCMV) model has been used for decades to study mechanisms influencing CMV pathogenesis *in vivo*, including how cytokines orchestrate antiviral immunity [summarized in detail elsewhere (15)]. Herein, we examine evidence from both clinical studies and experimental models of CMV infection showing that although cytokines are required to limit viral replication, they can cause host damage. We discuss these findings in the context of different tissues where damage during CMV infection can ensue and describe the mechanisms that restrict these harmful processes (see **Figure 1** for summary).

PRO-INFLAMMATORY CYTOKINES, SYSTEMIC CYTOMEGALOVIRUS-INDUCED DISEASE, AND ORGAN DAMAGE

Cytokine responses during HCMV viremia have been mostly studied in the transplantation setting where time of virus exposure is known. Following initial replication, sustained type 1 cytokine signatures are observed that are characterized by production of IFNγ [in some but not all studies (16)], IL-18 and IL-6, and is further accompanied by acute phase protein and chemokine (IP-10) secretion (16, 17). T-cells are implicated as a significant source of type 1 cytokines (18, 19). Furthermore, numerous pro-inflammatory chemokines and cytokines, including IL-6, are secreted directly following HCMV infection (20). HCMV triggers cytokine production through the stimulation of pattern recognition receptors (PRRs), most notably Toll-like receptor 2 (21), the cytoplasmic DNA sensor STING (22) and IFI16 (23). Mice defective in PRRs mount reduced cytokine responses to MCMV *in vivo* (24–26). Although differences in the relative contributions of PRRs to the recognition of MCMV and HCMV may exist, these data suggest that innate immune recognition of viral infection by PRRs contributes to HCMV-induced cytokine profiles. Furthermore, *in vitro*, HCMV stimulation of peripheral blood-derived monocytes increases expression of TLRs, CD14, and adaptor molecules and transcription factors downstream of TLRs (27). Thus, active HCMV replication likely induces systemic pro-inflammatory cytokine responses both following via direct host recognition but also, potentially, by priming the host immune response to respond strongly to unrelated microbial signals.

Given the established role for type 1 cytokines in antiviral immunity, is such a response to CMV infection a bad thing for the host? Certainly, substantial evidence from clinical and experimental studies point toward a protective role for type 1 cytokine responses in cytomegalovirus infections (28–30). However, studies using MCMV show that T-cell responses, particularly $CD8^+$ T-cells, known to be induced by type 1 cytokines cause substantial tissue damage if insufficiently regulated (31, 32). Also, severe inflammatory cytokine responses or "cytokine storms" occur during MCMV hepatitis (33). Thus, these processes may drive acute HCMV-associated diseases. Furthermore, HCMV is implicated in organ rejection (34, 35) and, in cardiac transplants, graft atherosclerosis (36). Experimental studies using MCMV have recapitulated the observation that acute infection and viral reactivation can influence graft longevity (37, 38). MCMV reactivation induces expression within the graft of IFNα and IL-12 (37), implying that viral infection may elicit cytokine responses that activate cellular immunity capable of mediating graft rejection. Furthermore, HCMV induces IP-10 and fractalkine production during infection (17, 39), both of which are markers of allograft rejection (40).

HCMV establishes life-long infection within multiple host tissues (41) where some genomes are silent but others are transcriptionally active and express many genes (41–43). Immunological data highlights the likelihood that frequent reactivation events occur that re-stimulate the host immune system (44). Subsequently, HCMV may contribute to cytokine mediated inflammatory diseases in latently-infected immune competent individuals via continued gene transcription and reactivation, stimulating immune recognition and subsequent cytokine production. For example, HCMV is implicated in cardiac diseases (45) including atherosclerosis (46) where plaque formation and instability is an inflammatory-driven processes initiated by IFNγ (47). HCMV also induces accumulation of virus-specific cytotoxic $CD4^+$ T-cells expressing CX3CR1 (48). CX3CR1 binds fractalkine which is expressed by activated endothelium in response to TNFα and IFNγ produced by HCMV-specific T-cells (39). Interestingly, the HCMV chemokine receptor homolog US28 also binds fractalkine (49) and may contribute to localized inflammation. Thus, HCMV-induced cytokine and T-cell responses may mediate endothelial damage that in turn promotes vascular diseases and contributes to damage in multiple tissues and organs. Whether such processes underpin other harmful associations of HCMV, such as increased frailty in elderly individuals (4), is unclear.

Cytokines may also indirectly enhance tissue damage by promoting CMV reactivation and subsequent replication. IL-6 promotes HCMV reactivation in dendritic cells via ERK-MAPK

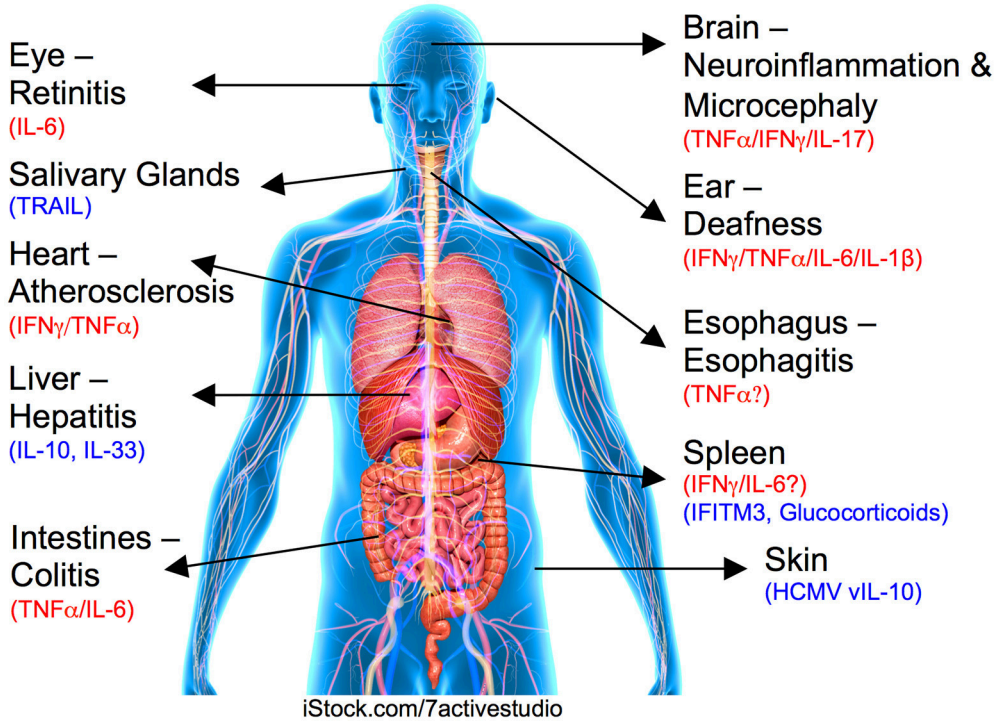

FIGURE 1 | Role for cytokines in CMV-induced organ pathologies. Organ or tissue and associated CMV-induced disease is labeled with inflammatory pathogenic cytokines highlighted in red and regulatory/suppressive pathways shown in blue.

mediated transcriptional induction of major immediate early (IE) genes (50, 51). TNFα and IL-1β also induce IE gene transcription by latent HCMV (52–54) and are implicated in reactivation of HCMV and/or MCMV *in vitro* and *in vivo* (55–59). An additional role for IFNγ in initiating HCMV reactivation has been described (56, 58). Data from MCMV suggest that overt pro-inflammatory cytokine responses may also impinge on innate antiviral immunity. Inadequate pro-inflammatory cytokine regulation can promote activation-induced NK cell death (60, 61) in a process involving IL-6 (60). Thus, inflammatory cytokines may directly and indirectly promote virus replication, which in turn drives peripheral tissue damage.

CYTOKINES AND DAMAGE IN IMMUNE PRIVILEGED SITES

When HCMV accesses immune privileged organs, immune-mediated pathology can ensue. HCMV-induced retinitis is a significant problem in AIDS/HIV patients (7–9). Interestingly, elevated expression of type 1 cytokines including IL-6 and IFNγ in aqueous and/or vitreous fluids from patients is detectable (62–64). Systemic CMV infection in immune competent mice induces significant myeloid cell and T-cell infiltrations into ocular tissue including the neural retina (65). Although cytokines likely play a role in mediating these inflammatory processes in immune competent hosts, this has yet to be investigated.

A role for inflammation in HCMV-induced hearing loss in infants is suggested by autopsies showing inner ear inflammation (66, 67). In mice, systemic infection of newborns induces progressive hearing loss and decreased spiral ganglia neuron density that is indicative of congenital HCMV infection (68). In MCMV, hearing loss does not correlate with the presence of virus in the cochlea but rather associates with persistent expression of chemokines and pro-inflammatory cytokines including TNFα, IL-6, and IL-1β (68). Similarly, intracranial MCMV infection induces hearing loss and chronic inflammatory cytokine expression (69).

Murine neonatal infection models have also been used to recapitulate central nervous system pathology triggered by congenital HCMV infection. After systemic infection, MCMV induces widespread focal encephalitis accompanied by mononuclear inflammation and microglial activation (70, 71), including TNFα expression (72). This is accompanied by STAT1 activation and IFN (type I and II) expression, in addition to TNFα (73). Interestingly, glucocorticoid treatment of these mice reduced cytokine expression and associated morphogenic abnormalities and cellular inflammation without influencing virus load, suggesting that virus-induced inflammation could be safely targeted to improve CMV-induced CNS pathogenesis (73). Indeed, neutralization of TNFα reduced expression of cytokines and myeloid cell activation and accumulation in the brain, and corrected cerebellar abnormalities and developmental gene expression (74). These important studies provide proof-of-concept that anti-inflammatory approaches

can be safely utilized to ameliorate CMV pathogenesis *in vivo*.

HCMV is implicated in esophagitis in HIV-infected individuals and associates with elevated TNFα production (75). Inflammatory bowel diseases are common during HIV co-infection (7) and HCMV maintains active replication in the gastrointestinal epithelium of individuals treated with antiretroviral therapy, where replication disrupts epithelial integrity in a manner partially dependent upon IL-6 (76). HCMV also associates with gastrointestinal inflammation in healthy individuals (77), where the virus may drive local production of cytokines such as TNFα (78) via induction of pattern recognition receptor expression and/or downstream, adaptor molecules (27, 79).

HCMV may also impact on neurological diseases in adults, with associations with HIV-associated neurological disorder (HAND) and impaired cognitive performance in HIV-infected individuals being reported [reviewed in (10)]. The link between HCMV and multiple sclerosis in immune competent hosts is controversial, with contradicting findings regarding the association between HCMV seropositivity and disease occurrence (80–82). In the murine experimental autoimmune encephalomyelitis (EAE) experimental model, MCMV worsens disease in genetically susceptible mice (83) and increases EAE occurrence in resistant (BALB/c) strains. Here, infection increases CD4 T-cell-dependent disease that is associated with IFNγ- and IL-17-expressing T-cells (84), further demonstrating that CMV can exacerbate tissue damage in the central nervous system.

Like many herpesviruses, HCMV is implicated as a risk factor in Alzheimer's Disease (AD) and cognitive decline (85). PBMCs from HCMV seropositive AD subjects produce more IFNγ following polyclonal and viral protein stimulation than non-AD subjects (86), and IFNγ is detectable only in cerebrospinal fluid of HCMV seropositive but not seronegative AD patients (87). Thus, although the role of HCMV in AD development is controversial, (88) it appears that HCMV-infected AD sufferers exhibit heightened cytokine responses which in turn could contribute to disease development and/or progression.

REGULATION OF CYTOKINE-DRIVEN CMV-INDUCED PATHOGENESIS

Despite its inflammatory potential, HCMV rarely causes inflammatory conditions in healthy individuals. Furthermore, infection in immune compromised and immunologically immature hosts does not always cause overt tissue damage, suggesting that virus-induced inflammatory cytokine responses are tightly regulated.

Regulatory T-Cells

The association between inducible regulatory T-cell (iTregs) expansions and reduced vascular pathology in elderly HCMV-infected individuals suggests a protective function for Tregs in HCMV infection (89). In MCMV, Tregs (promoted by IL-33) restrict liver pathology following systemic MCMV infection (32) and chronic reactive gliosis triggered by MCMV encephalitis (90). Although hepatic Tregs are known to be dependent upon IL-33 (32), whether Treg-mediated control of pathogenic T-cell responses involves restriction of inflammatory cytokine secretion is currently unknown.

Cytokines

Inflammatory cytokine responses during acute HCMV infection are accompanied by secretion of the immune modulatory cytokine IL-10 (16, 91). HCMV re-programmes human hematopoietic progenitor cells (HPCs) into immune-suppressive monocytes that express IL-10 in a process requiring US28 (92). In mice, genetic and pharmacological targeting of IL-10 demonstrates that IL-10 limits systemic inflammatory cytokine responses induced by CMV, including IL-6 and TNFα (61, 93, 94). This alleviates MCMV-induced disease, assessed using body weight (93, 94), and weight loss in IL-$10^{-/-}$ mice is alleviated by TNFα neutralization (93). IL-10 also restricts MCMV-induced hepatic inflammation and preserves liver function by limiting inflammatory effector cell infiltration, hepatocyte apoptosis and necrosis (95, 96). Experiments performed in perforin-deficient mice that are unable to control MCMV replication reveal that IL-10 restricts liver inflammation primarily by limiting pathogenic $CD8^+$ T-cell responses (31), a conclusion supported by data derived from immune competent Il-$10^{-/-}$ mice (95). Following injection of MCMV into the brain, IL-10 limits fatal immunopathology characterized by pro-inflammatory cytokine production and neutrophil infiltration (97, 98). Although the physiological relevance of some of these experiments in terms of HCMV pathogenesis is unclear, these data clearly highlight that IL-10R signaling can suppress CMV-induced immune pathology.

Importantly, genetic variation within the human IL-10 gene correlates with altered HCMV disease occurrence following allogeneic stem cell transplantation (99) and during HIV co-infection (100). This suggests that host genetic variation may influence tissue damage caused by HCMV-induced cytokines. Furthermore, HCMV encodes a functional IL-10 otholog (UL111A, vIL-10) that is expressed in lytic replication (101) and an alternate isoform in latency [LAcmvIL-10 (102)]. vIL-10 suppresses numerous innate and adaptive host immune responses including pro-inflammatory cytokine secretion (103, 104). Given that cellular IL-10 promotes MCMV carriage (93, 105–107), one may predict that HCMV vIL-10 facilitates virus persistence. However, using rhesus macaque CMV (rhCMV) that, like HCMV but not MCMV, expresses *UL111A*, it has been demonstrated that vIL-10 restricts acute inflammation at the initial site of infection, the skin. Interestingly, UL111A had no obvious impact on virus shedding in these experiments. This implies that virus persistence may not be influenced by UL111A *in vivo* (108) but instead that restriction of tissue pathology is an important function of viral IL-10 orthologs and perhaps other immune evasion gene products expressed by HCMV. Intriguingly, certain clinically-isolated HCMV strains have disrupted UL111A genes (109, 110). It will be interesting to investigate whether these HCMV strains preferentially associate with overt inflammatory responses.

IL-27 is an IL-12 family member that restricts numerous infection-induced pathologies (111). IL-27 facilitates MCMV persistence in the mucosa by suppressing IFNγ$^+$ (107) and/or cytotoxic (112) CD4$^+$ T-cells. Given that cytotoxic CD4$^+$ T-cells are implicated in tissue damage (113), IL-27-faciliated shedding of virions may be a necessary evil to restrict the development of these cells. Data regarding the function of IL-27 during HCMV infection is limited. Spector and colleagues identified that IL-27 limits IFNγ expression by virus-specific T-cells in HIV$^+$ and HIV$^-$ HCMV-infected individuals. This was accompanied by IL-27-mediated induction of IL-10 secreting CD4$^+$ T-cells (114). Whether IL-27 also alters the development of HCMV-specific cytotoxic T-cells is unknown. However, overall these data are consistent with the idea that IL-27 restricts chronic tissue damage by limiting HCMV-specific T-cell responses.

Data from HCMV and MCMV highlights that the cytokine TNF-related apoptosis-inducing ligand (TRAIL) contributes to control of virus replication (115–117). During persistent MCMV infection in the salivary glands, however, TRAIL expression by NK cells restricts pathogenic CD4$^+$ T-cell responses in this tissue. TRAIL-deficient mice exhibit hallmarks of Sjogren's syndrome (SS), an autoimmune disease of the salivary glands that is characterized by ectopic germinal center-like structures in the glands, elevated autoantibody production and impaired saliva secretion (113). Thus, TRAIL can limit both viral replication and potentially harmful infection-induced inflammatory responses.

Antiviral Restriction Factors

Interferon induced transmembrane protein 3 (IFITM3) is an antiviral restriction factor that inhibits endocytosis-dependent cell entry of numerous viruses (118). IFITM3 polymorphisms associated with reduced function are linked to increased risk of severe viral pathogenesis, most notably influenza-induced disease (119–121). Although IFITM3 does not directly impinge on either MCMV or HCMV replication (60, 122), *Ifitm3*$^{-/-}$ mice are dramatically more susceptible to MCMV-driven pathogenesis (60). Disease, which can be fatal, consists of extensive weight loss, transient pulmonary and hepatic mononuclear inflammation, and extensive and irreversible splenic damage. Blocking the action of IL-6 alleviates pathogenesis in MCMV-infected *Ifitm3*$^{-/-}$ mice and also inhibits activation-induced NK cell death and promotes NK cell immunity (60). Thus, it is unclear whether IL-6 drives CMV-induced pathology by promoting tissue damage and/or by impairing cellular antiviral innate immune responses and subsequent control of virus replication. Irrespective, these data again highlight the possible role for genetics in determining host cytokine responsiveness to HCMV and the subsequent disease outcome.

Glucocorticoids

Endogenous glucocorticoids are steroid hormones produced in the adrenal cortex following activation of the hypothalamic-pituitary-adrenal (HPA) axis. Initial inflammatory cytokine responses during acute MCMV infection are accompanied by robust glucocorticoid production (123, 124), the maximal release of which is dependent upon virus-induced IL-6 (123). The importance of glucocorticoids in modulating CMV-induced pathogenesis is highlighted in studies where mice are rendered globally deficient in glucocorticoids by adrenalectomy and display increased production of pro-inflammatory cytokines and susceptibility to TNFα-mediated lethal disease (125). Furthermore, glucocorticoid receptor signaling in NK cells, via an axis involving the inhibitory PD-1 receptor, exerts tissue-specific regulation of IFNγ production. Here, unrestricted NK cell expression of IFNγ in spleens of mice lacking the glucocorticoid receptor in NCR1$^+$ cells results in necrotizing splenitis and destruction of the white pulp (124). Although pathology in medically important sites of CMV pathogenesis like the liver were unaffected by this process (124), these data suggest that neuro-immune pathways may be critical for control of cytokine-driven pathogenesis during CMV infection.

CONCLUSIONS

Many associations exist between production of inflammatory cytokines and CMV-associated pathologies in humans and in experimental systems. Experimental models like MCMV have their limitations in terms of variations in virus genetics (including lacking key immune regulatory genes like vIL-10) and the imperfect recreation in mice of HCMV-induced pathologies. However, important predictions regarding roles that cytokines play in virus-induced tissue damage and how inflammatory cytokines are regulated can be derived from these studies. Moving forward, these models will be critical to examine whether targeting CMV-induced inflammation is an effective, safe and viable approach to alleviating pathogenesis. Understanding exactly how cytokines cause tissue damage and how production of these cytokines is regulated will hopefully lead to more refined and effective strategies to help alleviate the pathological consequences of HCMV infection. These studies may also help identify host genetic variations that influence cytokine responsiveness and susceptibility to HCMV disease. Finally, these studies may help form novel hypotheses regarding the possible influence of genetic variation in virus-encoded immune evasion genes on HCMV pathogenesis.

AUTHOR CONTRIBUTIONS

IRH defined the manuscript focus and structure. MC and IRH wrote and edited the manuscript.

FUNDING

This work was funded by a Welcome Trust Senior Research Fellowship to Ian Humphreys (207503/Z/17/Z).

ACKNOWLEDGMENTS

The authors wish to thank Dr. Matthew Reeves for critical reading of this manuscript.

REFERENCES

1. Jackson SE, Mason GM, Wills MR. Human cytomegalovirus immunity and immune evasion. *Virus Res.* (2011) 157:151–60. doi: 10.1016/j.virusres.2010.10.031
2. Stack G, Stacey MA, Humphreys IR. Herpesvirus exploitation of host immune inhibitory pathways. *Viruses* (2012) 4:1182–201. doi: 10.3390/v4081182
3. Dupont L, Reeves MB. Cytomegalovirus latency and reactivation: recent insights into an age old problem. *Rev Med Virol.* (2016) 26:75–89. doi: 10.1002/rmv.1862
4. Thomasini RL, Pereira DS, Pereira FSM, Mateo EC, Mota TN, Guimaraes GG, et al. Aged-associated cytomegalovirus and Epstein-Barr virus reactivation and cytomegalovirus relationship with the frailty syndrome in older women. *PLoS ONE* (2017) 12:e0180841. doi: 10.1371/journal.pone.0180841
5. Spyridopoulos I, Martin-Ruiz C, Hilkens C, Yadegarfar ME, Isaacs J, Jagger C, et al. CMV seropositivity and T-cell senescence predict increased cardiovascular mortality in octogenarians: results from the Newcastle 85+ study. *Aging Cell* (2016) 15:389–92. doi: 10.1111/acel.12430
6. Crough T, Khanna R. Immunobiology of human cytomegalovirus: from bench to bedside. *Clin Microbiol Rev.* (2009) 22:76–98. doi: 10.1128/CMR.00034-08
7. Jacobson MA, Mills J. Serious cytomegalovirus disease in the acquired immunodeficiency syndrome (AIDS). Clinical findings, diagnosis, and treatment. *Ann Intern Med.* (1988) 108:585–94. doi: 10.7326/0003-4819-108-4-585
8. Hoover DR, Peng Y, Saah A, Semba R, Detels RR, Rinaldo CR Jr, et al. Occurrence of cytomegalovirus retinitis after human immunodeficiency virus immunosuppression. *Arch Ophthalmol.* (1996) 114:821–7. doi: 10.1001/archopht.1996.01100140035004
9. Jabs DA, Van Natta ML, Holland GN, Danis R, Studies of the Ocular Complications of AIDS Research Group. Cytomegalovirus retinitis in patients with acquired immunodeficiency syndrome after initiating antiretroviral therapy. *Am J Ophthalmol.* (2017) 174:23–32. doi: 10.1016/j.ajo.2016.10.011
10. Gianella S, Letendre S. Cytomegalovirus and HIV: A Dangerous Pas de Deux. *J Infect Dis.* (2016) 214:S67–74. doi: 10.1093/infdis/jiw217
11. Griffiths PD. Burden of disease associated with human cytomegalovirus and prospects for elimination by universal immunisation. *Lancet Infect Dis.* (2012) 12:790–8. doi: 10.1016/S1473-3099(12)70197-4
12. Hagay ZJ, Biran G, Ornoy A, Reece EA. Congenital cytomegalovirus infection: a long-standing problem still seeking a solution. *Am J Obstet Gynecol.* (1996) 174:241–5. doi: 10.1016/S0002-9378(96)70401-5
13. Fowler KB. Congenital cytomegalovirus infection: audiologic outcome. *Clin Infect Dis.* (2013) 57:S182–4. doi: 10.1093/cid/cit609
14. Britt W. Manifestations of human cytomegalovirus infection: proposed mechanisms of acute and chronic disease. *Curr Top Microbiol Immunol.* (2008) 325:417–70. doi: 10.1007/978-3-540-77349-8_23
15. Biron CA, Tarrio ML. Immunoregulatory cytokine networks: 60 years of learning from murine cytomegalovirus. *Med Microbiol Immunol.* (2015) 204:345–54. doi: 10.1007/s00430-015-0412-3
16. Sadeghi M, Daniel V, Naujokat C, Schnitzler P, Schmidt J, Mehrabi A, et al. Dysregulated cytokine responses during cytomegalovirus infection in renal transplant recipients. *Transplantation* (2008) 86:275–85. doi: 10.1097/TP.0b013e31817b063d
17. van de Berg PJ, Heutinck KM, Raabe R, Minnee RC, Young SL, van Donselaar-van der Pant KA, et al. Human cytomegalovirus induces systemic immune activation characterized by a type 1 cytokine signature. *J Infect Dis.* (2010) 202:690–9. doi: 10.1086/655472
18. Villacres MC, Longmate J, Auge C, Diamond DJ. Predominant type 1 CMV-specific memory T-helper response in humans: evidence for gender differences in cytokine secretion. *Hum Immunol.* (2004) 65:476–85. doi: 10.1016/j.humimm.2004.02.021
19. Gamadia LE, Rentenaar RJ, van Lier RA, ten Berge IJ. Properties of CD4(+) T cells in human cytomegalovirus infection. *Hum Immunol.* (2004) 65:486–92. doi: 10.1016/j.humimm.2004.02.020
20. Dumortier J, Streblow DN, Moses AV, Jacobs JM, Kreklywich CN, Camp D, et al. Human cytomegalovirus secretome contains factors that induce angiogenesis and wound healing. *J Virol.* (2008) 82:6524–35. doi: 10.1128/JVI.00502-08
21. Compton T, Kurt-Jones EA, Boehme KW, Belko J, Latz E, Golenbock DT, et al. Human cytomegalovirus activates inflammatory cytokine responses via CD14 and Toll-like receptor 2. *J Virol.* (2003) 77:4588–96. doi: 10.1128/JVI.77.8.4588-4596.2003
22. Ishikawa H, Ma Z, Barber GN. Sting regulates intracellular DNA-mediated, type I interferon-dependent innate immunity. *Nature* (2009) 461:788–92. doi: 10.1038/nature08476
23. Li T, Chen J, Cristea IM. Human cytomegalovirus tegument protein pUL83 inhibits IFI16-mediated DNA sensing for immune evasion. *Cell Host Microbe.* (2013) 14:591–9. doi: 10.1016/j.chom.2013.10.007
24. Krug A, French AR, Barchet W, Fischer JA, Dzionek A, Pingel JT, et al. TLR9-dependent recognition of MCMV by IPC and DC generates coordinated cytokine responses that activate antiviral NK cell function. *Immunity* (2004) 21:107–19. doi: 10.1016/j.immuni.2004.06.007
25. Tabeta K, Georgel P, Janssen E, Du X, Hoebe K, Crozat K, et al. Toll-like receptors 9 and 3 as essential components of innate immune defense against mouse cytomegalovirus infection. *Proc Natl Acad Sci USA.* (2004) 101:3516–21. doi: 10.1073/pnas.0400525101
26. Zucchini N, Bessou G, Traub S, Robbins SH, Uematsu S, Akira S, et al. Cutting edge: Overlapping functions of TLR7 and TLR9 for innate defense against a herpesvirus infection. *J Immunol.* (2008) 180:5799–803. doi: 10.4049/jimmunol.180.9.5799
27. Smith PD, Shimamura M, Musgrove LC, Dennis EA, Bimczok D, Novak L, et al. Cytomegalovirus enhances macrophage TLR expression and MyD88-mediated signal transduction to potentiate inducible inflammatory responses. *J Immunol.* (2014) 193:5604–12. doi: 10.4049/jimmunol.1302608
28. Gamadia LE, Remmerswaal EB, Weel JF, Bemelman F, van Lier RA, Ten Berge IJ. Primary immune responses to human CMV: a critical role for IFN-gamma-producing CD4+ T cells in protection against CMV disease. *Blood* (2003) 101:2686–92. doi: 10.1182/blood-2002-08-2502
29. Tu W, Chen S, Sharp M, Dekker C, Manganello AM, Tongson EC, et al. Persistent and selective deficiency of CD4+ T cell immunity to cytomegalovirus in immunocompetent young children. *J Immunol.* (2004) 172:3260–7. doi: 10.4049/jimmunol.172.5.3260
30. Walton SM, Mandaric S, Torti N, Zimmermann A, Hengel H, Oxenius A. Absence of cross-presenting cells in the salivary gland and viral immune evasion confine cytomegalovirus immune control to effector CD4 T cells. *PLoS Pathog.* (2011) 7:e1002214. doi: 10.1371/journal.ppat.1002214
31. Lee SH, Kim KS, Fodil-Cornu N, Vidal SM, Biron CA. Activating receptors promote NK cell expansion for maintenance, IL-10 production, and CD8 T cell regulation during viral infection. *J Exp Med.* (2009) 206:2235–51. doi: 10.1084/jem.20082387
32. Popovic B, Golemac M, Podlech J, Zeleznjak J, Bilic-Zulle L, Lukic ML, et al. IL-33/ST2 pathway drives regulatory T cell dependent suppression of liver damage upon cytomegalovirus infection. *PLoS Pathog.* (2017) 13:e1006345. doi: 10.1371/journal.ppat.1006345
33. Trgovcich J, Stimac D, Polic B, Krmpotic A, Pernjak-Pugel E, Tomac J, et al. Immune responses and cytokine induction in the development of severe hepatitis during acute infections with murine cytomegalovirus. *Arch Virol.* (2000) 145:2601–18. doi: 10.1007/s007050070010
34. Hodson EM, Jones CA, Webster AC, Strippoli GF, Barclay PG, Kable K, et al. Antiviral medications to prevent cytomegalovirus disease and early death in recipients of solid-organ transplants: a systematic review of randomised controlled trials. *Lancet* (2005) 365:2105–15. doi: 10.1016/S0140-6736(05)66553-1
35. Cainelli F, Vento S. Infections and solid organ transplant rejection: a cause-and-effect relationship? *Lancet Infect Dis.* (2002) 2:539–49. doi: 10.1016/S1473-3099(02)00370-5
36. Grattan MT, Moreno-Cabral CE, Starnes VA, Oyer PE, Stinson EB, Shumway NE. Cytomegalovirus infection is associated with cardiac allograft rejection and atherosclerosis. *JAMA* (1989) 261:3561–6. doi: 10.1001/jama.1989.03420240075030
37. Cook CH, Bickerstaff AA, Wang JJ, Zimmerman PD, Forster MR, Nadasdy T, et al. Disruption of murine cardiac allograft

acceptance by latent cytomegalovirus. *Am J Transl.* (2009) 9:42–53. doi: 10.1111/j.1600-6143.2008.02457.x
38. Carlquist JF, Shelby J, Shao YL, Greenwood JH, Hammond ME, Anderson JL. Accelerated rejection of murine cardiac allografts by murine cytomegalovirus-infected recipients. lack of haplotype specificity. *J Clin Invest.* (1993) 91:2602–8. doi: 10.1172/JCI116499
39. Bolovan-Fritts CA, Trout RN, Spector SA. Human cytomegalovirus-specific CD4+-T-cell cytokine response induces fractalkine in endothelial cells. *J Virol.* (2004) 78:13173–81. doi: 10.1128/JVI.78.23.13173-13181.2004
40. Zhang Q, Liu YF, Su ZX, Shi LP, Chen YH. Serum fractalkine and interferon-gamma inducible protein-10 concentrations are early detection markers for acute renal allograft rejection. *Transl Proc.* (2014) 46:1420–5. doi: 10.1016/j.transproceed.2014.02.019
41. Shnayder M, Nachshon A, Krishna B, Poole E, Boshkov A, Binyamin A, et al. Defining the transcriptional landscape during cytomegalovirus latency with single-cell RNA sequencing. *MBio* (2018) 9:18. doi: 10.1128/mBio.00013-18
42. Cheng S, Caviness K, Buehler J, Smithey M, Nikolich-Zugich J, Goodrum F. Transcriptome-wide characterization of human cytomegalovirus in natural infection and experimental latency. *Proc Natl Acad Sci USA*. (2017) 114:E10586–95. doi: 10.1073/pnas.1710522114
43. Rossetto CC, Tarrant-Elorza M, Pari GS. Cis and trans acting factors involved in human cytomegalovirus experimental and natural latent infection of CD14 (+) monocytes and CD34 (+) cells. *PLoS Pathog*. (2013) 9:e1003366. doi: 10.1371/journal.ppat.1003366
44. Klenerman P, Oxenius A. T cell responses to cytomegalovirus. *Nat Rev Immunol*. (2016) 16:367–77. doi: 10.1038/nri.2016.38
45. Simanek AM, Dowd JB, Pawelec G, Melzer D, Dutta A, Aiello AE. Seropositivity to cytomegalovirus, inflammation, all-cause and cardiovascular disease-related mortality in the United States. *PLoS ONE* (2011) 6:e16103. doi: 10.1371/journal.pone.0016103
46. Weis M, Kledal TN, Lin KY, Panchal SN, Gao SZ, Valantine HA, et al. Cytomegalovirus infection impairs the nitric oxide synthase pathway: role of asymmetric dimethylarginine in transplant arteriosclerosis. *Circulation* (2004) 109:500–5. doi: 10.1161/01.CIR.0000109692.16004.AF
47. Hansson GK, Libby P. The immune response in atherosclerosis: a double-edged sword. *Nat Rev Immunol.* (2006) 6:508–19. doi: 10.1038/nri1882
48. Pachnio A, Ciaurriz M, Begum J, Lal N, Zuo J, Beggs A, et al. Cytomegalovirus infection leads to development of high frequencies of cytotoxic virus-specific CD4+ T Cells targeted to vascular endothelium. *PLoS Pathog.* (2016) 12:e1005832. doi: 10.1371/journal.ppat.1005832
49. Kledal TN, Rosenkilde MM, Schwartz TW. Selective recognition of the membrane-bound CX3C chemokine, fractalkine, by the human cytomegalovirus-encoded broad-spectrum receptor US28. *FEBS Lett.* (1998) 441:209–14. doi: 10.1016/S0014-5793(98)01551-8
50. Reeves MB, Compton T. Inhibition of inflammatory interleukin-6 activity via extracellular signal-regulated kinase-mitogen-activated protein kinase signaling antagonizes human cytomegalovirus reactivation from dendritic cells. *J Virol.* (2011) 85:12750–8. doi: 10.1128/JVI.05878-11
51. Hargett D, Shenk TE. Experimental human cytomegalovirus latency in CD14+ monocytes. *Proc Natl Acad Sci USA*. (2010) 107:20039–44. doi: 10.1073/pnas.1014509107
52. Forte E, Swaminathan S, Schroeder MW, Kim JY, Terhune SS, Hummel M. Tumor necrosis factor alpha induces reactivation of human cytomegalovirus independently of myeloid cell differentiation following posttranscriptional establishment of latency. *MBio* (2018) 9:e01560–18. doi: 10.1128/mBio.01560-18
53. O'Connor CM, Murphy EA. A myeloid progenitor cell line capable of supporting human cytomegalovirus latency and reactivation, resulting in infectious progeny. *J Virol.* (2012) 86:9854–65. doi: 10.1128/JVI.01278-12
54. Hummel M, Zhang Z, Yan S, DePlaen I, Golia P, Varghese T, et al. Allogeneic transplantation induces expression of cytomegalovirus immediate-early genes *in vivo*: a model for reactivation from latency. *J Virol.* (2001) 75:4814–22. doi: 10.1128/JVI.75.10.4814-4822.2001
55. Simon CO, Seckert CK, Dreis D, Reddehase MJ, Grzimek NK. Role for tumor necrosis factor alpha in murine cytomegalovirus transcriptional reactivation in latently infected lungs. *J Virol.* (2005) 79:326–40. doi: 10.1128/JVI.79.1.326-340.2005
56. Hahn G, Jores R, Mocarski ES. Cytomegalovirus remains latent in a common precursor of dendritic and myeloid cells. *Proc Natl Acad Sci USA*. (1998) 95:3937–42. doi: 10.1073/pnas.95.7.3937
57. Docke WD, Prosch S, Fietze E, Kimel V, Zuckermann H, Klug C, et al. Cytomegalovirus reactivation and tumour necrosis factor. *Lancet* (1994) 343:268–9. doi: 10.1016/S0140-6736(94)91116-9
58. Soderberg-Naucler C, Streblow DN, Fish KN, Allan-Yorke J, Smith PP, Nelson JA. Reactivation of latent human cytomegalovirus in CD14(+) monocytes is differentiation dependent. *J Virol.* (2001) 75:7543–54. doi: 10.1128/JVI.75.16.7543-7554.2001
59. Cook CH, Trgovcich J, Zimmerman PD, Zhang Y, Sedmak DD. Lipopolysaccharide, tumor necrosis factor alpha, or interleukin-1beta triggers reactivation of latent cytomegalovirus in immunocompetent mice. *J Virol.* (2006) 80:9151–8. doi: 10.1128/JVI.00216-06
60. Stacey MA, Clare S, Clement M, Marsden M, Abdul-Karim J, Kane L et al. The antiviral restriction factor IFN-induced transmembrane protein 3 prevents cytokine-driven CMV pathogenesis. *J Clin Invest*. (2017) 127:1463–74. doi: 10.1172/JCI84889
61. Stacey MA, Marsden M, Wang EC, Wilkinson GW, Humphreys IR. IL-10 restricts activation-induced death of NK cells during acute murine cytomegalovirus infection. *J Immunol.* (2011) 187:2944–52. doi: 10.4049/jimmunol.1101021
62. Schrier RD, Song MK, Smith IL, Karavellas MP, Bartsch DU, Torriani FJ, et al. Intraocular viral and immune pathogenesis of immune recovery uveitis in patients with healed cytomegalovirus retinitis. *Retina* (2006) 26:165–9. doi: 10.1097/00006982-200602000-00007
63. Iyer JV, Agrawal R, Yeo TK, Gunasekeran DV, Balne PK, Lee B, et al. Aqueous humor immune factors and cytomegalovirus (CMV) levels in CMV retinitis through treatment - The CRIGSS study. *Cytokine* (2016) 84:56–62. doi: 10.1016/j.cyto.2016.05.009
64. Iyer JV, Connolly J, Agrawal R, Yeo TK, Lee B, Au B, et al. Cytokine analysis of aqueous humor in HIV patients with cytomegalovirus retinitis. *Cytokine* (2013) 64:541–7. doi: 10.1016/j.cyto.2013.08.006
65. Voigt V, Andoniou CE, Schuster IS, Oszmiana A, Ong ML, Fleming P, et al. Cytomegalovirus establishes a latent reservoir and triggers long-lasting inflammation in the eye. *PLoS Pathog.* (2018) 14:e1007040. doi: 10.1371/journal.ppat.1007040
66. Davis LE, Johnsson LG, Kornfeld M. Cytomegalovirus labyrinthitis in an infant: morphological, virological, and immunofluorescent studies. *J Neuropathol Exp Neurol.* (1981) 40:9–19. doi: 10.1097/00005072-198101000-00002
67. Boppana SBW. Cytomegalovirus. in: Newton VE, Vallely PJ, editors. *Infection and Hearing Impairment*. Sussex: John Wiley and Sons (2006). p. 67–93.
68. Bradford RD, Yoo YG, Golemac M, Pugel EP, Jonjic S, Britt WJ. Murine CMV-induced hearing loss is associated with inner ear inflammation and loss of spiral ganglia neurons. *PLoS Pathog.* (2015) 11:e1004774. doi: 10.1371/journal.ppat.1004774
69. Schachtele SJ, Mutnal MB, Schleiss MR, Lokensgard JR. Cytomegalovirus-induced sensorineural hearing loss with persistent cochlear inflammation in neonatal mice. *J Neurovirol.* (2011) 17:201–11. doi: 10.1007/s13365-011-0024-7
70. Koontz T, Bralic M, Tomac J, Pernjak-Pugel E, Bantug G, Jonjic S, et al. Altered development of the brain after focal herpesvirus infection of the central nervous system. *J Exp Med.* (2008) 205:423–35. doi: 10.1084/jem.20071489
71. Cekinovic D, Golemac M, Pugel EP, Tomac J, Cicin-Sain L, Slavuljica I, et al. Passive immunization reduces murine cytomegalovirus-induced brain pathology in newborn mice. *J Virol.* (2008) 82:12172–80. doi: 10.1128/JVI.01214-08
72. Mutnal MB, Hu S, Little MR, Lokensgard JR. Memory T cells persisting in the brain following MCMV infection induce long-term microglial activation via interferon-gamma. *J Neurovirol.* (2011) 17:424–37. doi: 10.1007/s13365-011-0042-5
73. Kosmac K, Bantug GR, Pugel EP, Cekinovic D, Jonjic S, Britt WJ. Glucocorticoid treatment of MCMV infected newborn mice attenuates CNS inflammation and limits deficits in cerebellar development. *PLoS Pathog.* (2013) 9:e1003200. doi: 10.1371/journal.ppat.1003200

74. Seleme MC, Kosmac K, Jonjic S, Britt WJ. Tumor necrosis factor alpha-induced recruitment of inflammatory mononuclear cells leads to inflammation and altered brain development in murine cytomegalovirus-infected newborn mice. *J Virol.* (2017) 91:e01983–16. doi: 10.1128/JVI.01983-16
75. Wilcox CM, Harris PR, Redman TK, Kawabata S, Hiroi T, Kiyono H, et al. High mucosal levels of tumor necrosis factor alpha messenger RNA in AIDS-associated cytomegalovirus-induced esophagitis. *Gastroenterology* (1998) 114:77–82. doi: 10.1016/S0016-5085(98)70635-3
76. Maidji E, Somsouk M, Rivera JM, Hunt PW, Stoddart CA. Replication of CMV in the gut of HIV-infected individuals and epithelial barrier dysfunction. *PLoS Pathog.* (2017) 13:e1006202. doi: 10.1371/journal.ppat.1006202
77. Kandiel A, Lashner B. Cytomegalovirus colitis complicating inflammatory bowel disease. *Am J Gastroenterol.* (2006) 101:2857–65. doi: 10.1111/j.1572-0241.2006.00869.x
78. Smith PD, Saini SS, Raffeld M, Manischewitz JF, Wahl SM. Cytomegalovirus induction of tumor necrosis factor-alpha by human monocytes and mucosal macrophages. *J Clin Invest.* (1992) 90:1642–8. doi: 10.1172/JCI116035
79. Dennis EA, Smythies LE, Grabski R, Li M, Ballestas ME, Shimamura M, et al. Cytomegalovirus promotes intestinal macrophage-mediated mucosal inflammation through induction of Smad7. *Mucosal Immunol.* (2018) 1694–704. doi: 10.1038/s41385-018-0041-4
80. Sanadgol N, Ramroodi N, Ahmadi GA, Komijani M, Moghtaderi A, Bouzari M, et al. Prevalence of cytomegalovirus infection and its role in total immunoglobulin pattern in Iranian patients with different subtypes of multiple sclerosis. *N Microbiol.* (2011) 34:263–74.
81. Horakova D, Zivadinov R, Weinstock-Guttman B, Havrdova E, Qu J, Tamano-Blanco M, et al. Environmental factors associated with disease progression after the first demyelinating event: results from the multi-center SET study. *PLoS ONE* (2013) 8:e53996. doi: 10.1371/journal.pone.0053996
82. Sundqvist E, Bergstrom T, Daialhosein H, Nystrom M, Sundstrom P, Hillert J, et al. Cytomegalovirus seropositivity is negatively associated with multiple sclerosis. *Mult Scler*. (2014) 20:165–73. doi: 10.1177/1352458513494489
83. Vanheusden M, Broux B, Welten SPM, Peeters LM, Panagioti E, Van Wijmeersch B, et al. Cytomegalovirus infection exacerbates autoimmune mediated neuroinflammation. *Sci Rep*. (2017) 7:663. doi: 10.1038/s41598-017-00645-3
84. Milovanovic J, Popovic B, Milovanovic M, Kvestak D, Arsenijevic A, Stojanovic B, et al. Murine cytomegalovirus infection induces susceptibility to EAE in resistant BALB/c mice. *Front Immunol.* (2017) 8:192. doi: 10.3389/fimmu.2017.00192
85. Barnes LL, Capuano AW, Aiello AE, Turner AD, Yolken RH, Torrey EF, et al. Cytomegalovirus infection and risk of Alzheimer disease in older black and white individuals. *J Infect Dis.* (2015) 211:230–7. doi: 10.1093/infdis/jiu437
86. Westman G, Berglund D, Widen J, Ingelsson M, Korsgren O, Lannfelt L, et al. Increased inflammatory response in cytomegalovirus seropositive patients with Alzheimer's disease. *PLoS ONE* (2014) 9:e96779. doi: 10.1371/journal.pone.0096779
87. Lurain NS, Hanson BA, Martinson J, Leurgans SE, Landay AL, Bennett DA, et al. Virological and immunological characteristics of human cytomegalovirus infection associated with Alzheimer disease. *J Infect Dis.* (2013) 208:564–72. doi: 10.1093/infdis/jit210
88. Itzhaki RF, Klapper P. Cytomegalovirus: an improbable cause of Alzheimer disease. *J Infect Dis.* (2014) 209:972–3. doi: 10.1093/infdis/jit665
89. Terrazzini N, Bajwa M, Vita S, Cheek E, Thomas D, Seddiki N, et al. A novel cytomegalovirus-induced regulatory-type T-cell subset increases in size during older life and links virus-specific immunity to vascular pathology. *J Infect Dis.* (2014) 209:1382–92. doi: 10.1093/infdis/jit576
90. Lokensgard JR, Schachtele SJ, Mutnal MB, Sheng WS, Prasad S, Hu S. Chronic reactive gliosis following regulatory T cell depletion during acute MCMV encephalitis. *Glia* (2015) 63:1982–96. doi: 10.1002/glia.22868
91. Nordoy I, Muller F, Nordal KP, Rollag H, Lien E, Aukrust P, et al. The role of the tumor necrosis factor system and interleukin-10 during cytomegalovirus infection in renal transplant recipients. *J Infect Dis.* (2000) 181:51–7. doi: 10.1086/315184
92. Zhu D, Pan C, Sheng J, Liang H, Bian Z, Liu Y, et al. Human cytomegalovirus reprogrammes haematopoietic progenitor cells into immunosuppressive monocytes to achieve latency. *Nat Microbiol.* (2018) 3:503–13. doi: 10.1038/s41564-018-0131-9
93. Mandaric S, Walton SM, Rulicke T, Richter K, Girard-Madoux MJ, Clausen BE, et al. vIL-10 suppression of NK/DC crosstalk leads to poor priming of MCMV-specific CD4 T cells and prolonged MCMV persistence. *PLoS Pathog.* (2012) 8:e1002846. doi: 10.1371/journal.ppat.1002846
94. Oakley OR, Garvy BA, Humphreys S, Qureshi MH, Pomeroy C. Increased weight loss with reduced viral replication in interleukin-10 knock-out mice infected with murine cytomegalovirus. *Clin Exp Immunol.* (2008) 151:155–64. doi: 10.1111/j.1365-2249.2007.03533.x
95. Tang-Feldman YJ, Lochhead GR, Lochhead SR, Yu C, Pomeroy C. Interleukin-10 repletion suppresses pro-inflammatory cytokines and decreases liver pathology without altering viral replication in murine cytomegalovirus (MCMV)-infected IL-10 knockout mice. *Inflamm Res.* (2011) 60:233–43. doi: 10.1007/s00011-010-0259-4
96. Gaddi PJ, Crane MJ, Kamanaka M, Flavell RA, Yap GS, Salazar-Mather TP. IL-10 mediated regulation of liver inflammation during acute murine cytomegalovirus infection. *PLoS ONE* (2012) 7:e42850. doi: 10.1371/journal.pone.0042850
97. Cheeran MC, Mutnal MB, Hu S, Armien A, Lokensgard JR. Reduced lymphocyte infiltration during cytomegalovirus brain infection of interleukin-10-deficient mice. *J Neurovirol.* (2009) 15:334–42. doi: 10.1080/13550280903062797
98. Mutnal MB, Cheeran MC, Hu S, Little MR, Lokensgard JR. Excess neutrophil infiltration during cytomegalovirus brain infection of interleukin-10-deficient mice. *J Neuroimmunol.* (2010) 227:101–10. doi: 10.1016/j.jneuroim.2010.06.020
99. Loeffler J, Steffens M, Arlt EM, Toliat MR, Mezger M, Suk A, et al. Polymorphisms in the genes encoding chemokine receptor 5, interleukin-10, and monocyte chemoattractant protein 1 contribute to cytomegalovirus reactivation and disease after allogeneic stem cell transplantation. *J Clin Microbiol.* (2006) 44:1847–50. doi: 10.1128/JCM.44.5.1847-1850.2006
100. Sezgin E, Jabs DA, Hendrickson SL, Van Natta M, Zdanov A, Lewis RA, et al. Effect of host genetics on the development of cytomegalovirus retinitis in patients with AIDS. *J Infect Dis.* (2010) 202:606–13. doi: 10.1086/654814
101. Kotenko SV, Saccani S, Izotova LS, Mirochnitchenko OV, Pestka S. Human cytomegalovirus harbors its own unique IL-10 homolog (cmvIL-10). *Proc Natl Acad Sci USA.* (2000) 97:1695–700. doi: 10.1073/pnas.97.4.1695
102. Jenkins C, Garcia W, Godwin MJ, Spencer JV, Stern JL, Abendroth A, et al. Immunomodulatory properties of a viral homolog of human interleukin-10 expressed by human cytomegalovirus during the latent phase of infection. *J Virol.* (2008) 82:3736–50. doi: 10.1128/JVI.02173-07
103. Spencer JV, Lockridge KM, Barry PA, Lin G, Tsang M, Penfold ME, et al. Potent immunosuppressive activities of cytomegalovirus-encoded interleukin-10. *J Virol.* (2002) 76:1285–92. doi: 10.1128/JVI.76.3.1285-1292.2002
104. Slobedman B, Barry PA, Spencer JV, Avdic S, Abendroth A. Virus-encoded homologs of cellular interleukin-10 and their control of host immune function. *J Virol.* (2009) 83:9618–29. doi: 10.1128/JVI.01098-09
105. Humphreys IR, de Trez C, Kinkade A, Benedict CA, Croft M, Ware CF. Cytomegalovirus exploits IL-10-mediated immune regulation in the salivary glands. *J Exp Med.* (2007) 204:1217–25. doi: 10.1084/jem.20062424
106. Jones M, Ladell K, Wynn KK, Stacey MA, Quigley MF, Gostick E, et al. IL-10 restricts memory T cell inflation during cytomegalovirus infection. *J Immunol.* (2010) 185:3583–92. doi: 10.4049/jimmunol.1001535
107. Clement M, Marsden M, Stacey MA, Abdul-Karim J, Gimeno Brias S, Costa Bento D, et al. Cytomegalovirus-Specific IL-10-Producing CD4+ T cells are governed by type-I IFN-induced IL-27 and promote virus persistence. *PLoS Pathog.* (2016) 12:e1006050. doi: 10.1371/journal.ppat.1006050
108. Chang WL, Barry PA. Attenuation of innate immunity by cytomegalovirus IL-10 establishes a long-term deficit of adaptive antiviral immunity. *Proc Natl Acad Sci USA.* (2010) 107:22647–52. doi: 10.1073/pnas.1013794108
109. Cunningham C, Gatherer D, Hilfrich B, Baluchova K, Dargan DJ, Thomson M, et al. Sequences of complete human cytomegalovirus genomes from infected cell cultures and clinical specimens. *J Gen Virol.* (2010) 91:605–15. doi: 10.1099/vir.0.015891-0
110. Sijmons S, Thys K, Mbong Ngwese M, Van Damme E, Dvorak J, Van Loock M, et al. High-throughput analysis of human cytomegalovirus

genome diversity highlights the widespread occurrence of gene-disrupting mutations and pervasive recombination. *J Virol.* (2015). 89:7673–95. doi: 10.1128/JVI.00578-15

111. Yoshida H, Hunter CA. The immunobiology of interleukin-27. *Annu Rev Immunol.* (2015) 33:417–43. doi: 10.1146/annurev-immunol-032414-112134
112. Wehrens EJ, Wong KA, Gupta A, Khan A, Benedict CA, Zuniga EI. IL-27 regulates the number, function and cytotoxic program of antiviral CD4 T cells and promotes cytomegalovirus persistence. *PLoS ONE* (2018) 13:e0201249. doi: 10.1371/journal.pone.0201249
113. Schuster IS, Wikstrom ME, Brizard G, Coudert JD, Estcourt MJ, Manzur M, et al. TRAIL+ NK cells control CD4+ T cell responses during chronic viral infection to limit autoimmunity. *Immunity* (2014) 41:646–56. doi: 10.1016/j.immuni.2014.09.013
114. Garg A, Trout R, Spector SA. Human Immunodeficiency virus type-1 myeloid derived suppressor cells inhibit cytomegalovirus inflammation through interleukin-27 and B7-H4. *Sci Rep.* (2017) 7:44485. doi: 10.1038/srep44485
115. Verma S, Loewendorf A, Wang Q, McDonald B, Redwood A, Benedict CA, et al. Inhibition of the TRAIL death receptor by CMV reveals its importance in NK cell-mediated antiviral defense. *PLoS Pathog.* (2014) 10:e1004268. doi: 10.1371/journal.ppat.1004268
116. Smith W, Tomasec P, Aicheler R, Loewendorf A, Nemcovicova I, Wang EC, et al. Human cytomegalovirus glycoprotein UL141 targets the TRAIL death receptors to thwart host innate antiviral defenses. *Cell Host Microbe.* (2013) 13:324–35. doi: 10.1016/j.chom.2013.02.003
117. Stacey MA, Marsden M, Pham NT, Clare S, Dolton G, Stack G, et al. Neutrophils recruited by IL-22 in peripheral tissues function as TRAIL-dependent antiviral effectors against MCMV. *Cell Host Microbe.* (2014) 15:471–83. doi: 10.1016/j.chom.2014.03.003
118. Diamond MS, Farzan M. The broad-spectrum antiviral functions of IFIT and IFITM proteins. *Nat Rev Immunol.* (2013) 13:46–57. doi: 10.1038/nri3344
119. Allen EK, Randolph AG, Bhangale T, Dogra P, Ohlson M, Oshansky CM, et al. SNP-mediated disruption of CTCF binding at the IFITM3 promoter is associated with risk of severe influenza in humans. *Nat Med.* (2017) 23:975–83. doi: 10.1038/nm.4370
120. Everitt AR, Clare S, Pertel T, John SP, Wash RS, Smith SE, et al. IFITM3 restricts the morbidity and mortality associated with influenza. *Nature* (2012) 484:519–23. doi: 10.1038/nature10921
121. Zhang YH, Zhao Y, Li N, Peng YC, Giannoulatou E, Jin RH, et al. Interferon-induced transmembrane protein-3 genetic variant rs12252-C is associated with severe influenza in Chinese individuals. *Nat Commun.* (2013) 4:1418. doi: 10.1038/ncomms2433
122. Xie M, Xuan B, Shan J, Pan D, Sun Y, Shan Z, et al. Human cytomegalovirus exploits interferon-induced transmembrane proteins to facilitate morphogenesis of the virion assembly compartment. *J Virol.* (2015) 89:3049–61. doi: 10.1128/JVI.03416-14
123. Ruzek MC, Miller AH, Opal SM, Pearce BD, Biron CA. Characterization of early cytokine responses and an interleukin (IL)-6-dependent pathway of endogenous glucocorticoid induction during murine cytomegalovirus infection. *J Exp Med.* (1997) 185:1185–92. doi: 10.1084/jem.185.7.1185
124. Quatrini L, Wieduwild E, Escaliere B, Filtjens J, Chasson L, Laprie C, et al. Endogenous glucocorticoids control host resistance to viral infection through the tissue-specific regulation of PD-1 expression on NK cells. *Nat Immunol.* (2018) 19:954–62. doi: 10.1038/s41590-018-0185-0
125. Ruzek MC, Pearce BD, Miller AH, Biron CA. Endogenous glucocorticoids protect against cytokine-mediated lethality during viral infection. *J Immunol.* (1999) 162:3527–33.

Conflict of Interest Statement: The authors declare that the research was conducted in the absence of any commercial or financial relationships that could be construed as a potential conflict of interest.

frontiers in Immunology

MINI REVIEW
published: 15 October 2019
doi: 10.3389/fimmu.2019.02447

Nef-induced CCL2 Expression Contributes to HIV/SIV Brain Invasion and Neuronal Dysfunction

Michael H. Lehmann[1,2]*, *Jonas M. Lehmann*[3] *and Volker Erfle*[1]

[1] *Institute of Virology, Technische Universität München, Munich, Germany,* [2] *Institute for Infectious Diseases and Zoonoses, Ludwig-Maximilians-Universität München, Munich, Germany,* [3] *Department of Informatics, Technische Universität München, Munich, Germany*

C-C motif chemokine ligand 2 (CCL2) is a chemoattractant for leukocytes including monocytes, T cells, and natural killer cells and it plays an important role in maintaining the integrity and function of the brain. However, there is accumulating evidence that many neurological diseases are attributable to a dysregulation of CCL2 expression. Acquired immune deficiency syndrome (AIDS) encephalopathy is a severe and frequent complication in individuals infected with the human immunodeficiency virus (HIV) or the simian immunodeficiency virus (SIV). The HIV and SIV Nef protein, a progression factor in AIDS pathology, can be transferred by microvesicles including exosomes and tunneling nanotubes (TNT) within the host even to uninfected cells, and Nef can induce CCL2 expression. This review focuses on findings which collectively add new insights on how Nef-induced CCL2 expression contributes to neurotropism and neurovirulence of HIV and SIV and elucidates why adjuvant targeting of CCL2 could be a therapeutic option for HIV-infected persons.

Keywords: AIDS, astrocyte, autophagy, chemokine, dementia, inflammation, neuron, virus

OPEN ACCESS

Edited by:
Serge Benichou, Centre National de la Recherche Scientifique (CNRS), France

Reviewed by:
Laura Fantuzzi, National Institute of Health (ISS), Italy
Tetsuo Tsukamoto, Kindai University, Japan
Fan Wu, Fudan University, China
Matthias Clauss, Indiana University Bloomington, United States

***Correspondence:**
Michael H. Lehmann
Orlataler@web.de

Specialty section:
This article was submitted to Viral Immunology, a section of the journal Frontiers in Immunology

Received: *27 June 2019*
Accepted: *01 October 2019*
Published: *15 October 2019*

Citation:
Lehmann MH, Lehmann JM and Erfle V (2019) Nef-induced CCL2 Expression Contributes to HIV/SIV Brain Invasion and Neuronal Dysfunction. Front. Immunol. 10:2447. doi: 10.3389/fimmu.2019.02447

INTRODUCTION

Acquired immune deficiency syndrome (AIDS), caused by the human immunodeficiency virus (HIV) (1, 2), has to date resulted in the deaths of over 32 million people. According to the 2019 UNAIDS Global AIDS Update, 1.7 million people became newly infected with HIV in 2018 resulting in a total number of 37.9 million people living with HIV worldwide. To date, there is no effective protective vaccine against HIV or even a feasible cure available for HIV-infected patients (3, 4).

In the mid-1990s combined anti-retroviral therapy (ART) was introduced, which considerably reduced the mortality of HIV-infected patients. However, since then, the prevalence of HIV-associated diseases has increased. A major obstacle toward the development of therapies against these diseases that affect a number of organs such as the heart, lungs, kidneys, and the brain is due mainly to the fact that the disease pathogenesis is poorly understood (5–8). In the meantime, there exists at best a consensus that a systemic and persistent activation of the immune system plays a major role in the disease pathogenesis (9–11). Moreover, it is difficult to accurately differentiate between age-related neurodegeneration, other neurodegenerative diseases and HIV-associated neurocognitive disorders (HAND) (12). However, attempts have been made to identify biomarkers to diagnose neurocognitive impairment in HIV-infected persons and activated

monocytes/macrophages and C-C motif chemokine ligand 2 (CCL2) appear to be the most promising amongst them (13).

CCL2, also named monocyte chemoattractant protein 1, is a chemotactic cytokine for monocytes (14) and T cells (15), which are the main target cells of HIV-1. CCL2 decreases interferon-alpha expression (16), and promotes HIV/SIV replication by up-regulation of surface C-X-C motif chemokine receptor 4 expression (17).

CCL2 binds to the C-C motif chemokine receptor 2 (CCR2), which is expressed by neurons (18), human fetal astrocytes (19) and brain microvascular endothelial cells (BMECs) (20). CCL2 also binds to the D6 chemokine decoy receptor, which is expressed on adult human astrocytes (21).

The CCL2-CCR2 axis has been shown to play a key role in multiple sclerosis and in experimental autoimmune encephalomyelitis (22), in addition to exacerbating neuronal damage after status epilepticus (23), eliciting itch- and pain-like behavior in allergic contact dermatitis (24), as well as mediating alcohol-induced neuroinflammation and neurotoxicity (25).

HIV AND SIV ASSOCIATED DEMENTIA, ENCEPHALITIS AND NEURONAL DAMAGE

Without combined ART, HIV causes dementia which is characterized by deficiencies in cognition, motor disorders, and behavior abnormalities (26). Pathological manifestations of HIV-associated dementia (HAD) appear as meningitis, encephalitis and vacuolar myelopathy (27). A similar clinical picture has been observed in the SIV/macaque model (28, 29). Even after the introduction of combined ART, HAND remain (8), and, in fact SIV-infected macaques treated with suppressive ART also show ongoing neurodegeneration and inflammation (30). The reason for this phenomenon is unknown although several explanations have been proposed, e.g., that anti-retroviral drugs cannot access the central nervous system (CNS), are not effective in eliminating viral reservoirs, or themselves contribute to HAND (31, 32). However, since specific CNS-targeted ART failed to improve neurocognition in HIV-infected patients compared to non-CNS-targeted (33), it has been hypothesized that early events after primary infection with HIV/SIV are critical for initiating the development of HAND (8).

Indeed, SIV was detected in the brains of macaques within a few days after intravenous infection (34, 35). Further, HIV nucleic acid was detected in the brain of an HIV naïve patient who died 15 days after intravenous inoculation of indium-111-labeled white blood cells, which originated from an HIV-infected individual (36). Additionally, a more recent study showed that HIV RNA is present in the cerebrospinal fluid (CSF) of humans as early as 8 days after HIV infection (37). This suggests that HIV/SIV is capable of exploiting a distinct mechanism to enter the brain rapidly.

Entry of SIV into the brain and induction of neuropathology does not appear to depend on a sustained high viral load because the SIVmac32H(pC8) strain, whose replication is attenuated *in vivo* (38, 39), was detected in the brain 3 days after infection of macaques where it caused persisting neuroinflammation (40). The attenuated phenotype of SIVmac32H(pC8) is most probably due to a 12 base-pair deletion in its *nef* gene, which results in an in-frame deletion of the amino acids 143–146 of the translational product (38). Although this Nef variant was detected at lower levels *in vitro* compared to other variants (41), it was definitely detected in the brain of macaques infected with SIVmac32H(pC8) (42). However, SIV strains containing nucleotide deletions in the *nef* long-terminal repeat (*nef*/LTR) overlap region, analogous to the HIV strain of the Sydney blood bank cohort (SBBC), could not be detected in the brains of macaques despite viral replication in the periphery (43). Of note, members of the SBBC who had become infected with an HIV strain containing the nucleotide sequence deletions in the *nef*/LTR region that results in a truncated Nef protein of 24 amino acids (44), did not or only slowly progressed to AIDS including HAD (45).

THE NEF PROTEIN OF HIV/SIV: IMPORTANCE FOR AIDS PROGRESSION AND ITS INTERCELLULAR TRANSFER

The importance of Nef for AIDS progression was confirmed in SIV-infected rhesus monkeys and HIV-transgenic mice (46, 47). Additionally, it was shown that Nef is required for high viral load *in vivo* (47). These findings have stimulated a series of studies aiming to identify the mechanistic background with the ultimate goal to exploit the knowledge for therapeutic intervention. Indeed, numerous cellular interaction partners and pathophysiological functions of Nef have been detected (48, 49), and several models of how Nef executes its role in HIV/SIV replication and immunopathogenesis have been proposed (50). In 2009, Kyei et al. showed that HIV Nef inhibits autophagic maturation in human macrophages and thereby provided a convincing explanation of how Nef acts at the molecular level to enable efficient replication of HIV (51). Inhibition of autophagy increases the production of proinflammatory cytokines (52, 53) including CCL2 (54, 55). Thus, Nef also seems to contribute to chronic inflammation, which occurs in HIV-infected persons (56).

HIV Nef was found in supernatants of *nef*-expressing BHK cells (57), yeast (58), and HEK293 cells (59), which was surprising at the time of these discoveries because *nef* does not code for an N-terminal signal sequence that would direct the protein to the cell secretory pathway leading to export. Thus, the mechanism by which Nef is released from infected cells was regarded as an open question. In the past, on analyzing the supernatants of BHK cells infected with recombinant vaccinia virus expressing HIV Nef, it was assumed that Nef could be released by vesicles (57). Today, it is recognized that not only proteins but also lipids and RNA can be released from a cell by extracellular vesicles (60).

In 2003, it was shown that HIV Nef induces an accumulation of multivesicular bodies (MVBs) and that Nef itself is present in MVBs (61). MVBs can fuse with the cell plasma membrane, leading to the release of 40–90 nm diameter vesicles, termed

exosomes, into the extracellular environment (62). Consequently, it was tempting to speculate that Nef could be released from cells by exosomes. However, it was challenging to test this hypothesis in HIV-infected cells because Nef is incorporated in virions (63, 64).

The astrocytoma cell line TH4-7-5 is persistently infected with the HIV isolate TH4-7-5 which has a mutation in the *nef* gene (GenBank accession number: L31963.1), resulting in a myristoylation-deficient Nef (65). However, myristoylation of Nef is required for optimal HIV replication *in vitro* (66). Thus, a myristoylation-deficient Nef and a block in HIV Rev function most probably effected a very low production of infectious virus but a high production of Nef in astrocytoma TH4-7-5 cells (65, 67). We took advantage of the astrocytoma cell line TH4-7-5 and examined whether Nef is present in the supernatants of these cells. Application of a two-step centrifugation protocol, previously shown to enable the enrichment of microvesicles including exosomes from cellular supernatants (68), resulted in the detection of Nef in the pellets of centrifuged supernatants of these cells (69).

It was later confirmed that Nef is released from HIV-infected cells (70, 71) by microvesicles and it was even claimed that this occurs via exosomes (72). However, there is still an ongoing debate regarding the type of vesicle by which Nef leaves the cell (73, 74). Further, Nef was detected in microvesicles and exosomes isolated from the plasma of HIV-infected persons despite them receiving ART, and it has been shown that exosomes derived from HAD patients can transfer *nef* mRNA to cells, leading to Nef expression and subsequent induction of cellular genes (75, 76).

Nef was also found in uninfected human peripheral blood mononuclear cells (PBMCs), which can transfer Nef to human umbilical cord vein endothelial cells (77). A recent study not only reported that Nef is released by vesicles from HIV-infected cells, but also confirmed the result for SIV-infected cells and has additionally shown that extracellular vesicles containing Nef circulate in the blood of SIV-infected macaques (78). Meanwhile, the process of protein and mRNA transfer by exosomes and other extracellular vesicles even between different types of cells is well understood (79). In summary, irrespective of the type of extracellular vesicle from which Nef is released by HIV/SIV infected cells, Nef is present in the extracellular environment independently of virions and can enter uninfected cells where it affects cellular functions and gene expression.

Additionally, cells can exchange molecules and organelles directly via tunneling nanotubes (TNTs), which are about 50–200 nm long thin actin rich membrane conduits, even between different types of cells (80). Nef can induce TNT formation (81, 82), and it can also be transferred to B cells via TNTs from HIV-infected macrophages (83), from macrophages to T cells (82), from *nef*-expressing T cells to hepatocytic cells (84) and also between macrophages (81). Importantly, Nef is transferred from T cells and monocytes to human coronary arterial endothelial cells via TNTs, leading to apoptosis and CCL2 expression (85).

NEF-INDUCED CCL2 EXPRESSION AND THE FUNCTION OF THE BLOOD-BRAIN-BARRIER

CCL2 increases the blood-brain barrier (BBB) permeability (86, 87), and much progress has been made in revealing the molecular mechanism of how leukocytes, governed by CCL2, pass the BBB (88). Therein, astrocyte and BMEC-derived CCL2 play complementary roles (89).

A natural repair mechanism to restore damaged brain tissue after experimentally-induced ischemia starts with the recruitment of $CCR2^{+}Iba1^{+}$ monocytes from the periphery, which then differentiate into brain $Iba1^{+}NG2^{+}$ cells within the brain parenchyma (90, 91). Transmigration of $CCR2^{+}Iba1^{+}$ monocytes through the BBB is enabled by a transient expression of CCL2 in astrocytes and endothelial cells that lasts for only 2 days (92). Indeed, under normal physiological conditions, the BBB is impermeable for circulating monocytes (93, 94), and therefore invasion of a healthy brain by HIV/SIV should not happen as fast as it has been observed. But a specific HIV/SIV-triggered mechanism leading to CCL2 expression in BMECs may enable HIV/SIV to get access to the brain either in the form of free virions or via infected $CCR2^{+}$ cells. In this respect, it was significant to observe that Nef (i) can be transferred from human PBMC to human endothelial cells (77), (ii) was detected in endothelial cells of *nef*-transgenic mice and macaques infected with SHIV-nefSF33, and (iii) induces CCL2 expression in endothelial cells (85).

Invasion of the brain by leukocytes would additionally require an upregulation of adhesion molecules on both endothelial and infected cells. Indeed, it has been shown that HIV Nef upregulates the intercellular adhesion molecule 1 (ICAM-1) in vascular endothelial cells (95). ICAM-1 interacts with the lymphocyte function-associated antigen 1 (LFA-1), and its subunits, CD11a and CD18, are upregulated in HIV-infected monocytes (96, 97). Endothelial-derived CCL2 activates CD11a, leading to a firm arrest of monocytes on endothelial cells (98, 99), and mediates the subsequent transendothelial migration (100).

In summary, the findings collectively result in a model in which Nef-containing PBMCs and extracellular vesicles carrying Nef attach to and transfer Nef into endothelial cells, leading to CCL2 production that can cause BBB leakiness and subsequent entry of HIV/SIV by infected cells into the brain (**Figure 1**). Of note, this provides a simple explanation of why SIV with a deleted *nef* gene cannot enter the brain (43).

NEF-INDUCED CCL2 EXPRESSION AND NEURONAL DYSFUNCTIONS

Once in the brain, HIV/SIV cannot be eliminated by ART. The virus persists and triggers a chronic inflammation leading to sustained leukocyte infiltration, astrogliosis and neuronal degeneration (102, 103). In brain tissues of HIV-infected patients, HIV DNA was detected in the cells of the macrophage lineage and in astrocytes, the most abundant cell type in the brain. However, it was not found in neurons (104), which is in accordance with

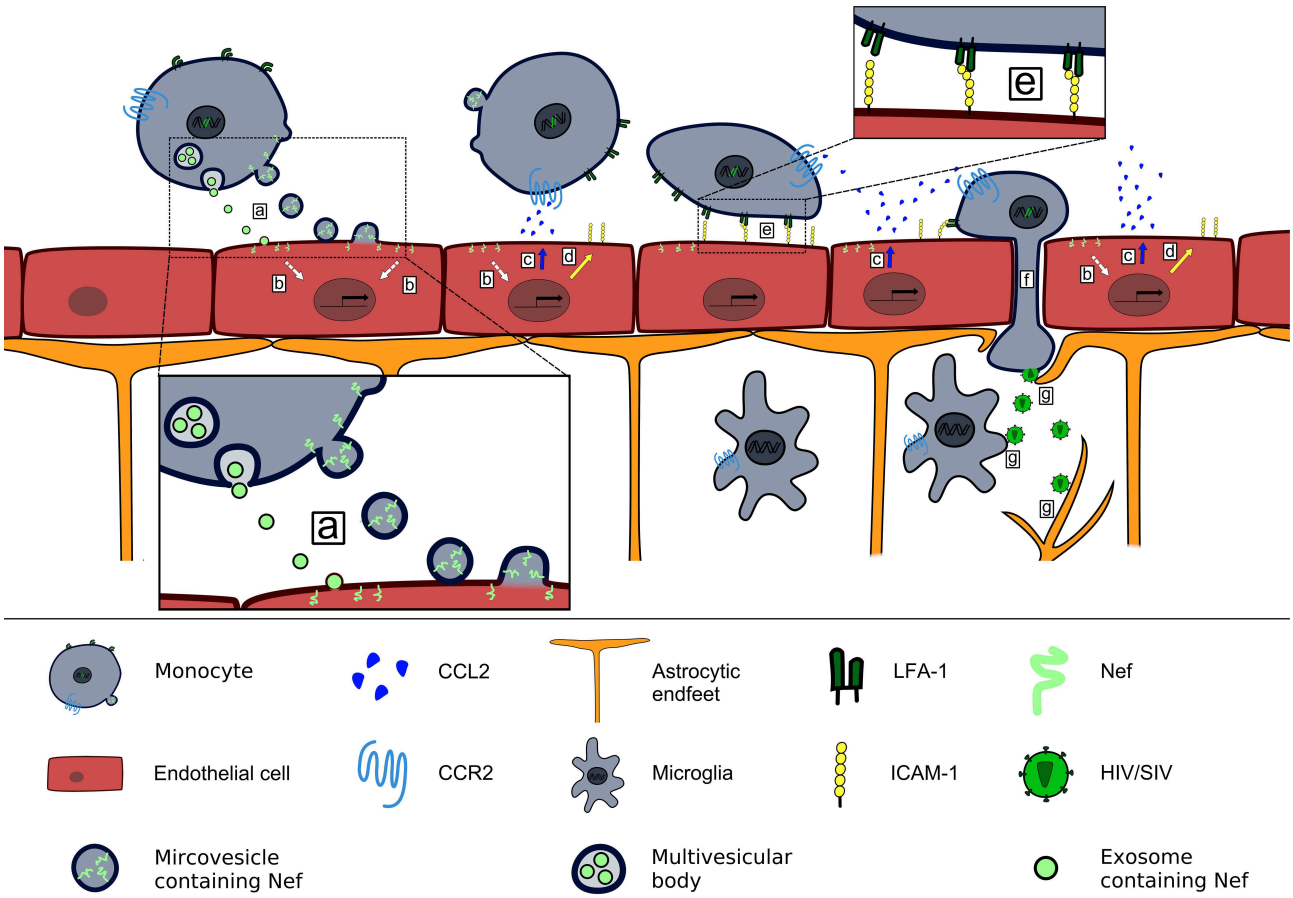

FIGURE 1 | Contribution of Nef-induced CCL2 expression to HIV/SIV neurotropism. HIV/SIV infected monocytes release microvesicles and exosomes that transfer Nef into brain endothelial cells (a), where Nef induces a signaling pathway (b) that leads to release of CCL2 at the luminal side of the BBB (c) and upregulation of ICAM-1 (d). CCL2 binding to $CCR2^{+}$cells triggers a conformational change of LFA-1 that enables their firm adhesion to brain endothelial cells via LFA-1–ICAM-1 interaction (e). Endothelial CCL2 expression enables transendothelial migration of HIV/SIV-infected $CCR2^{+}$monocytes into the brain parenchyma (101) (f). There HIV/SIV infects astrocytes and microglia (g).

the finding that perivascular macrophages and microglia, but not neurons, can be productively infected with HIV/SIV (105, 106). These findings indicate that an indirect mechanism causes neuronal dysfunction and damage, and microglia that release exosomes and microvesicles containing Nef (107) may play an important role therein. It has long been known that HIV and SIV antigens are present in astrocytes of primary infected tissues (106, 108). Recently, a hypothesis was proposed that explains this finding (109) and challenges the consensus that HIV/SIV can infect astrocytes (110).

Significantly, Nef is highly expressed in astrocytes (111), promotes replication of HIV (112), and is also released by exosomes (113) or any other extracellular vesicle (114). Human astrocytes infected with recombinant Sindbis virus vector encoding *HIV nef* produced elevated CCL2 mRNA levels, which was independent of the *nef* variant tested (115). Induction of CCL2 expression by HIV Nef was confirmed in U-251 MG astroglioma cells transfected stably with *nef* (116), in primary rat astrocytes *in vivo* (117), and in primary murine macrophages and microglia (118). Animal models have provided evidence that there is a direct link between Nef-induced CCL2 expression and neuronal dysfunction and damage. Macrophages expressing HIV Nef, which were implanted into the rat hippocampus, triggered immigration of monocytes/macrophages, tumor necrosis factor expression, and astrogliosis, a hallmark of HIV encephalitis (HIVE). In addition, the neurotoxicity triggered by Nef was associated with cognitive deficits (119). Cognitive deficits in particular spatial and recognition memory were observed in rat brains in which primary astrocytes were implanted that expressed HIV Nef. This was associated with Nef-induced CCL2 expression, which resulted in immigration of macrophages in the hippocampus and loss of hippocampal CA3 neurons in these animals (117). In transgenic mice, in which HIV Nef was expressed specifically in macrophages and microglia, CCL2 was increased in the brain, and the dopamine system was affected, leading to mania-like behavior, especially in males (118).

There are several studies demonstrating that increased CCL2 concentrations correlate with HAD/HAND. Elevated levels of CCL2 were detected in the CSF of HIV-infected individuals positively diagnosed with HAD (120, 121). Microglia and astrocytes of HIV-infected persons suffering from HIVE produce CCL2 (122), which was confirmed for SIV infected macaques (123). Additionally, a specific small nucleotide polymorphism in the CCL2 promoter, which leads to increased CCL2 expression and infiltration of mononuclear phagocytes into tissues correlates positively with the risk of HAD (124). Cocaine, known to exacerbate neurodegeneration in persons infected with HIV, induces CCL2 expression in microglia and leads to increased transmigration of monocytes into the brain (125).

It is now also known that CCL2 affects neurons directly in addition to enhancing the transmigration of infected leukocytes through the BBB (126). For example, over-induction of CCL2 in astrocytes causes dopaminergic neurodegeneration in 1-methyl-4-phenyl-1,2,3,6-tetrahydropyridine mice (127), and an inhibition of CCL2 expression protects neurons against amyloid-beta-induced toxicity (128). Indeed, CCL2 mediates cell death

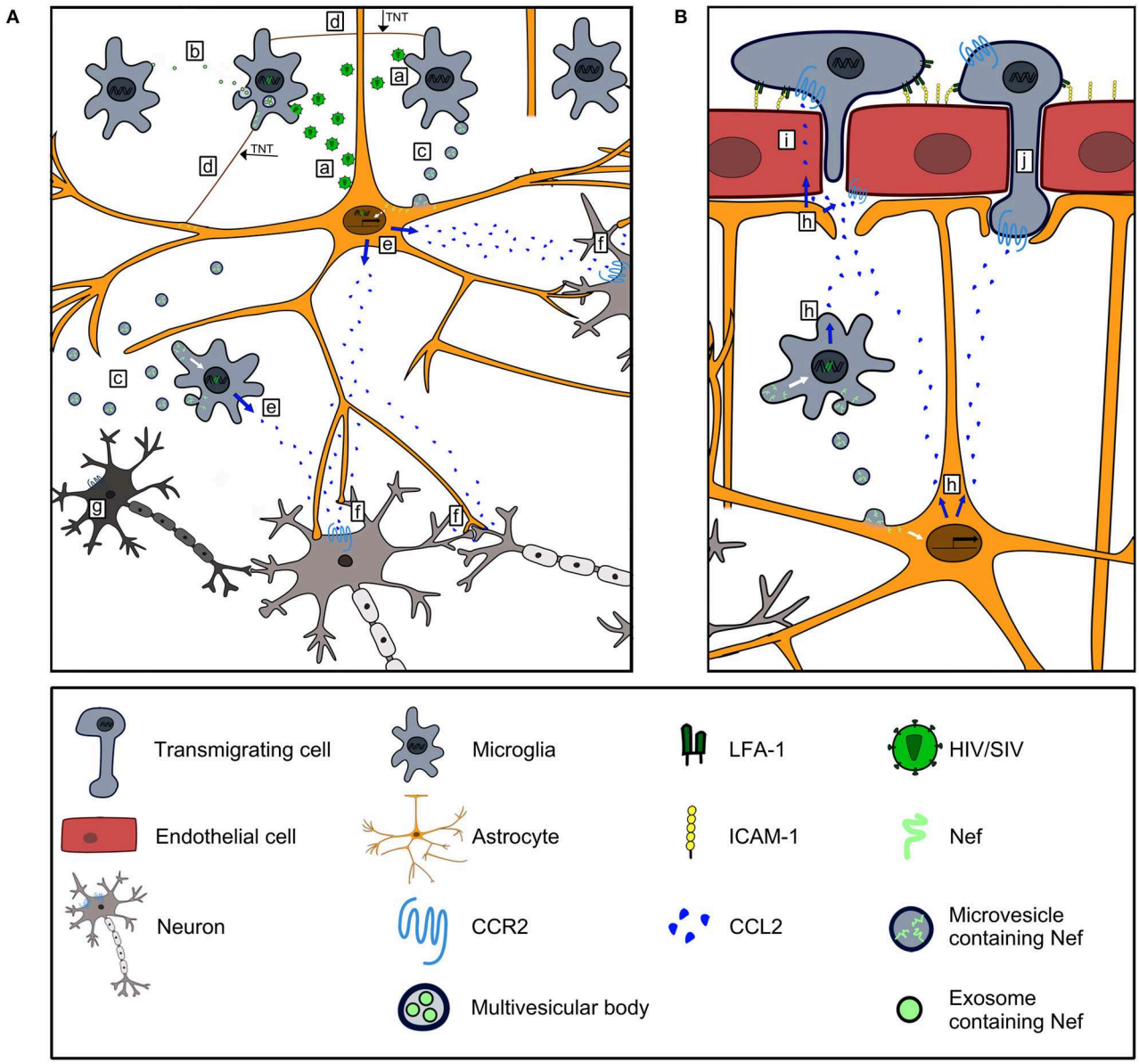

FIGURE 2 | Contribution of Nef-induced CCL2 expression to HIV/SIV neurovirulence. **(A)** HIV/SIV-infected microglia and astrocytes infect uninfected microglia and astrocytes (a), and disseminate Nef via exosomes (b), microvesicles (c) and TNTs (d) to uninfected cells. Nef harboring astrocytes and microglia express CCL2 (e). CCL2 stimulates CCR2 signaling in neurons leading to their dysfunction (f) and death (g). **(B)** CCL2 produced by Nef harboring astrocytes and microglia (h) is transported transcellularly across BMEC (136) to act on $CCR2^+$cells along the luminal side of the BBB (i). CCL2 binds to CCR2 on BMEC and mediates disruption of endothelial junctions (86, 87) to foster invasion of $CCR2^+$cells into the brain (j).

in neurons of the hippocampal CA3 region after kainic acid-induced seizures in mice. Neuronal degeneration was associated with behavioral impairment, memory decline, and anxiety (129), all characteristics which have been observed early after infection of humans with HIV and even in HIV-infected persons receiving ART (130–132).

CCR2, the receptor of CCL2, is present on neurons (18), and its absence reduced brain damage as well as BBB permeability in an experimental stroke model in mice (133). Similar to the process in an HIV/SIV infection, CCR2 plays a key role in the accumulation of myeloid cells in the brain and the activation of hippocampal myeloid cells upon infection with Theiler's murine encephalitis virus (TMV). Notably, CCR2 deficient mice had almost no hippocampal damage during TMV infection (134). Thus, CCL2 represents a convincing candidate to explain neuronal dysfunction and damage (135) which occur in HIV/SIV infected humans and animals (**Figure 2**). Additionally, CCL2 is major mediator of pain (137), and chronic pain is a common burden in people living with HIV/AIDS (138).

SUMMARY

The findings summarized herein not only integrate well into the "Trojan horse" model that states that a cell infected with HIV/SIV enters the brain leading to a persistent infection and consequently HAND (139) but also add to this model the fact that the transfer of Nef by microvesicles into endothelial cells and the subsequent induction of CCL2, mimics a pathophysiological state of the brain to which monocytes are recruited normally. Nef, in combination with other HIV/SIV proteins and even anti-retroviral drugs, possibly work together more efficiently to enable a rapid entry of HIV/SIV-infected cells into the brain (140). This interplay presumably plays a general role in HIV-associated diseases (141).

In the brain, HIV/SIV-infected cells such as astrocytes and microglia distribute Nef to uninfected cells via microvesicles and TNTs. Thereby, there is a steady increase in the number of Nef-bearing, non-infected cells which produce CCL2. HIV Tat in astrocytes seems to contribute to an increase in the levels of CCL2 in the brain (142, 143). The persistent non-physiological expression of CCL2 leads to sustained cell infiltration into the brain and a disturbance of neuronal functions. If a person is infected with HIV subtype B then Tat could enhance CCR2 activation through its acidic region (144, 145). Moreover, when present in sufficiently high concentrations in the brain, Tat could definitely exacerbate neuronal dysfunctions through its basic region (146). Moreover, besides CCL2, the C-X-C motif chemokine 10 (CXCL10) has also been identified as a biomarker for HAND (13), especially in HIV-infected women (147) and this chemokine can also be induced by Nef (115).

CONCLUSION

The findings summarized here classify HIV/SIV Nef-induced CCL2 expression in the complex pathogenesis of HAND, and once again highlight the special role which the CCL2-CCR2 axis can play in a neurological disease. Consequently, drugs which have been developed to target this chemokine or its receptor could also be an option for an adjuvant therapy in HIV-infected persons.

AUTHOR CONTRIBUTIONS

ML wrote the initial draft. ML and VE discussed the manuscript. JL, ML, and VE edited the manuscript. JL and ML designed and drew the illustrations.

FUNDING

This work was supported by the German Research Foundation (DFG) and the Technical University of Munich (TUM) in the framework of the Open Access Publishing Program.

ACKNOWLEDGMENTS

The authors would like to thank Jacqueline Weber-Lehmann for critical reading of the manuscript.

REFERENCES

1. Barre-Sinoussi F, Chermann JC, Rey F, Nugeyre MT, Chamaret S, Gruest J, et al. Isolation of a T-lymphotropic retrovirus from a patient at risk for acquired immune deficiency syndrome (AIDS). *Science*. (1983) 220:868–71. doi: 10.1126/science.6189183
2. Gallo RC, Salahuddin SZ, Popovic M, Shearer GM, Kaplan M, Haynes BF, et al. Frequent detection and isolation of cytopathic retroviruses (HTLV-III) from patients with AIDS and at risk for AIDS. *Science*. (1984) 224:500–3. doi: 10.1126/science.6200936
3. Kent SJ, Davenport MP. Moving the HIV vaccine field forward: concepts of protective immunity. *Lancet HIV*. (2019) 6:e406–10. doi: 10.1016/S2352-3018(19)30134-1
4. Lopez-Galindez C, Pernas M, Casado C, Olivares I, Lorenzo-Redondo R. Elite controllers and lessons learned for HIV-1 cure. *Curr Opin Virol*. (2019) 38:31–6. doi: 10.1016/j.coviro.2019.05.010
5. Fitzpatrick ME, Kunisaki KM, Morris A. Pulmonary disease in HIV-infected adults in the era of antiretroviral therapy. *AIDS*. (2018) 32:277–92. doi: 10.1097/QAD.0000000000001712
6. Naicker S, Rahmanian S, Kopp JB. HIV and chronic kidney disease. *Clin Nephrol*. (2015) 83(suppl. 1):32–8. doi: 10.5414/CNP83S032
7. Pinto DSM, da Silva M. Cardiovascular disease in the setting of human immunodeficiency virus infection. *Curr Cardiol Rev*. (2018) 14:25–41. doi: 10.2174/1573403X13666171129170046
8. Saylor D, Dickens AM, Sacktor N, Haughey N, Slusher B, Pletnikov M, et al. HIV-associated neurocognitive disorder–pathogenesis and prospects for treatment. *Nat Rev Neurol*. (2016) 12:234–48. doi: 10.1038/nrneurol.2016.27
9. Paiardini M, Muller-Trutwin M. HIV-associated chronic immune activation. *Immunol Rev*. (2013) 254:78–101. doi: 10.1111/imr.12079
10. Plaeger SF, Collins BS, Musib R, Deeks SG, Read S, Embry A. Immune activation in the pathogenesis of treated chronic HIV disease: a workshop summary. *AIDS Res Hum Retroviruses*. (2012) 28:469–77. doi: 10.1089/aid.2011.0213

11. Younas M, Psomas C, Reynes J, Corbeau P. Immune activation in the course of HIV-1 infection: causes, phenotypes and persistence under therapy. *HIV Med*. (2016) 17:89–105. doi: 10.1111/hiv.12310
12. Rosenthal J, Tyor W. Aging, comorbidities, and the importance of finding biomarkers for HIV-associated neurocognitive disorders. *J Neurovirol*. (2019). doi: 10.1007/s13365-019-00735-0. [Epub ahead of print].
13. Bandera A, Taramasso L, Bozzi G, Muscatello A, Robinson JA, Burdo TH, et al. HIV-associated neurocognitive impairment in the modern ART era: are we close to discovering reliable biomarkers in the setting of virological suppression? *Front Aging Neurosci*. (2019) 11:187. doi: 10.3389/fnagi.2019.00187
14. Robinson EA, Yoshimura T, Leonard EJ, Tanaka S, Griffin PR, Shabanowitz J, et al. Complete amino acid sequence of a human monocyte chemoattractant, a putative mediator of cellular immune reactions. *Proc Natl Acad Sci USA*. (1989) 86:1850–4. doi: 10.1073/pnas.86.6.1850
15. Loetscher P, Seitz M, Clark-Lewis I, Baggiolini M, Moser B. Monocyte chemotactic proteins MCP-1, MCP-2, and MCP-3 are major attractants for human CD4+ and CD8+ T lymphocytes. *FASEB J*. (1994) 8:1055–60. doi: 10.1096/fasebj.8.13.7926371
16. Williams DW, Askew LC, Jones E, Clements JE. CCR2 signaling selectively regulates IFN-alpha: role of beta-arrestin 2 in IFNAR1 internalization. *J Immunol*. (2019) 202:105–18. doi: 10.4049/jimmunol.1800598
17. Campbell GR, Spector SA. CCL2 increases X4-tropic HIV-1 entry into resting CD4+ T cells. *J Biol Chem*. (2008) 283:30745–53. doi: 10.1074/jbc.M804112200
18. Coughlan CM, McManus CM, Sharron M, Gao Z, Murphy D, Jaffer S, et al. Expression of multiple functional chemokine receptors and monocyte chemoattractant protein-1 in human neurons. *Neuroscience*. (2000) 97:591–600. doi: 10.1016/S0306-4522(00)00024-5
19. Andjelkovic AV, Song L, Dzenko KA, Cong H, Pachter JS. Functional expression of CCR2 by human fetal astrocytes. *J Neurosci Res*. (2002) 70:219–31. doi: 10.1002/jnr.10372
20. Dzenko KA, Andjelkovic AV, Kuziel WA, Pachter JS. The chemokine receptor CCR2 mediates the binding and internalization of monocyte chemoattractant protein-1 along brain microvessels. *J Neurosci*. (2001) 21:9214–23. doi: 10.1523/JNEUROSCI.21-23-09214.2001
21. Fouillet A, Mawson J, Suliman O, Sharrack B, Romero IA, Woodroofe MN. CCL2 binding is CCR2 independent in primary adult human astrocytes. *Brain Res*. (2012) 1437:115–26. doi: 10.1016/j.brainres.2011.11.049
22. Mahad DJ, Ransohoff RM. The role of MCP-1 (CCL2) and CCR2 in multiple sclerosis and experimental autoimmune encephalomyelitis (EAE). *Semin Immunol*. (2003) 15:23–32. doi: 10.1016/S1044-5323(02)00125-2
23. Varvel NH, Neher JJ, Bosch A, Wang W, Ransohoff RM, Miller RJ, et al. Infiltrating monocytes promote brain inflammation and exacerbate neuronal damage after status epilepticus. *Proc Natl Acad Sci USA*. (2016) 113:E5665–74. doi: 10.1073/pnas.1604263113
24. Jiang H, Cui H, Wang T, Shimada SG, Sun R, Tan Z, et al. CCL2/CCR2 signaling elicits itch- and pain-like behavior in a murine model of allergic contact dermatitis. *Brain Behav Immun*. (2019) 80:464–73. doi: 10.1016/j.bbi.2019.04.026
25. Zhang K, Luo J. Role of MCP-1 and CCR2 in alcohol neurotoxicity. *Pharmacol Res*. (2019) 139:360–6. doi: 10.1016/j.phrs.2018.11.030
26. Price RW, Brew B, Sidtis J, Rosenblum M, Scheck AC, Cleary P. The brain in AIDS: central nervous system HIV-1 infection and AIDS dementia complex. *Science*. (1988) 239:586–92. doi: 10.1126/science.3277272
27. Petito CK. Review of central nervous system pathology in human immunodeficiency virus infection. *Ann Neurol*. (1988) 23:S54–7. doi: 10.1002/ana.410230715
28. Rausch DM, Murray EA, Eiden LE. The SIV-infected rhesus monkey model for HIV-associated dementia and implications for neurological diseases. *J Leukoc Biol*. (1999) 65:466–74. doi: 10.1002/jlb.65.4.466
29. Zink MC, Spelman JP, Robinson RB, Clements JE. SIV infection of macaques–modeling the progression to AIDS dementia. *J Neurovirol*. (1998) 4:249–59. doi: 10.3109/13550289809114526
30. Beck SE, Queen SE, Metcalf Pate KA, Mangus LM, Abreu CM, Gama L, et al. An SIV/macaque model targeted to study HIV-associated neurocognitive disorders. *J Neurovirol*. (2018) 24:204–12. doi: 10.1007/s13365-017-0582-4
31. Nabha L, Duong L, Timpone J. HIV-associated neurocognitive disorders: perspective on management strategies. *Drugs*. (2013) 73:893–905. doi: 10.1007/s40265-013-0059-6
32. Fois AF, Brew BJ. The potential of the CNS as a reservoir for HIV-1 infection: implications for HIV eradication. *Curr HIV AIDS Rep*. (2015) 12:299–303. doi: 10.1007/s11904-015-0257-9
33. Ellis RJ, Letendre S, Vaida F, Haubrich R, Heaton RK, Sacktor N, et al. Randomized trial of central nervous system-targeted antiretrovirals for HIV-associated neurocognitive disorder. *Clin Infect Dis*. (2014) 58:1015–22. doi: 10.1093/cid/cit921
34. Chakrabarti L, Hurtrel M, Maire MA, Vazeux R, Dormont D, Montagnier L, et al. Early viral replication in the brain of SIV-infected rhesus monkeys. *Am J Pathol*. (1991) 139:1273–80.
35. Matsuda K, Dang Q, Brown CR, Keele BF, Wu F, Ourmanov I, et al. Characterization of simian immunodeficiency virus (SIV) that induces SIV encephalitis in rhesus macaques with high frequency: role of TRIM5 and major histocompatibility complex genotypes and early entry to the brain. *J Virol*. (2014) 88:13201–11. doi: 10.1128/JVI.01996-14
36. Davis LE, Hjelle BL, Miller VE, Palmer DL, Llewellyn AL, Merlin TL, et al. Early viral brain invasion in iatrogenic human immunodeficiency virus infection. *Neurology*. (1992) 42:1736–9. doi: 10.1212/WNL.42.9.1736
37. Valcour V, Chalermchai T, Sailasuta N, Marovich M, Lerdlum S, Suttichom D, et al. Central nervous system viral invasion and inflammation during acute HIV infection. *J Infect Dis*. (2012) 206:275–82. doi: 10.1093/infdis/jis326
38. Rud EW, Cranage M, Yon J, Quirk J, Ogilvie L, Cook N, et al. Molecular and biological characterization of simian immunodeficiency virus macaque strain 32H proviral clones containing nef size variants. *J Gen Virol*. (1994) 75:529–43. doi: 10.1099/0022-1317-75-3-529
39. Stahl-Hennig C, Dittmer U, Nisslein T, Petry H, Jurkiewicz E, Fuchs D, et al. Rapid development of vaccine protection in macaques by live-attenuated simian immunodeficiency virus. *J Gen Virol*. (1996) 77:2969–81. doi: 10.1099/0022-1317-77-12-2969
40. Ferguson D, Clarke S, Berry N, Almond N. Attenuated SIV causes persisting neuroinflammation in the absence of a chronic viral load and neurotoxic antiretroviral therapy. *AIDS*. (2016) 30:2439–48. doi: 10.1097/QAD.0000000000001178
41. Carl S, Iafrate AJ, Skowronski J, Stahl-Hennig C, Kirchhoff F. Effect of the attenuating deletion and of sequence alterations evolving *in vivo* on simian immunodeficiency virus C8-Nef function. *J Virol*. (1999) 73:2790–7.
42. Clarke S, Berry N, Ham C, Alden J, Almond N, Ferguson D. Neuropathology of wild-type and nef-attenuated T cell tropic simian immunodeficiency virus (SIVmac32H) and macrophage tropic neurovirulent SIVmac17E-Fr in cynomolgus macaques. *J Neurovirol*. (2012) 18:100–12. doi: 10.1007/s13365-012-0084-3
43. Thompson KA, Kent SJ, Gahan ME, Purcell DF, McLean CA, Preiss S, et al. Decreased neurotropism of nef long terminal repeat (nef/LTR)-deleted simian immunodeficiency virus. *J Neurovirol*. (2003) 9:442–51. doi: 10.1080/13550280390218715
44. Deacon NJ, Tsykin A, Solomon A, Smith K, Ludford-Menting M, Hooker DJ, et al. Genomic structure of an attenuated quasi species of HIV-1 from a blood transfusion donor and recipients. *Science*. (1995) 270:988–91. doi: 10.1126/science.270.5238.988
45. Gorry PR, Churchill M, Learmont J, Cherry C, Dyer WB, Wesselingh SL, et al. Replication-dependent pathogenicity of attenuated nef-deleted HIV-1 *in vivo*. *J Acquir Immune Defic Syndr*. (2007) 46:390–4. doi: 10.1097/QAI.0b013e31815aba08
46. Hanna Z, Kay DG, Rebai N, Guimond A, Jothy S, Jolicoeur P. Nef harbors a major determinant of pathogenicity for an AIDS-like disease induced by HIV-1 in transgenic mice. *Cell*. (1998) 95:163–75. doi: 10.1016/S0092-8674(00)81748-1
47. Kestler HW III, Ringler DJ, Mori K, Panicali DL, Sehgal PK, Daniel MD, et al. Importance of the nef gene for maintenance of high virus loads and for development of AIDS. *Cell*. (1991) 65:651–62. doi: 10.1016/0092-8674(91)90097-I
48. Fackler OT, Baur AS. Live and let die: Nef functions beyond HIV replication. *Immunity*. (2002) 16:493–7. doi: 10.1016/S1074-7613(02)00307-2

49. Quaranta MG, Mattioli B, Giordani L, Viora M. The immunoregulatory effects of HIV-1 Nef on dendritic cells and the pathogenesis of AIDS. *FASEB J.* (2006) 20:2198–208. doi: 10.1096/fj.06-6260rev
50. Kirchhoff F, Schindler M, Specht A, Arhel N, Munch J. Role of Nef in primate lentiviral immunopathogenesis. *Cell Mol Life Sci*. (2008) 65:2621–36. doi: 10.1007/s00018-008-8094-2
51. Kyei GB, Dinkins C, Davis AS, Roberts E, Singh SB, Dong C, et al. Autophagy pathway intersects with HIV-1 biosynthesis and regulates viral yields in macrophages. *J Cell Biol*. (2009) 186:255–68. doi: 10.1083/jcb.200903070
52. Nakahira K, Haspel JA, Rathinam VA, Lee SJ, Dolinay T, Lam HC, et al. Autophagy proteins regulate innate immune responses by inhibiting the release of mitochondrial DNA mediated by the NALP3 inflammasome. *Nat Immunol*. (2011) 12:222–30. doi: 10.1038/ni.1980
53. Saitoh T, Fujita N, Jang MH, Uematsu S, Yang BG, Satoh T, et al. Loss of the autophagy protein Atg16L1 enhances endotoxin-induced IL-1beta production. *Nature*. (2008) 456:264–8. doi: 10.1038/nature07383
54. Ghosh AK, Mau T, O'Brien M, Garg S, Yung R. Impaired autophagy activity is linked to elevated ER-stress and inflammation in aging adipose tissue. *Aging*. (2016) 8:2525–37. doi: 10.18632/aging.101083
55. Xu W, Wei Q, Han M, Zhou B, Wang H, Zhang J, et al. CCL2-SQSTM1 positive feedback loop suppresses autophagy to promote chemoresistance in gastric cancer. *Int J Biol Sci*. (2018) 14:1054–66. doi: 10.7150/ijbs.25349
56. Appay V, Sauce D. Immune activation and inflammation in HIV-1 infection: causes and consequences. *J Pathol*. (2008) 214:231–41. doi: 10.1002/path.2276
57. Guy B, Riviere Y, Dott K, Regnault A, Kieny MP. Mutational analysis of the HIV nef protein. *Virology*. (1990) 176:413–25. doi: 10.1016/0042-6822(90)90011-F
58. Macreadie IG, Castelli LA, Lucantoni A, Azad AA. Stress- and sequence-dependent release into the culture medium of HIV-1 Nef produced in Saccharomyces cerevisiae. *Gene*. (1995) 162:239–43. doi: 10.1016/0378-1119(95)00316-X
59. James CO, Huang MB, Khan M, Garcia-Barrio M, Powell MD, Bond VC. Extracellular Nef protein targets CD4+ T cells for apoptosis by interacting with CXCR4 surface receptors. *J Virol*. (2004) 78:3099–109. doi: 10.1128/JVI.78.6.3099-3109.2004
60. Robbins PD, Morelli AE. Regulation of immune responses by extracellular vesicles. *Nat Rev Immunol*. (2014) 14:195–208. doi: 10.1038/nri3622
61. Stumptner-Cuvelette P, Jouve M, Helft J, Dugast M, Glouzman AS, Jooss K, et al. Human immunodeficiency virus-1 Nef expression induces intracellular accumulation of multivesicular bodies and major histocompatibility complex class II complexes: potential role of phosphatidylinositol 3-kinase. *Mol Biol Cell*. (2003) 14:4857–70. doi: 10.1091/mbc.e03-04-0211
62. Denzer K, Kleijmeer MJ, Heijnen HF, Stoorvogel W, Geuze HJ. Exosome: from internal vesicle of the multivesicular body to intercellular signaling device. *J Cell Sci*. (2000) 113:3365–74.
63. Pandori MW, Fitch NJ, Craig HM, Richman DD, Spina CA, Guatelli JC. Producer-cell modification of human immunodeficiency virus type 1: Nef is a virion protein. *J Virol*. (1996) 70:4283–90.
64. Welker R, Kottler H, Kalbitzer HR, Krausslich HG. Human immunodeficiency virus type 1 Nef protein is incorporated into virus particles and specifically cleaved by the viral proteinase. *Virology*. (1996) 219:228–36. doi: 10.1006/viro.1996.0240
65. Brack-Werner R, Kleinschmidt A, Ludvigsen A, Mellert W, Neumann M, Herrmann R, et al. Infection of human brain cells by HIV-1: restricted virus production in chronically infected human glial cell lines. *AIDS*. (1992) 6:273–85. doi: 10.1097/00002030-199203000-00004
66. Chowers MY, Spina CA, Kwoh TJ, Fitch NJ, Richman DD, Guatelli JC. Optimal infectivity *in vitro* of human immunodeficiency virus type 1 requires an intact nef gene. *J Virol*. (1994) 68:2906–14.
67. Neumann M, Felber BK, Kleinschmidt A, Froese B, Erfle V, Pavlakis GN, et al. Restriction of human immunodeficiency virus type 1 production in a human astrocytoma cell line is associated with a cellular block in Rev function. *J Virol*. (1995) 69:2159–67.
68. Raposo G, Nijman HW, Stoorvogel W, Liejendekker R, Harding CV, Melief CJ, et al. B lymphocytes secrete antigen-presenting vesicles. *J Exp Med*. (1996) 183:1161–72. doi: 10.1084/jem.183.3.1161
69. Lehmann MH, Walter S, Ylisastigui L, Striebel F, Kohleisen B, Ovod V, et al. Exogenous HIV-1 Nef protein increases migration of monocytes. In: *XXII Symposium of the International Association for Comparative Research on Leukemia and Related Diseases*. Heidelberg (2005).
70. Campbell TD, Khan M, Huang MB, Bond VC, Powell MD. HIV-1 Nef protein is secreted into vesicles that can fuse with target cells and virions. *Ethn Dis*. (2008) 18(suppl. 2):S2–14–9.
71. Muratori C, Cavallin LE, Kratzel K, Tinari A, De Milito A, Fais S, et al. Massive secretion by T cells is caused by HIV Nef in infected cells and by Nef transfer to bystander cells. *Cell Host Microbe*. (2009) 6:218–30. doi: 10.1016/j.chom.2009.06.009
72. Lenassi M, Cagney G, Liao M, Vaupotic T, Bartholomeeusen K, Cheng Y, et al. HIV Nef is secreted in exosomes and triggers apoptosis in bystander CD4+ T cells. *Traffic*. (2010) 11:110–22. doi: 10.1111/j.1600-0854.2009.01006.x
73. Luo X, Fan Y, Park IW, He JJ. Exosomes are unlikely involved in intercellular Nef transfer. *PLoS ONE*. (2015) 10:e0124436. doi: 10.1371/journal.pone.0124436
74. Ellwanger JH, Veit TD, Chies JAB. Exosomes in HIV infection: a review and critical look. *Infect Genet Evol*. (2017) 53:146–54. doi: 10.1016/j.meegid.2017.05.021
75. Khan MB, Lang MJ, Huang MB, Raymond A, Bond VC, Shiramizu B, et al. Nef exosomes isolated from the plasma of individuals with HIV-associated dementia (HAD) can induce Abeta(1–42) secretion in SH-SY5Y neural cells. *J Neurovirol*. (2016) 22:179–90. doi: 10.1007/s13365-015-0383-6
76. Raymond AD, Campbell-Sims TC, Khan M, Lang M, Huang MB, Bond VC, et al. HIV Type 1 Nef is released from infected cells in CD45(+) microvesicles and is present in the plasma of HIV-infected individuals. *AIDS Res Hum Retroviruses*. (2011) 27:167–78. doi: 10.1089/aid.2009.0170
77. Wang T, Green LA, Gupta SK, Amet T, Byrd DJ, Yu Q, et al. Intracellular Nef detected in peripheral blood mononuclear cells from HIV patients. *AIDS Res Hum Retroviruses*. (2015) 31:217–20. doi: 10.1089/aid.2013.0250
78. McNamara RP, Costantini LM, Myers TA, Schouest B, Maness NJ, Griffith JD, et al. Nef secretion into extracellular vesicles or exosomes is conserved across human and simian immunodeficiency viruses. *MBio*. (2018) 9:e02344-17. doi: 10.1128/mBio.02344-17
79. Mathieu M, Martin-Jaular L, Lavieu G, Thery C. Specificities of secretion and uptake of exosomes and other extracellular vesicles for cell-to-cell communication. *Nat Cell Biol*. (2019) 21:9–17. doi: 10.1038/s41556-018-0250-9
80. Dupont M, Souriant S, Lugo-Villarino G, Maridonneau-Parini I, Verollet C. Tunneling nanotubes: intimate communication between myeloid cells. *Front Immunol*. (2018) 9:43. doi: 10.3389/fimmu.2018.00043
81. Hashimoto M, Bhuyan F, Hiyoshi M, Noyori O, Nasser H, Miyazaki M, et al. Potential role of the formation of tunneling nanotubes in HIV-1 spread in macrophages. *J Immunol*. (2016) 196:1832–41. doi: 10.4049/jimmunol.1500845
82. Uhl J, Gujarathi S, Waheed AA, Gordon A, Freed EO, Gousset K. Myosin-X is essential to the intercellular spread of HIV-1 Nef through tunneling nanotubes. *J Cell Commun Signal*. (2018) 13:209–24. doi: 10.1007/s12079-018-0493-z
83. Xu W, Santini PA, Sullivan JS, He B, Shan M, Ball SC, et al. HIV-1 evades virus-specific IgG2 and IgA responses by targeting systemic and intestinal B cells via long-range intercellular conduits. *Nat Immunol*. (2009) 10:1008–17. doi: 10.1038/ni.1753
84. Park IW, Fan Y, Luo X, Ryou MG, Liu J, Green L, et al. HIV-1 Nef is transferred from expressing T cells to hepatocytic cells through conduits and enhances HCV replication. *PLoS ONE*. (2014) 9:e99545. doi: 10.1371/journal.pone.0099545
85. Wang T, Green LA, Gupta SK, Kim C, Wang L, Almodovar S, et al. Transfer of intracellular HIV Nef to endothelium causes endothelial dysfunction. *PLoS ONE*. (2014) 9:e91063. doi: 10.1371/journal.pone.0091063
86. Roberts TK, Eugenin EA, Lopez L, Romero IA, Weksler BB, Couraud PO, et al. CCL2 disrupts the adherens junction: implications for neuroinflammation. *Lab Invest*. (2012) 92:1213–33. doi: 10.1038/labinvest.2012.80
87. Stamatovic SM, Keep RF, Kunkel SL, Andjelkovic AV. Potential role of MCP-1 in endothelial cell tight junction 'opening': signaling via Rho and Rho kinase. *J Cell Sci*. (2003) 116:4615–28. doi: 10.1242/jcs.00755

88. Yao Y, Tsirka SE. Monocyte chemoattractant protein-1 and the blood-brain barrier. *Cell Mol Life Sci*. (2014) 71:683–97. doi: 10.1007/s00018-013-1459-1
89. Paul D, Ge S, Lemire Y, Jellison ER, Serwanski DR, Ruddle NH, et al. Cell-selective knockout and 3D confocal image analysis reveals separate roles for astrocyte-and endothelial-derived CCL2 in neuroinflammation. *J Neuroinflammation*. (2014) 11:10. doi: 10.1186/1742-2094-11-10
90. Matsumoto H, Kumon Y, Watanabe H, Ohnishi T, Shudou M, Chuai M, et al. Accumulation of macrophage-like cells expressing NG2 proteoglycan and Iba1 in ischemic core of rat brain after transient middle cerebral artery occlusion. *J Cereb Blood Flow Metab*. (2008) 28:149–63. doi: 10.1038/sj.jcbfm.9600519
91. Smirkin A, Matsumoto H, Takahashi H, Inoue A, Tagawa M, Ohue S, et al. Iba1(+)/NG2(+) macrophage-like cells expressing a variety of neuroprotective factors ameliorate ischemic damage of the brain. *J Cereb Blood Flow Metab*. (2010) 30:603–15. doi: 10.1038/jcbfm.2009.233
92. Tei N, Tanaka J, Sugimoto K, Nishihara T, Nishioka R, Takahashi H, et al. Expression of MCP-1 and fractalkine on endothelial cells and astrocytes may contribute to the invasion and migration of brain macrophages in ischemic rat brain lesions. *J Neurosci Res*. (2013) 91:681–93. doi: 10.1002/jnr.23202
93. Ajami B, Bennett JL, Krieger C, McNagny KM, Rossi FM. Infiltrating monocytes trigger EAE progression, but do not contribute to the resident microglia pool. *Nat Neurosci*. (2011) 14:1142–9. doi: 10.1038/nn.2887
94. Ajami B, Bennett JL, Krieger C, Tetzlaff W, Rossi FM. Local self-renewal can sustain CNS microglia maintenance and function throughout adult life. *Nat Neurosci*. (2007) 10:1538–43. doi: 10.1038/nn2014
95. Fan Y, Liu C, Qin X, Wang Y, Han Y, Zhou Y. The role of ERK1/2 signaling pathway in Nef protein upregulation of the expression of the intercellular adhesion molecule 1 in endothelial cells. *Angiology*. (2010) 61:669–78. doi: 10.1177/0003319710364215
96. Dhawan S, Weeks BS, Soderland C, Schnaper HW, Toro LA, Asthana SP, et al. HIV-1 infection alters monocyte interactions with human microvascular endothelial cells. *J Immunol*. (1995) 154:422–32.
97. Stent G, Crowe SM. Effects of HIV-1 on the surface expression of LFA-1 on cultured monocytes. *J Acquir Immune Defic Syndr Hum Retrovirol*. (1997) 15:95–103. doi: 10.1097/00042560-199706010-00001
98. Maus U, Henning S, Wenschuh H, Mayer K, Seeger W, Lohmeyer J. Role of endothelial MCP-1 in monocyte adhesion to inflamed human endothelium under physiological flow. *Am J Physiol Heart Circ Physiol*. (2002) 283:H2584–91. doi: 10.1152/ajpheart.00349.2002
99. Weber KS, Klickstein LB, Weber C. Specific activation of leukocyte beta2 integrins lymphocyte function-associated antigen-1 and Mac-1 by chemokines mediated by distinct pathways via the alpha subunit cytoplasmic domains. *Mol Biol Cell*. (1999) 10:861–73. doi: 10.1091/mbc.10.4.861
100. Dzenko KA, Song L, Ge S, Kuziel WA, Pachter JS. CCR2 expression by brain microvascular endothelial cells is critical for macrophage transendothelial migration in response to CCL2. *Microvasc Res*. (2005) 70:53–64. doi: 10.1016/j.mvr.2005.04.005
101. Williams DW, Veenstra M, Gaskill PJ, Morgello S, Calderon TM, Berman JW. Monocytes mediate HIV neuropathogenesis: mechanisms that contribute to HIV associated neurocognitive disorders. *Curr HIV Res*. (2014) 12:85–96. doi: 10.2174/1570162X12666140526114526
102. Kraft-Terry SD, Stothert AR, Buch S, Gendelman HE. HIV-1 neuroimmunity in the era of antiretroviral therapy. *Neurobiol Dis*. (2010) 37:542–8. doi: 10.1016/j.nbd.2009.12.015
103. Mangus LM, Beck SE, Queen SE, Brill SA, Shirk EN, Metcalf Pate KA, et al. Lymphocyte-dominant encephalitis and meningitis in simian immunodeficiency virus-infected macaques receiving antiretroviral therapy. *Am J Pathol*. (2018) 188:125–34. doi: 10.1016/j.ajpath.2017.08.035
104. Churchill MJ, Gorry PR, Cowley D, Lal L, Sonza S, Purcell DF, et al. Use of laser capture microdissection to detect integrated HIV-1 DNA in macrophages and astrocytes from autopsy brain tissues. *J Neurovirol*. (2006) 12:146–52. doi: 10.1080/13550280600748946
105. Hurtrel B, Chakrabarti L, Hurtrel M, Montagnier L. Target cells during early SIV encephalopathy. *Res Virol*. (1993) 144:41–6. doi: 10.1016/S0923-2516(06)80010-5
106. Michaels J, Sharer LR, Epstein LG. Human immunodeficiency virus type 1 (HIV-1) infection of the nervous system: a review. *Immunodefic Rev*. (1988) 1:71–104.
107. Raymond AD, Diaz P, Chevelon S, Agudelo M, Yndart-Arias A, Ding H, et al. Microglia-derived HIV Nef+ exosome impairment of the blood-brain barrier is treatable by nanomedicine-based delivery of Nef peptides. *J Neurovirol*. (2016) 22:129–39. doi: 10.1007/s13365-015-0397-0
108. Ward JM, O'Leary TJ, Baskin GB, Benveniste R, Harris CA, Nara PL, et al. Immunohistochemical localization of human and simian immunodeficiency viral antigens in fixed tissue sections. *Am J Pathol*. (1987) 127:199–205.
109. Russell RA, Chojnacki J, Jones DM, Johnson E, Do T, Eggeling C, et al. Astrocytes resist HIV-1 fusion but engulf infected macrophage material. *Cell Rep*. (2017) 18:1473–83. doi: 10.1016/j.celrep.2017.01.027
110. Al-Harti L, Joseph J, Nath A. Astrocytes as an HIV CNS reservoir: highlights and reflections of an NIMH-sponsored symposium. *J Neurovirol*. (2018) 24:665–9. doi: 10.1007/s13365-018-0691-8
111. Ranki A, Nyberg M, Ovod V, Haltia M, Elovaara I, Raininko R, et al. Abundant expression of HIV Nef and Rev proteins in brain astrocytes *in vivo* is associated with dementia. *AIDS*. (1995) 9:1001–8. doi: 10.1097/00002030-199509000-00004
112. Bencheikh M, Bentsman G, Sarkissian N, Canki M, Volsky DJ. Replication of different clones of human immunodeficiency virus type 1 in primary fetal human astrocytes: enhancement of viral gene expression by Nef. *J Neurovirol*. (1999) 5:115–24. doi: 10.3109/13550289909021993
113. Puzar Dominkus P, Ferdin J, Plemenitas A, Peterlin BM, Lenassi M. Nef is secreted in exosomes from Nef.GFP-expressing and HIV-1-infected human astrocytes. *J Neurovirol*. (2017) 23:713–24. doi: 10.1007/s13365-017-0552-x
114. Sami Saribas A, Cicalese S, Ahooyi TM, Khalili K, Amini S, Sariyer IK. HIV-1 Nef is released in extracellular vesicles derived from astrocytes: evidence for Nef-mediated neurotoxicity. *Cell Death Dis*. (2017) 8:e2542. doi: 10.1038/cddis.2016.467
115. van Marle G, Henry S, Todoruk T, Sullivan A, Silva C, Rourke SB, et al. Human immunodeficiency virus type 1 Nef protein mediates neural cell death: a neurotoxic role for IP-10. *Virology*. (2004) 329:302–18. doi: 10.1016/j.virol.2004.08.024
116. Lehmann MH, Masanetz S, Kramer S, Erfle V. HIV-1 Nef upregulates CCL2/MCP-1 expression in astrocytes in a myristoylation- and calmodulin-dependent manner. *J Cell Sci*. (2006) 119:4520–30. doi: 10.1242/jcs.03231
117. Chompre G, Cruz E, Maldonado L, Rivera-Amill V, Porter JT, Noel RJ Jr. Astrocytic expression of HIV-1 Nef impairs spatial and recognition memory. *Neurobiol Dis*. (2013) 49:128–36. doi: 10.1016/j.nbd.2012.08.007
118. Acharjee S, Branton WG, Vivithanaporn P, Maingat F, Paul AM, Dickie P, et al. HIV-1 Nef expression in microglia disrupts dopaminergic and immune functions with associated mania-like behaviors. *Brain Behav Immun*. (2014) 40:74–84. doi: 10.1016/j.bbi.2014.02.016
119. Mordelet E, Kissa K, Cressant A, Gray F, Ozden S, Vidal C, et al. Histopathological and cognitive defects induced by Nef in the brain. *FASEB J*. (2004) 18:1851–61. doi: 10.1096/fj.04-2308com
120. Cinque P, Vago L, Mengozzi M, Torri V, Ceresa D, Vicenzi E, et al. Elevated cerebrospinal fluid levels of monocyte chemotactic protein-1 correlate with HIV-1 encephalitis and local viral replication. *AIDS*. (1998) 12:1327–32. doi: 10.1097/00002030-199811000-00014
121. Conant K, Garzino-Demo A, Nath A, McArthur JC, Halliday W, Power C, et al. Induction of monocyte chemoattractant protein-1 in HIV-1 Tat-stimulated astrocytes and elevation in AIDS dementia. *Proc Natl Acad Sci USA*. (1998) 95:3117–21. doi: 10.1073/pnas.95.6.3117
122. Persidsky Y, Ghorpade A, Rasmussen J, Limoges J, Liu XJ, Stins M, et al. Microglial and astrocyte chemokines regulate monocyte migration through the blood-brain barrier in human immunodeficiency virus-1 encephalitis. *Am J Pathol*. (1999) 155:1599–611. doi: 10.1016/S0002-9440(10)65476-4
123. Zink MC, Coleman GD, Mankowski JL, Adams RJ, Tarwater PM, Fox K, et al. Increased macrophage chemoattractant protein-1 in cerebrospinal fluid precedes and predicts simian immunodeficiency virus encephalitis. *J Infect Dis*. (2001) 184:1015–21. doi: 10.1086/323478
124. Gonzalez E, Rovin BH, Sen L, Cooke G, Dhanda R, Mummidi S, et al. HIV-1 infection and AIDS dementia are influenced by a mutant MCP-1 allele linked to increased monocyte infiltration of tissues and MCP-1 levels. *Proc Natl Acad Sci USA*. (2002) 99:13795–800. doi: 10.1073/pnas.202357499
125. Yao H, Yang Y, Kim KJ, Bethel-Brown C, Gong N, Funa K, et al. Molecular mechanisms involving sigma receptor-mediated induction of

MCP-1: implication for increased monocyte transmigration. *Blood*. (2010) 115:4951–62. doi: 10.1182/blood-2010-01-266221
126. Eugenin EA, Osiecki K, Lopez L, Goldstein H, Calderon TM, Berman JW. CCL2/monocyte chemoattractant protein-1 mediates enhanced transmigration of human immunodeficiency virus (HIV)-infected leukocytes across the blood-brain barrier: a potential mechanism of HIV-CNS invasion and NeuroAIDS. *J Neurosci*. (2006) 26:1098–106. doi: 10.1523/JNEUROSCI.3863-05.2006
127. Parillaud VR, Lornet G, Monnet Y, Privat AL, Haddad AT, Brochard V, et al. Analysis of monocyte infiltration in MPTP mice reveals that microglial CX3CR1 protects against neurotoxic over-induction of monocyte-attracting CCL2 by astrocytes. *J Neuroinflammation*. (2017) 14:60. doi: 10.1186/s12974-017-0830-9
128. Severini C, Passeri PP, Ciotti M, Florenzano F, Possenti R, Zona C, et al. Bindarit, inhibitor of CCL2 synthesis, protects neurons against amyloid-beta-induced toxicity. *J Alzheimers Dis*. (2014) 38:281–93. doi: 10.3233/JAD-131070
129. Tian DS, Peng J, Murugan M, Feng LJ, Liu JL, Eyo UB, et al. Chemokine CCL2-CCR2 signaling induces neuronal cell death via STAT3 activation and IL-1beta production after status epilepticus. *J Neurosci*. (2017) 37:7878–92. doi: 10.1523/JNEUROSCI.0315-17.2017
130. Brandt C, Zvolensky MJ, Woods SP, Gonzalez A, Safren SA, O'Cleirigh CM. Anxiety symptoms and disorders among adults living with HIV and AIDS: a critical review and integrative synthesis of the empirical literature. *Clin Psychol Rev*. (2017) 51:164–84. doi: 10.1016/j.cpr.2016.11.005
131. Prakash A, Hou J, Liu L, Gao Y, Kettering C, Ragin AB. Cognitive function in early HIV infection. *J Neurovirol*. (2017) 23:273–82. doi: 10.1007/s13365-016-0498-4
132. Smail RC, Brew BJ. HIV-associated neurocognitive disorder. *Handb Clin Neurol*. (2018) 152:75–97. doi: 10.1016/B978-0-444-63849-6.00007-4
133. Dimitrijevic OB, Stamatovic SM, Keep RF, Andjelkovic AV. Absence of the chemokine receptor CCR2 protects against cerebral ischemia/reperfusion injury in mice. *Stroke*. (2007) 38:1345–53. doi: 10.1161/01.STR.0000259709.16654.8f
134. Kaufer C, Chhatbar C, Broer S, Waltl I, Ghita L, Gerhauser I, et al. Chemokine receptors CCR2 and CX3CR1 regulate viral encephalitis-induced hippocampal damage but not seizures. *Proc Natl Acad Sci USA*. (2018) 115:E8929–38. doi: 10.1073/pnas.1806754115
135. Conductier G, Blondeau N, Guyon A, Nahon JL, Rovere C. The role of monocyte chemoattractant protein MCP1/CCL2 in neuroinflammatory diseases. *J Neuroimmunol*. (2010) 224:93–100. doi: 10.1016/j.jneuroim.2010.05.010
136. Ge S, Song L, Serwanski DR, Kuziel WA, Pachter JS. Transcellular transport of CCL2 across brain microvascular endothelial cells. *J Neurochem*. (2008) 104:1219–32. doi: 10.1111/j.1471-4159.2007.05056.x
137. Van Steenwinckel J, Reaux-Le Goazigo A, Pommier B, Mauborgne A, Dansereau MA, Kitabgi P, et al. CCL2 released from neuronal synaptic vesicles in the spinal cord is a major mediator of local inflammation and pain after peripheral nerve injury. *J Neurosci*. (2011) 31:5865–75. doi: 10.1523/JNEUROSCI.5986-10.2011
138. Parker R, Stein DJ, Jelsma J. Pain in people living with HIV/AIDS: a systematic review. *J Int AIDS Soc*. (2014) 17:18719. doi: 10.7448/IAS.17.1.18719
139. Fischer-Smith T, Rappaport J. Evolving paradigms in the pathogenesis of HIV-1-associated dementia. *Expert Rev Mol Med*. (2005) 7:1–26. doi: 10.1017/S1462399405010239
140. Marincowitz C, Genis A, Goswami N, De Boever P, Nawrot TS, Strijdom H. Vascular endothelial dysfunction in the wake of HIV and ART. *FEBS J*. (2019) 286:1256–70. doi: 10.1111/febs.14657
141. Covino DA, Sabbatucci M, Fantuzzi L. The CCL2/CCR2 axis in the pathogenesis of HIV-1 infection: a new cellular target for therapy? *Curr Drug Targets*. (2016) 17:76–110. doi: 10.2174/1389450117011512171109 17
142. Dickens AM, Yoo SW, Chin AC, Xu J, Johnson TP, Trout AL, et al. Chronic low-level expression of HIV-1 Tat promotes a neurodegenerative phenotype with aging. *Sci Rep*. (2017) 7:7748. doi: 10.1038/s41598-017-07570-5
143. Khiati A, Chaloin O, Muller S, Tardieu M, Horellou P. Induction of monocyte chemoattractant protein-1 (MCP-1/CCL2) gene expression by human immunodeficiency virus-1 Tat in human astrocytes is CDK9 dependent. *J Neurovirol*. (2010) 16:150–67. doi: 10.3109/13550281003735691
144. Campbell GR, Watkins JD, Singh KK, Loret EP, Spector SA. Human immunodeficiency virus type 1 subtype C Tat fails to induce intracellular calcium flux and induces reduced tumor necrosis factor production from monocytes. *J Virol*. (2007) 81:5919–28. doi: 10.1128/JVI.01938-06
145. Albini A, Ferrini S, Benelli R, Sforzini S, Giunciuglio D, Aluigi MG, et al. HIV-1 Tat protein mimicry of chemokines. *Proc Natl Acad Sci USA*. (1998) 95:13153–8. doi: 10.1073/pnas.95.22.13153
146. Sabatier JM, Vives E, Mabrouk K, Benjouad A, Rochat H, Duval A, et al. Evidence for neurotoxic activity of tat from human immunodeficiency virus type 1. *J Virol*. (1991) 65:961–7. doi: 10.1007/978-94-011-2264-1_282
147. Burlacu R, Umlauf A, Marcotte TD, Soontornniyomkij B, Diaconu CC, Bulacu-Talnariu A, et al. Plasma CXCL10 correlates with HAND in HIV-infected women. *J Neurovirol*. (2019). doi: 10.1007/s13365-019-00785-4. [Epub ahead of print].

Conflict of Interest: The authors declare that the research was conducted in the absence of any commercial or financial relationships that could be construed as a potential conflict of interest.

frontiers in Immunology

REVIEW
published: 20 December 2018
doi: 10.3389/fimmu.2018.03022

Fine Tuning the Cytokine Storm by IFN and IL-10 Following Neurotropic Coronavirus Encephalomyelitis

*Carine Savarin and Cornelia C. Bergmann**

Department of Neuroscience, Cleveland Clinic Foundation, Lerner Research Institute, Cleveland, OH, United States

The central nervous system (CNS) is vulnerable to several viral infections including herpes viruses, arboviruses and HIV to name a few. While a rapid and effective immune response is essential to limit viral spread and mortality, this anti-viral response needs to be tightly regulated in order to limit immune mediated tissue damage. This balance between effective virus control with limited pathology is especially important due to the highly specialized functions and limited regenerative capacity of neurons, which can be targets of direct virus cytolysis or bystander damage. CNS infection with the neurotropic strain of mouse hepatitis virus (MHV) induces an acute encephalomyelitis associated with focal areas of demyelination, which is sustained during viral persistence. Both innate and adaptive immune cells work in coordination to control virus replication. While type I interferons are essential to limit virus spread associated with early mortality, perforin, and interferon-γ promote further virus clearance in astrocytes/microglia and oligodendrocytes, respectively. Effective control of virus replication is nonetheless associated with tissue damage, characterized by demyelinating lesions. Interestingly, the anti-inflammatory cytokine IL-10 limits expansion of tissue lesions during chronic infection without affecting viral persistence. Thus, effective coordination of pro- and anti-inflammatory cytokines is essential during MHV induced encephalomyelitis in order to protect the host against viral infection at a limited cost.

Keywords: central nervous system, viral infection, JHMV, IFNα/β, IFNγ, IL-10, demyelination

OPEN ACCESS

Edited by:
Michael H. Lehmann, Ludwig Maximilian University of Munich, Germany

Reviewed by:
Lauren Alene O'Donnell, Duquesne University, United States
Tian Wang, The University of Texas Medical Branch at Galveston, United States

****Correspondence:***
Cornelia C. Bergmann
bergmac@ccf.org

Specialty section:
This article was submitted to Viral Immunology, a section of the journal Frontiers in Immunology

Received: *16 October 2018*
Accepted: *06 December 2018*
Published: *20 December 2018*

Citation:
Savarin C and Bergmann CC (2018) Fine Tuning the Cytokine Storm by IFN and IL-10 Following Neurotropic Coronavirus Encephalomyelitis. Front. Immunol. 9:3022. doi: 10.3389/fimmu.2018.03022

INTRODUCTION

The central nervous system (CNS) is susceptible to various neurotropic viral infections associated with acute inflammation. Depending on the distinct anatomical regions infected, inflammation is referred to as meningitis (meninges), encephalitis (brain), myelitis (spinal cord), or meningoencephalitis and encephalomyelitis if multiple sites are afflicted (1). Viral meningitis is overall more clinically benign, whereas encephalitis is associated with clinical evidence of neurological dysfunctions, which can range from behavioral changes to seizures and paralysis. Many encephalitic viruses such as insect borne viruses, enteroviruses, and non-endogenous retroviruses can rapidly invade the CNS early following peripheral infection. However, encephalitis caused by members of the herpes viruses, e.g., Herpes Simplex Virus (HSV)-2, cytomegalovirus (CMV), or the polyomavirus John Cunningham virus (JC virus) are more commonly caused by immune suppression allowing re-activation of otherwise controlled chronic or latent peripheral infections and invasion of, or reactivation within the brain, resulting in severe disability and death (2). For example, premature death of multiple sclerosis patients treated with

Natalizumab due to JC-virus mediated progressive multifocal leukoencephalopathy emphasizes the importance of CNS immune surveillance to prevent viral recrudescence (3, 4).

As many neurotropic viruses predominantly target highly specialized and/or non-renewable cells controlling cognitive and vital physiological functions, an efficient anti-viral immune response is essential to limit viral CNS dissemination to prevent lethal outcomes. However, the anti-viral immune response needs to be tightly regulated to minimize bystander tissue damage and neurological dysfunction, which can be long term sequela even after virus control (2). Given the limitations in obtaining human CNS samples, several murine models of viral encephalitis provide complementary tools to unravel activation, effector function and regulation of protective immune responses within the CNS; these include Vesicular stomatitis virus (VSV), Sindbis virus, West Nile virus, Theiler's encephalomyelitis virus (TMEV) and mouse hepatitis virus (MHV). This review primarily focuses on encephalomyelitis induced by neurotropic MHV, namely the sublethal glia tropic variant of the John Howard Muller MHV strain, designated v2.2-1, and the non-lethal dual liver and neurotropic MHV-A59 strain (5). Both viruses are characterized by an acute encephalomyelitis which resolves into a persistent infection characterized by demyelination and sustained detection of viral RNA in the absence of infectious virus. As demyelination is immune-mediated and neuronal infection is sparse in the v2.2-1 model, it provides a useful tool to study the dynamics and regulation of antiviral host immune responses associated with ongoing immune-mediated tissue damage balanced by repair during chronic infection.

MOUSE HEPATITIS VIRUS

Mouse hepatitis viruses (MHV), members of the positive-strand RNA enveloped *Coronaviridae*, are natural murine pathogens that infect the liver, gastrointestinal tract and CNS (6, 7). Virus tropism and pathogenesis depends upon virus strains and variants, as well as inoculation route (8). The attenuated MHV-JHM v2.2-1 referred as v2.2-1 from hereon is a monoclonal antibody derived variant of the lethal MHV-JHM strain (9), which has been extensively used to unravel immune correlates of protection and viral-induced demyelination. Upon intracranial infection the MHV-A59 strain is more neuronotropic than v2.2-1, but also infects glia and causes immune mediated demyelination, although clinical disease severity in immune competent adult infected mice is less severe (10). Unless otherwise stated, this review pertains to encephalomyelitis induced by v2.2-1. Following intracranial administration, v2.2-1 infects the ependymal cells lining the ventricles before spreading to microglia, astrocytes, and oligodendrocytes (OLG); neurons are largely spared. Peak virus replication around day (d) 5 post-infection (p.i.) correlates with activation of astrocytes and microglia, disruption of the blood brain barrier (BBB) and CNS recruitment of neutrophils, NK cells and predominantly bone marrow derived monocytes (6, 11). Monocytes and neutrophils enhance BBB disruption (12) and pave the way for infiltration of T and B cells. T cell recruitment is associated with signs of encephalitis observed around d7 p.i. Both CD8 and CD4 T cells are essential for reducing infectious virus below detectable levels 2 weeks p.i. (6, 13). T cell mediated antiviral function also correlates with onset of demyelination, which peaks 2–3 weeks after control of infectious virus. While virus replication is no longer detectable in chronically infected mice, persisting viral RNA remains present in spinal cords at slowly declining levels. Deprivation of local humoral immunity constitutes the only manipulation resulting in reemergence or lack of clearance of infectious v2.2-1 or A59 virus (14), suggesting virus persists in a replication competent form controlled by local Ab (15).

Induction of cytokines and chemokines, as well as CNS recruitment of innate and adaptive immune cells, is highly regulated during neurotropic MHV infection, emphasizing the orchestration of specific functions at times critical to efficiently control infectious various, while restraining subsequent tissue destruction. This review discusses findings from our colleagues and own laboratories on the role of signature cytokines associated with effective, yet dampened anti-viral responses and limited tissue damage with focus on Interferon (IFN)α/β, IFNγ and IL-10.

TYPE I IFN: CONDUCTOR OF THE EARLY ANTI-VIRAL RESPONSE

The induction of innate immune responses, including type I IFNs, provides the first critical line of immune defense in stemming viral spread throughout the CNS (16, 17). Although coronaviruses are known to be poor IFNα/β inducers, the importance of IFNα/β signaling following both MHV-A59 and v2.2-1 infection, became apparent following infection of IFNα/β receptor deficient ($IFNAR^{-/-}$) mice. Uncontrolled viral replication, extensive viral dissemination throughout the CNS, and expanded tropism to neurons coincided with rapid mortality (18, 19). Early viral replication also induces cytokines and chemokines, some of which are IFNα/β dependent (20). Together, the early response regulates the adaptive immune response essential for reducing viral replication.

Since the naïve CNS is devoid of plasmacytoid dendritic cells, potent peripheral IFNα/β inducers, IFNα/β production relies on sensing of virus invasion by glial and neuronal cells. Although glia and neurons are known to express pattern recognition receptors (PRRs), which recognize diverse pathogen associated molecular patterns (PAMPs) and endogenous danger signals (DAMPs), the diversity and magnitude varies not only between CNS cell type, but also their regional anatomical localization within the CNS (2, 21–23). While all CNS cell types have been shown to be capable of producing IFNα/β *in vitro,* the ability to induce IFNα/β *in vivo* depends on the specific virus, its replication cycle, cellular tropism and respective repertoire of PRRs and associated signaling factors. The disparities between CNS cells in their ability to produce and respond to IFNα/β *in vivo* have recently been reviewed (20). Our own studies with v2.2-1 revealed that oligodendrocytes (OLG) are poor inducers of IFNα/β relative to microglia consistent with low basal levels and limited diversity of PRRs detecting viral RNAs (24). The low expression of IFNα/β receptor chains further coincides

with reduced and delayed expression of interferon sensitive genes (ISG) encoding factors with anti-viral activity, including interferon-induced protein with tetratricopeptide repeats 1 and 2 (Ifit1 and Ifit2). Both their reduced ability to establish an antiviral state and upregulate IFNα/β-induced major histocompatibility complex (MHC) class I presentation components may enhance their propensity to become the predominantly infected glia cells and set the stage for establishment of persistent infection (24, 25).

Cell types, which are not effective initial type I IFN inducers, may nevertheless be protected after inducing ISG, which also include PRRs, in response to IFNα/β produced by heterologous cells. Similar to OLG, lower constitutive PRR, and ISG levels were found in astrocytes relative to microglia. However, studies with MHV-A59 revealed delayed but substantial upregulation of IFNα/β pathway genes within astrocytes following infection (26). Some PRRs, ISGs and IFNα were even expressed at higher levels in astrocytes at d5 p.i. compared to microglia, indicating that astrocytes are critical to the innate antiviral activity through amplification of the IFNα/β response. The importance of IFNα/β signaling within astrocytes was confirmed by uncontrolled viral replication and premature death (1 week p.i.) of mice lacking IFNAR expression specifically on astrocytes (26). However, delayed mortality compared to total IFNAR deficiency indicated that other CNS cells, presumably microglia, contribute early to limiting virus dissemination. Analysis using the v2.2-1 virus will determine whether the astrocytic contribution to IFNAR mediated protection remains similar in a model with sparse astrocyte infection.

Altogether, these data shed light on the individual *in vivo* contribution of glial cells in overall IFNα/β mediated early protection against MHV CNS infection. More studies using conditional ablation of IFNAR and selected ISGs in various encephalitic virus models will be beneficial in unraveling the importance of autocrine and paracrine protective IFNα/β effects on subsequent adaptive responses and potential establishment of cell type specific persistence.

IFNγ AND PERFORIN: WHEN ADAPTIVE IMMUNITY TAKES THE RELAY

Although innate anti-viral immune responses are critical in containing initial CNS virus spread, virus-specific T cell effector functions are essential to eliminate or reduce infectious virus load during most acute infections (27–29). Importantly, CNS cells appear to shape the adaptive immune response to avert direct T cell cytolytic effector mechanisms, especially targeted to neurons, as recently reviewed by Miller at al. (2). While various mechanisms, including intrinsic deviation from cellular targets of lytic granules, T cell inhibitory molecules, as well as anti-inflammatory factors have been demonstrated to dampen T cell effector functions, the same mechanisms also favor establishment of persistent infection.

The requirement for adaptive immune responses to control neurotropic MHV was evidenced by uncontrolled viral replication and mortality of v2.2-1 infected immunodeficient Rag2$^{-/-}$ or SCID mice (30, 31). However, the absence of adaptive immunity also revealed that virus itself does not cause demyelination (6, 9, 32), supporting T cell effector function in mediating pathology. T cell depletion studies subsequently revealed that v2.2-1 control required both CD4$^+$ and CD8$^+$ T cells, with CD4$^+$ T cells providing helper function for CD8$^+$ T cells, which are the primary effector T cells within the CNS (13, 33). Efforts to define prominent anti-viral effector function further demonstrated that mice deficient in perforin-mediated cytolysis could not control viral replication in microglia and astrocytes, while virus control in oligodendrocytes (OLG) was unaffected (34). In contrast, IFNγ$^{-/-}$ mice exhibited loss of viral control specifically in OLG (35). The requirement for IFNγ mediated control in OLG was further confirmed by specifically abrogating IFNγ receptor signaling in OLG (36). These data thus demonstrated that T cell mechanisms affecting viral control *in vivo* were clearly cell type dependent, although CD8$^+$ T cells isolated from the infected CNS exerted both potent cytolytic activity and produced IFNγ *ex vivo*. The distinct susceptibilities of glia cells to CD8$^+$ T cell effector functions was further confirmed by adoptive transfer of virus-specific CD8$^+$ T cells deficient in either IFNγ or perforin into infected T cell-deficient mice (13, 31). The overall higher dependency on IFNγ for MHV control may also reside in the differential dependence of glia on IFNγ to upregulate MHC class I and antigen processing components. Whereas, class I surface expression by microglia coincides with IFNα/β expression, OLG appear to require IFNγ to upregulate class I (25). This delayed class I expression coinciding with enhanced expression of the inhibitory receptor B7-H1 may protect OLG from CD8$^+$ T cell cytolysis (37).

Analysis of the relative contribution of CD8$^+$ vs. CD4$^+$ T cells to express IFNγ following v2.2-1 infection surprisingly revealed that CD4$^+$ T cell express higher levels of IFNγ mRNA at the population levels than CD8$^+$ T cells (38). However, the APC triggering IFNγ production by CD4$^+$ T cells have not been identified, but may be meningeal or perivascular DC. CD4$^+$ T cells can indeed mediate direct anti-viral activity in addition to enhancing CD8$^+$ T cell migration and survival within the CNS (39). However, adoptive transfer of perforin- or IFNγ-deficient CD4$^+$ T cells into infected immunodeficient recipients revealed that viral control was independent of either anti-viral function (13, 17). Moreover, sparse MHC class II upregulation on microglia in the absence of IFNγ, and lack of MHC class II expression on astrocytes and OLG suggest that CD4$^+$ T cells contribute to viral control indirectly via a viral antigen cross presenting APC or via an MHC class II-independent mechanisms (17). Cell types presenting viral antigen to activate CD4$^+$ T or CD8$^+$ T cells in the CNS *in vivo* requires more extensive investigation not only in the MHV model, but also models of neuronotropic infection.

Although the anti-viral T cell response is vital to protect the host following neurotropic infection, it induces tissue damage characterized by demyelination and modest axonal damage. A role for cytolytic infection of OLG was discounted based on the lack of tissue damage in immunodeficient mice, as well as restored myelin loss by transfer of virus specific CD4$^+$ or CD8$^+$ T cells (7). Direct T cell-mediated cytolysis of OLG is also unlikely given the IFNγ dependent control

of infectious virus and difficulties to detect apoptotic OLG (30). Delayed virus control in both perforin$^{-/-}$ as well as IFNγ$^{-/-}$ mice did not alter pathology compared to wt mice, indicating that these effector molecules did not play a role in demyelination (34, 35). Similarly, enhanced OLG infection in the absence of IFNγR signaling in OLG did not result in increased demyelination even in the presence of intact T cell function (36). These studies gave the first indication that IFNγ signaling in OLG, independent of their virus load, does not directly affect demyelination.

The role of IFNγ in demyelination nevertheless still remains unresolved. T cell transfer studies with select virus primed T cell populations further indicate that the source of IFNγ in CD4$^+$ or CD8$^+$ T cells influences pathogenesis. Less demyelination after transfer of IFNγ$^{-/-}$ CD8$^+$ T cells into RAG$^{-/-}$ mice correlated with decreased macrophage/microglia activation and recruitment into white matter areas (40). By contrast, transfer of IFNγ$^{-/-}$ CD4$^+$ T cells into RAG$^{-/-}$ mice correlated with increased demyelination and mortality (41). The dichotomy of enhanced demyelination in RAG$^{-/-}$ recipient of IFNγ$^{-/-}$ CD4$^+$ T cells, which also exhibit selectively increased OLG infection, is likely due to increased IFNγ-regulated neutrophil infiltration and induction of pathogenic Th17 cells (42–44), which had not been uncovered at the time. Distinct from the later studies, lack of IFNγ production by CD4$^+$ T cells partially protected SCID recipients from myelin loss, but led to premature mortality (17). Decreased demyelination in SCID recipients of IFNγ$^{-/-}$ CD4$^+$ T cells nevertheless also correlated with reduced macrophage infiltration and microglia activation. A direct toxic effect of CD4$^+$ T cells on OLG is unlikely due to their lack of MHC class II expression. Some inconsistencies between results in RAG$^{-/-}$ vs. SCID recipients remain to be resolved and may reside in different genetic backgrounds or activation state of transferred T cells (17, 41). Irrespectively, together these data indicate that while IFNγ is vital to reduce MHV virus load, the side effect of extensive macrophages/microglia activation promotes myelin destruction. On the other hand, the total absence of IFNγ not only enhanced virus load, but also maintained neutrophil function and activated Th17 cells (44), which normally do not play a role during a strongly Th1 skewed response during neurotropic MHV infection. More in depth analysis of the role of IFNγ, specifically its cellular targets, is expected to reveal a better understanding of IFNγ as a major regulator of inflammation by promoting MHC class II and iNOS expression and shaping the composition of CNS inflammatory response by regulating chemokine expression. Although iNOS upregulation and oxidative damage have been implicated as factors contributing to CNS tissue damage during demyelination (45), neither genetic ablation of iNOS or pharmacological inhibition of NO affected viral control, demyelination or mortality following infection with v2.2-1 or the neuro attenuated MHV-OBLV60 (46, 47). By contrast, compounds reducing reactive oxygen species (ROS) reduced neuronal loss and demyelination during MHV-A59 induced optic neuritis (48). The contribution of ROS to pathogenesis thus requires more in depth analysis.

IL-10: THE GAMEKEEPER OF TISSUE DAMAGE DURING CHRONIC JHMV INFECTION

Incomplete control of neurotropic MHV results in persistent infection characterized by low levels of viral RNA in spinal cord, sustained detection of cytokine and chemokine expression, retention of CD4$^+$ and CD8$^+$ T cells and ongoing primary demyelination balanced by remyelination (6, 7, 11). The inability to completely eliminate virus suggested an important host response to dampen myelin loss at the expense of virus persistence. One checkpoint molecule was the T cell inhibitory molecule B7-H1, strongly upregulated on OLG. The severity of tissue destruction within lesions in the absence of B7-H1 coincided with increased mortality, although viral control was accelerated (37). Another molecule counteracting tissue damage is the anti-inflammatory cytokine IL-10, known to be a master regulator of immunity to infection (49) as well as balancing immune responses and neurodegeneration in the brain (50). IL-10 is upregulated during acute v2.2-1 infection, at which time it is mainly produced by CD4$^+$ and to a lesser extent CD8$^+$ T cells (51). While IL-10 expression by CD8$^+$ T cells wanes during persistence, it is maintained by CD4$^+$ T cells (52, 53). Both Foxp3 regulatory CD4$^+$ T cells (Tregs) and virus-specific IFNγ$^+$IL-10$^+$ CD4$^+$ T cells (Tr1) are sources of IL-10 throughout the course of JHMV infection and their role have been recently reviewed by Perlman et al. (54). V2.2-1 infection of IL-10$^{-/-}$ mice resulted in faster control of virus replication during acute infection and reduced initial demyelination; surprisingly however, the severity of demyelination increased 2 weeks after viral control without altering viral persistence (55). IL-10 deficiency was also associated with sustained MHC class II expression on Iba1$^+$ myeloid cells and increased iNOS levels in lesions. These data suggested a critical role of IL-10 in limiting tissue damage, despite similar levels of persisting virus. Increased IL-10 production following CNS infection using an engineered IL-10 expressing v2.2-1 variant also resulted in decreased demyelination while virus clearance was slightly delayed (56).

The confirmation of IL-10 as a critical regulator of demyelination questioned whether Tr1 and Foxp3 Tregs played a distinct role. As IL-10 induction in Tr1 cells is IL-27-dependent, mice deficient in IL-27 signaling (IL-27R$^{-/-}$) infected with v2.2-1 were analyzed for a role of Tr1 cells (57). Infected IL-27R$^{-/-}$ displayed drastically reduced Tr1 cells as anticipated, and significantly reduced IL-10 levels at d7 p.i. consistent with faster viral control, similar to IL-10$^{-/-}$ mice. However, impaired IL-27R signaling also correlated with decreased demyelination distinct from the IL-10$^{-/-}$ infected mice. While these findings implied that IL-10 mediated suppression of demyelination is Tr1-independent, it is noted that IL-27R$^{-/-}$ mice have several other dysregulated immune pathways (58, 59). Switching the focus on Foxp3 Tregs, transfer of naïve Foxp3 Tregs into wt or RAG1$^{-/-}$ recipients during acute infection ameliorated tissue damage without affecting virus control (52, 60). These results from a gain of function approach were supported by depletion of CD25$^+$ Tregs prior to infection, which resulted in increased

demyelination (57). While the effect of Foxp3 Tregs on tissue damage is manifested during chronic infection, their regulatory function may already be initiated during acute infection. Indeed, depletion of Foxp3 Tregs during chronic infection had no effect on the extent of myelin loss (61). Similarly, IL-10 neutralization coincident with CNS infection induced increased demyelination whereas delayed IL-10 inhibition did not affect tissue damage (56). Lastly, although Foxp3 Treg transfer during acute infection decreased CNS tissue damage, they were not detected within the CNS. They rather exerted their functions within CNS draining cervical lymph nodes (CLN) by dampening dendritic cell activation and T cell proliferation (60). These data are consistent with a critical regulatory role of Foxp3 Tregs at the time of initial T cell activation with remote consequences on tissue damage.

Irrespective of Treg effects on effector T cells, increased demyelination in IL-$10^{-/-}$ mice correlated with sustained microglia activation and impaired glial scar formation (55). These results supported a local regulatory role of IL-10 acting directly on CNS resident cells. The downregulation of IL-10Rα expression on microglia, yet upregulation on lesion associated astrocytes further highlights the complex dynamics of the CNS environment in responding to IL-10 (55). The identity of the Foxp3 Treg population limiting tissue damage also requires further investigation. A small population of virus-specific Foxp3 Tregs was detected in both CLN and CNS, where they effectively regulated the pro-inflammatory T cell response at both sites (62). Whether these virus-specific Foxp3 Tregs also play a role in directly regulating demyelination remains to be ascertained. Foxp3 Tregs may also prevent tissue damage during chronic

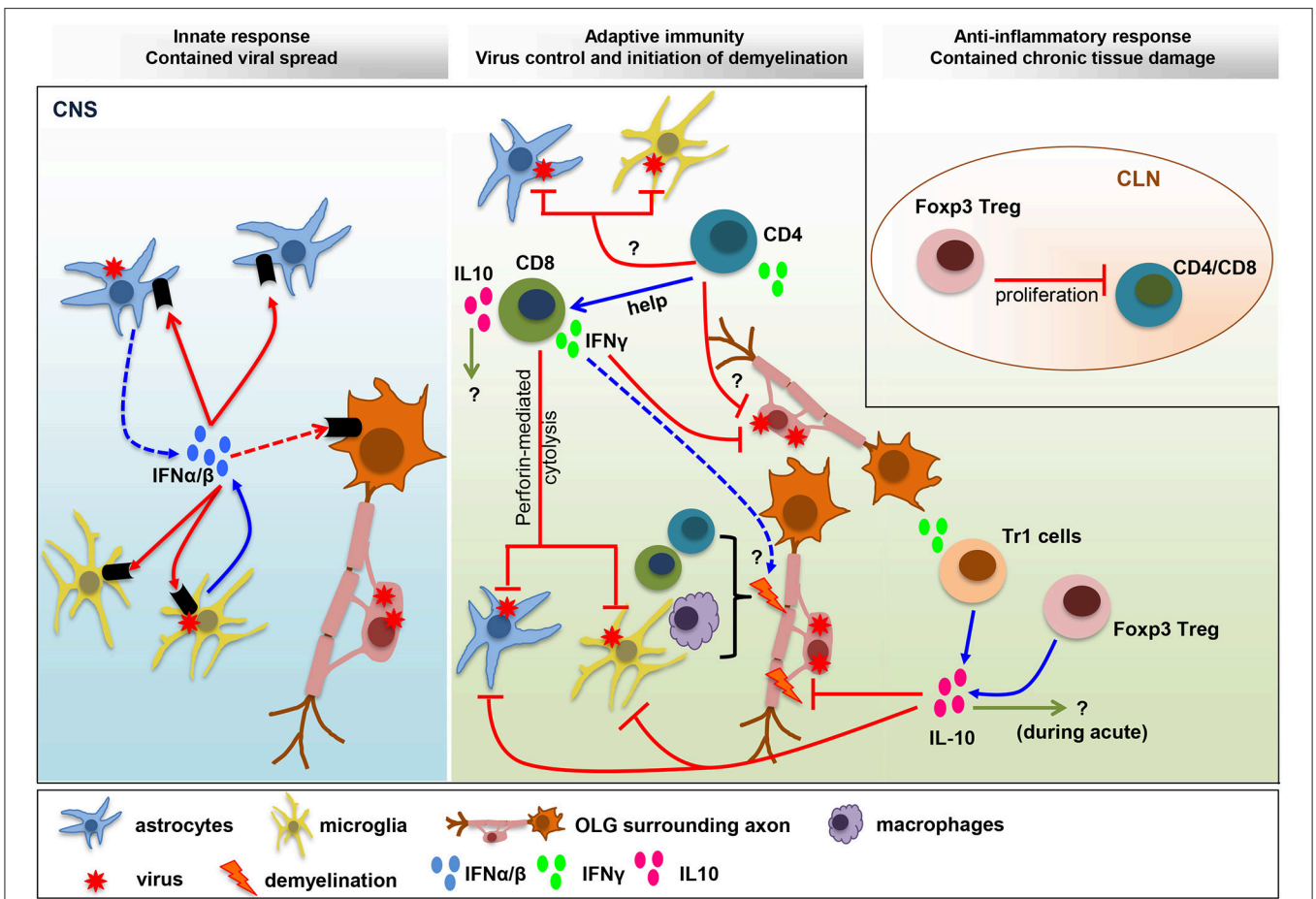

FIGURE 1 | Balance IFN and IL-10 responses determine viral control and pathology. IFNα/β limits viral spread throughout the CNS following MHV infection. The collaboration of microglia as early IFNα/β inducers, and astrocytes as amplifiers of IFNα/β, is crucial to protect from viral dissemination and expanded tropism. The innate response promotes virus-specific T cell recruitment and anti-viral activity critical to eliminate infectious virus below detection limits. $CD4^+$ T cells enhance $CD8^+$ T cell functions and survival and exhibit uncharacterized anti-viral activity. Virus-specific $CD8^+$ T cells eliminate virus using perforin-dependent mechanism in astrocyte/microglia and IFNγ in OLG. CNS T cell recruitment also correlates with initiation of demyelination. Both $CD4^+$ and $CD8^+$ T cells participate in tissue destruction by instructing myeloid cells to initiate tissue damage. The adverse effects mediated by the pro-inflammatory anti-viral response are balanced by IL-10, a master regulator of immunity to infection. While the role of IL-10 during acute infection remains unknown, it limits myelin loss during chronic infection without affecting viral persistence. Both Foxp3 Tregs and Tr1 cells produce IL-10, which restrain demyelination by regulating microglia activation and astroglial scar formation. A direct role of Foxp3 Treg on peripheral T cell activation, with remote temporal effects on tissue damage, has been suggested by T cell transfer studies.

MHV infection by limiting the autoimmune response (63). Global Foxp3 Treg depletion during acute infection correlated with increased proliferation of transferred self-reactive T cells within both CLN and CNS (64). A correlation with potential expansion of demyelinated lesions was however not evaluated. The interplay of various IL-10 secreting Tregs acting at specific sites and on selective target cells at critical time points emphasizes the complex role of IL-10 in dampening JHMV-induced tissue damage without affecting viral clearance and persistence.

Pronounced effects of IL-10 on pathogenesis and clinical outcome rather than viral control in the CNS are also clearly evident in other viral encephalitis models. In the TMEV-mediated transient polioencephalitis model using SJL mice, peak virus load in the hippocampus coincides with peak expression of *IL-10, IL-10ra*, and relates genes. IL-10R neutralization resulted in increased loss of mature neurons and axonal damage, which correlated with enhanced inflammation, although virus load was not altered (65). Further, increased accumulation of Foxp3 Tregs and arginase-1 expressing microglia/macrophages suggested unsuccessful efforts of the host to compensate for the abrogated IL-10 signaling. IL-10 signaling also protects from CNS damage in mice infected with a virulent strain of the mosquito borne alphavirus Sindbis virus by mitigating detrimental Th17 cell functions (66). By contrast, using a more attenuated Sindbis virus, IL-10 deficiency led to longer morbidity, higher mortality, and delayed viral clearance without affecting Th17 cells. Morbidity was rather associated with increased Th1 and decreased Th2 T cells and delayed humoral immunity (67). Along with TNF-α and IL-2, IL-10 is also a key factor for disease remission from fatal encephalitis due to infection with Oshima strain of Tick born encephalitis virus (68). In a murine model of Japanese encephalitis virus infection, elevated IL-10 and reduced IFNγ also correlated with better survival (69). Lastly, IL-10 treatment has been shown to reduce levels of proinflammatory cytokines and infiltrate in murine HSV keratitis without impairing viral clearance (70). *In vivo* results further suggest that IL-10 has the ability to regulate microglial cell production of immune mediators and thereby dampen the pro-inflammatory response to HSV-1 (71).

CONCLUSION

Animal models of viral CNS infection have been crucial in revealing mechanisms of viral control, establishment of persistence and tissue damage. A common theme, not only applying to neurotropic MHV encephalomyelitis, are the protective activities of IFNα/β signaling in limiting initial viral dissemination and predominantly non-cytolytic T cell effector functions in reducing infectious virus load (1, 2). While some viruses are cytolytic to their target cells, the immune response also actively contributes to bystander damage manifested in glia and neuronal dysfunction or demyelination associated with axonal damage. The neurotropic MHV model specifically highlights the critical role of IFNα/β signaling in a single cell type in stemming overwhelming viral dissemination despite no evident defects in T cell function (**Figure 1**). It further demonstrates that maximal T cell anti-viral activity during acute infection coincides with maximal anti-inflammatory IL-10 expression, suggesting that an overaggressive adaptive immune response is already counterbalanced during the viral clearance phase, and does not necessarily emerge as a result of tissue damage (**Figure 1**). Most importantly, the lack of this anti-inflammatory activity can manifest in exacerbated tissue damage remote from acute infection. An immune mediated imbalance early during encephalomyelitis may thus also explain distinct severities of neurological sequelae following human viral disease. For example, IL-6 and IFNγ levels in CSF may be associated with enterovirus (EV)71-induced neuropathology (72). Further, analysis of serum and CSF samples from patients with acute encephalitis syndrome, including with Japanese encephalitis virus supported that higher IL-10 levels in both serum and CSF correlates with protection (73). Similarly, a distinct study of encephalitis patients, including a subcohort with HSV-1, revealed that IL-10 levels were associated with a better coma score on admission in the overall cohort. Elevated IL-10 levels were also associated with a lesser degree of BBB permeability (74). IL-10 signaling also supports BBB integrity following traumatic CNS injury in rodent models (75). With respect to human virus induced encephalitis, it is also interesting to note IL-10 gene polymorphisms as potential susceptibility factors (76). Mutations in IL-10Ra have also been identified as a risk factor of severe influenza-associated encephalopathy (77).

The imprinting of the innate immune response on subsequent adaptive immunity and its effects on bystander cells such as microglia and infiltrating myeloid cells make it difficult to tease apart critical checkpoints determining disease progression or resolution. However, the availability of numerous conditional knockout mice blocking cytokine responses in distinct cell types and in a temporal fashion promise to shed more light on pathways ameliorating pathology while preserving viral control. Confirmation of similar pathways in multiple viral encephalomyelitis models will ultimately enhance targeted treatment options at early stages of disease manifestation. Accumulating literature in both rodent models and human encephalitis implicate that manipulation of IL-10 and IFNγ may have broad implications to treat encephalitis more broadly.

AUTHOR CONTRIBUTIONS

CS and CB contributed to the writing, editing of the manuscript and approved the final version for publication.

FUNDING

This work was supported by the National Institutes of Health grant NS091183.

REFERENCES

1. Swanson PA. II, Mcgavern DB. Viral diseases of the central nervous system. *Curr Opin Virol.* (2015) 11:44–54. doi: 10.1016/j.coviro.2014.12.009
2. Miller KD, Schnell MJ, Rall GF. Keeping it in check: chronic viral infection and antiviral immunity in the brain. *Nat Rev Neurosci.* (2016) 17:766–76. doi: 10.1038/nrn.2016.140
3. Khalili K, White MK, Lublin F, Ferrante P, Berger JR. Reactivation of JC virus and development of PML in patients with multiple sclerosis. *Neurology* (2007) 68:985–90. doi: 10.1212/01.wnl.0000257832.38943.2b
4. Ransohoff RM. Natalizumab for multiple sclerosis. *NE J Med.* (2007) 356:2622–9. doi: 10.1056/NEJMct071462
5. Cowley TJ, Weiss SR. Murine coronavirus neuropathogenesis: determinants of virulence. *J Neurovirol.* (2010) 16:427–34. doi: 10.1007/BF03210848
6. Bergmann CC, Lane TE, Stohlman SA. Coronavirus infection of the central nervous system: host-virus stand-off. *Nat Rev Microbiol.* (2006) 4:121–32. doi: 10.1038/nrmicro1343
7. Lane TE, Hosking MP. The pathogenesis of murine coronavirus infection of the central nervous system. *Cri Rev Immunol.* (2010) 30:119–30. doi: 10.1615/CritRevImmunol.v30.i2.20
8. Weiss SR, Leibowitz JL. Coronavirus pathogenesis. *Adv Virus Res.* (2011) 81:85–164. doi: 10.1016/B978-0-12-385885-6.00009-2
9. Fleming JO, Trousdale MD, El-Zaatari FA, Stohlman SA, Weiner LP. Pathogenicity of antigenic variants of murine coronavirus JHM selected with monoclonal antibodies. *J Virol.* (1986) 58:869–75.
10. Butchi NB, Hinton DR, Stohlman SA, Kapil P, Fensterl V, Sen GC, et al. Ifit2 deficiency results in uncontrolled neurotropic coronavirus replication and enhanced encephalitis via impaired alpha/beta interferon induction in macrophages. *J Virol.* (2014) 88:1051–64. doi: 10.1128/JVI.02272-13
11. Templeton SP, Perlman S. Pathogenesis of acute and chronic central nervous system infection with variants of mouse hepatitis virus, strain JHM. *Immunol Res.* (2007) 39:160–72. doi: 10.1007/s12026-007-0079-y
12. Savarin C, Stohlman SA, Atkinson R, Ransohoff RM, Bergmann CC. Monocytes regulate T cell migration through the glia limitans during acute viral encephalitis. *J Virol.* (2010) 84:4878–88. doi: 10.1128/JVI.00051-10
13. Wu GF, Dandekar AA, Pewe L, Perlman S. CD4 and CD8 T cells have redundant but not identical roles in virus-induced demyelination. *J Immunol.* (2000) 165:2278–86. doi: 10.4049/jimmunol.165.4.2278
14. Lin MT, Hinton DR, Marten NW, Bergmann CC, Stohlman SA. Antibody prevents virus reactivation within the central nervous system. *J Immunol.* (1999) 162:7358–68.
15. Matthews AE, Weiss SR, Shlomchik MJ, Hannum LG, Gombold JL, Paterson Y. Antibody is required for clearance of infectious murine hepatitis virus A59 from the central nervous system, but not the liver. *J Immunol.* (2001) 167:5254–63. doi: 10.4049/jimmunol.167.9.5254
16. Paul S, Ricour C, Sommereyns C, Sorgeloos F, Michiels T. Type I interferon response in the central nervous system. *Biochimie* (2007) 89:770–8. doi: 10.1016/j.biochi.2007.02.009
17. Savarin C, Bergmann CC, Hinton DR, Ransohoff RM, Stohlman SA. Memory CD4+ T-cell-mediated protection from lethal coronavirus encephalomyelitis. *J Virol.* (2008) 82:12432–40. doi: 10.1128/JVI.01267-08
18. Cervantes-Barragan L, Zust R, Weber F, Spiegel M, Lang KS, Akira S, et al. Control of coronavirus infection through plasmacytoid dendritic-cell-derived type I interferon. *Blood* (2007) 109:1131–7. doi: 10.1182/blood-2006-05-023770
19. Ireland DD, Stohlman SA, Hinton DR, Atkinson R, Bergmann CC. Type I interferons are essential in controlling neurotropic coronavirus infection irrespective of functional CD8 T cells. *J Virol.* (2008) 82:300–10. doi: 10.1128/JVI.01794-07
20. Hwang M, Bergmann CC. Intercellular communication is key for protective ifnalpha/beta signaling during viral central nervous system infection. *Viral Immunol.* (2018) 31. doi: 10.1089/vim.2018.0101
21. Cahoy JD, Emery B, Kaushal A, Foo LC, Zamanian JL, Christopherson KS, et al. A transcriptome database for astrocytes, neurons, and oligodendrocytes: a new resource for understanding brain development and function. *J Neuroscience* (2008) 28:264–78. doi: 10.1523/JNEUROSCI.4178-07.2008
22. Russo MV, Mcgavern DB. Immune Surveillance of the CNS following Infection and Injury. *Trends Immunol.* (2015) 36:637–50. doi: 10.1016/j.it.2015.08.002
23. Zegenhagen L, Kurhade C, Koniszewski N, Overby AK, Kroger A. Brain heterogeneity leads to differential innate immune responses and modulates pathogenesis of viral infections. *Cytokine Growth Fac Rev.* (2016) 30:95–101. doi: 10.1016/j.cytogfr.2016.03.006
24. Kapil P, Butchi NB, Stohlman SA, Bergmann CC. Oligodendroglia are limited in type I interferon induction and responsiveness *in vivo*. *Glia* (2012) 60:1555–66. doi: 10.1002/glia.22375
25. Malone KE, Stohlman SA, Ramakrishna C, Macklin W, Bergmann CC. Induction of class I antigen processing components in oligodendroglia and microglia during viral encephalomyelitis. *Glia* (2008) 56:426–35. doi: 10.1002/glia.20625
26. Hwang M, Bergmann CC. Alpha/Beta Interferon (IFN-alpha/beta) signaling in astrocytes mediates protection against viral encephalomyelitis and regulates IFN-gamma-dependent responses. *J Virol.* 92. doi: 10.1128/JVI.01901-17
27. Hufford MM, Kim TS, Sun J, Braciale TJ. The effector T cell response to influenza infection. *Curr Topics Microbiol Immunol.* (2015) 386:423–55. doi: 10.1007/82_2014_397
28. Griffin DE. The immune response in measles: virus control, clearance and protective immunity. *Viruses* 8:E282. doi: 10.3390/v8100282
29. Zhou Y. Immunobiology and Host Response to HEV. *Adv Exp Med Biol.* (2016) 948:113–41. doi: 10.1007/978-94-024-0942-0_7
30. Wu GF, Perlman S. Macrophage infiltration, but not apoptosis, is correlated with immune-mediated demyelination following murine infection with a neurotropic coronavirus. *J Virol.* (1999) 73:8771–80.
31. Bergmann CC, Parra B, Hinton DR, Ramakrishna C, Dowdell KC, Stohlman SA. Perforin and gamma interferon-mediated control of coronavirus central nervous system infection by CD8 T cells in the absence of CD4 T cells. *J Virol.* (2004) 78:1739–50. doi: 10.1128/JVI.78.4.1739-1750.2004
32. Bender SJ, Weiss SR. Pathogenesis of murine coronavirus in the central nervous system. *J Neuroimmune Pharmacol.* (2010) 5:336–54. doi: 10.1007/s11481-010-9202-2
33. Phares TW, Stohlman SA, Hwang M, Min B, Hinton DR, Bergmann CC. CD4 T cells promote CD8 T cell immunity at the priming and effector site during viral encephalitis. *J Virol.* (2012) 86:2416–27. doi: 10.1128/JVI.06797-11
34. Lin MT, Stohlman SA, Hinton DR. Mouse hepatitis virus is cleared from the central nervous systems of mice lacking perforin-mediated cytolysis. *J Virol.* (1997) 71:383–91.
35. Parra B, Hinton DR, Marten NW, Bergmann CC, Lin MT, Yang CS, et al. IFN-gamma is required for viral clearance from central nervous system oligodendroglia. *J Immunol.* (1999) 162:1641–7.
36. Gonzalez JM, Bergmann CC, Ramakrishna C, Hinton DR, Atkinson R, Hoskin J, et al. Inhibition of interferon-gamma signaling in oligodendroglia delays coronavirus clearance without altering demyelination. *Am J Pathol.* (2006) 168:796–804. doi: 10.2353/ajpath.2006.050496
37. Phares TW, Ramakrishna C, Parra GI, Epstein A, Chen L, Atkinson R, et al. Target-dependent B7-H1 regulation contributes to clearance of central nervous system infection and dampens morbidity. *J Immunol.* (2009) 182:5430–8. doi: 10.4049/jimmunol.0803557
38. Phares TW, Stohlman SA, Hinton DR, Atkinson R, Bergmann CC. Enhanced antiviral T cell function in the absence of B7-H1 is insufficient to prevent persistence but exacerbates axonal bystander damage during viral encephalomyelitis. *J Immunol.* (2010) 185:5607–18. doi: 10.4049/jimmunol.1001984
39. Lane TE, Liu MT, Chen BP, Asensio VC, Samawi RM, Paoletti AD, et al. A central role for CD4(+) T cells and RANTES in virus-induced central nervous system inflammation and demyelination. *J Virol.* (2000) 74:1415–24. doi: 10.1128/JVI.74.3.1415-1424.2000
40. Pewe L, Perlman S. Cutting edge: CD8 T cell-mediated demyelination is IFN-gamma dependent in mice infected with a neurotropic coronavirus. *J Immunol.* (2002) 168:1547–51. doi: 10.4049/jimmunol.168.4.1547
41. Pewe L, Haring J, Perlman S. CD4 T-cell-mediated demyelination is increased in the absence of gamma interferon in mice infected with mouse hepatitis virus. *J Virol.* (2002) 76:7329–33. doi: 10.1128/JVI.76.14.7329-7333.2002
42. Tran EH, Prince EN, Owens T. IFN-gamma shapes immune invasion of the central nervous system via regulation of chemokines. *J Immunol.* (2000) 164:2759–68. doi: 10.4049/jimmunol.164.5.2759
43. Cua DJ, Sherlock J, Chen Y, Murphy CA, Joyce B, Seymour B, et al. Interleukin-23 rather than interleukin-12 is the critical cytokine

for autoimmune inflammation of the brain. *Nature* (2003) 421:744–8. doi: 10.1038/nature01355
44. Savarin C, Stohlman SA, Hinton DR, Ransohoff RM, Cua DJ, Bergmann CC. IFN-gamma protects from lethal IL-17 mediated viral encephalomyelitis independent of neutrophils. *J Neuroinflammation* (2012) 9:104. doi: 10.1186/1742-2094-9-104
45. Sun N, Grzybicki D, Castro RF, Murphy S, Perlman S. Activation of astrocytes in the spinal cord of mice chronically infected with a neurotropic coronavirus. *Virology* (1995) 213:482–93. doi: 10.1006/viro.1995.0021
46. Lane TE, Paoletti AD, Buchmeier MJ. Disassociation between the in vitro and in vivo effects of nitric oxide on a neurotropic murine coronavirus. *J Virol*. (1997) 71:2202–10.
47. Wu GF, Pewe L, Perlman S. Coronavirus-induced demyelination occurs in the absence of inducible nitric oxide synthase. *J Virol*. (2000b) 74:7683–6. doi: 10.1128/JVI.74.16.7683-7686.2000
48. Khan RS, Dine K, Das Sarma J, Shindler KS. SIRT1 activating compounds reduce oxidative stress mediated neuronal loss in viral induced CNS demyelinating disease. *Acta Neuropathol Commun*. (2014) 2:3. doi: 10.1186/2051-5960-2-3
49. Couper KN, Blount DG, Riley EM. IL-10: the master regulator of immunity to infection. *J Immunol.* (2008) 180:5771–7. doi: 10.4049/jimmunol.180.9.5771
50. Lobo-Silva D, Carriche GM, Castro AG, Roque S, Saraiva M. Balancing the immune response in the brain: IL-10 and its regulation. *J Neuroinflammation* (2016) 13:297. doi: 10.1186/s12974-016-0763-8
51. Puntambekar SS, Bergmann CC, Savarin C, Karp CL, Phares TW, Parra GI, et al. Shifting hierarchies of interleukin-10-producing T cell populations in the central nervous system during acute and persistent viral encephalomyelitis. *J Virol.* (2011) 85:6702–13. doi: 10.1128/JVI.00200-11
52. Anghelina D, Zhao J, Trandem K, Perlman S. Role of regulatory T cells in coronavirus-induced acute encephalitis. *Virology* (2009) 385:358–67. doi: 10.1016/j.virol.2008.12.014
53. Trandem K, Zhao J, Fleming E, Perlman S. Highly activated cytotoxic CD8 T cells express protective IL-10 at the peak of coronavirus-induced encephalitis. *J Immunol.* (2011) 186:3642–52. doi: 10.4049/jimmunol.1003292
54. Perlman S, Zhao J. Roles of regulatory T cells and IL-10 in virus-induced demyelination. *J Neuroimmunol.* (2017) 308:6–11. doi: 10.1016/j.jneuroim.2017.01.001
55. Puntambekar SS, Hinton DR, Yin X, Savarin C, Bergmann CC, Trapp BD, et al. Interleukin-10 is a critical regulator of white matter lesion containment following viral induced demyelination. *Glia* (2015) 63:2106–20. doi: 10.1002/glia.22880
56. Trandem K, Jin Q, Weiss KA, James BR, Zhao J, Perlman S. Virally expressed interleukin-10 ameliorates acute encephalomyelitis and chronic demyelination in coronavirus-infected mice. *J Virol.* (2011) 85:6822–31. doi: 10.1128/JVI.00510-11
57. De Aquino MT, Kapil P, Hinton DR, Phares TW, Puntambekar SS, Savarin C, et al. IL-27 limits central nervous system viral clearance by promoting IL-10 and enhances demyelination. *J Immunol.* (2014) 193:285–94. doi: 10.4049/jimmunol.1400058
58. Hall AO, Silver JS, Hunter CA. The immunobiology of IL-27. *Adv Immunol.* (2012) 115:1–44. doi: 10.1016/B978-0-12-394299-9.00001-1
59. Aparicio-Siegmund S, Garbers C. The biology of interleukin-27 reveals unique pro- and anti-inflammatory functions in immunity. *Cytokine Growth Factor Rev* (2015) 26:579–86. doi: 10.1016/j.cytogfr.2015.07.008
60. Trandem K, Anghelina D, Zhao J, Perlman S. Regulatory T cells inhibit T cell proliferation and decrease demyelination in mice chronically infected with a coronavirus. *J Immunol.* (2010) 184:4391–400. doi: 10.4049/jimmunol.0903918
61. Savarin C, Bergmann CC, Hinton DR, Stohlman SA. Differential regulation of self-reactive CD4(+) T cells in cervical lymph nodes and central nervous system during viral encephalomyelitis. *Front Immunol.* (2016) 7:370. doi: 10.3389/fimmu.2016.00370
62. Zhao J, Fett C, Trandem K, Fleming E, Perlman S. IFN-gamma- and IL-10-expressing virus epitope-specific Foxp3$^+$ T reg cells in the central nervous system during encephalomyelitis. *J Exp Med.* (2011) 208:1571–7. doi: 10.1084/jem.20110236
63. Savarin C, Bergmann CC, Gaignage M, Stohlman SA. Self-reactive CD4$^+$ T cells activated during viral-induced demyelination do not prevent clinical recovery. *J Neuroinflammation* (2015) 12:207. doi: 10.1186/s12974-015-0426-1
64. Cervantes-Barragan L, Firner S, Bechmann I, Waisman A, Lahl K, Sparwasser T, et al. Regulatory T cells selectively preserve immune privilege of self-antigens during viral central nervous system infection. *J Immunol.* (2012) 188:3678–85. doi: 10.4049/jimmunol.1102422
65. Uhde AK, Ciurkiewicz M, Herder V, Khan MA, Hensel N, Claus P, et al. Intact interleukin-10 receptor signaling protects from hippocampal damage elicited by experimental neurotropic virus infection of SJL mice. *Sci Rep*. 8:6106. doi: 10.1038/s41598-018-24378-z
66. Kulcsar KA, Baxter VK, Greene IP, Griffin DE. Interleukin 10 modulation of pathogenic Th17 cells during fatal alphavirus encephalomyelitis. *Proc Natl Acad Sci USA*. (2014) 111:16053–8. doi: 10.1073/pnas.1418966111
67. Martin NM, Griffin DE. Interleukin-10 modulation of virus clearance and disease in mice with alphaviral encephalomyelitis. *J Virol*. 92. doi: 10.1128/JVI.01517-17
68. Tun MM, Aoki K, Senba M, Buerano CC, Shirai K, Suzuki R, et al. Protective role of TNF-alpha, IL-10 and IL-2 in mice infected with the Oshima strain of Tick-borne encephalitis virus. *Sci Rep* 4:5344. doi: 10.1038/srep05344
69. Biswas SM, Kar S, Singh R, Chakraborty D, Vipat V, Raut CG, et al. Immunomodulatory cytokines determine the outcome of Japanese encephalitis virus infection in mice. *J Med Virol*. (2010) 82:304–10. doi: 10.1002/jmv.21688
70. Tumpey TM, Elner VM, Chen SH, Oakes JE, Lausch RN. Interleukin-10 treatment can suppress stromal keratitis induced by herpes simplex virus type 1. *J Immunol*. (1994) 153:2258–65.
71. Marques CP, Hu S, Sheng W, Cheeran MC, Cox D, Lokensgard JR. Interleukin-10 attenuates production of HSV-induced inflammatory mediators by human microglia. *Glia* (2004) 47:358–66. doi: 10.1002/glia.20045
72. Li H, Li S, Zheng J, Cai C, Ye B, Yang J, et al. Cerebrospinal fluid Th1/Th2 cytokine profiles in children with enterovirus 71-associated meningoencephalitis. *Microbiol Immunol*. (2015) 59:152–9. doi: 10.1111/1348-0421.12227
73. Singh K, Kulshreshtha D, Singh K, Maurya K, Thacker K. Acute encephalitis syndrome in adults and its correlation with cytokine levels in the serum and cerebrospinal fluid. *Jpn J Infect Dis*. (2017) 70:374–7. doi: 10.7883/yoken.JJID.2016.063
74. Michael BD, Griffiths MJ, Granerod J, Brown D, Keir G, Wnek G, et al. The Interleukin-1 balance during encephalitis is associated with clinical severity, blood-brain barrier permeability, neuroimaging changes, and disease outcome. *J Infect Dis*. (2016) 213:1651–60. doi: 10.1093/infdis/jiv771
75. Chen X, Duan XS, Xu LJ, Zhao JJ, She ZF, Chen WW, et al. Interleukin-10 mediates the neuroprotection of hyperbaric oxygen therapy against traumatic brain injury in mice. *Neuroscience* (2014) 266:235–43. doi: 10.1016/j.neuroscience.2013.11.036
76. Yu Y, Chen Y, Wang FL, Sun J, Li HJ, Liu JM. Cytokines Interleukin 4 (IL-4) and Interleukin 10 (IL-10) gene polymorphisms as potential host susceptibility factors in virus-induced encephalitis. *Med Sci Monit*. (2017) 23:4541–8. doi: 10.12659/MSM.904364
77. Ishige, T., Igarashi, Y., Hatori, R., Tatsuki, M., Sasahara, Y., Takizawa, T., et al. (2018). IL-10RA Mutation as a risk factor of severe influenza-associated encephalopathy: a case report. *Pediatrics* 141:e20173548 doi: 10.1542/peds.2017-3548

Conflict of Interest Statement: The authors declare that the research was conducted in the absence of any commercial or financial relationships that could be construed as a potential conflict of interest.

frontiers in Immunology

ORIGINAL RESEARCH
published: 25 October 2018
doi: 10.3389/fimmu.2018.02479

TRIM21 Restricts Coxsackievirus B3 Replication, Cardiac and Pancreatic Injury via Interacting With MAVS and Positively Regulating IRF3-Mediated Type-I Interferon Production

*Hui Liu†, Min Li†, Yahui Song and Wei Xu**

Jiangsu Provincial Key Laboratory of Infection and Immunity, Institute of Biology and Medical Sciences, Soochow University, Suzhou, China

OPEN ACCESS

Edited by:
Michael H. Lehmann, Ludwig-Maximilians-Universität München, Germany

Reviewed by:
Antje Beling, Charité Universitätsmedizin Berlin, Germany
Haizhen Zhu, Hunan University, China

***Correspondence:**
Wei Xu
xuweifd828@126.com

†These authors have contributed equally to this work

Specialty section:
This article was submitted to Viral Immunology, a section of the journal Frontiers in Immunology

Received: *22 May 2018*
Accepted: *08 October 2018*
Published: *25 October 2018*

Citation:
Liu H, Li M, Song Y and Xu W (2018) TRIM21 Restricts Coxsackievirus B3 Replication, Cardiac and Pancreatic Injury via Interacting With MAVS and Positively Regulating IRF3-Mediated Type-I Interferon Production. Front. Immunol. 9:2479. doi: 10.3389/fimmu.2018.02479

Tripartite motif-containing 21 (TRIM21) is a regulator of tissue inflammation and pro-inflammatory cytokine production, and has been implicated in negative regulation of IRF3-dependent type I interferon signaling. However, the antiviral activity of TRIM21 varies among diverse viruses and its role on regulation of type I interferon remains inconsistent in different microbial infections. Here, we investigate the potential role for TRIM21 in controlling Coxsackievirus B3 (CVB3) replication and susceptible organ pathology. We found that CVB3 infection up-regulated the expression of TRIM21 in hearts of mice and cardiomyocytes at early phase of infection. Knock-down of TRIM21 resulted in increased viral replication, while overexpression led to increased phosphorylation and dimerization of IRF3, increased IFN-β transcription and reduced viral replication *in vitro*. We demonstrate that TRIM21 promotes the activation of IRF3 in CVB3-infected cells via interacting with MAVS and catalyzing the K27-linked polyubiquitination of MAVS, thereby enhancing type I interferon signaling. The RING domain of ubiquitin ligase activity and PRY-SPRY domain of TRIM21 are critical for its anti-viral effect. *In vivo* overexpression of TRIM21 significantly protected mice against viral myocarditis by suppressing CVB3 replication and reducing cardiac inflammatory cytokine production. While TRIM21 deficient mice exhibited a decreased IFN-β production, an increased cardiac and pancreatic CVB3 replication, and aggravated pancreatic injury as well as myocarditis during acute infection. Thus, our results demonstrate TRIM21 as a positive regulator of IFN-β signaling by targeting MAVS during CVB3 infection and suggest it as a potent host defense against CVB3 infection and viral-induced injury in hearts and pancreas.

Keywords: TRIM21, coxsackievirus B3 (CVB3), viral myocarditis, IFN-β, IRF3

INTRODUCTION

Coxsackievirus is a single-Stranded RNA non-enveloped virus of the Enterovirus genus within Picornaviridae associated with several human and mammalian diseases, of which B3 type Coxsackievirus (CVB3) is well-identified as a major causative agent of viral myocarditis (VMC) (1, 2). CVB3 has been involved in 25–27% cases of acute myocarditis and dilated cardiomyopathy in children and young adults (3). VMC has been identified as an important etiology of heart failure and dilated cardiomyopathy, which contribute to nearly 50% of the indication for the heart transplantation (4). CVB3 infection also involves brain and pancreas, resulting in aseptic meningitis and pancreatitis (5, 6). Early direct virus-induced cytopathic effect and intense inflammatory injury followed by host immune responses are the main pathological processes of VMC and pancreatitis. Although excessive activation of immune response triggered by virus infection maybe a major factor contributing to tissue injuries, the virus itself is critical to the progression of VMC via direct attack on cardiomyocytes (7, 8). Despite considerable effort for decades, the fundamental mechanism responsible for the pathogenesis of viral myocarditis has not been well-understood and no effective therapies for VMC are currently available. During acute phase, CVB3 replication leads to myocardial and pancreatic injury directly through inducing apoptosis and necrosis of cardiomyocytes and pancreatic acinar cells. CVB3 RNA can be detected in the chronic stages in infected animals by 21 days post-infection, initiating the disease progression to more severe myocardial fibrosis and DCM (8, 9). In this sense, development of novel anti-viral compounds and early intervention represents an alternative way to treat CVB3 myocarditis and related cardiomyopathy.

The tripartite motif (TRIM) protein family contains over 70 members of TRIM protein family in human and is structurally characterized by a RING domain, one or two B-boxes, and a coiled-coil domain (10). TRIM proteins have been reported to be involved in multiple biological processes including the regulating innate immunity, carcinogenesis, cell differentiation and apoptosis, which are mainly dependent on the RING domain of ubiquitin ligase activity and B-box domain of interacting motif (11, 12). Recently, a growing body of evidence suggests that many TRIM proteins play important roles in direct antiviral activities and in the regulation of antiviral innate immunity. TRIM5α was found to inhibit HIV-1 replication by directly interacting with viral proteins (13). TRIM22 has been reported to exert antiviral activity against several viruses, such as hepatitis B virus (HBV), encephalomyocarditis virus (ECMV), and human immunodeficiency virus (HIV-1) (14–16).

TRIM21, initially known as an autoantigen Ro52/SS-A, is an ubiquitously expressed cytosolic E3 ubiquitin ligase and plays important roles in immune regulation and microbial restriction. TRIM21 has been well known as a regulator for type I interferon (IFN) production, however it may positively or negatively modulate the antiviral innate signaling according to the types of viruses. TRIM21 has been reported to be a positive regulator of IRF3 signaling by preventing its ubiquitination and degradation, thus enhancing IRF3 mediated antiviral responses (17).On the other hand, Higgs et al. claimed that TRIM21 catalyzed IRF3 ubiquitination and promoted its degradation leading to inhibition of interferon-β (IFN-β) production post-pathogen recognition (18). TRIM21 also serves as a negative regulator of IFN-β during Japanese encephalitis virus (JEV) infection in human microglial cells (19).Recently, Xue et al. report that TRIM21 is upregulated upon RNA virus infection and promotes K27-linked polyubiquitination of MAVS to upregulate type-I interferon signaling, thereby inhibiting viral infection (20). Thus, the antiviral activity of TRIM21 varies among different viral infection. Up to the present, there is no report of TRMI21 on CVB3 infection; and almost no biological function of TRIM21 has been confirmed in animal models of viral infection. It is of great interest to explore the possible antiviral function of TRIM21 on CVB3 infection and its role in the disease progression of CVB3-induced VMC and pancreatitis.

Here, we investigate the antiviral activity of TRIM21 against CVB3 replication and its role in CVB3-induced acute vial myocarditis and pancreatic injury. Our results indicate that TRIM21 inhibits CVB3 replication via interacting with MAVS for promoting the K27 polyubiquitination of MAVS, thereby enhancing IRF3-mediated type I IFN signaling pathway and protecting mice against CVB3-induced myocarditis as well as pancreatic acinar cell necrosis.

MATERIALS AND METHODS

Mice and Virus

Six–eight weeks old male BALB/c mice were purchased from the Shanghai Slac Animal Inc. TRIM21$^{-/-}$ mice were constructed from Cyagen Biotech (Guangzhou, China).CVB3 (Nancy strain) was a kind gift from Professor Yingzhen Yang (Key Laboratory of Viral Heart Diseases, Zhongshan Hospital, Shanghai Medical College of Fudan University).

Cell Culture

HeLa cells and HEK-293 cells were grown and maintained in DMEM medium supplemented with 10% FBS (Gibco) and 100 units/ml penicillin and streptomycin in a 5% CO_2 incubator at 37°C.

Virus Titers Assays

The viral titer was determined by $TCID_{50}$ assay on HeLa cell monolayers with standard methodology (AdEasy Application Manual, version 1.4; Qbiogene, Carlsbad, CA, United States).Cell culture and tissue lysis supernatants were diluted serially using 10-fold dilutions and titered on HeLa cell monolayers by the $TCID_{50}$ assay.

Plasmids and Transfection

The Flag-MAVs or HA-K27Ub plasmids were the gifts from Prof. Hui Zheng (Institute of biological and medical sciences, Soochow University). Human TRIM21 cDNA was amplified from RNA of HeLa cells using primers: For: 5′-GCCA CCATGGATTACAAGGATGACGACCGATAAGGCTTCAGC

ACGC-3′ and Rev: 5′-AAAGCCATCAATAGTCAG-3′. Mouse TRIM21 cDNA was amplified from RNA of cardiomyocytes using primers:5′-ATGGATTACAAGGATGACGATAAGCAC CCTCTACAACCTCAAAA-3′ and 5′-CCTGGCTCCTGACCA TCACA-3′. cDNA of truncated forms of TRIM21 lacking N-terminal RING,B-box C-terminal and PRY-SPRY domain were amplified using primers: ΔRING-For: 5′-CCGGCAGCGCTT TATGCTGCTC-3′ and ΔRING-Rev: 5′-AAAGCCATCAAT AGTCAG-3′; ΔB-box-For: 5′-ATGCGGTGTGCAGTGCAT GGA-3′ and ΔB-box-Rev: 5′-AAAGCCATCAATAGTCAG-3′; ΔPRY/SPRY-For: 5′-GCCACCATGGCTTCAGCAGCACGC-3′ and ΔPRY/SPRY-Rev: 5′-TCACACATGGCACACACTC-3′. For the transfection experiment, HeLa cells were seeded into 24-well plates and transient transfection was performed by Lipofectamine 2000 according to the manufacturer's instruction. Cells were cultured for 24 h before infection of CVB3.

Quantitative Real-Time PCR (Q-PCR)

Total RNA was isolated from cells or tissues using RNAiso reagent (Takara, Cat. No. 9109), and cDNA was prepared using reverse transcriptase (Takara, Cat. No. DRR063A). Quantitative real-time RT-PCR (Q-PCR) was performed using SYBR green real-time PCR kits (TaKaRa, Cat. No. DRR041A)on a Bio-Rad iCycler using the following primers:

	For (5′-3′)	Rev (5′-3′)
human-TRIM21	TGGTGTGTGCCC AGTCT	CATCGTGAGATCCAT TTCCA
mouse-TRIM21	AGGGTTAGAGGGGC TGTGTT	GACCATGGCTCCCTC ATCTA
human-IFN-α	GCCTCGCCCTTTG CTTTACT	CTGTGGGTCTCAGGG AGATCA
human-IFN-β	ATGACCAACAAGTGT CTCCTCC	GCTCATGGAAAGAGC TGTAGTG
mouse- IFN-β	CCCTATGGAGATG ACGGAGA	CTGTCTGCTGGTGGA GTTCA
ISG15	TCCTGGTGAGGAATAAC AAGG	GTCGTCGTCAGCCA GAACAG
ISG54	ATGTGCAACCTACTG GCCTAT	TGAGAGTCGGCCCAT GTGATA
human-GAPDH	CATGAGAAGTATGACA ACAGCCT	AGTCCTTCCACGATAC CAAAGT
mouse-GAPDH	TGGATTTGGACGCAT TGGTC	TTTGCACTGGTACGT GTTGAT

The $2^{-\Delta\Delta CT}$ method was used to normalize the transcription of the detected gene mRNA to that of the GAPDH mRNA and calculate the fold induction relative to the control.

Short Interference RNA (siRNA)

Human siRNA oligonucleotides targeting sequences named as TRIM21 siRNA1 (UCAUUGUCAAGCGUGCUGC) and TRIM21 siRNA2 (UGGCAUGGAGGCACCUGAAGGUGG) were ordered from GenePharma.Inc (Shanghai, China). The siRNA was transfected into HeLa cells using INTERFERin *in vitro* siRNA transfection reagent (Polyplus, NewYork, United States).

Western Blotting

HEK293 cells were transfected with plasmids containing human or murine TRIM21 (1 μg) using the Lipofectamine Plus reagent (Invitrogen) for 24 h, and then infected by CVB3 (MOI = 5) for 18 h. Samples were resuspended in sample lysis buffer (Bio-Rad). Lysates were resolved by SDS-polyacrylamide gel electrophoresis and transferred to PVDF membranes. The blots were probed primary antibodies for Flag (1:1,000, CST 8146S), IRF3 (1:1,000, CST, D8389), pIRF3 (1:1,000, CST, S396), actin (1:2,000, ABGEN, SG140609AB), GAPDH (1:10,000, Sigma, G9545), and VP-1 (1:2,000, Dako, M706401). HRP-conjugated anti-rabbit (1:4,000, CST, 7074) or anti-mouse IgG (Bioworld, AB54151) was used as a secondary antibody. Proteins were detected by chemiluminescence (Pierce). The intensities of the bands in the blots were quantified by densitometry using the Image Studio Lite program according to the developer's instructions.

IP and Immunoblotting

HEK293 cells were transfected with an expression plasmid encoding full-length of Flag-tagged MAVS. Cell lysates were collected using radioimmunoprecipitation assay (RIPA) lysis buffer with protease inhibitors (1 mM phenylmethylsulfonyl fluoride, Roche complete protease inhibitor), followed by immunoprecipitation with anti-Flag beads. Proteins were eluted from the beads after washing six times with PBS. The protein binding to the beads was subjected to Western blot with anti-TRIM21 (1:2,000 Santa Cruz Biotechnology, SC25351) or anti-Flag (1:1,000, CST 8146S).

Ubiquitination Assays and Native Page

For analysis of ubiquitination of MAVS in HeLa cells, cells were co-transfected with TRIM21, HA-K27ub or Flag-MAVS, followed by infection with CVB3. Cell lysates were immunoprecipitated with anti-Flag and analyzed by immunoblotting with the anti-HA antibody. Native page for the detection of IRF3 dimerization was performed on acrylamide gel without SDS. Cells were lysed with ice-cold lysis buffer including 50 mM of Tris-Hcl at PH = 7.5, 150 mM of NaCl and 0.5% NP-40 containing protease inhibitor cocktail. After centrifugation at 13,000 g for 15 min, proteins in the supernatant were quantified and diluted with 5x native PAGE sample buffer (312.5 mM Tris-HCl, pH = 6.8; 75% glycerol; 0.25% bromophenol blue). The gel was pre-run for 30 min at 40 mA on ice with 25 mM Tris-HCL (pH = 8.4), and 192 mM glycine with or without 1% of deoxycholate in the cathode chamber and anode chamber, respectively. The unboiled total protein was added into the gel for 80 min at 25 mA on ice.

Luciferase Reporter Assay

HEK293 cells were co-transfected with 100 ng luciferase reporter plasmid, 10 ng thymidine kinase promoter-Renilla luciferase reporter plasmid, and the TRIM21-expression or control vector plasmid using the Lipofectamine 2000 transfection reagent (Invitrogen,Cat.No.116688-019). 48 hrs later, cell lysates were prepared and the luciferase activities were determined by the Dual-Luciferase Reporter Assay System

(Promega,Cat.No.E10910) according to the manufacturer's instructions.

CVB3 Infection

Mice were infected intraperitoneally (i.p.) with 100 μl PBS containing 1000 $TCID_{50}$ dose of CVB3. Body weight and mortality of mice were recorded upon the termination of experiment. Individual experiments were conducted at least three times with 7 to 10 mice per group.

Histopathological Analysis

Three hearts and pancreas of each group of mice were collected 7 days post infection. The apical parts of the tissues were fixed in 10% phosphate-buffered formalin, embedded in paraffin wax, sectioned at 5 μm and stained with hematoxylin–eosin (H&E). Stained sections were used for image analysis with a Nikon Eclipse TE2000-S microscope and five images were captured under high power fields randomly.

Immunohistochemistry

Hearts were fixed with 10% formalin in 0.1 M phosphate buffer, pH 7.4. Sections were deparaffinized and irradiated at 750 W in a microwave oven in 10 mM sodium citrate buffer, pH 6.0. Sections were then treated with 3% hydrogen peroxide to inhibit endogenous peroxidases. After washing in TBS with 0.025% Triton X-100, the sections were blocked with 10% BSA. Following blocking, sections were incubated with goat polyclonal antibody against TRIM21 (sc-21362; 1:500; Santa Cruz Biotechnology) diluted in TBS-1% BSA overnight at 4°C. After washing, sections were incubated with a biotinylated anti-goat secondary antibody (Jackson immunoresearch) for 1 h and a peroxidase-labeled streptavidin for 5 min at room temperature. Peroxidase activity was detected with DAB (Mouse and Rabbit Specific HRP/DAB Detection IHC Kit, ab64264, Abcam), and sections were counter stained with hematoxylin. The level of protein accumulation was estimated as the percentage of the total counterstained area that was positively stained for the protein of interest, which was determined using Image Jsoftware (Nikon Eclipse TE2000-S microscope).

Primary Cardiomyocyte Culture

Neonatal cardiomyocytes were isolated from 1 to 3 days BALB/c mice. The ventricles obtained from 1 to 3 days BALB/c mice were removed rapidly into cold Hanks' balanced salt solution (Gibco). After washing and mincing, tissues were digested in 0.05% trypsin (Gibco) for 30 min at 4°C with rotation before transfer into DMEM (Gibco) containing 20% FBS (Fetalbovine serum, Gibco) to terminate the digestion. After washing with HBSS, the tissues were incubated with Liberase TH (0.1 U/mL, Roche, Germany) at 37°C for 5 min, and the dissociated cells were collected into 20% FBS DMEM. This procedure was repeated until most of the cells were released. The isolated cells were incubated with 5% CO_2 at 37°C for 2 h. The unattached cardiomyocytes were seeded into fibronectin-coated 8-well Live Cell Imaging Culture Dish (Bestmagsystem Medical Co. Ltd., Suzhou, China) and experiments were performed when the cardiomyocytes formed a confluent monolayer and beat in synchrony at 72 h.

Immunofluorescence

Immunofluorescence was performed to assess the cellular expression and location of TRIM21 and viral RNA expression according to the manufacturer's instructions. Freshly cultured cardiomyocytes were infected with CVB3 (MOI = 5) for 0, 12, and 24 hrs. Heart tissues of infected mice were embedded in OCT and made into 5 μm cryo section. Cells were fixed with 4% paraformaldehyde for 1 h before blocking (2% BSA) for 1 h. Cells were then incubated with primary antibodies against TRIM21 (1:200, Santa Cruz Biotechnology) and anti-dsRNA (1:300, J2 mAb, English and Scientific Consulting) at 4°C overnight. Fluorochrome-conjugated secondary antibodies (1:200, goat anti-rabbit IgG, goat anti-mouse IgG, Southern Biotech) and DAPI were used for immunofluorescent staining. Images were captured and analyzed with Nikon A1 confocal microscope.

Enzyme-Linked Immunosorbent Assay (ELISA)

Levels of TNF-α, IL-6, IL-10, IFN-γ, MCP-1 were determined using sensitive mouse, IL-6, IL-10, and IFN-γ kits according to the manufacturers' instructions (eBioscience, San Diego, USA).

In vivo Overexpression of TRIM21

Mice were retro-orbitally injected with 1.0 ml reagent containing 50 μg of mouse TRIM21-expression plasmid or vector plasmid using *in vivo*-JetPEITM–Gal transfection agent according to the manufacturer's instructions (Polyplus-transfection Inc., USA). Mice received 2 doses of TRIM21 plasmids 2 days before and 1 day after CVB3 infection to sustain *in vivo* over-expression of TRIM21.

Statistical Analysis

Data were presented as the mean ± SEM and statistical analysis was analyzed by GraphPadPrism 5 software. For two-group comparisons, statistical significance was determined by Student's *t*-test. Survival curves were estimated from Kaplan-Meier procedure with the Lonrank test to compare survival among groups. $P < 0.05$ was considered to be statistically significant and are indicated as follows: *, $0.05 \geq P > 0.01$; **, $0.01 \geq P > 0.001$; ***, $P \leq 0.01$.

RESULTS

TRIM21 Is Up-Regulated in Hearts of Mice and in the Murine Cardiomyocytes Upon CVB3 Infection

To explore the role of TRIM21 in CVB3 infection, first we investigate whether TRIM21 is induced in heart tissues of mice by CVB3 infection. After 1000 $TCID_{50}$ CVB3 i.p.

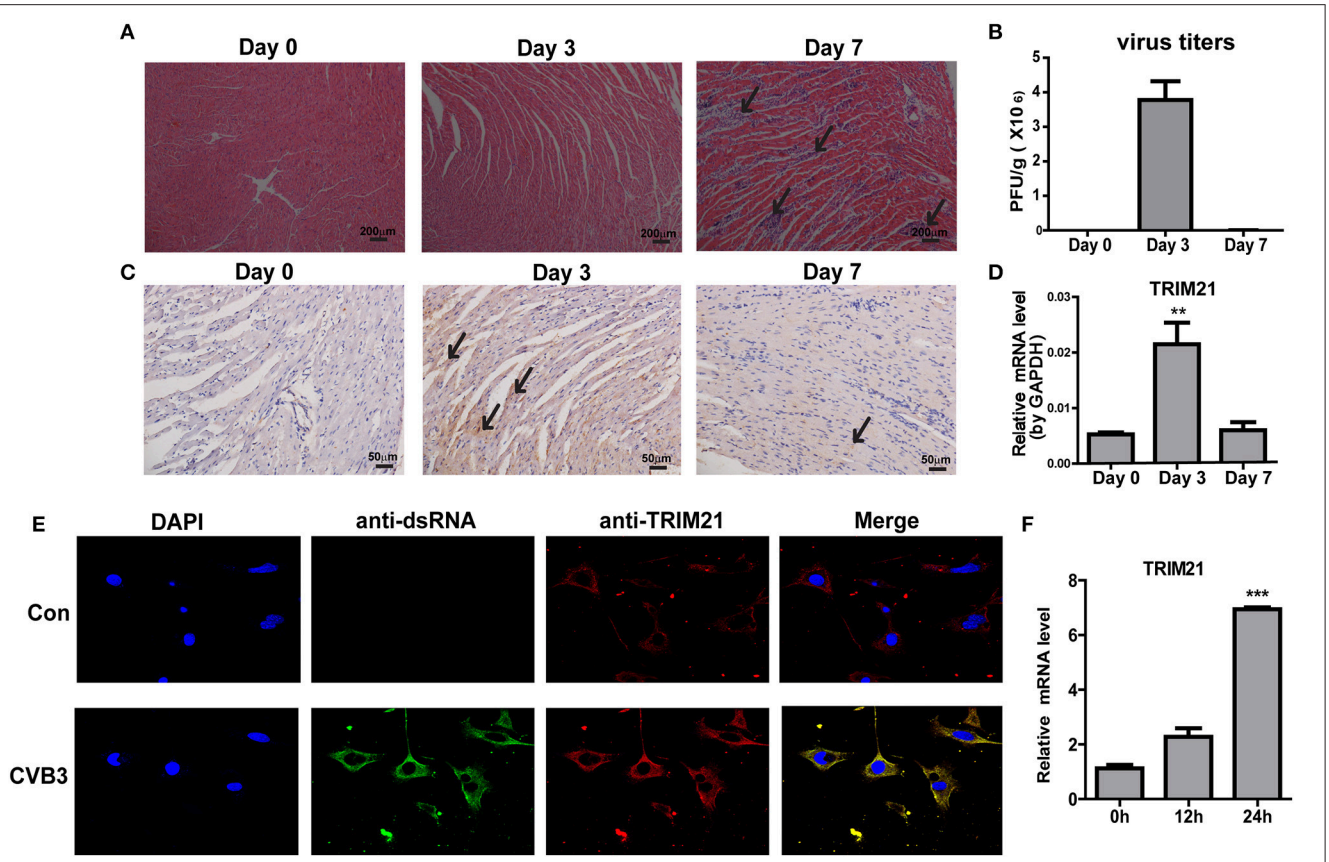

FIGURE 1 | TRIM21 is up-regulated in heart tissues of CVB3-induced VMC mice. Male BALB/c mice were intraperitoneally injected with 1000 $TCID_{50}$ dose of CVB3 and the tissues were collected at the indicated time. **(A)** Paraffin sections of heart tissues were prepared and subjected to H&E staining (200 × magnifications). **(B)** The viral titers were analyzed by $TCID_{50}$ assay. Data were presented as mean ± SEM of three representative independent experiments. **(C)** TRIM21 protein level in heart tissues was evaluated by IHC assay. Five photomicrographs were captured at each time under high power fields (400× magnifications) randomly and one representative image was shown. **(D)** TRIM21 mRNA level was analyzed by Q-PCR. Data were presented as mean ± SEM of three representative independent experiments. The GAPDH expression levels of heart tissues was set 1.0. **(E,F)** Primary cardiomyocytes of mice were mock infected or infected by CVB3 (MOI = 5) for 24 h. CVB3 dsRNA, endogenous TRIM21 protein and nucleus were stained with anti-dsRNA antibody (green), anti-TRIM21Ab (red) and DAPI dye (blue) and observed under confocal microscope. Photomicrographs were captured under high power fields (100 × magnifications) **(E)**.TRIM21 mRNA level were analyzed by Q-PCR. Data were presented as mean ± SEM of three representative independent experiments. The GAPDH expression level of heart tissues was set as 1.0 **(F)**. $^{**}p < 0.01$; $^{***}p < 0.001$.

infection, a massive inflammatory infiltration and cardiomyocye necrosis were observed in hearts at day 7 p.i. (**Figure 1A**). The viral load in myocardium increased and peaked at day 3 p.i., then declined at day 7 p.i. (**Figure 1B**). Then we detected the expression kinetics of TRIM21 by Q-PCR and immunohistochemistry. The protein and mRNA levels of TRIM21 in hearts of mice were significantly increased and peaked at day 3 p.i. (**Figures 1C,D**). To confirm the expression and localization of TRIM21 in cardiomyocytes, we cultured primary cardiomyocytes from newborn mice and infected cells with CVB3. The immunofluorescence assay showed that TRIM21 was localized in cytoplasm and CVB3 infection enhanced its expression at protein and RNA levels (**Figures 1E,F**).Therefore, our result demonstrate that cardiac TRIM21 expression is up-regulated by CVB3 infection, which may be involved in the regulation of CVB3 infection and the progression of viral myocarditis.

TRIM21 Suppresses CVB3 Replication *in vitro*

To investigate the role of TRIM21 on CVB3 replication, HeLa cells were transiently transfected with a plasmid expressing TRIM21 or vector alone and then infected with CVB3 at MOI of 5. The efficiency of overexpression of TRIM21 was confirmed by real-time PCR and Western blot (**Figure 2A**). The supernatant was subjected to $TCID_{50}$ assay to determine the role of TRIM21 on viral progeny release. As shown in **Figure 2B**, TRIM21 overexpression significantly reduced the virus particle release. Furthermore, the protein level of CVB3 capsid VP1 was significantly inhibited by TRIM21 overexpression (**Figure 2C**).

To further verify the antiviral effect of TRIM21, we designed and screened two specific siRNA targeting the open reading frame of TRIM21, which led to a 75–80% reductions in the overall levels of the TRIM21 mRNA and

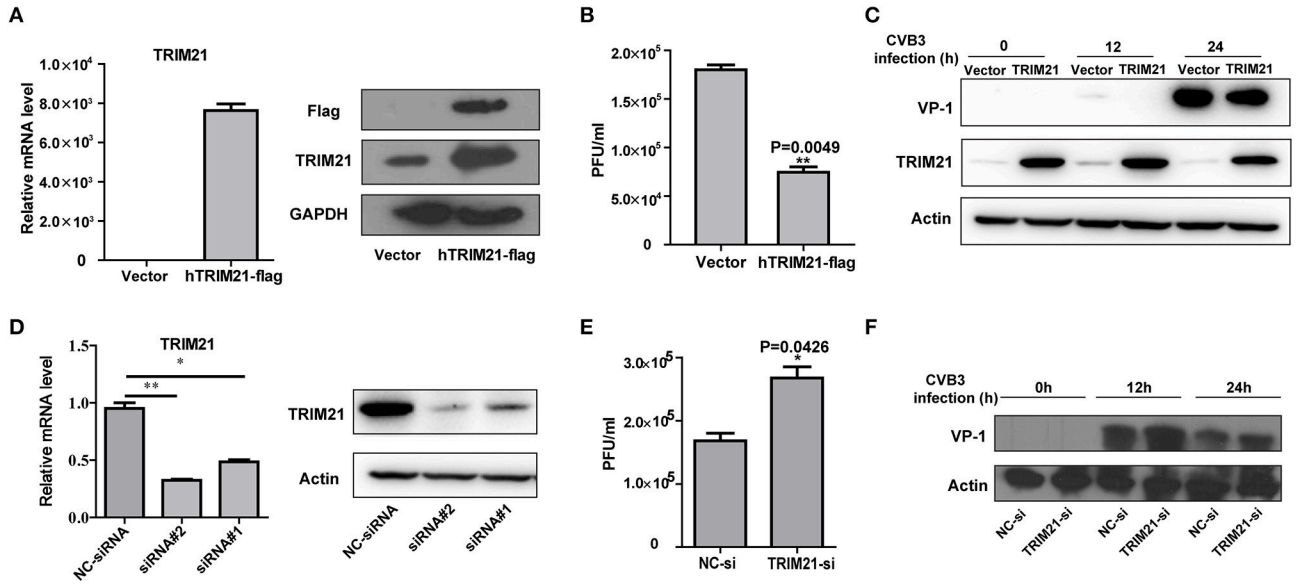

FIGURE 2 | TRIM21 inhibits CVB3 infection *in vitro*. **(A)** HeLa cells were transiently transfected with human TRIM21-flag, or mock plasmids and 24 h later cells were subjected to Q-PCR and Western blot for detecting TRIM21 mRNA and protein levels. **(B–D)** HeLa cells were transiently transfected with human TRIM21-flag, or mock plasmids and 24 h later cells were infected with CVB3 at an MOI of 5 for the indicated time. Supernatants were collected and subjected to $TCID_{50}$ **(B)**.Caspid protein of virus was analyzed by Western blot **(C)**. **(D)** HeLa cells were transfected with negative-control siRNA or TRIM21 siRNAs. 24 h later, cells were collected and subjected to Q-PCR and Western blot for analysis of TRIM21 expression.**(E,F)** HeLa cells were transfected with negative-control siRNA or TRIM21 siRNA and 24 h later, cells were infected with CVB3 (MOI = 5) for the indicated times. Supernatants were collected and subjected to $TCID_{50}$ **(E)**. VP1caspid protein of virus were analyzed by Western blot **(F)**. $^{*}p < 0.05$; $^{**}p < 0.01$.

protein (**Figure 2D**). Knockdown of TRIM21 increased CVB3 progeny production (**Figure 2E**) and viral capsid protein VP1 expression (**Figure 2F**) significantly, compared to the effect of NC siRNA. Collectively, these results confirm that TRIM21 significantly restricts CVB3 replication *in vitro*.

TRIM21 Increases IFN-α/β Activation Pathway

Type I interferons (IFNs) play an important part in the resistance to viral infection. TRIM21 is reported to be involved in modulating host innate type I signaling against viral replication. Thus, we first examined the IFN-β mRNA production in HeLa cells overexpressing TRIM21 upon CVB3 infection by real-time PCR. Cells transfected with an empty vector were used as a control. In comparison to vector-transfect cells, a moderate promotion in IFN-β mRNA levels was observed in the TRIM21-overexpressed cells infected with CVB3. Additionally, IFN-α mRNA level was increased significantly by TRIM21 overexpression (**Figure 3A**). To confirm IFN-α/β promoting role of TRIM21, HeLa cells were co-transfected with TRIM21 vector and IFN-β promoter-luciferase plasmid. As demonstrated in **Figure 3B**, overexpression of TRIM21 enhanced the activity of IFN-β promoter in a dose-dependent manner after CVB3 infection. Furthermore, co-transfection of TRIM21 increased MAVS-activated and MAD5-activated IFN-β reporter gene expression. Next, we detected IFN-stimulated genes (ISGs) expression and found TRIM21 also up-regulated the expression of ISG15 and ISG54 upon CVB3 infection (**Figure 3C**). Thus, our data suggest that TRIM21 up-regulates the activation of IFN-β signaling pathway.

TRIM21 Positively Regulates IRF3 Activation via K27-Linked Polyubiquitination of MAVS Upon CVB3 Infection

Since TRIM21 promotes IFN-β activation after CVB3 infection, we suggest that TRIM21 might positively modulate the upstream molecules of type I interferon signaling pathway. RIG-I and MDA-5 recognition of CVB3 RNA leads to the activation of IRF3 and transcription factors required for transcription activation of IFN-α/β. We next explored the effect of TRIM21 on IRF3 activation upon CVB3 infection. As shown in **Figure 3D**, overexpression of TRIM21 significantly enhanced the reporter activity of IRF3 at basal level and after CVB3 infection. Then, native page assay was performed and demonstrated that TRIM21 overexpression promoted the dimerization and phosphorylation of IRF3 (**Figures 3E,F**). Recently, Xue et al. reported that TRIM21 catalyzed the K27-linked polyubiquitination of MAVS to upregulate type-I interferons signaling upon RNA virus infection. So we examined the interaction between TRIM21 and MAVS. The CO-IP experiments revealed that TRIM21 interacted with MAVS while CVB3 infection reduced MAVS expression (**Figure 3G**). Degradation of MAVS by CVB3 pro2A

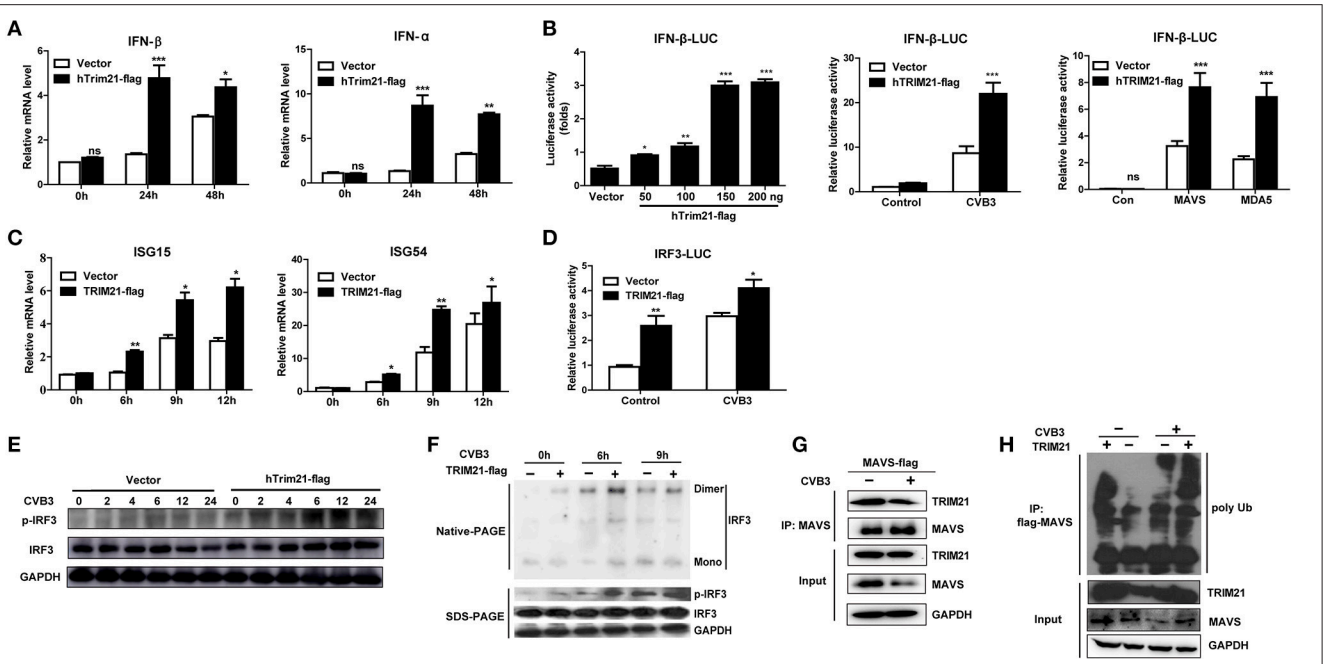

FIGURE 3 | Overexpression of TRIM21 activates the virus-induced type I IFN signaling via catalyzing the K27-linked polyubiquitination of MAVS and increases IRF3 phosphorylation. **(A)** HeLa cells were transfected with TRIM21 expression or vector plasmids. 24 h after transfection, cells were infected with CVB3 (MOI = 5) for the indicated time. The mRNA levels of endogenous IFN-β and IFN-α were detected by Q-PCR assay. Data were presented as mean ± SEM of three representative independent experiments. **(B)** HEK293 cells were co-transfected with the IFN-β promoter reporter plasmids and the indicated amounts of TRIM21 expression plasmid or 100 ng vector plasmid. 24 h later, the luciferase activity was determined. HEK293 cells were co-transfected with the IFN-β promoter reporter plasmids and TRIM21 expression plasmid or mock vector. 24 h later, cells were infected with CVB3 (MOI = 5) for 12 h and the luciferase activity was determined. HEK293 cells were co-transfected with the IFN-β promoter reporter plasmids and TRIM21 expression plasmid or mock vector, together with MAVS or MDA5 expression plasmids. 24 h later, cells were infected with CVB3 (MOI = 5) for 12 h and the luciferase activity was determined. Data were presented as mean ± SEM of three representative independent experiments. **(C)** HeLa cells were transfected with TRIM21 expression or vector plasmids for 24 h before infection with CVB3 (MOI = 5). The mRNA levels of endogenous ISG15 and ISG54 were detected by Q-PCR assay. **(D)** HEK293 cells were co-transfected with the IRF3 promoter reporter plasmids and TRIM21 expression plasmid or mock vector. 24 h later, cells were infected with CVB3 (MOI = 5) for 12 h and the luciferase activity was determined and data were presented as mean ± SEM of three representative independent experiments. **(E,F)** HeLa cells were transfected with TRIM21 expression or vector plasmids for 24 h before infection with CVB3 (MOI = 5). Cell lysates were subjected to probe withanti-IRF3, anti-pIRF3 and anti-GAPDH antibodies by Western blotting and Native page for the detection of IRF3 dimerization. **(G)** HeLa cells were transfected with Flag-MAVS plasmids as indicated, 24 h later cells were infected with CVB3 (MOI = 5). Cellular lysates were immunoprecipitated with anti-Flag. Immunoprecipitates were analyzed by WB with anti-Flag and anti-TRIM21. **(H)** HeLa cells were co-transfected with TRIM21, Flag-MAVS, and HA-K27Ub for 24 h and treated with CVB3 for additional 12 h. Ubiquitination and immunoblotting assays were performed with indicated antibodies. $^{*}p < 0.05$; $^{**}p < 0.01$; $^{***}p < 0.001$.

(21) may counteract the effect of CVB3 on TRIM21 up-regulation and TRIM21-MAVS interaction *in vitro*. Furthermore, we observed that TRIM21 catalyzed the formation of K27-linked polyubiquitin chains on MAVS (**Figure 3H**, lane 1–2). Importantly, CVB3 infection enhanced the formation of the K27-linked polyubiquitinon MAVS by TRIM21 (**Figure 3H**, lane 3–4).Our data suggest that TRIM21 positively regulates type I IFN pathway during CVB3 infection via interacting with and promoting the ubiquitination of MAVS, thereby enhancing IRF3 activation.

The Ring and PRY-SPRY Domains Are Required to Facilitate the TRIM21-Mediated Anti-viral Activity

TRIM21 contains three classical motifs including a RING finger domain, a B-box domain and a B30.2 domain. We constructed various domain mutants of TRIM21 to define which part was involved in its antiviral role (**Figure 4A**). As compared with the full-length TRIM21, B-Box mutant showed similar anti-CVB3 effects, while RING and PRY-SPRY domain mutants abolished the antiviral effects as measured by western blot of viral VP-1 protein (**Figure 4B**). Furthermore, dysfunction of RING domain and PRY-SPRY domain obstructed the activating role of TRIM21 on the promoter of IFN-β and IRF3, while B-box mutant and B30.2 mutant had no effect (**Figure 4C**). Collectively, the RING domain with E3 ubiquitin ligase and the PRY-SPRY domain were required for the TRIM21-mediated type I IFN activation and anti-viral effect.

In vivo Overexpression of TRIM21 Protects Mice Against CVB3-Induced Myocarditis

We next evaluate the antiviral effect of TRIM21 *in vivo* according to an *in vivo*-JetPEI^{TM} strategy (22) and one retroorbital injection of 50 μg TRIM21- plasmids led to an enhanced protein

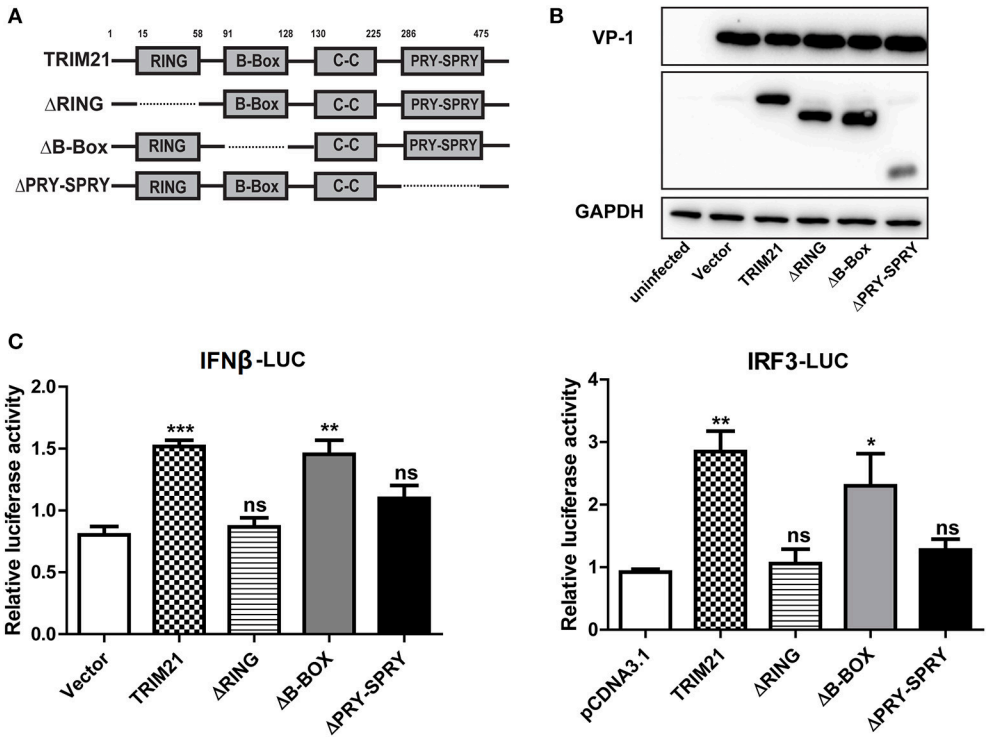

FIGURE 4 | The RING domain and PRY-SPRY domain are essential for its antiviral effect against CVB3. **(A)** Schematic of domain organization and deletion mutants of TRIM21. Approximate amino acid positions of domains are shown at the top. Various domains are boxed and discontinuous lines represent deletion of those regions. **(B)** HeLa cells were transiently transfected with TRIM21 expression plasmid, or indicated domain deletion mutants and 24 h later cells were infected with CVB3 (MOI = 5) for 24 h. The expression efficiency of domain deletion mutants and VP-1 production were analyzed by Western blot. **(C)** HEK293 cells were transfected with the IFN-β or IRF3 promoter reporter plasmids, together with TRIM21 expression plasmid or the indicated domain deletion mutants. The luciferase activity was determined after 24 h and data were presented as mean ± SEM of three representative independent experiments. $^{*}p < 0.05$; $^{**}p < 0.01$; $^{***}p < 0.001$.

expression of cardiac TRIM21 which sustained for 2–3 days confirmed by IHC analysis (**Figure 5A**). Therefore, groups of mice were retro-orbitally injected with 50 μg TRIM21-plasmids or vector-plasmids using *in vivo*-Jet PEI reagent 2 days before and 1 day after CVB3 infection (**Figure 5B**), and susceptibility to CVB3 myocarditis as well as viral replication were evaluated in a course of 7 days infection. The survival rate and bodyweight loss of mice were monitored by day 7 p.i. and a significantly improved disease condition and reduced mortality were observed in mice with *in vivo* TRIM21 overexpression. More than 60% mice injected with mock plasmids died by day 7 and lost their 28% bodyweight; while TRIM21-overexpressed mice underwent a gentle decline loss of bodyweight (∼17%) and ∼70% mice survived by day 7 p.i. (**Figures 5C,D**). Consistently, histological analysis revealed that mice with mock plasmids developed severe myocarditis with diffuse inflammation and necrotic lesions, whereas TRIM21 treatment attenuated myocarditis with restricted inflammation and necrosis (**Figure 5E**). By analyzing the levels of cardiac inflammatory cytokines we found that inflammatory cytokines, such as IL-1β, TNF-α, IL-6, IL-10, and MCP-1, were significantly reduced by TRIM21 overexpression while IFN-γ level was not affected (**Figure 5F**).

To test whether differences in CVB3 disease susceptibility were due to differences in viral titers, CVB3 burden in the hearts of mice were measured. As shown in **Figure 5G**, CVB3 titer was significantly reduced in hearts of mice with TRIM21 over-expression at day 3 p.i. Immunofluorescent staining of the heart sections also confirmed dramatically reduced viral RNA level in hearts (**Figure 5I**). In accordance with that, a significantly up-regulated mRNA expression of IFN-β in heart was confirmed in TRIM21 overexpressed mice at day 3 p.i.(**Figure 5H**).

TRIM21 Deficient Mice Exhibits Increased Cardiac and Pancreatic Viral Burden and Aggravated Myocarditis as Well as Pancreatic Necrosis

To further confirm the antiviral effect of TRIM21 *in vivo*, we constructed deficient mice by CRISPR-CAS9 strategy (**Figure 6A**) and confirmed the deletion of mRNA and protein level of TRIM21 in tissues of mice (**Figures 6B,C**). Next, WT and TRIM21-deficient mice were infected i.p. with CVB3. Throughout the 7 days infection, TRIM21-deficient mice exhibited greater signs of sickness at day3 p.i. and lost weight more promptly by day 7 p.i. (14.8 vs. 5.1%, TRIM21-deficient vs. WT, $p < 0.05$, **Figure 6D**). Histopathology analysis revealed that TRIM21-deficient mice exhibited a significantly aggravated coagulative necrosis and acinar cell necrosis in the pancreas

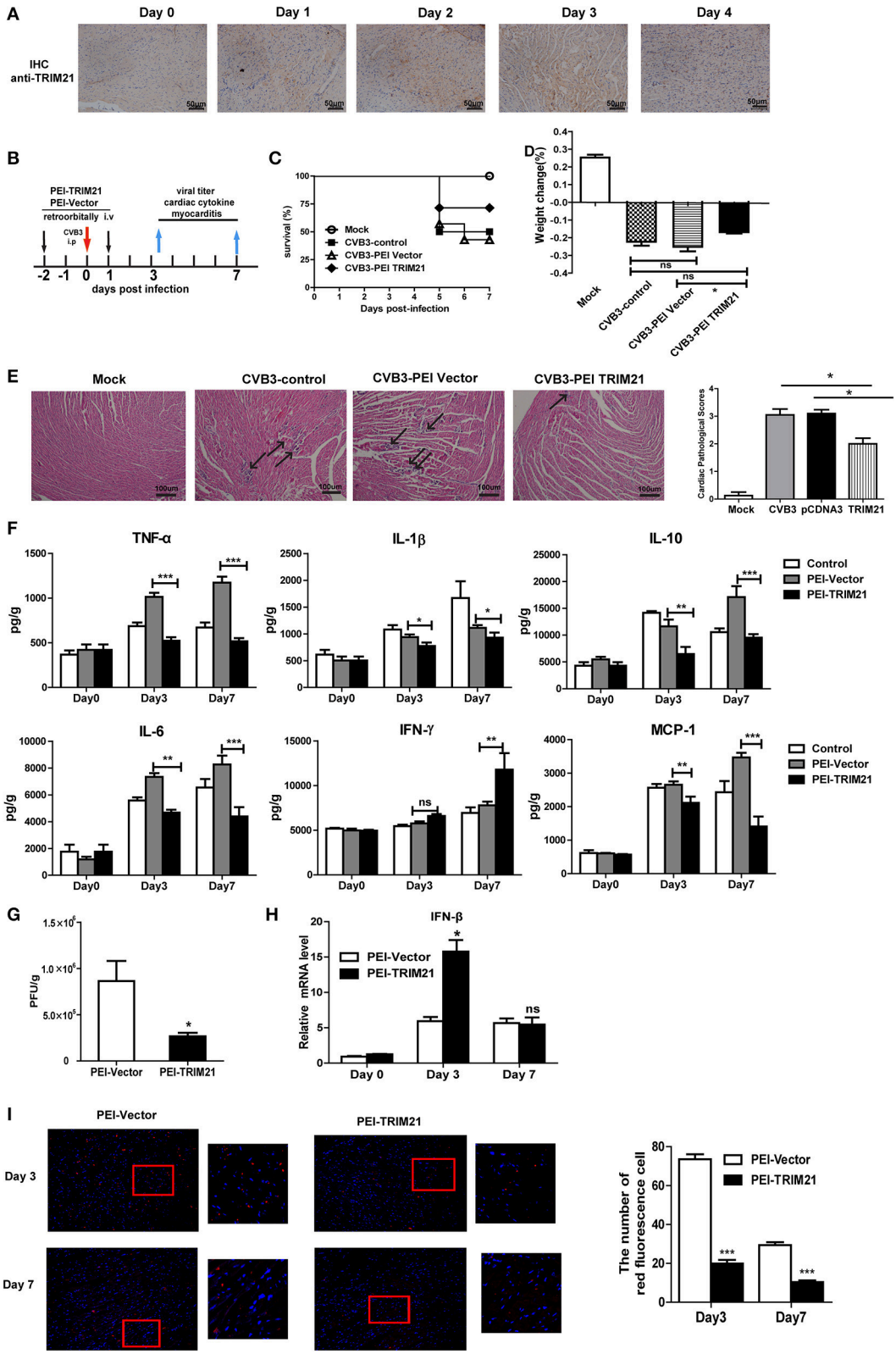

FIGURE 5 | Overexpression of TRIM21 *in vivo* significantly reduces viral load and alleviates CVB3-induced viral myocarditis. **(A)** Male BALB/c mice were retroorbitally injected 50 μg TRIM21 plasmids using *in vivo*-jet PEI and were sacrificed daily till day 4. Protein level of cardiac TRIM21was measured by IHC assay. **(B)** Mice were

(Continued)

FIGURE 5 | injected retroordibitally with 2 doses of 50 μg PEI-packaged mock or TRIM21 plasmids on day −2 and 1 and subjected to 1000$TCID_{50}$ CVB3 on day 0($n = 6$). The survival rate **(C)** and body weight change **(D)** were monitored daily until day 7 p.i. **(E)** Representative image of HE-staining hearts of CVB3-infected mice (day 7 p.i.) treated with PEI-TRIM21 or PEI-vector, showing intra-cardiac immune infiltrates (marked with arrows). Scale bar: 100 μm. Pathological scores of the heart of mice are shown. Results are presented as mean ± SEM; $^{*}p < 0.05$. **(F)** Protein levels of inflammatory cytokines in the homogenates of heart were measured by ELISA. Data were presented as mean ± SEM of three representative independent. **(G)** The cardiac CVB3 titer at day 3 p.i. were determined by $TCID_{50}$ assay. Data represent mean values of CVB3 PFU per gram of the heart tissues. Results are presented as mean ± SEM; Data pooled from 3 independent experiments. $^{*}p < 0.05$; $^{**}p < 0.01$. **(H)** Relative mRNA level of IFN-β (day 3 and 7p.i.) was detected by Q-PCR. Data were normalized to GAPDH expression and presented as mean ± SEM of three representative independent. **(I)** Hearts of mice at day 3 and 7 p.i. were OCT-embedded and cyrosections (5 μM) were subjected to fluorescent staining. Composite confocal represented images show dsRNA (red, anti-dsRNA Ab) and nuclear (blue, DAPI).Low magnification (magnification, × 100) and higher magnification of the boxed areas (magnification, × 200) are shown. The number of red-stained viral-infected cells in the heart sections of mice were numerated. Data are expressed as mean ± SEM from three repeated experiments ($n = 3$). $^{***}p < 0.001$.

at day3 p.i., and an increased cardiac immune infiltration at day 7 p.i. (**Figure 6E**) compared to WT mice. Consistent with enhanced tissue pathology, the levels of cardiac inflammatory cytokines were significantly increased in TRIM21 KO mice than in WT mice (**Figure 6F**).To test whether differences in CVB3 disease susceptibility were due to differences in viral replication, CVB3 burden in the hearts and pancreas of mice were measured. At 3 dpi, the peak of viral replication, TRIM21 deficient mice exhibited significantly increased viral titers in hearts and pancreas compared to WT mice (**Figure 6G**). To confirm the anti-viral effect of TRIM21 *in vivo*, the mRNA and protein level of IFN-β in hearts were measured and were found significantly decreased in TRIM21 deficiency mice at early infection stage compared to those in WT mice (**Figure 6H**). These data confirm that TRIM21 effectively suppresses CVB3 replication *in vivo*. We thus propose a model depicting the role of TRIM21 in CVB3 infection: CVB3 infection up-regulates the expression of TRIM21 in cardiomyocytes, which interacts with MAVS and promotes IRF3-mediated IFN-I signaling to suppress viral replication *in vivo,* thereby decreasing virus-induced inflammatory injury in both hearts and pancreas of mice (**Figure 6I**).

DISCUSSION

In this study, we try to explore the role of TRIM21 in the susceptibility of mice to CVB3 induced myocarditis. TRIM21 expression is significantly up-regulated in hearts of mice on day 3 post infection, and systemic TRIM21 effectively inhibits CVB3 replication *in vivo*. TRIM21 restricts CVB3 replication by positively regulating IRF3 activation and IFN-β production after CVB3 infection via interacting with and promoting K27-linked polyubiquitination of MAVS. Silencing of TRIM21 significantly enhances CVB3 replication in tissues and alleviates virus-induced cardiac and pancreatic injury. Treatment with CVB3-infected mice with TRIM21 significantly reduces CVB3 replication in hearts and the severity of viral myocarditis.

TRIM21, initially known as an autoantigen Ro52/SS-A, is an ubiquitously expressed cytosolic E3 ubiquitin ligase and plays important roles in immune regulation and microbial restriction (23, 24). It has been reported that TRIM21 is constitutively and broadly expressed in various organs and cell types, but with highly divergent levels of expression. Highest expression is seen in cells of the immune system with particularly high levels in T cells, macrophages and DCs, where the expression is further augmented by stimulation with IFNs and TLR ligation (25). Previous study finds that TRIM21 expression is substantially increased in human primary lymphocytes and monocyte-derived macrophages in response to interferons (IFNs, type I and II), suggesting TRIM21 as an interferon-induced gene (26). It has been reported that SeV, NDV or HCV infection could significantly induce the expression of TRIM21 through JAK/STAT signaling pathway (27). Thus, although CVB3 infection does not induce robust production of IFN-β, a significant induction of TRIM21 protein is observed in heart tissues upon CVB3 infection. More convincingly, TRIM21 expression is significantly enhanced in primary cardiomyocytes upon CVB3 infection (**Figures 1E,F**) which is localized in cytoplasm of cells.

The host cells activate a series of signaling events that lead to induction of type I interferons (IFNs), including IFN-β and IFN-α. Type I IFNs further induce the expression of downstream proteins, which mediate innate immune responses, such as suppression of viral replication, clearance of virus-infected cells (28, 29). The role of TRIM21 in regulating the type I interferon signaling has been controversial. Sunit K Singh demonstrates TRIM21 as a negative regulator of IFN-β production mediated by IRF-3 during JEV infection in human microglial cells (19). In 2015, another study finds that TRIM21 facilitates Nmi-mediated negative regulation of the innate antiviral response (32). And Liu Y's group reports that TRIM21 as an E3 ligase which induces the Lys48 (K48)-linked ubiquitination and degradation of DDX41 and negatively regulates the innate immune response to intracellular dsDNA in myeloid dendritic cells (30). All the above data indicate that TRIM21 is a negative regulator of IRF3 (or DD41) activation and IFN-β production. However, Chen Wang reports that TRIM21 is induced and interacts with IRF3, preventing IRF3 ubiquitination and degradation thus playing an anti-viral effect during SeV infection (17). Recently, Xue et.al have reported (20) that TRIM21 is upregulated upon RNA virus (SeV, VSV) infection, interacts with MAVS and catalyzes the K27-linked polyubiquitination of MAVS, thereby promoting the activation of IRF3 and inhibiting viral infection. In our study, we confirm the co-immunoprecipitation and polyubiquitination of TRIM21 with MAVS (**Figures 3G,H**), which is in consistency with Xue's report that TRIM21 interacts with MAVS and promotes K27-linked polyubiquitination of MAVS. It also supports our conclusion that the anti-viral effect of TRIM21 is RING domain dependent (**Figure 4C**). Finally we propose a model depicting the role of TRIM21 in CVB3 infection:

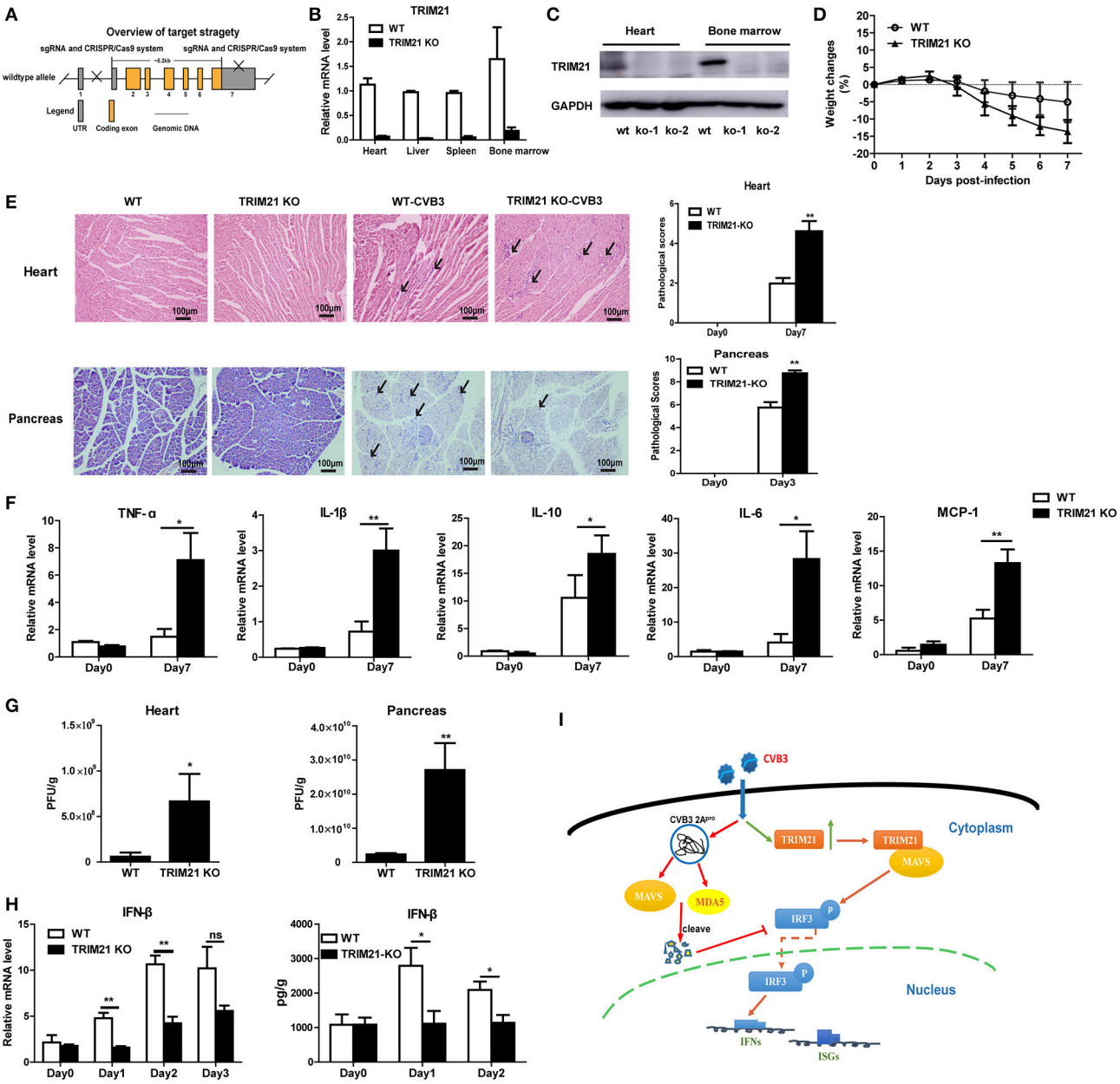

FIGURE 6 | TRIM21 deficient mice increases CVB3 replication in organs and aggravates pancreatic acinar cell necrosis as well as myocarditis. **(A)** Schematic diagram of deficient mice construction by CRISPR-CAS9 strategy. **(B,C)** Q-PCR and Western blot analysis of TRIM21 expression from tissues and BM cells of wild-type (WT) and TRIM21-/- mice, GAPDH was used as a loading control. **(D-H)** WT and TRIM21-deficient mice were infected i.p. with CVB3 ($n = 6$).The body weight change were monitored daily until day 7 p.i. **(D).** Representative image of HE-staining hearts and pancreas of CVB3-infected WT or TRIM21-/-mice (day 7 p.i.), showing intra-cardiac immune infiltrates or intactpancreatic acini (marked with arrows). Scale bar: 100 μm. Pathological scores of the heart and pancreas of mice are shown. Results are presented as mean ± SEM; Data pooled from 3 independent experiments **(E)**.The mRNA levels of inflammatory cytokines in the homogenates of heart (day 7 p.i.) were measured by Q-PCR. Data were presented as mean ± SEM of three representative independent **(F)**.Viral loadin pancreas and hearts of mice(day 3p.i.) was assessed by $TCID_{50}$ assay. Results are presented as mean ± SEM;Data pooled from 3 independent experiments. *$p < 0.05$; **$p < 0.01$ **(G)**.The mRNA and protein level of IFN-β (day 1–3 p.i.) in hearts of mice was detected by Q-PCR and ELISA. Data as mean ± SEM of three representative independent. *$p < 0.05$; **$p < 0.01$ **(H)**. **(I)** Proposed model depicting the role of TRIM21 in positive regulation of IFN-I production during CVB3 infection. TRIM21 targets and promotes the activity of MAVS, leading to the increased phosphorylation and translocation of p-IRF3 into the nucleus, leading to enhanced transcription and production of IFNs and IFN-stimulated genes (ISGs) that limits CVB3 infection.

CVB3 infection up-regulates the expression of TRIM21 in mice, TRIM21 interacts with MAVS and promotes the activation of IRF3 resulting in an up-regulation of type I innate signaling during CVB3 infection (**Figure 6I**).Although MDA5, MAVS and RIG-I are cleaved by CVB3 2Apro and 3Cpro (21) indicating TRIM21, one of ISGs, might be hardly up-regulated during CVB3

infection and TRIM21-mediated IFN-I response enhancing effect might be counteracted, there is article suggesting that enhancing IFNs production might be an alternative prescription in CVB3-related syndromes (33). And our *in vivo* over-expression and deficiency experiment in mice confirm TRIM21 supplementation as a promising strategy to limit CVB3 infection and related cardiac and pancreatic pathology.

CVB3 has evolved many strategies to suppress host innate immunity therefore does not cause robust interferon release and ISG expression. As shown in **Figure 3A**, the mRNA expressions of IFN-α and IFN-β in cells at 24 h after CVB3 infection were quite low (as similar as the level seen before infection). 48 h after infection, CVB3 did not induce IFN-α expression while induced a very modest up-regulation of IFN-β. Only upon transfection with TRIM21 plasmid, the mRNA expressions of IFN-α/β were significantly up-regulated at both 24 and 48 h post infection. The induced up-regulation of ISG15 by CVB3 was also very moderate, only TRIM21 overexpression significantly promoted ISG15 expression. It seems that upregulation of IFN-α/β may be a TRIM21-mediated effect. However, our data demonstrate that CVB3 infection significantly increases expression of TRIM21 in hearts of mice (**Figures 1 A–D**) and in primary cardiomyocytes (**Figures 1E,F**). Therefore, the upregulation of IFN-α/β signaling by TRIM21 is at least partially dependent on CVB3 infection. And the interaction of TRIM21 with MAVS (**Figures 3G,H**) further supports our data that CVB3-induced TRIM21 could enhance the phosphorylation of IRF3 upon CVB3 infection leading to elevated IFN-β production.

As a member of tripartite motif (TRIM) family protein, TRIM21 contains a RNIG motif in the N-terminal domain, a B-box motif, a coiled-coil domain. And TRIM21 protein also contains a carboxy-terminal B30.2 (SPRY) domain (31). Previous study demonstrates that TRIM21 interacts with IRF3 directly via its C-terminal SPRY domain, resulting in the polyubiquitination and proteasomal degradation of IRF3 and reduced IFN-β promoter activity (18). Liu Y's group report that TRIM21 cannot interact with IRF3 in mDC but interact with DD41 for promoting the ubiquitination and degradation of DDX41 therefore negatively regulates IFN-I response to DNA virus (HSV) (30). In 2015, another study finds that during SeV and VSV infection, up-regulated TRIM21 interacts with both Nmi and IFI35 and activates K63-linked ubiquitination on K22 residue of Nmi (SPRY domain dependent) which facilitates the negative regulatory function of the Nmi-IFI35 complex on innate antiviral signaling (32). Yang et al. report in their study that upon RNA virus infection TRIM21 interacts with IRF3, interferes with the interaction between Pin1 and IRF3, thus preventing IRF3 ubiquitination and degradation via its B30.2 domain (17). Xue et al. reports that TRIM21 interacts with MAVS and catalyzes the K27-linked polyubiquitination of MAVS through its RING domain (20). In our study, we confirmed (**Figure 3G**) that TRIM21 interacts with and promotes the K27-ubiquitination of MAVS, and the anti-viral effect of TRIM21 is RING and PRY-SPRY domain dependent (**Figure 4**), which is in consistency with the recent report (20).

Currently, there is only limited report of antiviral effect of TRIM21 in mice model. Our study demonstrate the *in vivo* effect of TRIM21 on CVB3 replication and tissue pathology. By using *in vivo*-Jet PEI-transfection of TRIM21-plasmids and TRIM21 deficient mice, we demonstrated that the viral replication and CVB3-induced cardiac immune infiltration, cardiac proinflammatory cytokines production and injuries were significantly decreased upon *in vivo* over-expression of TRIM21 (**Figure 5**). In accordance with that, cardiac and pancreatic CVB3 replication as well as virus-induced pancreatic acinar cell necrosis and myocarditis were significantly aggravated in TRIM21 deficient mice (**Figure 6**). Our data identify TRIM21 as a potent viral inhibitory factor during CVB3 infection. Recently, TRIM21 is also identified as an intracellular Fc receptor linking cytosolic antibody recognition to the ubiquitin proteasome system (34–36).So we cannot rule out the antiviral effect of TRIM21 is partially dependent on antibody-dependent intracellular neutralization (ADIN) effect of TRIM21 *in vivo*. And our preliminary data show that TRIM21 has IgA-mediated ADIN effect on CVB3 replication *in vitro* (data not shown). So in further study we will focus on clarifying whether TRIM21 exerts IgA-mediated ADIN function on intestinal CVB3 replication considering CVB3 as an oral-fecal disseminating virus.

Overall, our study identifies cytosolic TRIM21 as a positive regulator of CVB3-triggered MAVS-mediated type I Interferon signaling pathway that restricts viral infection. TRIM21 expression is up-regulated by CVB3 infection at early phase of viral infection. TRIM21 inhibits CVB3 replication *in vivo* and *in vitro* through interacting with MAVS thereby promoting the activation of IRF3 and Type I Interferon production. The anti-viral effect of TRIM21 is dependent on RING and PRY-SPRY domain. We also demonstrate the antiviral effect of systemic TRIM21 *in vivo* which leads to the increased resistance to CVB3-induced myocarditis and pancreatic injury. Our data help to clarify the biological role of TRIM21 in severe tissue pathology caused by viral infection and indicating a therapeutic target potential for TRIM21.

ETHICS STATEMENT

All animal experiments were performed in accordance with Soochow University institutional guidelines, and the study was approved by the Ethics Committee of Soochow University in written form (SYXK2015-0036).

AUTHOR CONTRIBUTIONS

WX conceived and supervised the project. HL and YS performed the experiments. HL and ML interpreted data and wrote the manuscript. All authors approved the final version of the paper.

FUNDING

This work was supported by NSFC grant (31870903, 31670930, 31470869, 31270973), the Natural Science Foundation of Jiangsu Province Higher education (14KJA310005), the Jiangsu Provincial Innovative Research Team, and Program for Changjiang Scholars and Innovative Research Team in University (grant PCSIRTIRT1075).

REFERENCES

1. Esfandiarei M, McManus BM. Molecular biology and pathogenesis of viral myocarditis. *Ann Rev Pathol.* (2008) 3:127–55. doi: 10.1146/annurev.pathmechdis.3.121806.151534
2. Tam PE. Coxsackievirus myocarditis: interplay between virus and host in the pathogenesis of heart disease. *Viral Immunol.* (2006) 19:133–46. doi: 10.1089/vim.2006.19.133
3. Gaaloul I, Riabi S, Harrath R, Hunter T, Hamda KB, Ghzala AB, et al. Coxsackievirus B detection in cases of myocarditis, myopericarditis, pericarditis and dilated cardiomyopathy in hospitalized patients. *Molecul Med Rep.* (2014) 10:2811–8. doi: 10.3892/mmr.2014.2578
4. Sagar S, Liu PP, Cooper LT Jr. Myocarditis. *Lancet* (2012) 379:738–47. doi: 10.1016/s0140-6736(11)60648-x
5. Cheung PK, Yuan J, Zhang HM, Chau D, Yanagawa B, Suarez A, et al. Specific interactions of mouse organ proteins with the 5'untranslated region of coxsackievirus B3: potential determinants of viral tissue tropism. *J Med Virol.* (2005) 77:414–24. doi: 10.1002/jmv.20470
6. Harvala H, Kalimo H, Bergelson J, Stanway G, Hyypia T. Tissue tropism of recombinant coxsackieviruses in an adult mouse model. *J General Virol.* (2005) 86(Pt 7):1897–907. doi: 10.1099/vir.0.80603-0
7. Huber SA, Gauntt CJ, Sakkinen P. Enteroviruses and myocarditis: viral pathogenesis through replication, cytokine induction, and immunopathogenicity. *Adv Virus Res.* (1998) 51:35–80.
8. McManus BM, Chow LH, Wilson JE, Anderson DR, Gulizia JM, Gauntt CJ, et al. Direct myocardial injury by enterovirus: a central role in the evolution of murine myocarditis. *Clin Immunol Immunopathol.* (1993) 68:159–69.
9. Kawai C. From myocarditis to cardiomyopathy: mechanisms of inflammation and cell death: learning from the past for the future. *Circulation* (1999) 99:1091–100.
10. Short KM, Cox TC. Subclassification of the RBCC/TRIM superfamily reveals a novel motif necessary for microtubule binding. *J Biol Chem.* (2006) 281:8970–80. doi: 10.1074/jbc.M512755200
11. Hatakeyama S. TRIM family proteins: roles in autophagy, immunity, and carcinogenesis. *Trends Biochem Sci.* (2017) 42:297–311. doi: 10.1016/j.tibs.2017.01.002
12. Kano S, Miyajima N, Fukuda S, Hatakeyama S. Tripartite motif protein 32 facilitates cell growth and migration via degradation of Abl-interactor 2. *Cancer Res.* (2008) 68:5572–80. doi: 10.1158/0008-5472.can-07-6231
13. Imran M, Manzoor S, Saalim M, Resham S, Ashraf J, Javed A, et al. HIV-1 and hijacking of the host immune system: the current scenario. *APMIS* (2016) 124:817–31. doi: 10.1111/apm.12579
14. Vicenzi E, Poli G. The interferon-stimulated gene TRIM22: a double-edged sword in HIV-1 infection. *Cytokine Growth Factor Rev.* (2018) 40:10–7. doi: 10.1016/j.cytogfr.2018.02.001
15. Lim KH, Park ES, Kim DH, Cho KC, Kim KP, Park YK, et al. Suppression of interferon-mediated anti-HBV response by single CpG methylation in the 5'-UTR of TRIM22. *Gut* (2018) 67:166–78. doi: 10.1136/gutjnl-2016-312742
16. Di Pietro A, Kajaste-Rudnitski A, Oteiza A, Nicora L, Towers GJ, Mechti N, et al. TRIM22 inhibits influenza a virus infection by targeting the viral nucleoprotein for degradation. *J Virol.* (2013) 87:4523–33. doi: 10.1128/jvi.02548-12
17. Yang K, Shi HX, Liu XY, Shan YF, Wei B, Chen S, et al. TRIM21 is essential to sustain IFN regulatory factor 3 activation during antiviral response. *J Immunol.* (2009) 182:3782–92. doi: 10.4049/jimmunol.0803126
18. Higgs R, Ni Gabhann J, Ben Larbi N, Breen EP, Fitzgerald KA, Jefferies CA. The E3 ubiquitin ligase Ro52 negatively regulates IFN-beta production post-pathogen recognition by polyubiquitin-mediated degradation of IRF3. *J Immunol.* (2008) 181:1780–6. doi: 10.4049/jimmunol.181.3.1780
19. Manocha GD, Mishra R, Sharma N, Kumawat KL, Basu A, Singh SK. Regulatory role of TRIM21 in the type-I interferon pathway in Japanese encephalitis virus-infected human microglial cells. *J Neuroinflamm.* (2014) 11:24. doi: 10.1186/1742-2094-11-24
20. Xue B, Li H, Guo M, Wang J, Xu Y, Zou X, et al. TRIM21 Promotes innate immune response to RNA viral infection through Lys27-Linked Polyubiquitination of MAVS. *J Virol.* (2018) 92. doi: 10.1128/jvi.00321-18
21. Feng Q, Langereis MA, Lork M, Nguyen M, Hato SV, Lanke K, et al. Enterovirus 2Apro targets MDA5 and MAVS in infected cells. *J Virol.* (2014) 88:3369–78. doi: 10.1128/jvi.02712-13
22. Li M, Yan K, Wei L, Yang J, Lu C, Xiong F, et al. Zinc finger antiviral protein inhibits coxsackievirus B3 virus replication and protects against viral myocarditis. *Antiviral Res.* (2015) 123:50–61. doi: 10.1016/j.antiviral.2015.09.001
23. Espinosa A, Dardalhon V, Brauner S, Ambrosi A, Higgs R, Quintana FJ, et al. Loss of the lupus autoantigen Ro52/Trim21 induces tissue inflammation and systemic autoimmunity by disregulating the IL-23-Th17 pathway. *J Exp Med.* (2009) 206:1661–71. doi: 10.1084/jem.20090585
24. Kong HJ, Anderson DE, Lee CH, Jang MK, Tamura T, Tailor P, et al. Cutting edge: autoantigen Ro52 is an interferon inducible E3 ligase that ubiquitinates IRF-8 and enhances cytokine expression in macrophages. *J Immunol.* (2007) 179:26–30. doi: 10.4049/jimmunol.179.1.26
25. Oke V, Vassilaki I, Espinosa A, Strandberg L, Kuchroo VK, Nyberg F, et al. High Ro52 expression in spontaneous and UV-induced cutaneous inflammation. *J Invest Dermatol.* (2009) 129:2000–10. doi: 10.1038/jid.2008.453
26. Brauner S, Zhou W, Backlin C, Green TM, Folkersen L, Ivanchenko M, et al. Reduced expression of TRIM21/Ro52 predicts poor prognosis in diffuse large B-cell lymphoma patients with and without rheumatic disease. *J Internal Med.* (2015) 278:323–32. doi: 10.1111/joim.12375
27. Jiang MX, Hong X, Liao BB, Shi SZ, Lai XF, Zheng HY, et al. Expression profiling of TRIM protein family in THP1-derived macrophages following TLR stimulation. *Sci Rep.* (2017) 7:42781. doi: 10.1038/srep42781
28. Kawai T, Akira S. The roles of TLRs, RLRs and NLRs in pathogen recognition. *Int Immunol.* (2009) 21:317–37. doi: 10.1093/intimm/dxp017
29. Zhou Y, He C, Wang L, Ge B. Post-translational regulation of antiviral innate signaling. *Eur J Immunol.* (2017) 47:1414–26. doi: 10.1002/eji.201746959
30. Zhang Z, Bao M, Lu N, Weng L, Yuan B, Liu YJ. The E3 ubiquitin ligase TRIM21 negatively regulates the innate immune response to intracellular double-stranded DNA. *Nat Immunol.* (2013) 14:172–8. doi: 10.1038/ni.2492
31. Ozato K, Shin DM, Chang TH, Morse HC III. TRIM family proteins and their emerging roles in innate immunity. *Nat Rev Immunol.* (2008) 8:849–60. doi: 10.1038/nri2413
32. Das A, Dinh PX, Pattnaik AK. Trim21 regulates Nmi-IFI35 complex-mediated inhibition of innate antiviral response. *Virology* (2015) 485:383–92. doi: 10.1016/j.virol.2015.08.013
33. Rahnefeld A, Klingel K, Schuermann A, Diny NL, Althof N, Lindner A, et al. Ubiquitin-like protein ISG15 (interferon-stimulated gene of 15 kDa) in host defense against heart failure in a mouse model of virus-induced cardiomyopathy. *Circulation* (2014) 130:1589–600. doi: 10.1161/circulationaha.114.009847
34. Watkinson RE, Tam JC, Vaysburd MJ, James LC. Simultaneous neutralization and innate immune detection of a replicating virus by TRIM21. *J Virol.* (2013) 87:7309–13. doi: 10.1128/jvi.00647-13
35. Rakebrandt N, Lentes S, Neumann H, James LC, Neumann-Staubitz P. Antibody- and TRIM21-dependent intracellular restriction of Salmonella enterica. *Pathog Dis.* (2014) 72:131–7. doi: 10.1111/2049-632x.12192
36. Bottermann M, James LC. Intracellular antiviral immunity. *Adv Virus Res.* (2018) 100:309–54. doi: 10.1016/bs.aivir.2018.01.002

Conflict of Interest Statement: The authors declare that the research was conducted in the absence of any commercial or financial relationships that could be construed as a potential conflict of interest.

frontiers in Immunology

ORIGINAL RESEARCH
published: 08 October 2018
doi: 10.3389/fimmu.2018.02303

Silencing the CSF-1 Axis Using Nanoparticle Encapsulated siRNA Mitigates Viral and Autoimmune Myocarditis

Ingmar Sören Meyer[1,2†], Carl Christoph Goetzke[3,4†], Meike Kespohl[3,4], Martina Sauter[5], Arnd Heuser[6], Volker Eckstein[7], Hans-Peter Vornlocher[8], Daniel G. Anderson[9,10,11], Jan Haas[1,2], Benjamin Meder[1,2], Hugo Albert Katus[1,2], Karin Klingel[5], Antje Beling[3,4†] and Florian Leuschner[1,2*†]*

[1] Internal Medicine III, University Hospital Heidelberg, Heidelberg, Germany, [2] DZHK (German Centre for Cardiovascular Research), Partner Site Heidelberg-Mannheim, Heidelberg, Germany, [3] Institute of Biochemistry, Charité - Universitätsmedizin Berlin, Corporate Member of Freie Universität Berlin, Humboldt-Universität zu Berlin, and Berlin Institute of Health, Berlin, Germany, [4] DZHK (German Centre for Cardiovascular Research), Partner Site Berlin, Berlin, Germany, [5] Cardiopathology, Institute for Pathology and Neuropathology, University Hospital Tuebingen, Tuebingen, Germany, [6] Max-Delbrueck-Center for Molecular Medicine Berlin, Berlin, Germany, [7] Internal Medicine V, University Hospital Heidelberg, Heidelberg, Germany, [8] Axolabs GmbH, Kulmbach, Germany, [9] David H. Koch Institute for Integrative Cancer Research, Massachusetts Institute of Technology, Cambridge, MA, United States, [10] Cardiovascular Division, Department of Medicine, Brigham and Women's Hospital, Boston, MA, United States, [11] Department of Chemical Engineering, Massachusetts Institute of Technology (MIT), Cambridge, MA, United States

OPEN ACCESS

Edited by:
Michael H. Lehmann, Ludwig-Maximilians-Universität München, Germany

Reviewed by:
Milena Botelho Pereira Soares, Instituto Gonçalo Moniz (IGM), Fiocruz Bahia, Brazil
Yasushi Fujio, Osaka University, Japan

***Correspondence:**
Antje Beling
antje.beling@charite.de
Florian Leuschner
florian.leuschner@med.uni-heidelberg.de

† These authors have contributed equally to this work and are share first and senior authorship

Specialty section:
This article was submitted to Cytokines and Soluble Mediators in Immunity, a section of the journal Frontiers in Immunology

Received: *17 July 2018*
Accepted: *17 September 2018*
Published: *08 October 2018*

Citation:
Meyer IS, Goetzke CC, Kespohl M, Sauter M, Heuser A, Eckstein V, Vornlocher H-P, Anderson DG, Haas J, Meder B, Katus HA, Klingel K, Beling A and Leuschner F (2018) Silencing the CSF-1 Axis Using Nanoparticle Encapsulated siRNA Mitigates Viral and Autoimmune Myocarditis. Front. Immunol. 9:2303. doi: 10.3389/fimmu.2018.02303

Myocarditis is an inflammatory disease of the heart muscle most commonly caused by viral infection and often maintained by autoimmunity. Virus-induced tissue damage triggers chemokine production and, subsequently, immune cell infiltration with pro-inflammatory and pro-fibrotic cytokine production follows. In patients, the overall inflammatory burden determines the disease outcome. Following the aim to define specific molecules that drive both immunopathology and/or autoimmunity in inflammatory heart disease, here we report on increased expression of colony stimulating factor 1 (CSF-1) in patients with myocarditis. CSF-1 controls monocytes originating from hematopoietic stem cells and subsequent progenitor stages. Both, monocytes and macrophages are centrally involved in mediating tissue damage and fibrotic scarring in the heart. CSF-1 influences monocytes via engagement of CSF-1 receptor, and it is also produced by cells of the mononuclear phagocyte system themselves. Based on this, we sought to modulate the virus-triggered inflammatory response in an experimental model of Coxsackievirus B3-induced myocarditis by silencing the CSF-1 axis in myeloid cells using nanoparticle-encapsulated siRNA. siCSF-1 inverted virus-mediated immunopathology as reflected by lower troponin T levels, a reduction of accumulating myeloid cells in heart tissue and improved cardiac function. Importantly, pathogen control was maintained and the virus was efficiently cleared from heart tissue. Since viral heart disease triggers heart-directed autoimmunity, in a second approach we investigated the influence of CSF-1 upon manifestation of heart tissue inflammation during experimental autoimmune myocarditis (EAM). EAM was induced in Balb/c mice by immunization with a myocarditogenic myosin-heavy chain-derived peptide dissolved in complete Freund's adjuvant. siCSF-1 treatment initiated upon established disease inhibited monocyte infiltration into heart tissue and this suppressed cardiac injury

as reflected by diminished cardiac fibrosis and improved cardiac function at later states. Mechanistically, we found that suppression of CSF-1 production arrested both differentiation and maturation of monocytes and their precursors in the bone marrow. In conclusion, during viral and autoimmune myocarditis silencing of the myeloid CSF-1 axis by nanoparticle-encapsulated siRNA is beneficial for preventing inflammatory tissue damage in the heart and preserving cardiac function without compromising innate immunity's critical defense mechanisms.

Keywords: inflammation and immunmodulation, innate immunity, cytokines, monocytes/macrophages, RNA interference, virus, infection-immunology, myocarditis

INTRODUCTION

Myocarditis and its sequela, dilated cardiomyopathy, are leading causes of heart failure and sudden death in young adults (1). While various agents may provoke cardiac inflammation, viral infections are the most common trigger of myocardial inflammation in the Western world. Although various viruses are putative invaders of heart tissue, most of our knowledge on disease pathology comes from infection with enteroviruses, in particular CoxsackievirusB3 (CVB3). CVB3 had been reported among the most prevalent pathogens causing viral myocarditis in North America and Europe in the past (2, 3). Mouse models using different strains with divergent susceptibility for cardiotropic CVB3 elegantly reflect human disease with highly diverse disease outcome (4, 5). The hereditary susceptibility involves a certain immune-anchored genetic phenotype leading either to altered virus control and/or to induction of deleterious immunopathology (6–8). Severe virus-induced inflammation can result in a subsequent loss of self-tolerance against cardiac proteins, which contributes to additive auto-destructive activity of infiltrating cells and exaggerates heart tissue damage (9, 10). Cardiac myosin is such a crucial autoantigen in both human and murine virus-induced myocarditis (9). Administration of cardiac myosin or its pathogenic epitope in combination with an adjuvant induces experimental autoimmune myocarditis (EAM) in mice, a model that mimics certain aspects of myocarditis and heart failure in humans (11).

Treatment options for patients with myocarditis are sparse and both conventional immunosuppressive as well as anti-viral approaches have not yielded the desired results in clinical trials (12). Recent data suggest that it is not the presence and/or replicative activity of invading viruses in the myocardium that determines outcome, but the virus-triggered abundance of infiltrating leukocytes is an independent risk factor (13, 14). At the acute state of myocarditis in mice, the majority of accumulating leukocytes in inflamed heart tissue are $CD11b^+$ monocytes and macrophages (15, 16). Consistently, the presence of $CD68^+$ macrophages is a diagnostic hallmark for human myocarditis (3). Infiltration of immune cells is cytokine/chemokine-dependent. Consistent with previous findings (17), we have demonstrated that not CVB3-mediated cytotoxicity itself, but the overwhelming cytokine response initiated by viral PAMPs is responsible for disease severity. Lower pro-inflammatory cytokine/chemokine production during the early phase of infection paralleled in reduced inflammatory heart tissue damage and protected mice from cardiac failure (14). As monocytes and macrophages are key players that secrete pro-inflammatory and pro-fibrotic cytokines thereby exacerbating acute and chronic inflammatory injury during myocarditis (4, 18), effector molecules that modulate their differentiation, activity, and cytokine secretion might be putative drug targets for myocarditis. We have previously described the precise targeting of inflammatory monocytes and their precursors by optimized lipid nanoparticles which were encapsulated with siRNA directed against CCR2 or CD115 (19, 20). Injection of mice with these nanoparticles resulted in rapid blood clearance, accumulation in spleen and bone marrow, and localization to monocytes (19).

Here, we demonstrate RNA sequencing data obtained from endomyocardial biopsies of patients with myocarditis indicating a significantly increased production of Colony Stimulating Factor 1 (CSF-1). The development of monocytes depends on CSF-1 (21) and its receptor CSF-1R/CD115. CSF-1 can be expressed and produced by various cells including monocytes themselves (22). Local production of CSF-1 stimulates tissue-resident macrophage proliferation and reduces apoptosis, thereby influencing cellular survival (23). CSF-1R is expressed on monocytes, macrophages, dendritic cells and their precursors, including "granulocyte-macrophage progenitors" (GMP), "monocyte-macrophage DC progenitors" (MDP) and "common monocyte progenitors" (cMoP) (24, 25). CSF-1 receptor signaling is a well-described mechanism that leads to monocyte production from progenitors and stimulates mature monocytes screwing them into a pro-inflammatory state (26). Based on this, we hypothesized that disruption of the CSF-1 axis in myeloid cells attenuates heart muscle inflammation and the resulting organ damage during myocarditis. Using mouse models of CVB3-induced myocarditis and experimental autoimmune myocarditis, we have found that silencing of CSF-1 upon treatment of mice with CSF-1 siRNA encapsulated nanoparticles substantially mitigated inflammatory heart muscle damage leading to less fibrosis formation and improved heart muscle function without the risk of exacerbating direct viral pathology.

MATERIALS AND METHODS

Study Approval

All subjects gave written informed consent in accordance with the Declaration of Helsinki. The study protocol was approved by the ethic committee of the Medical Faculty—University of Heidelberg—project 390/2011 "Central biobank of Department

Internal Medicine III for research on molecular and genetic markers in patients with cardiovascular disease."

RNA-Seq Analysis, Read Processing and Mapping

Patient enrollment and biomaterial processing for RNA-seq analysis of heart biopsies was performed as previously described (27). In detail, biopsy specimens were obtained from the apical part of the free LV wall during cardiac catheterization using a standardized protocol. Biopsies of 1- to 2-mm diameter were immediately washed in ice-cold saline (0.9% NaCl), transferred and stored in liquid nitrogen until RNA extraction. After diagnostic workup of the biopsies (histopathology), the remaining material was used to isolate RNA with an Allprep Kit (Qiagen). RNA purity and concentration were determined using the Bioanalyzer 2100 (Agilent Technologies) with a Eukaryote Total RNA Pico assay for RNA from biopsies. Sequencing libraries were generated using the TruSeq Stranded Total RNA Sample Preparation Kit with Ribo-Zero Human/Mouse/Rat from Illumina, adhering to the standard protocol of the kit. Sequencing was performed using 2 × 75 bp paired end sequencing on an Illumina HiSeq2000 instrument. For transcriptome analysis, raw read files were mapped with STAR v2.4.1c5 using GRCh37/hg19 and the Gencode 19 gene model (http://www.gencodegenes.org/). Read counts were generated with help of subread's feature counts program 6 (subread version 1.4.6.p1), using uniquely mapped reads only (28). Normalization was performed with help of rlog-normalization (29). RNA seq data were deposited to the public repository Gene Expression Omnibus (GEO) - NCBI, accession number GSE120567. RNA seq data for DCM patients are partially demonstrated in (30).

Differential Gene Expression- and Gene Set Enrichment Analysis

Differential gene expression analysis of RNA-seq data was carried out within the RStudio framework using the edgeR package (31). Gene set enrichment analysis was performed with KEGG gene sets.

Histology and Immunohistochemistry

Human endomyocardial biopsy tissue and murine tissue was stained as described elsewhere (32). For AVM, paraffin embedded organ tissue sections were stained with hematoxylin/eosin (HE) or Masson's trichrome according to standard protocols. Immunohistochemical stains for CSF-1 (rabbit polyclonal, abcam), T lymphocytes (CD3 and CD4) and mononuclear phagocytes (Mac-3) was performed as previously described (32). For EAM, hearts were excised 30 days after primary immunization. Hearts were rinsed in PBS, fixed in 10% formaline for 24 h and embedded in paraffin. Serial 5 μm sections were stained with Masson's trichrome staining to quantify fibrotic tissue formation. Severity of EAM was evaluated according to a 6-tier scoring system as previously described (19, 20). All slides were counterstained with hematoxylin. Sections were mounted with Pertex mounting media (Medite). Slides were viewed with a Zeiss Axioskop 40 microscope.

Candidate Identification of CSF-1 siRNA

Lysates of several murine cell lines were tested on CSF1 expression. NIH-3T3 cells showed high CSF1 expression, are readily to be transfected, and were therefore used in candidate identification experiments. siRNA loaded lipid-based nanoparticles were generated by Axolabs GmbH (Kulmbach, Germany) as previously described (19). siRNA targeting CSF-1 receptor (CSF-1R, CD115) is described elsewhere (33). To generate siRNAs that target the CSF-1 transcript, NIH 3T3 cells were transfected with siRNAs targeting CSF-1 or non-targeting control siRNA complexed with Lipofectamine2000 Transfection Reagent at 5 and 50 nM final concentration in quadruplicates. Values for CSF-1 were normalized to GAPDH and related to the mean value of three different control siRNAs (100% expression). Optimal siRNA concentration yielding most efficient knockdown of CSF-1 production was obtained with RNA transfections starting at 100 nM in 6-fold dilution steps down to 10 fM. CSF-1 siRNAs that showed the best knockdown in both the dual concentration screen and the concentration response curve screen were used for nanoparticle encapsulation and *in vivo* experiments.

Induction of Acute Viral Myocarditis (AVM) and Experimental Autoimmune Myocarditis (EAM)

For induction of AVM, 5–7 weeks old male A.BY/SnJ mice were infected intraperitoneally (i.p.) with 5×10^5 PFU CVB3 (cardiotropic Nancy strain) provided by Klingel (15) and Rahnefeld et al. (32). Original breeding stocks for A.BY/SnJ mice were purchased from the Jackson Laboratory. For EAM, male BALB/c were purchased from Janvier (Saint-Berthevin, France). Myocarditis was induced by subcutaneous injection of an emulsion containing 150 μg myosin peptide SLKLMATLFSTYASAD (PSL GmbH, Heidelberg, Germany) supplemented with complete Freund's adjuvant (CFA) (Sigma-Aldrich, Taufkirchen, Germany) and 5 mg/ml *Mycobacterium tuberculosis* H37Ra (Sigma-Aldrich, Taufkirchen, Germany). Directly after the initial immunization, mice were injected with 500 ng pertussis toxin (Sigma-Aldrich, Taufkirchen, Germany) i.p. Seven days after the primary immunization, mice received a second subcutaneous injection of 150 μg myosin peptide supplemented with CFA and complemented with *Mycobacterium tuberculosis*. All mice were housed under standard laboratory conditions with a 12-h light-dark cycle and access to water and food *ad libitum*. For AVM, the protocol was approved by the Committee on the Ethics of Animal Experiments of Berlin State authorities [G0034/16]. EAM experimental protocols were approved by the institutional review board of the University of Heidelberg, Germany, and the responsible government authority of Baden-Württemberg, Germany (project number 35-9185.81/G-209/12). All mouse studies were carried out in accordance with the recommendations in the Guide for the Care and Use of Laboratory Animals of the German animal welfare act, which is based on the directive of the European parliament and of the council on the protection of animals used for scientific purposes. All efforts were made to minimize suffering.

In vivo Silencing of CSF-1 During AVM and EAM

The optimal CSF-1–targeted siRNA (siCSF-1) was scaled up for *in vivo* studies. For viral myocarditis, mice were intravenously treated with 0.5 mg/kg nanoparticle encapsulated siLUC or siCSF-1 immediately prior to CVB3 infection and 2, 4, and 6 days after infection. For EAM, nanoparticle treatment started 14 days after the primary immunization with myosin peptide. Animals received four i.v. injections of 0.5 mg/kg siCSF-1 or siLuciferase (LUC)-nanoparticles (control siCD115) per week.

Evaluation of Knockdown Efficacy of siCSF-1

Male BALB/c mice received single injections of 1.5 mg/kg lipid-based nanoparticle containing either siLUC or siCSF-1 on three consecutive days. Animals were sacrificed 24 h after the third injection. Bone marrow cells were isolated and prepared for flow cytometry-based sorting of monocytes, which were identified as Lin^-(CD90;B220;CD49b;NK1.1;Ly6G,Ter119);F4/80$^-$; CD11c$^-$; CD11b$^+$. Cell sorting was performed on a FACS ARIAII (BD Bioscience, Heidelberg, Germany). RNA from sorted cells was isolated using Trizol (Life Technologies, Darmstadt, Germany). Knockdown efficacy was evaluated using quantitative real-time PCR. Gene expression was normalized to HPRT. The following primers were used: CSF-1: TCCCAT ATGTCTCCTTCCATAAA (fwd), GGTGGAACTGCCAGT ATAGAAAG (rev); CD115: CGAGGGAGATCTCAGCTACA (fwd), GACTGGAGAAGCCACTGTCC (rev). HPRT: GTCAAC GGGGGACATAAAAG (fwd), TGCATTGTTTTACCAGTG TCAA (rev). For the AVM model, spleen tissue was isolated 8 days after virus inoculation and tissue homogenization was performed using a lysis buffer containing 20 mM HEPES, 1 % (v/v) Triton X-100, 4 mM EDTA, 1 mM EGTA, 5 mM TCEP, 50 mM NaF, 5 mM NaPP, 2 mM Na-*o*-vanadate and Complete® protease inhibitor cocktail (Roche). Western blot analysis was performed following standard procedures. After blocking with 5% milk/PBS-Tween at 4 °C overnight, membranes were probed with the primary antibody α-CD115 (ab32633, Cell Signalling) and α-actin (Merck Millipore). The bound primary antibodies were detected using IRDye800CW labeled goat anti-mouse secondary antibodies in conjunction with an Odyssey CLx infrared imaging system (Li-Cor Biosciences, Bad Homburg, Germany).

Echocardiography

Cardiac function and morphology of mice with AVM were assessed with a VisualSonics Vevo 770 High-Frequency Imaging System with the use of a high-resolution (RMV-707B; 15–45 MHz) transducer during anesthesia with 1.5–2% isoflurane. Temperature and ECG were continuously monitored. For the EAM model, echocardiography was performed in conscious animals on a VisualSonics Vevo 2100 30 days after the first immunization. Standard imaging planes, M-mode, and functional calculations were obtained. For AVM, the parasternal long-axis four-chamber view of the left ventricle (LV) was used to guide calculations of percentage fractional shortening, ventricular dimensions and volumes. M-mode echocardiographic images were recorded at the level of the papillary muscles from the parasternal short-axis view. An experienced reader blinded to treatment performed all measurements. Ejection fraction (EF) and fractional shortening (FS) were calculated based on M-mode measurements.

Flow Cytometry

Flow cytometric analysis was performed 8 days after infection in AVM and 21 days after the first immunization in EAM. Single cell suspension of bone marrow, spleen and heart tissue were prepared as previously described (34). Hearts were flushed with PBS and homogenized in RPMI 1,640 medium (Biochrom) containing 10% (v/v) fetal calf serum (FCS) (Biochrom), 1% (v/v) penicillin/streptomycin (Pan Biotech), 30 mM HEPES, 0.1 % (w/v) collagenase type 2 (Worthington) and 0.015% (w/v) DNase I (Sigma-Aldrich) at 37°C at 800 rpm for 30 min. Afterwards, 10 mM EDTA was added. Cells were washed with PBS and passed through a 70 μm cell strainer as described in reference (35). For the identification of myeloid cells, cell suspensions were stained with a cocktail of PE-conjugated anti-mouse antibodies targeting hematopoietic lineage markers (B220 for B cells (RA3-6B2, BD Bioscience), CD90.2 for T cells (53-2.1, BD Bioscience), CD49b for NK cells (DX5, eBioscience), NK-T/NK Cell Antigen for NK cells (U5A2-13, BD Bioscience) and Ter-119 for erythroid cells (TER-119, BD Bioscience)) and fluorescent-dye conjugated antibodies against the following cell surface markers: CD45.2 (104, Brilliant Violet 711™, BioLegend), CD11b (M1/70, PE-CF594, BD Bioscience), Ly6G (1A8, PerCP/Cy5.5, BioLegend), Ly6C (HK1.4, Pacific Blue™, BioLegend), CD11c (N418, Brilliant Violet 510™, BioLegend), I-A[b] (AF6-120.1, FITC, BD Bioscience) and F4/80 (BM8, APC, BioLegend). Cells were stained in PBS containing 2% FCS, 2 mM EDTA for 20 min at 4°C. For the identification of lymphoid cells, cell suspensions were stained with fluorescent-dye conjugated anti-mouse antibodies against CD45.2 (104, Brilliant Violet 711™, BioLegend), CD3e (145-2C11, PerCP/Cy5.5, BioLegend), CD4 (RM4-5, V500, BD Bioscience), CD8a (53-6.7, Pacific Blue™, BD Bioscience), B220 (RA3-6B2, FITC, BioLegend) and CD19 (6D5, APC, BioLegend). The antibody staining was followed by a cell viability stain (Fixable Viability Dye eFluor® 780, eBioscience) according to the manufacturer's protocol.

Monocytes were identified as Lin^{low} (CD90;B220;CD49b;NK1.1;Ly6G,Ter119), F4/80^{low}, CD11c^{low}, CD11b^{high}; or Fixable Viability Dye^{low}, CD45.2^{high}, CD11b^{high}, (B220, CD90.2, CD49, NK-T/NK Cell Antigen, Ter-119)^{low}, Ly6G^{low}, SSC^{low}, F4/80^{low} and CD11c^{low} and further differentiated according to Ly6C-expression. Inflammatory monocytes express high levels of Ly6C and patrolling monocytes express low levels of Ly6C. Macrophages were identified as Fixable Viability Dye^{low}, CD45.2^{high}, CD11b^{high}, Lin^{low}, Ly6G^{low}, SSC^{low}, F4/80^{high} and CD11c$^{low/high}$. Dendritic cells were identified as Fixable Viability Dye^{low}, CD45.2^{high}, CD11b^{high}, Lin^{low}, CD11c^{high} and MHC II^{high} (compared to isotype control). Neutrophils were identified as Fixable Viability Dye^{low}, CD45.2^{high}, CD11b^{high}, Lin^{low}, Ly6G^{high} and SSC^{high}. B

cells were gated as Fixable Viability Dye^{low}, CD45.2^{high}, CD3^{low}, B220^{high} and CD19^{high}. T cells were gated as Fixable Viability Dye^{low}, CD45.2^{high}, B220^{low}, CD3^{high} and either CD4^{high} or CD8^{high}. For identifying proliferating GMPs mice received two s.c. injections of 1 mg/kg Bromdesoxyuridin (BrdU) 12 and 24 h before the animals were sacrificed. BrdU was stained using BrdU flow kit (BD Biosciences). Proliferating GMPs were identified as (CD90;B220;CD49b;NK1.1;Ly6G;CD11b;CD11c;IL-7R;Sca-1)^{low} and (CD117;CD34;CD16/32;BrdU)^{high}.

For the assessment of quantitative data, 123 count eBeads (eBioscience) were used according to manufacturer's protocol. Data were acquired on a FACS Verse (BD Biosciences, Heidelberg, Germany) or on a LSR II (BD Bioscience) and analyzed with FlowJo v10.0 software (FLOWJO, Ashland, United States). Reported cell numbers were normalized to the weight of total hearts, yielding the number of respective cell fraction per mg tissue.

Determination of Viral Load in Heart Tissue

Plaque assays were performed in triplicates on sub-confluent green monkey kidney cell monolayers as described recently (32). *In situ* hybridization of CVB3 RNA was performed using probes generated with the DIGoxigenin (DIG) RNA labeling kit (Roche) and the pCVB3-R1 plasmid. Plasmid cDNA was linearized with SmaI (36); all other steps were conducted as previously described (37). DIG-labeled CVB3 RNA was detected using a horseradish-peroxidase-conjugated DIG antibody (Roche 1:100). HistoGreen (Linaris) was used as a substrate. All slides were counterstained with hematoxylin.

High-Sensitive (hs)-Troponint (TnT)

Blood was sampled by facial vein puncture and collected in a heparinized capillary. Thereby obtained plasma was diluted 1:15 in PBS. hs-TnT was determined by the electrochemiluminescence method (ECLIA; Elecsys 2010 analyzer) according to the method described in reference (38).

Statistics

Statistical analysis of the data was performed in GraphPad Prism v6.00/v.700 for Windows (GraphPad Software, La Jolla, California, United States). Logarithmic data (virus titer, semi-quantitative RNA quantification) measured on a linear scale was transformed logarithmically prior to data plotting and data analysis. Data summary is indicated on plots as mean ± SD unless stated otherwise. Unpaired *t*-tests were used for two group comparisons. If samples had unequal variances (determined by an *F*-test), an unpaired *t*-test with Welch's correction was used. For multiple group comparison unequal variance versions of ANOVA (1-way or 2-way ANOVA) were performed followed by a Sidak-Holm's multiple comparison test. The significance threshold for all tests was set at the 0.05 level.

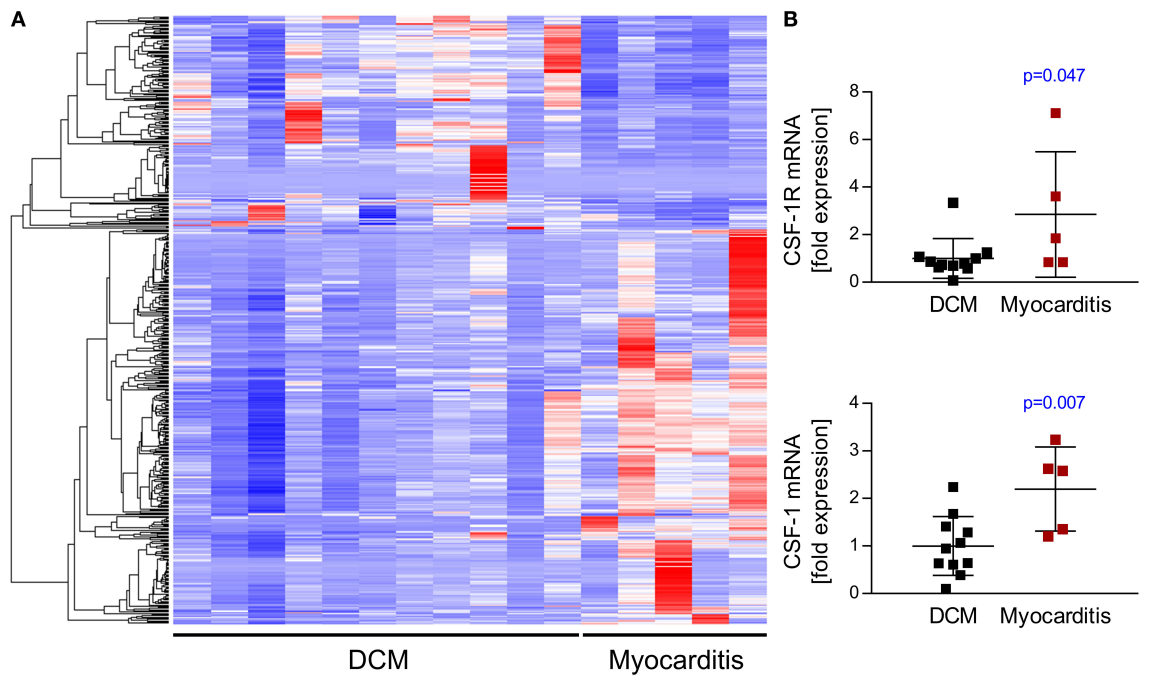

FIGURE 1 | Transcriptome analysis of endomyocardial specimen from patients with dilated cardiomyopathy and myocarditis**.** RNA-Sequencing data from endomyocardial biopsies obtained from patients with clinically diagnosed myocarditis or dilated cardiomyopathy as a control were analyzed for relative expression of different gene sets. **(A)** RNA-seq analyses revealed differential expression of 1963 genes. Heatmap depicts top 500 differentially expressed genes hierarchically clustered by using Euclidean distance measures. **(B)** CSF-1 and CSF-1R expression taken from RNA-seq data. Unpaired *t*-tests were used; *p*-values are indicated on the graph and significant differences ($p < 0.05$) are marked with blue color.

RESULTS

Increased Abundance of CSF-1 in Heart Muscle Tissue During Myocarditis/Inflammatory Cardiomyopathy

RNA-seq analyses revealed that myocarditis results in a diverse transcriptional response in the patient's heart tissue. We observed 1963 differentially expressed genes in biopsies taken from patients with acute myocarditis vs. patients with a non-inflammatory dilated cardiomyopathy (DCM) (**Figure 1A**). Gene set enrichment analysis (GSEA) revealed that a decent amount of differentially expressed genes participates in inflammatory processes (especially cytokines and cytokine receptors) and differentiation of hematopoietic cell lineages (**Table 1**). Myocarditis leads to a massive infiltration with immune cells into heart tissue. Monocytes represent the most prominent leukocyte population both during virus-mediated and experimental autoimmune myocarditis (16, 32). Monocyte production and maturation is strongly dependent on CSF-1 and CSF-1R, and, both effector molecules were identified in two gene sets mentioned above. Our data indicate a pronounced up-regulation particularly of CSF-1 and CSF-1R in endomyocardial specimen from patients with myocarditis/inflammatory cardiomyopathy (**Figure 1B**). Immunohistochemical stain of heart tissue from patients with myocarditis revealed CSF-1 expressing cells only within inflammatory foci, with a strong focus on mononuclear immune cells (**Figure 2A**). Altogether, these data argued toward a significant contribution of monocytes/macrophages to the cardiac CSF-1 expression, which we found in patients with inflammatory heart disease.

Local production of CSF-1 stimulates tissue-resident macrophage proliferation and reduces apoptosis (23). In addition to this function and a direct role of CSF-1 during monocyte development, it might also influence pro-fibrotic processes under inflammatory conditions. Since inflammation and fibrosis are hallmarks of inflammatory heart disease, we aimed to investigate the pathophysiological influence of CSF-1 with respect to manifestation of inflammatory heart tissue injury. First, we determined CSF-1 production in a mouse model of CVB3-induced myocarditis. We performed immunohistochemical stains to evaluate CSF-1 abundance during viral myocarditis. Consistent with our findings in patients, CSF-1 production was increased within inflammatory foci at the acute state of myocarditis in mice (**Figure 2B**). Since monocytes/macrophages represent the major infiltrating cell population in acute myocarditis, it is very likely that these cells are also involved in CSF-1 production. By double labeling immunohistochemistry we found CSF-1 protein expression in a part of Mac-3 positive mononuclear phagocytes within the cardiac inflammatory lesions (**Figure 2C**).

Nanoparticle-Encapsulated siRNA Effectively Downregulates CSF-1 Production in Monocytes

CSF-1 can be expressed and produced by various cells including monocytes themselves (22). siRNA encapsulated in lipid-based nanoparticles has been shown to effectively downregulate target genes in monocytes and their lineage progenitors (19, 20). Furthermore, *in vivo* knockdown of CSF-1R and monocyte depletion with nanoparticle-encapsulated siRNA has recently been demonstrated for ischemic heart disease (33). Thus, in order to investigate the pathophysiological function of CSF-1 production by monocytes/macrophages on inflammatory tissue damage during myocarditis, we decided to use a nanoparticle-encapsulated siRNA approach to target CSF-1 production in myeloid cells. To identify siRNAs leading to highly efficacious suppression of CSF-1 production, 24 different siRNAs targeting CSF-1 were investigated regarding their influence on CSF-1 mRNA levels *in vitro* (**Figure 3A**). Six different siRNAs, which yielded optimal *in vitro* suppression of CSF-1 mRNA production, were further investigated for their knockdown efficacy. Next, we screened the respective CSF-1 directed siRNA regarding to the concentration-dependent knockdown efficacy (**Figure 3B**) and selected the most efficacious siRNA for *in vivo* nanoparticle studies. Naive BALB/c mice were intravenously inoculated with

TABLE 1 | Top 10 C2 curated gene sets (KEGG Database) significantly enriched in human biopsies.

Gene set name (KEGG database)	Description	*p*-value	FDR *q*-value
CYTOKINE_CYTOKINE_RECEPTOR_INTERACTION	Cytokine-cytokine receptor interaction	2.11E−20	3.93E−18
SYSTEMIC_LUPUS_ERYTHEMATOSUS	Systemic lupus erythematosus	5.61E−19	5.22E−17
CELL_ADHESION_MOLECULES_CAMS	Cell adhesion molecules (CAMs)	1.3E−17	8.07E−16
HEMATOPOIETIC_CELL_LINEAGE	Hematopoietic cell lineage	2.08E−15	9.67E−14
VIRAL_MYOCARDITIS	Viral myocarditis	5.19E−14	1.93E−12
NEUROACTIVE_LIGAND_RECEPTOR_INTERACTION	Neuroactive ligand-receptor interaction	2.81E−13	8.71E−12
LEISHMANIA_INFECTION	Leishmania infection	4.67E−13	1.24E−11
COMPLEMENT_AND_COAGULATION_CASCADES	Complement and coagulation cascades	2.62E−11	6.1E−10
RIBOSOME	Ribosome	1.91E−10	3.96E−9
CHEMOKINE_SIGNALING_PATHWAY	Chemokine signaling pathway	2.61E−10	4.64E−9

RNA-Sequencing data of endomyocardial biopsies from patients with clinically diagnosed myocarditis or dilated cardiomyopathy as a control were analyzed for relative expression of different gene sets. Indicated are the names, description and p-values (with FDR-adjustment) of the most relevant gene sets.

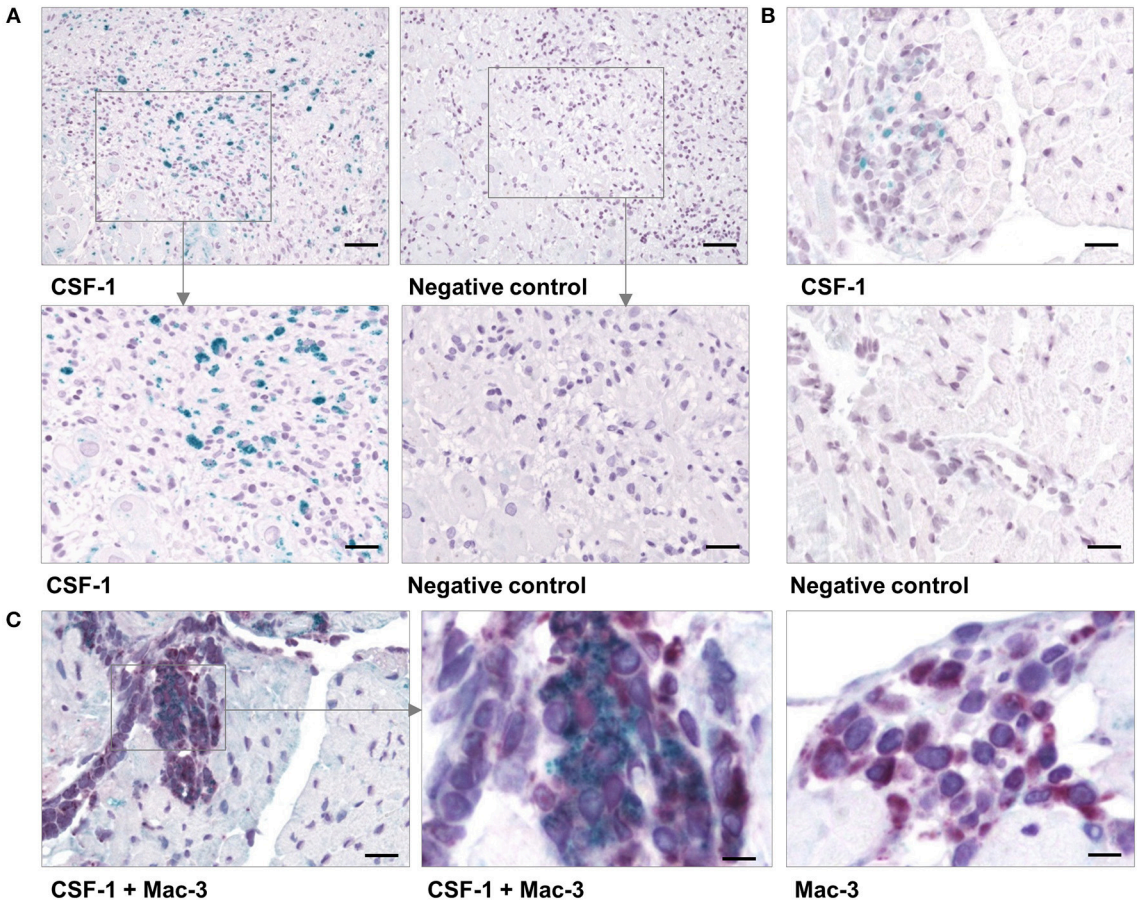

FIGURE 2 | CSF-1 production in cardiac tissue during viral myocarditis. Paraffin-embedded tissue sections from endomyocardial biopsies that had been obtained from patients with acute myocarditis were stained by immunohistochemistry. **(A)** Representative micrographs stained with an anti-CSF-1 antibody [left column] or with a secondary antibody only [right column] are depicted. top: scale bar = 120 μm; bottom: scale bar = 60 μm. **(B)** Heart tissue sections were obtained from CVB3-infected A.BY/SnJ mice on day 8 *p.i.* Representative micrographs of anti-CSF-1 stained heart tissue are shown [scale bar = 36 μm]. **(C)** In addition, cardiac sections from mice were double-stained with an antibody directed against Mac-3 (red) [left: scale bar = 36 μm; center: scale bar = 12 μm] and against CSF-1 (green). As control, Mac-3 stained tissue sections were counterstained omitting the anti-CSF-1 directed antibody [right: scale bar = 12 μm].

1 mg/kg of this nanoparticle-encapsulated siRNA (termed siCSF-1) on three consecutive days. Expression of CSF-1 was found to be effectively downregulated in monocytes that were sorted from spleen of siCSF-1 treated mice and further evaluated by quantitative PCR analysis (**Figure 3C**). Since pathogens are frequently involved in the pathogenesis of myocarditis (5), as a next step we set up an experimental approach to decipher the CSF-1 axis using nanoparticle-encapsulated siRNA in a mouse model of virus-mediated myocarditis. A.BY/SnJ mice with high hereditary susceptibility for the development of acute viral myocarditis (AVM) were treated with siCSF-1 or respective controls directly prior to infection with cardiotropic CVB3 (Nancy). siCSF-1 treatment was repeated every other day until mice were sacrificed 8 days after infection at the respective peak of infiltration in heart muscle (**Figure 3D**) (6–8). Following this protocol, we monitored the abundance of CSF-1 receptor levels in spleens of infected mice, which allowed us to conclude on the efficiency of siCSF-1 treatment during infection. Consistent with virus-mediated mobilization of monocytes/macrophages from bone-marrow sources, viral infection resulted in increased CSF-1R levels in the spleen. In siCSF-1-treated mice, we found reduced CSF-1R levels being indicative of suppressed myeloid cell mobilization upon siCSF-1 injection during AVM (**Figure 3E**).

siRNA-Mediated Knockdown of CSF-1 Attenuates Virus-Mediated Pathology

Since we found reduced mobilization of monocytes/macrophages in siCSF-1-treated mice during CVB3 infection, this mouse model allowed us to delineate the pathophysiological role of CSF-1 production particularly by monocytes/macrophages during viral myocarditis. First, we questioned whether siCSF-1 treatment manipulated the viral load during AVM. The viral burden as reflected by the amount of infectious viral particles (**Figure 4A**) was not substantially influenced by siCSF-1 in heart tissue at the acute state of infection. Thus, targeting the CSF-1 axis represents a safe approach regarding to control of virus dissemination and replication in A.BY/SnJ mice. During virus-mediated myocarditis, there is a strong spatial-temporal relation

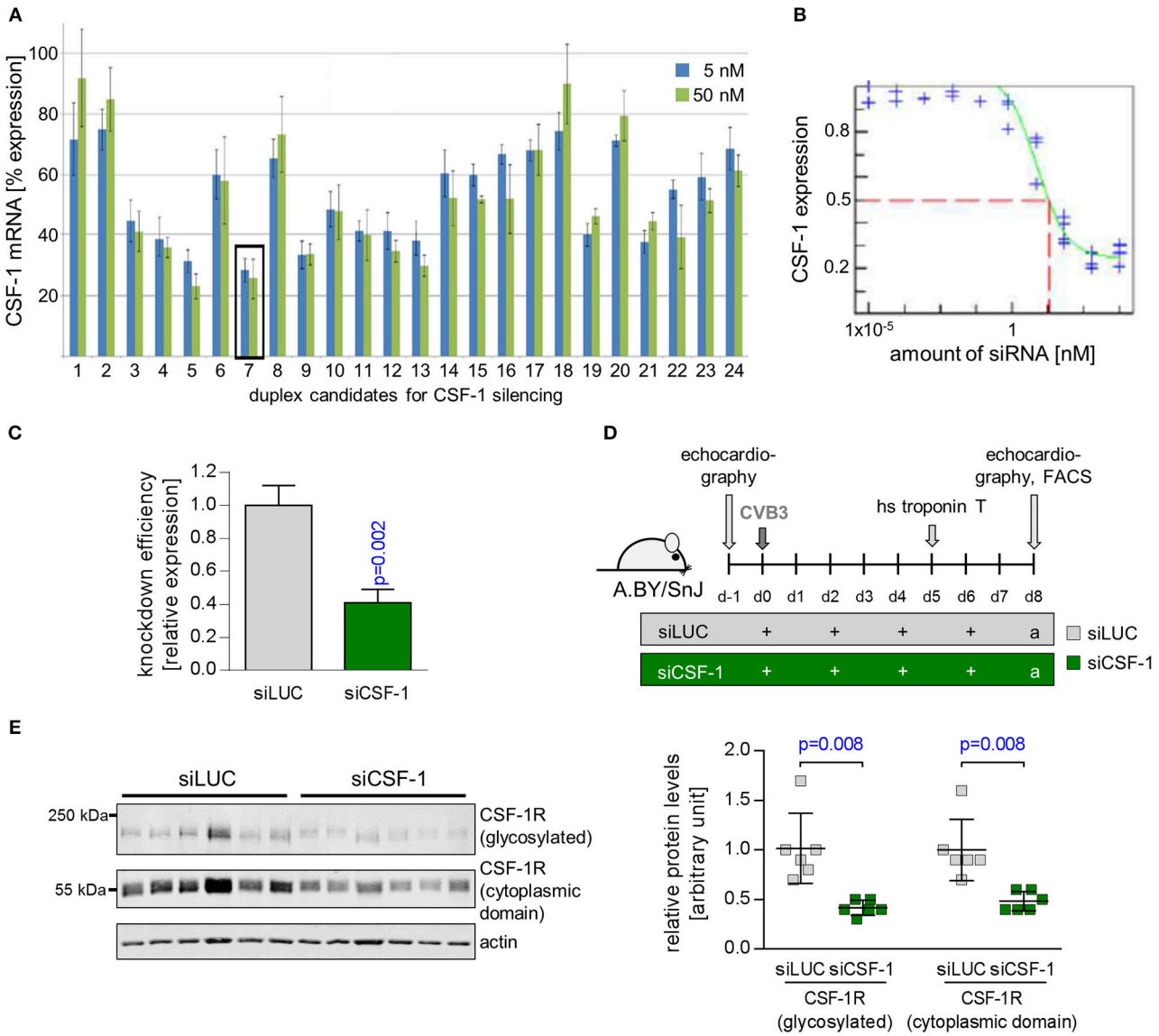

FIGURE 3 | Suppression of CSF-1 production by siRNA-encapsulated nanoparticles. **(A)** NIH-3T3 cells were transfected with 24 siRNA candidates directed against CSF-1. siRNA #7 was most efficient to reduce CSF-1 mRNA expression both at 5 and 50 nM and was selected for further studies. **(B)** CSF-1-directed siRNA # 7 was titrated and the respective CSF-1 knockdown efficacy was determined. **(C)** Knockdown efficacy of nanoparticle-encapsulated CSF-1 candidate siRNA pool 7 after injection into naive Balb/c mice ($n = 3$). **(D)** A.BY/SnJ mice were intravenously treated with nanoparticle encapsulated siRNA targeting either luciferase ($n = 7$ siLUC, gray color) or CSF-1 siRNA #7 ($n = 8$ siCSF-1, green color) directly prior to CVB3 inoculation. siRNA treatment was repeated after 2, 4, and 6 days. **(E)** The overall efficacy of siCSF-1 treatment during AVM as indicated by the presence of CSF-1-R)-positive cells was monitored by Western blot analysis of spleen tissue homogenates ($n = 6$ mice per group) 8 day after virus inoculation. CSF-1R (high molecular weight band) and the cytoplasmic domain of CSF-1R (around 55 kDa) are depicted. Fluorescence was quantified by the Image Studio Lite Ver 5.2 software. Signal intensity was normalized to actin and is depicted as relative expression levels compared to siLUC-treated mice in the bar graph. Unpaired *t*-tests were used; *p*-values are indicated on the graph and significant differences ($p < 0.05$) are marked with blue color.

between virus-induced cellular injury and the emergence of inflammatory foci in heart tissue (39). Likewise, viral genome abundance as detected by CVB3 *in situ* hybridization was spatially connected with high-grade inflammation and most impressive in siLUC-treated mice (**Figure 4B**). Since CVB3 does not only target the heart, but also replicates in the pancreas, we also determined the magnitude of virus-induced pancreas destruction and found similar tissue injury in both siLUC- and siCSF-1-treated groups (**Figure S1**).

Next, CVB3-infected mice that received siCSF-1 or siLUC as a control were followed for global signs of acute infection. siCSF-1 treatment profoundly attenuated overall virus-induced pathology as represented by significantly less pronounced body weight reduction (**Figure 4C**) and only a minor loss of body temperature

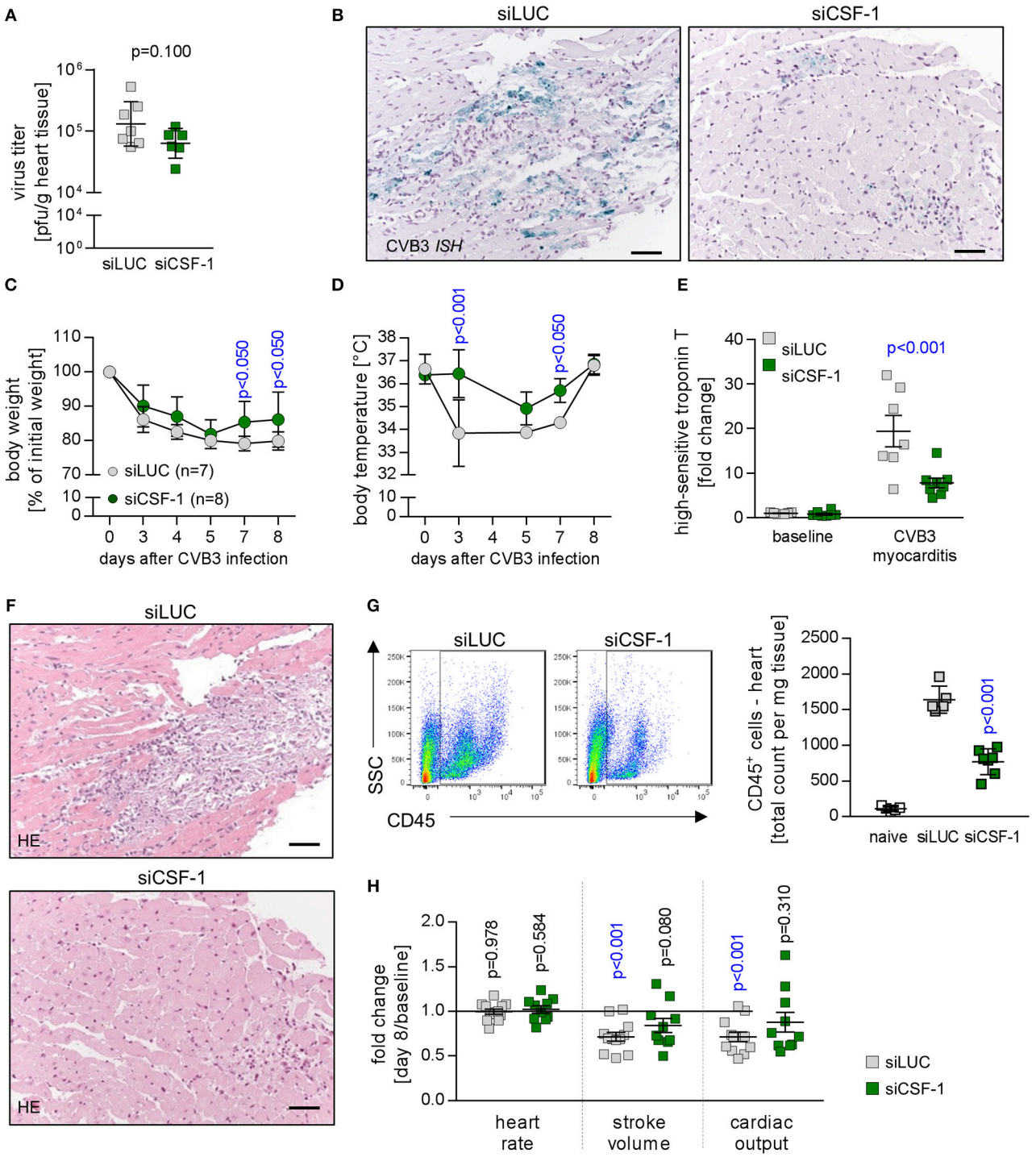

FIGURE 4 | Depletion of CSF-1 attenuates virus-mediated pathology. Mice with AVM were subjected to CSF-1 siRNA treatment as indicated in **Figure 3D**. **(A)** Infectious virus particles were determined in heart tissue homogenates by plaque assay. Data summary is mean ± SEM. A student's *t*-test was conducted and the *p*-value is shown. **(B)** To localize viral RNA in infected heart tissue, *in situ* hybridization for the detection of the CVB3 genome was performed and slides were counterstained with hematoxylin/eosin. Representative micrographs are depicted (scale bar = 60 μm). During viral infection, mice were monitored for body weight **(C)** and body temperature **(D)** at the indicated points in time. Dots represent mean ± SEM. Repeated measurements versions of two-way ANOVA were performed followed by a Sidak- Holm multiple comparison procedure. P values are indicated (blue color indicates $p < 0.05$; only significant results are depicted on the graph). **(E)** To assess injury of cardiomyocytes prior to peak of inflammation, blood was sampled 5 days after infection by facial vein puncture and high sensitive (hs) troponin T plasma levels were determined. Obtained results were normalized to the results obtained with blood samples from non-infected siLUC-treated mice and are depicted

(Continued)

FIGURE 4 | as fold changes. Data summary is mean + SD. Repeated measurements two-way ANOVA was performed followed by a Sidak-Holm's multiple comparison test and the p value is depicted. **(F)** After sacrificing mice 8 days after infection, heart tissue sections were stained with hematoxylin/eosin. **(G)** To quantify cell infiltration, single cell suspensions of heart tissue obtained from naive mice (uninfected mice that did not receive siRNA treatment; white bars, $n = 4$) as well as AVM and siRNA-treated mice (siLUC: gray squares, $n = 7$; siCSF-1: green squares, $n = 8$) were stained with CD45 antibodies to quantify total leukocyte count in the heart. **(H)** Cardiac function was assessed by echocardiography prior to CVB3 infection in A.BY/SnJ mice (baseline) by an experienced and blinded investigator. Mice were allocated to respective groups: siLUC and siCSF-1. In all CVB3-infected mice, echocardiography was repeated 8 days after CVB3 infection (siLUC $n = 16$; siCSF-1 $n = 17$ mice). Data were analyzed regarding putative alteration during AVM in the respective treatment groups (day 8 after infection vs. baseline measurements of the same cohort). Relative changes of stroke volume, heart rate and cardiac output compared to baseline measurements were calculated for each group and these fold changes are depicted for siLUC and siCSF-1-treated groups. One-sample *t*-tests were performed to compare baseline measurements and values obtained 8 days after infection. All p values are depicted, $p < 0.05$ are in blue color.

during infection in comparison to controls that received siLUC (**Figure 4D**). Overall diminution of virus-mediated pathology under siCSF-1 influence was further corroborated by a significant reduction of cardiac troponin T serum levels as a heart-specific sign of tissue damage (**Figure 4E**). Cardiac troponin T at an early state of myocarditis might reflect both direct virus-induced cytotoxicity and tissue destruction by innate mediators of the immune response. In line with this, analysis of heart tissue obtained from siCSF-1 treated animals sacrificed 8 days p.i. revealed distinct differences. Histological staining of heart tissue (**Figure 4F**) demonstrated a profound myocarditis in siLUC-treated A.BY/SnJ mice and in contrast to that only moderate signs of myocarditis after siCSF-1 treatment. Since viral injury of cardiomyocytes provokes an inflammatory response that significantly contributes to tissue damage and functional impairment of the heart (32), next we quantified infiltration with $CD45^+$ immune cells into hearts from siCSF-1 and siLUC-treated mice by flow cytometry. We found a significant reduction of infiltrating leucocytes in siCSF-1 treated mice (**Figure 4G**), thus indicating reduced inflammatory organ damage under suppression of the CSF-1 axis. Following up on observed systemic and heart-tissue specific responses to siCSF-1 treatment, siCSF-1 effects on cardiac performance were assessed by echocardiography during the inflammatory peak of viral myocarditis. In siLUC-treated, infected A.BY/SnJ mice, both the stroke volume and cardiac output were significantly reduced in comparison to baseline measurements (**Figure 4H**) and **Table S1**. Consistent with its heart-directed effects, siCSF-1 treatment mitigated these detrimental changes and CVB3 infection in this group resulted only in minor, non-significant reduction of cardiac performance (**Table S1**).

siRNA-Mediated Knockdown of CSF-1 Diminishes Immune Cell Infiltration During Acute Viral Myocarditis

As a next step, we aimed to determine whether siCSF-1 specifically influenced infiltration with monocytes/macrophages or whether other immune cells were affected as well. Immunohistochemistry using antibodies directed against marker proteins for myeloid (Mac3) and T cells (CD3 and CD4) indicated reduced infiltration of these respective immune cell populations in siCSF-1-treated mice during AVM (**Figures 5A,B**). These findings were corroborated by the results obtained from a quantitative flow cytometry-based analysis of the different immune cell populations in infected mouse hearts. We detected 756 ± 63 $CD11b^+$/$lineage^-$ cells in siLUC- vs. 273.3 ± 30.8 $CD11b^+$/$lineage^-$ cells/mg heart tissue in siCSF-1 treated mice ($p < 0.0001$) and 198 ± 34 T cells in siLUC- vs. 95 ± 12 T cells/mg heart tissue in siCSF-1 treated mice ($p = 0.02$; **Figures 5C,E**). The vast majority of infiltrating myeloid cells belonged to the pool of inflammatory monocytes (**Figure 5D**). Consistent with the influence of CSF-1 on monocyte recruitment and differentiation, inflammatory monocytes were highly significantly reduced in infected mouse hearts upon siCSF-1 treatment. siCSF-1 also led to a significant reduction of patrolling monocytes, macrophages and dendritic cells (**Figure 5D**), which might all originate from inflammatory monocytes. In correspondence to previous reports (15), the pool of invading T cells during AVM was majorly comprised of $CD4^+$ T cells. Comparable to siCSF-1-induced effects on myeloid cell infiltration, we also found a significant reduction of the $CD4^+$ T cell count in heart tissue upon siCSF-1-treatment (**Figure 5E**).

siRNA-Mediated Knockdown of CSF-1 Mitigates Inflammatory Heart Tissue Damage in a Mouse Model of Experimental Autoimmune Myocarditis

siCSF-1 treatment impressively improved cardiac function upon mitigating the inflammatory damage response during acute viral myocarditis. A high inflammatory disease burden at the acute state might directly translate into the manifestation of a chronic functional impairment. Long-term sequela of acute myocarditis involve cardiac remodeling processes with substantial fibrosis formation and a reduction of systolic cardiac function (4). Experimental autoimmune myocarditis (EAM) represents an excellent model that enables researchers to follow inflammatory disease progression from acute to chronic states of myocardial dysfunction (40). Therefore, we investigated the pathophysiological role of CSF-1 also in EAM, and started siCSF-1 treatment upon manifestation of myosin-heavy chain-directed autoimmunity 14 days after the first immunization (**Figure 6**). This application strategy might also be considered as a therapeutic regime starting upon manifestation of acute disease. Similar to the AVM model, intravenous siCSF-1 nanoparticle application was repeated every 48 h for a 1-week course. First, we performed a quantitative flow cytometry-based analysis of inflammatory monocytes in the injured hearts directly after this siCSF-1 treatment period. As expected from our results obtained in AVM, we indeed found a reduced number of inflammatory $Ly6C^{high}$ monocytes in siCSF-1-treated animals compared to the siLUC-treated controls during EAM (**Figure 6B**). To investigate

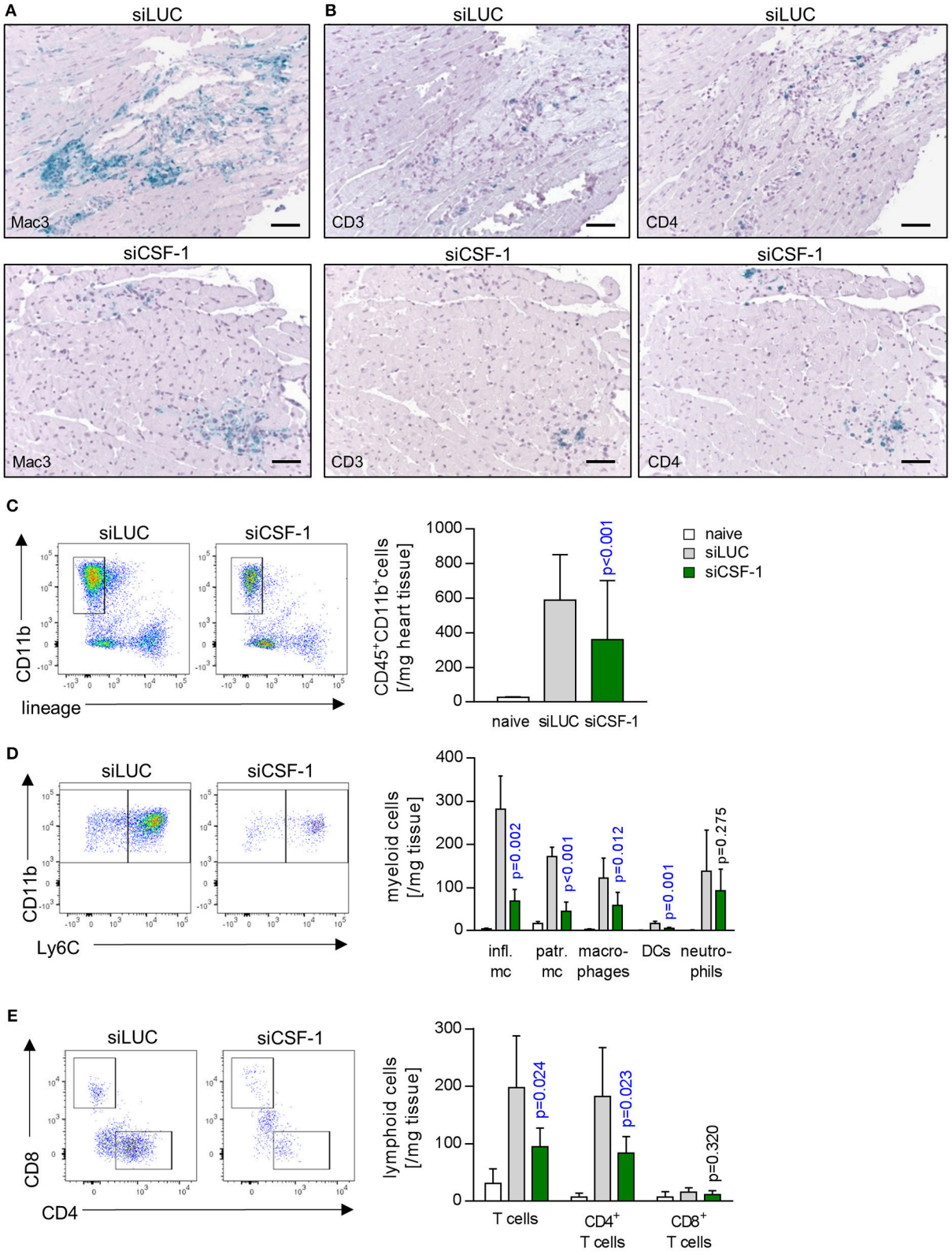

FIGURE 5 | Influence of CSF-1 on immune cell infiltration into heart tissue during AVM. To further differentiate immune cell infiltration, immunohistochemical stain for **(A)** mononuclear phagocytes using antibodies directed against Mac-3 and **(B)** T-cells using antibodies directed against CD3 and CD4 were performed (scale

(Continued)

FIGURE 5 | bars = 60 μm). Further differentiation by flow cytometry (**Figure S2**) was performed. **(C)** Total infiltrating myeloid cells (identified as $CD45^+$, $CD11b^+$, lymphoid lineage$^-$ life single cells) were quantified. **(D)** Myeloid cells were further differentiated according to the gating strategy depicted in **Figure S2A**. **(E)** Equally, lymphoid cells were further analyzed. Representative flow cytometry dot blots of siLUC- and siCSF-1-treated groups are depicted. Unpaired *t*-tests were performed between siLUC- and siCSF-1-treated groups and *p*-values are shown. Significant differences ($p < 0.05$) are marked with blue color.

whether CSF-1 promotes monocyte development from bone-marrow sources during EAM, we next evaluated the influence of CSF-1 knockdown on granulocyte-monocyte progenitor (GMP) cell numbers. siRNA-mediated knockdown of CSF-1 led to markedly increased numbers of GMPs in the bone marrow during EAM (**Figure 6C**). However, proliferation rates of GMPs did not differ significantly between siLUC- and siCSF-1-treated groups (**Figure 6D**). To further validate that CSF-1 knockdown leads to an arrest of progenitor cells in the bone marrow, we measured myeloid cell numbers in the blood and found reduced numbers 21 days after EAM induction (**Figure 6E**).

Based on our finding of reduced infiltration with inflammatory monocytes upon siCSF-1 treatment, next we followed mice for a total of 30 days after EAM induction and determined the formation of fibrotic scars as an integral hallmark of cardiac remodeling at this chronic disease state (**Figure 7A**). Knockdown of CSF-1 production resulted in a significant reduction of fibrosis formation in the heart muscle as indicated by quantitative assessment of Masson's trichrome stains (**Figure 7B**). Consistent with this reduction of long-term, inflammation-mediated tissue damage in the siCSF-1 group, functional investigation of cardiac performance by echocardiography revealed an improved ejection fraction in siCSF-1-treated animals compared to siLUC-treated control animals (**Figure 7C**). Chronic disease in siLUC-treated mice was mirrored by a substantial reduction of cardiac contractility. As a proof of principle, we also tested whether knockdown of CSF-1R expression could exert similar effects during disease course. Therefore, upon establishment of autoimmune myocarditis mice were treated with a nanoparticle-encapsulated siRNA that specifically targets CSF-1R (33). Formation of cardiac fibrosis assessed 30 days after EAM induction was found to be diminished in comparison to siLUC-treated controls, and was reduced to similar levels as achieved by siCSF-1-treatment (**Figure 7B**). Likewise, echocardiographic imaging of siCSF-1R-treated animals demonstrated significant improvement of cardiac performance as indicated by higher left ventricular ejection fraction in comparison to siLUC nanoparticle-treated animals (**Figure 7C**). Altogether, our data demonstrate that silencing the CSF-1 axis hampers monocyte development and substantially mitigates inflammatory heart tissue damage both in a mouse model of viral and autoimmune-mediated myocarditis. Moreover, initiation of CSF-1 knockdown upon manifestation of inflammatory tissue damage attenuates the manifestation of debilitating long-term sequela of acute inflammatory injury, and this parallels in preserved systolic contractility of the heart muscle (**Figure 8**).

DISCUSSION

One of the major causes of heart failure particularly in young patients is myocarditis. Direct viral cytotoxicity stimulates infiltration and immune response activation leading to pathogen clearance and resolution of organ damage. Nevertheless, in immune-genetically predisposed individuals there is also an adverse scenario where pathogen-induced immune response activation subsequently induces overwhelming inflammatory cytokine response and detrimental immunopathology or autoimmune processes, both leading to cardiac remodeling and fibrotic scarring. It appears to be a slim line between the induction of inflammation to fight the virus and exaggerated immune responses that begin to be deleterious. We here downregulated an important branch of the innate immunity—the development of monocytes/macrophages—by siCSF-1 treatment for approximately a week during the acute phase of a viral infection, yet found no impairment on pathogen control. In fact, silencing CSF-1 production impressively mitigated acute inflammatory heart tissue damage and attenuated the development of a debilitating long-term sequela of acute inflammatory injury to the heart. This nanoparticle-mediated immune-modulation improved the course of disease both in acute viral myocarditis and autoimmune inflammatory heart disease and importantly, did not adversely influence viral burden and clearance of infectious particles. As it might be hypothesized that attenuating inflammatory activity could allow for enhanced virus-induced cell death, this is not what we observed with siCSF-1 treatment. Our finding is in line with previous data: out of 46 studies that intervened the immune response, more than 90% found no adverse effect on viral load (4). In line with this, we could recently demonstrate that inhibition of cellular proteolysis in immune cells by the immunoproteasome inhibitor ONX 0914 is highly efficient to reverse high grade AVM and this protective effect was attributed to maintained immune cell homeostasis, but not to direct antiviral aspects (14).

A.BY/SnJ mice that were used in this study for AVM are characterized by a high hereditary susceptibility to CVB3-induced cardiomyopathy (6, 15, 41). Upon viral infection of cardiomyocytes, heart tissue injury during the first days is mainly attributed to direct virus-induced cytotoxicity, while the activation of local type I interferon responses (T1IFN) is substantially hampered in this strain (7, 8). This phase of ongoing viral replication is accompanied and succeeded by the recruitment of cells of the innate immune response such as NK cells and monocytes (42). Later on, infiltration with immune cells of the adaptive immune response such as T and B cells follows (15). Analysis of the composition of leukocytes in the heart revealed that 8 days after viral infection a general reduction in invading immune cells was observed which suggests that hampering early responders, such as monocytes e.g., by reduced production of lymphocyte-attracting chemokines might dampen the infiltration and activation of subsequent populations as well. Although we found an overall reduction of $CD4^+$ T cells in the heart in siCSF-1 treated mice, we cannot conclude on the influence of silencing the CSF-1 axis on $CD4^+$ T cell

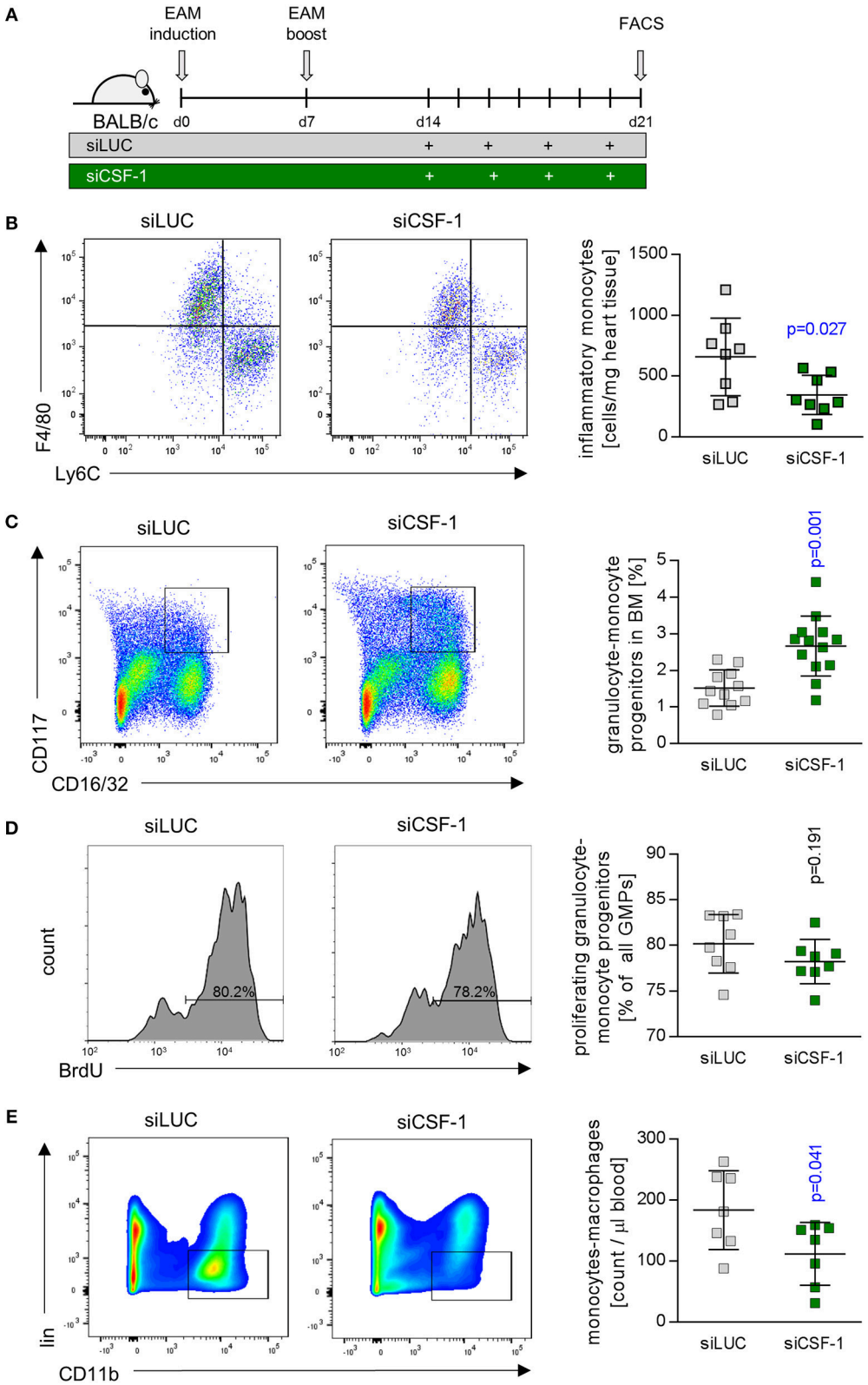

FIGURE 6 | CSF-1 silencing during EAM diminishes infiltration of inflammatory monocytes into injured mouse hearts. **(A)** EAM was induced by inoculation of myosin peptide in conjunction with Freud's adjuvant and mice were boosted after 7 days. Nanoparticle-encapsulated CSF-1 siRNA #7 (**Figure 3**) was investigated regarding

(Continued)

FIGURE 6 | to its potential to manipulate EAM in comparison to siLUC (control). Therefore, mice were treated with 0.5 mg/kg siRNA intravenously every other day starting 14 days after EAM induction, and mice were sacrificed 21 days after the first immunization. **(B)** Representative dot plots (left) and enumeration (right) of inflammatory Ly6C^{hi} monocytes in heart tissue of siLUC- and siCSF-1-treated mice ($n = 8$). **(C)** Representative dot plots (left) and quantification of granulocyte-monocyte progenitors (GMPs) (right) found in bone marrow of siLUC- and siCSF-1-treated mice during EAM ($n = 12$). **(D)** Representative FACS plots (left) and quantification (right) of BrdU incorporation in GMPs of the bone marrow in siLUC- and siCSF-1 treated mice ($n = 8$). **(E)** Representative FACS density plots (left) and quantification of monocytes/macrophages (right) in the blood of siLUC- and siCSF-1- treated mice ($n = 7$). Unpaired *t*-tests were used. *p*-values are indicated on the graph and significant differences ($p < 0.05$) are marked with blue color.

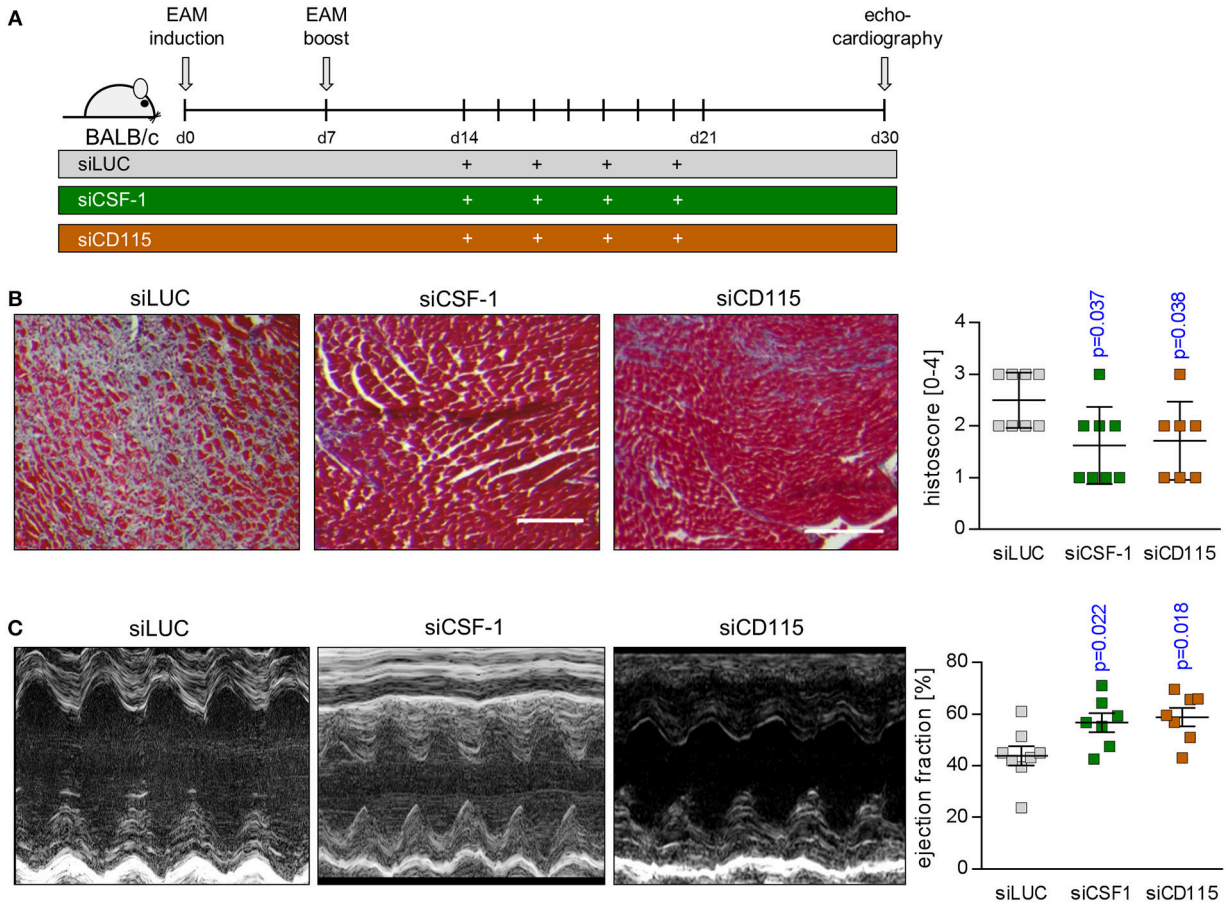

FIGURE 7 | siRNA-mediated knockdown of CSF-1 during acute EAM attenuates the development of chronic disease states**. (A)** EAM induction and siRNA treatment was conducted as shown in **A**. Mice were sacrificed after 30 days. **(B)** Representative Masson's trichrome stains of heart tissue sections obtained 30 days after EAM induction are depicted (left: scale bar = 150 nm). Fibrosis was scored microscopically ($n = 8$ for siLUC and siCSF-1 as well as $n = 7$ for siCSF-1R). **(C)** Heart function was evaluated 30 days after the initial immunization by echocardiography. Representative M-mode echocardiographic images are shown during late state EAM. Calculated left ventricular ejection fraction (EF) ($n = 8$ for siLUC and siCSF-1 as well as $n = 7$ for siCSF-1) is shown. One-way-ANOVA was performed. Since ANOVA was significant, a Sidak-Holm-multiple comparison was performed. *p*-values of multiple comparison are indicated. Blue color indicates $p < 0.05$.

differentiation e.g., into regulatory T cells or Th1 and Th17 cells. From our data we cannot conclude on possible additional effects e.g., of regulatory CD4$^+$ T cells that are known to mitigate the inflammatory tissue damage in the heart (43, 44). CSF-1 facilitates myeloid cell differentiation, monocyte survival, and macrophage proliferation. It was recently shown that CSF-1R also plays a role in splenic monocytopoiesis (33). Monocytes are also important producers of CSF-1 themselves. Hume and MacDonald suggested that modulation of the CSF-1 axis may be beneficial under pathological conditions (45). We here show that siRNA-mediated knockdown of CSF-1 in monocytes and its imminent precursors leads to a significant reduction of inflammatory Ly6C^{hi} monocyte numbers in the inflamed heart. We speculate that this observation results from arresting the CSF-1-dependent monocyte/myeloid cell development at precursor stages. This hypothesis is supported by detection of increased GMP cell numbers in the bone marrow in siCSF-1-treated animals during EAM. Although increased cell numbers may also arise from increased proliferation rates, this situation seems to be unlikely, since the percentages of proliferating GMPs in the bone marrow of siCSF-1- and siLUC-treated animals did not differ. Consistently, the numbers of myeloid cells were reduced

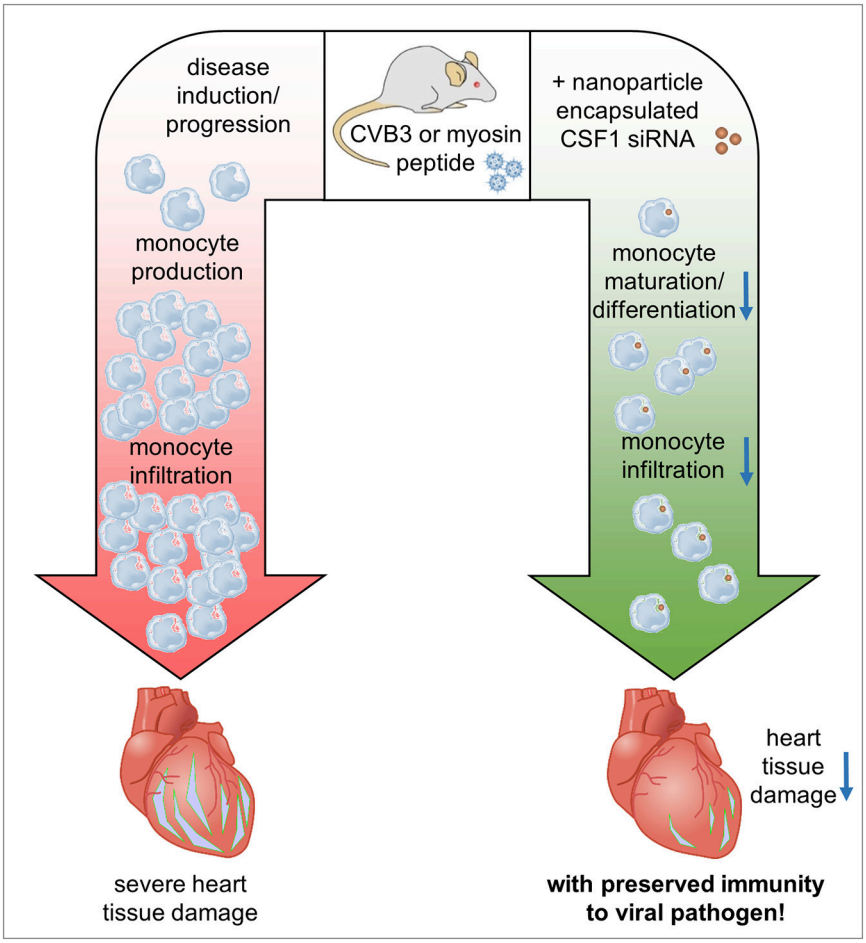

FIGURE 8 | Graphical synopsis: The CSF-1 axis is induced in patients with acute myocarditis. Based on the preponderant role of CSF-1 for monocyte differentiation/maturation and the disease-modifying function of monocytes during the course of inflammatory heart disease, we investigated how silencing of CSF-1 in monocytes/macrophages using nanoparticle encapsulated siRNA influences heart tissue damage during the onset of acute viral myocarditis and upon manifestation of acute inflammation in an autoimmune myocarditis model. Silencing of the myeloid CSF-1 axis was beneficial for preventing inflammatory tissue damage in the heart and preserving cardiac function at acute and chronic disease states without compromising innate immunity's critical defense mechanisms.

in the blood stream of siCSF-1-treated animals during EAM. In agreement with this and the fact that other than in siLUC-treated mice enhanced monocyte counts were not observed in the blood in siCSF-1-treated mice during AVM (data not shown), we found a reduction of CSF-1R abundance in the spleen during AVM in the siCSF-1 group. The spleen itself is a source for monocytes with local production and from which they are recruited to the site of inflammation (34). CSF-1R is expressed throughout the mononuclear phagocyte system, which is primarily composed of monocytes and macrophages (22, 46). A reduction of CSF-1R expression might also be indicative for reduced numbers of monocytes and macrophages. These findings further underscore our assumption of a halted monocyte/macrophage production due to CSF-1 knockdown during inflammation. Mice that carry a deleterious mutation in CSF-1 develop characteristic skeletal malformation, caused by defective osteoclasts. In the context of an inflammatory disease, such as atherosclerosis however, deletion of CSF-1 results in dramatically reduced atherosclerotic plaque size (47, 48). After myocardial infarction an upregulation of CSF-1 is observed in ischemic areas for more than 5 days after the injury (49). In this context, CSF-1 also appears to exhibit indirect effects by regulating chemokine production (49). In the absence of CSF-1, GM-CSF controls the differentiation of selected macrophage subsets and may lead to an enhancement of macrophage lineage numbers (50). Under certain conditions, GM-CSF induces an inflammatory program marked by increased IL-1, IL-6 and TNF-α secretion, whereas the presence of CSF-1 suppresses the production of pro-inflammatory signals (51). Others have reported that administration of CSF-1 in EAM between days 21 and 29 after disease induction ameliorated cardiac fibrosis and left ventricular dysfunction by preventing the accumulation of fibroblasts (52). Notably, no effects were observed in the above mentioned study when CSF-1 was administered at later stages. These conflicting results stress the importance of timing in CSF-1 modulation. The reduced numbers of inflammatory

monocytes due to silencing myeloid CSF-1 from days 14 to 21 observed in this study may outweigh the beneficial effects of CSF-1 in the inflamed heart at these early stages. In addition, macrophages have been shown to release pro-fibrotic cytokines such as TGF-β, which causes the differentiation of fibroblasts to myofibroblasts and a massive deposition of extracellular matrix proteins such as collagens (53). Since we see a reduction of myeloid cells during myocarditis in response to siCSF-1 treatment and this includes macrophages, we propose that thereby achieved reduction of pro-fibrotic signals most likely contributes to lower scar formation as observed at advanced states of EAM.

It has been reported that other cell types beyond cells of the myeloid lineage are capable of CSF-1 expression under inflammatory conditions, including fibroblasts and endothelial cells (54, 55). These cells may also influence monocyte production/proliferation during myocarditis. Nevertheless, at the acute state of virus-mediated myocarditis, we observed that Mac-3 positive cells like monocytes/macrophages, which infiltrate the heart, may represent the main producers of CSF-1. Many studies using different pathogenic models of bacterial, viral and fungal infections have highlighted the importance and requirement of TNF- and NO-producing monocytes as facilitators of the resolution of an infection (56). Also, during inflammation bone-marrow derived monocytes can mature into macrophages (56) and macrophage-depletion results in increased virus titers in infected mouse hearts (17). Therefore, it was somewhat surprising at the first glance that depletion of monocytes upon siCSF-1 treatment actually improved virus-mediated pathology. We found no experimental evidence that virus dissemination, control and elimination had been adversely affected by such immune-modulating intervention. Since virus titers were not significantly influenced by siCSF-1-treatment, the impressively reduced inflammatory injury and preserved cardiac function in this group is not influenced by direct virus-mediated effects. These data suggest that virus-induced inflammation can be segregated from pathways that promote and limit virus infection and CSF-1-induced monocyte maturation. Monocytes can be directly activated by CVB3 infection resulting in the production of pro-inflammatory cytokines (57). Thereby, these cells can contribute to a strong inflammatory response and eventual tissue damage in the myocardium. Further experimental evidence for an adverse function of myeloid immune cells comes from macrophage depletion studies, where myocardial injury and formation of cardiac fibrosis were substantially diminished despite and in clear contrast to increased viral burden during AVM (17). Interestingly and in line with our findings in siCSF-1 treated A.BY/SnJ mice, macrophage depletion did not adversely affect clearance of infectious virus particles (17). We conclude that attenuated innate immune cell mobilization and hampered CSF-1-driven differentiation of innate myeloid cells in siCSF-1-treated mice directly suppresses cytotoxicity induced by cytokine production and/or infiltration with lymphocytes in viral myocarditis. Although there is a clear causal relationship between T1IFN-mediated suppression of viral load in infected cardiac cells and attenuation of inflammation and chronic tissue damage (8, 32), several publications including work of our group support the concept that—independent of direct virus-induced cell injury—particularly monocytes and macrophages are important players in inflammation and chronic organ damage in response to Coxsackievirus infection (4, 14, 58, 59).

Taken together, modulation of the CSF-1 axis in the myeloid cell lineage with siRNAs at early stages has beneficial acute and long-term effects in both viral and autoimmune myocarditis. Our data support the notion that particularly infiltrating myeloid cells contribute to acute and chronic functional impairment in inflammatory heart disease. Since pathogen control was not influenced upon suppression of the CSF-1 axis in myeloid cells, this study yields important insights for translating the pathophysiological role of CSF-1 from animal models to putative novel therapeutic targets for patients with inflammatory heart disease.

ETHICS STATEMENT

The requested information is provided in the material and method section of the manuscript.

AUTHOR CONTRIBUTIONS

AB and FL conceptualization. AB, FL, IM, CG, MK, MS, BM, JH, and KK methodology. IM, CG, KK, MS, AH, VE, H-PV, DA, JH, and MK investigation. IM and CG formal analysis. CG and IM visualization. FL, AB, IM, and CG writing-original draft. HK drafting/revising critically. AB, FL, and HK funding acquisition. AB and FL supervision.

FUNDING

AB is supported by the Foundation for Experimental Biomedicine Zurich, Switzerland. CG received a MD scholarship from the Berlin Institute of Health. This project was additionally supported by DFG VO 1602/4-1 to AB, DFG KL 595/2-3 to KK, and CRC 1292/project 2 to AB. FL is supported by the DZHK (German Centre for Cardiovascular Research), the German Research Foundation (DFG, LE 2530/2-1), the German Heart Research Foundation, and the BMBF (German Ministry of Education and Research; Project DeCaRe).

ACKNOWLEDGMENTS

We appreciate the excellent technical support of Anika Lindner, Karolin Voß and Sandra Bundschuh, Stefanie Schelenz und Martin Taube. We acknowledge support from the German Research Foundation (DFG) and the Open Access Publication Fund of Charité–Universitätsmedizin Berlin.

SUPPLEMENTARY MATERIAL

The Supplementary Material for this article can be found online at: https://www.frontiersin.org/articles/10.3389/fimmu.2018.02303/full#supplementary-material

REFERENCES

1. Cooper LT Jr. Myocarditis. *N Engl J Med.* (2009) 360:1526–38. doi: 10.1056/NEJMra0800028
2. Feldman AM, Mcnamara D. Myocarditis. *N Engl J Med.* (2000) 343:1388–98. doi: 10.1056/NEJM200011093431908
3. Sagar S, Liu PP, Cooper LT Jr. Myocarditis. *Lancet* (2012) 379:738–47. doi: 10.1016/S0140-6736(11)60648-X
4. Corsten MF, Schroen B, Heymans S. Inflammation in viral myocarditis: friend or foe? *Trends Mol Med.* (2012) 18:426–37. doi: 10.1016/j.molmed.2012.05.005
5. Epelman S, Liu PP, Mann DL. Role of innate and adaptive immune mechanisms in cardiac injury and repair. *Nat Rev Immunol.* (2015) 15:117–29. doi: 10.1038/nri3800
6. Szalay G, Meiners S, Voigt A, Lauber J, Spieth C, Speer N, et al. Ongoing coxsackievirus myocarditis is associated with increased formation and activity of myocardial immunoproteasomes. *Am J Pathol.* (2006a) 168:1542–52. doi: 10.2353/ajpath.2006.050865
7. Jakel S, Kuckelkorn U, Szalay G, Plotz M, Textoris-Taube K, Opitz E, et al. Differential interferon responses enhance viral epitope generation by myocardial immunoproteasomes in murine enterovirus myocarditis. *Am J Pathol.* (2009) 175:510–8. doi: 10.2353/ajpath.2009.090033
8. Rahnefeld A, Ebstein F, Albrecht N, Opitz E, Kuckelkorn U, Stangl K, et al. Antigen-presentation capacity of dendritic cells is impaired in ongoing enterovirus myocarditis. *Eur J Immunol.* (2011) 41:2774–81. doi: 10.1002/eji.201041039
9. Neumann DA, Rose NR, Ansari AA, Herskowitz A. Induction of multiple heart autoantibodies in mice with coxsackievirus B3- and cardiac myosin-induced autoimmune myocarditis. *J Immunol.* (1994) 152:343–50.
10. Rose NR. Myocarditis: infection versus autoimmunity. *J Clin Immunol.* (2009) 29:730–7. doi: 10.1007/s10875-009-9339-z
11. Leuschner F, Katus HA, Kaya Z. Autoimmune myocarditis: past, present and future. *J Autoimmun.* (2009) 33:282–9. doi: 10.1016/j.jaut.2009.07.009
12. Caforio AL, Pankuweit S, Arbustini E, Basso C, Gimeno-Blanes J, Felix SB, et al. Current state of knowledge on aetiology, diagnosis, management, and therapy of myocarditis: a position statement of the European Society of Cardiology Working Group on Myocardial and Pericardial Diseases. *Eur Heart J.* (2013) 2636-48, 2648a-2648d. doi: 10.1093/eurheartj/eht210
13. Kindermann I, Kindermann M, Kandolf R, Klingel K, Bultmann B, Muller T, et al. Predictors of outcome in patients with suspected myocarditis. *Circulation* (2008) 118:639–48. doi: 10.1161/CIRCULATIONAHA.108.769489
14. Althof N, Goetzke CC, Kespohl M, Voss K, Heuser A, Pinkert S, et al. The immunoproteasome-specific inhibitor ONX 0914 reverses susceptibility to acute viral myocarditis. *EMBO Mol Med.* (2018) 10:200–18. doi: 10.15252/emmm.201708089
15. Klingel K, Hohenadl C, Canu A, Albrecht M, Seemann M, Mall G, et al. Ongoing enterovirus-induced myocarditis is associated with persistent heart-muscle infection - quantitative-analysis of virus-replication, tissue-damage, and inflammation. *Proc Natl Acad Sci USA* (1992) 89:314–8. doi: 10.1073/pnas.89.1.314
16. Afanasyeva M, Georgakopoulos D, Belardi DF, Ramsundar AC, Barin JG, Kass DA, et al. Quantitative analysis of myocardial inflammation by flow cytometry in murine autoimmune myocarditis: correlation with cardiac function. *Am J Pathol.* (2004) 164:807–15. doi: 10.1016/S0002-9440(10)63169-0
17. Jaquenod De Giusti C, Ure AE, Rivadeneyra L, Schattner M, Gomez RM. Macrophages and galectin 3 play critical roles in CVB3-induced murine acute myocarditis and chronic fibrosis. *J Mol Cell Cardiol.* (2015) 85:58–70. doi: 10.1016/j.yjmcc.2015.05.010
18. Zimmermann O, Homann JM, Bangert A, Muller AM, Hristov G, Goeser S, et al. Successful use of mRNA-nucleofection for overexpression of interleukin-10 in murine monocytes/macrophages for anti-inflammatory therapy in a murine model of autoimmune myocarditis. *J Am Heart Assoc.* (2012) 1:e003293. doi: 10.1161/JAHA.112.003293
19. Leuschner F, Dutta P, Gorbatov R, Novobrantseva TI, Donahoe JS, Courties G, et al. Therapeutic siRNA silencing in inflammatory monocytes in mice. *Nat Biotechnol.* (2011) 29:1005–10. doi: 10.1038/nbt.1989
20. Leuschner F, Courties G, Dutta P, Mortensen LJ, Gorbatov R, Sena B, et al. Silencing of CCR2 in myocarditis. *Eur Heart J.* (2015) 36:1478–88. doi: 10.1093/eurheartj/ehu225
21. Auffray C, Sieweke MH, Geissmann F. Blood monocytes: development, heterogeneity, and relationship with dendritic cells. *Annu Rev Immunol.* (2009) 27:669–92. doi: 10.1146/annurev.immunol.021908.132557
22. Chitu V, Stanley ER. Colony-stimulating factor-1 in immunity and inflammation. *Curr Opin Immunol.* (2006) 18:39–48. doi: 10.1016/j.coi.2005.11.006
23. Shaposhnik Z, Wang X, Lusis AJ. Arterial colony stimulating factor-1 influences atherosclerotic lesions by regulating monocyte migration and apoptosis. *J Lipid Res.* (2010) 51:1962–70. doi: 10.1194/jlr.M005215
24. Lieu YK, Reddy EP. Impaired adult myeloid progenitor CMP and GMP cell function in conditional c-myb-knockout mice. *Cell Cycle* (2012) 11:3504–12. doi: 10.4161/cc.21802
25. Hettinger J, Richards DM, Hansson J, Barra MM, Joschko AC, Krijgsveld J, et al. Origin of monocytes and macrophages in a committed progenitor. *Nat Immunol.* (2013) 14:821–30. doi: 10.1038/ni.2638
26. Warren MK, Ralph P. Macrophage growth factor CSF-1 stimulates human monocyte production of interferon, tumor necrosis factor, and colony stimulating activity. *J Immunol.* (1986) 137:2281–5.
27. Meder B, Haas J, Sedaghat-Hamedani F, Kayvanpour E, Frese K, Lai A, et al. Epigenome-wide association study identifies cardiac gene patterning and a novel class of biomarkers for heart failure. *Circulation* (2017) 136:1528–44. doi: 10.1161/CIRCULATIONAHA.117.027355
28. Liao Y, Smyth GK, Shi W. Featurecounts: an efficient general purpose program for assigning sequence reads to genomic features. *Bioinformatics* (2014) 30:923–30. doi: 10.1093/bioinformatics/btt656
29. Love MI, Huber W, Anders S. Moderated estimation of fold change and dispersion for RNA-seq data with DESeq2. *Genome Biol.* (2014) 15:550. doi: 10.1186/s13059-014-0550-8
30. Bischoff FC, Werner A, John D, Boeckel JN, Melissari MT, Grote P, et al. Identification and functional characterization of hypoxia-induced endoplasmic reticulum stress regulating incRNA (HypERlnc) in pericytes. *Circ Res.* (2017) 121:368–75. doi: 10.1161/CIRCRESAHA.116.310531
31. Robinson MD, Mccarthy DJ, Smyth GK. edgeR: a Bioconductor package for differential expression analysis of digital gene expression data. *Bioinformatics* (2010) 26:139–40. doi: 10.1093/bioinformatics/btp616
32. Rahnefeld A, Klingel K, Schuermann A, Diny NL, Althof N, Lindner A, et al. Ubiquitin-Like Protein ISG15 (Interferon-Stimulated Gene of 15 kDa) in host defense against heart failure in a mouse model of virus-induced cardiomyopathy. *Circulation* (2014) 130:1589–600. doi: 10.1161/CIRCULATIONAHA.114.009847
33. Dutta P, Hoyer FF, Grigoryeva LS, Sager HB, Leuschner F, Courties G, et al. Macrophages retain hematopoietic stem cells in the spleen via VCAM-1. *J Exp Med.* (2015) 212:497–512. doi: 10.1084/jem.20141642
34. Leuschner F, Rauch PJ, Ueno T, Gorbatov R, Marinelli B, Lee WW, et al. Rapid monocyte kinetics in acute myocardial infarction are sustained by extramedullary monocytopoiesis. *J Exp Med.* (2012) 209:123–37. doi: 10.1084/jem.20111009
35. Molawi K, Wolf Y, Kandalla PK, Favret J, Hagemeyer N, Frenzel K, et al. Progressive replacement of embryo-derived cardiac macrophages with age. *J Exp Med.* (2014) 211:2151–8. doi: 10.1084/jem.20140639
36. Hohenadl C, Klingel K, Mertsching J, Hofschneider PH, Kandolf R. Strand-specific detection of enteroviral RNA in myocardial tissue by in situ hybridization. *Mol Cell Probes* (1991) 5:11–20. doi: 10.1016/0890-8508(91)90033-G
37. Zieba J, Forlenza KN, Khatra JS, Sarukhanov A, Duran I, Rigueur D, et al. TGFbeta and BMP dependent cell fate changes due to loss of filamin b produces disc degeneration and progressive vertebral fusions. *PLoS Genet.* (2016) 12:e1005936. doi: 10.1371/journal.pgen.1005936
38. Andrassy M, Volz HC, Maack B, Schuessler A, Gitsioudis G, Hofmann N, et al. HMGB1 is associated with atherosclerotic plaque composition and burden in patients with stable coronary artery disease. *PLoS ONE* (2012) 7:e52081. doi: 10.1371/journal.pone.0052081
39. Althof N, Harkins S, Kemball CC, Flynn CT, Alirezaei M, Whitton JL. *In vivo* ablation of type I interferon receptor from cardiomyocytes delays

coxsackieviral clearance and accelerates myocardial disease. *J Virol.* (2014) 88:5087–99. doi: 10.1128/JVI.00184-14
40. Kaya Z, Leib C, Katus HA. Autoantibodies in heart failure and cardiac dysfunction. *Circ Res.* (2012) 110:145–58. doi: 10.1161/CIRCRESAHA.111.243360
41. Szalay G, Sauter M, Hald J, Weinzierl A, Kandolf R, Klingel K. Sustained nitric oxide synthesis contributes to immunopathology in ongoing myocarditis attributable to interleukin-10 disorders. *Am. J. Pathol.* (2006b) 169:2085–93. doi: 10.2353/ajpath.2006.060350
42. Klingel K, Fabritius C, Sauter M, Goldner K, Stauch D, Kandolf R, et al. The activating receptor NKG2D of natural killer cells promotes resistance against enterovirus-mediated inflammatory cardiomyopathy. *J Pathol.* (2014) 234:164–77. doi: 10.1002/path.4369
43. Shi Y, Fukuoka M, Li G, Liu Y, Chen M, Konviser M, et al. Regulatory T cells protect mice against coxsackievirus-induced myocarditis through the transforming growth factor beta-coxsackie-adenovirus receptor pathway. *Circulation* (2010). 121:2624–34. doi: 10.1161/CIRCULATIONAHA.109.893248
44. Pappritz K, Savvatis K, Miteva K, Kerim B, Dong F, Fechner H, et al. Immunomodulation by adoptive regulatory T-cell transfer improves Coxsackievirus B3-induced myocarditis. *Faseb j.* (2018). doi: 10.1096/fj.201701408R. [Epub ahead of print].
45. Hume DA, Macdonald KP. Therapeutic applications of macrophage colony-stimulating factor-1 (CSF-1) and antagonists of CSF-1 receptor (CSF-1R) signaling. *Blood* (2012) 119:1810–20. doi: 10.1182/blood-2011-09-379214
46. Sasmono RT, Oceandy D, Pollard JW, Tong W, Pavli P, Wainwright BJ, et al. A macrophage colony-stimulating factor receptor-green fluorescent protein transgene is expressed throughout the mononuclear phagocyte system of the mouse. *Blood* (2003) 101:1155–63. doi: 10.1182/blood-2002-02-0569
47. Qiao JH, Tripathi J, Mishra NK, Cai Y, Tripathi S, Wang XP, et al. Role of macrophage colony-stimulating factor in atherosclerosis: studies of osteopetrotic mice. *Am J Pathol.* (1997) 150:1687–99.
48. Rajavashisth T, Qiao JH, Tripathi S, Tripathi J, Mishra N, Hua M, et al. Heterozygous osteopetrotic (op) mutation reduces atherosclerosis in LDL receptor- deficient mice. *J Clin Invest.* (1998) 101:2702–10. doi: 10.1172/JCI119891
49. Frangogiannis NG, Mendoza LH, Ren G, Akrivakis S, Jackson PL, Michael LH, et al. MCSF expression is induced in healing myocardial infarcts and may regulate monocyte and endothelial cell phenotype. *Am J Physiol Heart Circ Physiol.* (2003) 285:H483–492. doi: 10.1152/ajpheart.01016.2002
50. Naito M, Hayashi S, Yoshida H, Nishikawa S, Shultz LD, Takahashi K. Abnormal differentiation of tissue macrophage populations in 'osteopetrosis' (op) mice defective in the production of macrophage colony-stimulating factor. *Am J Pathol.* (1991) 139:657–67.
51. Fleetwood AJ, Lawrence T, Hamilton JA, Cook AD. Granulocyte-macrophage colony-stimulating factor (CSF) and macrophage CSF-dependent macrophage phenotypes display differences in cytokine profiles and transcription factor activities: implications for CSF blockade in inflammation. *J Immunol.* (2007) 178:5245–52. doi: 10.4049/jimmunol.178.8.5245
52. Blyszczuk P, Berthonneche C, Behnke S, Glonkler M, Moch H, Pedrazzini T, et al. Nitric oxide synthase 2 is required for conversion of pro-fibrogenic inflammatory CD133(+) progenitors into F4/80(+) macrophages in experimental autoimmune myocarditis. *Cardiovasc Res.* (2013) 97:219–29. doi: 10.1093/cvr/cvs317
53. Ogle ME, Segar CE, Sridhar S, Botchwey EA. Monocytes and macrophages in tissue repair: implications for immunoregenerative biomaterial design. *Exp Biol Med.* (2016) 241:1084–97. doi: 10.1177/1535370216650293
54. Stanley ER, Berg KL, Einstein DB, Lee PSW, Pixley FJ, Wang Y, et al. Biology and action of colony-stimulating factor-1. *Molecul Reprod Dev.* (1997) 46:4–10. doi: 10.1002/(SICI)1098-2795(199701)46:1<4::AID-MRD2>3.0.CO;2-V
55. Garcia S, Hartkamp LM, Malvar-Fernandez B, Van Es IE, Lin H, Wong J, et al. Colony-stimulating factor (CSF) 1 receptor blockade reduces inflammation in human and murine models of rheumatoid arthritis. *Arthritis Res Ther.* (2016) 18:75. doi: 10.1186/s13075-016-0973-6
56. Jakubzick CV, Randolph GJ, Henson PM. Monocyte differentiation and antigen-presenting functions. *Nat Rev Immunol.* (2017) 17:349–62. doi: 10.1038/nri.2017.28
57. Henke A, Mohr C, Sprenger H, Graebner C, Stelzner A, Nain M, et al. Coxsackievirus B3-induced production of tumor necrosis factor-alpha, IL-1 beta, and IL-6 in human monocytes. *J Immunol.* (1992) 148:2270–7.
58. Opitz E, Koch A, Klingel K, Schmidt F, Prokop S, Rahnefeld A, et al. Impairment of immunoproteasome function by beta5i/LMP7 subunit deficiency results in severe enterovirus myocarditis. *PLoS Pathog.* (2011) 7:1–13. doi: 10.1371/journal.ppat.1002233
59. Paeschke A, Possehl A, Klingel K, Voss M, Voss K, Kespohl M, et al. The immunoproteasome controls the availability of the cardioprotective pattern recognition molecule Pentraxin3. *Eur J Immunol.* (2016) 46:619–33. doi: 10.1002/eji.201545892

Conflict of Interest Statement: The authors declare that the research was conducted in the absence of any commercial or financial relationships that could be construed as a potential conflict of interest.

frontiers in Immunology

REVIEW
published: 28 November 2018
doi: 10.3389/fimmu.2018.02620

Proteasomal Protein Degradation: Adaptation of Cellular Proteolysis With Impact on Virus—and Cytokine-Mediated Damage of Heart Tissue During Myocarditis

Antje Beling[1,2]* *and Meike Kespohl*[1,2]

[1] *Charité—Universitätsmedizin Berlin, Corporate Member of Freie Universität Berlin, Humboldt-Universität zu Berlin, and Berlin Institute of Health (BIH), Institute of Biochemistry, Berlin, Germany,* [2] *Deutsches Zentrum für Herz-Kreislauf-Forschung (DZHK), Partner Site Berlin, Berlin, Germany*

OPEN ACCESS

Edited by:
Michael H. Lehmann, Ludwig-Maximilians-Universität München, Germany

Reviewed by:
George W. Booz, University of Mississippi Medical Center School of Dentistry, United States
Jason Brice Weinberg, University of Michigan, United States

***Correspondence:**
Antje Beling
antje.beling@charite.de

Specialty section:
This article was submitted to Viral Immunology, a section of the journal Frontiers in Immunology

Received: *19 September 2018*
Accepted: *24 October 2018*
Published: *28 November 2018*

Citation:
Beling A and Kespohl M (2018) Proteasomal Protein Degradation: Adaptation of Cellular Proteolysis With Impact on Virus—and Cytokine-Mediated Damage of Heart Tissue During Myocarditis. Front. Immunol. 9:2620. doi: 10.3389/fimmu.2018.02620

Viral myocarditis is an inflammation of the heart muscle triggered by direct virus-induced cytolysis and immune response mechanisms with most severe consequences during early childhood. Acute and long-term manifestation of damaged heart tissue and disturbances of cardiac performance involve virus-triggered adverse activation of the immune response and both immunopathology, as well as, autoimmunity account for such immune-destructive processes. It is a matter of ongoing debate to what extent subclinical virus infection contributes to the debilitating sequela of the acute disease. In this review, we conceptualize the many functions of the proteasome in viral myocarditis and discuss the adaptation of this multi-catalytic protease complex together with its implications on the course of disease. Inhibition of proteasome function is already highly relevant as a strategy in treating various malignancies. However, cardiotoxicity and immune-related adverse effects have proven significant hurdles, representative of the target's wide-ranging functions. Thus, we further discuss the molecular details of proteasome-mediated activity of the immune response for virus-mediated inflammatory heart disease. We summarize how the spatiotemporal flexibility of the proteasome might be tackled for therapeutic purposes aiming to mitigate virus-mediated adverse activation of the immune response in the heart.

Keywords: virus, myocarditis, proteasome, cytokine, immunopathology, heart failure

INTRODUCTION

Myocarditis and its debilitating sequela, inflammatory cardiomyopathy, are leading causes of heart failure and sudden cardiac death particularly in infants, children, and young adults (1) with viral infections being the most common trigger of non-ischemic myocardial inflammation in the Western world (2). Acute injury of the heart muscle upon viral infection stimulates infiltration of

immune cells, aiming to support pathogen clearance and alleviate organ damage. However, this pathogen-induced immune response can result subsequently in overwhelming immunopathology or the development of auto-aggressive immunity against cardiac self-antigens. These processes comprise fibrotic scarring and cardiac remodeling (3, 4). Both the high mortality of acute viral myocarditis in childhood and the putative progression of acute myocarditis to chronic disease support the need to define precisely the underlying mechanisms.

Most of our knowledge on the pathology of viral myocarditis comes from infection with enteroviruses, in particular coxsackievirus B3 (CVB3) in mice. CVB belong to the picornavirus family and have a non-enveloped, icosahedral capsid surrounding a positive-strand RNA genome. CVB3 used to be among the most prevalent pathogens known to cause viral myocarditis in North America and Europe (3, 5). Infection of laboratory mouse strains mirrors the variable manifestation of the disease in man (6, 7) by causing susceptibility for cardiac pathogenesis to a highly varying degree. A certain genetic background determines both control of viral pathogens and the activation of deleterious immune response pathways (6, 8). Recent observational studies suggest that it is not primarily the presence and/or replicative activity of invading viruses in the myocardium that determines outcome. In fact, the virus-triggered abundance of infiltrating leukocytes is an independent risk factor for adverse outcome (9). Although it is indisputable that primary encounter of virus in the heart triggers death of cardiomyocytes, the pathogenic role of persisting viral genomes was poorly defined in the past. Recently, experimental mouse data demonstrated that persisting enteroviral RNAs do not actively contribute to ongoing myocardial disease after viral myocarditis (10).

Mice with high susceptibility to severe virus-induced inflammation are pre-disposed also to a loss of self-tolerance against cardiac proteins (11). Additionally, viral infection of cardiomyocytes can trigger auto-destructive activity of infiltrating cells, as well as, the formation of autoantibodies directed against antigens of cardiac origin (12, 13) further exaggerating heart tissue damage. Establishment of autoimmune myocarditis in mice by priming with cardiac antigens revealed that the same strains of inbred mice, who develop post-viral inflammatory heart tissue injury are also prone to autoimmune-triggered heart pathology. This indicates that the background genetics and involved immune response pathways for both diseases might be overlapping (13, 14). Others have reviewed in detail how type B coxsackievirus interacts with the innate and adaptive immune system and inflammatory responses (7, 15). Our primary interest herein is to discuss how cellular proteolysis by the proteasome affects the innate and adaptive immune response during CVB3-induced inflammatory damage of heart tissue, and our focus will broaden to the adaptation of this multi-catalytic protease in different cells during infection and inflammation. We will specifically discuss recent findings regarding the functional importance of a specific proteasome subtype expressed in hematopoietic cells and its possible implications for cytokine-mediated pathogenesis and therapeutic interference during viral myocarditis.

THE PROTEASOME: A DRUGGABLE MULTI-CATALYTIC PROTEASE

Several avenues of research have implicated the ubiquitin-proteasome system (UPS) as a major regulator of cell signaling and transcription. It controls also antigen processing, apoptosis and cellular proliferation. The ubiquitination machinery tags degradation-prone proteins in a highly regulated system for processing by the proteasome. As an integral part of cellular proteostasis, proteasome-mediated protein degradation is the primary route for intracellular removal of misfolded, damaged, or short-lived proteins (16). Proteasomes are multi-subunit enzymes with a barrel-shaped structure and internal active sites are accessible through a gated pore (17, 18). Proteasome-destined cargoes are recognized by regulatory particles (19S regulator) associated with the proteasome core complex (20S proteasome). The recognition, de-ubiquitination, and unfolding of substrates in direct proximity to the gated entry channel made up of the outer α ring of the 20S proteasome is required for degradation (19). Peptide hydrolysis is restricted to three β subunits, β1, β2, and β5, within the interior of the 2-fold symmetric core 20S proteasome. In addition to the aforementioned functions of the proteasome, the UPS is also of particular importance under conditions of cellular stress, where a rapid elimination of unfolded and potentially toxic proteins is required to prevent formation of cytotoxic aggregates (16, 20). Restrained function of the UPS might lead to accumulation of harmful proteins to toxic levels, causing disease (21). Cells have several ways to meet such increased demand for protein turnover. In response to Interferon (IFN)-γ (22, 23), tumor necrosis factor (TNF)-α (24), doxorubicin (25), or H_2O_2 exposure (26), others and we demonstrated an increased abundance of the immunoproteasome (i-proteasome), a specific proteasome isoform that contains alternative catalytic subunits (β1i/low molecular weight protein (LMP) 2; β2i/multicatalytic endopeptidase complex (Mecl)-1, β5i/LMP7) (27). I-proteasomes at least partially replace their constitutively expressed standard proteasome counterpart in different tissues upon infection (28, 29). During viral myocarditis, the i-proteasome is upregulated strongly in heart tissue and its induction involves IFN-γ (30, 31), as well as, type 1 interferon (T1IFN)-mediated signaling (8). In the heart, i-proteasome formation results in increased peptide hydrolysis capacity (8). This adaptation within the proteolytic core of the 20S proteasome complex is advantageous since it contributes to maintenance of protein homeostasis during inflammation (23, 32, 33). I-proteasome assembly is very similar to the formation of the standard proteasome [reviewed recently by (34)]. Additional proteasome subtypes like the thymoproteasome with tissue-specific β5t subunit expression (35) and mixed proteasomes that contain only one (β5i) or two (β1i and β5i) of the three inducible catalytic subunits of the i-proteasome (36) contribute to the variety of proteasome-mediated proteolysis.

Both facts—the close vicinity of genes encoding β1i/LMP2, β5i/LMP7, and the transporter associated with antigen

presentation (TAP) within the major histocompatibility (MHC) II region, as well as, the regulatory function of IFNγ for these molecules—were indicative for a specialized function of the i-proteasome during MHC class I antigen presentation (37). The finding that β1i/LMP2 and β5i/LMP7 enhance substrate cleavage after basic and hydrophobic amino acid residues further strengthened the notion for a specific role of the i-proteasome in the generation of antigenic peptides (22, 38). In fact, there are numerous examples for viral, bacterial, and parasitic pathogens for which *in vitro* peptide processing studies revealed facilitated MHC class I epitope liberation by the i-proteasome complex in comparison to lower epitope abundance upon processing of model polypeptides with the standard proteasome (39). This altered prevalence of antigenic peptide generation by the i-proteasome is attributed to different peptide cleavage site usage (40), and can elicit to altered $CD8^+$ T cell-mediated immune surveillance also (41–46). Nevertheless, these findings appear to be restricted to a defined pool of immunodominant epitopes with no effect of the i-proteasome on other epitopes (28, 47, 48).

During the last three decades, the experimental landscape investigating i-proteasome biology substantially broadened with the availability of knockout mice lacking either single immunosubunits (47, 49) or a combinatory deletion of the three genes encoding β5i/LMP7, β1i/LMP2, and β2i/MECL-1 (45). Because deletion of a single i-proteasome subunit might be outweighed by increased formation of standard proteasome complexes (50), research on the i-proteasome improved further with the availability of i-proteasome subunit-selective inhibitors. Kisselev and Groettrup provided a detailed overview on inhibitors of the respective subunits of the immunoproteasome (51). Structure-guided optimization of such inhibitory compounds with subunit selectivity is actually an ongoing objective. Initially, development of i-proteasome-selective inhibitors was pursued with regard to the profound benefit in patients with multiple myeloma (MM) upon the implementation of non-selective proteasome inhibitors like bortezomib or carfilzomib (52–55). Despite their high efficacy for MM cells, targeting the proteasome in other organs like the heart constitutes a risk for heart failure (56). In comparison to heart tissue (57), MM cells are unique regarding the preferential expression of the i-proteasome in these cancer cells. Therefore, compounds with selective i-proteasome subunit specificity represent an alternative strategy for more selective tumor-directed targeting (54, 58). ONX 0914 initially known as PR957 is a potent i-proteasome-selective inhibitor that predominantly targets the β5i/LMP7 and to a lower degree the β1i/LMP2 i-proteasome subunit as well (29, 59). Beyond the tumor-suppressive potential of ONX 0914 (60, 61), pre-clinical research utilizing this compound and other i-proteasome-selective inhibitors revealed additional putative clinical scenarios, where such drugs might improve current medical treatment. Pioneering work by the Groettrup group and others highlighted the therapeutic potential of i-proteasome inhibitors for mitigation of autoimmune-driven inflammatory tissue damage (50, 59, 62–64). KZR-616—an ortholog of ONX 0914 with high selectivity for the human i-proteasome—passed successfully phase I trials and is now in phase II trials for patients with systemic lupus erythematosus. Since i-proteasome activity controls alloantibody production by B cells and influences processes resulting in T cell exhaustion, i-proteasome-selective compounds could be used to prevent allograft rejection upon organ transplantation as well (65, 66). All these recent reports shed light onto several previously unappreciated biological functions of the i-proteasome and support the requirement for a detailed overview on the pathological function of the proteasome during virus-induced inflammatory heart tissue injury.

VIRAL ENTRY, REPLICATION, AND RELEASE: CONTROL MECHANISMS BY THE PROTEASOME

Viruses subvert cellular processes to favor viral propagation. Given its central role in a wide range of cellular functions by maintaining a critical level of essential regulatory proteins, it is expected that the proteasome is involved in viral replication, and numerous examples have indeed been reported. Several viral proteins direct host-cell proteins to proteolytic degradation by the proteasome (67). Viruses have evolved e.g., by encoding specific ubiquitin ligase activity to employ the proteasome for degradation of host proteins that would impede viral growth. Since this review mainly focuses on the immunomodulatory function of the proteasome complex itself during manifestation of virus-mediated inflammatory damage of heart tissue, the reader is encouraged to refer to an excellent review recently provided by Honglin Luo on interactions between ubiquitin/ubiquitin family proteins and viral growth (68). Here, we will summarize examples of viruses with known cardiac tropism, where the proteasome complex is exploited for virus progeny formation and/or where inhibitors of proteasome activity affect viral replication (**Table 1**).

Approximately 20 viruses have been implicated in human myocarditis and some of them interfere directly with the UPS. Among them, parvovirus B19 is detected often in endomyocardial biopsies obtained from patients with clinically suspected myocarditis (9). Parvoviruses follow multiple strategies for nuclear transport, some of them requiring active proteasomes. Replication of minute virus of mice—a murine parvovirus—is disrupted in the presence of proteasome inhibitors (81). In addition to parvoviruses, members of the herpesviridae family like human herpesvirus 6 (HHV6) are commonly detected pathogens in cardiac biopsies (9). HHV6 causes accumulation of p53 in the cytoplasm (86), and among many mechanisms regulating p53 activity, the cellular abundance of p53 is controlled by UPS-dependent turnover (87). In herpes simplex virus (HSV) infection, proteasome activity directly affects virus progeny formation. Since inhibitors of the proteasome block HSV entry at a step occurring after capsid penetration into the cytosol but prior to capsid arrival at the nuclear periphery, it was concluded that cellular proteasome activity facilitates virus entry at this early stage (74). The human cytomegalovirus (HCMV) pp71 protein stimulates quiescent cells to enter the cell cycle by targeting

TABLE 1 | Effect of the proteasome on the propagation of viral particles.

Virus	Cell type	Treatment/condition	Effect on viral replication	Targeted step in life cycle of virus	References
Adenovirus	HeLa cells	MG132	Reduced	Late gene expression	(69)
Mouse adenovirus[1]	C57BL/6 mice	LMP7$^{-/-}$	No effect	n.r.	(31)
Coxsackie-virus B3 (CVB3)	Murine myxoma cell line HL-1	MG132, lactacystin	Reduced	Post entry	(70)
	A/J mice	MLN353	No effect	n.r.	(71)
	C57BL/6 mice	LMP7$^{-/-}$	No effect	n.r.	(23)
	Murine embryonic cardiomyocytes	ONX 0914	No effect	n.r.	(72)
	C57BL/6 mice	ONX 0914	Increased cardiac titers		
	A/J mice	ONX 0914	No effect on cardiac titers		
	HeLa cells	PA28α/β siRNA	Increased	n.r.	(73)
	HeLa cells	PA28α/β overexpression	Reduced		
	Murine embryonic cardiomyocytes	PA28α/β$^{-/-}$	Increased		
	C57BL/6 mice	PA28α/β$^{-/-}$	No effect on cardiac titers		
Herpes simplex virus 1 (HSV-1)	Monkey kidney epithelial cells (Vero cells) Hamster ovary cells (CHO-cells)	MG132 epoxomicin lactacystin	Reduced	Virus entry/post penetration step	(74)
	HeLa derivative HEp-2	MG132, MG115, epoxomicin	Reduced	Immediate-early and late viral proteins	(75)
Human cytomegalo-virus (HCMV)	Human embryonic lung fibroblasts	MG132	Reduced	All stages of viral replication	(76)
	Human embryonic lung fibroblasts	MG132	Reduced	Immediate early protein synthesis	(77)
Human immuno-deficiency virus 1/2 (HIV1/2)	HeLa cells, human T cell line A3.01	MG132, lactacystin	Reduced	Gag processing and virus particle release	(78)
	Human CD4$^+$ T cells, human CD4$^+$ cell line OM-10.1	Bortezomib, lactacystin, MG132	Reduced	Infectivity of the virion and viral latency	(79)
Influenza A virus	Canine kidney cells MDCK	MG132, bortezomib	Reduced	Post fusion	(80)
Minute virus of mice[1]	Murine B cells A9	MG132, lactacystin, epoxomicin	Reduced	Post endosomal escape	(81)
Polio virus	HeLa cells	MG132, bortezomib	Reduced	Post entry (no effect on translation)	(82)
Vaccinia virus	HeLa cells	MG132, epoxomicin	Reduced	Post entry (viral genome replication; intermediate and late gene expression)	(83)
	HeLa cells	MG132, bortezomib	Reduced	Genome uncoating, replication, late viral gene expression, virus assembly	(84)

The table summarizes viruses with known cardiac tropism and the impact of different proteasome inhibitors (bortezomib, MG132, lactacystin, MLN353, MG115, as well as, the immunoproteasome-selective inhibitor ONX 0914 (59)), of the proteasome activator PA28 (85), as well as, of the i-proteasome (cell culture and mouse studies using LMP7$^{-/-}$ mice or cell lines obtained from these mice (47) on viral replication. CHO, chinese hamster ovary; MDCK, madin-darby canine kidney; Gag, group-specific antigen; n.r., not reported; MLN353, Millennium353 (proteasome inhibitor); ONX 0914, immunoproteasome-specific inhibitor; PA28α/β, proteasome activator α/β of 28 kDa.

[1]*Murine pathogens.*

proteins of the retinoblastoma (Rb) family for proteasome-dependent degradation (88) and proteasome inhibitors block viral DNA replication, as well as, assembly of HCMV (76). The annual influenza virus (IV) season also calls upon some cases of IV-induced myocarditis in man. Proteasome inhibitors attenuate virus progeny formation at a post-fusion step upon influenza A virus (IAV) infection, and UPS activity is required for RNA synthesis of the virus (80). A similar function of the proteasome machinery at a post-entry step during viral replication applies to DNA replication and expression of intermediate and late genes of the vaccinia virus (83). Work is still in progress to unravel the role of the proteasome in the replication of human immunodeficiency virus (HIV). Thus far, it was shown that proteasome inhibition interferes with gag polyprotein processing, release and maturation of HIV-1 and HIV-2 (78, 79).

Although the frequency of adenovirus and coxsackie B virus detection in human myocarditis has gradually declined in adults in Western Europe during the last two decades, they are still a common cause of myocarditis in children or reported in small regional outbreaks. The adenovirus (Ad) E4 protein requires active proteasomes to promote late gene expression (69). Moreover, the Ad E1A protein regulates proteasomal activity, but is also a substrate for proteasome-mediated degradation (89). Recently, the Weinberg group established a mouse model of pediatric Ad-mediated myocarditis following intranasal infection of neonatal C57BL/6 mice with mouse adenovirus 1 (MAV-1) (90). MAV-1-myocarditis induces IFN-γ-mediated i-proteasome

formation in infected heart tissue, but the catalytic activity of the β5i/LMP7 i-proteasome subunit had no effect on viral genome copy numbers in heart tissue (31). Therefore, it is unlikely that MAV-1 replication is affected by i-proteasome activity. In addition to *in vivo* models for the investigation of viral heart disease, *in vitro* studies have substantial advantages to provide information on the function of the proteasome regarding virus progeny formation. Most detailed information on the proteasome during the replicative phase of a human cardiotropic virus is available for CVB3. The McManus/Luo group was first to report a substantial suppression of CVB3 replication in HL-1 cells upon treatment with pan-specific proteasome inhibitors. This inhibitory effect was independent of the blockade of viral entry into host cells and rather attributed to reduced genome replication (70). The Luo group followed proteasome inhibition also during CVB3-induced myocarditis using A/J mice, which are known to be highly susceptible for CVB3-induced pathogenesis. In their study, MLN353 was introduced as a novel proteasome inhibitor for *in vivo* application. In contrast to the robust suppression of viral replication upon MG132 treatment in the HL-1 myxoma cell line (70), MLN353 treatment of mice did not influence virus titers (71). These somewhat controversial findings indicate that other essential pathways for CVB3 control might possibly be adversely influenced by MLN353, and this could outweigh the suppressive effect of proteasome inhibitors in cells targeted by virus infection. Our group investigated the contribution of specific proteasome subunits on the replication cycle of CVB3 *in cellulo* under one-step conditions using both HeLa cells and murine primary embryonic cardiomyocytes. PR825, as well as, ONX 0914 were applied at non-toxic concentrations to specifically block the catalytic activity of either β5 or β5i/LMP7, respectively. The CVB3 replication cycle involving the adsorption, penetration, replication of the parent virus, and release of progeny virus was not altered by the selective inhibition of these proteasome subunits (72). In addition to diverging peptidase activities of the six catalytic subunits, proteasome activity can be regulated upon binding to regulatory particles like the proteasome activator of 28 kDa (PA28). PA28-capped proteasome complexes are equipped with increased peptide hydrolysis capacity (91), and by as yet unknown mechanisms PA28 suppresses the CVB3 replication machinery (73). Altogether, a broad spectrum of various viral pathogens exploits the proteasome machinery in cells of the host organism.

INNATE IMMUNITY: HOW THE PROTEASOME AFFECTS THE FIRST DEFENSE WAVE

Type I Interferons During Viral Myocarditis: Control by Proteasome Activity

During viral infection, viral RNAs and replication intermediates bind to their respective intracellular pattern recognition receptors, including Toll-like receptors (TLRs) and retinoic acid-inducible gene I (RIG-I), and, mediated by several distinct signaling pathways, this increases the production of T1IFNs [refer to (92) for a detailed review on T1IFNs in infectious disease]. T1IFNs are an effective first line of defense against viral infections and as such, a robust T1IFN response is highly beneficial to counteract early CVB3 infection in mice (93–95). Results from a pilot trial indicated a putative beneficial therapeutic influence of T1IFN substitution in patients with coxsackieviral myocarditis (96, 97). Following activation of the IFNα/β receptor (IFNAR), a diverse repertoire of antiviral proteins is expressed including protein kinase R (PKR), 2,5 oligoadenylate synthetase-like protein 2 (OASL-2), IFN-induced proteins with tetratricopeptide repeats (IFITs), as well as, IFN-stimulated genes like ISG15. The latter is an ubiquitin family protein, which is strongly induced by T1IFNs and NF-κB signaling in cardiomyocytes (98, 99), suppresses coxsackieviral replication, mitigates profoundly viral myocarditis and blocks the progression to its debilitating sequela (99).

Plasmacytoid dendritic cells (pDCs) are a major source for T1IFNs during viral myocarditis (100) and unique regarding their TLR7 or TLR9-dependent activation of IFN regulatory factor 7 (IRF7)-mediated IFNα/β production (101). Whereas, molecular accounts on the influence of ubiquitin modifications on pattern recognition receptor (PRR)-mediated signaling are available (102), less is known about the role of the different peptidase activities of the proteasome during the process from engagement of PRR to T1IFN production. Pan-specific inhibitors of the proteasome like bortezomib or carfilzomib, which target both the standard proteasome and i-proteasome, are potent suppressors of TLR9 activation in murine bone marrow cells, as well as, human peripheral blood mononuclear cells (PBMCs), but other TLR-mediated pathways like Toll/interleukin-1 receptor-domain-containing adapter-inducing IFNβ (TRIF)-mediated IRF3 activation are affected as well (63). Selective i-proteasome inhibitors assigned specifically the control of IFNα/β production in pDCs to i-proteasome peptidase activity (59, 63). Correspondingly, i-proteasome inhibition in CVB3-infected C57BL/6 (B6) mice substantially reduces T1IFN production. Thereby, i-proteasome inhibition aggravates disease parameters like viral load in B6 mice (72). On the other hand, ISGs in germline LMP7$^{-/-}$ mouse models are as active as in wild-type controls during viral myocarditis (23). Indisputably, numerous studies indicate that the effects of T1IFN on the host response to infection are not limited to the acute, cell-intrinsic antiviral response described above. IFNα/β are also involved at various stages in the activation of adaptive immune cell responses e.g., by evolving antigen presenting DCs into a mature state (92). Similar to this, in hosts exhibiting high susceptibility for development of severe acute and chronic heart pathology like A.BY/SnJ mice, a shifted and overall significantly impaired T1IFN response (9, 100) leads to reduced DC activation and lower cross-presentation (100, 103). Genetic defects of i-proteasome subunits in mice that lead to impaired i-proteasome formation or proteasome inhibitor treatment decrease DC activation, thus, influencing the immune-stimulatory capacity of DCs as reflected by altered co-stimulatory molecule and C-C chemokine receptor 7 (CCR7) expression, as well as, cytokine production, respectively

(104, 105). Thereby, i-proteasome-mediated proteolysis might directly control the antigen presentation capacity of DCs.

In contrast to the classical antiviral function of T1IFNs, there is increasing appreciation that IFNα/β can also be harmful, e.g., by triggering excessive inflammation and tissue damage (106). Likewise, IFNα/β is a classical disease-trigger of autoimmunity and auto-inflammation, and a reduced IFNα/β production as achieved upon administration of i-proteasome-selective inhibitors attenuates disease manifestation in models of lupus erythematosus (63). Defects in the DNA three prime repair exonuclease 1 (Trex1), which result in high cyclic guanosine monophosphate–adenosine monophosphate synthase (cGAS) induced IFNα/β production, lead to spontaneous inflammatory myocarditis in mice and Aicardi-Goutières syndrome in man (107, 108). Similarly, mutations in different genes encoding protein subunits of the human proteasome restrain T1IFN production, and this commences to a syndrome involving chronic atypical neutrophilic dermatosis with lipodystrophy and elevated temperature (CANDLE) (109–111).

Effect of the Proteasome for Humoral Innate Immunity

In addition to the cellular branch of innate immunity that comprises cell-associated pattern recognition receptors, its humoral branch includes molecules such as the classic short pentraxin C-reactive protein (CRP), the long pentraxin PTX3, and complement recognition molecules (112). During viral myocarditis, PTX3 is produced mainly by monocytes and macrophages (113, 114). PTX3 promotes the engulfment of cellular debris by immune cells (115), and acts as a safeguard mechanism dampening myocardial injury induced upon pattern-associated molecular pattern (PAMP)/damage-associated molecular pattern (DAMP) signaling (112). Although, the detailed molecular aspects are unresolved, the peptidase activity of the i-proteasome controls PTX3 expression in TLR4-activated macrophages during viral myocarditis (114) and pneumococcal pneumonia (116), a function of the i-proteasome which cannot be compensated by enhanced formation of standard proteasome in LMP7$^{-/-}$ mice (114).

The Proteasome Balances Protein Homeostasis

Myocarditis in CVB3 (Nancy)-infected LMP7$^{-/-}$ mice on a B6 background lacking intact i-proteasomes is not only mirrored by reduced PTX3 production (114), but it also comprises high-grade inflammation and increased cell death (23). In cells with high rate of protein synthesis e.g., in response to cytokine signaling, a reduction of translational fidelity often occurs, generating defective ribosomal products (16). Cells in general and cardiomyocytes in particular that produce higher amounts of i-proteasomes are equipped with increased proteolytic activity and can efficiently degrade defective proteins (32, 33, 117). Thereby, the i-proteasome diminishes tissue damage in mouse hearts of CVB3-infected wild-type B6 mice (23). Nevertheless, this finding in B6 mice is in clear contrast to findings made in A/J mice, which exhibit high susceptibility for virus-mediated inflammation of heart tissue (118, 119) and generally present with increased viral burden in the heart. Here, i-proteasome activity constitutes severe cytokine-mediated inflammatory heart tissue injury. I-proteasome inhibition blocks chemokine and cytokine production, and consequently reduces the appearance of misfolded proteins (72). The use of selective inhibitors targeting i-proteasome activity does not necessarily reflect the findings obtained in respective germ-line gene deficient mouse models (23, 50, 72). As an example, contrary to what was reported in LMP7$^{-/-}$ B6 mice, inhibition of i-proteasome activity by ONX 0914 in CVB3-infected wild-type B6 mice disrupts the T1IFN defense against the invading pathogen, facilitates virus-mediated tissue damage and exacerbates PAMP/DAMP-signaling in the heart. Thereby, the production of chemokines, infiltration with immune cells, as well as, cytokine release increase (72). Such discrepancies between specific inhibitors for proteasome subunits and their knockout models might be due to a compensatory formation of standard proteasomes in LMP7$^{-/-}$ mice (50, 59), which is not observed at a similar level in ONX 0914-treated mice.

Innate Myeloid Cells: Proteasome Activity Regulates Chemokine and Cytokine Production

Neutrophils are the first and most abundant cell population of the host's innate immune response with well-known function in the defense against bacterial and fungal pathogens. Moreover, neutrophil recruitment in virus infection can be part of a protective strategy leading to prevention of viral disease (120). The i-proteasome influences the abundance of these cells in blood and spleen, but it controls the activation status of neutrophils as well (72, 121). Nevertheless, neutrophils have no disease modifying impact on CVB3-induced myocarditis (72, 122, 123). During myocarditis, particularly monocytes/macrophages—that emigrate the bone marrow, then sequester and differentiate in the spleen—infiltrate the infected mouse heart (23, 99). Chemokines attract these cells to the injured heart, where they are indispensable for waste removal and healing (7, 124). On the other hand, many studies have highlighted the requirement of monocytes/macrophages for the manifestation of the detrimental consequences of viral myocarditis—inflammatory injury and formation of fibrotic scar (72, 125–128). Similar to monocytes, macrophages also exacerbate inflammatory injury in infected mouse hearts (127). Monocytes and macrophages secrete pro-inflammatory and pro-fibrotic cytokines (7, 126). Therefore, molecules involved in innate immune cell mobilization and differentiation or in the control of cytokine/chemokine production by these cells present putative drug targets for future investigation. Resembling their effects on neutrophils, i-proteasome inhibitors stimulate also monocyte/macrophage emigration from the bone marrow and increase the abundance particularly of Ly6C^{high} monocytes in the spleen (72, 121), where they differentiate to macrophages under inflammatory conditions (129). These findings might be indicative for a pro-inflammatory function of the i-proteasome.

In contrast, there is considerable experimental evidence from various *in vitro* and *in vivo* approaches that argues substantially against this notion and rather advocates i-proteasome-selective inhibitors as anti-inflammatory drugs e.g., for autoimmunity or to prevent transplant rejection (50, 59, 62, 65, 66). As summarized in **Figure 1**, selective inhibitors of the i-proteasome suppress the production of pro-inflammatory cytokines such as TNF-α and IL-6 in TLR4 and TLR7 activated immune cells. Similar results were obtained in IFNγ and TLR4 activated mouse macrophages (137), TLR4 stimulated splenocytes (59, 138), TLR4 activated PBMCs from healthy donors and patients with rheumatoid arthritis (59), as well as, TLR7 engaged macrophages (72). Consistently, in CVB3 infected A/J mice, the i-proteasome affects cytokine production also (72). Nevertheless, it needs to be recalled that under conditions where i-proteasome activity is needed for pathogen control like during *Candida albicans* or CVB3 infection of B6 mice, this influence of i-proteasome proteolysis on cytokine production seems to be outweighed by a higher PAMP burden (72, 121). In this case, the pathogen load is presumably a much stronger effector of cytokine production than the cellular content of the i-proteasome.

Influence of Proteasome Peptidase Activity on TLR Signaling

In A/J mice, CVB3 replicates to about 10-fold increased titers in the heart in comparison to B6 mice (72). One might speculate that the overall increase in viral RNA ultimately stimulates PRR signaling in mouse hearts, thereby facilitating cytokine/chemokine production. In fact, the inflammatory response in infected heart tissue is higher in A/J mice if directly compared to B6 mice. It remains an enigma how i-proteasome catalyzed proteolysis controls PRR signaling at a molecular level. In addition, it is unclear why the i-proteasome affects differently the cardiac phenotype during MAV-1 and CVB3-induced myocarditis in B6 mice (31, 72). CVB3 as a single-stranded RNA virus is a bona fide activator of TLR7 and TLR8 (139) [in mice only TLR7 is active (140)]. Viral DNA from Ad however triggers the TLR9 pathway. Alternatively, Ad escaping the endosome reveals viral DNA complexes to the cytosolic compartment and sensors like cGAS, which acts by the stimulator of interferon genes (STING)-controlled immune pathway (141). Thereby induced signaling stimulates transcription factors like IRF7 (TLR7, TLR9) activator protein 1 (AP-1) (TLR7, TLR9), NF-κB (TLR7, TLR9, STING), and IRF3 (STING) leading to the induction of target genes that—in addition to IFNs and other ISGs - also encode pro-inflammatory cytokines and chemokines (101, 142). Therefore, we have summarized the current understanding on how the i-proteasome influences e.g., TLR mediated cellular signaling in **Figure 1**.

The NF-κB family of transcription factors, which acts downstream of TLR7, TLR9, and STING, plays a central role in regulation of inflammation. In the canonical pathway of NF-κB activation, the proteasome degrades IκBα, releasing the active NF-κB dimer (usually p65/p50) and allowing translocation to the nucleus (**Figure 2**). The impact of the different proteasome isoforms on NF-κB signaling is reported controversially (summarized in **Table 2**). A defective NF-κB activation as a response to reduced LMP2 expression in non-obese mice was attributed to reduced processing of the NF-κB precursor p105 (143, 145), but two different laboratories rebutted these findings (146, 150). Other data confirmed the initial findings and suggested an altered stimulation of canonical NF-κB activation by the i-proteasome in comparison to the standard proteasome. 20S i-proteasomes accelerate IκBα degradation (144), p65 nuclear translocation is lower in IFN-γ activated murine embryonic fibroblasts from LMP7$^{-/-}$ mice (149), and LPS-activated B cells from LMP2$^{-/-}$ degrade IκBα less efficiently than controls do (147). However, different groups revisited these aspects and novel data reported on contradictory findings arguing that the i-proteasome plays no obligatory role in the degradation of IκBα and activation of the canonical NF-κB pathway (59, 114, 137, 148). Different model systems and heterogeneous read outs for the activation of canonical NF-κB activation might attribute to these controversial findings. As illustrated in **Table 2**, more recent reports utilized advanced models such as primary cells obtained from different i-proteasome deficient mouse strains (LMP7$^{-/-}$, LMP7$^{-/-}$/Mecl-1$^{-/-}$, LMP2$^{-/-}$), and, more importantly, applied selective proteasome inhibitors in diverse immune and non-immune cells. Moreover, the majority of these reports focused on transcriptional activity of the canonical NF-κB pathway, whereas earlier reports indicated effects on signaling primarily at the level of p105 processing and Iκ-Bα degradation.

Similar to TLR4-stimulated cells, cytokine/chemokine production in TLR 7 activated cells also involves MyD88 signaling, which in addition to NF-κB activates mitogen-activated protein kinase kinases (MAPKK) resulting in phosphorylation of p38, c-Jun N-terminal kinases (JNKs), and extracellular signal-regulated kinases 1/2 (ERK1/2), culminating in activation of AP-1 (101, 151). Pan-specific proteasome inhibition influences this MAPKK pathway in lipopolysaccharide (LPS)-stimulated DCs (104). Since the pool of proteasomes in DCs is mostly comprised of the i-proteasome (136), such findings are indicative for a specific effect of the i-proteasome. And indeed, data from more recent work showed that the i-proteasome controls specifically the abundance and/or activity of certain kinases, phosphatases and/or regulatory proteins involved in the complex MAPK signaling network, resulting in increased MAPK phosphorylation upon engagement of TLR4 and TLR7 (72, 114). A comprehensive system biology-based approach might be most appropriate to dissect the involved effectors that rely on functional i-proteasome activity. If and how i-proteasome activity influences mRNA transcription of genes that are under the control of IRF3, IRF8, and IRF7 is still a matter of ongoing investigation. TLR4-activated DCs from LMP7$^{-/-}$/Mecl-1$^{-/-}$ mice show unaltered phosphorylation of IRF3 (105). The pan-specific inhibitor of the proteasome bortezomib interferes with IRF-3 and IRF-8 activation in response to LPS in human DCs (104), suggesting a selective effect of proteasome inhibition on the IRF-3 pathway as well.

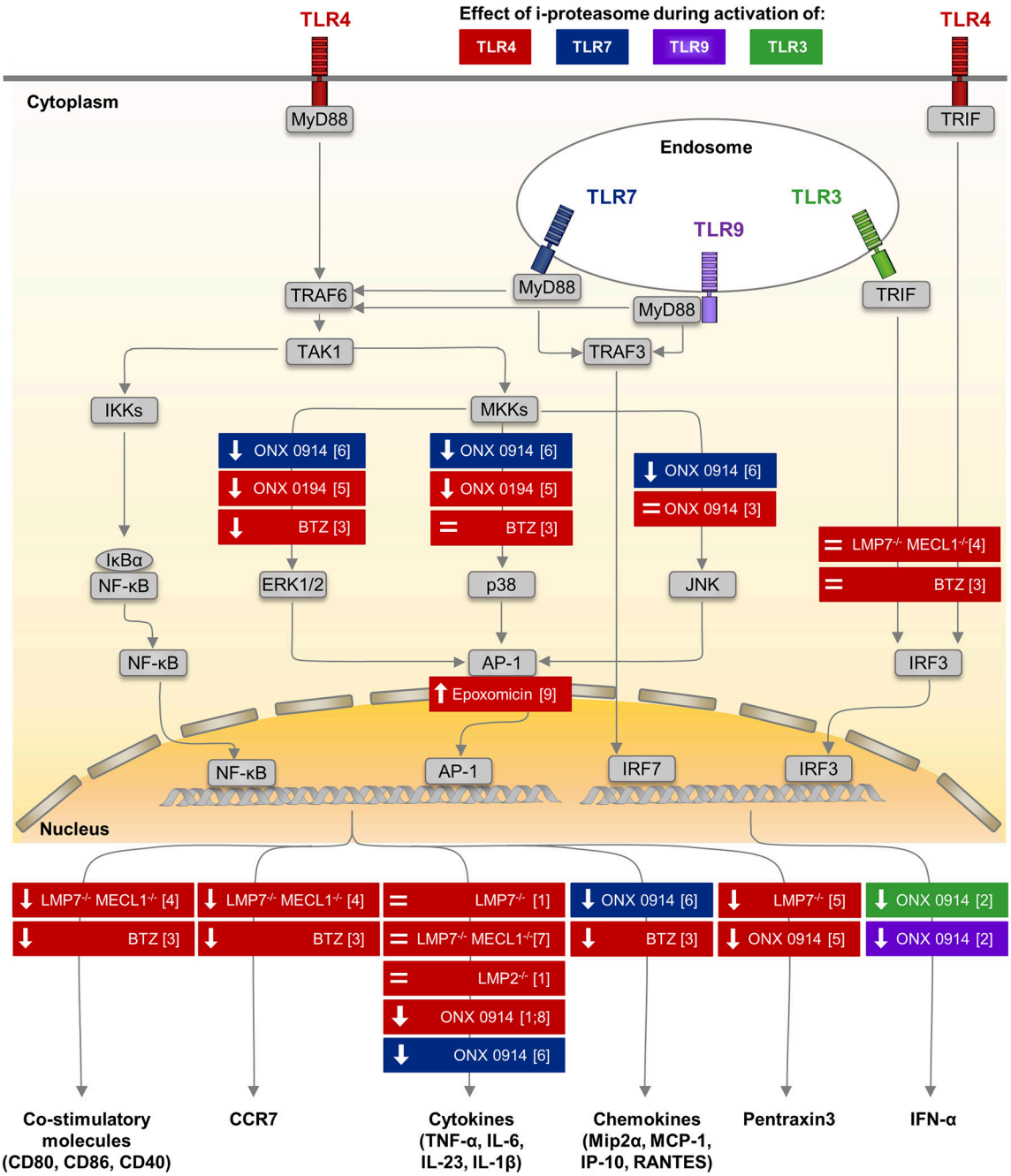

FIGURE 1 | Impact of i-proteasome subunits on innate immune signaling in myeloid cells. Among many different pattern recognition receptors, TLRs are sensors of microbial antigens on monocytes/macrophages and dendritic cells. These membrane-bound receptors are located both on the cellular surface (TLR4—colored in red) and in endosomes (TLR3—green, TLR7—blue, TLR9—purple) (101). Signaling pathways down-stream of TLR4, TLR7, and TLR9 involve the common adaptor molecule MyD88 (130, 131). Upon TLR stimulation, the ubiquitin E3 ligase TRAF6 engages with the TLR/MyD88 complex and generates poly-ubiquitin scaffolds (132), thereby recruiting the TAK1 complex (133). TAK1 then activates the IKK complex, which in turn phosphorylates IκBα. Ubiquitination of IκBα marks it for degradation by the proteasome. Thereafter, NF-κB translocates into the nucleus. Simultaneously, TAK1 induces MAP kinase signaling (134), which results in the phosphorylation of ERK1/2, p38, and JNK and thereby activates the transcription factor AP-1. Both NF-κB and AP-1 induce the expression of co-stimulatory molecules (CD80, CD86, CD40) and migration signals (CCR7) on DCs, the secretion of pro-inflammatory cytokines (e.g., TNF-α, IL-6, IL-23, IL-1β), chemokines (e.g., Mip2α, MCP-1, IP-10, RANTES), and of Pentraxin3 by monocytes/macrophages (cytokines partially also by DCs). MyD88-dependent TLR7/9 signaling induces the phosphorylation of IRF7, which is a key regulator of T1IFN (IFNα, IFNβ) expression in pDCs (135). Signals from TLR3 and TLR4 are transmitted by a MyD88-independent, TRIF-dependent pathway involving activating kinases (131). Phosphorylation of IRF-3 induces translocation into the nucleus. Results obtained from *in vitro* studies, in which the impact of the different peptidase activities of the proteasome isoforms regarding to TLR signaling or the expression of effector molecules were investigated by different

(Continued)

FIGURE 1 | approaches, are summarized. Colors indicate the type of TLR stimulated to activate innate immune cells of different origin including human PBMCs, murine splenocytes, bone marrow cells and peritoneal macrophages. Each box illustrates both the model used to alter a specific peptidase activity of the proteasome—innate myeloid cells isolated from knock out mice or proteasome inhibitors with different specificity studied in innate myeloid cells, as well as, the observed effect either on the respective signaling pathway or on the production of respective effector molecules. (↓): reduced phosphorylation of a key molecule in the indicated signaling pathway or lower production of the effector molecule, = no alteration of signaling or production of the effector molecule. AP-1, activator protein 1; BTZ, bortezomib—a pan-specific proteasome inhibitor included because the i-proteasome is highly abundant in DCs (136), CCR7, C-C chemokine receptor type 7; DC, dendritic cell; ERK, extracellular signal–regulated kinases; IκBs, inhibitors of κB; IKK, IκB kinase; IP-10, interferon-gamma induced protein 10; IRF3, interferon regulatory factor 3; JNK, c-Jun N-terminal kinase; MAPK, mitogen-activated protein kinase; MCP-1, monocyte chemoattractant protein 1; Mip2α, macrophage inflammatory protein 2α; MKK, mitogen-activated protein kinase kinase; MyD88, myeloid differentiation primary response 88; NF-κB, nuclear factor-κB; ONX 0914, immunoproteasome inhibitor (59); RANTES, regulated on activation; normal T cell expressed and secreted; T1IFN, type I interferon; TAK1, transforming growth factor-β activated kinase 1; TLR, Toll-like receptor; TNF-α, tumor necrosis factor α; TRAF, TNF receptor associated factor; TRIF, TIR-domain-containing adapter inducing IFNβ. (1) (59) (2) (63) (3) (104) (4) (105) (5) (114) (6) (72) (7) (137) (8) (138) (9) (116).

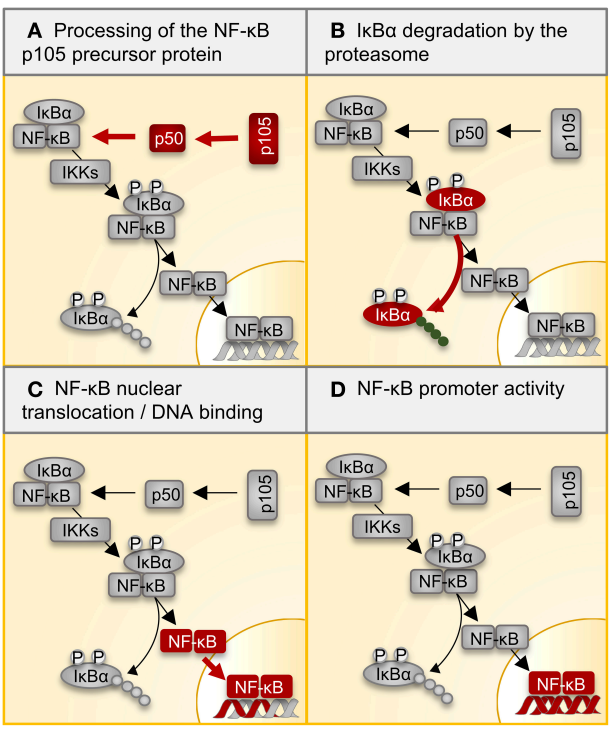

FIGURE 2 | Regulation of NF-κB signaling by the proteasome. Multiple inflammatory signals result in the activation of the transcription factor NF-κB through a variety of adapter proteins and kinases. The most abundant form of the NF-κB dimer is the p50/p65 heterodimer. **(A)** The p105 precursor is processed by the proteasome, thereby liberating the NF-kB p50 subunit for dimerization with p65. IκB retains the NF-κB heterodimer in the cytoplasm. **(B)** Ligand binding to cellular receptors like TLRs activates the IKK complex, which catalyzes the phosphorylation of IκB, inducing its poly-ubiquitination and degradation by the proteasome. **(C)** Activated NF-κB translocates into the nucleus, where it **(D)** activates target gene expression. **Table 2** summarizes all reported effects of i-proteasome activity on the different steps in this canonical NF-κB signaling pathway. NF-kB, nuclear factor kappa B; IκBs, inhibitors of κB; IKK, IκB kinase.

Natural Killer Cells

Natural killer (NK) cells as lymphoid effectors of the rapidly acting antiviral immune response are among the first cells to sense pro-inflammatory cytokines. More than two decades ago, the importance of NK cells for CVB3 clearance and disease progression was highlighted in mice (152, 153). More recently, this pathobiological significance could be extended by providing firm evidence for a protective role of the NK cell receptor NKG2D, which upon activation triggers effective virus clearance in myocarditis (154). Knowledge regarding the impact of proteasome activity on NK cell function is incomplete and data are mainly available from tumor models. Immune surveillance of tumor cells involves a tumor necrosis factor-related apoptosis-inducing ligand (TRAIL)-mediated cytotoxic pathway used by NK cells leading to tumor cell lysis. Proteasome inhibitors like bortezomib can sensitize tumor cells to TRAIL-mediated lysis (155). If findings in tumor models might be transferable to viral myocarditis, is unknown. There is no evidence for a specific influence of the different proteasome isoforms on NK cell abundance within the inflamed heart of mice after CVB3 infection (23). Nevertheless, our current comprehension of the role of proteasome activity on NK cell function during viral myocarditis remains incomplete.

INFLUENCE OF THE PROTEASOME ON ESTABLISHMENT OF ADAPTIVE IMMUNITY

The migration of NK cells and myeloid cells to the site of injury in conjunction with a considerable increase in pro-inflammatory cytokines is followed by a second wave of infiltration with $CD4^+$ and to a lesser extent B and $CD8^+$ T lymphocytes as well. Similar to innate immunity, virtually all knowledge about the biological function of the adaptive immune response with regard to the manifestation of viral myocarditis is based on the mouse model of CVB3-induced myocarditis. Experiments with immune-deficient mice revealed that both humoral and cellular immune responses are required to control CVB3 infection. Accordingly, mice with severe combined immunodeficiency, which lack mature B and T cell function, develop extensive myocarditis with high mortality rates (156). In this review, we expand upon established knowledge about the function of the proteasome in adaptive immunity and attempt to illuminate the implication of the different isoforms in virus control. For further details on interactions of coxsackievirus and adaptive immune system, we refer the reader to an excellent review by (15).

TABLE 2 | Regulation of NF-κB signaling by the i-proteasome.

Affected part of NF-κB pathway	Implicated subunit	Shown in/by	Cell type/stimulus	Determined by	References
Processing of the NF-κB p105 precursor protein—(A)	LMP2	NOD and LMP2$^{-/-}$ mice	Splenocytes	WB, IVP	(143)
	LMP2, MECL-1	IBD patients	Isolated proteasomes from colonic mucosa	IVP	(144)
	LMP2, LMP7	Cells lacking LMP2 and LMP7	T2 cells (human)	WB, IVP	(145)
	LMP2, LMP7	Cells lacking LMP2 and LMP7	T2 cells	WB	(146)
IκBα degradation by the proteasome—(B)	LMP2	LMP2$^{-/-}$ mice	B cells + LPS	WB	(147)
	LMP2	NOD and LMP2$^{-/-}$ mice	Splenocytes + TNF-α	WB	(143)
	LMP2, MECL-1	IBD patients	Isolated proteasomes from colonic mucosa	WB	(144)
	LMP2, LMP7	Cells lacking LMP2 and LMP7	T2 cells + TNF-α	WB	(145)
	LMP7	ONX 0914	Cardiomyocytes (murine) + IFN-γ/TNF-α	WB	(114)
	LMP2, LMP7	UK-101, LSK01	Lung cells H23 (human) + TNF-α	WB	(148)
	LMP7	LMP7$^{-/-}$ mice, ONX 0914	BM macrophages + LPS	WB	(114)
	LMP2, LMP7, MECL-1	LMP7$^{-/-}$ MECL-1$^{-/-}$ and LMP2$^{-/-}$ mice	Perit. Macrophages + IFN-γ/TNF-α or LPS, MEFs +IFN-γ/LPS	WB	(137)
NF-κB nuclear translocation and DNA binding—(C)	LMP2	NOD and LMP2$^{-/-}$ mice	Splenocytes + TNF-α	EMSA	(143)
	LMP2, LMP7	Cells lacking LMP2 and LMP7	T2 cells + TNF-α	EMSA	(145)
	LMP7	LMP7$^{-/-}$ mice	MEFs +IFN-γ/TNF-α	IF	(149)
	LMP7	LMP7$^{-/-}$ mice	Cardiomyocytes + IFN-γ/TNF-α	TransAM® NFκB p50	(23)
	LMP7	ONX 0914	Cardiomyocytes (murine) + IFN-γ/TNF-α	WB	(114)
	LMP7	ONX 0914	BM macrophages + LPS	TransAM® NFκB p50, WB	(114)
	LMP2, LMP7	UK-101, LSK01	Lung cells H23 (human) + TNF-α	WB, IF, EMSA	(148)
	LMP2, LMP7, MECL-1	LMP7$^{-/-}$ MECL-1$^{-/-}$ and LMP2$^{-/-}$ mice	MEFs +IFN-γ/TNF-α	EMSA, TransAM® NFκB p65	(137)
NF-κB promoter activity—(D)	LMP2, LMP7	Cells lacking LMP2 and LMP7	T2 cells + TNF-α	Luciferase assay	(145)
	LMP2	UK-101	Lung cells H23 + TNF-α	Luciferase assay	(148)
	LMP7	LSK01	Lung cells H23 + TNF-α	Luciferase assay	(148)
	LMP7	ONX 0914	Lung cells A549 + IFN-γ/TNF-α	Luciferase assay	(59)
	LMP7	ONX 0914	Macrophages RAW264.7 (murine) + LPS	Luciferase assay	(114)

*Known effects of the i-proteasome are summarized for each step of the NF-κB signaling pathway. These steps involve: (A) processing of the NF-κB p105 precursor protein, (B) IκBα degradation by the proteasome, (C) NF-κB nuclear translocation and DNA binding, and (D) NF-κB promoter activity, respectively (**Figure 2**). Results that indicate a specific role of the i-proteasome for canonical NF-κB signaling are colored in light blue. Controversial findings arguing against the notion that the i-proteasome has a specific effect on canonical NF-κB signaling are colored in dark blue. NF-kB: nuclear factor kappa B, IκBs, inhibitors of κB; T2 cells, human lymphoblast cell line defective in LMP2 and LMP7; UK-101, LMP2-specific inhibitor; LSK-01, LMP7-specific inhibitor; ONX 0914, immunoprotesome-specific inhibitor. WB, Western blotting; IF, immuno-fluorescence; EMSA, electrophoretic mobility shift assay; IVP, p105 in vitro processing assay, perit. macrophages: peritoneal macrophages; BM macrophages, bone marrow-derived macrophages; MEFs, mouse embryonic fibroblasts; LPS, lipopolysaccharide.*

Influence of CD8$^+$ T Cells on Viral Myocarditis and Role of the Proteasome

In contrast to the preponderant significance of B cell and CD4$^+$ T cell responses for CVB3 clearance (157, 158), the pathophysiological significance of CD8$^+$ T cells for CVB3 clearance and inflammatory injury is less clear. The protective function of CD8$^+$ T cells (159) involves the production of cytokines like IFNγ, yet is clearly separated from the direct cytolytic effect mediated by perforin, a classic hallmark of virus-specific CD8$^+$ T cells (160). CD8$^+$ T cells acting by perforin cause extensive destruction of myocardial tissue (160, 161). Evidence arguing in favor of a protective function of CD8$^+$ T cells during myocarditis was obtained from CD8$^+$ T cell-deficient β2-microglobulin$^{-/-}$ mice, in which injury of cardiac tissue exacerbates due to insufficient confinement of the initial viral load in the heart muscle (160). One needs to keep in mind that constitutive knockout models for perforin and β2-microglobulin do not only mirror the function of these molecules in CD8$^+$ T cells. Both perforin and β2-microglobulin affect also NK cell activation and function. Nevertheless, the finding that CD8$^+$ T cells restrain CVB3 in mice indicates that the virus could induce detectable CD8$^+$ T cell responses. However, the Whitton group provided data that coxsackieviruses do not elicit strong CD8$^+$ T cell responses. Investigation of mice infected with a recombinant CVB3 encoding known lymphocytic choriomeningitis virus (LCMV) derived CD8$^+$ T cell epitopes failed to trigger a marked expansion of CD8$^+$ T effector cells (162, 163). This is mainly due to the inhibition of antigen presentation by virus-induced disruption of host protein trafficking in infected cells (164, 165). The virus almost completely blocks antigen presentation via the MHC class I pathway, thereby evading CD8$^+$ T cell immunity (163). Our group followed a complementary approach employing prediction tools for proteasomal cleavage sites, MHC binding studies and *in vitro* peptide processing assays with the proteasome to identify MHC class I epitopes originating from CVB3 proteins (8, 166). Concordant with the findings by the Whitton group, expansion of respective CD8$^+$ T effector cells was weak in mice (8). Similarly, adoptive transfer of CD8$^+$ T cells isolated from mice with CVB3 myocarditis did not affect the manifestation of viral myocarditis in recipient mice (23).

Based on these virus-specific aspects, the role for the i-proteasome with regard to induction of CD8$^+$ T cell responses needs to be revisited for viral myocarditis. Following up on robust i-proteasome formation in hearts of both MAV-1 and CVB3-infected mice (30, 31), the Weinberg lab and our workgroup investigated the role of the i-proteasome concerning virus clearance in myocarditis. The i-proteasome facilitates the release of peptides harboring hydrophobic or basic C-terminal amino acids typical for MHC class I epitopes (22, 27). By facilitating such specific peptide cleavages, the i-proteasome augments the pool of antigenic peptides (40). Nevertheless, we found uniformly that the i-proteasome can be adequately compensated by its standard proteasome counterpart during viral myocarditis (23, 31). Although the i-proteasome provides an increased capacity to liberate CVB3 epitopes for MHC class I antigen presentation (40, 166), it cannot compensate for the disruption of MHC class I presentation by the virus. If detectable at all, CD8$^+$ effector T cell responses remain weak during CVB3 infection (163).

CD4$^+$ T Cells and Antibody Responses in CVB3 Myocarditis: Impact of the Proteasome

Infections with CVB3 trigger a rapid and effective antibody response. Neutralizing antibodies appear 4 days after CVB3 infection (167) and are essential for controlling virus dissemination and clearance in the heart (158). CD4$^+$ T cells activate B cells for production of protective antibodies. In contrast to MHC class I, MHC class II epitopes are presented efficiently upon infection with CVB3 and CD4$^+$ T cells mature quickly into effector and later on into memory T cells (163). The proteasome is involved in multiple cellular processes needed for antibody production. As outlined above, it controls the maturation and activation of DCs (104), but the proteasome regulates also B cell function (147). The canonical pathway for MHC class II antigen presentation is located within the endolysosomal compartment and thereby spatially separated from the proteasome. However, there is also a non-canonical cytosolic pathway of MHC class II-restricted antigen processing involving proteasome-dependent peptide processing. In addition to DCs exposed to exogenous influenza and vaccinia virus (168), cancer cells present peptides on MHC class II by such non-classical antigen-processing pathways (169). It is unknown whether the cleavage site preference of the different proteasome isoforms determine a specific CD4$^+$ T cell repertoire as reported for CD8$^+$ T cells. To dissect the function of the i-proteasome in CVB3 myocarditis, our group applied the i-proteasome-specific inhibitor ONX 0914, and alternatively utilized LMP7$^{-/-}$ mice. We found a strong induction of CVB3-directed immunoglobulins and neutralizing antibodies in mice lacking intact i-proteasome function (23). In fact, neutralizing antibody titers were higher in mice with ONX 0914 treatment, an observation that might be attributed to maintained survival of CD4$^+$ T cells during infection in response to i-proteasome inhibition (72). The latter finding during CVB3 infection was specific for A/J mice and did not occur in B6 mice. In B6 mice, i-proteasome inhibition resulted in a reduction of lymphocyte abundance in blood and spleen at the acute phase of the disease. In fact, other groups demonstrated also a pro-survival function of the i-proteasome in T cells during viral infection with IV and LCMV (147, 170).

The fact that re-infection of B6 mice with CVB3 4 weeks after primary virus inoculation completely revokes disease manifestation emphasizes the importance of memory immune status, as well as, antibody formation during CVB3 infection (72). Upon encountering CVB3, memory T and B cells initiate cell division much more rapidly than their naive counterparts do. These data suggest that the level of MHC/peptide complex upon initial infection is sufficient to trigger memory T cells (163). In CVB3-infected B6 mice, displaying impaired i-proteasome function, adequate immune memory develops unhindered as well (23, 72). Similarly, protective immunity to MAV-1 is preserved in LMP7$^{-/-}$ mice (31). Conclusively, the specific peptidase

activities of the i-proteasome are not essential for establishment of an adaptive immune response in mouse models of viral myocarditis.

CVB-specific $CD4^+$ T cells show an effector phenotype with a Th1 cytokine profile (163). In addition, A/J mice induce an autoreactive $CD4^+$ T cell repertoire that contains IL-17-producing cells (11). The availability of i-proteasome selective inhibitors shed new light onto the role of the i-proteasome during $CD4^+$ T cell differentiation. Under Th17 skewing conditions, inhibition of the LMP7 subunit downregulates RORγt activity leading to reduced Th17 counts, whereby lower STAT1 phosphorylation reduces IFN-γ production under Th1 skewing conditions indicative for lower Th1 counts (171). Whether or not these *in vitro* findings are relevant during viral myocarditis needs further investigation—a challenging task given the relatively weak IL-17 signal obtained from $CD4^+$ T cells during acute myocarditis (11).

FUTURE PERSPECTIVES

Several mechanisms have been proposed for CVB3-mediated myocarditis in mice, including direct virus-mediated cell damage and destruction of heart tissue in response to the action of immune effector cells (7). Being the major cellular mechanism for protein degradation, the proteasomal system adapts to augmented protein turnover by increased formation of i-proteasomes (32, 33). Based on structural information (17, 18, 29), site-specific inhibitors targeting particular subunits of the major proteasome isoforms have become available [reviewed in (51)] and our understanding about the pathophysiological role of the proteasome during CVB3-mediated myocarditis has thereby improved. In our concluding remarks, we discuss whether subunit-selective inhibitors might be applicable to suppress manifestation or progression of virus-induced cardiac injury.

Inactivation of the highly abundant β5 standard proteasome subunit in murine cardiomyocytes augments apoptosis in myocardial ischemia/reperfusion injury (172) or due to doxorubicin treatment. In contrast, even under conditions with cytokine-induced i-proteasome expression, selective i-proteasome inhibitors are advantageous in reducing cardiomyocyte death in comparison to compounds targeting either the standard or both the standard and the i-proteasome with similar efficacy (25). During viral myocarditis, i-proteasome formation and to a minor extent induction of PA28β also enhance cellular protein turnover reducing the accumulation of oxidant-damaged proteins (23, 73). The notion of a minor influence of the i-proteasome regarding the control of pathogens was supported by elimination of virus despite a reduction of T1IFN (63, 72) upon i-proteasome inhibitor treatment and induction of immune memory in CVB3 heart disease (72). This is consistent with findings for other pathogens as well (48, 59) and in addition, i-proteasome inhibitors are well tolerated in other viral infection models (31, 173). In none of these models, i-proteasome inhibition alters significantly the abundance of toxic aggregates. Most strikingly, in mice susceptible for CVB3 myocarditis, i-proteasome inhibition is highly beneficial. ONX 0914 treatment improves cardiac function and mortality by efficient suppression of cardiac and systemic chemokine and cytokine production (72).

In addition to myocarditis, experimental infection of susceptible mice with CVB3 results in severe systemic disease as well, with the pancreas being the primary and most affected organ (174). Early upon infection, mice become hypoglycemic, most likely due to pancreatitis and digestive dysfunction (175). With the release of cytokines, such systemic pathology alters the vascular tone and impairs diastolic filling as well. Systemic disease in A/J mice is reminiscent of a distributive shock in sepsis (118). Importantly, given the high abundance of i-proteasome in immune cells, i-proteasome specific inhibitors affect systemic pathology as well and this has immediate impact on the cardiac output and immune-mediated damage of heart tissue (72). Other than in the experimental mouse model, myocarditis in man usually follows a benign respiratory, gastrointestinal or urogenital infection, and pancreatitis is reported only occasionally (3). Therefore, our current understanding of i-proteasome biology during myocarditis needs further clarification. Additional research ought to elucidate the contribution of the i-proteasome once virus-mediated injury of the heart muscle has developed. In addition, we need detailed knowledge on molecular and cellular aspects of i-proteasome biology and the underlying mechanisms that contribute to the protective outcome if the i-proteasome is blocked prior to the occurrence of viral heart disease. As the i-proteasome has wide-ranging functions, toxicity and immune-related adverse effects may represent significant hurdles regarding the application of i-proteasome inhibitors. A detailed comprehension of i-proteasome function at an advanced stage of myocarditis is particularly important, because the resolution of acute CVB3 myocarditis is followed by the onset of chronic inflammation, which has been attributed to autoimmunity, as shown in genetically susceptible mice (176). Whether the i-proteasome affects also manifestation of autoimmune heart disease is unknown. Nonetheless, our current understanding of i-proteasome biology encourages a continued look at this context to define novel treatment options for viral heart disease.

AUTHOR CONTRIBUTIONS

All authors listed have made a substantial, direct and intellectual contribution to the work, and approved it for publication.

FUNDING

Funding was funded by the Foundation for Experimental Biomedicine (Zurich, Switzerland), by the German Research Foundation DFG BE 6335/4-1 and DFG BE 6335/6-1, CRC 1292 project 02, as well as, by the Federal Ministry of Education and Research (BacVirISG15 031L0123B) to AB. We acknowledge Martin Voss and Hannah Louise Neumaier for critical discussion of the manuscript. Publication was supported by the German Research Foundation (DFG) and the Open Access Publication Fund of Charité—Universitätsmedizin Berlin.

REFERENCES

1. Cooper LT Jr. Myocarditis. *N Engl J Med.* (2009) 360:1526–38. doi: 10.1056/NEJMra0800028
2. Epelman S, Liu PP, Mann DL. Role of innate and adaptive immune mechanisms in cardiac injury and repair. *Nat Rev Immunol.* (2015) 15:117–29. doi: 10.1038/nri3800
3. Sagar S, Liu PP, Cooper LT Jr. Myocarditis. *Lancet* (2012) 379:738–47. doi: 10.1016/S0140-6736(11)60648-X
4. Caforio AL, Pankuweit S, Arbustini E, Basso C, Gimeno-Blanes J, Felix SB, et al. Current state of knowledge on aetiology, diagnosis, management, and therapy of myocarditis: a position statement of the European Society of Cardiology Working Group on Myocardial and Pericardial Diseases. *Eur Heart J.* (2013) 34:2636–48. doi: 10.1093/eurheartj/eht210
5. Feldman AM, Mcnamara D. Myocarditis. *N Engl J Med.* (2000) 343:1388–98. doi: 10.1056/NEJM200011093431908
6. Klingel K, Hohenadl C, Canu A, Albrecht M, Seemann M, Mall G, et al. Ongoing enterovirus-induced myocarditis is associated with persistent heart-muscle infection - quantitative-analysis of virus-replication, tissue-damage, and inflammation. *Proc Natl Acad Sci USA.* (1992) 89:314–8. doi: 10.1073/pnas.89.1.314
7. Corsten MF, Schroen B, Heymans S. Inflammation in viral myocarditis: friend or foe? *Trends Mol Med.* (2012) 18:426–37. doi: 10.1016/j.molmed.2012.05.005
8. Jakel S, Kuckelkorn U, Szalay G, Plotz M, Textoris-Taube K, Opitz E, et al. Differential interferon responses enhance viral epitope generation by myocardial immunoproteasomes in murine enterovirus myocarditis. *Am J Pathol.* (2009) 175:510–8. doi: 10.2353/ajpath.2009.090033
9. Kindermann I, Kindermann M, Kandolf R, Klingel K, Bultmann B, Muller T, et al. Predictors of outcome in patients with suspected myocarditis. *Circulation* (2008) 118:639–48. doi: 10.1161/CIRCULATIONAHA.108.769489
10. Flynn CT, Kimura T, Frimpong-Boateng K, Harkins S, Whitton JL. Immunological and pathological consequences of coxsackievirus RNA persistence in the heart. *Virology* (2017) 512:104–12. doi: 10.1016/j.virol.2017.09.017
11. Gangaplara A, Massilamany C, Brown DM, Delhon G, Pattnaik AK, Chapman N, et al. Coxsackievirus B3 infection leads to the generation of cardiac myosin heavy chain-alpha-reactive CD4 T cells in A/J mice. *Clin Immunol.* (2012) 144:237–49. doi: 10.1016/j.clim.2012.07.003
12. Neumann DA, Rose NR, Ansari AA, Herskowitz A. Induction of multiple heart autoantibodies in mice with coxsackievirus B3- and cardiac myosin-induced autoimmune myocarditis. *J Immunol.* (1994) 152:343–50.
13. Rose NR. Myocarditis: infection versus autoimmunity. *J Clin Immunol.* (2009) 29:730–7. doi: 10.1007/s10875-009-9339-z
14. Kaya Z, Leib C, Katus HA. Autoantibodies in heart failure and cardiac dysfunction. *Circ Res.* (2012) 110:145–58. doi: 10.1161/CIRCRESAHA.111.243360
15. Kemball CC, Alirezaei M, Whitton JL. Type B coxsackieviruses and their interactions with the innate and adaptive immune systems. *Fut Microbiol.* (2010) 5:1329–47. doi: 10.2217/fmb.10.101
16. Goldberg AL. Protein degradation and protection against misfolded or damaged proteins. *Nature* (2003) 426:895–9. doi: 10.1038/nature02263
17. Groll M, Ditzel L, Lowe J, Stock D, Bochtler M, Bartunik HD, et al. Structure of 20S proteasome from yeast at 2.4 angstrom resolution. *Nature* (1997) 386:463–71. doi: 10.1038/386463a0
18. Groll M, Bajorek M, Kohler A, Moroder L, Rubin DM, Huber R, et al. A gated channel into the proteasome core particle. *Nat Struct Biol.* (2000) 7:1062–7. doi: 10.1038/80992
19. Pickart CM, Cohen RE. Proteasomes and their kin: proteases in the machine age. *Nat Rev Mol Cell Biol.* (2004) 5:177–87. doi: 10.1038/nrm1336
20. Dantuma NP, Lindsten K. Stressing the ubiquitin-proteasome system. *Cardiovasc Res.* (2010) 85:263–71. doi: 10.1093/cvr/cvp255
21. Dikic I. Proteasomal and autophagic degradation systems. *Annu Rev Biochem.* (2017) 86:193–224. doi: 10.1146/annurev-biochem-061516-044908
22. Gaczynska M, Rock KL, Goldberg AL. Gamma-interferon and expression of Mhc genes regulate peptide hydrolysis by proteasomes. *Nature* (1993) 365:264–7. doi: 10.1038/365264a0
23. Opitz E, Koch A, Klingel K, Schmidt F, Prokop S, Rahnefeld A, et al. Impairment of immunoproteasome function by beta5i/LMP7 subunit deficiency results in severe enterovirus myocarditis. *PloS Pathog.* (2011) 7:1–13. doi: 10.1371/journal.ppat.1002233
24. Hallermalm K, Seki K, Wei C, Castelli C, Rivoltini L, Kiessling R, et al. Tumor necrosis factor-alpha induces coordinated changes in major histocompatibility class I presentation pathway, resulting in increased stability of class I complexes at the cell surface. *Blood* (2001) 98:1108–15. doi: 10.1182/blood.V98.4.1108
25. Spur EM, Althof N, Respondek D, Klingel K, Heuser A, Overkleeft HS, et al. Inhibition of chymotryptic-like standard proteasome activity exacerbates doxorubicin-induced cytotoxicity in primary cardiomyocytes. *Toxicology* (2016) 353–354:34–47. doi: 10.1016/j.tox.2016.04.010
26. Pickering AM, Koop AL, Teoh CY, Ermak G, Grune T, Davies KJA. The immunoproteasome, the 20S proteasome and the PA28 alpha beta proteasome regulator are oxidative-stress-adaptive proteolytic complexes. *Biochem J.* (2010) 432:585–94. doi: 10.1042/BJ20100878
27. Aki M, Shimbara N, Takashina M, Akiyama K, Kagawa S, Tamura T, et al. Interferon-gamma induces different subunit organizations and functional diversity of proteasomes. *J Biochem.* (1994) 115:257–69. doi: 10.1093/oxfordjournals.jbchem.a124327
28. Strehl B, Joeris T, Rieger M, Visekruna A, Textoris-Taube K, Kaufmann SH, et al. Immunoproteasomes are essential for clearance of *Listeria monocytogenes* in nonlymphoid tissues but not for induction of bacteria-specific CD8(+) T cells. *J Immunol.* (2006) 177:6238–44. doi: 10.4049/jimmunol.177.9.6238
29. Huber EM, Basler M, Schwab R, Heinemeyer W, Kirk CJ, Groettrup M, et al. Immuno- and constitutive proteasome crystal structures reveal differences in substrate and inhibitor specificity. *Cell* (2012) 148:727–38. doi: 10.1016/j.cell.2011.12.030
30. Szalay G, Meiners S, Voigt A, Lauber J, Spieth C, Speer N, et al. Ongoing coxsackievirus myocarditis is associated with increased formation and activity of myocardial immunoproteasomes. *Am J Pathol.* (2006a) 168:1542–52. doi: 10.2353/ajpath.2006.050865
31. Mccarthy MK, Malitz DH, Molloy CT, Procario MC, Greiner KE, Zhang L, et al. Interferon-dependent immunoproteasome activity during mouse adenovirus type 1 infection. *Virology* (2016) 498:57–68. doi: 10.1016/j.virol.2016.08.009
32. Seifert U, Bialy LP, Ebstein F, Bech-Otschir D, Voigt A, Schroter F, et al. Immunoproteasomes preserve protein homeostasis upon interferon-induced oxidative stress. *Cell* (2010) 142:613–24. doi: 10.1016/j.cell.2010.07.036
33. Ebstein F, Voigt A, Lange N, Warnatsch A, Schroter F, Prozorovski T, et al. Immunoproteasomes are important for proteostasis in immune responses. *Cell* (2013) 152:935–7. doi: 10.1016/j.cell.2013.02.018
34. Murata S, Yashiroda H, Tanaka K. Molecular mechanisms of proteasome assembly. *Nat Rev Mol Cell Biol.* (2009) 10:104–15. doi: 10.1038/nrm2630
35. Murata S, Sasaki K, Kishimoto T, Niwa S, Hayashi H, Takahama Y, et al. Regulation of CD8+ T cell development by thymus-specific proteasomes. *Science* (2007) 316:1349–53. doi: 10.1126/science.1141915
36. Guillaume B, Chapiro J, Stroobant V, Colau D, Van Holle B, Parvizi G, et al. Two abundant proteasome subtypes that uniquely process some antigens presented by HLA class I molecules. *Proc Natl Acad Sci USA.* (2010) 107:18599–604. doi: 10.1073/pnas.1009778107
37. Kloetzel PM, Ossendorp F. Proteasome and peptidase function in MHC-class-I-mediated antigen presentation. *Curr Opin Immunol.* (2004) 16:76–81. doi: 10.1016/j.coi.2003.11.004
38. Gaczynska M, Rock KL, Spies T, Goldberg AL. Peptidase activities of proteasomes are differentially regulated by the major histocompatibility complex-encoded genes for LMP2 and LMP7. *Proc Natl Acad Sci USA.* (1994) 91:9213–7. doi: 10.1073/pnas.91.20.9213
39. Sijts EJ, Kloetzel PM. The role of the proteasome in the generation of MHC class I ligands and immune responses. *Cell Mol Life Sci.* (2011) 68:1491–502. doi: 10.1007/s00018-011-0657-y
40. Mishto M, Liepe J, Textoris-Taube K, Keller C, Henklein P, Weberruss M, et al. Proteasome isoforms exhibit only quantitative differences in cleavage and epitope generation. *Eur J Immunol.* (2014) 44:3508–21. doi: 10.1002/eji.201444902

41. Schwarz K, Van Den Broek M, Kostka S, Kraft R, Soza A, Schmidtke G, et al. Overexpression of the proteasome subunits LMP2, LMP7, and MECL-1, but not PA28 alpha/beta, enhances the presentation of an immunodominant lymphocytic choriomeningitis virus T cell epitope. *J Immunol.* (2000) 165:768–78. doi: 10.4049/jimmunol.165.2.768
42. Chen WS, Norbury CC, Cho YJ, Yewdell JW, Bennink JR. Immunoproteasomes shape immunodominance hierarchies of antiviral CD8(+) T cells at the levels of T cell repertoire and presentation of viral antigens. *J Exp Med.* (2001) 193:1319–26. doi: 10.1084/jem.193.11.1319
43. Deol P, Zaiss DM, Monaco JJ, Sijts AJ. Rates of processing determine the immunogenicity of immunoproteasome-generated epitopes. *J Immunol.* (2007) 178:7557–62. doi: 10.4049/jimmunol.178.12.7557
44. Tu L, Moriya C, Imai T, Ishida H, Tetsutani K, Duan XF, et al. Critical role for the immunoproteasome subunit LMP7 in the resistance of mice to *Toxoplasma gondii* infection. *Eur J Immunol.* (2009) 39:3385–94. doi: 10.1002/eji.200839117
45. Kincaid EZ, Che JW, York I, Escobar H, Reyes-Vargas E, Delgado JC, et al. Mice completely lacking immunoproteasomes show major changes in antigen presentation. *Nat Immunol.* (2012) 13:129–35. doi: 10.1038/ni.2203
46. Ersching J, Vasconcelos JR, Ferreira CP, Caetano BC, Machado AV, Bruna-Romero O, et al. The combined deficiency of immunoproteasome subunits affects both the magnitude and quality of pathogen- and genetic vaccination-induced CD8+ T cell responses to the human protozoan parasite *Trypanosoma cruzi*. *PLoS Pathog.* (2016) 12:e1005593. doi: 10.1371/journal.ppat.1005593
47. Fehling HJ, Swat W, Laplace C, Kuhn R, Rajewsky K, Muller U, et al. Mhc class-I expression in mice lacking the proteasome subunit Lmp-7. *Science* (1994) 265:1234–7. doi: 10.1126/science.8066463
48. Nussbaum AK, Rodriguez-Carreno MP, Benning N, Botten J, Whitton JL. Immunoproteasome-deficient mice mount largely normal CD8(+) T cell responses to lymphocytic choriomeningitis virus infection and DNA vaccination. *J Immunol.* (2005) 175:1153–60. doi: 10.4049/jimmunol.175.2.1153
49. Vankaer L, Ashtonrickardt PG, Eichelberger M, Gaczynska M, Nagashima K, Rock KL, et al. Altered peptidase and viral-specific T-cell response in Lmp2 mutant mice. *Immunity* (1994) 1:533–41. doi: 10.1016/1074-7613(94)90043-4
50. Basler M, Mundt S, Muchamuel T, Moll C, Jiang J, Groettrup M, et al. Inhibition of the immunoproteasome ameliorates experimental autoimmune encephalomyelitis. *EMBO Mol Med.* (2014) 6:226–38. doi: 10.1002/emmm.201303543
51. Kisselev AF, Groettrup M. Subunit specific inhibitors of proteasomes and their potential for immunomodulation. *Curr Opin Chem Biol.* (2014) 23:16–22. doi: 10.1016/j.cbpa.2014.08.012
52. Richardson PG, Barlogie B, Berenson J, Singhal S, Jagannath S, Irwin D, et al. A phase 2 study of bortezomib in relapsed, refractory myeloma. *N Engl J Med.* (2003) 348:2609–17. doi: 10.1056/NEJMoa030288
53. Richardson PG, Sonneveld P, Schuster MW, Irwin D, Stadtmauer EA, Facon T, et al. Bortezomib or high-dose dexamethasone for relapsed multiple myeloma. *N Eng J Med.* (2005) 352:2487–98. doi: 10.1056/NEJMoa043445
54. Parlati F, Lee SJ, Aujay M, Suzuki E, Levitsky K, Lorens JB, et al. Carfilzomib can induce tumor cell death through selective inhibition of the chymotrypsin-like activity of the proteasome. *Blood* (2009) 114:3439–47. doi: 10.1182/blood-2009-05-223677
55. Stewart AK, Rajkumar SV, Dimopoulos MA, Masszi T, Spicka I, Oriol A, et al. Carfilzomib, lenalidomide, and dexamethasone for relapsed multiple myeloma. *N Engl J Med.* (2015) 372:142–52. doi: 10.1056/NEJMoa1411321
56. Dimopoulos MA, Goldschmidt H, Niesvizky R, Joshua D, Chng WJ, Oriol A, et al. Carfilzomib or bortezomib in relapsed or refractory multiple myeloma (ENDEAVOR): an interim overall survival analysis of an open-label, randomised, phase 3 trial. *Lancet Oncol.* (2017) 18:1327–37. doi: 10.1016/S1470-2045(17)30578-8
57. Gomes AV, Zong C, Edmondson RD, Li X, Stefani E, Zhang J, et al. Mapping the murine cardiac 26S proteasome complexes. *Circul Res.* (2006) 99:362–71. doi: 10.1161/01.RES.0000237386.98506.f7
58. De Bruin G, Xin BT, Kraus M, Van Der Stelt M, Van Der Marel GA, Kisselev AF, et al. A set of activity-based probes to visualize human (Immuno)proteasome activities. *Angew Chem Int Ed Engl.* (2015) 55:4199–203. doi: 10.1002/anie.201509092
59. Muchamuel T, Basler M, Aujay MA, Suzuki E, Kalim KW, Lauer C, et al. A selective inhibitor of the immunoproteasome subunit LMP7 blocks cytokine production and attenuates progression of experimental arthritis. *Nat Med.* (2009) 15:781–7. doi: 10.1038/nm.1978
60. Koerner J, Brunner T, Groettrup M. Inhibition and deficiency of the immunoproteasome subunit LMP7 suppress the development and progression of colorectal carcinoma in mice. *Oncotarget* (2017) 8:50873–88. doi: 10.18632/oncotarget.15141
61. Vachharajani N, Joeris T, Luu M, Hartmann S, Pautz S, Jenike E, et al. Prevention of colitis-associated cancer by selective targeting of immunoproteasome subunit LMP7. *Oncotarget* (2017) 8:50447–59. doi: 10.18632/oncotarget.14579
62. Basler M, Dajee M, Moll C, Groettrup M, Kirk CJ. Prevention of experimental colitis by a selective inhibitor of the immunoproteasome. *J Immunol.* (2010) 185:634–41. doi: 10.4049/jimmunol.0903182
63. Ichikawa HT, Conley T, Muchamuel T, Jiang J, Lee S, Owen T, et al. Beneficial effect of novel proteasome inhibitors in murine lupus via dual inhibition of type I interferon and autoantibody-secreting cells. *Arthritis Rheum.* (2012) 64:493–503. doi: 10.1002/art.33333
64. Basler M, Lindstrom MM, Lastant JJ, Bradshaw JM, Owens TD, Schmidt C, et al. Co-inhibition of immunoproteasome subunits LMP2 and LMP7 is required to block autoimmunity. *EMBO Rep.* (2018) 19:e46512. doi: 10.15252/embr.201846512
65. Sula Karreci E, Fan H, Uehara M, Mihali AB, Singh PK, Kurdi AT, et al. Brief treatment with a highly selective immunoproteasome inhibitor promotes long-term cardiac allograft acceptance in mice. *Proc Natl Acad Sci USA.* (2016) 113:E8425–32. doi: 10.1073/pnas.1618548114
66. Li J, Basler M, Alvarez G, Brunner T, Kirk CJ, Groettrup M. Immunoproteasome inhibition prevents chronic antibody-mediated allograft rejection in renal transplantation. *Kidney Int.* (2018) 93:670–80. doi: 10.1016/j.kint.2017.09.023
67. Banks L, Pim D, Thomas M. Viruses and the 26S proteasome: hacking into destruction. *Trends Biochem Sci.* (2003) 28:452–9. doi: 10.1016/S0968-0004(03)00141-5
68. Luo H. Interplay between the virus and the ubiquitin-proteasome system: molecular mechanism of viral pathogenesis. *Curr Opin Virol.* (2016) 17:1–10. doi: 10.1016/j.coviro.2015.09.005
69. Corbin-Lickfett KA, Bridge E. Adenovirus E4-34kDa requires active proteasomes to promote late gene expression. *Virology* (2003) 315:234–44. doi: 10.1016/S0042-6822(03)00527-0
70. Luo HL, Zhang JC, Cheung C, Suarez A, Mcmanus BM, Yang DC. Proteasome inhibition reduces coxsackievirus B3 replication in murine cardiomyocytes. *Am J Pathol.* (2003) 163:381–5. doi: 10.1016/S0002-9440(10)63667-X
71. Gao G, Zhang JC, Si XN, Wong J, Cheung C, Mcmanus B, et al. Proteasome inhibition attenuates coxsackievirus-induced myocardial damage in mice. *Am J Physiol Heart Circul Physiol.* (2008) 295:H401–8. doi: 10.1152/ajpheart.00292.2008
72. Althof N, Goetzke CC, Kespohl M, Voss K, Heuser A, Pinkert S, et al. The immunoproteasome-specific inhibitor ONX 0914 reverses susceptibility to acute viral myocarditis. *EMBO Mol Med.* (2018) 10:200–18. doi: 10.15252/emmm.201708089
73. Respondek D, Voss M, Kuhlewindt I, Klingel K, Kruger E, Beling A. PA28 modulates antigen processing and viral replication during coxsackievirus B3 infection. *PLoS ONE* (2017) 12:e0173259. doi: 10.1371/journal.pone.0173259
74. Delboy MG, Roller DG, Nicola AV. Cellular proteasome activity facilitates herpes simplex virus entry at a postpenetration step. *J Virol.* (2008) 82:3381–90. doi: 10.1128/JVI.02296-07
75. La Frazia S, Amici C, Santoro MG. Antiviral activity of proteasome inhibitors in herpes simplex virus-1 infection: role of nuclear factor-kappaB. *Antivir Ther.* (2006) 11:995–1004.
76. Kaspari M, Tavalai N, Stamminger T, Zimmermann A, Schilf R, Bogner E. Proteasome inhibitor MG132 blocks viral DNA replication and assembly of human cytomegalovirus. *FEBS Lett.* (2008) 582:666–72. doi: 10.1016/j.febslet.2008.01.040

77. Prösch S, Priemer C, Hoflich C, Liebenthaf C, Babel N, Kruger DH, et al. Proteasome inhibitors: a novel tool to suppress human cytomegalovirus replication and virus-induced immune modulation. *Antivir Ther.* (2003) 8:555–67.
78. Schubert U, Ott DE, Chertova EN, Welker R, Tessmer U, Princiotta MF, et al. Proteasome inhibition interferes with gag polyprotein processing, release, and maturation of HIV-1 and HIV-2. *Proc Natl Acad Sci USA.* (2000) 97:13057–62. doi: 10.1073/pnas.97.24.13057
79. Miller LK, Kobayashi Y, Chen CC, Russnak TA, Ron Y, Dougherty JP. Proteasome inhibitors act as bifunctional antagonists of human immunodeficiency virus type 1 latency and replication. *Retrovirology* (2013) 10:120. doi: 10.1186/1742-4690-10-120
80. Widjaja I, De Vries E, Tscherne DM, Garcia-Sastre A, Rottier PJ, De Haan CA. Inhibition of the ubiquitin-proteasome system affects influenza A virus infection at a postfusion step. *J Virol.* (2010) 84:9625–31. doi: 10.1128/JVI.01048-10
81. Ros C, Burckhardt CJ, Kempf C. Cytoplasmic trafficking of minute virus of mice: low-pH requirement, routing to late endosomes, and proteasome interaction. *J Virol.* (2002) 76:12634–45. doi: 10.1128/JVI.76.24.12634-12645.2002
82. Neznanov N, Dragunsky EM, Chumakov KM, Neznanova L, Wek RC, Gudkov AV, et al. Different effect of proteasome inhibition on vesicular stomatitis virus and poliovirus replication. *PLoS ONE* (2008) 3:e1887. doi: 10.1371/journal.pone.0001887
83. Satheshkumar PS, Anton LC, Sanz P, Moss B. Inhibition of the ubiquitin-proteasome system prevents vaccinia virus DNA replication and expression of intermediate and late genes. *J Virol.* (2009) 83:2469–79. doi: 10.1128/JVI.01986-08
84. Mercer J, Snijder B, Sacher R, Burkard C, Bleck CK, Stahlberg H, et al. RNAi screening reveals proteasome- and Cullin3-dependent stages in vaccinia virus infection. *Cell Rep.* (2012) 2:1036–47. doi: 10.1016/j.celrep.2012.09.003
85. Murata S, Udono H, Tanahashi N, Hamada N, Watanabe K, Adachi K, et al. Immunoproteasome assembly and antigen presentation in mice lacking both PA28 alpha and PA28 beta. *Embo J.* (2001) 20:5898–907. doi: 10.1093/emboj/20.21.5898
86. Takemoto M, Mori Y, Ueda K, Kondo K, Yamanishi K. Productive human herpesvirus 6 infection causes aberrant accumulation of p53 and prevents apoptosis. *J Gen Virol.* (2004) 85:869–79. doi: 10.1099/vir.0.19626-0
87. Scheffner M, Werness BA, Huibregtse JM, Levine AJ, Howley PM. The E6 oncoprotein encoded by human papillomavirus types 16 and 18 promotes the degradation of p53. *Cell* (1990) 63:1129–36. doi: 10.1016/0092-8674(90)90409-8
88. Kalejta RF, Shenk T. Proteasome-dependent, ubiquitin-independent degradation of the Rb family of tumor suppressors by the human cytomegalovirus pp71 protein. *Proc Natl Acad Sci USA.* (2003) 100:3263–8. doi: 10.1073/pnas.0538058100
89. Turnell AS, Grand RJ, Gorbea C, Zhang X, Wang W, Mymryk JS, et al. Regulation of the 26S proteasome by adenovirus E1A. *Embo J.* (2000) 19:4759–73. doi: 10.1093/emboj/19.17.4759
90. Mccarthy MK, Procario MC, Twisselmann N, Wilkinson JE, Archambeau AJ, Michele DE, et al. Proinflammatory effects of interferon gamma in mouse adenovirus 1 myocarditis. *J Virol.* (2015) 89:468–79. doi: 10.1128/JVI.02077-14
91. Cascio P. PA28alphabeta: the enigmatic magic ring of the proteasome? *Biomolecules* (2014) 4:566–84. doi: 10.3390/biom4020566
92. Mcnab F, Mayer-Barber K, Sher A, Wack A, O'garra A. Type I interferons in infectious disease. *Nat Rev Immunol.* (2015) 15:87–103. doi: 10.1038/nri3787
93. Wessely R, Klingel K, Knowlton KU, Kandolf R. Cardioselective infection with coxsackievirus B3 requires intact type I interferon signaling - implications for mortality and early viral replication. *Circulation* (2001) 103:756–61. doi: 10.1161/01.CIR.103.5.756
94. Deonarain R, Cerullo D, Fuse K, Liu PP, Fish EN. Protective role for interferon-beta in coxsackievirus B3 infection. *Circulation* (2004) 110:3540–3. doi: 10.1161/01.CIR.0000136824.73458.20
95. Althof N, Harkins S, Kemball CC, Flynn CT, Alirezaei M, Whitton JL. *In vivo* ablation of type I interferon receptor from cardiomyocytes delays coxsackieviral clearance and accelerates myocardial disease. *J Virol.* (2014) 88:5087–99. doi: 10.1128/JVI.00184-14
96. Kuhl U, Pauschinger M, Schwimmbeck PL, Seeberg B, Lober C, Noutsias M, et al. Interferon-beta treatment eliminates cardiotropic viruses and improves left ventricular function in patients with myocardial persistence of viral genomes and left ventricular dysfunction. *Circulation* (2003) 107:2793–8. doi: 10.1161/01.CIR.0000072766.67150.51
97. Kuhl U, Lassner D, Von SJ, Poller W, Schultheiss HP. Interferon-Beta improves survival in enterovirus-associated cardiomyopathy. *J Am Coll Cardiol.* (2012) 60:1295–6. doi: 10.1016/j.jacc.2012.06.026
98. Maier HJ, Schips TG, Wietelmann A, Kruger M, Brunner C, Sauter M, et al. Cardiomyocyte-specific IkappaB kinase (IKK)/NF-kappaB activation induces reversible inflammatory cardiomyopathy and heart failure. *Proc Natl Acad Sci USA.* (2012) 109:11794–9. doi: 10.1073/pnas.1116584109
99. Rahnefeld A, Klingel K, Schuermann A, Diny NL, Althof N, Lindner A, et al. Ubiquitin-like protein ISG15 (interferon-stimulated gene of 15 kDa) in host defense against heart failure in a mouse model of virus-induced cardiomyopathy. *Circulation* (2014) 130:1589–600. doi: 10.1161/CIRCULATIONAHA.114.009847
100. Weinzierl AO, Szalay G, Wolburg H, Sauter M, Rarnmensee HG, Kandolf R, et al. Effective chemokine secretion by dendritic cells and expansion of cross-presenting CD4(-)/CD8(+) dendritic cells define a protective phenotype in the mouse model of coxsackievirus myocarditis. *J Virol.* (2008) 82:8149–60. doi: 10.1128/JVI.00047-08
101. Blasius AL, Beutler B. Intracellular toll-like receptors. *Immunity* (2010) 32:305–15. doi: 10.1016/j.immuni.2010.03.012
102. Heaton SM, Borg NA, Dixit VM. Ubiquitin in the activation and attenuation of innate antiviral immunity. *J Exp Med.* (2016) 213:1–13. doi: 10.1084/jem.20151531
103. Rahnefeld A, Ebstein F, Albrecht N, Opitz E, Kuckelkorn U, Stangl K, et al. Antigen-presentation capacity of dendritic cells is impaired in ongoing enterovirus myocarditis. *Eur J Immunol.* (2011) 41:2774–81. doi: 10.1002/eji.201041039
104. Nencioni A, Schwarzenberg K, Brauer KM, Schmidt SM, Ballestrero A, Grunebach F, et al. Proteasome inhibitor bortezomib modulates TLR4-induced dendritic cell activation. *Blood* (2006) 108:551–8. doi: 10.1182/blood-2005-08-3494
105. De Verteuil DA, Rouette A, Hardy MP, Lavallee S, Trofimov A, Gaucher E, et al. Immunoproteasomes shape the transcriptome and regulate the function of dendritic cells. *J Immunol.* (2014) 193:1121–32. doi: 10.4049/jimmunol.1400871
106. Davidson S, Crotta S, Mccabe TM, Wack A. Pathogenic potential of interferon alphabeta in acute influenza infection. *Nat Commun.* (2014) 5:3864. doi: 10.1038/ncomms4864
107. Stetson DB, Ko JS, Heidmann T, Medzhitov R. Trex1 prevents cell-intrinsic initiation of autoimmunity. *Cell* (2008) 134:587–98. doi: 10.1016/j.cell.2008.06.032
108. Gray EE, Treuting PM, Woodward JJ, Stetson DB. Cutting edge: cGAS is required for lethal autoimmune disease in the Trex1-deficient mouse model of aicardi-goutieres syndrome. *J Immunol.* (2015) 195:1939–43. doi: 10.4049/jimmunol.1500969
109. Agarwal AK, Xing C, Demartino GN, Mizrachi D, Hernandez MD, Sousa AB, et al. PSMB8 encoding the beta 5i proteasome subunit is mutated in joint contractures, muscle atrophy, microcytic anemia, and panniculitis-induced lipodystrophy syndrome. *Am J Hum Genet.* (2010) 87:866–72. doi: 10.1016/j.ajhg.2010.10.031
110. Kitamura A, Maekawa Y, Uehara H, Izumi K, Kawachi I, Nishizawa M, et al. A mutation in the immunoproteasome subunit PSMB8 causes autoinflammation and lipodystrophy in humans. *J Clin Invest.* (2011) 121:4150–60. doi: 10.1172/JCI58414
111. Brehm A, Liu Y, Sheikh A, Marrero B, Omoyinmi E, Zhou Q, et al. Additive loss-of-function proteasome subunit mutations in CANDLE/PRAAS patients promote type I IFN production. *J Clin Invest.* (2015) 125:4196–211. doi: 10.1172/JCI81260
112. Magrini E, Mantovani A, Garlanda C. The dual complexity of PTX3 in health and disease: a balancing act? *Trends Mol Med.* (2016) 22:497–510. doi: 10.1016/j.molmed.2016.04.007
113. Nebuloni M, Pasqualini F, Zerbi P, Lauri E, Mantovani A, Vago L, et al. PTX3 expression in the heart tissues of patients with myocardial

infarction and infectious myocarditis. *Cardiovasc Pathol.* (2011) 20:e27–35. doi: 10.1016/j.carpath.2010.02.005
114. Paeschke A, Possehl A, Klingel K, Voss M, Voss K, Kespohl M, et al. The immunoproteasome controls the availability of the cardioprotective pattern recognition molecule Pentraxin3. *Eur J Immunol.* (2016) 46:619–33. doi: 10.1002/eji.201545892
115. Rovere P, Peri G, Fazzini F, Bottazzi B, Doni A, Bondanza A, et al. The long pentraxin PTX3 binds to apoptotic cells and regulates their clearance by antigen-presenting dendritic cells. *Blood* (2000) 96:4300–6. Available online at: www.bloodjournal.org/
116. Kirschner F, Reppe K, Andresen N, Witzenrath M, Ebstein F, Kloetzel PM. Proteasome beta5i subunit deficiency affects opsonin synthesis and aggravates pneumococcal pneumonia. *PLoS ONE* (2016) 11:e0153847. doi: 10.1371/journal.pone.0153847
117. Yun YS, Kim KH, Tschida B, Sachs Z, Noble-Orcutt KE, Moriarity BS, et al. mTORC1 coordinates protein synthesis and immunoproteasome formation via PRAS40 to prevent accumulation of protein stress. *Mol Cell* (2016) 61:625–39. doi: 10.1016/j.molcel.2016.01.013
118. Chow LH, Gauntt CJ, Mcmanus BM. Differential effects of myocarditic variants of Coxsackievirus B3 in inbred mice. A pathologic characterization of heart tissue damage. *Lab Invest.* (1991) 64:55–64.
119. Opavsky MA, Martino T, Rabinovitch M, Penninger J, Richardson C, Petric M, et al. Enhanced ERK-1/2 activation in mice susceptible to coxsackievirus-induced myocarditis. *J Clin Invest.* (2002) 109:1561–9. doi: 10.1172/JCI0213971
120. Jenne CN, Kubes P. Virus-induced NETs–critical component of host defense or pathogenic mediator? *PLoS Pathog.* (2015) 11:e1004546. doi: 10.1371/journal.ppat.1004546
121. Mundt S, Basler M, Buerger S, Engler H, Groettrup M. Inhibiting the immunoproteasome exacerbates the pathogenesis of systemic *Candida albicans* infection in mice. *Sci Rep.* (2016a) 6:19434. doi: 10.1038/srep19434
122. Hiraoka Y, Kishimoto C, Takada H, Suzaki N, Shiraki K. Colony-stimulating factors and coxackievirus B3 myocarditis in mice: macrophage colony-stimulating factor suppresses acute myocarditis with increasing interferon-alpha. *Am Heart J.* (1995) 130:1259–64. doi: 10.1016/0002-8703(95)90152-3
123. Xu D, Wang P, Yang J, Qian Q, Li M, Wei L, et al. Gr-1+ cells other than Ly6G+ neutrophils limit virus replication and promote myocardial inflammation and fibrosis following coxsackievirus B3 infection of mice. *Front Cell Infect Microbiol.* (2018) 8:157. doi: 10.3389/fcimb.2018.00157
124. Jakubzick CV, Randolph GJ, Henson PM. Monocyte differentiation and antigen-presenting functions. *Nat Rev Immunol.* (2017) 17:349–62. doi: 10.1038/nri.2017.28
125. Goser S, Ottl R, Brodner A, Dengler TJ, Torzewski J, Egashira K, et al. Critical role for monocyte chemoattractant protein-1 and macrophage inflammatory protein-1alpha in induction of experimental autoimmune myocarditis and effective anti-monocyte chemoattractant protein-1 gene therapy. *Circulation* (2005) 112:3400–7. doi: 10.1161/CIRCULATIONAHA.105.572396
126. Zimmermann O, Homann JM, Bangert A, Muller AM, Hristov G, Goeser S, et al. Successful use of mRNA-nucleofection for overexpression of interleukin-10 in murine monocytes/macrophages for anti-inflammatory therapy in a murine model of autoimmune myocarditis. *J Am Heart Assoc.* (2012) 1:e003293. doi: 10.1161/JAHA.112.003293
127. Jaquenod De Giusti C, Ure AE, Rivadeneyra L, Schattner M, Gomez RM. Macrophages and galectin 3 play critical roles in CVB3-induced murine acute myocarditis and chronic fibrosis. *J Mol Cell Cardiol.* (2015) 85:58–70. doi: 10.1016/j.yjmcc.2015.05.010
128. Leuschner F, Courties G, Dutta P, Mortensen LJ, Gorbatov R, Sena B, et al. Silencing of CCR2 in myocarditis. *Eur Heart J.* (2015) 36:1478–88. doi: 10.1093/eurheartj/ehu225
129. Ginhoux F, Jung S. Monocytes and macrophages: developmental pathways and tissue homeostasis. *Nat Rev Immunol.* (2014) 14:392–404. doi: 10.1038/nri3671
130. Takeda K, Akira S. TLR signaling pathways. *Semin Immunol.* (2004) 16:3–9. doi: 10.1016/j.smim.2003.10.003
131. Kawai T, Akira S. The role of pattern-recognition receptors in innate immunity: update on Toll-like receptors. *Nat Immunol.* (2010) 11:373–84. doi: 10.1038/ni.1863
132. Deng L, Wang C, Spencer E, Yang L, Braun A, You J, et al. Activation of the IkappaB kinase complex by TRAF6 requires a dimeric ubiquitin-conjugating enzyme complex and a unique polyubiquitin chain. *Cell* (2000) 103:351–61. doi: 10.1016/S0092-8674(00)00126-4
133. Ajibade AA, Wang HY, Wang RF. Cell type-specific function of TAK1 in innate immune signaling. *Trends Immunol.* (2013) 34:307–16. doi: 10.1016/j.it.2013.03.007
134. Arthur JS, Ley SC. Mitogen-activated protein kinases in innate immunity. *Nat Rev Immunol.* (2013) 13:679–92. doi: 10.1038/nri3495
135. Akira S, Uematsu S, Takeuchi O. Pathogen recognition and innate immunity. *Cell* (2006) 124:783–801. doi: 10.1016/j.cell.2006.02.015
136. Macagno A, Kuehn L, De Giuli R, Groettrup M. Pronounced up-regulation of the PA28 alpha/beta proteasome regulator but little increase in the steady-state content of immunoproteasome during dendritic cell maturation. *Eur J Immunol.* (2001) 31:3271–80. doi: 10.1002/1521-4141(200111)31:113.0.CO;2-2
137. Bitzer A, Basler M, Krappmann D, Groettrup M. Immunoproteasome subunit deficiency has no influence on the canonical pathway of NF-kappaB activation. *Mol Immunol.* (2017) 83:147–53. doi: 10.1016/j.molimm.2017.01.019
138. Basler M, Beck U, Kirk CJ, Groettrup M. The antiviral immune response in mice devoid of immunoproteasome activity. *J Immunol.* (2011) 187:5548–57. doi: 10.4049/jimmunol.1101064
139. Triantafilou K, Orthopoulos G, Vakakis E, Ahmed MA, Golenbock DT, Lepper PM, et al. Human cardiac inflammatory responses triggered by Coxsackie B viruses are mainly Toll-like receptor (TLR) 8-dependent. *Cell Microbiol.* (2005) 7:1117–26. doi: 10.1111/j.1462-5822.2005.00537.x
140. Jurk M, Heil F, Vollmer J, Schetter C, Krieg AM, Wagner H, et al. Human TLR7 or TLR8 independently confer responsiveness to the antiviral compound R-848. *Nat Immunol.* (2002) 3:499. doi: 10.1038/ni0602-499
141. Lam E, Stein S, Falck-Pedersen E. Adenovirus detection by the cGAS/STING/TBK1 DNA sensing cascade. *J Virol.* (2014) 88:974–81. doi: 10.1128/JVI.02702-13
142. Barber GN. STING: infection, inflammation and cancer. *Nat Rev Immunol.* (2015) 15:760–70. doi: 10.1038/nri3921
143. Hayashi T, Faustman D. NOD mice are defective in proteasome production and activation of NF-kappa B. *Mol Cell Biol.* (1999) 19:8646–59. doi: 10.1128/MCB.19.12.8646
144. Visekruna A, Joeris T, Seidel D, Kroesen A, Loddenkemper C, Zeitz M, et al. Proteasome-mediated degradation of I kappa B alpha and processing of p105 in Crohn disease and ulcerative colitis. *J Clin Invest.* (2006) 116:3195–203. doi: 10.1172/JCI28804
145. Hayashi T, Faustman D. Essential role of human leukocyte antigen-encoded proteasome subunits in NF-kappa B activation and prevention of tumor necrosis factor-alpha-induced apoptosis. *J Biol Chem.* (2000) 275:5238–47. doi: 10.1074/jbc.275.7.5238
146. Runnels HA, Watkins WA, Monaco JJ. LMP2 expression and proteasome activity in NOD mice. *Nat Med.* (2000) 6:1064–5. doi: 10.1038/80349
147. Hensley SE, Zanker D, Dolan BP, David A, Hickman HD, Embry AC, et al. Unexpected role for the immunoproteasome subunit LMP2 in antiviral humoral and innate immune responses. *J Immunol.* (2010) 184:4115–22. doi: 10.4049/jimmunol.0903003
148. Jang ER, Lee NR, Han S, Wu Y, Sharma LK, Carmony KC, et al. Revisiting the role of the immunoproteasome in the activation of the canonical NF-kappaB pathway. *Mol Biosyst.* (2012) 8:2295–302. doi: 10.1039/c2mb25125f
149. Schmidt N, Gonzalez E, Visekruna A, Kuhl AA, Loddenkemper C, Mollenkopf H, et al. Targeting the proteasome: partial inhibition of the proteasome by bortezomib or deletion of the immunosubunit LMP7 attenuates experimental colitis. *Gut* (2010) 59:896–906. doi: 10.1136/gut.2009.203554
150. Kessler BM, Lennon-Dumenil AM, Shinohara ML, Lipes MA, Ploegh HL. LMP2 expression and proteasome activity in NOD mice. *Nat Med.* (2000) 6:1064. doi: 10.1038/80346
151. Ronkina N, Kotlyarov A, Dittrich-Breiholz O, Kracht M, Hitti E, Milarski K, et al. The mitogen-activated protein kinase (MAPK)-activated protein kinases MK2 and MK3 cooperate in stimulation of tumor necrosis factor

biosynthesis and stabilization of p38 MAPK. *Mol Cell Biol.* (2007) 27:170–81. doi: 10.1128/MCB.01456-06
152. Godeny EK, Gauntt CJ. Involvement of natural killer cells in coxsackievirus B3-induced murine myocarditis. *J Immunol.* (1986) 137:1695–702.
153. Godeny EK, Gauntt CJ. Murine natural killer cells limit coxsackievirus B3 replication. *J Immunol.* (1987) 139:913–8.
154. Klingel K, Fabritius C, Sauter M, Goldner K, Stauch D, Kandolf R, et al. The activating receptor NKG2D of natural killer cells promotes resistance against enterovirus-mediated inflammatory cardiomyopathy. *J Pathol.* (2014) 234:164–77. doi: 10.1002/path.4369
155. Hallett WH, Ames E, Motarjemi M, Barao I, Shanker A, Tamang DL, et al. Sensitization of tumor cells to NK cell-mediated killing by proteasome inhibition. *J Immunol.* (2008) 180:163–70. doi: 10.4049/jimmunol.180.1.163
156. Chow LH, Beisel KW, Mcmanus BM. Enteroviral infection of mice with severe combined immunodeficiency. Evidence for direct viral pathogenesis of myocardial injury. *Lab Invest.* (1992) 66:24–31.
157. Leipner C, Borchers M, Merkle I, Stelzner A. Coxsackievirus B3-induced myocarditis in MHC class II-deficient mice. *J Hum Virol.* (1999) 2:102–14.
158. Mena I, Perry CM, Harkins S, Rodriguez F, Gebhard J, Whitton JL. The role of B lymphocytes in coxsackievirus B3 infection. *Am J Pathol.* (1999) 155:1205–15. doi: 10.1016/S0002-9440(10)65223-6
159. Henke A, Huber S, Stelzner A, Whitton JL. The Role of Cd8(+) T-Lymphocytes in Coxsackievirus B3-Induced Myocarditis. *J Virol.* (1995) 69:6720–8.
160. Klingel K, Schnorr JJ, Sauter M, Szalay G, Kandolf R. beta 2-microglobulin-associated regulation of interferon-gamma and virus-specific immunoglobulin G confer resistance against the development of chronic coxsackievirus myocarditis. *Am J Pathol.* (2003) 162:1709–20. doi: 10.1016/S0002-9440(10)64305-2
161. Gebhard JR, Perry CM, Harkins S, Lane T, Mena I, Asensio VC, et al. Coxsackievirus B3-induced myocarditis: perforin exacerbates disease, but plays no detectable role in virus clearance. *Am J Pathol.* (1998) 153:417–28. doi: 10.1016/S0002-9440(10)65585-X
162. Kemball CC, Harkins S, Whitton JL. Enumeration and functional evaluation of virus-specific CD4(+) and CD8(+) T cells in lymphoid and peripheral sites of coxsackievirus B3 infection. *J Virol.* (2008) 82:4331–42. doi: 10.1128/JVI.02639-07
163. Kemball CC, Harkins S, Whitmire JK, Flynn CT, Feuer R, Whitton JL. Coxsackievirus B3 inhibits antigen presentation *in vivo*, exerting a profound and selective effect on the MHC class I pathway. *PLoS Pathog.* (2009) 5:e1000618. doi: 10.1371/journal.ppat.1000618
164. Cornell CT, Kiosses WB, Harkins S, Whitton JL. Inhibition of protein trafficking by coxsackievirus B3: multiple viral proteins target a single organelle. *J Virol.* (2006) 80:6637–47. doi: 10.1128/JVI.02572-05
165. Cornell CT, Mosses WB, Harkins S, Whitton L. Coxsackievirus B3 proteins directionally complement each other to downregulate surface major histocompatibility complex class I. *J Virol.* (2007) 81:6785–97. doi: 10.1128/JVI.00198-07
166. Voigt A, Jakel S, Textoris-Taube K, Keller C, Drung I, Szalay G, et al. Generation of *in silico* predicted coxsackievirus B3-derived MHC class I epitopes by proteasomes. *Amino Acids* (2010) 39:243–55. doi: 10.1007/s00726-009-0434-5
167. Szalay G, Sauter M, Hald J, Weinzierl A, Kandolf R, Klingel K. Sustained nitric oxide synthesis contributes to immunopathology in ongoing myocarditis attributable to interleukin-10 disorders. *Am J Pathol.* (2006b) 169:2085–93. doi: 10.2353/ajpath.2006.060350
168. Tewari MK, Sinnathamby G, Rajagopal D, Eisenlohr LC. A cytosolic pathway for MHC class II-restricted antigen processing that is proteasome and TAP dependent. *Nat Immunol.* (2005) 6:287–94. doi: 10.1038/ni1171
169. Matsuzaki J, Tsuji T, Luescher I, Old LJ, Shrikant P, Gnjatic S, et al. Nonclassical antigen-processing pathways are required for MHC class II-restricted direct tumor recognition by NY-ESO-1-specific CD4(+) T cells. *Cancer Immunol Res.* (2014) 2:341–50. doi: 10.1158/2326-6066.CIR-13-0138
170. Moebius J, Van Den Broek M, Groettrup M, Basler M. Immunoproteasomes are essential for survival and expansion of T cells in virus-infected mice. *Eur J Immunol.* (2010) 40:3439–49. doi: 10.1002/eji.201040620
171. Kalim KW, Basler M, Kirk CJ, Groettrup M. Immunoproteasome subunit LMP7 deficiency and inhibition suppresses Th1 and Th17 but enhances regulatory T cell differentiation. *J Immunol.* (2012) 189:4182–93. doi: 10.4049/jimmunol.1201183
172. Tian Z, Zheng H, Li J, Li Y, Su H, Wang X. Genetically induced moderate inhibition of the proteasome in cardiomyocytes exacerbates myocardial ischemia-reperfusion injury in mice. *Circ Res.* (2012) 111:532–42. doi: 10.1161/CIRCRESAHA.112.270983
173. Mundt S, Engelhardt B, Kirk CJ, Groettrup M, Basler M. Inhibition and deficiency of the immunoproteasome subunit LMP7 attenuates LCMV-induced meningitis. *Eur J Immunol.* (2016b) 46:104–13. doi: 10.1002/eji.201545578
174. Horwitz MS, La Cava A, Fine C, Rodriguez E, Ilic A, Sarvetnick N. Pancreatic expression of interferon-gamma protects mice from lethal coxsackievirus B3 infection and subsequent myocarditis. *Nat Med.* (2000) 6:693–7. doi: 10.1038/76277
175. Mena I, Fischer C, Gebhard JR, Perry CM, Harkins S, Whitton JL. Coxsackievirus infection of the pancreas: evaluation of receptor expression, pathogenesis, and immunopathology. *Virology* (2000) 271:276–88. doi: 10.1006/viro.2000.0332
176. Esfandiarei M, Mcmanus BM. Molecular biology and pathogenesis of viral myocarditis. *Annu Rev Pathol.* (2008) 3:127–55. doi: 10.1146/annurev.pathmechdis.3.121806.151534

Conflict of Interest Statement: The authors declare that the research was conducted in the absence of any commercial or financial relationships that could be construed as a potential conflict of interest.

frontiers in Immunology

HYPOTHESIS AND THEORY
published: 10 December 2018
doi: 10.3389/fimmu.2018.02870

Theiler's Virus-Mediated Immunopathology in the CNS and Heart: Roles of Organ-Specific Cytokine and Lymphatic Responses

*Seiichi Omura[1,2], Eiichiro Kawai[2], Fumitaka Sato[1,2], Nicholas E. Martinez[2], Alireza Minagar[3], Mahmoud Al-Kofahi[4], J. Winny Yun[4], Urska Cvek[5], Marjan Trutschl[5], J. Steven Alexander[3,4] and Ikuo Tsunoda[1,2,3]**

[1] Department of Microbiology, Kindai University Faculty of Medicine, Osaka, Japan, [2] Department of Microbiology and Immunology, Center for Molecular and Tumor Virology, Center for Cardiovascular Diseases and Sciences, Louisiana State University Health Sciences Center-Shreveport, Shreveport, LA, United States, [3] Department of Neurology, Louisiana State University Health Sciences Center-Shreveport, Shreveport, LA, United States, [4] Department of Molecular and Cellular Physiology, Louisiana State University Health Sciences Center-Shreveport, Shreveport, LA, United States, [5] Department of Computer Science, Louisiana State University Shreveport, Shreveport, LA, United States

OPEN ACCESS

Edited by:
Michael H. Lehmann,
Ludwig Maximilian University of Munich, Germany

Reviewed by:
Jun-ichi Kira,
Kyushu University, Japan
Andreas Beineke,
University of Veterinary Medicine Hannover, Germany

***Correspondence:**
Ikuo Tsunoda
itsunoda@med.kindai.ac.jp

Specialty section:
This article was submitted to Viral Immunology, a section of the journal Frontiers in Immunology

Received: 28 September 2018
Accepted: 21 November 2018
Published: 10 December 2018

Citation:
Omura S, Kawai E, Sato F, Martinez NE, Minagar A, Al-Kofahi M, Yun JW, Cvek U, Trutschl M, Alexander JS and Tsunoda I (2018) Theiler's Virus-Mediated Immunopathology in the CNS and Heart: Roles of Organ-Specific Cytokine and Lymphatic Responses. Front. Immunol. 9:2870. doi: 10.3389/fimmu.2018.02870

Theiler's murine encephalomyelitis virus (TMEV) induces different diseases in the central nervous system (CNS) and heart, depending on the mouse strains and time course, with cytokines playing key roles for viral clearance and immune-mediated pathology (immunopathology). In SJL/J mice, TMEV infection causes chronic TMEV-induced demyelinating disease (TMEV-IDD) in the spinal cord about 1 month post-inoculation (p.i.). Unlike other immunopathology models, both pro- and anti-inflammatory cytokines can play dual roles in TMEV-IDD. Pro-inflammatory cytokines play beneficial roles in viral clearance while they are also detrimental in immune-mediated demyelination. Anti-inflammatory cytokines suppress not only protective anti-viral immune responses but also detrimental autoreactive immune responses. Conversely, in C3H mice, TMEV infection induces a non-CNS disease, myocarditis, with three distinctive phases: phase I, viral pathology with interferon and chemokine responses; phase II, immunopathology mediated by acquired immune responses; and phase III, cardiac fibrosis. Although the exact mechanism(s) by which a single virus, TMEV, induces these different diseases in different organs is unclear, our bioinformatics approaches, especially principal component analysis (PCA) of transcriptome data, allow us to identify the key factors contributing to organ-specific immunopathology. The PCA demonstrated that *in vitro* infection of a cardiomyocyte cell line reproduced the transcriptome profile of phase I in TMEV-induced myocarditis; distinct interferon/chemokine-related responses were induced *in vitro* in TMEV-infected cardiomyocytes, but not in infected neuronal cells. In addition, the PCA of the *in vivo* CNS transcriptome data showed that decreased lymphatic marker expressions were weakly associated with inflammation in TMEV infection. Here, dysfunction of lymphatic vessels is shown to potentially contribute to immunopathology by delaying the clearance of cytokines and immune cells from the inflammatory site, although this can also confine the virus at these sites, preventing virus spread via lymphatic vessels. On the other hand, in the heart, dysfunction of lymphatics was associated with reduced lymphatic muscle contractility provoked by

pro-inflammatory cytokines. Therefore, TMEV infection may induce different patterns of cytokine expressions as well as lymphatic vessel dysfunction by rather different mechanisms between the CNS and heart, which might explain observed patterns of organ-specific immunopathology.

Keywords: adhesion molecules, animal models, blood-brain barrier, computational analysis, GLYCAM1, LYVE1, *Picornaviridae* infection, unsupervised analysis

INTRODUCTION

Theiler's Murine Encephalomyelitis Virus (TMEV) Induces Distinct Organ-Specific Diseases

Theiler's murine encephalomyelitis virus (TMEV) is a non-enveloped, single-stranded positive-sense RNA virus that belongs to the order *Picornavirales*, family *Picornaviridae*, genus *Cardiovirus*. Historically, Max Theiler discovered the Theiler's original (TO) strain of TMEV as an agent that induces acute polioencephalomyelitis in the central nervous system (CNS) of mice in 1934 (1–3). Since TMEV infects the gastrointestinal tract and induces an acute CNS disease similar to poliovirus (family *Picornaviridae*, genus *Enterovirus*), TMEV was originally classified into the genus *Enterovirus* and used as an animal model for poliomyelitis. In 1952, Joan Daniels reported that the Daniels (DA) strain of TMEV causes myositis in the skeletal muscle and a chronic inflammatory demyelinating disease in the spinal cord (4), the latter of which has been called TMEV-induced demyelinating disease (TMEV-IDD) and used as a viral model for multiple sclerosis (MS) (5–7), first by Howard Lipton in 1972. In 1996, Gómez et al. demonstrated that TMEV causes inflammation not only in the skeletal muscle (i.e., myositis) but also in the heart muscle (i.e., myocarditis) (8). Since 2014, TMEV-induced myocarditis has been applied as a viral model for myocarditis (9) (**Figure 1**). The resistance/susceptibility to TMEV-induced organ-specific pathology has been known to differ among mouse strains. The resistance to persistent CNS infection maps genetically to major histocompatibility complex (MHC) class I, *H-2D* region (3). The *H-2* background also appears to influence myositis and myocarditis, although studies using congenic mice are necessary to determine the precise role of MHC molecules (8).

In general, viruses infect limited species and induce diseases in an isolated group of organs. The determination of the mechanism(s) of such organ-specific tropism/pathogenesis of virus infections could powerfully inform the development of treatments and methods of prevention for viral infections: currently the precise mechanisms of many types of viral pathogenesis still remain unknown. TMEV is a natural enteric pathogen of mice (11) and has been isolated from trapped wild mice (12), while no TMEV-induced disease has been reported in the wild. TMEV has been shown to infect only mice, and not other species *in vivo* (with a few exceptions) and causes distinct maladies that mimic human diseases (3). In experimental mice, intracerebral inoculation of TMEV results in CNS viral infection as well as viremia and induces diseases in the CNS and the heart (13). On the other hand, peripheral inoculation, such as intraperitoneal or intravenous injection, causes myocarditis more efficiently (9), but rarely causes CNS infection. Thus, TMEV has high neurotropism and high neurovirulence, but low neuroinvasiveness, despite the fact that TMEV can use at least three routes to gain access to the CNS: neural spread, hematogenous spread, and olfactory route (14). Low neuroinvasiveness of peripherally inoculated TMEV can be explained by the fact that vascular endothelial cells are not permissive for TMEV infection *in vivo* (15). Here, although TMEV can still invade the CNS hematogenously, using infected macrophages as Trojan horse (3), this is not an efficient way to achieve fast and successful viral invasion into the CNS. TMEV infects only certain cell types in restricted organs *in vivo*, although TMEV can infect most cell lines derived from various organs and different host species, even insect cells (with the exception of T cells *in vitro*) (15).

TMEV-Induced CNS Disease

TMEV is divided into two subgroups: the TO and GDVII, based on its neurovirulence following intracerebral inoculation. The GDVII subgroup, including GDVII and FA strains, causes acute fatal polioencephalomyelitis and kills all mice following intracerebral infection. One plaque forming unit (PFU) of GDVII virus is enough to kill mice by induction of neuronal apoptosis and axonal injury without inducing acquired immune responses (16). The TO subgroup, including DA and BeAn strains, induces a biphasic disease in susceptible mouse strains (highly susceptible, SJL/J mice; and intermediate susceptible, C3H mice), following intracerebral injection (17). During the acute phase, about 1 week post-inoculation (p.i.), TMEV infects neurons and induces neuronal apoptosis, neuronophagia, and inflammation, mainly in the gray matter of the brain, including the hippocampus and cerebral cortex (polioencephalitis), while induction of TMEV-specific cellular and humoral immune responses is accompanied by the clearance of the virus from the brain. Thereafter, a low level of TMEV can persistently infect oligodendrocytes and microglia/macrophages in the white matter of the spinal cord of susceptible mice, and recruit anti-viral immune cells into the infected regions, particularly ventrolateral funiculus of the thoracic segments, leading to inflammatory demyelination during the chronic phase, about 1 month p.i. (3).

During the acute phase of TMEV infection, $CD4^+$ and $CD8^+$ T cells and anti-viral antibodies enter the CNS, contributing to viral clearance from the gray matter without causing overt immune-mediated tissue damage (immunopathology). During the chronic phase, however, these same immune effector components are detected in the white matter, and play key roles

TMEV-induced organ-specific pathology

Organ	CNS	Heart
Strain susceptibility	SJL/J > C3H > C57BL/6	C3H > C57BL/6 > SJL/J
Histology	Inflammation / Demyelination	Inflammation / Fibrosis
Acute infection	++	++
Virus persistence	+	−
Route	Intracerebral	Peripheral > Intracerebral

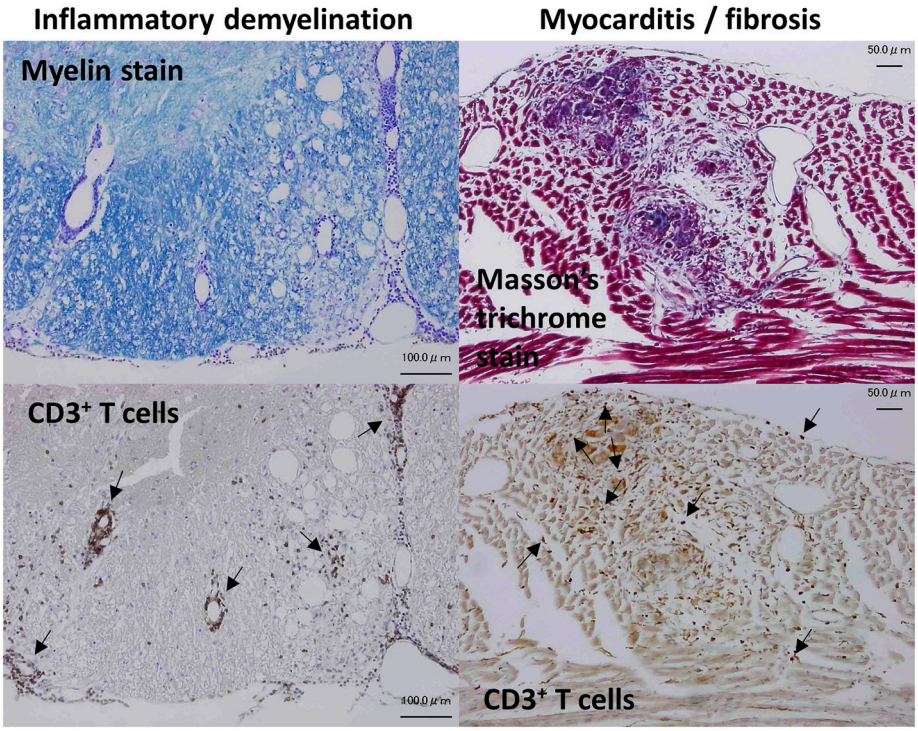

FIGURE 1 | Organ-specific pathology induced by Theiler's murine encephalomyelitis virus (TMEV). TMEV induces pathology in two organs: inflammatory demyelination in the central nervous system (CNS) and inflammation followed with fibrosis in the heart, whose susceptibilities differ among mouse strains (9, 10). Although TMEV can infect the CNS and the heart during the acute phase, persistent viral infection is observed only in the CNS. CNS disease can be induced only by intracerebral inoculation. On the other hand, both peripheral and intracerebral routes of viral inoculation result in myocarditis, while peripheral inoculation induces more severe cardiac disease. (**Left**) Inflammatory demyelination in the spinal cord of TMEV-induced demyelinating disease (TMEV-IDD). Luxol fast blue stain. CD3 immunohistochemical staining of consecutive sections showed that T cells were present in perivascular cuffing and meningitis (Arrows). Bar: 100 μm (**Right**) Inflammation and fibrosis in the heart during phase III of TMEV-induced myocarditis. Masson's trichrome stain. CD3 immunohistochemical staining showed T cell infiltration (Arrows) in the heart. Bar: 50 μm.

in immunopathology (18). Overall, gain-of-function and loss-of-function approaches to clarify the roles of immune effector cells, antibodies, and cytokines, have demonstrated that anti-viral pro-inflammatory effector molecules/cells, including $CD4^+$ T helper (Th)1, cells and $CD8^+$ cytotoxic T lymphocytes (CTLs), and antibodies play protective roles during the acute phase (7). For example, in GDVII virus infection, lack of CNS infiltrating immune cells results in acute fatal polioencephalitis (19), which has been associated with altered mRNA expression levels of cytokines, but not chemokines (20), as well as induction of transforming growth factor (TGF)-β1 protein in the neurons (21). On the other hand, during the chronic phase, these immune effector molecules/cells could play detrimental roles causing immunopathology in a bystander fashion and/or determinant (epitope) spreading to myelin antigens (22, 23), although the precise mechanisms of immunopathology remain unknown. While these immune effector molecules/cells (Th1, CTL, and antibody) seem to play both protective anti-viral and detrimental immunopathogenic roles in TMEV-IDD, anti-inflammatory cells including regulatory T cells (Tregs) can also be beneficial and detrimental depending on the disease phases in TMEV infection (24).

TMEV-Induced Myocarditis

Myocarditis is an inflammatory disease in the heart caused by microbial infections or autoimmunity and affects about 2 million people in the United States (25, 26). Among viruses, the picornavirus family, especially coxsackievirus B, is a well-known pathogen of myocarditis (27). In general, regardless of viral families or species, viral myocarditis has been proposed to be divided into three phases (28). In phase I (around 4 days p.i., experimentally), the virus infects and replicates in the heart, damaging cardiomyocytes, while innate immune responses against the virus are induced. In phase II, anti-viral T-cell and antibody responses are induced (after 5 or more days p.i.), with the penetration of these effector components into the heart. Under pathologic conditions, anti-viral immune responses not only clear the virus but also damage infected and uninfected cardiomyocytes by anti-viral CTLs and in a bystander fashion, respectively. This can be followed by induction of autoimmune responses to the heart reflecting determinant spreading and/or molecular mimicry between the virus and heart antigens. When the tissue damage caused in phase I and/or II is severe, cardiac remodeling and fibrosis with or without low-grade viral persistence occur, which can lead to dilated cardiomyopathy (phase III). Ideally, each patient with myocarditis should be treated depending on the phase (29): phase I, antiviral; phase II, immunomodulation; and phase III, standard heart failure therapy (e.g., immunosuppression may be appropriate for phase II, but will enhance virus replication in phase I). However, finding effective therapies has remained challenging because the phase-specific biomarkers and pathogenesis of myocarditis have not been conclusively identified (30), while serum cardiac troponin and creatine kinase, electrocardiogram and echocardiography, and the endomyocardial biopsy have been helpful, to some extent, for diagnosing myocarditis (31, 32).

To clarify the pathogenesis and discover the phase-specific biomarkers, we established a murine model for viral myocarditis using TMEV (9, 28, 33), which has unique characteristics not seen in most other animal models. For example, (1) most animal models don't have three phases; (2) fail to reproduce clinical and immunological findings in human viral myocarditis; and (3) fail to use a "natural" pathogen of the host, thus the TMEV model is possibly more relevant to human natural infections. Generally, peripheral injection (e.g., intraperitoneal) of TMEV in mice can efficiently cause inflammation in the heart, but not in the CNS (8, 13), while intracerebral injection of TMEV also causes myocarditis due to acute viremia. Susceptibilities to TMEV-induced myocarditis differ among mouse strains: the highly susceptible C3H strain, the intermediate susceptible C57BL/6 strain, and the highly resistant SJL/J strain. C3H mice develop all three phases, while SJL/J mice develop only phase I and C57BL/6 mice develop phases I and II; the different genetic susceptibilities to viral myocarditis has also been demonstrated in humans (34). TMEV-induced myocarditis can be divided into three phases as in human myocarditis. In phase I, innate immune molecules [interferon (IFN)-induced genes [e.g., interferon regulatory factor 7 (*Irf7*), interferon-induced protein with tetratricopeptide repeats 1 (*Ifit1*), and *Ifit3*] and chemokine genes [e.g., chemokine (C-X-C motif) ligand 9 (*Cxcl9*), *Cxcl10*, and chemokine (C-C motif) ligand 5 (*Ccl5*)] that can recruit Th1 and natural killer T (NKT) cells] were upregulated prior to immune cell infiltration in the heart. In phase II, T-cell infiltrates were observed with upregulation of pro-inflammatory IFN-γ pathway genes, followed by upregulation of cardiac remodeling genes (e.g., *Mmp12* and *Gpnmb*) in phase III. Among transgenic and knockout (KO) mice infected with TMEV, NKT KO mice developed more severe myocarditis with lower ejection fraction in echocardiography than wild-type mice (10).

Lymphatics and Viral Infections

The afferent lymphatic vessels transport interstitial fluid and antigens from tissues to lymph nodes and have specialized capillaries with an open structure; antigen transport to the draining lymph nodes is required to generate antigen-specific immune responses (35). Cancer cells and pathogens often "hijack" this transport system to achieve systemic spread (36), while dissemination to the blood circulation is first blocked at regional lymph nodes. In viral infections, while the mechanisms that limit systemic viral spread have not been studied extensively, several mechanisms have been proposed recently. Kastenmüller et al. (37) showed that vaccinia virus injected subcutaneously in mice was acquired by $CD169^+$ subcapsular sinus macrophages in the regional lymph nodes, but not in the spleen, 4 hours (h) p.i. Since local depletion of macrophages by clodronate-loaded liposomes resulted in viral spreading to the spleen, these results suggest that systemic viral spread ensues in the absence of effective viral capture by macrophages. On the other hand, Loo et al. (38) demonstrated that vaccinia virus infection by scarification, which did not spread the virus to draining lymph nodes, induced remodeling of the pre-existing cutaneous lymphatic vasculature, but not lymphangiogenesis. The remodeling was coincident with a rapid reduction in fluid transport, suggesting that lymphatic vessels negatively modulate fluid transport following viral infection in the skin, to limit the spread of viral particles into lymph nodes. Lymphatic vessel remodeling can result in not only compartmentalization of infectious virus, but also an accumulation of inflammatory mediators in the skin, which affect anti-viral immunity and immunopathology.

In the following sections, we will introduce our bioinformatics analyses of both supervised (such as heat map and *k*-means clustering) and unsupervised [particularly principal component analysis (PCA)] approaches to identify factors that contribute to organ-specific viral pathology. Previously, using these computational analyses, we were able to identify and rank key molecules involved in MS (39), stroke (40), and myocarditis (33). Here, we focus on two potential candidate factors contributing to organ-specific viral pathology: (1) innate immune responses by the major cell type of each organ, i.e., cardiomyocyte in the heart vs. neuron in the CNS; and (2) lymphatic vessel dysfunction induced by cytokines in the heart vs. downregulation of neuro-lymphatic molecules in the CNS.

CELL-TYPE SPECIFIC INNATE IMMUNE RESPONSES IN TMEV INFECTION

TMEV Infects and Damages Cardiomyocytes *in vitro*

The TMEV-induced myocarditis model *in vivo* is complemented by the *in vitro* model using a mouse cardiomyocyte cell line, HL-1, which was established by Dr. William C. Claycomb (Louisiana State University Health Sciences Center, New Orleans, LA) from an AT-1 subcutaneous tumor of a C57BL/6J mouse. HL-1 cells retain a differentiated cardiomyocyte phenotype and show contractile activity *in vitro* (41). To see the effects (innate immune responses and viral pathology) of direct virus infection without the involvement of immune cells (phase I mimic), we infected HL-1 cells, at a multiplicity of infection (MOI) = 1 or 10. TMEV infection induced cytopathic effects (CPE) on HL-1 cells, which became obvious 12 h p.i. (**Figure 2A**), while the cell viability started to decrease 8 h p.i., with most cells dying 36 h p.i. (**Figure 2B**). CPE was accompanied by the detection of cardiac troponin in the culture supernatants of HL-1 cells, which was measured by an enzyme-linked immunosorbent assay (ELISA) using the Ultra Sensitive Mouse Cardiac Troponin-I ELISA Kit (Life Diagnostics, West Chester, PA) (**Figure 2C**) (33). We also determined virus replication by plaque assays, using supernatants for cell-free virus and cell lysates for cell-associated virus (**Figure 2D**). Cell-free virus titers increased substantially 12 h p.i., which reflected a loss of plasma cell membrane integrity and showed similar kinetics with supernatant troponin concentrations. Cell-associated viral titers increased 8 h p.i. and peaked 12 h p.i., which was associated with the cell viability. In these assays, we also used a murine neuroblastoma cell line, Neuro-2a (43), since TMEV is known to infect neurons *in vitro* as well as during the acute phase following intracerebral infection *in vivo*. TMEV-infected Neuro-2a cells had similar kinetics of cell viability and viral replication to those of HL-1 cells, while cardiac troponin was not detectable in Neuro-2a cells regardless of infection, as expected (**Figures 2B–D**).

Innate Immunity-Related Genes Are Upregulated Only in Cardiomyocytes Infected With TMEV

To characterize gene expression patterns in cardiomyocytes infected with TMEV, we conducted a supervised analysis using the 2-way comparison of microarray data between TMEV-infected and control mock-infected HL-1 cell culture samples (**Supplementary Materials and Methods**). We visualized the numbers of up- or downregulated genes of infected HL-1 cells compared with controls, using a volcano plot (**Figures 3A–D**) (44–46). We identified substantial numbers of genes whose expressions changed 4 h p.i. (185 upregulated and 413 downregulated genes, >2-fold compared with controls), and their numbers were increased 8 h p.i. (251 upregulated and 1,211 downregulated genes).

To compare these gene expression patterns among samples, we generated the heat map for highly up- or downregulated genes (13), using top 20 of up- or downregulated genes of HL-1 samples 8 h p.i. (**Figure 3E**). At 8 h p.i., TMEV infection upregulated genes associated with innate immunity: IFN-induced genes, including *Ifit1*, and *Cxcl10* and *Ccl5*. TMEV-infected HL-1 samples 4 h p.i. showed a similar gene expression pattern to that of 8 h p.i. We categorized the genes up- or downregulated in TMEV-infected HL-1 cells, using the Database for Annotation, Visualization, and Integrated Discovery (DAVID) v6.8 (Laboratory of Human Retrovirology and Immunoinformatics, Leidos Biomedical Research, Inc., Frederick, MD). Among the upregulated genes, DAVID identified 18 pathways whose P values were <0.05 (**Supplementary Table 1**), including "chemokine-mediated signaling pathway," "cellular response to IFN-α and IFN-β," and "positive regulation of T cell migration." Among the downregulated genes, DAVID identified 28 pathways, including "cell division" and "heart morphogenesis."

To determine the requirement of live virus for the gene expression changes, we incubated HL-1 cells with ultraviolet (UV)-irradiated (replication inactive) TMEV (UV-TMEV) (47). Following 8 h incubation, UV-TMEV upregulated 41 genes, among which only one gene *Mir690* was identified, while none of the 41 genes significantly upregulated in live TMEV-infected HL-1 cells (**Figure 3C**; **Supplementary Table 2**). UV-TMEV also downregulated 10 genes whose immunological functions are unknown, while one gene [slingshot protein phosphatase 2 (*Ssh2*)] among the 10 genes was also downregulated in live TMEV-infected HL-1 cells. To identify cell-type specific gene expression, we conducted microarray analyses using TMEV- and mock-infected Neuro-2a cells (43). In Neuro-2a cells, TMEV infection did not upregulate any genes significantly, while two genes with unknown functions were downregulated (**Figure 3D**; **Supplementary Table 2**). No innate immunity-related genes were induced in HL-1 cells incubated with UV-TMEV or TMEV-infected Neuro-2a cells (**Figure 3E**; **Supplementary Table 2**). Thus, induction of innate immunity-related genes by TMEV requires live virus and is cell-type specific.

To identify sets of genes whose expression patterns were unique under the experimental conditions, we conducted *k*-means clustering (**Figure 3F**) (33). Among 10 clusters, three clusters (clusters 3, 4, and 6) showed differentially expressed patterns, which were visualized by radar chart showing the different expression patterns of cluster centers in each cluster. Most upregulated genes in TMEV-infected HL-1 cells 4 and 8 h p.i., including *Ifit1* and *Cxcl10,* were categorized in clusters 3, while the downregulated genes only 8 h p.i. or 4 and 8 h p.i. were categorized in cluster 4 or 6, respectively. Lists of genes in each cluster were shown in **Supplementary Table 3**.

PCA of Microarray Data Separates Between the TMEV-Infected HL-1 and Control Groups

To compare overall gene expression patterns among samples, we conducted unsupervised PCA by entering microarray data from each sample without labeling of grouping (33, 42). In PCA, each principal component (PC) is determined automatically, and PC values for each sample data are plotted, for example,

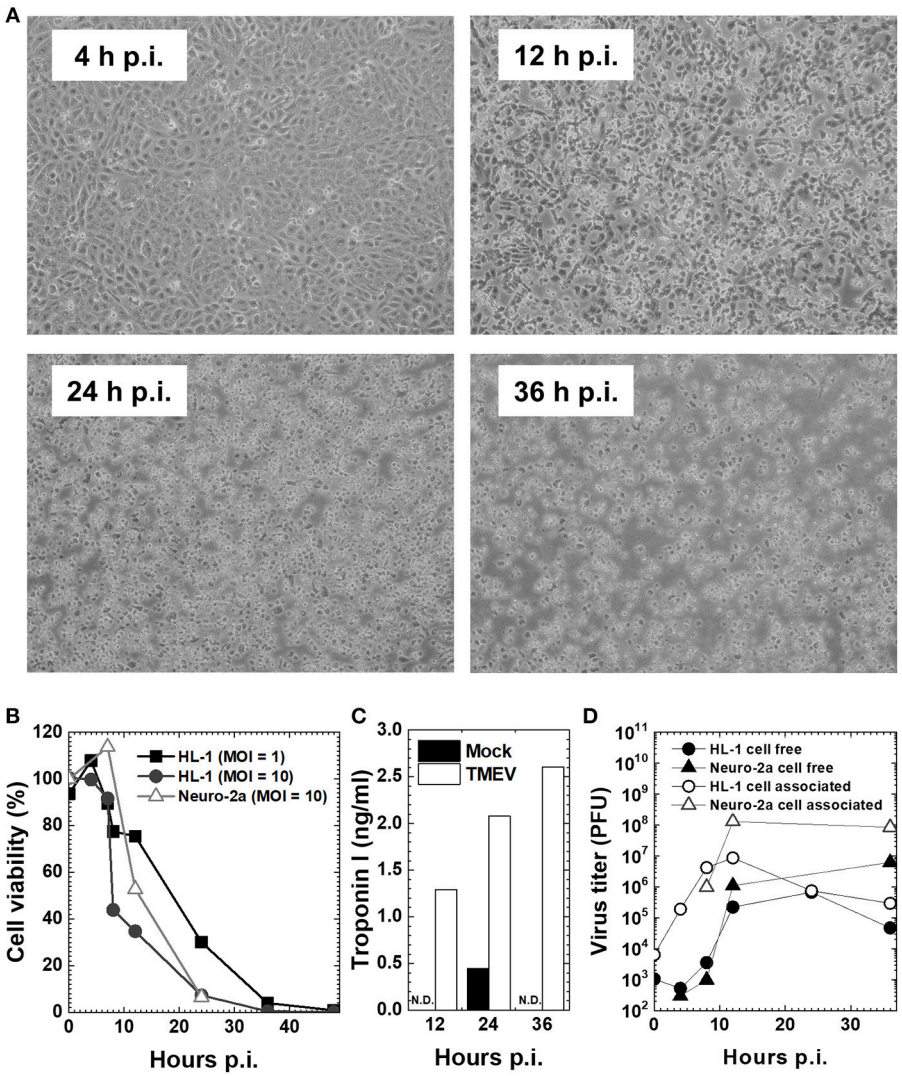

FIGURE 2 | Cardiomyocyte cell line HL-1 infection with the Daniels (DA) strain of TMEV (33, 42). **(A)** Confluent HL-1 cell monolayer infected with TMEV at a multiplicity of infection (MOI) = 10 showed no changes at 4 hours (h) post-inoculation (p.i.). Cytopathic effect (CPE), including the rounding up and detachment of cells from the culture dish, was observed at 12 h p.i., which developed cell lysis in most cells at 36 h p.i. **(B)** HL-1 cells and neuroblastoma cell line Neuro-2a were infected with TMEV at an MOI = 1 or 10. Cell viability was determined with trypan blue dye exclusion assays. Cell viability of both HL-1 and Neuro-2a cells decreased at 12 h p.i. and most cells died at 36 h p.i. **(C)** The concentration of cardiac troponin I in cell culture supernatants determined by an enzyme-linked immunosorbent assay (ELISA) was detectable in TMEV-infected HL-1 cells (open column), but not detectable (N.D.) in mock-infected HL-1 cells (closed column) or infected Neuro-2a cell culture (data not shown). **(D)** Viral titers of cell-free (•, ▲) and cell-associated virus (○, △) in HL-1 or Neuro-2a cell culture were determined by plaque assays with baby hamster kidney (BHK)-21 cells (24). In both HL-1 and Neuro-2a cells, cell-free virus titers increased substantially at 12 h p.i., while cell-associated viral titers increased at 8 h p.i. and peaked at 12 h p.i.

PC1 as the x-axis and PC2 as the y-axis. When the data of all HL-1 samples from mock-infection, TMEV-infection, and UV-TMEV incubation were entered, we found that the samples were separated into two distinct populations: live TMEV-infected samples vs. uninfected samples (mock-infection and UV-TMEV) (**Figure 4A**). According to the proportion of variance, PC1 explained 46% of the variation among samples (**Figure 4B**). Factor loading for PC1 showed that innate immunity-related genes, including *Cxcl10*, *Ccl5,* and *Ifit1*, contributed to PC1 positively, while a group of genes, including *Ssh2* (48), listerin E3 ubiquitin protein ligase 1 (*Ltn1*), and MINDY lysine 48 deubiquienase 2 (*Mindy2*) (49), contributed negatively (**Figure 4C**). Thus, both supervised and unsupervised analyses suggested that innate-immunity-related genes, including *Cxcl10*, *Ccl5,* and *Ifit1,* could be biomarkers for the differences between the TMEV-infected and control groups *in vitro*.

The gene expression changes in TMEV-infected HL-1 cells appeared to be similar to those found in the heart during phase I of *in vivo* TMEV infection. Thus, we conducted PCA by entering microarray data from TMEV-infected HL-1 cells

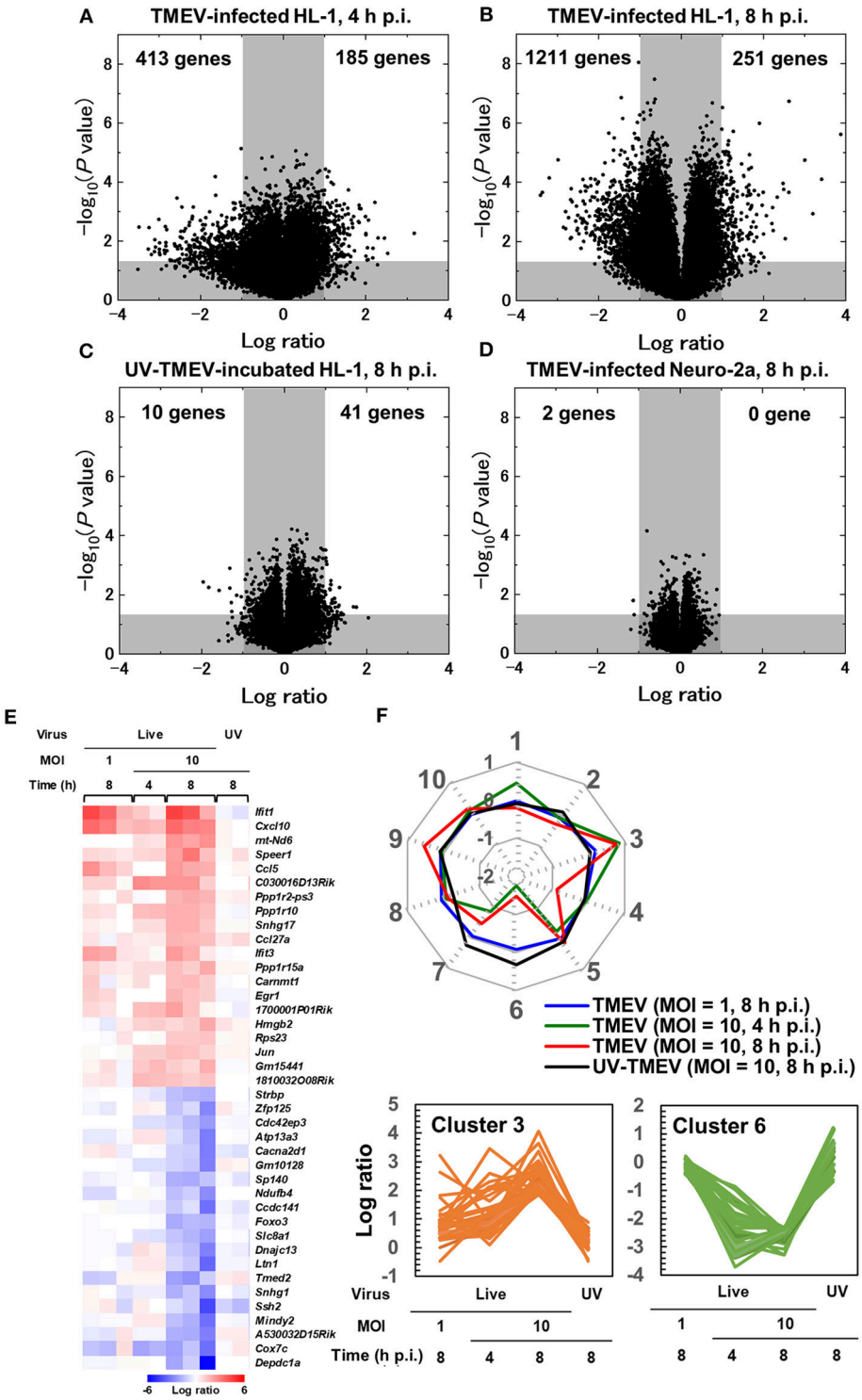

FIGURE 3 | Supervised bioinformatics analysis of transcriptome data from cardiomyocyte HL-1 cells infected with TMEV (33, 42). **(A–D)** Volcano plots of significantly up-regulated (upper right) or down-regulated genes (upper left) in TMEV-infected cells by the OriginPro 8.1 (OriginLab Corporation, Northampton, MA), to assess significance together with log ratio of transcriptome data (**Supplementary Materials and Methods**) (33). Log ratios of gene expression in the TMEV-infected cell culture compared with mock-infected cell culture were used as the x-axis and the logarithms of *P* values to base 10 were used as the y-axis. **(A)** TMEV-infected HL-1 cells at MOI = 10 at 4 h p.i. **(B)** TMEV-infected HL-1 cells at MOI = 10 at 8 h p.i. **(C)** HL-1 cells incubated with ultraviolet (UV)-irradiated TMEV for 8 h. **(D)** TMEV-infected Neuro-2a cells s at MOI = 10 at 8 h p.i. **(E)** Heat map of 20 up- or down-regulated genes in TMEV-infected HL-1 cells at MOI = 10 at 8 h p.i. by R

(Continued)

FIGURE 3 | version 3.4.3 and the R packages "gplots" and "genefilter." Red, blue, and white indicate up-regulation, down-regulation, and no change, respectively. Interferon-inducible genes (*Ifit1* and *Ifit3*) and chemokines (*Cxcl10* and *Ccl5*) were significantly up-regulated. While TMEV-infected HL-1 cells at MOI = 10 for 4 h or at MOI = 1 for 8 h showed a similar expression pattern in several genes, HL-1 cells incubated with UV-TMEV for 8 h did not up- or downregulated these genes. **(F)** Radar chart based on the values of cluster centers from *k*-means clustering. The number at each vertex is the cluster number (clusters 1 to 10), whereas the numbers along the axis (−2 to 1) are log ratios compared with mock-infected controls. Up-regulated genes in TMEV-infected HL-1 cells 4 and 8 h p.i., including *Cxcl10* and *Ifit1*, were categorized mostly in cluster 3, while the downregulated genes only 8 h p.i. or 4 and 8 h p.i. were categorized in cluster 4 or 6, respectively. In UV-TMEV-incubated HL-1 cells, most genes showed no change; the values of most cluster centers were log ratios = 0. List of genes in each cluster was shown in **Supplementary Table 3**.

and those from heart samples of all three phases in TMEV-infection *in vivo* (**Figure 4D**) (33, 42) to see whether the overall gene expression pattern of TMEV-infected HL-1 cells could be similar to those of TMEV-induced myocarditis *in vivo*. PCA clearly separated *in vivo* samples from three phases into three distinct groups by PC1 values; the PC1 values reflected distinct pathophysiology of three phases of myocarditis. Here, the PC1 values of *in vitro* TMEV-infected HL-1 cells 4 and 8 h p.i. were similar to that of heart samples of phase I in TMEV-induced myocarditis. On the other hand, PC2 values of *in vitro* TMEV-infected HL-1 cells were lower than those of *in vivo* samples. Thus, PC2 values could reflect the differences between *in vitro* and *in vivo* conditions, rather than phase-specific pathophysiology.

CYTOKINES AND LYMPHATICS IN TMEV INFECTION

Cytokines and Lymphatics in TMEV-Induced Myocarditis

Although several cytokines have been shown to influence lymphangiogenesis, the pro-lymphangiogenic cytokine, vascular endothelial growth factor (VEGF)-C or D (50), binds to VEGF receptor (VEGFR) 3 on lymphatic vessel endothelial cells to induce lymphangiogenesis during inflammation ("inflammation-associated lymphangiogenesis," IAL) (35), where macrophage-secreted VEGF induces sprouting of lymphatic vessels at the preexisting lymphatic vessels (51). The VEGF-A/VEGFR2, which is typically associated with angiogenesis (52), also induces lymphangiogenesis in a context-dependent manner, such as corneal lymphangiogenesis (50).

Cardiac lymphatic networks exist in all three layers of the heart, forming subendocardial, myocardial, and subepicardial plexuses, while these lymphatics share anatomical and physiological characteristics with those in other organs (53). Disturbed cardiac lymphatic drainage can contribute to many forms of cardiac pathology, such as dilated cardiomyopathy and heart failure. Myocarditis provokes myocardial edema and inflammatory infiltration of lymphocytes and macrophages; both can drive underlying lymphatic pumping disturbances. Lymphatic contraction is often impaired by inflammatory mediators, including cytokines, prostaglandins (PGs), and nitric oxide (54); inflammatory mediators produced during myocarditis could depress lymphatic pumping and drainage. In TMEV-induced myocarditis, we previously showed that pro-inflammatory cytokine interleukin (IL)-1β and tumor necrosis factor (TNF)-α upregulation was associated with myocarditis *in vivo* without induction of lymphatic markers, including lymphatic vessel endothelial hyaluronan receptor (LYVE)-1, or VEGFR3 (55). In addition, IL-1β reduced contractility of cardiac lymphatic muscle cells via cyclooxygenase (COX)-2/PGE_2 signaling with synergistic cooperation by TNF-α *in vitro*. These results suggest that a loss of cardiac lymphatic tonic contractility induced by IL-1β could exacerbate myocardial edema, leading to accumulation of inflammatory cytokines/chemokines and immune cells within the heart, while this may prevent viral spread to the systemic circulation.

Lymphatics and Virus Infection in the CNS

The CNS has been regarded as an immunologically privileged site due to several characteristics that isolate it from systemic immune responses under physiological conditions: lack of MHC molecules on most resident cells, the presence of the blood-brain barrier (BBB) with low adhesion molecule expression on blood vessels, and no conventional lymphatic system (56). Recently, meningeal lymphatic vessels have been identified in the CNS that may be used for clearance of not only soluble molecules (57) but also immune cells (58) from the CNS and drainage to the deep cervical lymph node. Although there have been many experimental reports showing the transport of soluble molecules, the cellular transport from the CNS to cervical lymph nodes is still controversial. For example, even highly malignant cancer cells in the CNS do not metastasize to any peripheral lymph nodes; cellular transport using the lymphatics from the CNS seems to be regulated with unknown mechanisms. Although the soluble antigens transported from the CNS to cervical lymph nodes can be used for antigen presentation, it is unclear whether this pathway is a major priming site for presentation of CNS antigens since cervical lymph node swelling is not seen in CNS microbial infections or CNS inflammatory diseases.

Using experimental intravenous injection of simian immunodeficiency virus (SIV) in rhesus macaques, Dave et al. (59) demonstrated the presence of SIV in the CNS and cervical lymph nodes with lower levels of virus in plasma, suggesting SIV spread from the CNS to draining cervical lymph nodes. Although the exit of SIV from the CNS via lymphatic vessels should be confirmed by future studies, including the comparison of viral genotypes between the CNS and lymph nodes, this study showed the possibility that lymphatics might be used for virus clearance and/or exit from the CNS to the periphery.

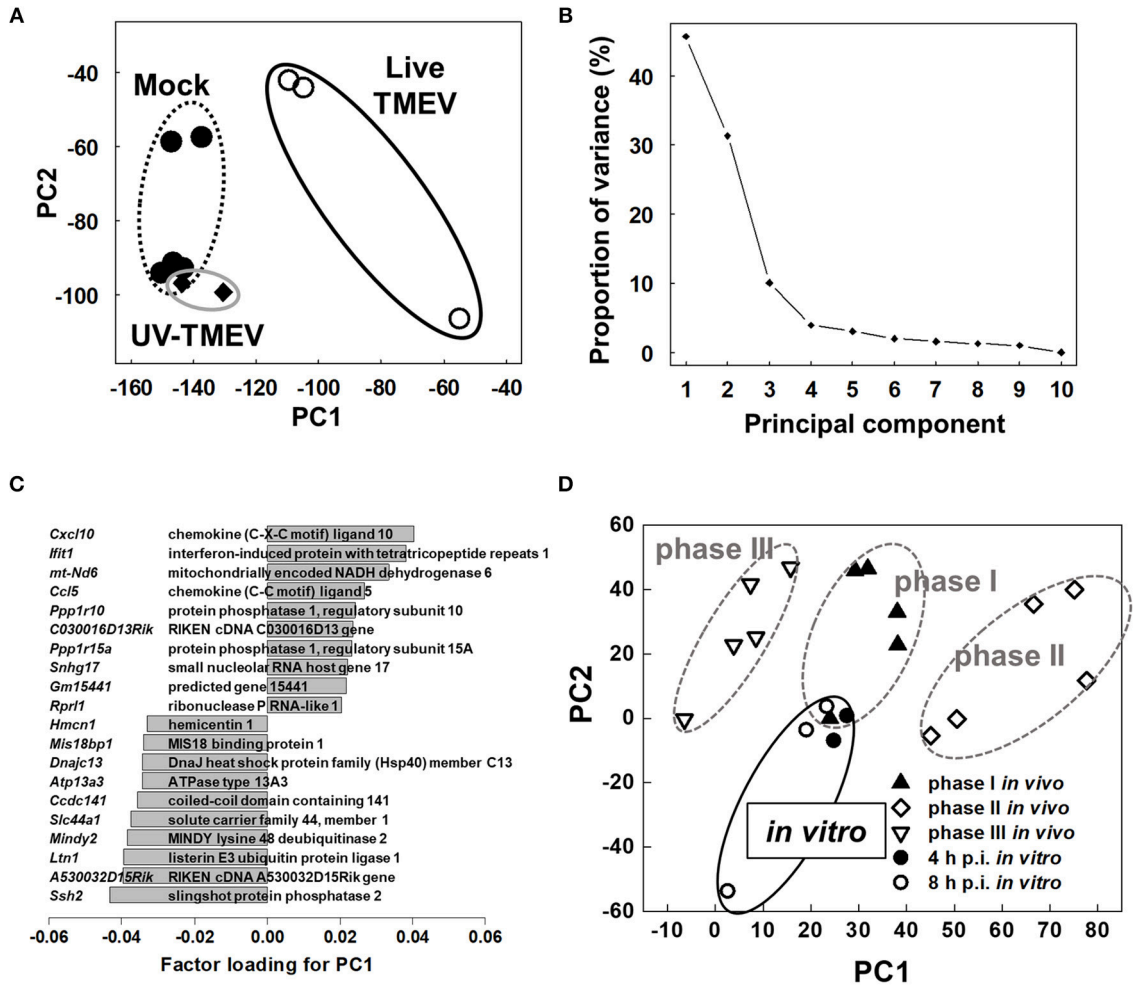

FIGURE 4 | Unsupervised principal component analysis (PCA) of transcriptome data of mock-infected, TMEV-infected, and UV-TMEV-incubated HL-1 cells (33, 42). **(A)** PCA separated samples into two groups: TMEV-infected samples vs. uninfected samples (mock infection and UV-TMEV), where principal component (PC) 1 reflected live virus infection. **(B)** The proportion of variance showed that PC1 explained 46% of the variance among the samples. **(C)** Factor loading for PC1 showed that chemokines (*Cxcl10* and *Ccl5*) and interferon-inducible genes (*Ifit1*) were correlated with PC1 positively, while several genes including slingshot protein phosphatase 2 (Ssh2) and listerin E3 ubiquitin protein ligase 1 (*Ltn1*) were correlated with PC1 negatively. **(D)** PCA of transcriptome data of TMEV-infected HL-1 cells 4 and 8 h p.i. and heart samples from phases I (4 days p.i.), II (7 days p.i.), and III (60 days p.i.) in TMEV-induced myocarditis *in vivo*. PCA showed that phase I samples and *in vitro* samples had similar PC1 values, compared with phases II and III samples. PCA was conducted using R version 3.4.3 (13). Microarray data were converted into tab-delimited text format and calculated using an R program "prcomp".

Lymphocyte Entry/Exit and Lymphatics in CNS TMEV Infection

In MS and its animal models, the presence of immune cell infiltrates, particularly lymphocytes, in the CNS has been correlated with disease activity and neuropathology. Lymphocyte entry into the CNS is accompanied by upregulation of adhesion molecules on lymphocytes and blood vessels as well as a breakdown of the BBB (60) (**Figure 5**). Among the adhesion molecules, the interactions between very late antigen (VLA)-4 (CD49d/CD29) and vascular cell adhesion molecule (VCAM)-1 (CD106) (63) as well as leukocyte function-associated antigen (LFA)-1 (CD11a/CD18) and intercellular adhesion molecule (ICAM)-1 (CD54) (64) have been shown to play a key role for lymphocyte extravasation into the CNS parenchyma (63). The BBB is composed of tight junctions of endothelial cells, the basement membrane, and astrocyte foot processes. Downregulation of tight junction proteins, including occludin and claudin, has been associated with BBB breakdown and disease activities in MS and its animal models (62). On the other hand, the pathophysiology of lymphocyte exit from the CNS is unclear, although newly identified CNS lymphatic vessels (58) might contribute to clearance of lymphocytes (and microbes) from the CNS, in theory.

In TMEV infection, we determined the extent of which expressions of the adhesion molecules, BBB and lymphatic molecules could be associated with CNS disease activity (53,

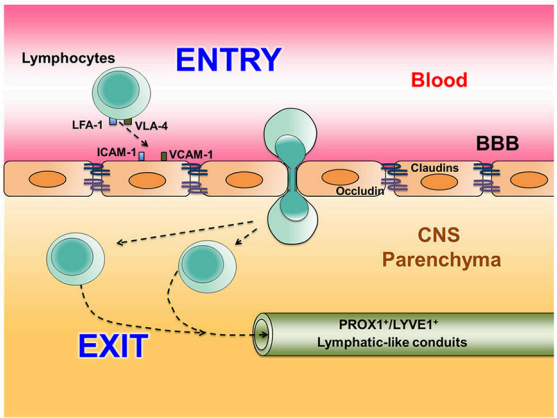

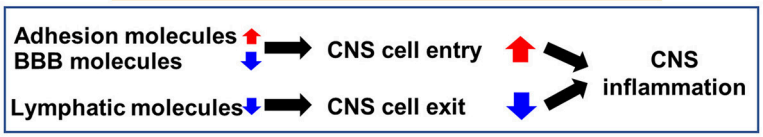

Representative 20 adhesion molecules, 14 BBB molecules, and 12 lymphatic molecules

Entrez ID	Symbol	Gene name
Adhesion molecules		
12481	Cd2	CD2 (lymphocyte function-associated antigen-2, LFA-2)
12490	Cd34	CD34
225825	Cd226	CD226 (DNAX accessory molecule-1, DNAM-1)
20340	Glg1	golgi apparatus protein 1 (E-selectin ligand)
14663	Glycam1	glycosylation dependent cell adhesion molecule 1
15894	Icam1	intercellular adhesion molecule 1 (ICAM-1, CD54)
15896	Icam2	intercellular adhesion molecule 2 (ICAM-2, CD102)
16401	Itga4	integrin α4 (very late antigen-4, VLA-4, CD49d)
16408	Itgal	integrin αL (LFA-1, CD11a)
16412	Itgb1	integrin β1 (fibronectin receptor β, VLA-4, CD29)
16414	Itgb2	integrin β2 (LFA-1, CD18)
16421	Itgb7	integrin β7
18613	Pecam1	platelet/endothelial cell adhesion molecule 1 (CD31)
52118	Pvr	poliovirus receptor (CD155)
19294	Pvrl2	poliovirus receptor-related 2 (Nectin2, CD112)
20339	Sele	selectin, endothelial cell (E-selectin, CD62E)
20343	Sell	selectin, lymphocyte (L-selectin, CD62L)
20344	Selp	selectin, platelet (p-selectin, CD62P)
20345	Selplg	selectin, platelet (p-selectin) ligand (PSGL-1, CD162)
22329	Vcam1	vascular cell adhesion molecule 1 (VCAM-1, CD106)
BBB molecules		
12562	Cdh5	cadherin 5 (CD144)
12737	Cldn1	claudin 1
65130	Cldn3	claudin 3
12741	Cldn5	claudin 5
58187	Cldn10	claudin 10
64945	Cldn12	claudin 12
75677	Cldn22	claudin 22
69524	Esam	endothelial cell-specific adhesion molecule (ESAM)
16456	F11r	F11 receptor (junctional adhesion molecule 1, JAM1, CD321)
67374	Jam2	junctional adhesion molecule 2 (JAM2, CD322)
83964	Jam3	junctional adhesion molecule 3 (JAM3)
18260	Ocln	occludin
19699	Reln	reelin
21872	Tjp1	tight junction protein 1 (zona occludens protein 1, ZO-1)
Lymphatic molecules		
11731	Ang2	angiogenin, ribonuclease A family, member 2
11600	Angpt1	angiopoietin 1
11601	Angpt2	angiopoietin 2
14205	Figf	c-fos induced growth factor (VEGF-D)
14257	Flt4	FMS-like tyrosine kinase 4 (VEGFR3)
14234	Foxc2	forkhead box C2
15898	Icam5	intercellular adhesion molecule 5, telencephalin (CD50)
104099	Itga9	integrin α9
114332	Lyve1	lymphatic vessel endothelial hyaluronan receptor 1 (LYVE1)
14726	Pdpn	podoplanin
19130	Prox1	prospero homeobox 1 (PROX1)
22341	Vegfc	vascular endothelial growth factor C (VEGF-C)

FIGURE 5 | Three components of lymphocyte entry into and exit from the CNS (61, 62). To initiate inflammation in the CNS, lymphocytes interact with endothelial cells of blood vessels via up-regulated adhesion molecules, particularly very late antigen (VLA)-4 and lymphocyte function-associated antigen (LFA)-1 on lymphocytes with vascular cell adhesion molecule (VCAM)-1 and intercellular adhesion molecule (ICAM)-1 on endothelia, respectively. Downregulation of molecules composed of the blood-brain barrier (BBB) also help in lymphocyte entry into the CNS parenchyma. While the precise mechanism of lymphocyte exit from the CNS is unknown, one hypothesis is the presence of vessels similar to peripheral lymphatic vessels, whose markers include prospero homeobox (PROX) 1 and lymphatic vessel endothelial hyaluronan receptor (LYVE) 1, may help in lymphocyte exit from the CNS to deep cervical lymph nodes. Increased lymphocyte entry together with decreased lymphocyte exit could lead to enhancement of CNS inflammation.

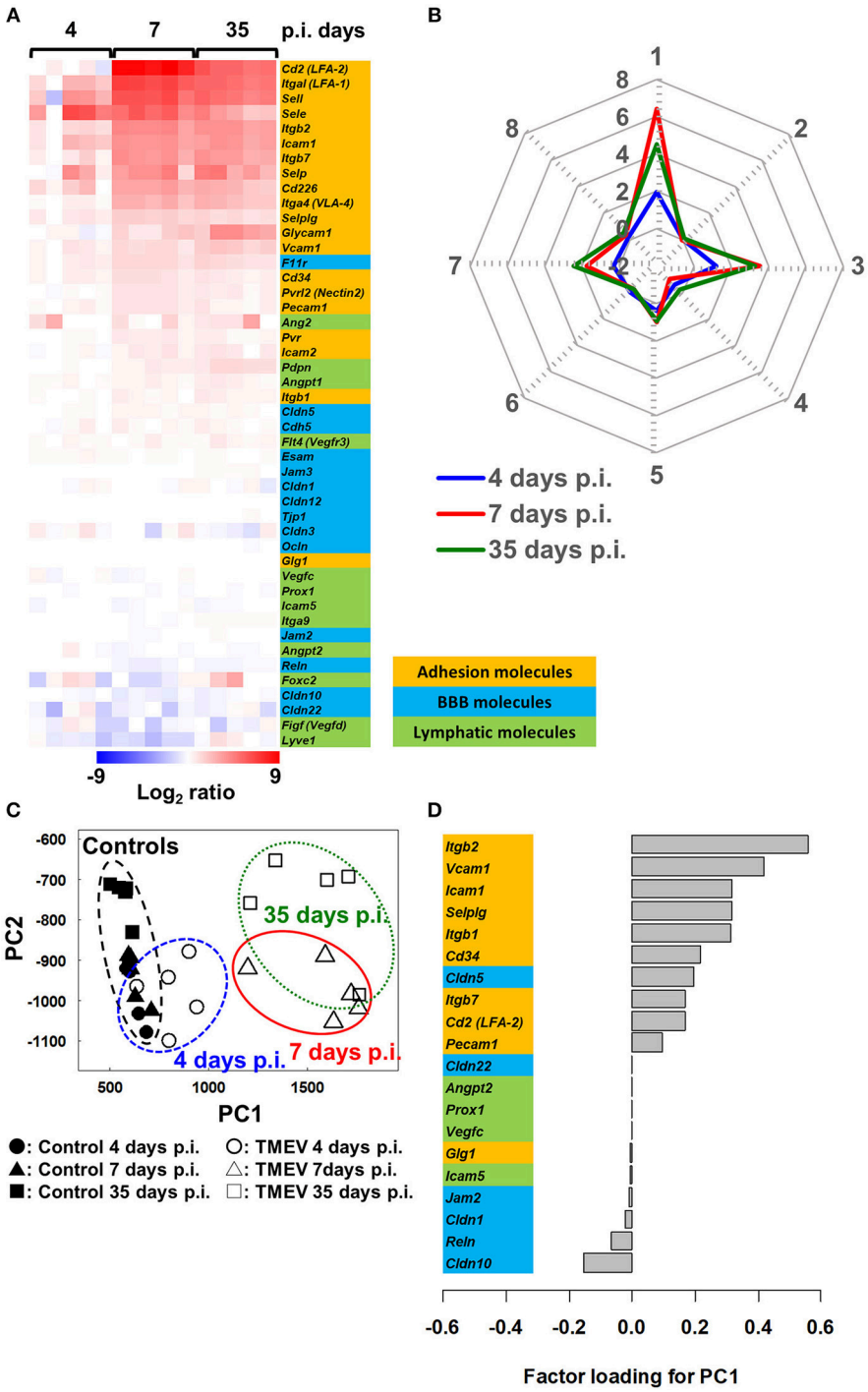

FIGURE 6 | Bioinformatics analyses of gene expression of three components associated with spinal cord inflammation in TMEV infection, 4 (prior to cell infiltration), 7 (acute polioencephalomyelitis) and 35 (TMEV-IDD) days p.i. (61). **(A)** We drew a heat map, using mRNA data of 20 adhesion molecules, 14 BBB molecules, and 12 lymphatic molecules listed in **Figure 5** (total 46 genes). Most adhesion molecule genes were upregulated 7 and 35 days p.i., while only a few adhesion molecules were upregulated 4 days p.i. BBB and lymphatic molecules showed no change or slight downregulation. **(B)** Radar chart based on the values of cluster centers from *k*-means clustering (**Supplementary Table 4**). The number of each vertex is the cluster number (clusters 1 to 8), whereas the number along the axis (−2 to 8) are log ratios compared with mock-infected controls. Radar chart showed that the expression patterns of sets of genes were similar between days 7 and 35 p.i. Upregulated genes were categorized mostly in clusters 1, 3, and 7. **(C)** PCA of the 46 genes listed in **Figure 5** separated controls/day 4 p.i. samples vs. days 7 and 35 p.i. samples based on PC1 values (proportion of variance was 85.9%), which reflect CNS cell infiltration. **(D)** Factor loading for PC1 showed that upregulation of adhesion molecules was associated with CNS inflammation, while downregulation of BBB and lymphatic molecules may play a minor role.

61). Using the RNA sequencing transcriptome data from the spinal cord of TMEV-infected mice harvested 4, 7, and 35 days p.i. (**Supplementary Materials and Methods**), we compared mRNA levels of representative 20 lymphocyte and vascular adhesion molecules, 14 BBB molecules, and 12 lymphatic molecules among samples (**Figure 5**). Both 7 and 35 days p.i., heat map showed that most adhesion molecules were upregulated, while lymphatic and BBB molecules showed no change or slight downregulation (**Figure 6A**). Since samples 7 days p.i. contain gray matter inflammatory lesions due to acute polioencephalomyelitis and those 35 days p.i. contain inflammatory demyelination in the white matter, we expected substantial difference in gene expression patterns between the two sample groups. Unexpectedly, however, the levels of most adhesion molecules 7 days p.i. were similar or slightly higher, compared with 35 days p.i. Only glycosylation-dependent cell adhesion molecule (GLYCAM) 1 was significantly upregulated from 7 to 35 days p.i. (65). Thus, GLYCAM1 may have a role in chronic demyelination. Most genes 4 days p.i. showed no or few changes, which is consistent with the histological finding that immune cell infiltrates become obvious 5 days p.i. in CNS TMEV infection. In radar chart that visualized gene expression patterns by *k*-means clustering, clusters 1, 3, and 7 were composed of highly upregulated genes 7 and 35 days p.i. (cluster 1, LFA-1 and 2, E- and L-selectin; cluster 3, ICAM-1, and other molecules; and cluster 7, VLA-4, VCAM-1, and GLYCAM1) (**Figure 6B**; **Supplementary Table 4**). Cluster 4 was composed of downregulated genes 4, 7, and 35 days p.i., including VEGF-C, LYVE1, and claudin 22.

We also conducted PCA using the same 46 gene expression data and found that expression patterns of molecules associated with CNS lymphocyte entry and exit could distinguish samples without CNS cell infiltration (control and 4 day p.i. samples) vs. with CNS cell infiltration (7 and 35 days p.i. samples) by PC1 values (**Figure 6C**). Factor loading for PC1 showed that upregulation of adhesion molecules (66) was correlated with PC1 values that reflect CNS inflammation 7 and 35 days p.i. (**Figure 6D**). Downregulation of several BBB molecules, including claudin 10 (67) and reelin, was weakly correlated with PC1 values. Downregulation of BBB may play a minor role in CNS inflammation induced with TMEV, although downregulation of BBB molecules has been reported not only in MS and autoimmune model for MS but also in another experimental CNS viral model induced with mouse hepatitis virus (68).

Inflammation has been reported to induce lymphangiogenesis in several organs and tissues. Following intracerebral TMEV infection in the CNS, however, most lymphatic markers were not upregulated at any time points, although the constitutive expression in control uninfected CNS tissues supports the presence of lymphatic-like structure in the CNS. This is consistent with our previous findings on the protein levels of lymphatic biomarkers, in which there was no increase in lymphatic markers, LYVE1 or prospero homeobox protein (PROX)1 in the CNS of TMEV-IDD (39). Most lymphatic molecules were actually downregulated slightly on 7 and 35 days p.i., while factor loading for PC1 showed that downregulation of lymphatic molecules was weakly correlated with PC1 values. This suggests that dysfunction of lymphatic-like structure might delay exit of inflammatory cytokines/chemokines and/or cells from the CNS, enhancing inflammation, only to some extent. On 14 days p.i. when inflammation had subsided in the CNS, the levels of most lymphatic molecules of the TMEV-infected spinal cord were similar to those of uninfected control spinal cord (data not shown); this may reflect that recovery of lymphatic flow from the CNS contributes to exit of inflammatory cytokines/chemokines and/or cells from the CNS around 2 weeks p.i.

TABLE 1 | Potential factors contributing to TMEV-induced organ-specific pathology.

	CNS	Heart
Infection of major cell type *in vitro*	+ (Neuro-2a)	+ (HL-1)
Innate immune response by major cell type *in vitro*	−	+
Infection *in vivo*	+	+
Lymphatics	Lymphatic molecule downregulation?	Cytokine-induced functional suppression

In TMEV-IDD, the balance between lymphocyte entry and exit could play a key role in inflammation in the CNS; upregulation of adhesion molecules rather than downregulation of BBB molecules could contribute to lymphocyte entry, while downregulation of lymphatic molecules may play a minor role in prolonged inflammation. In theory, dysfunction of the lymphatics results in the persistence of lymphocytes and cytokines/chemokines in the CNS (69). This would lead to chronic inflammation and immune-mediated demyelination by immunopathology, whereas such lymphostasis might confine TMEV to the CNS, limiting systemic viral spreading. Here, virus-specific lymphocytes among chronic cellular infiltrates in the CNS may also minimize virus replication in the CNS.

In summary, in TMEV infection, innate immune cytokines may play distinctive and diverse roles in lymphatic networks during inflammatory disease depending on the organs, which contribute to the levels of inflammation and to virus persistence (**Table 1**). Although TMEV can infect major cell types of the CNS (neurons) and the heart (cardiomyocytes), only infected cardiomyocytes expressed innate immunity-related molecules. In addition, lymphatic vessels in infected organs may also be differentially affected between the CNS and the heart. In the heart of TMEV-induced acute myocarditis, IL-1β with TNF-α could functionally alter lymphatics, while downregulation of lymphatic molecules might contribute to persistent virus infection and inflammation in the CNS of TMEV-IDD. These potential factors may contribute to organ-specific viral immunopathology in TMEV infection.

ETHICS STATEMENT

This study was carried out in accordance with the recommendations of the criteria outlined by the National Institutes of Health (NIH). The protocol was approved by the

Institutional Animal Care and Use Committee of LSUHSC-S and Kindai University.

AUTHOR CONTRIBUTIONS

IT and SO for substantial contributions to the conception or design of the work. SO, EK, FS for the acquisition of data. SO, UC, and MT for analysis of data. IT, AM, MA-K, and JA for interpretation of data for the work. IT, SO, NM, JY, and JA for drafting the work or revising it critically for important intellectual content.

FUNDING

This work was supported by the fellowships (FS and SO) from the Malcolm Feist Cardiovascular Research Endowment, LSU Health Sciences Center, Shreveport, and grants from the National Institute of General Medical Sciences COBRE Grant (8P20 GM 103433, IT), and the Science Research Promotion Fund from the Promotion and Mutual Aid Corporation for Private Schools of Japan (FS), the Faculty Assistance and Development Research Grants from the Kindai University Research Enhancement Grant (FS and SO), the KAKENHI from the Japan Society for the Promotion of Science [Grant-in-Aid for Young Scientists (B), JP17K15628 (FS), Grants-in-Aid for Research Activity Start-up, JP16H07356 (IT), Grant-in-Aid for Scientific Research on Innovative Areas Frontier Research on Chemical Communications (No 17H06400 and 17H06404, IT)] and Novartis Pharma Research Grants (IT).

ACKNOWLEDGMENTS

We thank John A. Vanchiere, M.D., Ph.D., Melody Cunningham Baddoo, Rona S. Scott, Ph.D., Mitsugu Fujita, M.D., Ph.D., and Ah-Mee Park, Ph.D. for helpful discussions, and Gloria B. McClure, Paula Polk, Elaine A. Cliburn, Sadie Faith Pearson and Lesya Ekshyyan for excellent technical assistance.

SUPPLEMENTARY MATERIAL

The Supplementary Material for this article can be found online at: https://www.frontiersin.org/articles/10.3389/fimmu.2018.02870/full#supplementary-material

REFERENCES

1. Theiler M. Spontaneous encephalomyelitis of mice–a new virus disease. *Science* (1934) 80:122. doi: 10.1126/science.80.2066.122-a
2. Theiler M. Spontaneous encephalomyelitis of mice, a new virus disease. *J Exp Med*. (1937) 65:705–19. doi: 10.1084/jem.65.5.705
3. Tsunoda I, Fujinami RS. Theiler's murine encephalomyelitis virus. In: Ahmed R and Chen ISY, editors. *Persistent Viral Infections*. New York, NY: John Wiley and Sons (1999). p. 517–36.
4. Daniels JB, Pappenheimer AM, Richardson S. Observations on encephalomyelitis of mice (DA strain). *J Exp Med*. (1952) 96:517–30. doi: 10.1084/jem.96.6.517
5. Sato F, Tanaka H, Hasanovic F, Tsunoda I. Theiler's virus infection: pathophysiology of demyelination and neurodegeneration. *Pathophysiology* (2011) 18:31–41. doi: 10.1016/j.pathophys.2010.04.011
6. Bjelobaba I, Savic D, Lavrnja I. Multiple sclerosis and neuroinflammation: the overview of current and prospective therapies. *Curr Pharm Des*. (2017) 23:693–730. doi: 10.2174/1381612822666161214153108
7. Sato F, Omura S, Martinez NE, Tsunoda I. Animal models of multiple sclerosis. In: Minagar A, editors. *Neuroinflammation*. 2nd ed. Burlington, MA: Academic Press (2018). p. 37–72.
8. Gómez RM, Rinehart JE, Wollmann R, Roos RP. Theiler's murine encephalomyelitis virus-induced cardiac and skeletal muscle disease. *J Virol*. (1996) 70:8926–33.
9. Sato F, Omura S, Kawai E, Martinez NE, Acharya MM, Reddy PC, et al. Distinct kinetics of viral replication, T cell infiltration, and fibrosis in three phases of myocarditis following Theiler's virus infection. *Cell Immunol*. (2014) 292:85–93. doi: 10.1016/j.cellimm.2014.10.004
10. Kawai E, Sato F, Omura S, Martinez NE, Reddy PC, Taniguchi M, et al. Organ-specific protective role of NKT cells in virus-induced inflammatory demyelination and myocarditis depends on mouse strain. *J Neuroimmunol*. (2015) 278:174–84. doi: 10.1016/j.jneuroim.2014.11.003
11. Lipton HL, Kim BS, Yahikozawa H, Nadler CF. Serological evidence that Mus musculus is the natural host of Theiler's murine encephalomyelitis virus. *Virus Res*. (2001) 76:79–86. doi: 10.1016/S0168-1702(01)00256-8
12. Williams SH, Che X, Garcia JA, Klena JD, Lee B, Muller D, et al. Viral diversity of house mice in New York City. *MBio* (2018) 9:e01354–17. doi: 10.1128/mBio.01354-17
13. Tsunoda I, McCright IJ, Kuang L-Q, Zurbriggen A, Fujinami RS. Hydrocephalus in mice infected with a Theiler's murine encephalomyelitis virus variant. *J Neuropathol Exp Neurol*. (1997) 56:1302–13. doi: 10.1097/00005072-199712000-00005
14. Flint J, Racaniello V, Rall G, Skalka A, Enquist L. Barriers to infection. In: *Principles of Virology*. Vol. 2. 4th ed. Washington, DC: ASM Press. (2015). pp. 24–51.
15. McCright IJ, Fujinami RS. Lack of correlation of Theiler's virus binding to cells with infection. *J Neurovirol*. (1997) 3 (Suppl. 1):S68–70.
16. Tsunoda I. Axonal degeneration as a self-destructive defense mechanism against neurotropic virus infection. *Future Virol*. (2008) 3:579–93. doi: 10.2217/17460794.3.6.579
17. Clatch RJ, Melvold RW, Miller SD, Lipton HL. Theiler's murine encephalomyelitis virus (TMEV)-induced demyelinating disease in mice is influenced by the H-2D region: correlation with TEMV-specific delayed-type hypersensitivity. *J Immunol*. (1985) 135:1408–14
18. Tsunoda I, Kuang L-Q, Fujinami RS. Induction of autoreactive $CD8^+$ cytotoxic T cells during Theiler's murine encephalomyelitis virus infection: implications for autoimmunity. *J Virol*. (2002) 76:12834–44. doi: 10.1128/JVI.76.24.12834-12844.2002
19. Tsunoda I, Iwasaki Y, Terunuma H, Sako K, Ohara Y. A comparative study of acute and chronic diseases induced by two subgroups of Theiler's murine encephalomyelitis virus. *Acta Neuropathol*. (1996) 91:595–602. doi: 10.1007/s004010050472
20. Theil DJ, Tsunoda I, Libbey JE, Derfuss TJ, Fujinami RS. Alterations in cytokine but not chemokine mRNA expression during three distinct Theiler's virus infections. *J Neuroimmunol*. (2000) 104:22–30. doi: 10.1016/S0165-5728(99)00251-9
21. Tsunoda I, Libbey JE, Fujinami RS. TGF-β1 suppresses T cell infiltration and VP2 puff B mutation enhances apoptosis in acute polioencephalitis induced by Theiler's virus. *J Neuroimmunol*. (2007) 190:80–9. doi: 10.1016/j.jneuroim.2007.07.026
22. Tsunoda I, Fujinami RS. TMEV and neuroantigens: Myelin genes and proteins, molecular mimicry, epitope spreading and autoantibody-mediated remyelination. In: Lavi E and Constantimescu C, editors. *Experimental Models of Multiple Sclerosis*. New York, NY: Springer (2005). pp. 593–616.

23. Sato F, Omura S, Jaffe SL, Tsunoda I. Role of $CD4^+$ T lymphocytes in pathophysiology of multiple sclerosis. In: Minagar A, editors. *Multiple Sclerosis: A Mechanistic View*. London: Elsevier Inc. (2016). pp. 41–69.
24. Martinez NE, Karlsson F, Sato F, Kawai E, Omura S, Minagar A, et al. Protective and detrimental roles for regulatory T cells in a viral model for multiple sclerosis. *Brain Pathol*. (2014) 24:436–51. doi: 10.1111/bpa.12119
25. Cooper LT. Jr. Myocarditis. *N Engl J Med*. (2009) 360:1526–38. doi: 10.1056/NEJMra0800028
26. Guglin M, Nallamshetty L. Myocarditis: diagnosis and treatment. *Curr Treat Options Cardiovasc Med*. (2012). doi: 10.1007/s11936-012-0204-7
27. Fairweather D, Stafford KA, Sung YK. Update on coxsackievirus B3 myocarditis. *Curr Opin Rheumatol*. (2012) 24:401–7. doi: 10.1097/BOR.0b013e328353372d
28. Martinez NE, Sato F, Kawai E, Omura S, Chervenak RP, Tsunoda I. Regulatory T cells and Th17 cells in viral infections: implications for multiple sclerosis and myocarditis. *Future Virol*. (2012) 7:593–608. doi: 10.2217/fvl.12.44
29. Liu PP, Mason JW. Advances in the understanding of myocarditis. *Circulation* (2001) 104:1076–82. doi: 10.1161/hc3401.095198
30. Corsten MF, Schroen B, Heymans S. Inflammation in viral myocarditis: friend or foe? *Trends Mol Med*. (2012) 18:426–37. doi: 10.1016/j.molmed.2012.05.005
31. Kindermann I, Barth C, Mahfoud F, Ukena C, Lenski M, Yilmaz A, et al. Update on myocarditis. *J Am Coll Cardiol*. (2012) 59:779–92. doi: 10.1016/j.jacc.2011.09.074
32. Shauer A, Gotsman I, Keren A, Zwas DR, Hellman Y, Durst R, et al. Acute viral myocarditis: current concepts in diagnosis and treatment. *ISR Med Assoc J*. (2013) 15:180–5.
33. Omura S, Kawai E, Sato F, Martinez NE, Chaitanya GV, Rollyson PA, et al. Bioinformatics multivariate analysis determined a set of phase-specific biomarker candidates in a novel mouse model for viral myocarditis. *Circ Cardiovasc Genet*. (2014) 7:444–54. doi: 10.1161/CIRCGENETICS.114.000505
34. Tang H, Pei H, Xia Q, Tang Y, Huang J, Huang J, et al. Role of gene polymorphisms/haplotypes and serum levels of interleukin-17A in susceptibility to viral myocarditis. *Exp Mol Pathol*. (2018) 104:140–5. doi: 10.1016/j.yexmp.2018.03.002
35. Proulx ST, Luciani P, Dieterich LC, Karaman S, Leroux J-C, Detmar M. Expansion of the lymphatic vasculature in cancer and inflammation: new opportunities for *in vivo* imaging and drug delivery. *J Control Release* (2013) 172:550–7. doi: 10.1016/j.jconrel.2013.04.027
36. Trevaskis NL, Kaminskas LM, Porter CJH. From sewer to saviour - targeting the lymphatic system to promote drug exposure and activity. *Nat Rev Drug Discov*. (2015) 14:781–803. doi: 10.1038/nrd4608
37. Kastenmüller W, Torabi-Parizi P, Subramanian N, Lämmermann T, Germain RN. A spatially-organized multicellular innate immune response in lymph nodes limits systemic pathogen spread. *Cell* (2012) 150:1235–48. doi: 10.1016/j.cell.2012.07.021
38. Loo CP, Nelson NA, Lane RS, Booth JL, Loprinzi Hardin SC, Thomas A, et al. Lymphatic vessels balance viral dissemination and immune activation following cutaneous viral infection. *Cell Rep*. (2017) 20:3176–87. doi: 10.1016/j.celrep.2017.09.006
39. Chaitanya GV, Omura S, Sato F, Martinez NE, Minagar A, Ramanathan M, et al. Inflammation induces neuro-lymphatic protein expression in multiple sclerosis brain neurovasculature. *J Neuroinflammation* (2013) 10:125. doi: 10.1186/1742-2094-10-125
40. Smith HK, Omura S, Vital SA, Becker F, Senchenkova EY, Kaur G, et al. Metallothionein I as a direct link between therapeutic hematopoietic stem/progenitor cells and cerebral protection in stroke. *FASEB J*. (2018) 32:2381–94. doi: 10.1096/fj.201700746R
41. Claycomb WC, Lanson NAJr, Stallworth BS, Egeland DB, Delcarpio JB, Bahinski A, et al. HL-1 cells: a cardiac muscle cell line that contracts and retains phenotypic characteristics of the adult cardiomyocyte. *Proc Natl Acad Sci USA*. (1998) 95:2979–84. doi: 10.1073/pnas.95.6.2979
42. Shafiei F, Omura S, Kawai E, Sato F, Martinez NE, Fernando, et al. Computational multivariate analyses for phase-specific biomarker identification in novel *in vivo* and *in vitro* viral myocarditis models induced by cardiovirus. *J Am Coll Cardiol*. (2014) 63:A971. doi: 10.1016/S0735-1097(14)60971-2
43. Tsunoda I, Kurtz CIB, Fujinami RS. Apoptosis in acute and chronic central nervous system disease induced by Theiler's murine encephalomyelitis virus. *Virology* (1997) 228:388–93. doi: 10.1006/viro.1996.8382
44. Chen JJ, Wang S-J, Tsai C-A, Lin C-J. Selection of differentially expressed genes in microarray data analysis. *Pharmacogenomics J*. (2007) 7:212–20. doi: 10.1038/sj.tpj.6500412
45. Oberg AL, Mahoney DW, Eckel-Passow JE, Malone CJ, Wolfinger RD, Hill EG, et al. Statistical analysis of relative labeled mass spectrometry data from complex samples using ANOVA. *J Proteome Res*. (2008) 7:225–33. doi: 10.1021/pr700734f
46. Li WT. Volcano plots in analyzing differential expressions with mRNA microarrays. *J Bioinform Comput Biol*. (2012) 10. doi: 10.1142/S0219720012310038
47. Tsunoda I, Tanaka T, Taniguchi M, Fujinami RS. Contrasting roles for $V\alpha14^+$ natural killer T cells in a viral model for multiple sclerosis. *J Neurovirol*. (2009) 15:90–8. doi: 10.1080/13550280802400684
48. Niwa R, Nagata-Ohashi K, Takeichi M, Mizuno K, Uemura T. Control of actin reorganization by Slingshot, a family of phosphatases that dephosphorylate ADF/cofilin. *Cell* (2002) 108:233–46. doi: 10.1016/S0092-8674(01)00638-9
49. Starnawska A, Demontis D, McQuillin A, O'Brien NL, Staunstrup NH, Mors O, et al. Hypomethylation of *FAM63B* in bipolar disorder patients. *Clin Epigenet*. (2016) 8:52. doi: 10.1186/s13148-016-0221-6
50. Wuest TR, Carr DJ. VEGF-A expression by HSV-1-infected cells drives corneal lymphangiogenesis. *J Exp Med*. (2010) 207:101–15. doi: 10.1084/jem.20091385
51. Kim H, Kataru RP, Koh GY. Inflammation-associated lymphangiogenesis: a double-edged sword? *J Clin Invest*. (2014) 124:936–42. doi: 10.1172/JCI71607
52. Religa P, Cao RH, Religa D, Xue Y, Bogdanovic N, Westaway D, et al. VEGF significantly restores impaired memory behavior in Alzheimer's mice by improvement of vascular survival. *Sci Rep*. (2013) 3:2053. doi: 10.1038/srep02053
53. Al-Kofahi M, Yun JW, Minagar A, Alexander JS. Anatomy and roles of lymphatics in inflammatory diseases *Clin Exp Neuroimmunol*. (2017) 8:4038–51. doi: 10.1111/cen3.12400
54. Becker F, Kurmaeva E, Gavins FN, Stevenson EV, Navratil AR, Jin L, et al. A Critical Role for monocytes/macrophages during intestinal inflammation-associated lymphangiogenesis. *Inflamm Bowel Dis*. (2016) 22:1326–45. doi: 10.1097/MIB.0000000000000731
55. Al-Kofahi M, Omura S, Tsunoda I, Sato F, Becker F, Gavins FN, et al. IL-1β reduces cardiac lymphatic muscle contraction via COX-2 and PGE_2 Induction: Potential role in myocarditis. *Biomed Pharmacother*. (2018) 107:1591–600. doi: 10.1016/j.biopha.2018.08.004
56. Johnson RT. Immune responses In: *Viral Infections of the Nervous System*. 2nd ed. Philadelphia, PA: Lippincott-Raven (1998). pp. 61–84.
57. Dave RS, Jain P, Byrareddy SN. Functional meningeal lymphatics and cerebrospinal fluid outflow. *J Neuroimmune Pharmacol*. (2018) 13:123–5. doi: 10.1007/s11481-018-9778-5
58. Louveau A, Smirnov I, Keyes TJ, Eccles JD, Rouhani SJ, Peske JD, et al. Structural and functional features of central nervous system lymphatic vessels. *Nature* (2015) 523:337–41. doi: 10.1038/nature14432
59. Dave RS, Sharma RK, Muir RR, Haddad E, Gumber S, Villinger F, et al. FDC:TFH interactions within cervical lymph nodes of SIV-infected rhesus macaques. *J Neuroimmune Pharmacol*. (2017) 13:204–18. doi: 10.1007/s11481-017-9775-0
60. Ortiz GG, Pacheco-Moisés FP, Macías-Islas MA, Flores-Alvarado LJ, Mireles-Ramírez MA, González-Renovato ED, et al. Role of the blood-brain barrier in multiple sclerosis. *Arch Med Res*. (2014) 45:687–97. doi: 10.1016/j.arcmed.2014.11.013
61. Omura S, Sato F, Fujita M, Park A-M, Alexander JS, Kilgore PCSR, et al. Computational analyses associate the CNS lymphatic molecules with disease progression of a viral model for multiple sclerosis. *Neuroinfection* (2018) 23:114–20.
62. Minagar A, Jy W, Jimenez JJ, Alexander JS. Multiple sclerosis as a vascular disease. *Neurol Res*. (2006) 28:230–5. doi: 10.1179/016164106X98080
63. Tsunoda I, Terry EJ, Marble BJ, Lazarides E, Woods C, Fujinami RS. Modulation of experimental autoimmune

encephalomyelitis by VLA-2 blockade. *Brain Pathol.* (2007) 17:45–55. doi: 10.1111/j.1750-3639.2006.00042.x
64. Inoue A, Koh CS, Yamazaki M, Ichikawa M, Isobe M, Ishihara Y, et al. Anti-adhesion molecule therapy in Theiler's murine encephalomyelitis virus-induced demyelinating disease. *Int Immunol.* (1997) 9:1837–47. doi: 10.1093/intimm/9.12.1837
65. Williams PA, Braine CE, Foxworth NE, Cochran KE, John SWM. GlyCAM1 negatively regulates monocyte entry into the optic nerve head and contributes to rediation-based protection in glaucoma. *J Neuroinflammation* (2017) 14:93. doi: 10.1186/s12974-017-0868-8
66. Hirano Y, Kobayashi K, Tomiki H, Inaba Y, Ichikawa M, Kim BS, et al. The role of α4 integrin in Theiler's murine encephalomyelitis virus (TMEV)-induced demyelinating disease: an infectious animal model for multiple sclerosis (MS). *Int Immunol.* (2016) 28:575–84. doi: 10.1093/intimm/dxw045
67. Ohtsuki S, Yamaguchi H, Katsukura Y, Asashima T, Terasaki T. mRNA expression levels of tight junction protein genes in mouse brain capillary endothelial cells highly purified by magnetic cell sorting. *J Neurochem.* (2008) 104:147–54. doi: 10.1111/j.1471-4159.2007.05008.x
68. Bleau C, Filliol A, Samson M, Lamontagne L. Brain invasion by mouse hepatitis virus depends on impairment of tight junctions and beta interferon production in brain microvascular endothelial cells. *J Virol.* (2015) 89:9896–908. doi: 10.1128/JVI.01501-15
69. Tsunoda I. Lymphatic system and gut microbiota affect immunopathology of neuroinflammatory diseases, including multiple sclerosis, neuromyelitis optica and Alzheimer's disease. *Clin Exp Neuroimmunol.* (2017) 8:177–9. doi: 10.1111/cen3.12405

Conflict of Interest Statement: The authors declare that the research was conducted in the absence of any commercial or financial relationships that could be construed as a potential conflict of interest.

frontiers in Immunology

REVIEW
published: 04 December 2018
doi: 10.3389/fimmu.2018.02862

Cytokine-Mediated Tissue Injury in Non-human Primate Models of Viral Infections

Cordelia Manickam[1], *Spandan V. Shah*[1], *Olivier Lucar*[1], *Daniel R. Ram*[1] and *R. Keith Reeves*[1,2]*

[1] Center for Virology and Vaccine Research, Beth Israel Deaconess Medical Center, Harvard Medical School, Boston, MA, United States, [2] Ragon Institute of Massachusetts General Hospital, MIT and Harvard, Cambridge, MA, United States

Viral infections trigger robust secretion of interferons and other antiviral cytokines by infected and bystander cells, which in turn can tune the immune response and may lead to viral clearance or immune suppression. However, aberrant or unrestricted cytokine responses can damage host tissues, leading to organ dysfunction, and even death. To understand the cytokine milieu and immune responses in infected host tissues, non-human primate (NHP) models have emerged as important tools. NHP have been used for decades to study human infections and have played significant roles in the development of vaccines, drug therapies and other immune treatment modalities, aided by an ability to control disease parameters, and unrestricted tissue access. In addition to the genetic and physiological similarities with humans, NHP have conserved immunologic properties with over 90% amino acid similarity for most cytokines. For example, human-like symptomology and acute respiratory syndrome is found in cynomolgus macaques infected with highly pathogenic avian influenza virus, antibody enhanced dengue disease is common in neotropical primates, and in NHP models of viral hepatitis cytokine-induced inflammation induces severe liver damage, fibrosis, and hepatocellular carcinoma recapitulates human disease. To regulate inflammation, anti-cytokine therapy studies in NHP are underway and will provide important insights for future human interventions. This review will provide a comprehensive outline of the cytokine-mediated exacerbation of disease and tissue damage in NHP models of viral infections and therapeutic strategies that can aid in prevention/treatment of the disease syndromes.

Keywords: viral infections, cytokines, animal model, tissue damage, non-human primates

OPEN ACCESS

Edited by:
Juliet Spencer,
Texas Woman's University,
United States

Reviewed by:
Vijayakumar Velu,
Emory University, United States
Cristian Apetrei,
University of Pittsburgh, United States

***Correspondence:**
R. Keith Reeves
rreeves@bidmc.harvard.edu

Specialty section:
This article was submitted to Viral Immunology, a section of the journal Frontiers in Immunology

Received: *22 September 2018*
Accepted: *20 November 2018*
Published: *04 December 2018*

Citation:
Manickam C, Shah SV, Lucar O, Ram DR and Reeves RK (2018) Cytokine-Mediated Tissue Injury in Non-human Primate Models of Viral Infections. Front. Immunol. 9:2862. doi: 10.3389/fimmu.2018.02862

INTRODUCTION

Microbial pathogens are constantly evolving to evade the host's immune system, and even with several decades of research and modern therapeutics, chronic diseases such as those caused by human immunodeficiency virus (HIV-1) and hepatitis C virus (HCV) are still globally prevalent. Viruses use multiple evasive strategies such as avoiding detection by pattern recognition receptors, T cell receptors and antibodies, mimicking or blocking cytokines, chemokines and other host proteins, and/or directly depleting immune cell subsets [reviewed in (1)]. Disruption of the cytokine milieu is also an important and commonly used strategy by viruses (2–4), since cytokines play important roles in shaping both innate and adaptive immunity. Cytokines are soluble proteins

secreted by cells during inflammation that act as key mediators of immune cell recruitment and modulators of the immune response via a complex network of cellular interactions and signaling pathways. So far, more than 300 cytokines including chemokines, interferons (IFN), and lymphokines have been described (5). While cytokines can be broadly classified based on the nature of the immune response as pro-inflammatory cytokines such as interleukin (IL)-1, IL-6, type 1 IFN, tumor necrosis factor (TNF)-α, and anti-inflammatory cytokines such as IL-4, IL-10, and transforming growth factor (TGF)-β, they have pleiotropic functions whereby individual cytokines can have either pro- or anti-inflammatory properties according to the cell system involved.

In viral infections, cytokines play central roles in the development of protective anti-viral responses, but also potential immunopathology associated with chronic viral diseases. Viral interactions with host cellular receptors triggers pro-inflammatory cytokine secretion which are essential for viral clearance. However, dysregulations in the cytokine type and quantitative levels can lead to overactivation of immune cells, which in turn cause tissue damage leading to fatal complications. For instance, extensive characterization of IFN-α and its direct antiviral activity since its discovery in 1957 (6), has led to successful treatment of "non-A, non-B (NANB) hepatitis" even before the actual identification of HCV as the causative agent (7). Combination therapy of pegylated IFN-α with ribavirin was the standard therapeutic regime for chronic HCV-infected patients until the recent introduction of directly acting antivirals. However, IFN-α therapy can induce side effects such as fever and headache to severe life threatening conditions including thyroid, visual, auditory, renal and cardiac impairments, and pulmonary interstitial fibrosis (8). The therapeutic use of cytokines for infectious diseases, autoimmune diseases and malignancies, may also come at a steep price, since prolonged use of cytokines present severe side-effects due to the pleiotropic nature of these molecules (9–14). While, it is necessary to understand cytokine dysregulations in viral diseases to anticipate potential tissue injury and deterioration, their pleotropic, rapid, and in some cases local and long term tissue effects make the study of cytokines in humans challenging with potential development of fatal complications. These challenges can be met by the use of animal models. Animal models have been used since more than 2400 years and currently are employed in all areas of biomedical research including basic biology, infections, immunology, cancer, metabolic diseases, and behavioral studies (15). This review is primarily focused on the virus mediated cytokine dysfunctions in animal models specifically non-human primates (NHP), which are already fundamental in the validation of human data.

NEED FOR ANIMAL MODELS IN STUDIES OF VIRAL IMMUNITY

Much of what is known regarding antiviral immunity and tissue inflammation comes from studies conducted in animal models of human diseases. Animal models act as preclinical and translational gatekeepers since they allow the study of cellular interactions *in vivo* and elucidation of disease pathogenesis in tissues that may be difficult to access in humans. While mouse models have provided tremendous benefits to immunologists in understanding immune responses in humans, 65 million years of divergent evolution has contributed to significant differences in cytokines and cytokine receptors for the two species. Studies have shown poor correlation in genomic responses to acute inflammatory stress between humans and mice (16), and engagement of different chemokine/cytokine pathways in response to oxygen and glucose deprivation by human neurons compared to murine neurons (17). IL-13 seems to induce B cell class switching for IgE production specifically in humans whereas mice require IL-4 (18, 19). Similarly, IL-7 receptor deficiency inhibits development of all T and B lymphocytes in mice (20), but only T cells in humans (21). Furthermore, a number of pathogens like influenza, HIV, or dengue are highly tropic to their respective hosts and do not mimic human pathologies in mice, potentially restricting the use of mice as models for some infectious diseases [reviewed in (22)].

NHP are perhaps the most commonly utilized models to study and understand immune responses against human infectious agents and for preclinical evaluation of therapeutics and vaccines (**Figure 1**). NHP have proven essential for research breakthroughs in maladies such as cancer, Parkinson's disease, heart diseases, and various infectious diseases such as HIV, Zika, Ebola, influenza, and others (23, 24). Even though NHP research accounts for <1% of the all the biomedical laboratories working in animal models (24), the advantages offered by NHP due to the genetic and physiological homology to humans are manifold. Indeed, human and NHP cytokines are relatively conserved with 95% amino acid identity of most cytokines such as IL-2 and IFN-γ for Old World NHP and up to 90% amino acid identity for New World NHP (25). In addition, many cross reactive reagents and monoclonal antibodies for the detection of cytokines have been evaluated and validated for NHP species (NIH Non-human Primate Reagents Resource; http://www.nhpreagents.org) (25–28), making NHP attractive animal models to study viral pathogenesis and disease progression.

NHP MODELS COMMONLY USED FOR VIRAL DISEASES

Great Apes

The great apes used previously as animal models include chimpanzees (*Pan troglodytes*), and to a lesser extent orangutans (*Pongo pygmaeus*) and gorillas (*Gorilla beringei*) (29). Chimpanzees share >98% DNA sequence homology to humans; and yet surprisingly, have immune systems that respond much more robustly to infections like HIV and hepatitis B virus (HBV). HBV and HCV can only pathogenically infect humans and chimpanzees, thus making chimpanzees, at one time, the primary animal model for therapeutics and vaccine research (30–32). However, the use of great apes in biomedical research has become increasingly restricted for ethical and cost reasons and therefore other NHP models are being increasingly utilized.

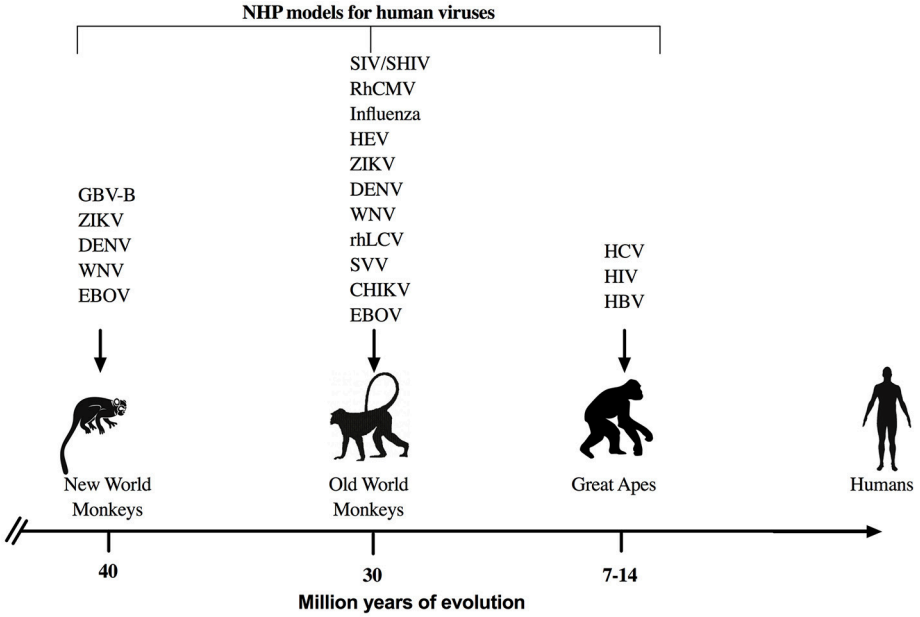

FIGURE 1 | NHP models for viral infections. Representation of NHP models that are used commonly to study human viral infections with respect to the evolutionary divergence from humans. GBV-B, GB virus-B; ZIKV, Zika virus; DENV, Dengue virus; WNV, West Nile virus; EBOV, Ebola virus; SIV, Simian Immunodeficiency virus; SHIV, Simian/Human Immunodeficiency virus; RhCMV, rhesus cytomegalovirus; HEV, Hepatitis E virus; rhLCV, rhesus lymphocryptovirus; SVV, simian varicella virus; CHIK, chikungunya virus, HIV, Human Imunodeficiency virus; HCV, Hepatitis C virus; and HBV, Hepatitis B virus are some of the most common examples for viral studies in NHP.

Old World Monkeys

The Old World monkeys are primarily found in the continents of Africa, Asia, and Europe with rhesus macaques *(Macaca mulatta)*, cynomolgus macaques *(Macaca fascicularis)*, sooty mangabeys (*Cercocebus atys)*, African green monkeys *(Chlorocebus aethiops),* and baboons *(Papio* spp.*)* being the predominant species used in biomedical research. Rhesus/cynomolgus macaques are perhaps the most widely utilized NHP animal models to study human infectious diseases. Besides HIV (33), macaque models have been used for infectious diseases such as influenza (34, 35), HBV (36, 37), HCV (38–40), measles (*Morbillivirus*) (41–43), cytomegalovirus (CMV) (44–46), among many others (47). Sooty mangabeys and African green monkeys are also used to study HIV and African green monkeys are used as a model for influenza (48). Less commonly used tree shrews *(Tupaia belangeri)* have also been explored as a model for HCV infection (49, 50).

New World Monkeys

New World monkeys or neotropical primates include cotton-top tamarins *(Saguinus Oedipus)*, common marmosets *(Callithrix jacchus)*, owl monkeys *(Aotus lemurimus)*, and squirrel monkeys (*Saimiri boliviensis)*, which are commonly located in Central and South America. Although, the New World monkeys are more divergent than Old World NHP from humans, they provide a distinct advantage in biomedical research due to their relatively smaller size and lower cost compared to other NHP. Marmosets and tamarins have been used to study many flaviviruses such as HCV, Dengue, and Zika (51–56). Owl monkeys can be infected with Hepatitis E Virus (57) and at least some individual animals might have HIV-1 compatible CD4 alleles (58) making them potentially useful for HIV research. Squirrel monkeys have been utilized as animal models for HTLV-1 pathogenesis and vaccine development (59, 60) and as an experimental model for Nipah Virus (61).

CYTOKINE DYSREGULATION IN VIRAL INFECTION MODELS

HIV/Acquired Immunodeficiency Syndrome (AIDS)

The emergence of HIV (Genus: Lentivirus, Family: Retroviridae) is the result of the combination of at least four simian immunodeficiency virus (SIV) transmission events from chimpanzees or gorillas to humans (62, 63). Therefore, SIV and simian/human immunodeficiency virus (SHIV) infections in NHP are commonly used to model HIV pathogenesis and development of vaccines and therapeutics. Specifically, rhesus macaques and sooty mangabeys have been critical in understanding the early phase of the infection (33, 64). Several studies (discussed below) have shown the principal involvement of an unusually vigorous immune activation leading to the progression and establishment of AIDS.

Based on plasma parameters from HIV-infected patients, the virus-mediated cytokine storm starts early in infection even before peak viremia is reached (65, 66). It rapidly initiates a

cascade of events characterized by the production of the early pro-inflammatory cytokines, IL-15, and IFN-α, quickly followed by the more sustained TNF-α and monocyte chemoattractant protein (MCP)-1 during infection. Other pro-inflammatory cytokines like IL-6, IL-8, IL-18, and IFN-γ are elevated 2 days post the first wave of proinflammatory cytokines. At the same time, the secretion of IL-10, an immunoregulatory cytokine exponentially increases until it peaks at 5 days of infection (65). While, the IL-10/IL10-R pathway has a major role in preventing tissue damage observed during HIV infection by inhibiting Th1 responses and the production of anti-viral cytokines (IFN-α, IFN-γ, IL-2), it also contributes to viral persistence. Furthermore, the expression of the PD-1/PDL-1 pathway drives the inhibition of T cell function (67) and indirectly up-regulates expression of IL-10 (68). Indeed, blockade of PD-1 by anti-PD-1 antibody in infected rhesus macaques augmented SIV specific IFN-γ responses in CD8+ T cells in the blood, and could be synergized with vaccination and anti-retroviral therapies (69, 70). However, more NHP studies are necessary to establish the importance of PD-1 blockade particularly in mucosal tissues.

The magnitude of the cytokine storm is broadly associated with the clinical outcome in infected rhesus macaques and sooty mangabeys (66, 71). Indeed, the progressive infection in rhesus macaques is associated with production of IL-15, IL-18, IFN-γ, granulocyte-colony stimulating factor (G-CSF), MCP-1 and macrophage inflammatory protein (MIP)-1β but not in non-progressive sooty mangabeys (66). Similar cytokine dysregulation evidenced as elevated IL-12 has also been reported in HIV seroconverts (72) and South African women who are high risk population for acquisition of HIV infection (73). Furthermore, the cytokine storm leads to immune activation with global damage in mucosal tissues, specifically the gut and gut-associated lymphoid tissue (GALT) which are the early and major sites of virus replication (74). Specifically, the virus targets the IL-17/Th-17 pathway that is essential for preservation of the gut barrier, maintenance of the gut microbial environment, and prevention of translocation of microbial products into the circulation that could otherwise cause immune activation (75, 76). However, it is shown that cART can partially restore effective CD4+ T cells (more than 50% compared to non-treated) in the gut and enhance the Th17 subset which is associated with a better clinical outcome (77). This further illustrates the importance of NHP to study gut immunity in HIV infection and evaluate therapeutic modalities at mucosal tissues (78).

SIV infection in sooty mangabeys leads to a long non-progressive infection as observed in some HIV-infected individuals (79). Sooty mangabeys do not develop disease symptoms due to a low level of immune activation despite high level of viral replication (80). Instead of an inflammatory immune response, elevated regulatory T cells (Treg) and associated cytokines, TGF-β and IL-10 limit the level of immune activation (80). Similarly in infected African green monkeys, an anti-inflammatory environment is rapidly established due to increases in Treg frequency, TGF-β, and IL-10 levels in the plasma (81). Interestingly, a comparison of acute infection in African green monkeys and rhesus macaques revealed that a rapid and elevated IFN-α is triggered in both models but return to baseline levels after 28 days of infection was observed only in African green monkeys (82). Further, no changes in the levels of pro-inflammatory cytokines such as IL-6, IL-18, and TNF-α were reported in infected African green monkeys compared to uninfected controls (83). It was also shown that sooty mangabeys have a unique genome that protects them from developing AIDS (84). Of importance, these animals possess a different TLR-4 gene compared to NHP that develop AIDS. TLR-4 is a pattern recognition receptor that senses lipopolysaccharides on bacteria and initiates pro-inflammatory cytokine induction. HIV can induce microbial translocation that elicited exacerbated TLR-4 stimulation and lead to chronic immune activation (85, 86). Therefore the differential cytokine response and an overall lower immune activation, in part confers immune protection, less tissue damage and maintenance of gut barrier in non-pathogenic SIV infection of sooty mangabeys as well as African green monkeys (87, 88).

Rhesus macaques are not natural hosts of SIV infection and therefore, some SIV strains can induce strong viral load and the development of AIDS similar to HIV-infected individual (89). In a rhesus macaque cohort infected with pathogenic or non-pathogenic strains of SIV/SHIV, the progressor cohort exhibited low IFN-γ induced by CD4+ T cells compared to CD8+ T cells whereas, the non-progressor monkeys did not develop a similar immunomodulation (90). Furthermore, infection with virulent SIVmac251 strain directly upregulated the cytokine production (IFN-α/β, IL-12, IL-18) and led to the activation of natural killer (NK) cells which are one of the major antiviral innate immune cells and also act as a bridge to the adaptive system. Interestingly, the production of antiviral cytokines (IFN-α, IFN-γ, IL-2) was also associated with viral establishment (91). An over production of IL-7 in the gut during the early days of acute SIV infection in rhesus macaques could contribute to the cytokine storm by inducing elevated chemokine expression triggering immune cell recruitment (92). Overall, the cytokine storm induces a vicious cycle by spreading the infection and causing tissue damage due to an extensive inflammation in SIV progressive NHP models. To overcome this cytokine mediated disease exacerbation, several therapeutic formulations that use cytokines including IL-12, IL-15, and IL-2 or block cytokine receptors are increasingly being tested in SIV infection models (discussed in later section).

Hepatitis B and C

Hepatitis B and C infections together are the leading causes of chronic liver disease worldwide (93). HBV (Genus: Orthohepadnavirus; Family: Hepadnaviridae) and HCV (Genus: Hepacivirus; Family: Flaviviridae) are hepatotropic viruses and cause both acute and chronic liver infections, which can progress to fibrosis and hepatocellular carcinoma. Interestingly, both viruses have a narrow host range (humans and chimpanzees) and have similar pathogenesis for progressive liver damage and persistence of infection. Studies in chimpanzees showed that HBV and HCV are not directly cytopathic (94–97) but instead cause liver injury due to chronic immune activation. Adaptive T cell and NK cell immunity are important in the control of viral hepatitis, but they can also prove detrimental in persistent infection. In cases of uncontrolled replication, infected

hepatocytes secrete cytokines IL-8, CXCL-9, and CXCL-10, which recruit T cells to the infected liver, all correlating with histological damage (98–100). Further, innate immune NK cells are activated and recruited by high levels of IFN-α and IL-8 in the liver and induction of cytotoxic TRAIL pathway leads to killing of hepatocytes and liver injury (101). HCV-mediated liver inflammation is promoted by IL-1β and the TNF superfamily cytokines such as TNF-α, TNF-β, TWEAK, and LIGHT through the activation of NF-kB and MLCK-signaling pathways to reduce hepatocellular tight junction integrity (102, 103). In HBV infection, TNF-α secretion was associated with significant fibrosis, and IL-10 and IFN-γ were associated with necroinflammation (104). Additionally, as a result of viral overload, induction of interferon stimulated genes and elevated IL-8 and chemokines such as CCL2, CXCL1, and CXCL5 results in cholestatic HCV, which is associated with metabolic dysregulation (105, 106).

Due to the narrow host range, chimpanzees were critical for initially understanding the natural history and pathogenesis of HCV and HBV (32, 107). However, because of the limited use of chimpanzees currently, other surrogate animal models are being employed. To model HBV, cynomolgus macaques have been used but with an indirect infection approach: *ex-vivo* baculovirus-mediated HBV genome transfer in hepatocytes to cross the species barrier (108). Recently, a new virus called the capuchin monkey hepatitis B virus (CMHBV) has been discovered in Brazilian capuchin monkeys, a neotropical primate and has potential implications in the development of the much needed animals model for hepatitis B (109). The more commonly used NHP models for HCV are infections of neotropical primates, marmosets and tamarins, with the surrogate hepacivirus GBV-B of the same family Flaviviridae (51, 110, 111). Several studies showed that activated T cell immune responses and IFN-γ secretion are important for clearance of GBV-B (112, 113). However, similar to HCV-infected liver, immune activation correlated with liver damage in primary infections and re-infections in marmosets (114, 115). Activated NK cells expressing IFN-γ and perforin were accumulated in the liver and in addition elevated plasma IFN-γ and RANTES were associated with acute hepatitis in infected animals (114). Further, infected marmosets developed metabolic dysfunctions associated with GBV-B infection even after clearance of viremia indicating that viral hepatitis induces a cascade of events toward hepatic and systemic inflammation. Particularly, imbalance in levels of pro-inflammatory adipocytokines such as resistin and plasminogen activator inhibitor-1 secreted by dysfunctional adipose tissues contribute to local, systemic, and metabolic malfunctions (116). Given the importance of liver immune responses in progression of viral hepatitis, limited access to liver tissues has severely impeded development of HCV vaccine and HBV therapeutics.

Zika

Infections with Zika virus (ZIKV; Genus: Flavivirus; Family: Flaviviridae) have recently caused a pandemic due to abortions, stillbirths, congenital birth defects, and neonate deaths called the congenital Zika syndrome (CZS) (117). ZIKV induced neuronal necrosis in the cortical layer of the brain is mediated by a complex array of cytokines and immune factors (118–120). While studies in brain tissue are limited, *in-situ* immunostaining of infected fetal brain samples showed that the predominant immune response was characterized by IL-4, IL-10, IL-33, iNOS, and arginase and therefore was generally skewed toward a Th2 response (118). IL-33, in particular is directly involved in pyroptosis, activation of inflammasomes, endoplasmic reticulum stress potentially leading to cellular damage (119). However, other cytokine responses indicative of Th1, Th17, Treg, Th9, and Th22 response were also involved to a lesser extent. Immune cells including microglia, CD4+ and CD8+ T cells, Treg, NK cells, M1/ M2 macrophages, and antigen-presenting cells contribute to the pathogenesis of the ZIKV induced inflammation (118). Thus, a complex relationship between different immune factors, cell damage, and direct viral action leads to ZIKV meningitis and encephalitis.

While ZIKV induced pathology and pathogenesis studies in humans are limited to samples obtained from autopsy of severe fatal cases, NHP have been tremendously helpful in elucidating pathogenesis and fast tracked development of several vaccine candidates (121–123). Indeed, fetal neuropathology, microcephaly, and other CZS symptoms were evidenced in several NHP models including rhesus, pigtail, and cynomolgus macaques, common marmosets, and squirrel monkeys infected during early pregnancy (55, 56, 124–128). Infection studies in common marmoset dams identified immune pathways in maternal viral responses. Interestingly, an increase in IFN-γ and pro-inflammatory cytokines as early as day 2 post-infection was reported. The pro-inflammatory response was maintained as elevated induction of type I/II IFN associated genes and pro-inflammatory cytokines even at day 7 post-infection and spontaneous abortion after 16–18 days of infection was reported with extensive viral infection in placenta and fetal tissues (56, 125). In infected rhesus macaques, viral persistence in the central nervous system and lymph nodes correlated with robust and early induction of pro-inflammatory responses and mTOR signaling pathways as evidenced by IFN-α induction at day 2, 4, and 6 post-infection and upregulation of transcript components of IFN-α and IFN-stimulated genes (ISGs) (OAS2, IFT1/2/3, ISG15, IRF7, IFI44, MX1, and MX2), pro-inflammatory cytokines and chemokines (TNF- α, IL-1, IL18, CCR7, CCL2, and CCL20), immunomodulatory pathways (IL-10, TGF-β, and T regulatory cells), and inflammasome pathways (NOD2, NLRP3, CXCL10, BTG2, BST2, OSM) at day 6 post-infection (129). As a result of these activated pathways, ZIKV persistence could contribute to the characteristic neuropathology associated with ZIKV. Further several experiments in NHP are currently underway for preclinical testing of vaccine candidates and Zika is an excellent example to illustrate the importance of NHP in developing vaccines within a short span of time.

Dengue

Dengue virus (DENV; Genus: Flavivirus; Family: Flavivirdae), is a major vector borne disease in tropical and subtropical countries affecting approximately 100 million people worldwide, which can progress from the typical Dengue fever to fatal conditions such as

Dengue hemorrhagic fever (DHF) and Dengue shock syndrome (DSS). Damage to vascular endothelium and uncontrolled activation of blood coagulation pathways in DHF can result in critical hypovolemic shock in DSS. Increased levels of cytokines, such as IFNs, IL-2, IL-8, TNF-α, and vascular endothelial growth factor A (VEGF-A) have all been reported to be associated with vascular leakage (130). Increased T cell activation and cytokine production in patients during both primary and secondary Dengue virus infections showed greater clinical severity of illness associated with cytokine storm characterized by elevated plasma pro-inflammatory cytokines such as IFN-γ, IL-6, IL-8, IL-10, CXCL9, CXCL10, CXCL11, MIF, TNF-α, and VEGF (130, 131).

Several NHP species are permissive to Dengue infection including chimpanzees, rhesus and cynomolgus macaques, sooty mangabeys, common marmosets, and owl monkeys, however the DENV induced hemorrhagic disease pattern is less common in NHP [reviewed in (132)]. In addition to elevated TGF-α and IFN-γ, increases in MCP-1, which drives immune cell recruitment, and potential cause of vascular damage was found elevated in rhesus macaques infected with DENV (133). A high dose intravenous inoculation of DENV induced classic dengue hemorrhage in infected rhesus macaques 3–5 days post-infection, with altered serum biochemical parameters indicative of coagulopathy (134). Similarly cytokine storm associated with enhanced dengue disease was detected in DENV infected marmosets, which showed a significant increase in plasma TNF-α as early as 3 days post-infection and significantly increased IFN-γ at 3, 6, and 20 days post-infection (52, 135). Indeed, antibody enhanced dengue disease in marmosets lead to CNS injury and was associated with intense TNF-α immunostaining in brain samples (135). Further, based on biomarker network analysis, two relevant strong axes during early stages of dengue fever were identified—a protective axis composed of TNF-α/lymphocytes/platelets, and a pathological axis IL-2/IL-6/monocyte/prothrombin time/viremia. Later time points post-infection showed the interaction of IFN-γ/platelets/DENV-3/prothrombin time, and the involvement of type-2 cytokines (IL-4, IL-5) (136). Overall, these studies indicate that elevated proinflammatory cytokines in dengue-infected NHP have a pathogenic role associated with disease severity.

Influenza

Influenza A virus (Genus: Influenzavirus A; Family: Orthomyxoviridae) causes acute and severe respiratory illness in more than 1 billion people worldwide. The severity of influenza infection derives from the interplay between the virus and the host's ability to control viral infection and spread. In severe cases the host's response is hyperactivated and the resulting inflammatory response produces a cytokine storm (137–139) that is responsible for tissue injury and potentially death. This was seen during the 1918 H1N1 pandemic and more recently via the spread of H5N1. Endothelial cells from the lung have been implicated as key players in propagating the cytokine storm, in part from having elevated levels of CCL2, CCL5, and CXCL10 (140). Further inhibiting S1P1 receptor signaling on pulmonary endothelial cells, which leads to downregulation of cytokine/chemokine signaling, has been shown to decrease the development of cytokine storm following infection with influenza (140, 141).

One of the major issues in NHP modeling of influenza is the result of low animal mortality as compared to what happens in humans. While NHP can be infected with seasonal influenza strains they do not always display symptoms akin to those seen in humans (142). Influenza infection in NHP may lead to a biphasic subclinical fever early during the infection (143, 144), but this seems to be dependent on the mode of infection and dosage utilized (145, 146). Aerosol delivery using the full head chamber (145) results in a more lethal outcome, whereas the facemask leads to less severe symptoms. Infection with highly pathogenic influenza strains can induce clinical symptoms such as fever, cough and lethargy, and even showing signs of acute respiratory distress syndrome (124), bronchointerstitial pneumonia, peribronchiolar alveolitis, edema, and hemorrhaging (147–150). Further, in this model and others, increased levels of IP-10 (CXCL10), MCP-1 (CCL2), and IL-6 have been observed, which have been characterized as hallmarks of H5N1 human infection (138, 139, 151–153). Gene expression analyses have also shown that CXCL10 and CXCL11 are highly upregulated early during infection with highly pathogenic H1N1 and H5N1 and associated with elevated tissue damage (151, 152, 154). Using the full head chamber allows for the macaques to develop fulminant pneumonia that rapidly progressed to acute respiratory distress syndrome, which is the result of widespread alveolar epithelial cell death as well as depletion of alveolar macrophages.

CMV

CMV (Genus: Cytomegalovirus; Family: Herpesviridae) can infect and persist lifelong in multiple cell types such as macrophages, neutrophils, fibroblasts, neuronal cells, hepatocytes and others (155–159). Human CMV (HCMV) infections are often reported in patients with suppressed immune system, including the elderly, AIDS patients, cancer patients, and transplant recipients. After infection, CMV hijacks cellular machinery, induces significant alterations in gene expression including IFN signaling genes, followed by a complex cascade of signaling events (160, 161) leading to upregulation of transcription factors like NF-κB and altered cytokine production, and thus successfully evades the host immune surveillance and disseminates to all organs (162–167). While the pathogenesis is not completely clear, elevated levels of MCP-1 and MIP-1α recruiting monocyte and macrophages to the site of infection could mediate tissue damage with uncontrolled viral replication in immunocompetent patients (168, 169). In congenital CMV infections, which cause severe birth defects in newborn babies, elevated MCP-1 and TNF-α in placenta could lead to adverse pregnancy outcomes or even death in utero (170, 171). Another group reported severe CNS abnormalities and brain vasculature damage in newborn babies due to proinflammatory cytokines IL-8, IL-6, TNF-α, and IL-1β upregulated by CMV infection of pericytes (172).

HCMV does not infect animals due to the species specificity of beta herpesviruses and interestingly the virus has co-evolved with its host species (173). Therefore, the study of specific CMV in their respective species of animal models has been

helpful in elucidating CMV specific immunity. Indeed, simian CMV seroprevalence was reported in baboons, African green monkeys, and rhesus macaques as early as 1971 (174) and currently, rhesus CMV (RhCMV) infections in rhesus macaques is more commonly used as a NHP model (175). Since the global prevalence of HCMV ranges from 60 to 100%, animal models offer a unique advantage of being specific pathogen free, in this case CMV-free, in order to understand CMV immunity in comparison to uninfected population. RhCMV is particularly useful to model congenital infections (176) and co-infections such as CMV and HIV infections in the same host (177). Intrauterine inoculation of pregnant dams and intraamniotic/intracranial inoculations of the fetuses with RhCMV led to severe neurological defects and CNS lesion similar to HCMV (45, 176, 178). Further, RhCMV studies helped identify that the primate CMV encodes and expresses IL-10 homolog genes *in vivo* (179). Interestingly, the viral homolog had evolved functions that are beneficial to viral replication, primarily through immunosuppressive and anti-proliferative effects on host immune cells (179). The CMV IL-10 could also play a role in CMV's ability to subvert NK cell reactivity, thus avoiding NK cell lysis (179). Further, exploration of RhCMV infections in CMV free animals can identify immunopathogenesis pathways and therapeutic targets.

IMMUNOTHERAPEUTIC APPROACHES

Recombinant cytokines and anti-cytokine antibodies have recently gained traction in the pharmaceutical arena as a novel class of drugs for therapeutic purposes especially in autoimmune disorders and cancer (180, 181). There are few cytokine therapies that are already in use for therapy against viral infections such as IFN-α for HBV and HCV therapy. To overcome the severe side effects of IFN-α therapy, recently type III IFNs namely IFN-λ which have similar biological functions as IFN-α, have been tested preclinically in rhesus macaques (182). IFN-λ demonstrated antiviral effects similar to IFN-α without hematologic toxicity and thus could be used as an alternative therapy in chronic hepatitis patients. IL-12 administration has been previously studied in chimpanzees and rhesus macaques for understanding IL-12 mediated pathways and antiviral protection in SIV infections respectively (183, 184). IL-15 agonist, which has immunomodulatory functions, activates innate and adaptive immunity, and has been well characterized in NHP (185–188). Recently, a novel IL-15 superagonist ALT 803 potentiated T cell and NK cell responses leading to transient viral suppression in ART naïve SIV infected rhesus macaques (189). While the viral suppression was transient, this study illustrates IL-15 as a potential therapeutic agent particularly in combination therapy and ALT 803 is already in clinical trials for cancer therapy (190, 191). Even in DNA vaccine studies, IL-2 administration augmented vaccine elicited HIV-1, and SIV-1 specific immune responses in SHIV challenged rhesus macaques (192) thus showing that cytokine co-administrations can potentiate both vaccines and therapeutics.

Blocking of cytokine receptors or administration of cytokine antagonists can also be helpful in control of viral replication. Antagonists of CCR5 (maraviroc and vicriviroc) and CXCR4 inhibitor (Plerixafor) are relevant as they block HIV entry in cells and therefore can be used for HIV treatment (193). In addition to these small molecule CCR5 inhibitors, CCR5 blocking antibodies have also been characterized in preclinical rhesus macaques model of SIV infection (194–196). Further, maraviroc prevented cardiac dysfunction and cardiomyopathy associated with AIDS by blocking CCL5 and its recruitment of inflammatory macrophages in the heart tissue of SIV infected rhesus macaques (197).

Cytokine-based therapeutics are increasingly tested for other non-viral disease models of NHP. IL-13 neutralization for prevention of IgE mediated allergic responses in airway inflammation model of cynomolgus macaques (198), IL-6 receptor blocking and anti-TNF agent, infliximab for treatment of rheumatoid arthritis in cynomolgus macaques and rhesus macaques, IFN-α treatment effects in rhesus macaques model of cytokine induced depression (199, 200) are some of the few examples and could have potential applications in viral immunity and therapy. While cytokine therapy is advantageous in controlling viral replication or preventing tissue damage, systemic administration of cytokine, or cytokine blocking can result in altered hematopoiesis and immune activation, and

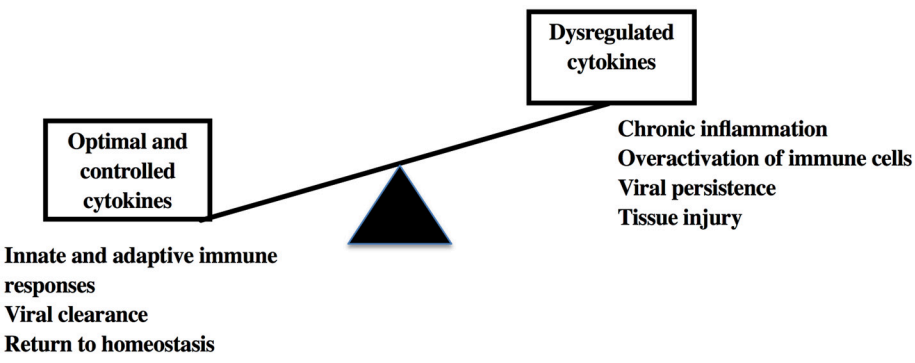

FIGURE 2 | Cytokine responses and sequelae in viral infections.

severe complications due to the pleiotropic nature of cytokines in long-term therapy. Even in co-inhibitor receptors/checkpoint blockade therapy such as anti-PD-1 or CTLA-4 therapy commonly used for reversion of exhausted T cells in cancer and chronic diseases, undue immune activation or autoimmune responses is a primary risk leading to systemic or organ toxicities associated with uncontrolled inflammatory cytokine secretion and cytotoxicity by activated immune cells, which in turn require additional or follow-up immunosuppressive treatment [reviewed in (201, 202)]. Therefore, development of site directed biologics or cytokine therapy targeting viral infected tissues would be more beneficial than systemic administration.

CONCLUSION

Within the last few years, cytokines have been identified as key diagnostic, prognostic, and therapeutic agents in human diseases. Their multifaceted roles in immunity, tissue protection, and remodeling, maintenance of systemic and metabolic homeostasis make them important biomarkers for understanding and treating infectious diseases, cancer, auto-immune diseases, metabolic dysfunctions and other inflammatory processes. However, it is very important that their use in conjunction with other therapeutic and preventative strategies needs to be tested in pre-clinical models due to their propensity to cause immunopathology and tissue injury leading to serious complications in certain conditions (**Figure 2**). The usage of NHP models will be helpful for early prevention of tissue injury and associated autoimmune and metabolic syndromes that arise in diseases caused by viral and non-viral causes.

AUTHOR CONTRIBUTIONS

CM and SVS performed most of the writing. OL and DRR contributed to writing of specific sections. RKR oversaw overall preparation of the manuscript, contributed to writing, and edited the final version of the manuscript.

FUNDING

This work was supported by National Institutes of Health (NIH) grants R01 DE026327, R01 DE026014, and R01 AI120828 to RKR. DRR was supported, in part, by T32 AI007387. The funders had no role in study design, data collection and analysis, decision to publish, or preparation of the manuscript.

REFERENCES

1. Vossen MT, Westerhout EM, Soderberg-Naucler C, Wiertz EJ. Viral immune evasion: a masterpiece of evolution. *Immunogenetics* (2002) 54:527–42. doi: 10.1007/s00251-002-0493-1
2. Sirskyj D, Theze J, Kumar A, Kryworuchko M. Disruption of the gamma c cytokine network in T cells during HIV infection. *Cytokine* (2008) 43:1–14. doi: 10.1016/j.cyto.2008.03.001
3. Bixler SL, Goff AJ. The role of cytokines and chemokines in filovirus infection. *Viruses* (2015) 7:5489–507. doi: 10.3390/v7102892
4. Beltra JC, Decaluwe H. *Cytokine*s and persistent viral infections. *Cytokine* (2016) 82:4–15. doi: 10.1016/j.cyto.2016.02.006
5. Becher B, Spath S, Goverman J. Cytokine networks in neuroinflammation. *Nat Rev Immunol.* (2017) 17:49–59. doi: 10.1038/nri.2016.123
6. Isaacs A, Lindenmann J. Virus interference. I The interferon. *Proc R Soc Lond B Biol Sci.* (1957) 147:258–67. doi: 10.1098/rspb.1957.0048
7. Hoofnagle JH, Mullen KD, Jones DB, Rustgi V, Di Bisceglie A, Peters M, et al. Treatment of chronic non-A,non-B hepatitis with recombinant human alpha interferon. *A preliminary report N Engl J Med.* (1986) 315:1575–8. doi: 10.1056/NEJM198612183152503
8. Dusheiko G. Side effects of alpha interferon in chronic hepatitis C. *Hepatology* (1997) 26:112S−121S. doi: 10.1002/hep.510260720
9. Bukowski, R. M., Olencki, T., Mclain, D., and Finke, J. H. (1994). Pleiotropic effects of cytokines: clinical and preclinical studies. *Stem Cells* 12(Suppl 1):129–40; discussion: 140–21.
10. Martin R. Interleukin 4 treatment of psoriasis: are pleiotropic cytokines suitable therapies for autoimmune diseases? *Trends Pharmacol Sci.* (2003) 24:613–6. doi: 10.1016/j.tips.2003.10.006
11. Liao W, Lin JX, Leonard WJ. IL-2 family cytokines: new insights into the complex roles of IL-2 as a broad regulator of T helper cell differentiation. *Curr Opin Immunol.* (2011) 23:598–604. doi: 10.1016/j.coi.2011.08.003
12. Xu L, Tian D, Zheng Y. Pleiotropic roles of TGFbeta/Smad signaling in the progression of chronic liver disease. *Crit Rev Eukaryot Gene Expr.* (2013) 23:237–55. doi: 10.1615/CritRevEukaryotGeneExpr.2013007490
13. Iwasaki Y, Fujio K, Okamura T, Yamamoto K. Interleukin-27 in T cell immunity. *Int J Mol Sci.* (2015) 16:2851–63. doi: 10.3390/ijms16022851
14. Yao X, Sun Y, Wang W, Sun Y. Interleukin (IL)-25: pleiotropic roles in asthma. *Respirology* (2016) 21:638–47. doi: 10.1111/resp.12707
15. Ericsson AC, Crim MJ, Franklin CL. A brief history of animal modeling. *Mo Med.* (2013) 110:201–5.
16. Seok J, Warren HS, Cuenca AG, Mindrinos MN, Baker HV, Xu W, et al. Genomic responses in mouse models poorly mimic human inflammatory diseases. *Proc Natl Acad Sci USA.* (2013) 110:3507–12. doi: 10.1073/pnas.1222878110
17. Du Y, Deng W, Wang Z, Ning M, Zhang W, Zhou Y, et al. Differential subnetwork of chemokines/cytokines in human, mouse, and rat brain cells after oxygen-glucose deprivation. *J Cereb Blood Flow Metab.* (2017) 37:1425–34. doi: 10.1177/0271678X16656199
18. Punnonen J, Aversa G, Cocks BG, Mckenzie AN, Menon S, Zurawski G, et al. Interleukin 13 induces interleukin 4-independent IgG4 and IgE synthesis and CD23 expression by human B cells. *Proc Natl Acad Sci USA.* (1993) 90:3730–4. doi: 10.1073/pnas.90.8.3730
19. Zurawski G, De Vries JE. Interleukin 13, an interleukin 4-like cytokine that acts on monocytes and B cells, but not on T cells. *Immunol Today* (1994) 15:19–26. doi: 10.1016/0167-5699(94)90021-3
20. Peschon JJ, Morrissey PJ, Grabstein KH, Ramsdell FJ, Maraskovsky E, Gliniak BC, et al. Early lymphocyte expansion is severely impaired in interleukin 7 receptor-deficient mice. *J Exp Med.* (1994) 180:1955–60. doi: 10.1084/jem.180.5.1955
21. Roifman CM, Zhang J, Chitayat D, Sharfe N. A partial deficiency of interleukin-7R alpha is sufficient to abrogate T-cell development and cause severe combined immunodeficiency. *Blood* (2000) 96:2803–7.
22. Coers J, Starnbach MN, Howard JC. Modeling infectious disease in mice: co-adaptation and the role of host-specific IFNgamma responses. *PLoS Pathog.* (2009) 5:e1000333. doi: 10.1371/journal.ppat.1000333
23. Carlsson HE, Schapiro SJ, Farah I, Hau J. Use of primates in research: a global overview. *Am J Primatol.* (2004) 63:225–37. doi: 10.1002/ajp.20054
24. Friedman H, Ator N, Haigwood N, Newsome W, Allan JS, Golos TG, et al. The critical role of nonhuman primates in medical research. *Pathog Immun.* (2017) 2:352–65. doi: 10.20411/pai.v2i3.186
25. Hoglind A, Arestrom I, Ehrnfelt C, Masjedi K, Zuber B, Giavedoni L, et al. Systematic evaluation of monoclonal antibodies and immunoassays

for the detection of Interferon-gamma and Interleukin-2 in old and new world non-human primates. *J Immunol. Methods* (2017) 441:39–48. doi: 10.1016/j.jim.2016.11.011
26. Makitalo B, Andersson M, Arestrom I, Karlen K, Villinger F, Ansari A, et al. ELISpot and ELISA analysis of spontaneous, mitogen-induced and antigen-specific cytokine production in cynomolgus and rhesus macaques. *J Immunol Methods* (2002) 270:85–97. doi: 10.1016/S0022-1759(02)00274-0
27. Giavedoni LD. Simultaneous detection of multiple cytokines and chemokines from nonhuman primates using luminex technology. *J Immunol Methods* (2005) 301:89–101. doi: 10.1016/j.jim.2005.03.015
28. Riccio EK, Pratt-Riccio LR, Bianco-Junior C, Sanchez V, Totino PR, Carvalho LJ, et al. Molecular and immunological tools for the evaluation of the cellular immune response in the neotropical monkey *Saimiri sciureus*, a non-human primate model for malaria research. *Malar J.* (2015) 14:166. doi: 10.1186/s12936-015-0688-1
29. Kalter SS. Nonhuman primates in viral research. *Ann N Y Acad Sci.* (1969) 162:499–528. doi: 10.1111/j.1749-6632.1969.tb56400.x
30. Abe K, Kurata T, Teramoto Y, Shiga J, Shikata T. Lack of susceptibility of various primates and woodchucks to hepatitis C virus. *J Med Primatol.* (1993) 22:433–4.
31. Eren R, Ilan E, Nussbaum O, Lubin I, Terkieltaub D, Arazi Y, et al. Preclinical evaluation of two human anti-hepatitis B virus (HBV) monoclonal antibodies in the HBV-trimera mouse model and in HBV chronic carrier chimpanzees. *Hepatology* (2000) 32:588–96. doi: 10.1053/jhep.2000.9632
32. Wieland SF. The chimpanzee model for hepatitis B virus infection. *Cold Spring Harb Perspect Med.* (2015) 5:a021469. doi: 10.1101/cshperspect.a021469
33. Letvin NL, Daniel MD, Sehgal PK, Desrosiers RC, Hunt RD, Waldron LM, et al. Induction of AIDS-like disease in macaque monkeys with T-cell tropic retrovirus STLV-III. *Science* (1985) 230:71–3. doi: 10.1126/science.2412295
34. Rimmelzwaan GF, Kuiken T, Van Amerongen G, Bestebroer TM, Fouchier RA, Osterhaus AD. Pathogenesis of influenza A (H5N1) virus infection in a primate model. *J Virol.* (2001) 75:6687–91. doi: 10.1128/JVI.75.14.6687-6691.2001
35. Baas T, Baskin CR, Diamond DL, Garcia-Sastre A, Bielefeldt-Ohmann H, Tumpey TM, et al. Integrated molecular signature of disease: analysis of influenza virus-infected macaques through functional genomics and proteomics. *J Virol.* (2006) 80:10813–28. doi: 10.1128/JVI.00851-06
36. Barker LF, Maynard JE, Purcell RH, Hoofnagle JH, Berquist KR, London WT. Viral hepatitis, type B, in experimental animals. *Am J Med Sci.* (1975) 270:189–95. doi: 10.1097/00000441-197507000-00026
37. Zuckerman AJ, Scalise G, Mazaheri MR, Kremastinou J, Howard CR, Sorensen K. Transmission of hepatitis B to the rhesus monkey. *Dev Biol Stand.* (1975) 30:236–9.
38. Li Q, Dong C, Wang J, Che Y, Jiang L, Wang J, et al. Induction of hepatitis C virus-specific humoral and cellular immune responses in mice and rhesus by artificial multiple epitopes sequence. *Viral Immunol.* (2003) 16:321–33. doi: 10.1089/088282403322396127
39. Rollier C, Verschoor EJ, Paranhos-Baccala G, Drexhage JA, Verstrepen BE, Berland JL, et al. Modulation of vaccine-induced immune responses to hepatitis C virus in rhesus macaques by altering priming before adenovirus boosting. *J Infect Dis.* (2005) 192:920–9. doi: 10.1086/432517
40. Capone S, Meola A, Ercole BB, Vitelli A, Pezzanera M, Ruggeri L, et al. A novel adenovirus type 6 (Ad6)-based hepatitis C virus vector that overcomes preexisting anti-ad5 immunity and induces potent and broad cellular immune responses in rhesus macaques. *J Virol.* (2006) 80:1688–99. doi: 10.1128/JVI.80.4.1688-1699.2006
41. Albrecht P, Burnstein T, Klutch MJ, Hicks HT, Ennis FA. Subacute sclerosing panencephalitis: experimental infection in primates. *Science* (1977) 195:64–6. doi: 10.1126/science.831255
42. Hicks JT, Sullivan JL, Albrecht P. Immune responses during measles infection in immunosuppressed rhesus monkeys. *J Immunol.* (1977) 119:1452–6.
43. Kobune F, Takahashi H, Terao K, Ohkawa T, Ami Y, Suzaki Y, et al. Nonhuman primate models of measles. *Lab Anim Sci.* (1996) 46:315–20.
44. Vogel P, Weigler BJ, Kerr H, Hendrickx AG, Barry PA. Seroepidemiologic studies of cytomegalovirus infection in a breeding population of rhesus macaques. *Lab Anim Sci.* (1994) 44:25–30.
45. Tarantal AF, Salamat MS, Britt WJ, Luciw PA, Hendrickx AG, Barry PA. Neuropathogenesis induced by rhesus cytomegalovirus in fetal rhesus monkeys (*Macaca mulatta*). *J Infect Dis.* (1998) 177:446–50. doi: 10.1086/514206
46. Lockridge KM, Sequar G, Zhou SS, Yue Y, Mandell CP, Barry PA. Pathogenesis of experimental rhesus cytomegalovirus infection. *J Virol.* (1999) 73:9576–83.
47. Gardner MB, Luciw PA. Macaque models of human infectious disease. *ILAR J.* (2008) 49:220–55. doi: 10.1093/ilar.49.2.220
48. Dinapoli JM, Yang L, Suguitan AJr, Elankumaran S, Dorward DW, Murphy BR, et al. Immunization of primates with a Newcastle disease virus-vectored vaccine via the respiratory tract induces a high titer of serum neutralizing antibodies against highly pathogenic avian influenza virus. *J Virol.* (2007) 81:11560–8. doi: 10.1128/JVI.00713-07
49. Xie ZC, Riezu-Boj JI, Lasarte JJ, Guillen J, Su JH, Civeira MP, et al. Transmission of hepatitis C virus infection to tree shrews. *Virology* (1998) 244:513–20. doi: 10.1006/viro.1998.9127
50. Zhao X, Tang ZY, Klumpp B, Wolff-Vorbeck G, Barth H, Levy S, et al. Primary hepatocytes of *Tupaia belangeri* as a potential model for hepatitis C virus infection. *J Clin Invest.* (2002) 109:221–32. doi: 10.1172/JCI0213011
51. Lanford RE, Chavez D, Notvall L, Brasky KM. Comparison of tamarins and marmosets as hosts for GBV-B infections and the effect of immunosuppression on duration of viremia. *Virology* (2003) 311:72–80. doi: 10.1016/S0042-6822(03)00193-4
52. Omatsu T, Moi ML, Hirayama T, Takasaki T, Nakamura S, Tajima S, et al. Common marmoset (*Callithrix jacchus*) as a primate model of dengue virus infection: development of high levels of viraemia and demonstration of protective immunity. *J Gen Virol.* (2011) 92:2272–80. doi: 10.1099/vir.0.031229-0
53. Yoshida T, Omatsu T, Saito A, Katakai Y, Iwasaki Y, Iijima S, et al. CD16(+) natural killer cells play a limited role against primary dengue virus infection in tamarins. *Arch Virol.* (2012) 157:363–8. doi: 10.1007/s00705-011-1178-6
54. Manickam C, Reeves RK. Modeling HCV disease in animals: virology, immunology and pathogenesis of HCV and GBV-B infections. *Front Microbiol.* (2014) 5:690. doi: 10.3389/fmicb.2014.00690
55. Chiu CY, Sanchez-San Martin C, Bouquet J, Li T, Yagi S, Tamhankar M, et al. Experimental Zika virus inoculation in a new world monkey model reproduces key features of the human infection. *Sci Rep.* (2017) 7:17126. doi: 10.1038/s41598-017-17067-w
56. Seferovic M, Martin CS, Tardif SD, Rutherford J, Castro ECC, Li T, et al. Experimental Zika virus infection in the pregnant common marmoset induces spontaneous fetal loss and neurodevelopmental abnormalities. *Sci Rep.* (2018) 8:6851. doi: 10.1038/s41598-018-25205-1
57. Ticehurst J, Rhodes LL Jr, Krawczynski K, Asher LV, Engler WF, Mensing TL, et al. Infection of owl monkeys (*Aotus trivirgatus*) and cynomolgus monkeys (*Macaca fascicularis*) with hepatitis E virus from Mexico. *J Infect Dis.* (1992) 165:835–45. doi: 10.1093/infdis/165.5.835
58. Meyerson NR, Sharma A, Wilkerson GK, Overbaugh J, Sawyer SL. Identification of Owl monkey CD4 receptors broadly compatible with early-stage HIV-1 isolates. *J Virol.* (2015) 89:8611–22. doi: 10.1128/JVI.00890-15
59. Kazanji M, Tartaglia J, Franchini G, De Thoisy B, Talarmin A, Contamin H, et al. Immunogenicity and protective efficacy of recombinant human T-cell leukemia/lymphoma virus type 1 NYVAC and naked DNA vaccine candidates in squirrel monkeys (*Saimiri sciureus*). *J Virol.* (2001) 75:5939–48. doi: 10.1128/JVI.75.13.5939-5948.2001
60. Mortreux F, Kazanji M, Gabet AS, De Thoisy B, Wattel E. Two-step nature of human T-cell leukemia virus type 1 replication in experimentally infected squirrel monkeys (*Saimiri sciureus*). *J Virol.* (2001) 75:1083–9. doi: 10.1128/JVI.75.2.1083-1089.2001
61. Marianneau P, Guillaume V, Wong T, Badmanathan M, Looi RY, Murri S, et al. Experimental infection of squirrel monkeys with nipah virus. *Emerg Infect Dis.* (2010) 16:507–10. doi: 10.3201/eid1603.091346
62. Tebit DM, Arts EJ. Tracking a century of global expansion and evolution of HIV to drive understanding and to combat disease. *Lancet Infect Dis.* (2011) 11:45–56. doi: 10.1016/S1473-3099(10)70186-9
63. D'arc M, Ayouba A, Esteban A, Learn GH, Boue V, Liegeois F, et al. Origin of the HIV-1 group O epidemic in western lowland gorillas. *Proc Natl Acad Sci USA.* (2015) 112:E1343–52. doi: 10.1073/pnas.1502022112

64. Johnson PR, Hirsch VM. SIV infection of macaques as a model for AIDS pathogenesis. *Int Rev Immunol.* (1992) 8:55–63. doi: 10.3109/08830189209056641
65. Stacey AR, Norris PJ, Qin L, Haygreen EA, Taylor E, Heitman J, et al. Induction of a striking systemic cytokine cascade prior to peak viremia in acute human immunodeficiency virus type 1 infection, in contrast to more modest and delayed responses in acute hepatitis B and C virus infections. *J Virol.* (2009) 83:3719–33. doi: 10.1128/JVI.01844-08
66. Keating SM, Heitman JW, Wu S, Deng X, Stacey AR, Zahn RC, et al. Magnitude and quality of cytokine and chemokine storm during acute infection distinguish nonprogressive and progressive simian immunodeficiency virus infections of nonhuman primates. *J Virol.* (2016) 90:10339–50. doi: 10.1128/JVI.01061-16
67. Kwon DS, Angin M, Hongo T, Law KM, Johnson J, Porichis F, et al. CD4+ CD25+ regulatory T cells impair HIV-1-specific CD4 T cell responses by upregulating interleukin-10 production in monocytes. *J Virol.* (2012) 86:6586–94. doi: 10.1128/JVI.06251-11
68. Brooks DG, Trifilo MJ, Edelmann KH, Teyton L, Mcgavern DB, Oldstone MB. Interleukin-10 determines viral clearance or persistence *in vivo*. *Nat Med.* (2006) 12:1301–9. doi: 10.1038/nm1492
69. Mylvaganam GH, Chea LS, Tharp GK, Hicks S, Velu V, Iyer SS, et al. Combination anti-PD-1 and antiretroviral therapy provides therapeutic benefit against SIV. *JCI Insight* (2018) 3:122940. doi: 10.1172/jci.insight.122940
70. Pan E, Feng F, Li P, Yang Q, Ma X, Chunxiu WU, et al. Immune protection of SIV challenge by PD-1 blockade during vaccination in rhesus monkeys. *Front Immunol.* (2018) 9:2415. doi: 10.3389/fimmu.2018.02415
71. Lifson JD, Nowak MA, Goldstein S, Rossio JL, Kinter A, Vasquez G, et al. The extent of early viral replication is a critical determinant of the natural history of simian immunodeficiency virus infection. *J Virol.* (1997) 71:9508–14.
72. Huang X, Liu X, Meyers K, Liu L, Su B, Wang P, et al. Cytokine cascade and networks among MSM HIV seroconverters: implications for early immunotherapy. *Sci Rep.* (2016) 6:36234. doi: 10.1038/srep36234
73. Roberts L, Passmore JA, Williamson C, Little F, Bebell LM, Mlisana K, et al. Plasma cytokine levels during acute HIV-1 infection predict HIV disease progression. *AIDS* (2010) 24:819–31. doi: 10.1097/QAD.0b013e3283367836
74. Mcmichael AJ, Borrow P, Tomaras GD, Goonetilleke N, Haynes BF. The immune response during acute HIV-1 infection: clues for vaccine development. *Nat Rev Immunol.* (2010) 10:11–23. doi: 10.1038/nri2674
75. Kolls JK, Linden A. Interleukin-17 family members and inflammation. *Immunity* (2004) 21:467–76. doi: 10.1016/j.immuni.2004.08.018
76. Hunt PW. Th17, gut, and HIV: therapeutic implications. *Curr Opin HIV AIDS* (2010) 5:189–93. doi: 10.1097/COH.0b013e32833647d9
77. Macal M, Sankaran S, Chun TW, Reay E, Flamm J, Prindiville TJ, et al. Effective CD4+ T-cell restoration in gut-associated lymphoid tissue of HIV-infected patients is associated with enhanced Th17 cells and polyfunctional HIV-specific T-cell responses. *Mucosal Immunol.* (2008) 1:475–88. doi: 10.1038/mi.2008.35
78. Ponte R, Mehraj V, Ghali P, Couedel-Courteille A, Cheynier R, Routy JP. Reversing gut damage in HIV infection: using non-human primate models to instruct clinical research. *EBioMed.* (2016) 4:40–9. doi: 10.1016/j.ebiom.2016.01.028
79. Hahn BH, Shaw GM, De Cock KM, Sharp PM. AIDS as a zoonosis: scientific and public health implications. *Science* (2000) 287:607–14. doi: 10.1126/science.287.5453.607
80. Silvestri G, Paiardini M, Pandrea I, Lederman MM, Sodora DL. Understanding the benign nature of SIV infection in natural hosts. *J Clin Invest.* (2007) 117:3148–54. doi: 10.1172/JCI33034
81. Kornfeld C, Ploquin MJ, Pandrea I, Faye A, Onanga R, Apetrei C, et al. Antiinflammatory profiles during primary SIV infection in African green monkeys are associated with protection against AIDS. *J Clin Invest.* (2005) 115:1082–91. doi: 10.1172/JCI23006
82. Jacquelin B, Mayau V, Targat B, Liovat AS, Kunkel D, Petitjean G, et al. Nonpathogenic SIV infection of African green monkeys induces a strong but rapidly controlled type I IFN response. *J Clin Invest.* (2009) 119:3544–55. doi: 10.1172/JCI40093
83. Jacquelin B, Petitjean G, Kunkel D, Liovat AS, Jochems SP, Rogers KA, et al. Innate immune responses and rapid control of inflammation in African green monkeys treated or not with interferon-alpha during primary SIVagm infection. *PLoS Pathog.* (2014) 10:e1004241. doi: 10.1371/journal.ppat.1004241
84. Palesch D, Bosinger SE, Tharp GK, Vanderford TH, Paiardini M, Chahroudi A, et al. Sooty mangabey genome sequence provides insight into AIDS resistance in a natural SIV host. *Nature* (2018) 553:77–81. doi: 10.1038/nature25140
85. Brenchley JM, Price DA, Schacker TW, Asher TE, Silvestri G, Rao S, et al. Microbial translocation is a cause of systemic immune activation in chronic HIV infection. *Nat Med.* (2006) 12:1365–71. doi: 10.1038/nm1511
86. Brenchley JM, Douek DC. HIV infection and the gastrointestinal immune system. *Mucosal Immunol.* (2008) 1:23–30. doi: 10.1038/mi.2007.1
87. Silvestri G, Sodora DL, Koup RA, Paiardini M, O'neil SP, Mcclure HM, et al. Nonpathogenic SIV infection of sooty mangabeys is characterized by limited bystander immunopathology despite chronic high-level viremia. *Immunity* (2003) 18, 441–452. doi: 10.1016/S1074-7613(03)00060-8
88. Brenchley JM, Paiardini M, Knox KS, Asher AI, Cervasi B, Asher TE, et al. Differential Th17 CD4 T-cell depletion in pathogenic and nonpathogenic lentiviral infections. *Blood* (2008) 112:2826–35. doi: 10.1182/blood-2008-05-159301
89. Naidu YM, Kestler HW III, Li Y, Butler CV, Silva DP, Schmidt DK, et al. Characterization of infectious molecular clones of simian immunodeficiency virus (SIVmac) and human immunodeficiency virus type 2: persistent infection of rhesus monkeys with molecularly cloned SIVmac. *J Virol.* (1988) 62:4691–6.
90. Mckay PF, Barouch DH, Schmitz JE, Veazey RS, Gorgone DA, Lifton MA, et al. Global dysfunction of CD4 T-lymphocyte cytokine expression in simian-human immunodeficiency virus/SIV-infected monkeys is prevented by vaccination. *J Virol.* (2003) 77:4695–702. doi: 10.1128/JVI.77.8.4695-4702.2003
91. Giavedoni LD, Velasquillo MC, Parodi LM, Hubbard GB, Hodara VL. Cytokine expression, natural killer cell activation, and phenotypic changes in lymphoid cells from rhesus macaques during acute infection with pathogenic simian immunodeficiency virus. *J Virol.* (2000) 74:1648–57. doi: 10.1128/JVI.74.4.1648-1657.2000
92. Ponte R, Rancez M, Figueiredo-Morgado S, Dutrieux J, Fabre-Mersseman V, Charmeteau-De-Muylder B, et al. Acute simian immunodeficiency virus infection triggers early and transient interleukin-7 production in the gut, leading to enhanced local chemokine expression and intestinal immune cell homing. *Front Immunol.* (2017) 8:588. doi: 10.3389/fimmu.2017.00588
93. El-Serag HB. Epidemiology of viral hepatitis and hepatocellular carcinoma. *Gastroenterology* (2012) 142:1264–73.e1. doi: 10.1053/j.gastro.2011.12.061
94. Walker CM. Comparative features of hepatitis C virus infection in humans and chimpanzees. *Springer Semin Immunopathol.* (1997) 19:85–98. doi: 10.1007/BF00945027
95. Guidotti LG, Rochford R, Chung J, Shapiro M, Purcell R, Chisari FV. Viral clearance without destruction of infected cells during acute HBV infection. *Science* (1999) 284:825–9. doi: 10.1126/science.284.5415.825
96. Lanford RE, Bigger C, Bassett S, Klimpel G. The chimpanzee model of hepatitis C virus infections. *ILAR J.* (2001) 42:117–26. doi: 10.1093/ilar.42.2.117
97. Thimme R, Wieland S, Steiger C, Ghrayeb J, Reimann KA, Purcell RH, et al. CD8(+) T cells mediate viral clearance and disease pathogenesis during acute hepatitis B virus infection. *J Virol.* (2003) 77:68–76. doi: 10.1128/JVI.77.1.68-76.2003
98. Apolinario A, Majano PL, Lorente R, Nunez O, Clemente G, Garcia-Monzon C. Gene expression profile of T-cell-specific chemokines in human hepatocyte-derived cells: evidence for a synergistic inducer effect of cytokines and hepatitis C virus proteins. *J Viral Hepat.* (2005) 12:27–37. doi: 10.1111/j.1365-2893.2005.00540.x
99. Akbar H, Idrees M, Butt S, Awan Z, Sabar MF, Rehaman I, et al. High baseline interleukine-8 level is an independent risk factor for the achievement of sustained virological response in chronic HCV patients. *Infect Genet Evol.* (2011) 11:1301–5. doi: 10.1016/j.meegid.2011.04.021
100. Zekri AR, Bahnassy AA, Mohamed WS, Alam El-Din HM, Shousha HI, Zayed N, et al. Dynamic interplay between CXCL levels in chronic hepatitis C patients treated by interferon. *Virol J.* (2013) 10:218. doi: 10.1186/1743-422X-10-218

101. Dunn C, Brunetto M, Reynolds G, Christophides T, Kennedy PT, Lampertico P, et al. Cytokines induced during chronic hepatitis B virus infection promote a pathway for NK cell-mediated liver damage. *J Exp Med.* (2007) 204:667–80. doi: 10.1084/jem.20061287
102. Fletcher NF, Sutaria R, Jo J, Barnes A, Blahova M, Meredith LW, et al. Activated macrophages promote hepatitis C virus entry in a tumor necrosis factor-dependent manner. *Hepatology* (2014) 59:1320–30. doi: 10.1002/hep.26911
103. Fletcher NF, Clark AR, Balfe P, Mckeating JA. TNF superfamily members promote hepatitis C virus entry via an NF-kappaB and myosin light chain kinase dependent pathway. *J Gen Virol.* (2017) 98:405–12. doi: 10.1099/jgv.0.000689
104. Poovorawan K, Tangkijvanich P, Chirathaworn C, Wisedopas N, Treeprasertsuk S, Komolmit P, et al. Circulating cytokines and histological liver damage in chronic hepatitis B infection. *Hepat Res Treat.* (2013) 2013:757246. doi: 10.1155/2013/757246
105. Deshpande V, Burd E, Aardema KL, Ma CK, Moonka DK, Brown KA, et al. High levels of hepatitis C virus RNA in native livers correlate with the development of cholestatic hepatitis in liver allografts and a poor outcome. *Liver Transpl.* (2001) 7:118–24. doi: 10.1053/jlts.2001.21278
106. Wald O, Weiss ID, Galun E, Peled A. Chemokines in hepatitis C virus infection: pathogenesis, prognosis and therapeutics. *Cytokine* (2007) 39:50–62. doi: 10.1016/j.cyto.2007.05.013
107. Dienstag JL, Popper H, Purcell RH. The pathology of viral hepatitis types A and B in chimpanzees. *A comparison Am J Pathol.* (1976) 85:131–48.
108. Lucifora J, Vincent IE, Berthillon P, Dupinay T, Michelet M, Protzer U, et al. Hepatitis B virus replication in primary macaque hepatocytes: crossing the species barrier toward a new small primate model. *Hepatology* (2010) 51:1954–60. doi: 10.1002/hep.23602
109. De Carvalho Dominguez Souza BF, Konig A, Rasche A, De Oliveira Carneiro I, Stephan N, Corman VM, et al. A novel hepatitis B virus species discovered in capuchin monkeys sheds new light on the evolution of primate hepadnaviruses. *J Hepatol.* (2018) 68:1114–22. doi: 10.1016/j.jhep.2018.01.029
110. Beames B, Chavez D, Lanford RE. GB virus B as a model for hepatitis C virus. *ILAR J.* (2001) 42:152–60. doi: 10.1093/ilar.42.2.152
111. Iwasaki Y, Mori K, Ishii K, Maki N, Iijima S, Yoshida T, et al. Long-term persistent GBV-B infection and development of a chronic and progressive hepatitis C-like disease in marmosets. *Front Microbiol.* (2011) 2:240. doi: 10.3389/fmicb.2011.00240
112. Beames B, Chavez D, Guerra B, Notvall L, Brasky KM, Lanford RE. Development of a primary tamarin hepatocyte culture system for GB virus-B: a surrogate model for hepatitis C virus. *J Virol.* (2000) 74:11764–72. doi: 10.1128/JVI.74.24.11764-11772.2000
113. Woollard DJ, Haqshenas G, Dong X, Pratt BF, Kent SJ, Gowans EJ. Virus-specific T-cell immunity correlates with control of GB virus B infection in marmosets. *J Virol.* (2008) 82:3054–60. doi: 10.1128/JVI.01153-07
114. Manickam C, Rajakumar P, Wachtman L, Kramer JA, Martinot AJ, Varner V, et al. Acute liver damage associated with innate immune activation in a small nonhuman primate model of hepacivirus infection. *J Virol.* (2016) 90:9153–62. doi: 10.1128/JVI.01051-16
115. Manickam C, Martinot AJ, Jones RA, Varner V, Reeves RK. Hepatic immunopathology during occult hepacivirus re-infection. *Virology* (2017) 512:48–55. doi: 10.1016/j.virol.2017.08.037
116. Manickam C, Wachtman L, Martinot AJ, Giavedoni LD, Reeves RK. Metabolic dysregulation in hepacivirus infection of common marmosets (*Callithrix jacchus*). *PLoS ONE* (2017) 12:e0170240. doi: 10.1371/journal.pone.0170240
117. Costa F, Sarno M, Khouri R, De Paula Freitas B, Siqueira I, Ribeiro GS, et al. Emergence of congenital Zika syndrome: viewpoint from the front lines. *Ann Intern Med.* (2016) 164:689–91. doi: 10.7326/M16-0332
118. Azevedo RSS, De Sousa JR, Araujo MTF, Martins Filho AJ, De Alcantara BN, Araujo FMC, et al. In situ immune response and mechanisms of cell damage in central nervous system of fatal cases microcephaly by Zika virus. *Sci Rep.* (2018) 8:1. doi: 10.1038/s41598-017-17765-5
119. De Sousa JR, Azevedo R, Martins Filho AJ, De Araujo MTF, Cruz E, Vasconcelos BCB, et al. *In situ* inflammasome activation results in severe damage to the central nervous system in fatal Zika virus microcephaly cases. *Cytokine* (2018) 111:255–64. doi: 10.1016/j.cyto.2018.08.008
120. De Sousa JR, Azevedo RSS, Martins Filho AJ, Araujo MTF, Moutinho ERC, Baldez Vasconcelos BC, et al. Correlation between apoptosis and in situ immune response in fatal cases of microcephaly caused by Zika virus. *Am J Pathol.* (2018). doi: 10.1016/j.ajpath.2018.07.009
121. Abbink P, Larocca RA, Dejnirattisai W, Peterson R, Nkolola JP, Borducchi EN, et al. Therapeutic and protective efficacy of a dengue antibody against Zika infection in rhesus monkeys. *Nat Med.* (2018) 24:721–3. doi: 10.1038/s41591-018-0056-0
122. Abbink P, Stephenson KE, Barouch DH. Zika virus vaccines. *Nat Rev Microbiol.* (2018). doi: 10.1038/s41579-018-0039-7
123. Alves Dos Santos E, Fink K. Animal models for dengue and zika vaccine development. *Adv Exp Med Biol.* (2018) 1062:215–39. doi: 10.1007/978-981-10-8727-1_16
124. Adams Waldorf KM, Stencel-Baerenwald JE, Kapur RP, Studholme C, Boldenow E, Vornhagen J, et al. Fetal brain lesions after subcutaneous inoculation of Zika virus in a pregnant nonhuman primate. *Nat Med.* (2016) 22:1256–9. doi: 10.1038/nm.4193
125. Dudley DM, Van Rompay KK, Coffey LL, Ardeshir A, Keesler RI, Bliss-Moreau E, et al. Miscarriage and stillbirth following maternal Zika virus infection in nonhuman primates. *Nat Med.* (2018) 24:1104–7. doi: 10.1038/s41591-018-0088-5
126. Hirsch AJ, Roberts VHJ, Grigsby PL, Haese N, Schabel MC, Wang X, et al. Zika virus infection in pregnant rhesus macaques causes placental dysfunction and immunopathology. *Nat Commun.* (2018) 9:263. doi: 10.1038/s41467-017-02499-9
127. Martinot AJ, Abbink P, Afacan O, Prohl AK, Bronson R, Hecht JL, et al. Fetal neuropathology in Zika virus-infected pregnant female rhesus monkeys. *Cell* (2018) 173:1111–22.e10. doi: 10.1016/j.cell.2018.03.019
128. Vanchiere JA, Ruiz JC, Brady AG, Kuehl TJ, Williams LE, Baze WB, et al. Experimental Zika virus infection of neotropical primates. *Am J Trop Med Hyg.* (2018) 98:173–7. doi: 10.4269/ajtmh.17-0322
129. Aid M, Abbink P, Larocca RA, Boyd M, Nityanandam R, Nanayakkara O, et al. Zika virus persistence in the central nervous system and lymph nodes of rhesus monkeys. *Cell* (2017) 169:610–20.e14. doi: 10.1016/j.cell.2017.04.008
130. Appanna R, Wang SM, Ponnampalavanar SA, Lum LC, Sekaran SD. Cytokine factors present in dengue patient sera induces alterations of junctional proteins in human endothelial cells. *Am J Trop Med Hyg.* (2012) 87:936–42. doi: 10.4269/ajtmh.2012.11-0606
131. Rothman AL. Immunity to dengue virus: a tale of original antigenic sin and tropical cytokine storms. *Nat Rev Immunol.* (2011) 11:532–43. doi: 10.1038/nri3014
132. Clark KB, Onlamoon N, Hsiao HM, Perng GC, Villinger F. Can non-human primates serve as models for investigating dengue disease pathogenesis? *Front Microbiol.* (2013) 4:305. doi: 10.3389/fmicb.2013.00305
133. Hickey AC, Koster JA, Thalmann CM, Hardcastle K, Tio PH, Cardosa MJ, et al. Serotype-specific host responses in rhesus macaques after primary dengue challenge. *Am J Trop Med Hyg.* (2013) 89:1043–57. doi: 10.4269/ajtmh.13-0145
134. Onlamoon N, Noisakran S, Hsiao HM, Duncan A, Villinger F, Ansari AA, et al. Dengue virus-induced hemorrhage in a nonhuman primate model. *Blood* (2010) 115:1823–34. doi: 10.1182/blood-2009-09-242990
135. Vasconcelos BC, Vieira JA, Silva GO, Fernandes TN, Rocha LC, Viana AP, et al. Antibody-enhanced dengue disease generates a marked CNS inflammatory response in the black-tufted marmoset *Callithrix penicillata*. *Neuropathology* (2016) 36:3–16. doi: 10.1111/neup.12229
136. Ferreira MS, De Castro PH, Silva GA, Casseb SM, Dias Junior AG, Rodrigues SG, et al. *Callithrix penicillata*: a feasible experimental model for dengue virus infection. *Immunol Lett.* (2014) 158:126–33. doi: 10.1016/j.imlet.2013.12.008
137. Peiris JS, Hui KP, Yen HL. Host response to influenza virus: protection versus immunopathology. *Curr Opin Immunol.* (2010) 22:475–81. doi: 10.1016/j.coi.2010.06.003
138. Safronetz D, Rockx B, Feldmann F, Belisle SE, Palermo RE, Brining D, et al. Pandemic swine-origin H1N1 influenza A virus isolates show heterogeneous virulence in macaques. *J Virol.* (2011) 85:1214–23. doi: 10.1128/JVI.01848-10

139. Liu Q, Zhou YH, Yang ZQ. The cytokine storm of severe influenza and development of immunomodulatory therapy. *Cell Mol Immunol.* (2016) 13:3–10. doi: 10.1038/cmi.2015.74
140. Teijaro JR, Walsh KB, Cahalan S, Fremgen DM, Roberts E, Scott F, et al. Endothelial cells are central orchestrators of cytokine amplification during influenza virus infection. *Cell* (2011) 146:980–91. doi: 10.1016/j.cell.2011.08.015
141. Oldstone MB, Teijaro JR, Walsh KB, Rosen H. Dissecting influenza virus pathogenesis uncovers a novel chemical approach to combat the infection. *Virology* (2013) 435:92–101. doi: 10.1016/j.virol.2012.09.039
142. Margine I, Krammer F. Animal models for influenza viruses: implications for universal vaccine development. *Pathogens* (2014) 3:845–74. doi: 10.3390/pathogens3040845
143. Skinner JA, Zurawski SM, Sugimoto C, Vinet-Oliphant H, Vinod P, Xue Y, et al. Immunologic characterization of a rhesus macaque H1N1 challenge model for candidate influenza virus vaccine assessment. *Clin Vaccine Immunol.* (2014) 21:1668–80. doi: 10.1128/CVI.00547-14
144. Itoh Y. Translational research on influenza virus infection using a nonhuman primate model. *Pathol Int.* (2016) 66:132–41. doi: 10.1111/pin.12385
145. Wonderlich ER, Swan ZD, Bissel SJ, Hartman AL, Carney JP, O'malley KJ, et al. Widespread virus replication in alveoli drives acute respiratory distress syndrome in aerosolized H5N1 influenza infection of Macaques. *J Immunol.* (2017) 198:1616–26. doi: 10.4049/jimmunol.1601770
146. Watanabe T, Iwatsuki-Horimoto K, Kiso M, Nakajima N, Takahashi K, Jose Da Silva Lopes T, et al. Experimental infection of Cynomolgus Macaques with highly pathogenic H5N1 influenza virus through the aerosol route. *Sci Rep.* (2018) 8:4801. doi: 10.1038/s41598-018-23022-0
147. Rimmelzwaan GF, Kuiken T, Van Amerongen G, Bestebroer TM, Fouchier RA, Osterhaus AD. A primate model to study the pathogenesis of influenza A (H5N1) virus infection. *Avian Dis.* (2003) 47:931–3. doi: 10.1637/0005-2086-47.s3.931
148. Bruder D, Srikiatkhachorn A, Enelow RI. Cellular immunity and lung injury in respiratory virus infection. *Viral Immunol.* (2006) 19:147–55. doi: 10.1089/vim.2006.19.147
149. Imai Y, Kuba K, Neely GG, Yaghubian-Malhami R, Perkmann T, Van Loo G, et al. Identification of oxidative stress and Toll-like receptor 4 signaling as a key pathway of acute lung injury. *Cell* (2008) 133:235–49. doi: 10.1016/j.cell.2008.02.043
150. Cilloniz C, Shinya K, Peng X, Korth MJ, Proll SC, Aicher LD, et al. Lethal influenza virus infection in macaques is associated with early dysregulation of inflammatory related genes. *PLoS Pathog.* (2009) 5:e1000604. doi: 10.1371/journal.ppat.1000604
151. Kobasa D, Jones SM, Shinya K, Kash JC, Copps J, Ebihara H, et al. Aberrant innate immune response in lethal infection of macaques with the 1918 influenza virus. *Nature* (2007) 445:319–23. doi: 10.1038/nature05495
152. Baskin CR, Bielefeldt-Ohmann H, Tumpey TM, Sabourin PJ, Long JP, Garcia-Sastre A, et al. Early and sustained innate immune response defines pathology and death in nonhuman primates infected by highly pathogenic influenza virus. *Proc Natl Acad Sci USA.* (2009) 106:3455–60. doi: 10.1073/pnas.0813234106
153. Moncla LH, Ross TM, Dinis JM, Weinfurter JT, Mortimer TD, Schultz-Darken N, et al. A novel nonhuman primate model for influenza transmission. *PLoS ONE* (2013) 8:e78750. doi: 10.1371/journal.pone.0078750
154. Jin S, Li Y, Pan R, Zou X. Characterizing and controlling the inflammatory network during influenza A virus infection. *Sci Rep.* (2014) 4:3799. doi: 10.1038/srep03799
155. Ruebner BH, Hirano T, Slusser RJ, Medearis DNJr. Human cytomegalovirus infection. electron microscopic and histochemical changes in cultures of human fibroblasts *Am J Pathol.* (1965) 46:477–96.
156. Fiala M, Austin T, Heiner DC, Imagawa DT, Guze LB, Payne JE. Cytomegalovirus infection of polymorphonuclear and mononuclear leukocytes in immunosuppressed transplant patients, patients with CMV mononucleosis and a patient with leukaemia. *IARC Sci Publ.* (1975) 109–12.
157. Margolis G, Kilham L. Neuronal parasitism and cell fusion in mouse cytomegalovirus encephalitis. *Exp Mol Pathol.* (1976) 25:20–30. doi: 10.1016/0014-4800(76)90013-7
158. Isom HC. DNA synthesis in isolated hepatocytes infected with herpesviruses. *Virology* (1980) 103:199–216. doi: 10.1016/0042-6822(80)90138-5
159. Dankner WM, Mccutchan JA, Richman DD, Hirata K, Spector SA. Localization of human cytomegalovirus in peripheral blood leukocytes by in situ hybridization. *J Infect Dis.* (1990) 161:31–6. doi: 10.1093/infdis/161.1.31
160. Garnett HM. Increased ability of human embryonic fibroblasts to accumulate Ca2+ due to cytomegalovirus infection. *Cytobios* (1981) 31:107–16.
161. Zhu H, Cong JP, Shenk T. Use of differential display analysis to assess the effect of human cytomegalovirus infection on the accumulation of cellular RNAs: induction of interferon-responsive RNAs. *Proc Natl Acad Sci USA.* (1997) 94:13985–90. doi: 10.1073/pnas.94.25.13985
162. Kowalik TF, Wing B, Haskill JS, Azizkhan JC, Baldwin ASJr, Huang ES. Multiple mechanisms are implicated in the regulation of NF-kappa B activity during human cytomegalovirus infection. *Proc Natl Acad Sci USA.* (1993) 90:1107–11. doi: 10.1073/pnas.90.3.1107
163. Waldman WJ, Knight DA, Huang EH, Sedmak DD. Bidirectional transmission of infectious cytomegalovirus between monocytes and vascular endothelial cells: an in vitro model. *J Infect Dis.* (1995) 171:263–72. doi: 10.1093/infdis/171.2.263
164. Fortunato EA, Mcelroy AK, Sanchez I, Spector DH. Exploitation of cellular signaling and regulatory pathways by human cytomegalovirus. *Trends Microbiol.* (2000) 8:111–9. doi: 10.1016/S0966-842X(00)01699-1
165. Gerna G, Percivalle E, Baldanti F, Sozzani S, Lanzarini P, Genini E, et al. Human cytomegalovirus replicates abortively in polymorphonuclear leukocytes after transfer from infected endothelial cells via transient microfusion events. *J Virol.* (2000) 74:5629–38. doi: 10.1128/JVI.74.12.5629-5638.2000
166. Haig DM. Subversion and piracy: DNA viruses and immune evasion. *Res Vet Sci.* (2001) 70:205–19. doi: 10.1053/rvsc.2001.0462
167. Noriega V, Redmann V, Gardner T, Tortorella D. Diverse immune evasion strategies by human cytomegalovirus. *Immunol Res.* (2012) 54:140–51. doi: 10.1007/s12026-012-8304-8
168. Goser S, Ottl R, Brodner A, Dengler TJ, Torzewski J, Egashira K, et al. Critical role for monocyte chemoattractant protein-1 and macrophage inflammatory protein-1alpha in induction of experimental autoimmune myocarditis and effective anti-monocyte chemoattractant protein-1 gene therapy. *Circulation* (2005) 112:3400–7. doi: 10.1161/CIRCULATIONAHA.105.572396
169. Riou R, Bressollette-Bodin C, Boutoille D, Gagne K, Rodallec A, Lefebvre M, et al. Severe symptomatic primary human cytomegalovirus infection despite effective innate and adaptive immune responses. *J Virol.* (2017) 91:e02245-16. doi: 10.1128/JVI.02245-16
170. Iwasenko JM, Howard J, Arbuckle S, Graf N, Hall B, Craig ME, et al. Human cytomegalovirus infection is detected frequently in stillbirths and is associated with fetal thrombotic vasculopathy. *J Infect Dis.* (2011) 203:1526–33. doi: 10.1093/infdis/jir121
171. Hamilton ST, Scott G, Naing Z, Iwasenko J, Hall B, Graf N, et al. Human cytomegalovirus-induces cytokine changes in the placenta with implications for adverse pregnancy outcomes. *PLoS ONE* (2012) 7:e52899. doi: 10.1371/journal.pone.0052899
172. Alcendor DJ, Charest AM, Zhu WQ, Vigil HE, Knobel SM. Infection and upregulation of proinflammatory cytokines in human brain vascular pericytes by human cytomegalovirus. *J Neuroinflammation* (2012) 9:95. doi: 10.1186/1742-2094-9-95
173. Mcgeoch DJ, Cook S, Dolan A, Jamieson FE, Telford EA. Molecular phylogeny and evolutionary timescale for the family of mammalian herpesviruses. *J Mol Biol.* (1995) 247:443–58. doi: 10.1006/jmbi.1995.0152
174. Swack NS, Liu OC, Hsiung GD. Cytomegalovirus infections of monkeys and baboons. *Am J Epidemiol.* (1971) 94:397–402. doi: 10.1093/oxfordjournals.aje.a121334
175. Powers C, Fruh K. Rhesus CMV: an emerging animal model for human CMV. *Med Microbiol Immunol.* (2008) 197:109–15. doi: 10.1007/s00430-007-0073-y
176. London WT, Martinez AJ, Houff SA, Wallen WC, Curfman BL, Traub RG, et al. Experimental congenital disease with simian cytomegalovirus in rhesus monkeys. *Teratology* (1986) 33:323–31. doi: 10.1002/tera.1420330311
177. Baskin GB. Disseminated cytomegalovirus infection in immunodeficient rhesus monkeys. *Am J Pathol.* (1987) 129:345–52.

178. Barry PA, Lockridge KM, Salamat S, Tinling SP, Yue Y, Zhou SS, et al. Nonhuman primate models of intrauterine cytomegalovirus infection. *ILAR J.* (2006) 47:49–64. doi: 10.1093/ilar.47.1.49
179. Lockridge KM, Zhou SS, Kravitz RH, Johnson JL, Sawai ET, Blewett EL, et al. Primate cytomegaloviruses encode and express an IL-10-like protein. *Virology* (2000) 268:272–80. doi: 10.1006/viro.2000.0195
180. Striz I, Brabcova E, Kolesar L, Sekerkova A. Cytokine networking of innate immunity cells: a potential target of therapy. *Clin Sci.* (2014) 126:593–612. doi: 10.1042/CS20130497
181. Cohen BL, Sachar DB. Update on anti-tumor necrosis factor agents and other new drugs for inflammatory bowel disease. *BMJ* (2017) 357:j2505. doi: 10.1136/bmj.j2505
182. Miller DM, Klucher KM, Freeman JA, Hausman DF, Fontana D, Williams DE. Interferon lambda as a potential new therapeutic for hepatitis C. *Ann N Y Acad Sci.* (2009) 1182:80–7. doi: 10.1111/j.1749-6632.2009.05241.x
183. Lauw FN, Dekkers PE, Te Velde AA, Speelman P, Levi M, Kurimoto M, et al. Interleukin-12 induces sustained activation of multiple host inflammatory mediator systems in chimpanzees. *J Infect Dis.* (1999) 179:646–52. doi: 10.1086/314636
184. Ansari AA, Mayne AE, Sundstrom JB, Bostik P, Grimm B, Altman JD, et al. Administration of recombinant rhesus interleukin-12 during acute simian immunodeficiency virus (SIV) infection leads to decreased viral loads associated with prolonged survival in SIVmac251-infected rhesus macaques. *J Virol.* (2002) 76:1731–43. doi: 10.1128/JVI.76.4.1731-1743.2002
185. Waldmann TA, Lugli E, Roederer M, Perera LP, Smedley JV, Macallister RP, et al. Safety (toxicity), pharmacokinetics, immunogenicity, and impact on elements of the normal immune system of recombinant human IL-15 in rhesus macaques. *Blood* (2011) 117:4787–95. doi: 10.1182/blood-2010-10-311456
186. Degottardi MQ, Okoye AA, Vaidya M, Talla A, Konfe AL, Reyes MD, et al. Effect of Anti-IL-15 administration on T Cell and NK cell homeostasis in rhesus Macaques. *J Immunol.* (2016) 197:1183–98. doi: 10.4049/jimmunol.1600065
187. Robinson TO, Schluns KS. The potential and promise of IL-15 in immuno-oncogenic therapies. *Immunol Lett.* (2017) 190:159–68. doi: 10.1016/j.imlet.2017.08.010
188. Hu Q, Ye X, Qu X, Cui D, Zhang L, Xu Z, et al. Discovery of a novel IL-15 based protein with improved developability and efficacy for cancer immunotherapy. *Sci Rep.* (2018) 8:7675. doi: 10.1038/s41598-018-25987-4
189. Ellis-Connell AL, Balgeman AJ, Zarbock KR, Barry G, Weiler A, Egan JO, et al. ALT-803 transiently reduces simian immunodeficiency virus replication in the absence of antiretroviral treatment. *J Virol.* (2000) 92:e01748-17. doi: 10.1128/JVI.01748-17
190. Romee R, Cooley S, Berrien-Elliott MM, Westervelt P, Verneris MR, Wagner JE, et al. First-in-human phase 1 clinical study of the IL-15 superagonist complex ALT-803 to treat relapse after transplantation. *Blood* (2018) 131:2515–27. doi: 10.1182/blood-2017-12-823757
191. Wrangle JM, Velcheti V, Patel MR, Garrett-Mayer E, Hill EG, Ravenel JG, et al. ALT-803, an IL-15 superagonist, in combination with nivolumab in patients with metastatic non-small cell lung cancer: a non-randomised, open-label, phase 1b trial. *Lancet Oncol.* (2018) 19:694–704. doi: 10.1016/S1470-2045(18)30148-7
192. Barouch DH, Santra S, Schmitz JE, Kuroda MJ, Fu TM, Wagner W, et al. Control of viremia and prevention of clinical AIDS in rhesus monkeys by cytokine-augmented DNA vaccination. *Science* (2000) 290:486–92. doi: 10.1126/science.290.5491.486
193. Henrich TJ, Kuritzkes DR. HIV-1 entry inhibitors: recent development and clinical use. *Curr Opin Virol.* (2013) 3:51–7. doi: 10.1016/j.coviro.2012.12.002
194. Billick E, Seibert C, Pugach P, Ketas T, Trkola A, Endres MJ, et al. The differential sensitivity of human and rhesus macaque CCR5 to small-molecule inhibitors of human immunodeficiency virus type 1 entry is explained by a single amino acid difference and suggests a mechanism of action for these inhibitors. *J Virol.* (2004) 78:4134–44. doi: 10.1128/JVI.78.8.4134-4144.2004
195. Este JA, Telenti A. HIV entry inhibitors. *Lancet* (2007) 370:81–8. doi: 10.1016/S0140-6736(07)61052-6
196. Taaffe JE, Bosinger SE, Del Prete GQ, Else JG, Ratcliffe S, Ward CD, et al. CCR5 blockade is well tolerated and induces changes in the tissue distribution of CCR5+ and CD25+ T cells in healthy, SIV-uninfected rhesus macaques. *J Med Primatol.* (2012) 41:24–42. doi: 10.1111/j.1600-0684.2011.00521.x
197. Kelly KM, Tocchetti CG, Lyashkov A, Tarwater PM, Bedja D, Graham DR, et al. CCR5 inhibition prevents cardiac dysfunction in the SIV/macaque model of HIV. *J Am Heart Assoc.* (2014) 3:e000874. doi: 10.1161/JAHA.114.000874
198. Duffen J, Zhang M, Masek-Hammerman K, Nunez A, Brennan A, Jones JEC, et al. Modulation of the IL-33/IL-13 axis in obesity by IL-13Ralpha2. *J Immunol.* (2018) 200:1347–59. doi: 10.4049/jimmunol.1701256
199. Yoshizaki K, Nishimoto N, Mihara M, Kishimoto T. Therapy of rheumatoid arthritis by blocking IL-6 signal transduction with a humanized anti-IL-6 receptor antibody. *Springer Semin Immunopathol.* (1998) 20:247–59. doi: 10.1007/BF00832010
200. Rojas JR, Taylor RP, Cunningham MR, Rutkoski TJ, Vennarini J, Jang H, et al. Formation, distribution, and elimination of infliximab and anti-infliximab immune complexes in cynomolgus monkeys. *J Pharmacol Exp Ther.* (2005) 313:578–85. doi: 10.1124/jpet.104.079277
201. Naidoo J, Page DB, Li BT, Connell LC, Schindler K, Lacouture ME, et al. Toxicities of the anti-PD-1 and anti-PD-L1 immune checkpoint antibodies. *Ann Oncol.* (2015) 26:2375–91. doi: 10.1093/annonc/mdv383
202. Okoye IS, Houghton M, Tyrrell L, Barakat K, Elahi S. Coinhibitory receptor expression and immune checkpoint blockade: maintaining a balance in CD8(+) T cell responses to chronic viral infections and cancer. *Front Immunol.* (2017) 8:1215. doi: 10.3389/fimmu.2017.01215

Conflict of Interest Statement: The authors declare that the research was conducted in the absence of any commercial or financial relationships that could be construed as a potential conflict of interest.

Advantages of publishing in Frontiers

OPEN ACCESS
Articles are free to read for greatest visibility and readership

FAST PUBLICATION
Around 90 days from submission to decision

HIGH QUALITY PEER-REVIEW
Rigorous, collaborative, and constructive peer-review

TRANSPARENT PEER-REVIEW
Editors and reviewers acknowledged by name on published articles

Frontiers
Avenue du Tribunal-Fédéral 34
1005 Lausanne | Switzerland

Visit us: www.frontiersin.org
Contact us: info@frontiersin.org | +41 21 510 17 00

REPRODUCIBILITY OF RESEARCH
Support open data and methods to enhance research reproducibility

DIGITAL PUBLISHING
Articles designed for optimal readership across devices

FOLLOW US
@frontiersin

IMPACT METRICS
Advanced article metrics track visibility across digital media

EXTENSIVE PROMOTION
Marketing and promotion of impactful research

LOOP RESEARCH NETWORK
Our network increases your article's readership